

**Best
Available
Copy**

AD-A284 276



AD _____

(1)

CONTRACT NO: DAMD17-90-C-0125

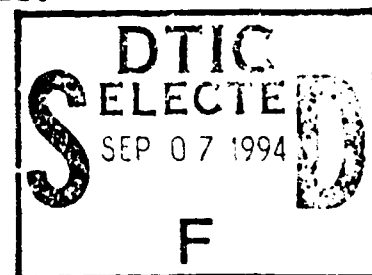
TITLE: MECHANISMS OF CYTOTOXICITY OF THE AIDS VIRUS

PRINCIPAL INVESTIGATOR: Lee Ratner, M.D., Ph.D.

CONTRACTING ORGANIZATION: Washington University
School of Medicine
660 S. Euclid Avenue
St. Louis, Missouri 63110

REPORT DATE: August 1, 1994

TYPE OF REPORT: Final Report



PREPARED FOR: U.S. Army Medical Research and Materiel
Command (Provisional), Fort Detrick,
Frederick, Maryland 21702-5012

DISTRIBUTION STATEMENT: Approved for public release;
distribution unlimited

The views, opinions and/or findings contained in this report are those of the author(s) and should not be construed as an official Department of the Army position, policy or decision unless so designated by other documentation.

94-29113



29113

5

1 August 1994 Final Report (9/17/90 - 7/16/94)

Mechanisms of Cytotoxicity of the Aids Virus

Contract No.
DAMD17-90-C-0125

Lee Ratner, M.D., Ph.D.

Washington University
School of Medicine
660 S. Euclid Avenue
St. Louis, Missouri 63110

U.S. Army Medical Research and Materiel
Command (Provisional)
Fort Detrick
Frederick, Maryland 21702-5012

Approved for public release;
Distribution unlimited

Regulatory genes of HIV-1, HIV-2, and SIV are important in modulating virus infection and infection and transmission in vivo. Viral proteins R. (VPR) and X (VPX) and the negative factor (NEF) are three of the least well characterized regulatory proteins. Identification of their functions, their mechanisms of actions, and structure-function relationships of each protein, in vitro and in vivo will assist in our understanding of the pathogenesis of HIV induced disease. This information will be critical in defining therapeutic approaches to suppression HIV-1 infection, replication, and transmission.

DISCLOSURE

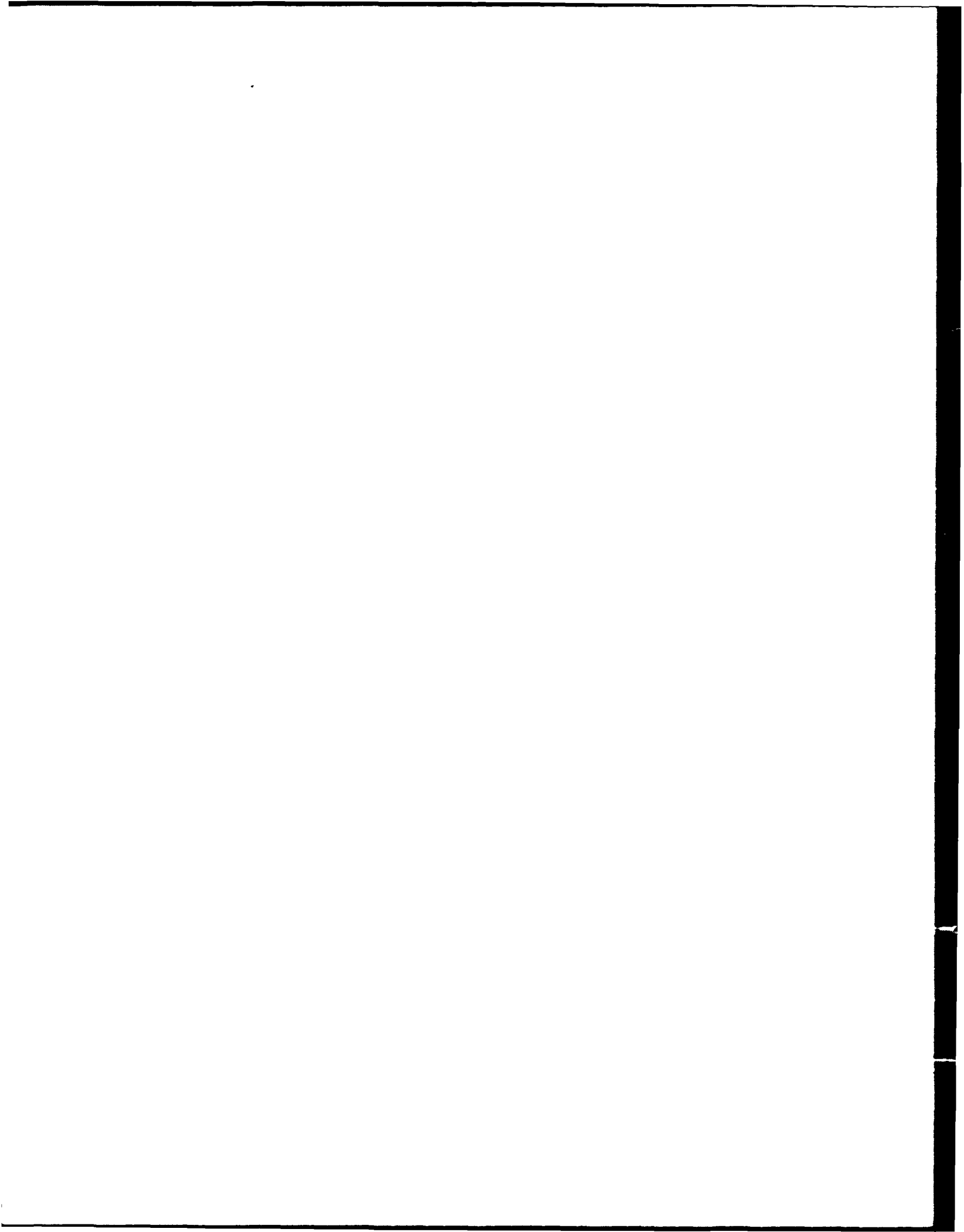
HIV, AIDS, Cytotoxicity, Biology, Biotechnology,
pr, Vpx, Nef, HIV-1, Vpu

Unclassified

Unclassified

Unclassified

Unlimited



Summary

The current study examined the functions of the Vpr, Vpx, and Nef regulatory proteins of human immunodeficiency viruses. Vpr was found to be important for productive infection of monocytes by HIV-1 but could be replaced by Vpu. Several Vpr mutants have been constructed in viral clones and expression vectors and a Vpr antibody raised for further structure-function studies of this protein. Vpr was shown to be packaged into virus particles, and this required only the Gag proteins of HIV-1. The C-terminus of the Pr55 Gag precursor, which includes the p6 domain, was necessary and sufficient for Vpr incorporation into the virus particle. Cellular localization studies for Vpr demonstrated that a significant proportion of the protein accumulated in the nucleus. The nuclear localization signal of Vpr was mapped to a basic domain in the C-terminus of the molecule. This activity of Vpr was critical for the nuclear import of newly synthesized viral DNA in quiescent cells. Studies of Vpx showed that it was associated with gag p27 in the virus particle. Furthermore, Vpx played a role in virus infection of primary lymphocytes at low multiplicities of infection. Studies of Nef demonstrated an inhibition of transcription of the HIV-1 LTR and IL2 promoter mediated by inhibition of NF-kB and AP-1 binding. However, the effects of Nef could be bypassed by activating T cells through the TNF receptor, IL1 receptor, or LPS receptor. Effects of Nef could also be overcome by the addition of phospholipase C, suggesting that the effects of Nef are on early T cell activation events. Studies of Nef mutants demonstrated a role for myristoylation in anchoring the protein to the cytoskeleton. Nef was also shown to mediate downmodulation of cell surface expression of CD4 through the lck binding domain of CD4.

Accepted	
NTIS	
DTIC	
Unannounced	
Justification	
E,	
Dist	
A-1	

FOREWORD

Opinions, interpretations, conclusions and recommendations are those of the author and are not necessarily endorsed by the U.S. Army.

✓ Where copyrighted material is quoted, permission has been obtained to use such material.

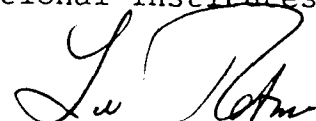
✓ Where material from documents designated for limited distribution is quoted, permission has been obtained to use the material.

N/A Citations of commercial organizations and trade names in this report do not constitute an official Department of the Army endorsement or approval of the products or services of these organizations.

N/A In conducting research using animals, the investigator(s) adhered to the "Guide for the Care and Use of Laboratory Animals," prepared by the Committee on Care and Use of Laboratory Animals of the Institute of Laboratory Animal Resources, National Research Council (NIH Publication No. 86-23, Revised 1985).

✓ For the protection of human subjects, the investigator(s) have adhered to policies of applicable Federal Law 45 CFR 46.

✓ In conducting research utilizing recombinant DNA technology, the investigator(s) adhered to current guidelines promulgated by the National Institutes of Health.



P.I. Signature

8-2-94

Date

TABLE OF CONTENTS

Page

Introduction

6 Technical Objectives

7 Hypotheses

7 Background

Body

11 To define the function of viral protein R (Vpr)

31 To define the function of viral protein X (Vpx)

36 To determine the function and mechanism of action of negative factor (Nef)

105 Conclusions

106 References

Appendix - Publications

Copy of all publications, numbered as listed in Publications Section

(5) INTRODUCTION - Derived from the original Contract Proposal

a) Technical Objectives

1. To define the function of viral protein R (VPR)

- a. Express HIV-1, HIV-2, and SIV vpr genes in E. coli
- b. Develop antibodies to recombinant VPR products
- c. Determine size(s) of VPR products in acute and chronically infected lymphoid and monocytoid cells infected with HIV-1, HIV-2, and SIV
- d. Determine cellular localization of VPR
- e. Assess co- and post-translational modifications of the VPR proteins
- f. Isolate cDNAs encoding VPR
- g. Determine role of VPR in HIV-1, HIV-2, and SIV replication in a variety of lymphoid and monocytoid cells
- h. Determine mechanism of action of VPR in enhancing HIV-1 infectivity and/or replication in MT4 lymphoid cells
- i. Determine role of VPR *in vivo* with appropriate model systems
- j. Determine role of VPR in modulating disease in HIV-1 infected humans

2. To determine the function of viral protein X (VPX)

- a. To assess effects of VPX on replication and cytopathicity of HIV-2 in T lymphoid and monocytoid cells
- b. To determine cellular localization of VPX in HIV-2 infected cells
- c. To determine if there are co- or post-translational modifications of VPX
- d. To assess whether VPX proviral mutants can be complemented *in trans* by a VPX expression clone
- e. To determine structure-function-relationships of VPX
- f. To assess effects of VPX on replication and cytopathicity of SIV in T lymphoid and monocytoid cells
- g. To assess role of VPX *in vivo* with animal model systems

3. To determine function and mechanism of action of NEF

- a. To determine relative effects of HIV-1 NEF on viral RNA transcription, degradation, and nuclear-cytoplasmic transport
- b. To characterize NEF responsive sequences
- c. To characterize mechanism of transcriptional suppression by NEF
- d. To determine role of phosphorylation, GTP binding, GTPase activity, and myristoylation acceptor activity in NEF activity
- e. To determine effects of NEF on cellular proteins including those which may modulate HIV-1 infectivity or replication
- f. To determine role of NEF in HIV-2 and SIV replication
- g. To determine role of NEF *in vivo* with animal model systems
- h. To determine role of NEF in modulating manifestations of HIV-1 infection in humans
- i. To determine therapeutic role of a retrovirus expressing NEF

b) Hypotheses

Regulatory genes of HIV-1, HIV-2, and SIV are important in modulating virus infection and transmission in vivo. Viral proteins R (Vrk) and X (VPX) and the negative factor (NEF) are three of the least well characterized regulatory proteins. Identification of their functions, their mechanisms of actions, and structure-function relationships of each protein, in vitro and in vivo will assist in our understanding of the pathogenesis of HIV induced disease. This information will be critical in defining therapeutic approaches to suppressing HIV-1 infection, replication, and transmission.

c) Background

i) Basis

HIV-1 and HIV-2 cause a slowly progressive immunosuppressive disorder in humans. One species of simian immunodeficiency virus (SIV) derived from rhesus macaques, SIV-MAC, can cause a similar disorder in this species of monkeys (Chakrabarti et al., 1987). Related lentiviruses are found in other species of monkeys including mandrills (Tsujiimoto et al., 1989), sooty mangabeys (Hirsch et al., 1989), and African green monkeys (Fukasawa et al., 1988). More distantly related lentiviruses causes immunosuppression in cats (feline immunodeficiency virus) (Pederson et al., 1987; Luciw et al., 1989), sheep (visna virus) (Haas et al., 1985), goats (caprine-arthritis encephalitis virus) (Narayan & Cork, 1985), and horses (equine infectious anemia virus (Issel et al., 1986).

These viruses are biologically and structurally related. They differ from avian and murine retroviruses in the complex nature of their genomes. In addition to genes encoding structural and enzymatic virion proteins, GAG, POL, and ENV, these viruses all encode a number of regulatory proteins (Haseltine et al., 1988). Seven regulatory proteins have been identified thus far.

TAT is a positive feedback regulator of expression of virion and regulatory proteins, working primarily at the level of transcriptional initiation or elongation, and to a lesser degree at a post-transcriptional level.

REV is a differential regulator that increases expression of virion proteins at the expense of regulatory proteins by increasing the transport of unspliced and singly spliced mRNAs from the nucleus to the cytoplasm and by increasing their stability. In addition, a fusion protein between TAT and REV has recently been described (Felber et al., 1989b); its function is unknown.

VIF is important for the infectivity of the virus particle by a post-translational mechanism that remains to be defined. VPU is important for mature virus assembly at the cell surface. VPR, VPX, and NEF are additional regulatory proteins whose functions will be the focus of this study, and will be discussed below.

Regulatory proteins are likely to be important in determining the level of virus replication at different stages of disease, in determining the types of interaction with the immune system, and in modulating virus infectivity and transmission. A better understanding of their structure, expression, and mechanism of action will undoubtedly improve our understanding of pathogenesis, lead to the development of new diagnostic assays, provide new insights into therapeutic maneuvers which may suppress virus replication and/or cytopathicity, and assist in the development of a vaccine for HIV prevention.

Viral Protein R (VPR)

The vpr gene is found in the genomes of HIV-1, HIV-2, simian immunodeficiency virus (SIV) of rhesus macaques (SIV-MAC), SIV of sooty mangabey (SIV-SM), but not SIV of African green monkeys (SIV-AGM), or SIV of mandrills (SIV-MN) (Wong-Staal et al., 1987; Guyader et al., 1987; Chakrabarti et al., 1987; Fukasawa et al., 1987; Tsujimoto et al., 1989; Hirsch et al., 1989). An open reading frame is also found in a similar position in the visna virus genome (Sonigo et al., 1985). The conservation of the predicted VPR proteins among these different lentiviruses is almost as great as that of GAG and POL proteins.

The HIV-1 VPR protein is 78 amino acids long in several strains, and 96 amino acids long in the remaining strains (Meyers et al., 1989). Functional proviral clones of HIV-1 have been identified with either form of the vpr gene (Dedera et al., 1989; Adachi et al., 1989). Among the first 70 amino acids, 50% conservation of amino acid sequences are noted (Meyers et al., 1989). The HIV-2 VPR protein is 105 amino acids in length, whereas that of SIV-MAC is 97 amino acids long (Guyader et al., 1987; Chakrabarti et al., 1987).

The VPR proteins of HIV-1, HIV-2, and SIV-MAC are expressed in vivo as evidenced by the presence of antibodies reactive with recombinant VPR products in 33-67% of infected humans or rhesus macaques (Wong-Staal et al., 1987; Lange et al., 1989; Yu et al., 1989). A single antibody to the 96 amino acid form of the HIV-1 VPR product has been developed and claimed to detect a 13 kd VPR protein in cells acutely infected with HIV-1 (Lange et al., 1989). The poor quality of the radioimmunoprecipitation analyses using this antibody suggest that the specificity and avidity of this antibody are poor. An antibody to the SIV-MAC VPR product has also recently been developed (Yu et al., 1989), but results with this antiserum have not yet been reported. No antibody to the HIV-2 VPR product has yet been developed.

Work from our laboratory has demonstrated that the HIV-1 and HIV-2 VPR products are dispensable for virus infectivity, replication, and cytopathicity (Dedera et al., 1989). Proviral clones have been constructed expressing a 2 (R2), 22 (R22), 31 (R31), 40 (R40), 78 (R78 or X), or 96 (R96) amino acid form of the VPR product. No differences in the above noted parameters were detected in H9, MOLT 3, CEM, U937, or SUP T1 cell lines, or peripheral blood lymphocytes. HIV-2 proviral clones have been constructed which express either a 105 (MR105 or SE) or 6 amino acid (MR7) form of VPR. No alterations in infectivity, replication, or cytopathicity were noted with viruses derived from these clones in H9, MOLT 3, CEM, SUP T1, Jurkat, or U937 cell lines, or primary human lymphocytes or monocytes.

However, recent data suggests a cell-type dependent effect of vpr expression or action. In MT4 cells, the kinetics or replication of virus derived from R2 were significantly different from that of R78, with retarded and diminished virus yield from the vpr mutant. This finding has now been obtained in 6 replicate experiments with 3 different preparations of R2 and R78. Cytopathicity was comparably depressed. The novel feature of this cell line which may account for this effect is unknown; there may be a relationship to human T-lymphotropic virus type 1 (HTLV-I) expression in MT4 cells.

In addition, we have noted subtle morphological differences of virus derived from vpr mutant infected cell lines compared to those infected with the parental virus. R2 virus particles appeared to be less homogenous and more immature than those derived from R78. This may suggest an effect of VPR in virus assembly or maturation. Possible alterations in the structure of the virus particle could account for possible changes in infectivity of the virus.

Viral Protein X (VPX)

The vpx gene is found in HIV-2, SIV-MAC, SIV-AGM, SIV-SM, but not HIV-1 or SIV-MN (Guyader et al., 1987; Chakrabarti et al., 1987; Fukasawa et al., 1988; Hirsch et al., 1989; Ratner et al., 1985a; Tsujimoto et al., 1989). It is an immunogenic protein expressed *in vivo*, to which 85% of HIV-2 infected humans and 20% of SIV-MAC infected rhesus macaques generate antibodies (Kappes et al., 1988; Yu et al., 1988).

The VPX product is a 112 amino acid proline-rich protein which is found in the virion in equimolar ratio to the GAG capsid (CA; p24) antigen (Henderson et al., 1988). It has also been found to be a nucleic acid binding protein, though specificity for this property remains to be investigated.

Four groups of investigators, including our own group, have now reported on findings of SIV or HIV-2 viruses with alterations in vpx (Yu et al., 1988; Guyader et al., 1989; Hu et al., 1989; Kappes et al., 1989). All groups agree that VPX is dispensable for virus infectivity, replication, and cytopathicity. For example, we have found no effect of VPX on replication of HIV-2 in CEM, H9, U937, SUP T1, and Jurkat cell lines. These studies were carried out with HIV-1 proviral clones capable of coding for the full-length VPX protein, or a clone with a serine substitution for the initiator methionine (MX1), a clone with a termination codon at position 22 (MX22), and a clone with the same mutation present in MX1 as well as a frameshift mutation at position 62 and another termination codon at position 70 (MX1+62).

However, divergent results were obtained in studies of vpx mutant replication on primary T lymphocytes. Whereas Guyader reported a 10-fold decrease in HIV-2 replication in the absence of VPX on T lymphocytes, our own studies have repeatedly failed to detect an alteration in infectivity, replication, or cytopathicity of HIV-2 viruses in primary human lymphocytes with or without vpx (Guyader et al., 1989; Hu et al., 1989). A more comprehensive examination of kinetics of HIV-2 and SIV replication in primary human and macaque lymphocytes and in primary monocytes is clearly indicated to resolve these potentially important discrepancies.

Our group has recently detected a particularly intriguing property of VPX to direct HIV-2 budding to particular sites in the cell. In the presence of VPX, HIV-2 was found in H9 cells to bud intracellularly and at the plasma membrane. The morphology of the virus particles was generally mature and rather homogeneous. In the absence of VPX, HIV-2 buds exclusively at the plasma membrane. The virus particles were generally less mature and less homogeneous.

Negative factor (NEF)

The nef gene, unlike the vpr and vpx genes, is poorly conserved between different strains of HIV-1 and other lentiviruses (Ratner et al., 1985;

Meyers et al., 1989). A similar open reading frame, however, has been described also in HIV-2, SIV-MAC, SIV-AGM, SIV-MN, and SIV-SM (Guyader et al., 1987; Chakrabarti et al., 1987; Fukasawa et al., 1987; Tsujimoto et al., 1989; Hirsch et al., 1989).

The NEF protein is immunogenic *in vivo* in infected humans. Both humoral and cell-mediated immune responses have been detected to this protein (Allan et al., 1985; Arya et al., 1986; Franchini et al., 1986 and 1987). Perhaps the most intriguing finding is the identification by several different investigators of antibodies reactive with NEF early after infection and frequently prior to the detection of other anti-HIV-1 antibodies (Ameisen et al., 1989a and b; Sabatier, et al., 1989; Reiss, et al., 1989; Ronde et al., 1989; Chengsong-Popov et al., 1989; Laure et al., 1989). This

suggests that NEF may be the first viral protein to be expressed in vivo. Recent data from tissue culture experiments confirm that NEF mRNA is expressed after infection earlier than mRNAs for other regulatory and structural proteins (Klotman et al., 1989).

Five laboratories, including our own, have now reported that NEF is a negative regulator of virus replication (Luciw et al., 1986; Terwilliger et al., 1986; Ahmad & Venketassen et al., 1988; Niederman et al., 1989 & Levy et al., 1989). However, one laboratory has failed to detect an effect of NEF (Kim & Baltimore, 1989). Differences in sequence of the NEF product expressed or other technical difficulties may explain the discrepancy. Differences in NEF expression, NEF action, or NEF responsiveness have been demonstrated for different HIV-1 clones (Levy et al., 1989). Kim & Baltimore have not yet carried out similar experiments with proviral clones obtained from any of the five laboratories which have described down-regulatory effects of NEF.

In studies of SIV-MAC clones, all of those which are capable of giving rise to virus in macaque lymphocytes have a defect in nef, whereas the single clone which is not functional has an intact nef gene (Desrosiers, personal communication).

Our own laboratory has recently localized the effect of NEF to an effect on viral RNA levels (Niederman et al., 1989). This effect is at least partially due to an effect on viral transcription as determined by nuclear run-off experiments. Effects on RNA transport or degradation have not been excluded. Confirmation of these results was reported by Ahmad & Venketessan (1988).

The NEF protein has also been reported to down-regulate human CD4 expression (Guy et al., 1987). However, this study was carried out with vaccinia expressed NEF, and only a single control experiment was done examining another lymphocyte surface antigen, 4B4, which was only minimally down-regulated. However, differences in stability of different antigens on the surface of lymphocytes could be reflected in vaccinia infected cells, and the effect may not be specific to NEF. Further studies of the effects of NEF on cellular protein expression and growth are warranted.

Nef is expressed as two proteins from the same mRNA due to utilization of different AUG codons (Ahmad & Venketessan, 1988). When the first AUG codon is recognized a 206 amino acid, N-myristoylated 27 kd protein is expressed. This protein may be phosphorylated at the threonine at position 15 by protein kinase C (Guy et al., 1988). A second NEF product is expressed from utilization of the second AUG codon to produce a 187 amino acid, 25 kd protein (Ahmad & Venketessan, 1988). Both proteins can bind and cleave GTP, and can autophosphorylate at a carboxyl terminal serine residue in the presence of GTP (Guy et al., 1988). Sequence similarities between amino acids 95 and 111 of NEF and other nucleotide binding proteins are readily apparent (Samuel et al., 1987; Guy et al., 1988). The possible relationships of these interesting biochemical activities with NEF activity remain to be investigated.

(6) BODY

1) To define the function of viral protein R (VPR)

a) Express HIV-1, HIV-2, and SIV vpr genes in E. coli

In the original application, we had proposed to express each form of vpr in E. coli, in order to obtain proteins that could be used for immunization of rabbits for antibody development. We have essentially bypassed this undertaking, by obtaining a purified synthetic HIV-1 Vpr protein from Dr. Gras-Maase. Furthermore, the current availability of antisera to the HIV-2 and SIV mac Vpr proteins (kindly provided by Dr. T.H. Lee, Harvard) also precluded the requirement for the expression of these proteins in E. coli for this purpose.

b) Develop antibodies to recombinant Vpr products

We have inoculated a single rabbit with the synthetic HIV-1 Vpr protein have now obtained over 100 ml of antiserum. This antiserum shows better reactivity with either [3H]-leucine labeled HIV-1 Vpr protein expressed in reticulocyte lysates or in transfected BSC40 cells than those provided by Dr. T.H. Lee, AIDS Repository, or Dr. George Shaw, and was utilized in all studies described below. We have provided 30 ml of our antiserum to the AIDS Reagent Repository.

c) Determine the size(s) of Vpr products in acute and chronically infected lymphoid and monocytoïd cells infected with HIV-1, HIV-2, and SIV

We have used the anti-vpr antibody to analyze 3H-leucine labeled proteins from reticulocyte lysates, HIV-1 infected primary lymphocytes, and vaccinia virus expressed vpr and have found no significant differences in sizes of the single 16 kDa product. No evidence for a precursor of a different size has been detected or for coimmunoprecipitation of other labeled proteins.

d) Determine the cellular localization of Vpr

We first examined the cellular localization of Vpr in HIV-1 infected primary lymphocytes. Cell fractionation studies demonstrated that about 50% of Vpr was present in the nucleus, 15% in the membrane fraction, and the remaining 35% was released from infected cells in virions (Fig 1).

Expression of Vpr in the absence of other HIV-1 proteins, using a SRalpha expression plasmid, demonstrated that the majority of Vpr was localized in the nucleus (Fig 2).

In BSC40 cells infected with VTF7-3 (vaccinia virus expressing T7 RNA polymerase) and transfected with pTM3(vpr), we have found that the majority of vpr was localized with the nuclear fraction (Fig 3). Co-expression of gag did not significantly effect the localization of vpr. In contrast, gag p24 was found primarily in the cytosol, and to a lower extent in the membrane and cell-free

supernatant under these labeling conditions.

We confirmed the results from the cell fractionation experiments by immunofluorescence studies (Fig 4). These data demonstrated that the majority of Vpr was in the nucleus. However, Vpr was also detected in a perinuclear localization, that was resistant to brefeldin treatment. This suggests that the latter location was probably not the Golgi apparatus.

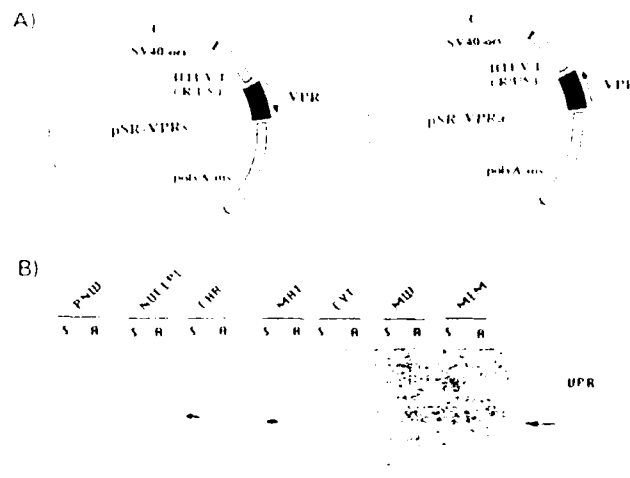


FIG. 2. Localization in COS-7 cells of Vpr expressed from pSR. (A) Vpr sense (pSR-VPRs) and antisense (pSR-VPRa) expression plasmids, which include a transcriptional enhancer (SV40-ori), a transcriptional promoter (HTLV-I long terminal repeat [RUS]), and a polyadenylation insertion sequence (polyA-ins). (B) Subcellular fractionation of Vpr expressed in transfected and [³H]leucine-labeled COS-7 cells from pSV-VPRs (S) and pSR-VPRa (A) in postnuclear wash (PNW), nucleoplasm (NUCLEI), chromatin (CHR), nuclear matrix (MAT), cytosol (CYT), membrane wash (MW), and membranes (MEM). Equivalent amounts of each fraction were immunoprecipitated with the anti-Vpr antiserum and analyzed by SDS-PAGE. The electrophoretic position of Vpr is shown by an arrow at the right.

Fig 1

Fig 2

We have also analyzed the cellular localization of mutant Vpr proteins using this vaccinia virus expression system. The distribution of the SRIG mutant, with a deletion of amino acid residues 79-82, closely mirror that seen with the parental form of Vpr, with primarily nuclear localization. In contrast, the CRST mutant, truncated after amino acid residue 77, was approximately equally distributed between nuclear, cytosol, and membrane fractions (Fig 3). This suggested that sequences between amino acids residues 78 and 96 may contribute to the localization with the nuclear fraction. We confirmed that these C-terminal sequences contain a nuclear localization sequence, based on the finding that a beta-galactosidase fusion protein to which amino acid residues 77-96 were added at the C-terminus resulted in translocation to the nucleus.

To assess the purity of each of these fractions, similar experiments were performed with marker proteins, for nuclear, membrane, Golgi, endoplasmic reticulum, and cytosolic proteins.

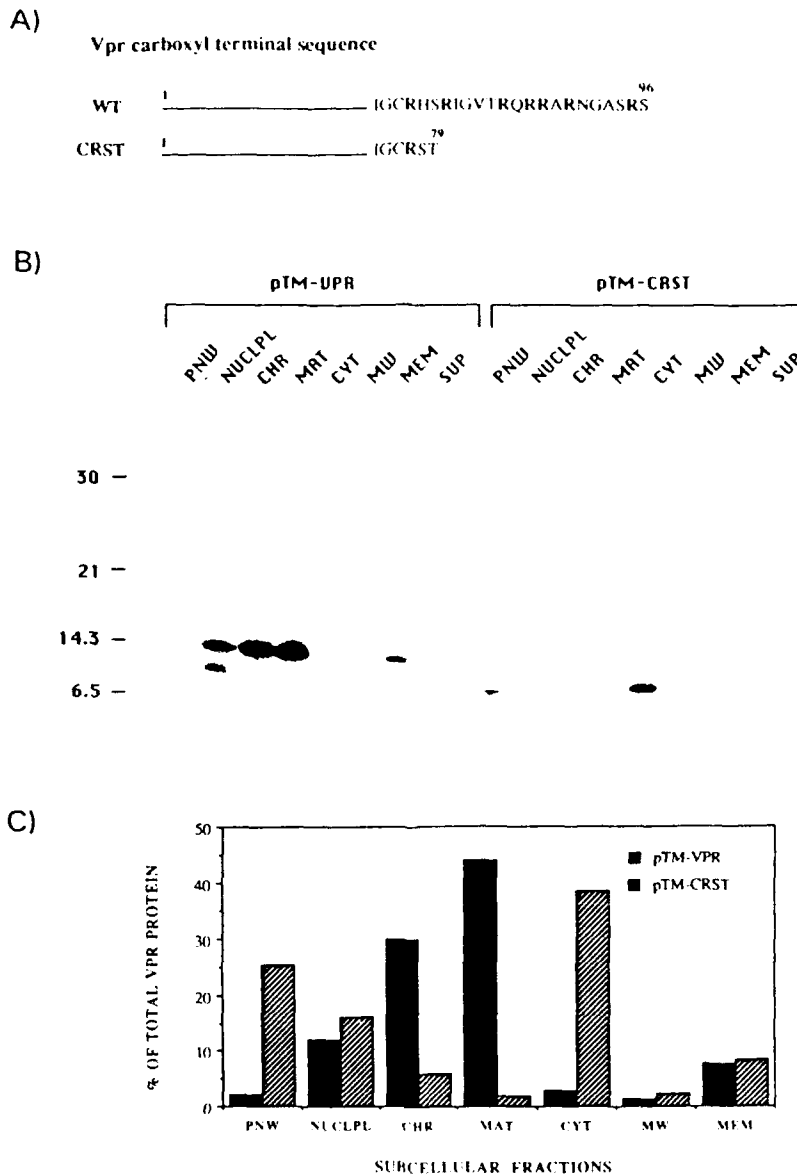


FIG. 3. Subcellular distribution of vaccinia virus-expressed parental Vpr and carboxyl-terminal truncation mutant CRST in BSC40 cells. (A) Schematic drawing of the Vpr protein, indicating the carboxyl-terminal arginine-rich sequence of the wild type (WT) and of the truncation mutant, CRST. (B) Vpr expressed from pTM3 in vTF7-3-infected cells. Cells were labeled with [³H]leucine and fractionated into postnuclear wash (PNW), nucleoplasm (NUCLEPL), chromatin (CHR), nuclear matrix (MAT), cytosol (CYT), membrane wash (MW), membranes (MEM), and cellular supernatant (SUP). Molecular mass markers are shown at the left in kilodaltons. (C) Proportion of VPR in each subcellular fraction as determined by laser densitometry from pTM-VPR (solid bars) or pTM-CRST (hatched bars)-transfected cells.

Fig 3

We have also performed immunogold localization studies with Vpr expressed in primary lymphocytes. First, we examined several vpr+ HIV-1 strains, and found in each case both intracellular (in vacuoles that resembled Golgi remnants) and extracellular virus particles (Fig 5). The average number of gold particles per virion was determined to be 1.15-1.79. For extracellular virions, the average number of gold particles per virion was 1.34-1.77, whereas for intracellular virions, the average number of gold particles per virion was 0.75-0.99. No significant effects on vpr packaging in the virus particle were found in the presence compared to the absence of co-expression of Vpu. The finding of decreased levels of Vpr per virion for intracellular versus extracellular virions was a consistent and interesting finding.

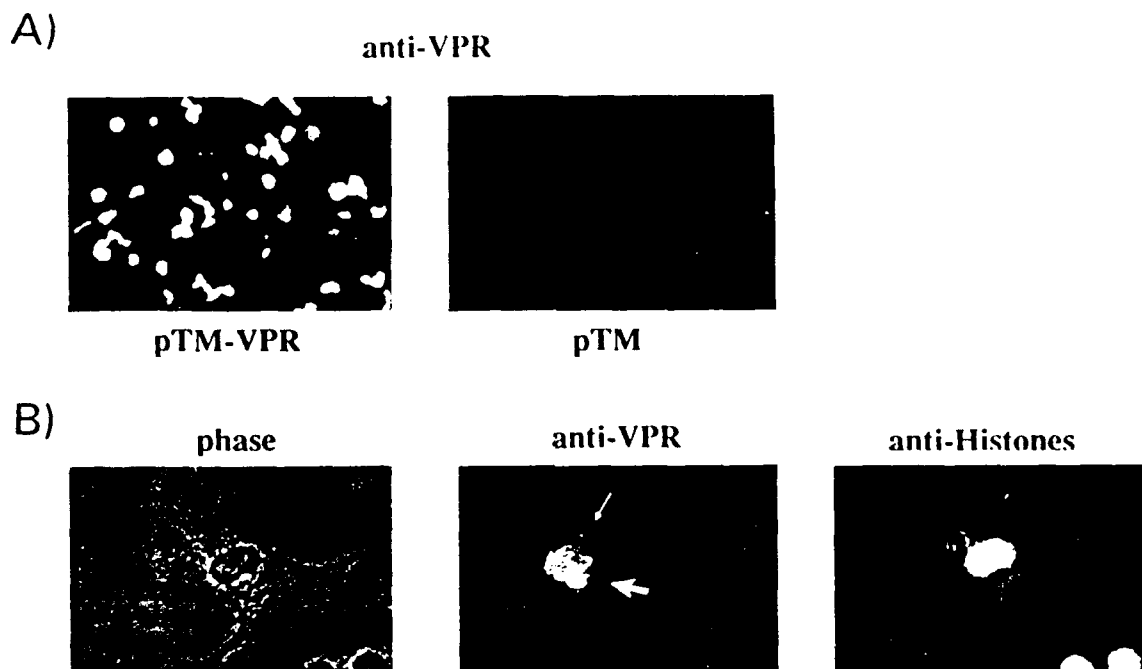


FIG. 4. Immunofluorescence localization of Vpr in BSC40 cells. (A) pTM-VPR (left)- or pTM (right)-transfected vTF7-3 infected cells were incubated with the anti-Vpr antiserum and an FITC-conjugated goat anti-rabbit immunoglobulin. Magnification, $\times 188$. (B) Higher magnification ($\times 752$) by phase-contrast microscopy (left) and fluorescence microscopy (middle and right) of a representative cell incubated with anti-Vpr antiserum and FITC-conjugated goat anti-rabbit immunoglobulin (middle; filter with excitation range of 450 to 490 nm and emission range of 520 to 560 nm) and antihistone antiserum and rhodamine-conjugated goat anti-mouse immunoglobulin (right; filter with excitation range of 510 to 560 nm and emission range of >590 nm). Diffuse nuclear (thin arrow) and focal perinuclear staining (thick arrow) are indicated in the middle panel.

Fig 4

In many cases the localization of Vpr in the virus particle appeared in a circular array, that resembled envelope localization (Fig 6,7). No such localization was seen with anti-vpx or anti-gag antisera. Experiments were performed with anti-gp120 antisera colabeling to demonstrate that vpr was situated beneath the viral envelope (Fig 7). In addition, we have constructed mutant

proviruses with frameshift deletions in vpr to examine whether vpr can still be packaged into the virions. Lymphocytes infected with a virus with a deletion of residues 79-82 of vpr showed preferential incorporation of vpr into intracellular compared to extracellular particles (Fig 8, 9). Lymphocytes infected with a virus with a deletion of residues 77-96 demonstrated less than 10% of vpr incorporation into virions. This result is not due to alteration in recognition by the antibody, since each of the mutant forms of Vpr has been expressed in reticulocyte lysates and vaccinia virus infected BSC40 cells and is detectable with the antiserum (Fig 10).

e) Assess co- and post-translational modifications of the Vpr protein

Experiments to examine whether HIV-1 or HIV-2 Vpr proteins are phosphorylated, O-glycosylated, sulfated, or palmitoylated were performed and showed no such modifications.

f) Isolate cDNAs encoding Vpr

The experiments on isolation of Vpr cDNAs in PBMCs from HIV-1 infected patients were carried out by RT PCR. We found the same mRNAs previously described by Schwartz et al (1991), and no fusion proteins of Vpr to other open reading frames were noted.

g) Determine role of Vpr in HIV-1, HIV-2, and SIV replication in a variety of lymphoid and monocytoid cells

We demonstrated that a discrete env determinant, including the V3 loop, but not the CD4-binding domain, is necessary and sufficient for HIV-1 infection of monocytes. Additionally, we have identified three virus replication phenotypes in monocytes in vitro using molecular defined proviral clones. These include productive infection, with the generation of high virus replication levels; silent infection, with low to undetectable virus replication in monocytes, despite ultimate virus recovery from infected monocytes following cocultivation with uninfected, phytohemagglutinin stimulated peripheral blood mononuclears (PBMCs [lymphoblasts]); and no infection, with neither virus replication in nor virus recovery from monocytes observed. We demonstrated that vpr and vpu are central to the regulation of virus replication in primary monocytes and together mediate the expression of silent versus productive infection (Fig 10).

To study viral regulation of monocyte infection, we utilized a panel of chimeric HIV-1 clones, constructed from the nonmonocyte-tropic clone HXB2, and the monocyetotropic clone ADA, as previously described. To correct a vpr defect in each of these clones, the result of a single base insertion in HXB2, 2.7 kb Sal I-Bam HI HXADA DNA fragments (nucleotides 5785-8474) were subcloned into the full-length proviral clone NL4-3, in which the vpr open reading frame is intact. The resultant NLHXADA clones contained the ADA-derived env determinant previously localized to nucleotides 7040-7323, flanked by other portions of env and vpu and small portions of tat and rev. A clone in which the entire 5785-8474 sequence was HXB2 derived (thus lacking a monocyte-tropic env determinant) was used as a negative control for

these experiments. Because HXB2 lacks a vpr initiator methionine codon, clones in which vpr was HXB2 derived were defective for that product, in contrast to clones with an ADA-encoded vpr. Finally, a vpr mutant corresponding to each NLHXADA clone was generated by introducing a frameshift mutation at codon 63.

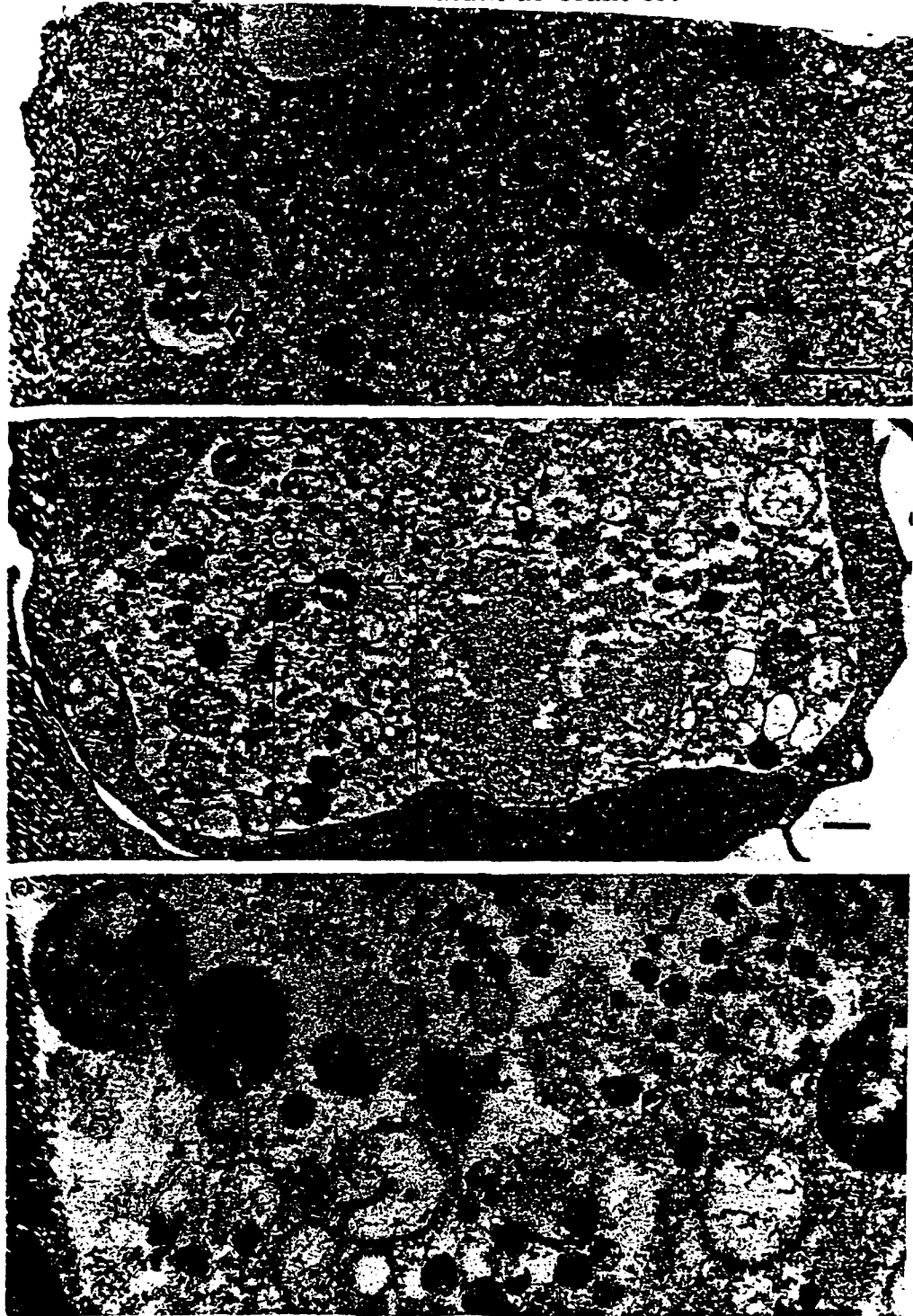


Fig 5

Immunogold localization of Vpr in virus particles. (a) Vpr-specific gold particles were seen in the wild-type HIV-1 virions in a vacuolar region (arrow 1) and in a cytoplasmic vacuole (arrow 2). Labelling was also found at a portion of the vacuolar region that showed higher density, consistent with that of a budding virus particle (arrow 3). The bar represents 500 nm. (b) Vpr-specific gold particles (15 nm diameter; arrowhead) were found in a large vacuole of an infected PBMC. N, nucleus. The bar represents 500 nm. (c) An enlarged area of the vacuole (boxed) in (b) is shown (rotated 90°) with Vpr-specific gold particles (15 nm diameter).

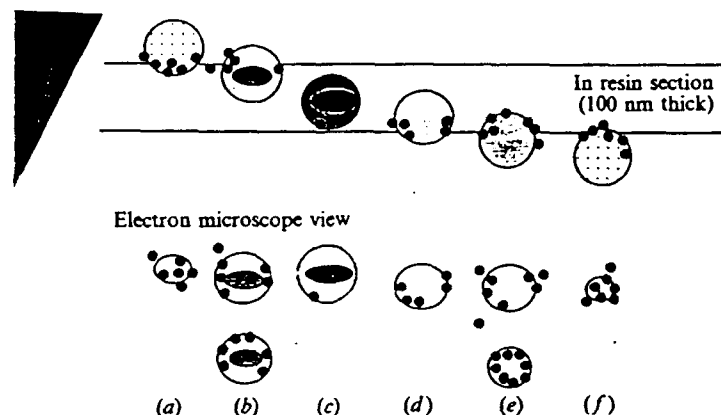


Fig. 3. Schematic representation of possible locations of Vpr-specific gold particles in HIV-1 virions embedded in thin resin sections. HIV-1 virions associated with infected cells were embedded in resin and cut into sections of 100 nm in thickness for post-embedding immunostaining and electron microscopic observations. Virions located at the upper (a) or lower portion of the section (f) would have been cut tangentially and the exposed Vpr antigen could be labelled with the antibody if Vpr was situated near or beneath the viral envelope. These virions would be predicted to appear smaller under the electron microscope and the gold particles would form a cluster. Virions cut through the centre would be predicted to appear larger and gold particles would form a ring-shaped pattern with (b) or without a core (d and e). The diameter of these virions would appear to be similar to that of typical virions. Virions embedded within the resin would not be accessible to H_2O_2 etching and their associated antigens would not be exposed. A typical virion diameter is approximately 100 nm.

Fig 6.

Virions from the recombinant clones, generated by transfection, were assayed for their ability to infect and replicate in primary monocytes by the presence of reverse transcriptase (RT) activity in culture supernatants and by the ultimate recovery of virus following cocultivation of monocytes with uninfected PEMCs. The results are summarized in Fig. 10. All clones containing the ADA-derived env determinants with an intact vpr gene generated high virus replication levels in monocytes. Inactivation of vpr in these clones, however, generated divergent results, depending upon the derivation of nucleotide sequences 5999-6345 (SK fragment). Clones in which this portion of the genome was ADA derived generated lower (but readily detectable) virus replication levels than did their wild-type vpr counterparts. However, vpr mutants in which the SK fragment was HXB2 derived typically failed to generate virus replication levels detectable above background in monocytes, despite subsequent virus recovery from these cultures onto uninfected PEMCs. The negative control clone, which carried a wild-type vpr but lacked the monocyte-tropic env determinant generated virions which neither replicated in nor were recovered from monocytes, as previously demonstrated. No significant differences were seen in the replication of each virus strain on PEMCs obtained from several different donors.

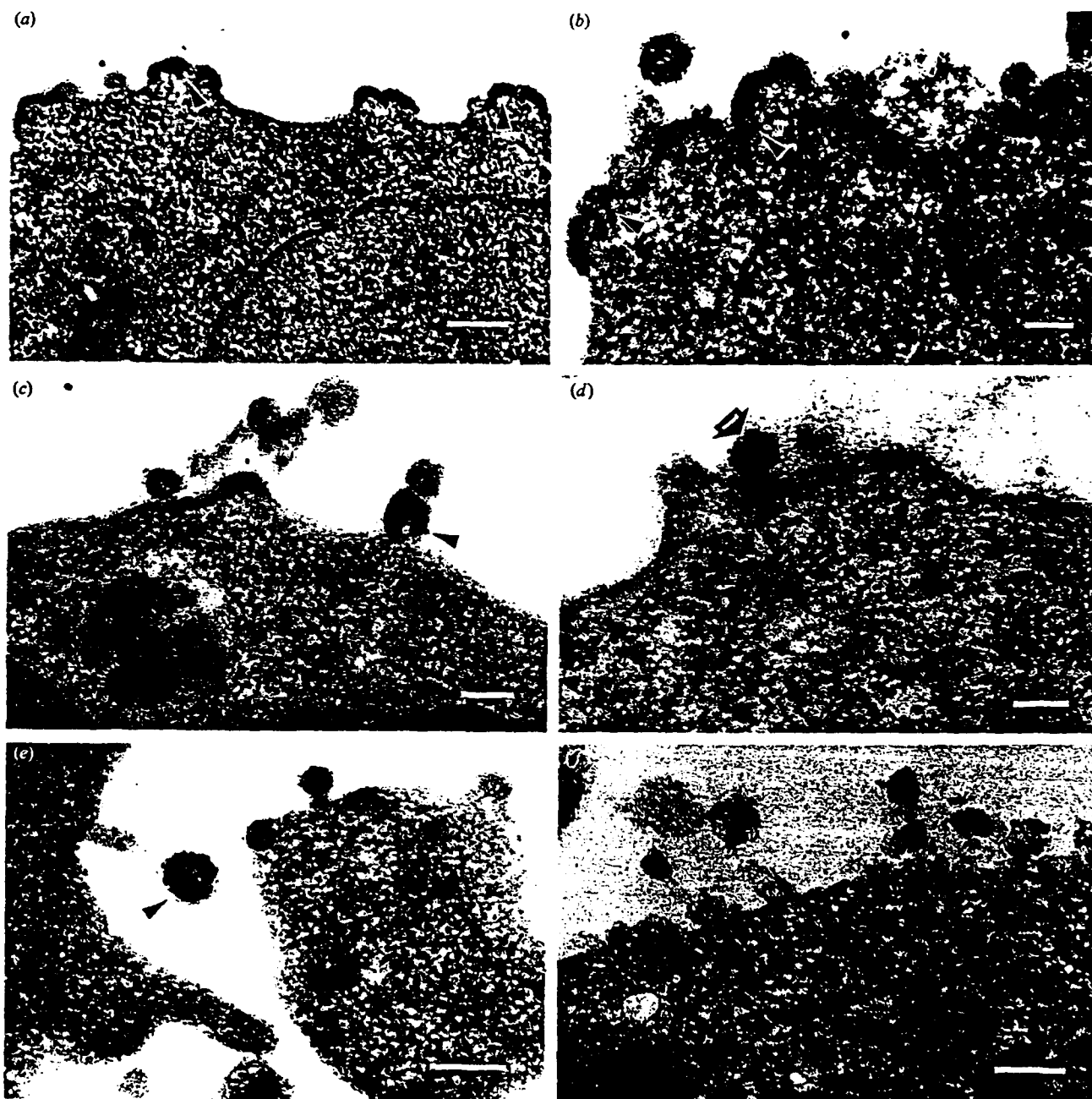


Fig 7.

Fig. 4. Vpr localization on budding virus particles. (a) Condensed plasma membrane structures are immunolabelled with Vpr-specific gold particles (arrowheads). The bar represents 200 nm. (b) Virus budding from a condensed area of the cell membrane was labelled with Vpr-specific gold particles (arrowheads). A single extracellular immature virion labelled weakly with these particles (15 nm), but better labelling with Gag p24-specific gold particles (5 nm) was observed. The bar represents 100 nm. (c) Other immature virions immunolabelled with Vpr-specific gold particles (arrowhead). The bar represents 100 nm. (d) Additional immature virions labelled with Vpr-specific gold particles (15 nm, arrow 1) under the virus envelope as well as Gag p24-specific gold particles (5 nm, arrow 2). (e) An immature virion near the cell surface was identified that labelled with Vpr-specific gold particles under the viral envelope (15 nm, arrowhead), whereas Gag p24-specific gold particles (5 nm) were seen in the central area of the virion. The bar represents 200 nm. (f) A ring-shaped distribution of Vpr-specific gold particles (15 nm) was evident on an extracellular virus particle, with Gag p24-specific gold particles (5 nm) localized in the central core of the virion.

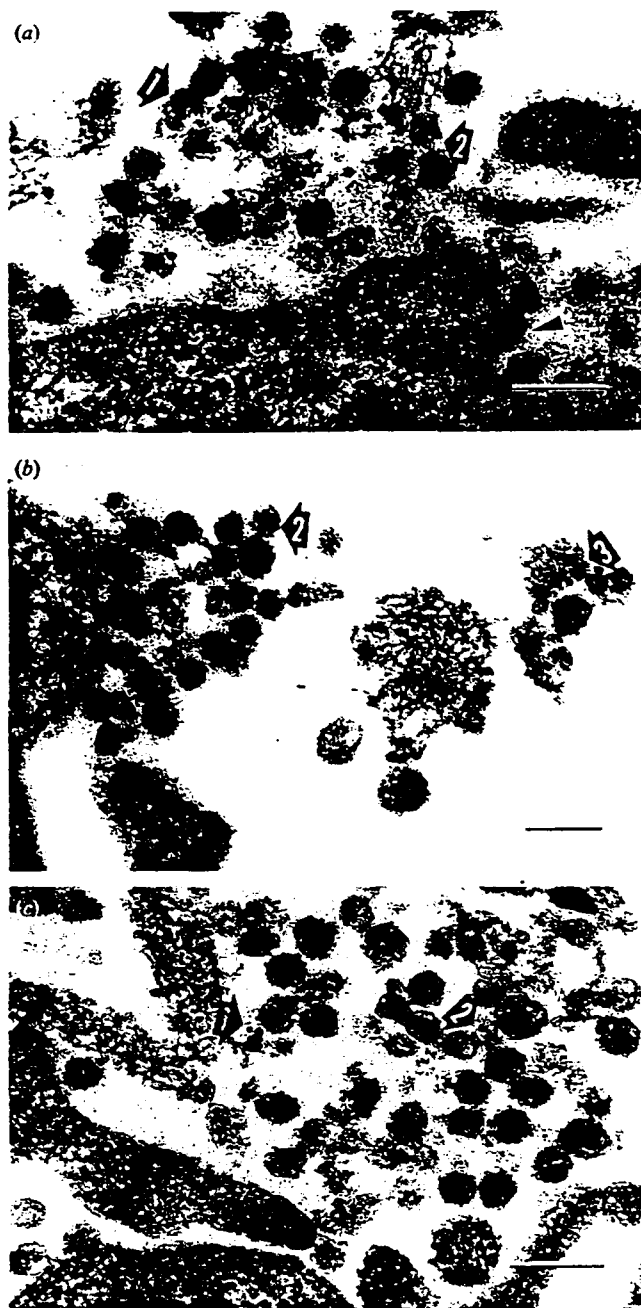


Fig. 5. Immunolabelling of wild-type and mutant forms of Vpr on HIV-1 virions. (a) Vpr-specific gold particles labelled extracellular wild-type virions (15 nm, arrow 1). Gag p24-specific gold particles (5 nm, arrow 2) were also observed in virions. An average of 1.5 Vpr-specific gold particles per virion was found. The bar represents 200 nm. (b) Vpr mutant SRIG virions also labelled with Vpr-specific gold particles (15 nm, arrow 1). Gag p24-specific gold particles (5 nm, arrow 2) and Env gp120-specific gold particles (10 nm, arrow 3) were also identified. An average of 1.1 Vpr-specific gold particles per virion was measured. The bar represents 200 nm. (c) Vpr mutant CRST virions showed very little Vpr-specific labelling (arrow 1), whereas Gag p24-specific gold particles were still observed (5 nm, arrow 2). An average of 0.1 Vpr-specific gold particles per virion was counted. The bar represents 200 nm.

Fig 8.

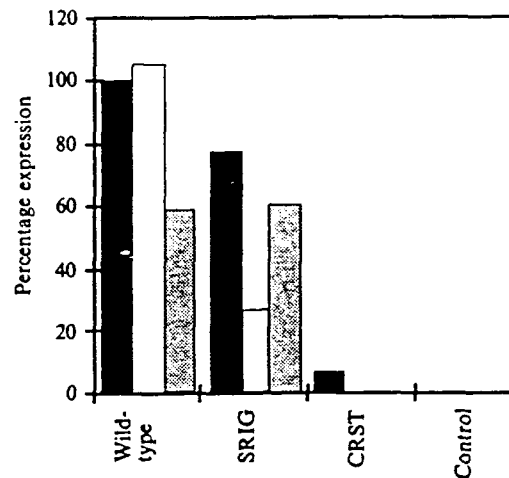


Fig. 6. Wild-type and mutant Vpr expression in virions as a percentage of the total expression in the wild-type in HIV-1-infected PBMCs infected for 7 days. Extracellular (□) and intracellular (■) Vpr expression are shown, together with the average number of Vpr-specific gold particles (on both extracellular and intracellular virions) as a percentage of the wild-type (▨).

Fig. 9

Monocytes were infected with recombinant HIV-1 clones containing a functional vpr gene, stained with toluidine blue, and examined by light microscopy (1 μ m thick plastic sections). Cultured infected with a noncytotoxic virus, NLHXADA-SK which contains a functional vpu gene, were indistinguishable from uninfected cells, with rare, small multinucleated cells (Fig 11a). Cultured productively infected with virus containing the monocyctotropic env determinant and a functional (NLHXADA-SM, Fig 11b) or nonfunctional (NLHXADA-GG, Fig 11c) vpu gene showed characteristic cytopathic effects. These consisted of the formation of multinucleated giant cells, often containing 10 or more nuclei per cell, and cell lysis. The frequencies and sizes of these cells were comparable in the NLHXADA-SM and NLHXADA-GG infected monocyte cultures. Virus production and cellular degeneration and necrosis were primarily confined to multinucleated cells. Transmission electron microscopy examination demonstrated typical budding and mature virions in intracellular vacuoles that were associated with the plasma membrane, in both the presence and absence of vpu, but not in the NLHXADA-SK infected cells (Fig 11d). Freeze fracture scanning electron microscopy demonstrated budding of virion particles from the plasma membrane of monocytes infected with virus which lacked a functional vpu (Fig 11e). No virus could be detected in monocytes infected with recombinant clones lacking both vpr and vpu (data not shown).

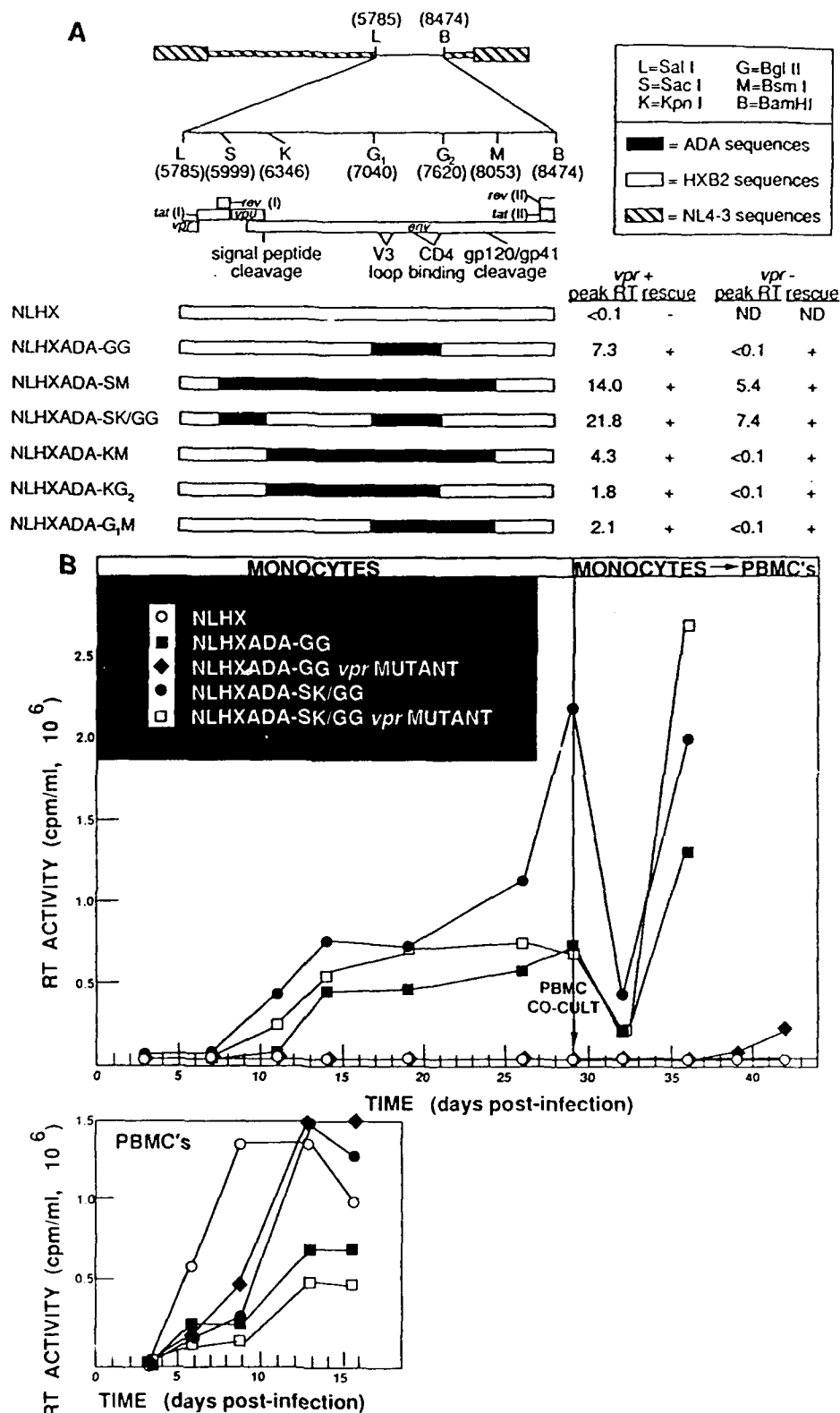


Fig 10.

FIG. 1. Replication of recombinant HIV-1 clones with both wild-type and mutant *vpr* genes. (A) The panel of recombinant NLXADA clones is represented diagrammatically. The region of the genome corresponding to the HXB2- and ADA-derived sequences (nucleotides 5785 to 8474) is expanded to highlight the relative positions of HXB2- and ADA-derived sequences. The open reading frames in this portion of the genome are represented above. Recombinant clones were generated by reciprocal DNA fragment exchanges of ADA- and HXB2-derived sequences into a *SalI*-*BamHI* fragment (5785 to 8474) from HXB2 subcloned into an intermediate shuttle vector, utilizing the restriction enzyme sites indicated on top. The resultant chimeric *SalI*-*BamHI* fragments were then subcloned into the clone NL4-3 to generate

recombinant NLHXADA clones. To inactivate *vpr*, clones were digested with *EcoRI* (nucleotide 5745), treated with Klenow fragment, and religated to generate a 4-bp insertion, as previously described (24). The replication levels of these clones in monocytes are summarized to the right of each clone. Monocytes were infected as previously described (36) by using filtered virus stocks generated by transfection of proviral DNA onto SW480 cell monolayers, and titers were determined by measuring RT activity. Infections were done at low multiplicities of infection (10 to 100 tissue culture infective doses per well) with monocytes plated at an initial density of 2×10^5 cells per well. Virus replication was monitored by serial determinations of RT activity in culture supernatants (25). Peak RT activities (days 26 to 29) are expressed as 10^5 counts per minute per milliliter. To determine virus rescue, fresh, uninfected PBMCs were added to monocyte cultures at 29 days postinfection, cocultivated (co-cult) for 2 days, and maintained separately for up to 12 additional days, while RT activity was monitored. Rescue was scored as positive with two successive RT results that were more than fivefold above background level. (B) The replication kinetics of representative NLHXADA clones is graphed. Similar results were obtained in three to five replicate experiments.

The SK fragment encoded the entire *vpu* gene product, 14 amino acids at the C termini of both the *tat* and the *rev* first exons, and the N-terminal 41 amino acids of *env* (Fig 12). Although the absence of a *vpu* initiator methionine codon in HXB2 is the most obvious difference between the SK portions of HXB2 and ADA, a role for *tat*, *rev*, or *env* could not be ruled out. The *env* sequences differ at 7 of 41 predicted amino acid positions, not including the nonaligned insertion of 3 residues and deletions of 4 residues in ADA. All but three of these differences are confined to the signal peptide, which varies by up to 30% between different HIV-1 clones. Furthermore, *tat* and *rev* both differ at 3 of 14 amino acid positions between the ADA and HXB2 SK fragments with four of these six changes being conservative in nature. Therefore, it is unlikely that these alterations in *env*, *tat*, or *rev* alter their function. However, to formally determine the specific requirement for *vpu* during HIV-1 infection of monocytes, the *vpu* initiator methionine codon of the silent infection clone NLHXADA-GG (*vpr* mutant) was restored by site-directed mutagenesis. The resultant clone was found to generate virus capable of productive infection of monocytes (data not shown).

HIV-1 and related lentiviruses are distinct from most other retroviruses in that besides the structural *gag*, *pol*, and *env* genes common to all retroviruses, they also encode a number of genes whose functions have been shown or are speculated to be regulatory in nature. In HIV-1, these genes include *tat*, *rev*, *vif*, *nef*, *vpu*, and *vpr*. While *tat*, *rev*, and *vif* are essential for viral gene expression or virion infectivity, the precise role and overall importance of *vpr*, *vpu*, and *nef* are unclear, since these genes are dispensable for virus infection and replication in CD4+ lymphocytes in vitro. The availability of molecular HIV-1 clones which infect and replicate in monocytes at levels comparable to those observed with many monocyctotropic virus isolates has facilitated investigation of the role that these viral genes may play in regulating the virus life cycle in monocytes. In the present study, we observed moderately decreased levels of virus replication in the absence of either *vpr* or *vpu*, whereas in the absence of both genes, virus replication in monocytes dropped to levels barely at or below the level of detection by the RT assay, such that infection of these cells usually could be detected only by virus rescue into PBMCs.

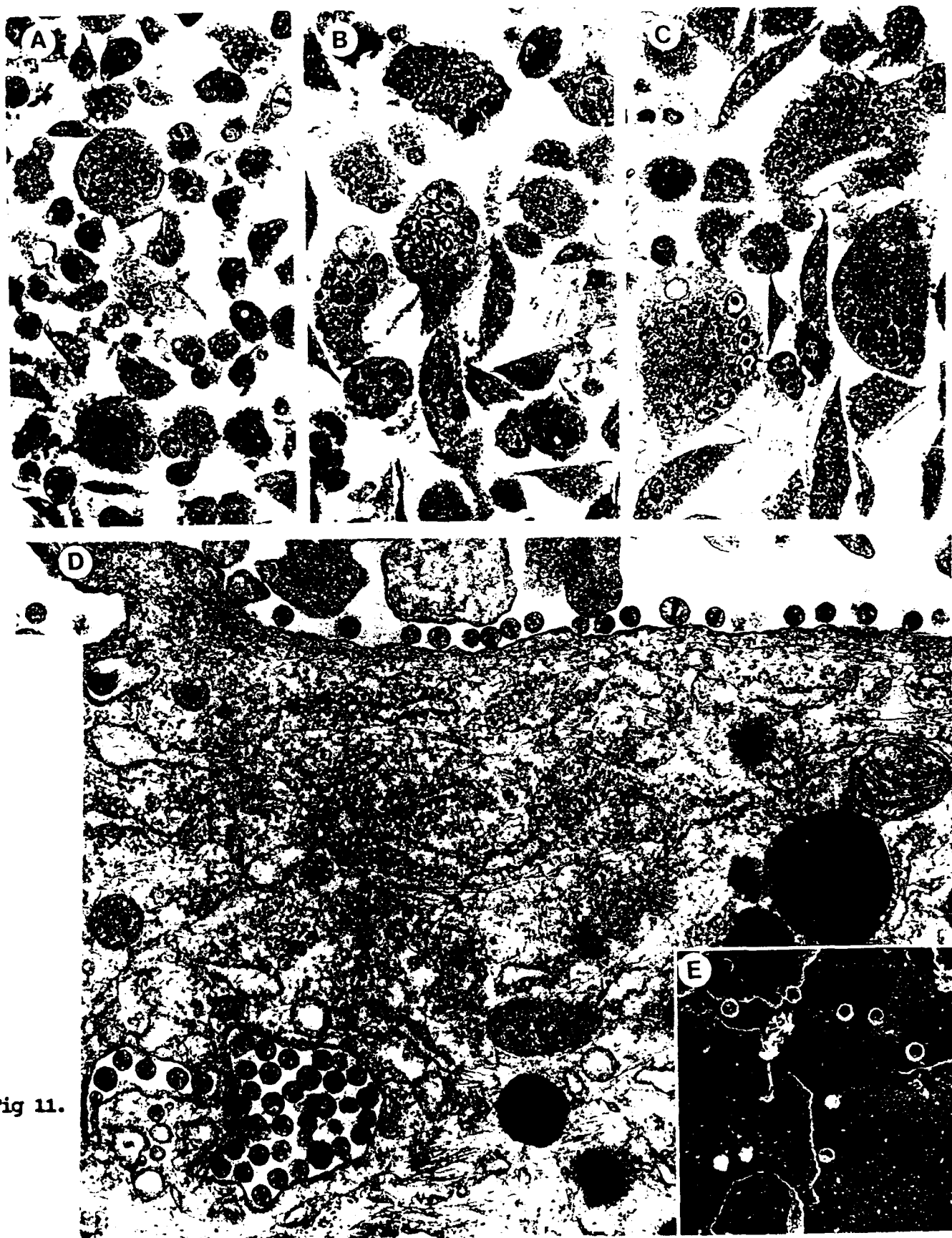


Fig 11.

FIG. 2. Light, transmission, and freeze fracture scanning electron microscopy of infected monocytes. Light micrographs of toluidine blue-stained semithin plastic sections showing typical fields of primary monocytes infected by nonmonocytotropic clone NLHXADA-SK (35) (A) and monocytotropic clones NLHXADA-SM (B) and NLHXADA-GG (C) are shown (15). The multinucleated giant cells were fewer and smaller in panel A than in panels B and C. Magnification, $\times 480$. Infected adherent cultured cells were carefully washed twice with phosphate-buffered saline (PBS), fixed in situ with 2% glutaraldehyde (pH 7.2) in PBS, scraped free with a rubber policeman, transferred to a 15-ml plastic conical tube, and pelleted for 10 min at $600 \times g$ centrifugation. The cells were mixed with warm agar, repelleted in the Microfuge for 1 min, and refrigerated overnight to form a firm agar block. The cell block was divided into small pieces and processed into Spurr's plastic, after osmification and block uranyl acetate staining (15). Sections ($1 \mu\text{m}$ thick) were stained with toluidine blue for light microscopy, while thin sections (600 \AA [60.0 nm]) were stained with uranyl acetate and lead citrate for transmission electron microscopy. (D) Transmission electron micrograph of a small portion of a multinucleated cell from NLHXADA-GG-infected monocytes showing a cytoplasmic vacuole (lower left) containing immature and mature virions and numerous typical mature particles associated with a stretch of plasma membrane. Magnification, $\times 34,000$. (E) Transmission electron microscopy view of NLHXADA-GG-infected monocytes, stabilized by formaldehyde fixation before quick-freezing, freeze-drying, and platinum replication (18). Budding from the convoluted surface are several 50-nm-diameter brightly outlined spherical virus particles. At higher magnification (not shown), these display characteristic surface coats of gp120 "pegs."

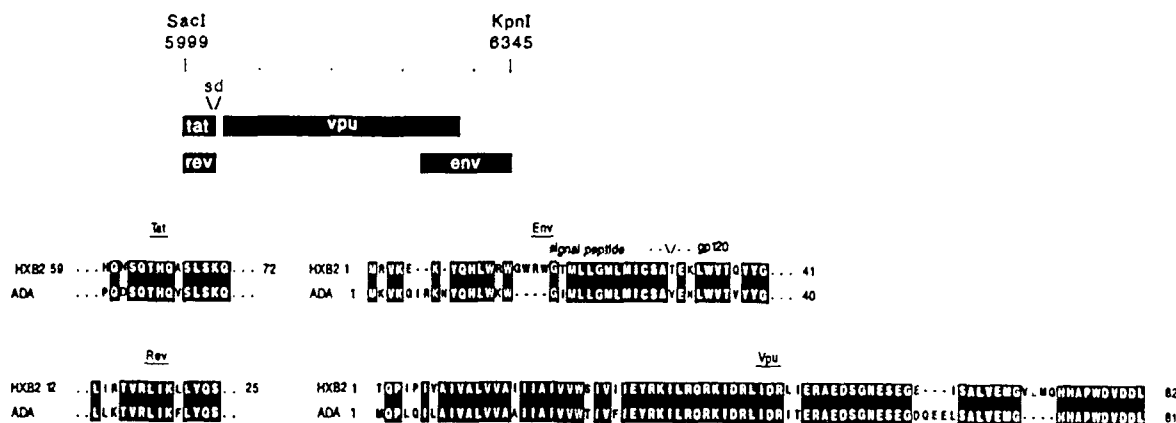


FIG. 3. Comparison of SK virus replication determinant from HXB2 and ADA. The predicted amino acid sequences of *vpr* and the portions of *tat*, *rev*, and *env* which are encoded by nucleotides 5999 to 6345 (SK fragment) from HXB2 and ADA are aligned by using single-letter amino acid designations. Identical residues are indicated within boxes.

Fig 12.

The *vpr* open reading frame encodes a protein of 96 amino acids in most HIV-1 clones and is conserved in other lentiviruses, including visna-maedi virus. Previous studies have shown that *vpr* is not required for HIV-1 infection or replication in CD4+ lymphocytic cell lines in vitro, although its inactivation led to slower replication kinetics and delayed cytopathogenicity in these cells. A recent study involving HIV-2 has shown that *vpr* is likewise dispensable during infection of PBMCs and T-cell lines but essential for productive infection of monocytes. The *vpr* protein has been demonstrated by radioimmunoprecipitation to be virion-associated, and thus it is speculated to function either late in the virus life cycle, during particle assembly or maturation, or early, during the initial stages of infection. The *vpu* gene encodes an 80-82 amino acid protein. It has not been reported whether the *vpu* protein is found in virion particles. *vpu* has been shown to augment virion particle release from infected cells, without affecting

levels of viral RNA or protein synthesis. In the absence of *vpu*, a higher ratio of immature to mature particles has been seen, with a shift in capsid formation from the plasma membrane to intracellular membranes. In monocytes, however, particle assembly and release occur both at the plasma membrane and in intracellular vacuoles in the presence or absence of *vpu* as shown in Fig. 11d.

HIV1 Vpu 39 ... IDRLIDRTERAEDSGNESGGQEE ... LSALVEMGHHPWDYDDL
HIV1 Vpr 1 ... MEAAQAPEDGQPRE PYNEWLELEELKSEAVRFPN ... IWLHNLQO HIYETYGDTWAGVEAIIA LQQLFFINIGG...
HIV2 Vpx 1 ... MTOPRETVPNGSGEETIGEAFANRTVEAINREAVNLDPELIFQVWDRBRYWDEQGMSESYTKRYLCI OKAVYMHVRXGC...

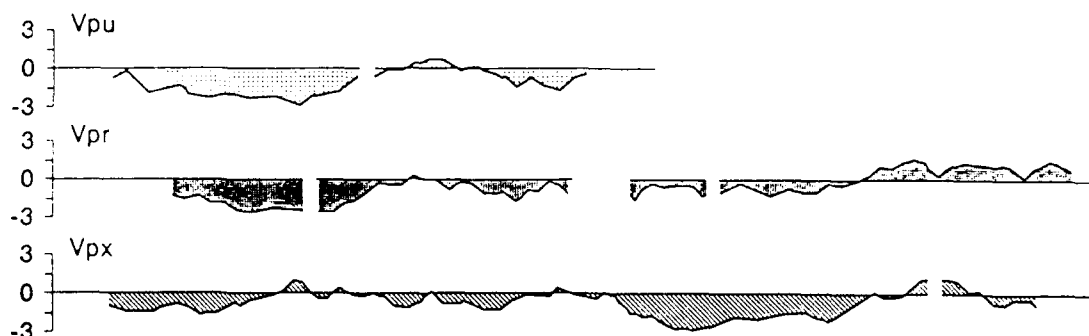


FIG. 4. Predicted amino acid homology between *vpr*, *vpu*, and *vpx*. The predicted amino acid sequence of the NL4-3-derived *vpr* gene is aligned with homologous regions of the ADA-derived *vpu* gene and the *vpx* gene encoded by the HIV-2_{ROD} clone, with single-letter amino acid designations. Identical residues are indicated within boxes. Hydrophilicity profiles for the corresponding segments of each protein are shown at the bottom.

Fig. 13.

It is intriguing that HIV-2 and SIV lack a *vpu* open reading frame but instead carry a gene designated *vpx*, which encodes a protein of 114-118 amino acids in these viruses. *vpu* and *vpx* occupy similar positions in their respective viral genomes, between *pol* and *env*, but have only distant amino acid homology. Recently, it has been suggested that *vpx* and *vpr* arose by duplication from a common progenitor in HIV-2 and SIV, on the basis of predicted amino acid sequence homology between the genes. To investigate the possibility of a similar link between *vpr* and *vpu* in HIV-1, the predicted amino acid sequences of both *vpu* and *vpx* were aligned with that of *vpr*. Although less compelling than the homology between *vpr* and *vpx*, a 38% identity was observed between *vpr* and *vpu* over a 24 residue overlap at the C-terminus of *vpu* and the N terminus of *vpr* (Fig. 12, top). These sequences were particularly rich in acidic residues. Similarity in the hydrophilicity profiles of these portions of the *vpu*, *vpr*, and *vpx* products was also noted (Fig. 12, bottom). The striking effect on virus replication levels in monocytes observed only when both genes were defective suggests that their gene products may perform similar roles and thus provide partial functional complementation. Alternatively, since lower replication levels were observed in the absence of either gene, the nearly complete attenuation observed in the absence of both may result from a compound effect of the loss of two relatively important but functionally unrelated genes. More detailed studies to determine the precise mechanisms of action of the *vpr* and *vpu* gene products will be required to address these alternatives. In either case, our data indicate that together, *vpr* and a second determinant, *vpu*, are more important for efficient HIV-1 infection and replication in primary monocytes than was observed

previously in lymphocytes. These observations provide a rationale for designing potential antiviral therapies to block the action of these gene products during HIV-1 infection of monocytes.

Persistent infection of tissue macrophages plays an important role in the pathogenic effects of other lentiviruses, including equine infectious anemia virus, visna-maedi virus, and caprine arthritis-encephalitis virus, providing a sanctuary for continuous virus replication in the face of a vigorous host immune response. The onset of increased virus replication has been correlated with the onset of clinical disease manifestations, such as encephalitis, pneumonitis, arthritis, and hemolytic anemia. The existence of poorly replicative HIV-1 variants may be essential for establishment of persistent macrophage infection during the early, asymptomatic stage of disease. Several studies have suggested a relationship between the in vitro replicative properties of HIV-1 isolates in T lymphocytes and clinical disease stage, with earlier isolates tending to replicate more slowly and to lower levels ("slow, low") than isolates from later stages of disease ("rapid, high"). Nonessential regulatory genes are ideally suited to act as "molecular switches" for control of replication phenotypes by their activation or inactivation, particularly in viruses such as HIV-1, which characteristically generate high levels of sequence heterogeneity. We demonstrate here that discrete genetic alterations in such accessory genes result in profoundly different replication rates in monocytes in vitro, which suggests a mechanism for transition from subclinical to clinical disease in vivo. These findings thus provide a rationale for addressing on a wider scale whether functional status of vpr and/or vpu correlates with disease stage or serves as a potential prognostic indicator of disease progression and outcome.

To further test the role of vpu and vpr in monocyte infection, several additional vpu mutant proviruses have been constructed. These include NLHXADA-SM and NLHXADA-SK/GG plasmids with a site-directed mutation at the initiator methionine codon of vpu. In addition, we have constructed NLHXADA-GG, NLHXADA-GP, NLHXU2-GP, and NLHXW1C1-GP plasmids in which we have inserted the vpu initiator methionine codon. Each of these clones were constructed with or without a frameshift mutation at the Eco RI site of vpr. Mutations in these plasmids were confirmed by nucleotide sequencing and then assayed for virus replication kinetics on monocytes. In addition, we used primary lymphocytes infected with these viruses to label with 3H-leucine and immunoprecipitated with anti-vpu or anti-vpr antiserum. Each of these mutants confirmed the role of vpr in productive macrophage infection.

To identify the function of vpr and vpu in macrophages, we have constructed a recombinant vaccinia virus that expresses vpr, and a recombinant vaccinia virus that expresses the vpu protein together with either the ADA or HXB2 envelope. The latter strategy was taken in light of the fact that vpu and envelope are expressed from a single bicistronic mRNA. Using these expression systems, we found no significant effect of vpr on env synthesis, processing, stability, cell surface transport, CD4 binding, release, oligomerization, or gp120 cleavage.

h) Determine mechanism of action of Vpr in enhancing HIV-1 infectivity and/or replication in MT4 lymphoid cells

The contract application describes 3-10-fold differences in the ability of HIV-1 clones with or without vpr to replicate in HTLV-I infected cell lines, MT4 and MT2. However, the much more dramatic differences in the presence of vpr in monocytes, and the particular relevance of monocytes to disease pathogenesis, suggested to us that much greater emphasis should be placed on examining the mechanism of action of Vpr in monocytes than in MT4 cells. Thus, the same analyses described in the original contract application for MT4 cell studies will still be performed, but these studies will take a lower priority to pursuing the much more exciting monocyte infection studies.

i) Determine effects of Vpr on HIV-1 infectivity

In collaboration with Drs Stevenson, Bukrinsky, and Emerman, we found that vpr was critical for preintegration complex transport to the nucleus in quiescent cells. In arrested T lymphocytes, neither the nuclear localization signal in p17 Gag or Vpr was critical for virus replication, but deletion of both signals arrested virus replication (Fig 14). Using PCR, we found that either signal was critical for the formation of LTR circle forms of viral DNA, a measurement of preintegration transport into the nucleus (Fig 15). Similarly, in macrophages, alteration of the nuclear localization signal in p17 Gag or Vpr alone, had a moderate effect on virus replication, whereas alteration of both signals abrogated replication (Fig 16). PCR data in monocytes showed very similar results to that obtained in quiescent T cells where at least one of these signals was required for formation of LTR circles (Fig 17).

ii) Determine effects of Vpr on HIV-1 production

The studies described above suggest that Vpr affects an early step in virus replication, and therefore the studies originally described for this section were not performed.

We have examined by transmission electron microscopy, monocytes infected productively or silently by a number of the virus strains described above. No virus particles were detected in silently infected monocytes, but this is being re-examined as described above. Thus, either the replication cycle is aborted prior to the step of virus assembly, or the level of expression was too low to be detected by electron microscopy.

iii) Determine if Vpr effects can be complemented in trans

The effects of Vpr could not be fully complemented in trans.

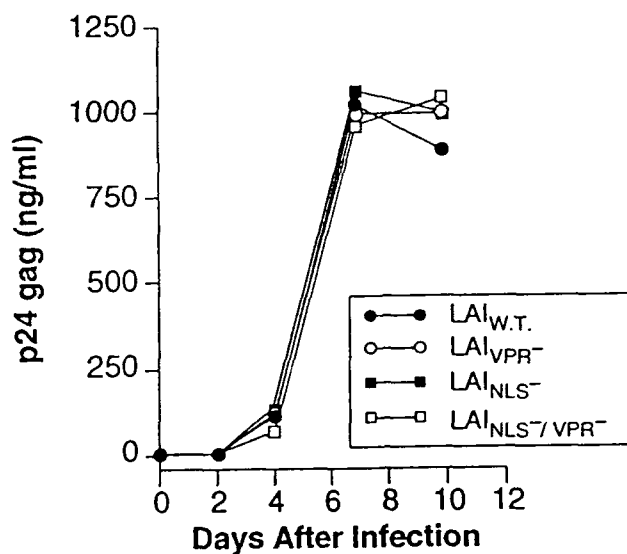


Fig 14.

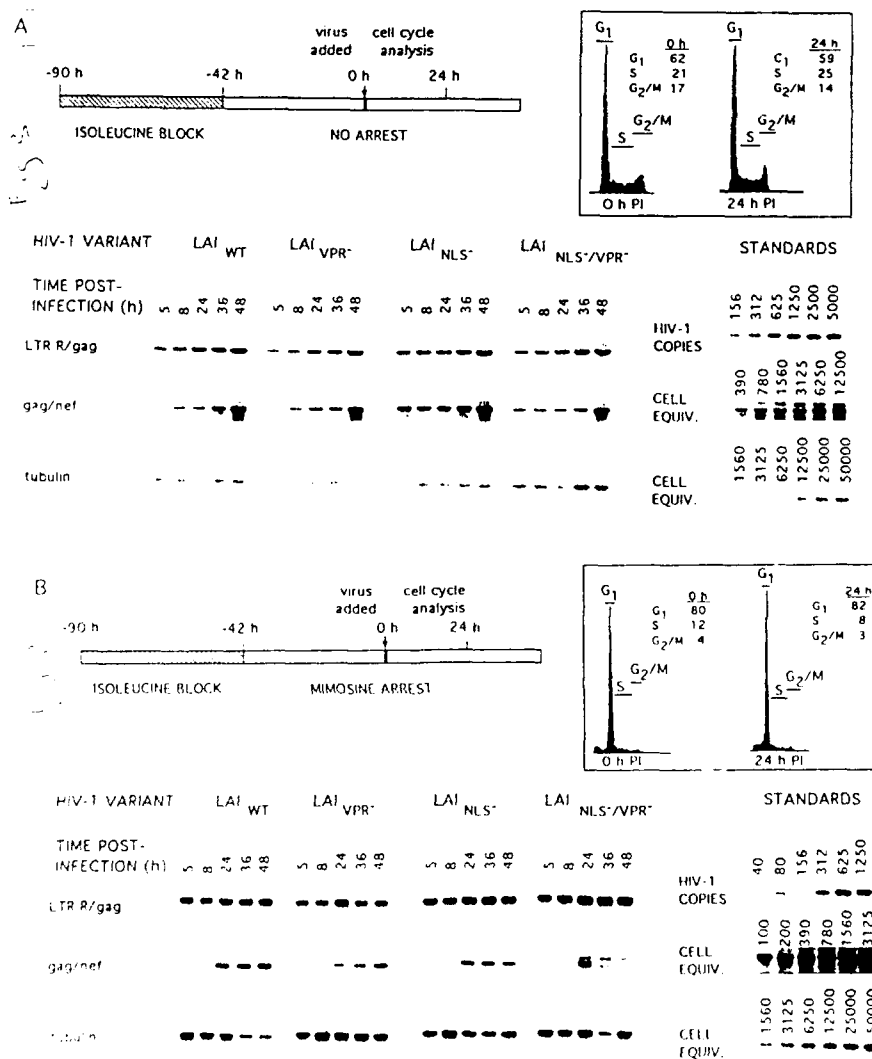


Fig 15.

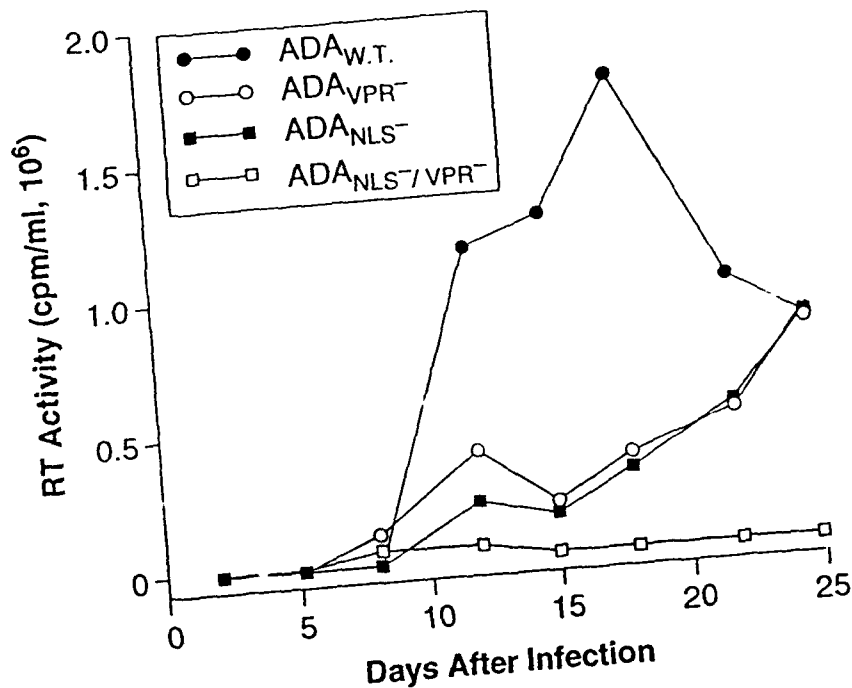


Fig 16.

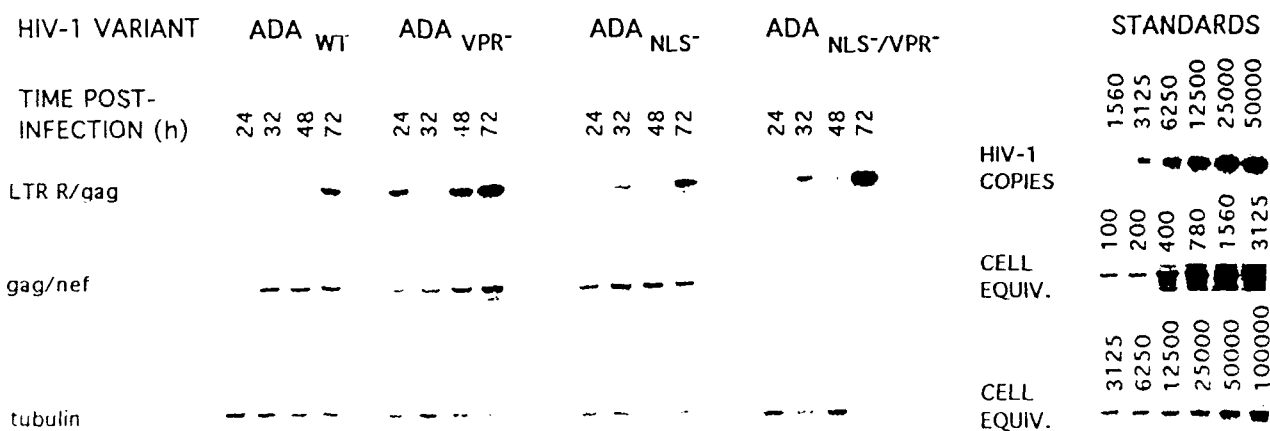


Fig 17.

iv) Determine if Vpr effects are independent of other regulatory proteins

We have already demonstrated a potential interaction between vpr, vpu, and vpx. Mutant strains of HIV-2 were constructed to examine if vpr and vpx effects are independent.

v) Determine the structure-function relationships of Vpr

Several additional vpr mutants have been constructed in regions conserved between HIV-1, HIV-2, and SIVmac. Mutants in the basic amino acid rich region of Vpr have been constructed to examine the role of this region in nuclear localization and virion packaging.

i) Determine the role of Vpr in vivo with appropriate model systems

We have initiated studies in scid/hu mice with constructs NLHX, NLHXADA-GG, and NLHXADA-GG vpr mutant in collaboration with R. Markham (Johns Hopkins). The first experiment showed successful replication and recovery from inoculated mice with each virus. Quantitative assays are now developed using in situ hybridization and PCR and will be applied in additional in vivo experiments of this type.

We have deferred work in the rabbit model system as advised by our collaborators, Drs. Tom Folks and Michael Lairmore (CDC and Ohio State University), since consistent infection results could not be reproduced with this model system.

Studies of vpr mutants in SIVmac239 are already underway in Dr. Desrosiers group at the New England Primate Research Center.

j) Determine the role of Vpr in modulating disease in HIV-1 infected humans

In collaboration with Dr. Richard Markham (Johns Hopkins), we have obtained samples from seven patients followed over the course of several years with three PBMC samples from each patient at times when the CD4>1000, CD4=250-750, and CD4<250, for this study. However, insufficient funds were available to complete this task, in light of the budgetary cuts that were imposed in the last six months of the project.

2. To determine the function of viral protein X (Vpx)

a) To assess the effects of Vpx on replication cytopathicity of HIV-2 in T lymphoid and monocytoid cells

i) To determine effects of Vpx on site of virus assembly in the cell

We have utilized immunogold electron microscopy to examine Vpx incorporation into virus particles. No detectable gold particles were found on virions generated from vpx mutant HIV-2 virus, MX, and vpx/vpr double mutant, MR/MX (Fig. 18). As with Vpr expression, intracellular particles were relatively depleted of Vpx compared to extracellular particles. Background gold labeling in cellular sites was too high to determine the localization of free vpx in the cell. Vpx had no effect on the site of virus assembly in PBLs or CEM cells. Preliminary immunofluorescence studies demonstrated that most vpx in the infected cells or in transfected cells was cytosolic.

ii) To determine the cellular localization of Vpx in HIV-2 infected cells

This is discussed above.

iii) To determine if there are co- or post-translational modifications of Vpx

No co- or post-translational modification of Vpx were identified.

d) To assess whether Vpx proviral mutants can be complemented in trans by a Vpx expression clone

Vpx could not be fully complemented in trans.

e) To determine structure-function relationships of Vpx

To examine Vpx binding to HIV-2 RNA, as noted previously, we have cloned HIV-2 vpx and vpr genes into pTM3 expression vectors to allow expression in reticulocyte lysates and in vTF7-3 infected BSC40 cells, and into pMON vectors for E. coli expression. Northwestern blots with the reticulocyte lysate expressed and vaccinia virus expressed Vpx proteins failed to demonstrate specific binding to viral RNA, but the amounts of protein expressed in these systems was quite low. Northwestern blot conditions have been established with the E. coli expressed proteins. As a control, we have shown that pMON expressed HIV-1 gag binds specifically HIV-1 RNA. We have therefore prepared blots with HIV-2 gag p55 and vpx proteins to examine binding to the HIV-2 RNAs that have been prepared.

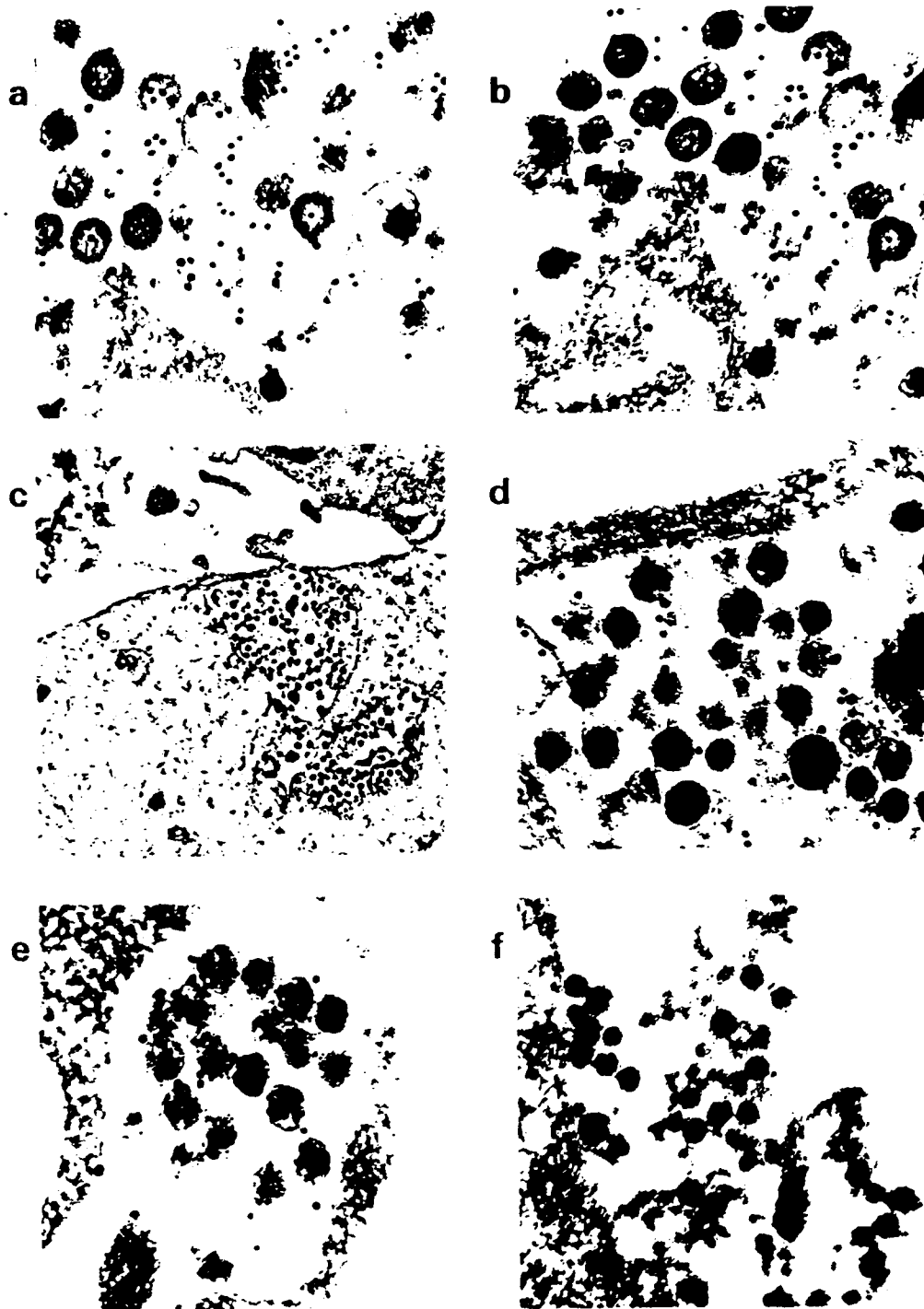


Fig 5. Immunogold electron microscopic localization of VPX. PBMCs were infected for 14 days with a-d) ES, e) MR, or f) MX viruses. a and b) VPX gold complexes in ES infected cells in extracellular virions. Magnification x 82,000, 1 cm bar = 0.122 μ m. c) VPX gold complexes in ES infected cells in intracellular virions, Magnification x 13,900, 1 cm bar = 0.72 μ m. d) VPX gold complexes in ES infected cells in intracellular virions (higher power view of c), Magnification x 78,000, 1 cm bar = 0.128 μ m. e) VPX gold complexes in MR infected cells and extracellular virions, Magnification x 79,000, 1 cm bar = 0.127 μ m. f) VPX gold complexes (a5 nm, double arrowhead) in MX infected cells and extracellular virions, and GAG p24 gold complexes (5 nm, single arrow) shown for comparison, Magnification x 38,000, 1 cm bar = 0.263 μ m.

Fig 18.

To assess the requirements for vpx packaging in virions, we have expressed vpx with a vaccinia virus expression system, in the presence or absence of gag. We found that p55 gag is sufficient for vpx packaging, and pol proteins, virion RNA, and proteolytic cleavage of gag was not required for vpx incorporation into virus particles (Fig 19). Moreover, we found that anti-vpx antiserum was capable of coprecipitating p27 capsid with vpx (Fig 19). The vpx-CA complex was resistant to boiling in 4% SDS, suggesting a covalent complex. However, the complex was dissociated by treatment with mercaptoethanol or DTT, suggesting a disulfide bond. Treatment of virions with iodoacetamide prior to processing did not affect complex formation, suggesting that this is not an artifact occurring during immunoprecipitation, but rather forms during virus particle assembly. Neither MA, NC, or p6 were involved in the vpx-CA complex.

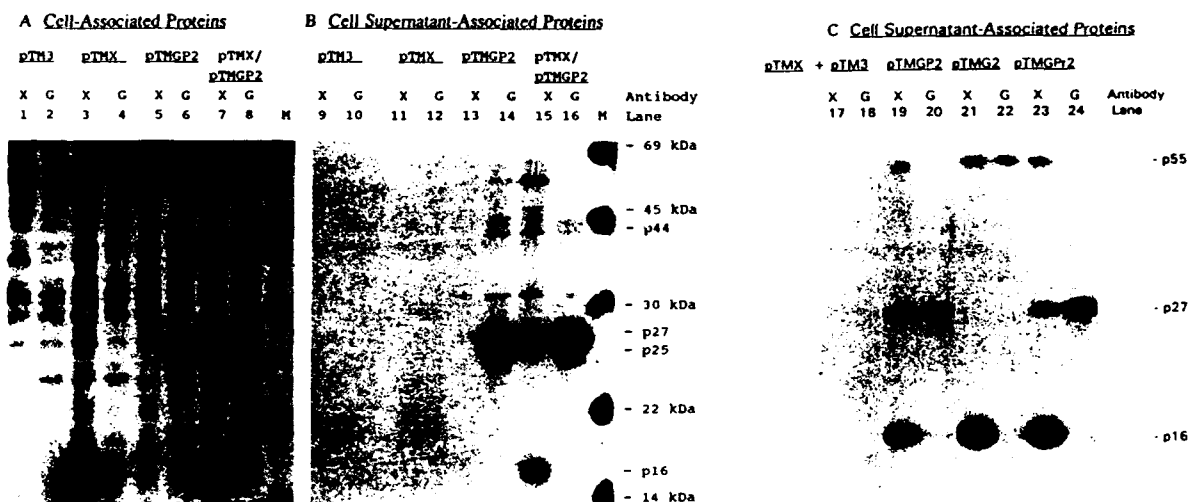


Fig. 1. Association of recombinant vaccinia virus expressed VPX with GAG p27. BSC40 cells were cotransfected 1 hr after infection with VTF7-3 with 20 μ g of pTM3 (lanes 1, 2, 9, 10), pTMX (lanes 3, 4, 11, 12, 17, 18), pTMGP2 (lanes 5, 6, 13, 14), pTMX and pTMGP2 (lanes 7, 8, 15, 16, 19, 20), pTMX and pTMGP2 (lanes 21, 22), or pTMX and pTMGP2 (lanes 23, 24). The calcium phosphate precipitation method was used for transfection for (A) and (B) and the lipofectin transfection method for (C), and equivalent amounts of DNA were transfected in each case (with the addition of pTM3). After 3 hr of cultivation in DMEM supplemented with 10% fetal calf serum, 50 μ g/ml penicillin, and 50 μ g/ml streptomycin the cells were placed in medium lacking methionine and cysteine, and labeled for 16 hr with 100 μ Ci/ml Trans³⁵S-label (ICN). Samples of conditioned medium (lanes 9-24) were cleared of cellular debris by centrifugation at 1000 rpm for 5 min and then 0.1 vol of 10X lysis buffer was added. Cells were washed with PBS and then PBS was added to the plates during scraping with a rubber policeman. 0.1 vol of 10X lysis buffer was added and the cells were vortexed at 4° for 1 min. Nuclei were removed by centrifugation at 2000 rpm for 10 min. Immunoprecipitation was performed with a rabbit anti-Vpx antiserum (odd-numbered lanes) or a mouse monoclonal anti-HIV-2 GAG antiserum (even-numbered lanes, provided by Dr. Paul Yoshihara through the NIH AIDS Reagent Repository). Immunoprecipitates were washed with 1X lysis buffer three times and then 30 μ l of 2X sample buffer was added. Samples were treated at 100° for 5 min and analyzed on 12% PAGE. Molecular weight markers are indicated (M) and the sizes are listed on the right of the figure in kDa.

Fig 19.

We found that HIV-1 virions were inefficient at incorporation of vpx (Fig 20). Therefore, we have constructed several HIV-1/2 Gag chimeric proteins to define the critical domain required for vpx incorporation. A construct with only the CA coding sequence of HIV-2 in place of that of HIV-1 CA coding sequence is capable of vpx incorporation. Further chimeras were constructed subdividing the CA sequence required for vpx packaging, as well as site-directed mutants in CA.

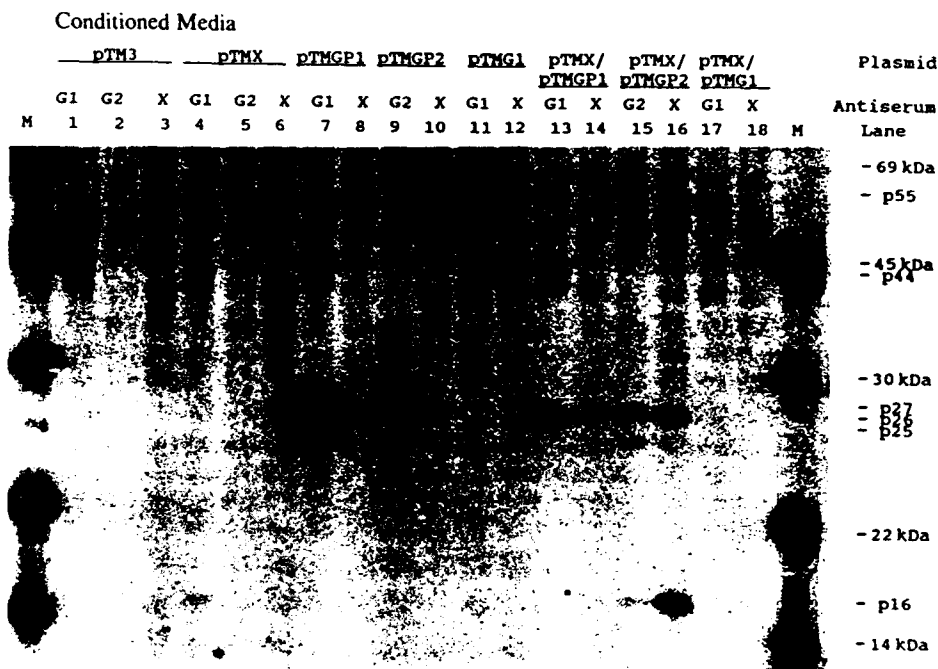


Fig. 4. Specificity of VPX for association with HIV-2 GAG but not HIV-1 GAG protein. BSC40 cells were transfected with pTM3 (lanes 1-3), pTMX (lanes 4-6), pTMGP1 (lanes 7, 8), pTMGP2 (lanes 9, 10), pTMG1 (lanes 11, 12), pTMX and pTMGP1 (lanes 13, 14), pTMX and pTMGP2 (lanes 15, 16), or pTMX and pTMG1 (lanes 17, 18). Cells were transfected with equivalent amounts of DNA and labeled with Trans³⁵S label, as described in Fig. 1 legend. Samples of conditioned media were immunoprecipitated with an anti-HIV-1 GAG antiserum (lanes 1, 4, 7, 11, 13, 17; produced in rabbits with a recombinant protein provided by the NIH AIDS Reagent Repository through American Biotech), the anti-HIV-2 p24 antiserum (lanes 2, 5, 9, 15), or the anti-VPX antiserum (lanes 3, 6, 8, 10, 12, 14, 16, 18). Samples were electrophoresed on SDS-PAGE and molecular weight standards (M) are shown on the right.

Fig 20.

We have also constructed deletion mutants of vpx to examine the critical domains required for incorporation into virions. These include deletion of the proline tail which was not essential for vpx incorporation. We have also deleted the cys-his domain as well as the amphipathic helix, alone or in combination with each other or the proline tail deletion. Since several of these constructs had reduced reactivity with the anti-vpx antiserum, they were tagged at the N-terminus with a hemagglutinin epitope, which neither altered vpx conformation or packaging activity.

In addition, mutation of each of the three cysteine residues in vpx was performed alone or in combination to examine their role in vpx activity, and complex formation with CA.

f) To assess effects of Vpx on replication and cytopathicity of SIV in T lymphoid and monocytoid cells

We have focused our initial work on the HIV-2 Vpx protein. We have found that mutation of vpx in HIV-2 leads to a decrease in HIV-2 replication in PBLs and HeLa/T4 cells, particularly at low multiplicities of infection. Minimal or no effects were found in CEM cells.

To further define the nature of the vpx defect in PBLs versus CEM cells was examined. For this purpose, we used PCR studies similar to those described above for vpr. In addition, studies were carried out in HeLa/T4/beta-galactosidase indicator cells.

g) To assess the role of Vpx in vivo with animal model systems

Animal model studies awaited initial data with the HIV-1 viruses in scid/hu mice (see 1.i.) and the initial data with the HIV-2 virus studies outlined in this section. Insufficient funds were available to complete this task, due to severe budgetary cuts in the last six months of the project.

3. To determine the function and mechanism of action of negative factor (NEF)

a) To determine relative effects of HIV-1 Nef on viral transcription, degradation, and nuclear-cytoplasmic transport

We have demonstrated that HIV-1 and SIVmac Nef affect viral transcription but not degradation or processing of viral transcripts. This work was reported in the first year's annual report and in our manuscript (Niederman, Hu, Ratner, Simian immunodeficiency virus negative factor (NEF) suppresses viral mRNA accumulation in COS cells. J. Virol. 65:3538-3546, 1991).

We have discussed the controversy concerning these results in a recent review by Niederman and Ratner, Functional analysis of HIV-1 and SIV nef proteins. Research in Virology 143:43-46, 1992. We found that the multiplicity of infection was critically important in assessing the effects of Nef in virus replication studies. It appeared reasonable to assess the relevance of the moi considering the relatively moderate effects of Nef compared to the effects of Tat or Rev. The hypothesis is that at relatively high moi, subtle effects of Nef may be masked due to an overload of viral DNA templates. That is, Nef may require a limited pool of cellular factors in order to maintain transcriptional suppression. Once a cascade of virus replication has occurred, and high-titer virus results, it may be impossible for Nef to reverse or even halt the cascade.

To assess the effect of the moi on Nef's suppressive capacity we compared the replication of Nef+ and Nef- viruses in lymphoid cells under conditions of varied moi. We found that at relatively high moi, replication of the Nef+ and Nef- viruses was indistinguishable as measured by reverse transcriptase activity. However, upon serial 10-fold dilutions of the initial virus inoculum, the replication of the Nef+ virus was significantly inhibited (up to 25-fold) in several T-cell lines compared to its Nef- counterpart. In addition to generating lower levels of reverse transcriptase activity, the Nef+ viruses lagged by 4-8 days in comparison to the Nef- virus with regards to detection of reverse transcriptase activity. This lag period may represent an in vitro form of latency. Similar experiments were carried out in macrophages. Recently other investigators compared the replicative capacities of SIV Nef+ versus Nef- viruses. They also found Nef-mediated suppression to be dependent upon low moi conditions and also observed a lag period for viral growth in the presence of Nef. Finally, there are other examples demonstrating the relevance of the moi when determining the function of other HIV-gene products, including Vpr and Vpx.

Other factors contributing to the differences observed between our laboratory and that of Kim and coworkers may involve different modes of virus transmission. In our system, Jurkat cells were cocultivated with COS cells which were constantly shedding extremely low concentrations of virus, too low to be detected by reverse transcriptase activity. Viral transmission may be either through cell-to-cell contact or via cell-free virus. In contrast, Kim and colleagues used virus derived from lymphocytes and adjusted the level of the virus inocula based on measurable reverse transcriptase activity; additionally, there are several amino acid

differences between of our nef allele and that of Kim et al, and it is interesting to note that the Nef proteins differed with respect to the mobilities on SDS PAGE.

b) To characterize Nef responsive sequences

Stimulation of T cells by T-cell-specific stimuli (e.g. antigen and antibody to CD2 or CD3) or nonspecific mitogens (e.g. phytohemagglutinin [PHA] and phorbol 12-myristate 13-acetate [PMA]) results in the induction of the DNA binding activity of the host transcription factor, NF-kB. The NF-kB family of proteins normally regulates the expression of genes involved in T-cell activation and proliferation, such as interleukin 2 (IL-2) and the alpha subunit of the IL-2 receptor. The human immunodeficiency virus type 1 (HIV-1) promoter possesses two adjacent NF-kB-binding sites, which allows the virus to subvert the normal activity of NF-kB to enhance its own replication.

Previous work suggests that the HIV-1-encoded Nef protein serves as a negative regulator of HIV-1 replication. Furthermore, we and others have found that Nef may suppress both HIV-1 and IL-2 transcription. To investigate whether Nef affects the DNA binding activity of NF-kB or other transcription factors implicated in HIV-1 regulation, we used the human T-cell lines stably transfected with the nef gene. Jurkat (J25) human T-cell clone 133 constitutively expresses the NL4-3 nef gene. 22F6 cells represent another antibiotic-resistant clone of J24 cells; however, these cells do not contain nef sequences and do not express Nef. Additionally, we used oligoclonal Jurkat E6-1 and HPB-ALL cells expressing the SF2 nef gene either in the correct orientation (Jurkat/LnefSN and HPB-ALL/LnefSNS1 cells) or in the reverse orientation (Jurkat/LfensN and HPB-ALL/LfensN cells) with respect to the Moloney murine leukemia virus promoter. These cells represent a mixed population of cells expressing Nef to various degrees and were used to exclude the possibility that clonal selection accounts for Nef effects observed in the J25 clones.

To determine the impact of T-cell activation on the expression of Nef, the human T-cell lines were stimulated with PHA and PMA. Cells were maintained in logarithmic growth in RPMI 1640 medium supplemented with 10% fetal bovine serum and 2 mM glutamine. J25 and Jurkat E6-1 cells (5×10^6) and HPB-ALL cells (1.5×10^7) were either not stimulated or stimulated with 13 ug of PHA-P (Sigma) and 75 ng of PMA (Sigma) per ml for 4 h. The cells were lysed in RIPA buffer, and lysates were immunoprecipitated with rabbit polyclonal anti-Nef sera. The immunoprecipitates were subjected to SDS-PAGE (12% polyacrylamide), and the proteins were transferred to nitrocellulose for Western blot analysis. The primary antibody was the rabbit anti-Nef-serum, and the secondary antibody was alkaline phosphatase-conjugated goat anti-rabbit immunoglobulin, sepcific for the heavy chain (Promega). The proteins were visualized by color development with nitroblue tetrazolium and 5-bromo-4-chloro-3-indoylphosphate toluidinium (Promega). Band intensity was determined by laser densitometry scanning of the Western blot and was in the linear range of analysis as established by a standard curve. Jurkat E6-1 cells were obtained from the AIDS Repository, American Type Culture Collection (Arthur Weiss), and were stably transduced with the SF2 nef gene as previously described.

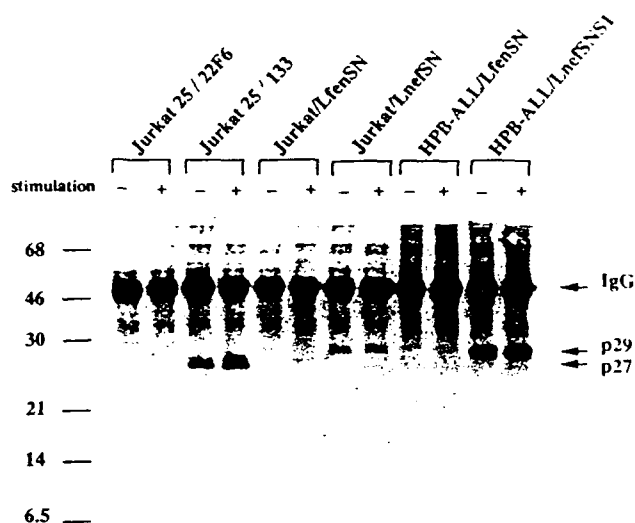


FIG. 1. Immunoblot analysis of the HIV-1 Nef protein in stably transfected and transduced human T-cell lines. Cell lysates were immunoprecipitated with rabbit anti-Nef polyclonal serum, electrophoresed, transferred to nitrocellulose, and immunoblotted with the same anti-Nef serum. The cells were either unstimulated (-) or stimulated (+) with PHA and PMA before cell harvesting. Prestained protein size markers are indicated on the left in kilodaltons. Nef protein in the 133 cells (21) was expressed from the *nef* gene of isolate pNL432 and had an apparent molecular mass of 27 kDa, whereas the Nef proteins expressed in the Jurkat E6-1 and HPB-ALL cells were encoded by the *nef* gene of isolate SF2 and demonstrated an apparent molecular mass of 29 kDa. Immunoglobulin G (IgG) heavy chain, which was present in the antiserum used for the immunoprecipitation step, is indicated at the right.

Fig 21

Immunoblot analysis with anti-Nef antibodies showed that stimulation caused a two- to threefold increase in Nef expression in clone 133 cells (Fig. 21). This increase was probably due to the inducibility of the chimeric simian virus 40 (SV40)-human T-cell leukemia virus type I promoter used to direct Nef expression. However, Nef expression was not induced in the Jurkat E6-1 or HPB-ALL cells (Fig. 21). The level of Nef expressed in these cells is comparable to the amount of Nef generated by HIV-1 in productively infected CEM human T cells (data not shown). The difference in the apparent molecular weight of the Nef produced in clone 133 cells and those produced in the Jurkat/LnefSN and HPB-ALL/LnefSNS1 cells is due to the presence of an alanine at amino acid position 54 in the NL4-3 *nef* gene compared with the presence of an aspartic acid at that position in the SF2 *nef* gene. The amount of lysate equivalents loaded in the HPB-ALL/LnefSNS1 lanes was threefold higher than that of the Jurkat/LnefSN lanes. Nevertheless, the amount of Nef expressed in the HPB-ALL/LnefSNS1 cells was approximately fourfold higher than the amount produced in the Jurkat/LnefSN cells (Fig. 21). Nef did not appear to be toxic in that Nef-

producing cells exhibited the same doubling time and morphology as the control cells.

Gel shift assays were performed with nuclear extracts prepared from stimulated and unstimulated cells. Nuclear extracts were prepared from 5×10^7 cells with a modified version of the method of Dignam and colleagues as adapted by Montminy and Bilezikjian. Following ammonium sulfate precipitation, nuclear proteins were resuspended in a 100 μ l solution containing 20 mM HEPES (N-2-hydroxyethylpiperazine-N'-2-ethanesulfonic acid, pH 7.9), 20 mM KCl, 1 mM $MgCl_2$, 2 mM DTT, and 17% glycerol with the addition of 10 mM NaF, 0.1 mM sodium vanadate, and 50 mM beta-glycerol-phosphate. Cytoplasmic extracts consisted of the supernatant resulting from the lysis of cells in hypotonic lysis solution, douncing, and low-speed centrifugation to pellet nuclei. Binding reaction mixtures contained 2 μ l (2 μ g) of nuclear extract (Fig. 22a through d) or 6 μ l (7 μ g) of cytoplasmic extract (Fig. 22e), 2 μ g of poly(dI-dC) (Pharmacia), 100-fold molar excess of unlabeled NF-kB mutant oligonucleotide (ACAATCAGTTTTCGCTGCTCAGTTTTCAGGGA), and 20,000 cpm of end-labeled oligonucleotide probe in DNA binding buffer in a final volume of 22 μ l. Reactions were performed at 30° C for 25 min, immediately loaded on a 4.5% polyacrylamide gel with 0.5 X Tris-borate-EDTA, and run at 200 V. Oligonucleotides used were as follows: NF-kB, ACAAGGGACTTTTCGCTGGGACTTTTCAGGGA; SP-1, CAGGGAGGGGTGGCTGG-GGGGACTGGGGAGTGGGGTCC. All DNA probes were gel purified and end labeled with gamma-32P-ATP. The intensity of the indicated bands was determined by laser densitometry and by measuring the radioactivity of excised bands in a liquid scintillation counter. There was a linear relationship between the amount of extract used and DNA-binding activity (data not shown). There was no NF-kB DNA binding activity with the cytoplasmic extracts in the absence of deoxycholic acid (data not shown). Protein concentration was determined with the Bradford reagent (Biorad) with bovine serum albumin as a standard. Nuclear extract preparations and binding reactions were repeated on three separate occasions with similar results.

The induction of NF-kB activity in stimulated 133 cells was suppressed 5-7-fold compared with that of the 22F6 cells. This inhibition was evident 40 min poststimulation and was sustained throughout the 4 h stimulation period (Fig. 22a). J25 clone 22D8 cells represent a distinct clonal cell line, which, like the 133 cells, also stably express Nef. NF-kB induction was suppressed 4-5-fold in the 22D8 cells compared with that of the 22F6 cells (Fig. 22b). NF-kB suppression was more profound in the 133 cells than in the 22D8 cells, which correlates with the observation that Nef expression was higher in the 133 cells. Similar to the Nef-expressing J25 clones, Nef inhibited NF-kB induction 3-4-fold in the Jurkat/LnefSN and HPB-ALL/Lnef-SNS1 cells compared with their non-Nef-expressing counterparts (Fig. 22c and d). Nef-mediated NF-kB suppression was more profound in the Jurkat/LnefSN cells than in the HPB-ALL/LnefSNS1 cells, even though the HPB-ALL/LnefSNS1 cells expressed several fold higher levels of Nef. This result is likely due to the biological differences that exist between the two cell lines. That is, Jurkat cells may be more sensitive to the effects of Nef than HPB-ALL cells because of differential expression of proteins involved in signal transduction. That Nef-mediated NF-kB suppression in the 133 and 22D8 cells was greater than in the Jurkat/LnefSN and HPB-ALL/LnefSNS1 cells

[illegible]

FIG. 2. Gel shift analysis of NF- κ B activity in nuclear extracts prepared from J25 (a and b), Jurkat E6-1 (c), or HPB-ALL (d) cells. (a) 22F6 and 133 cells were stimulated with PHA (13 μ g/ml) and PMA (75 ng/ml) for 0, 40, 80, 120, or 240 min; 22F6 and 22D8 (b), Jurkat E6-1 (c), or HPB-ALL (d) cells were not stimulated (0) or were stimulated with PHA and PMA as described above for 4 h (4). DNA probes used for binding are specified on the top of each panel. (e) Cytoplasmic protein extracts (7 μ g each) from the indicated cells were incubated with the NF- κ B DNA probe as described in the text, in the presence of 0.6% deoxycholic acid (Sigma). N, S, and P, NF- κ B-specific binding, SP-1-specific binding, and free probe, respectively. SP-1 binding served as a control for extract quality and specificity of Nef effects. Cold indicates that 100-fold molar excess of unlabeled DNA was added for competition. ns, nonspecific binding. Data represent at least three independent experiments.

NF- κ B activity in nuclei from unstimulated cells was extremely low but detectable, and no differences between the Nef-expressing and control cells were observed (data not shown). Additionally, when cytoplasmic extracts from unstimulated cells were treated with deoxycholic acid (which releases NF- κ B from its cytoplasmic inhibitor I κ B), they exhibited NF- κ B activity independent of Nef expression (Fig. 22e). Finally, that Nef suppressed the level of NF- κ B induction after only 40 min of stimulation suggests that Nef does not suppress p110 or p65 NF- κ B mRNA expression. These observations indicate that Nef affects the recruitment and not the cytoplasmic concentration of NF- κ B. The binding of SP-1 was independent of Nef expression and stimulation, and the amount of SP-1 probe used in these gel shift assays was not limited (Fig. 22a through e). In addition, no differences in binding to NFAT-, USF-, and URS-specific probes between 22F6 and 133 cells were observed (data not shown). These data suggest that Nef specifically inhibited the induction of NF- κ B activity.

To further demonstrate Nef's suppressive effect on NF- κ B recruitment, 22F6 cells were transiently transfected with DNA plasmids expressing Nef from the SV40 early promoter, pSVF/N, or the cytomegalovirus immediate-early promoter, pCMVF/N, or with plasmids containing frameshift mutations in the nef gene (pSVF/Nfs and pCMVF/Nfs, respectively). Nuclear extract preparation and DNA binding reactions were as described above. 22F6 cells (2×10^7) (Fig. 23a) were transfected with 30 μ g of the indicated plasmid DNA by using DEAE-dextran. Briefly, cells (10^7) were incubated with plasmid DNA suspended in a solution containing 10 ml of serum-free RPMI 1640, 0.25 M Tris, pH 7.3, and 125 μ g of DEAE-dextran (Sigma) per ml at 37°C for 40 min. Following centrifugation at $2,000 \times g$ for 7 min., the cells were maintained in growth medium for 60 h prior to stimulation and cell harvesting. Plasmid pSVF/N is similar to plasmid pSVF, except that HIV-1 nucleotides 8994-9213 (including the NF- κ B recognition sites) and 3' flanking cellular sequences were deleted. Plasmid pSVF/N was digested at the unique Bgl II site at codon 88 of the nef gene, the sticky ends were filled in with the Klenow fragment of DNA polymerase I, and the plasmid was religated with T4 DNA ligase. This plasmid was called pSVF/Nfs to indicate the introduction of a frameshift in the nef gene. The Bam HI fragment from pSVF/N and pSVF/Nfs, which includes the entire length of the HIV-1 sequences present in these clones was inserted into the vector pCB6 in the correct and incorrect orientation with respect to the cytomegalovirus immediate-early promoter to generate pCMVF/N and pCMVF/Nfs, respectively. Cells transfected with plasmids pSVF/N and pCMVF/N express Nef protein, but cells transfected with pSVF/Nfs and pCMVF/Nfs do not, as determined by Western blot and immunoprecipitation analysis (data not shown). Transfection efficiency was determined by cotransfection with 2 μ g of pSV2-CAT. Chloramphenicol acetyltransferase (CAT) activity (reported as the percent conversion to acetylated products) was determined as described below, and the values for the pSVF/N fs-0-, pSVF/N fs-4-, pSVF/N-4-, pCMVF/N fs-4-, and pCMVF/N-4-transfected cells were 51, 60, 61, 58, and 61%, respectively. A USF-specific DNA probe (corresponding to nucleotides -159 to -173 of the HIV-1 long terminal repeat, GCGCTAGCATTTTCATCAAGTGGGCGGAGAGCTGC) was used as a control for the specificity of Nef effects and extract integrity. Ionomycin (Sigma) (Fig. 22b) was used at a concentration of 2 μ M. Anti-p50, anti-p65, anti-v-rel and prebleed sera

(Fig. 23c) were kindly provided by Mark Hannik (University of Missouri, Columbia, Mo). Because the gels in Fig. 23a and b and Fig. 22 were run for a shorter length of time, the two bands indicated in Fig. 23c appear as one band in Fig. 23a and b, and Fig. 22.

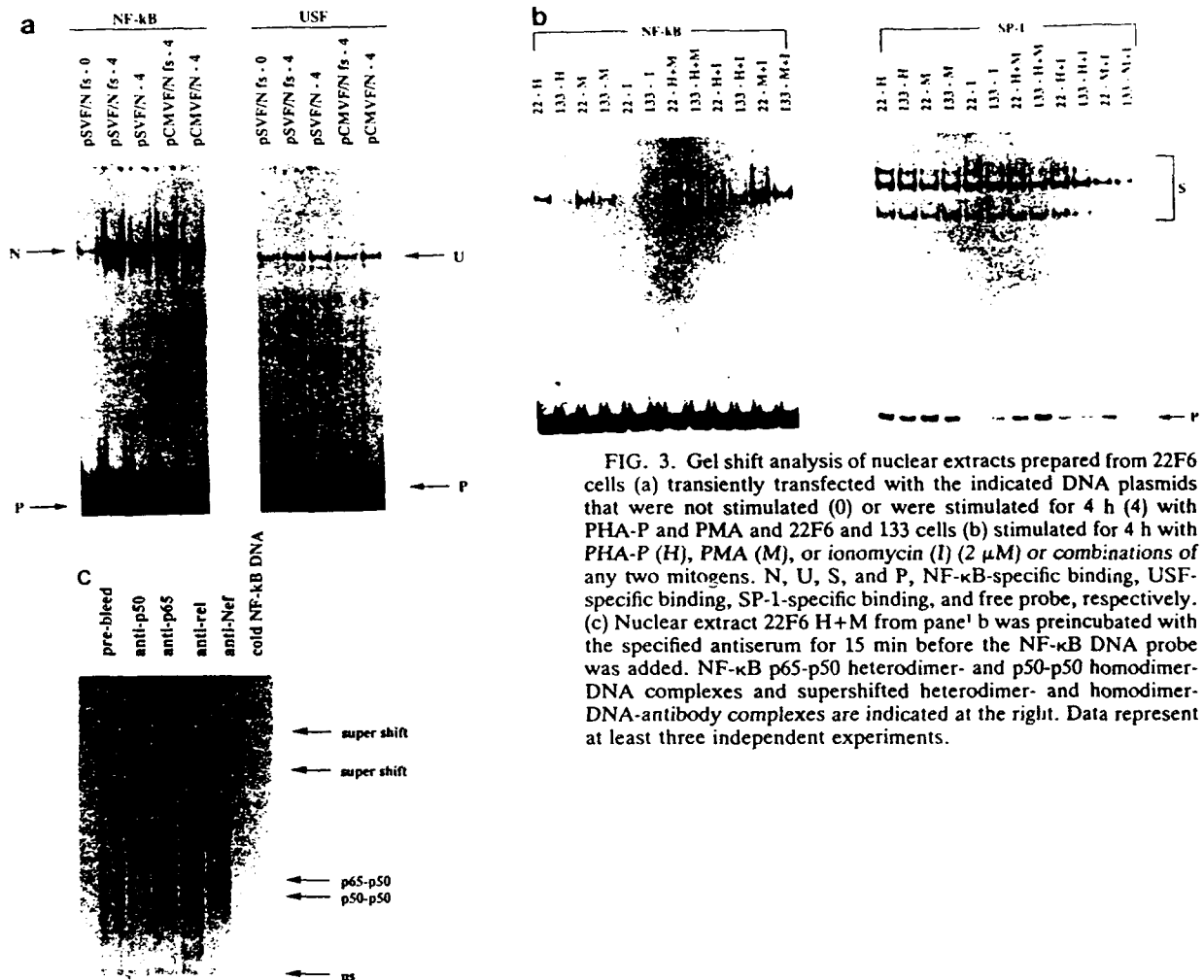


FIG. 3. Gel shift analysis of nuclear extracts prepared from 22F6 cells (a) transiently transfected with the indicated DNA plasmids that were not stimulated (0) or were stimulated for 4 h (4) with PHA-P (H), PMA (M), or ionomycin (I) (2 μ M) or combinations of any two mitogens. N, U, S, and P, NF- κ B-specific binding, USF-specific binding, SP-1-specific binding, and free probe, respectively. (c) Nuclear extract 22F6 H+M from pane¹ b was preincubated with the specified antiserum for 15 min before the NF- κ B DNA probe was added. NF- κ B p65-p50 heterodimer- and p50-p50 homodimer-DNA complexes and supershifted heterodimer- and homodimer-DNA-antibody complexes are indicated at the right. Data represent at least three independent experiments.

Fig 23.

NF- κ B induction was consistently inhibited at least two-fold in cells transfected with either pSVF/N or pCMVf/N compared with cells transfected with their nef mutant counterparts (Fig. 23a). Transfection efficiencies in these experiments were determined by cotransfecting cells with the pSV2-CAT plasmid and measuring CAT activity. No significant differences in transfection efficiency between the nef-expressing and the nef mutant plasmids were observed (Fig. 23a). The suppressive

effect of Nef in these transiently transfected cells was not as dramatic as the effects observed in the stably transfected and transduced cells. The more subtle effect of Nef in this experiment may be due to the expression of a nef allele which was derived from an HIV-1 isolate distinct from either the NL43 or the SF2 isolates. In addition, cells which did not receive the nef expression plasmid during the transient-transfection process were not eliminated (by antibiotic selection) from the total cell population.

To explore the relative contributions of individual mitogens to the recruitment of Nef-inhibitable complexes, cells were stimulated with either PHA, PMA, or ionomycin alone, or in combination. The maximal induction of NF- κ B activity occurred when PHA was combined with PMA (Fig. 23b). This result coupled with the observation that PHA mimics the effects of the natural ligand for the T-cell receptor (TCR) complex suggests that Nef may inhibit signal transduction emanating from the TCR complex. The addition of the Ca^{2+} ionophore, ionomycin, when coupled with PMA treatment partially substituted for the absence of PHA with respect to NF- κ B induction (Fig. 22b). However, ionomycin treatment did not significantly reduce Nef's inhibitory effects, suggesting that events other than Ca^{2+} mobilization may be disrupted by Nef. Using antibodies against the p50 and p65 NF- κ B subunits, we found that Nef-inhibitable complexes included both p50-p50 homodimers and p50-p65-heterodimers (Fig. 23c).

To determine whether Nef-mediated inhibition of NF- κ B binding activity correlated with a decrease in transcriptional activity, cells were transfected with DNA plasmids by using the HIV-1 long terminal repeat to direct expression of a heterologous gene product, CAT. Jurkat cells were transfected, as described above, with 15 μg of the CAT constructs indicated in Fig. 24. Following transfection, the cells were maintained in growth medium for 24 h. Cells were or were not treated with PHA-P (13 $\mu\text{g}/\text{ml}$) and PMA (75 ng/ml) and incubated for an additional 18 h. Cell extracts were prepared, and CAT activity was assessed by standard methods. Extract equivalent to 3×10^6 cells was used for each 18 h reaction. CAT activity was in the linear range of analysis with respect to extract amount and incubation time (data not shown). CAT assays were normalized to a noninducible control plasmid, RSV-CAT (2 μg), which was transfected in parallel with the HIV-1-CAT plasmids as described above. Assays were also normalized to protein concentrations as determined by Bradford reagent analysis (Biorad). The amount of CAT activity was quantitated by excising the spots corresponding to the unacetylated and acetylated forms of ^{14}C -chloramphenicol and measuring radioactivity in a liquid scintillation counter. CAT activity is expressed as the percent of radioactivity in the acetylated forms compared with the sum of that of the acetylated and unacetylated forms. The wild-type HIV-1-CAT (CD12-CAT) was derived by a small deletion in the nef coding sequence upstream of the long terminal repeat start site of clone C15-CAT), mutant NF- κ B HIV-CAT and IL-2-CAT plasmids were generously provided by Steven Josephs, Gary Nabel, and Gerald Crabtree, respectively. DeltaNRE-HIV-1-CAT was generated by excising the Ava I-Ava I fragment from HIV-1-CAT and therefore lacks the negative regulatory element sequences present in HIV-1-CAT.

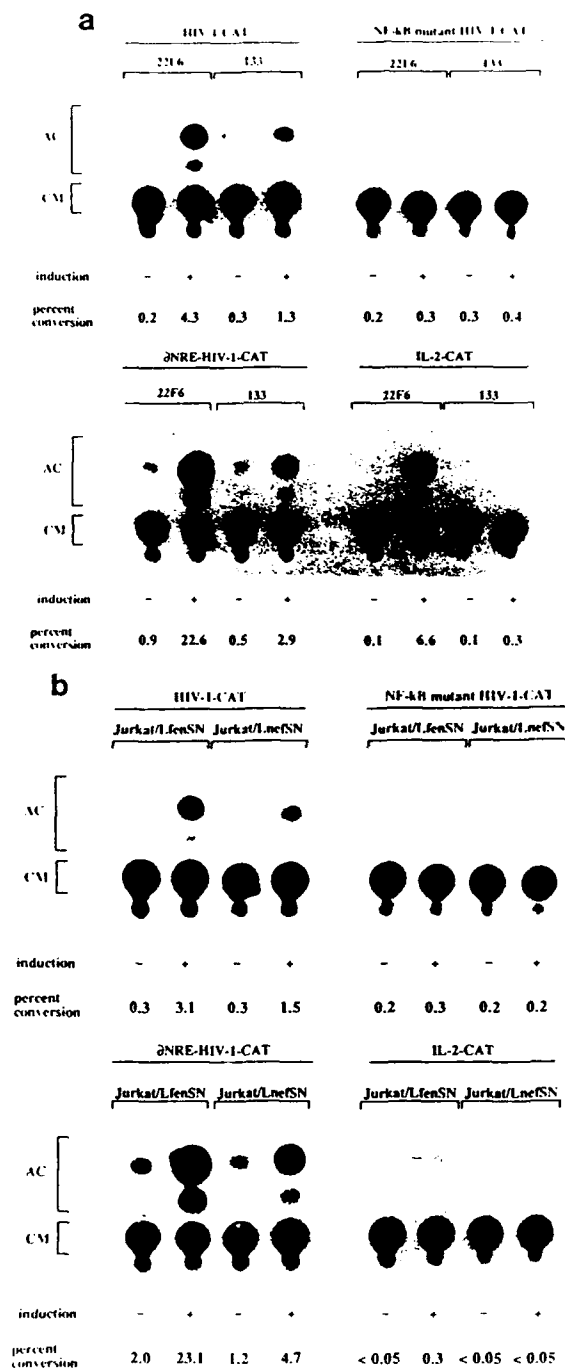


FIG. 4. CAT assays of extracts from cells transiently transfected with HIV-1-CAT and IL-2-CAT DNA plasmids. J25 (a) and Jurkat E6-1 (b) cells were transfected with the CAT constructs as indicated above each panel. Cells were not induced (-) or were induced (+) with PHA and PMA. CAT activity was determined by conversion of unacetylated [14 C]chloramphenicol (CM) to monoacetylated forms (AC). These data represent at least three independent experiments.

CAT activity correlated well with DNA-binding activity in that 133 cells exhibited a capacity to induce CAT activity that was fivefold less than that of 22F6 cells (Fig. 24a). Similarly, CAT activity induction was suppressed twofold in the Jurkat/LnefsN cells compared with that in the Jurkat/LfensN cells (Fig. 24b). This inhibition was demonstrated with both wild type HIV-1-CAT and the negative regulatory element deletion clone, deltaNRE-HIV-1-CAT, which lacks nucleotides -453 to -156 of the HIV-1 long terminal repeat (Fig. 24a and b). This result suggests that negative regulatory element sequences are not primary targets of Nef regulation in stimulated T cells. An HIV-1-CAT plasmid containing mutated NF-kB sequences was induced, at most, only twofold above basal levels, and induction was independent of cell type and Nef expression (Fig. 24a and b).

The importance of NF-kB with respect to the induction of IL-2 by T-cell mitogens was demonstrated by Hoyos and colleagues. These authors showed that the induction of CAT activity was prevented up to 80% with IL-2-CAT constructs bearing mutations in the NF-kB site compared with that of IL-2-CAT constructs containing wild-type NF-kB recognition sequences. As previously reported, we found that Nef profoundly suppressed the induction of CAT activity directed by the IL-2-CAT plasmid in the 133 cells (Fig. 24a). Where there was a 50- to 60-fold induction of CAT activity in the 22F6 cells, there was only a 2- to 3-fold induction in the 133 cells (Fig. 24a). Although NF-kB appears to play an important role in IL-2 induction, it is possible that Nef blocks other factors in addition to NF-kB which may be required for the efficient induction of IL-2 gene expression. This possibility may explain the dramatic suppressive effect of Nef on IL-2 induction compared with the results of Hoyos and colleagues. CAT activity generated by the IL-2-CAT construct was induced to a much lower extent in the Jurkat E6-1 cells. This result is likely due to differences that exist between Jurkat E6-1 and J25 cells. Despite the low level of induction of the IL-2 promoter in the Jurkat E6-1 cells, CAT activity was higher in the Jurkat/LfensN cells than in the Jurkat/LnefsN cells (Fig. 24b). Nef did not affect CAT activity driven by the SV40 early promoter or the promoters from Rous sarcoma virus, the cytomegalovirus, or the Mason-Pfizer monkey virus, indicating that Nef specifically suppressed the HIV-1 and IL-2 promoters (data not shown). The Jurkat E6-1 cells were transfected with equivalent efficiency; however, the Nef-expressing 133 cells were more easily transfected than were the control cells (22F6 cells). Therefore, CAT activity generated by an RSV-CAT plasmid that was transfected in parallel was used to assess the transfection efficiency and to normalize the CAT activity derived from the HIV-1-CAT and IL-2-CAT constructs.

The observation that Nef prevents IL-2 induction (Fig. 22a), coupled with the demonstrations that IL-2 induction requires CD4 and p56^{lck} and NF-kB recruitment, provides additional evidence to suggest that Nef uncouples signals originating from the TCR. Furthermore, the TCR complex induces NF-kB activity after treatment with antibodies to either CD2 or CD3. Nef inhibits the induction of IL-2 by both of these stimuli.

Interestingly, Nef has been reported to down-modulate the surface expression of CD4. Although Nef did not affect the rate of CD4 transcription or translation,

the mechanism by which Nef mediates the down-modulation of CD4 at the cell surface remains unclear. The connection between Nef-mediated negative effects on CD4 cell surface expression and HIV-1 and IL-2 regulation has not yet been established.

Previously, we and others reported that HIV-1 Nef mediated HIV-1 transcriptional suppression. Some investigators were unable to confirm this effect; however, differences in experimental approaches may explain the apparent discrepancy. For the first time, the data presented here suggest that the primary underlying event in Nef-mediated transcriptional repression in activated T cells is the inhibition of induction of NF- κ B activity. In vivo, this suppression may limit the production and cell surface expression of viral gene products in infected cells, thereby allowing the cells to evade clearance by the cellular and humoral arms of the immune response. This model for Nef-mediated viral persistence in vivo may be consistent with the results of Kestler and colleagues which demonstrated that the presence of an intact nef gene was required to prolong SIV infection and induce pathogenesis in infected macaques. Furthermore, we and others demonstrated that SIV Nef inhibited SIV replication in vitro in a way that was analogous to the way in which HIV-1 Nef inhibited HIV-1. It is possible that high-level Nef expression early after infection is sufficient to maintain HIV-1 in a relatively latent state, which may be critical for establishing a reservoir of HIV-1 infected cells and the eventual development of AIDS.

We also explored gel retarded complexes using a 32P-oligonucleotide corresponding to the HIV-1 AP-1 DNA recognition site. In the parental 22F6 Jurkat cells, an induced AP-1/DNA complex which was not present in unstimulated cells, was detected between 1 and 2 hr poststimulation and was abundant 4 hrs post-stimulation. In contrast, the recruitment of the same AP-1/DNA complex was inhibited 5-fold at 2 hr and 9-fold at 4 hr in the Nef expressing 133 cells compared to the 22F6 cells (Fig. 25). Addition of 100-fold molar excess of unlabeled AP-1 specific oligonucleotide inhibited the appearance of the major inducible complex (Fig. 25). However, an oligonucleotide with three nucleotide substitutions in the AP-1 recognition site did not compete away the inducible complex, and we included a 100-fold excess of the unlabeled mutant AP-1 oligonucleotide in all binding reactions as a non-specific inhibitor.

The presence of the constitutive AP-1/DNA complex (the slowest migrating complex in Fig. 25) was minimally if at all, affected by Nef and may be due to the constant presence of serum in the cell growth media. Moreover, this complex was not inducible (Fig. 25b). In addition, the constitutively active transcription factor SP-1 was not affected by the presence or absence of Nef, and was used as a control for extract quality (Fig. 25). Therefore, Nef inhibited the inducible AP-1/DNA complexes, specifically.

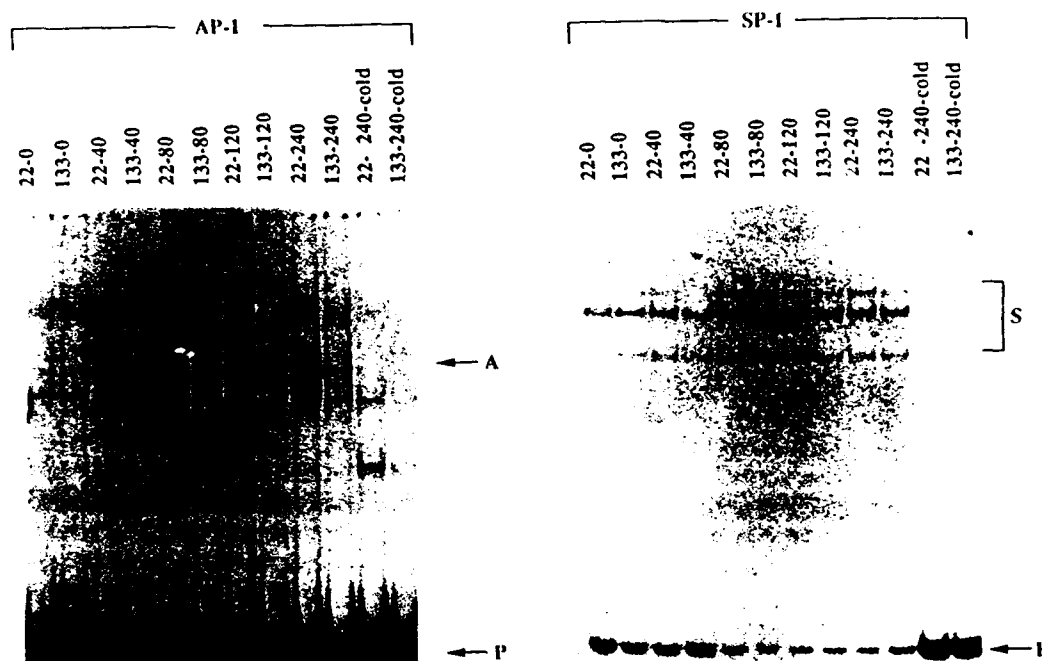


Fig. 1. Gel shift analysis of AP-1 DNA binding activity in extracts prepared from Jurkat 25 cells. Cells were stimulated with PHA-P (13 μ g/ml, [SIGMA]) and PMA (75 ng/ml, Sigma) for 0, 40, 80, 120, or 240 min. Oligonucleotide probes used for binding are specified on the top of each panel. A indicates the inducible AP-1/DNA complexes. S and P represent SP-1-specific binding and free probe, respectively. SP-1 binding served as a control for extract quality and specificity of Nef-mediated effects. Cold indicates that 100-fold molar excess of unlabeled DNA was added for competition. Methods: Cells were maintained in logarithmic growth in RPMI 1640 medium supplemented with 10% fetal calf serum and 2 mM glutamine. Nuclear extracts were prepared from 5×10^7 cells using a modified version of the method of Dignam *et al.* (36) as adapted by Montminy and Bilezikjian (37). Following ammonium sulfate precipitation, nuclear proteins were resuspended in 100 μ l of 20 mM HEPES (pH 7.9), 20 mM KCl, 1 mM $MgCl_2$, 2 mM DTT, and 17% glycerol (38) with the addition of 10 mM NaF, 0.1 mM sodium vanadate, and 50 mM β -glycerol-phosphate. Binding reactions contained 2 μ l (2 μ g) of nuclear extract, 2 μ g poly(dI-dC) (Pharmacia), 100-fold molar excess of unlabeled intragenic AP-1 mutant oligonucleotide (GATCTCAAAGCGGATATCAGCTGGTTAATCAATAAT), and 20–40,000 cpm of end-labeled oligonucleotide probe, in DNA binding buffer (39), in a final volume of 22 μ l. Reactions were performed at 30° for 30 min, immediately loaded onto a 4.5% polyacrylamide gel using 0.5X TBE, and run at 200 V. Oligonucleotides used were as follows: AP-1, CAGGGCCAGGAGTCAGATATCCACTGACCTTTGGATGGTGCT; SP-1, CAGGGAGGCGTGGCCTGGGCGGGAGTGGGAGTGGCGTCC. All DNA probes were gel purified and end-labeled with [γ - 32 P]ATP. The intensity of indicated bands was determined by laser densitometry scanning. There was a linear relationship between the amount of extract used and the DNA binding activity. Nuclear extract preparations and binding reactions were repeated on three separate occasions with similar results.

Fig 25.

Gel shift analysis with extracts prepared from stimulated and unstimulated HPB-ALL cells afforded results similar to those obtained with the Jurkat cells (Fig. 26). However, in contrast to the Jurkat cells, the mitogen-inducible AP-1/DNA complexes were present in unstimulated cells as well as the stimulated cells. Whereas the stimutable AP-1/DNA complexes in the HPB-ALL/LfensN cells were induced approximately 5-fold after 4 hrs of PHA and PMA treatment, there was no significant induction of these complexes in the HPB-ALL/LnefSNS1 cells (Fig. 26). In this experiment, the amount of AP-1 activity in the unstimulated HPB-ALL/LfensN cells was lower than the HPB-ALL/LnefSNS1 cells, however, this was not a consistent finding.

In this experiment, we included another Nef non-responsive transcription factor, USF, to demonstrate the specificity of Nef action and the integrity of the extract. The apparent difference in migration of the major inducible AP-1/DNA complexes between the HPB-ALL and the Jurkat cells probably reflects differences that exist between the different T-cell lines.

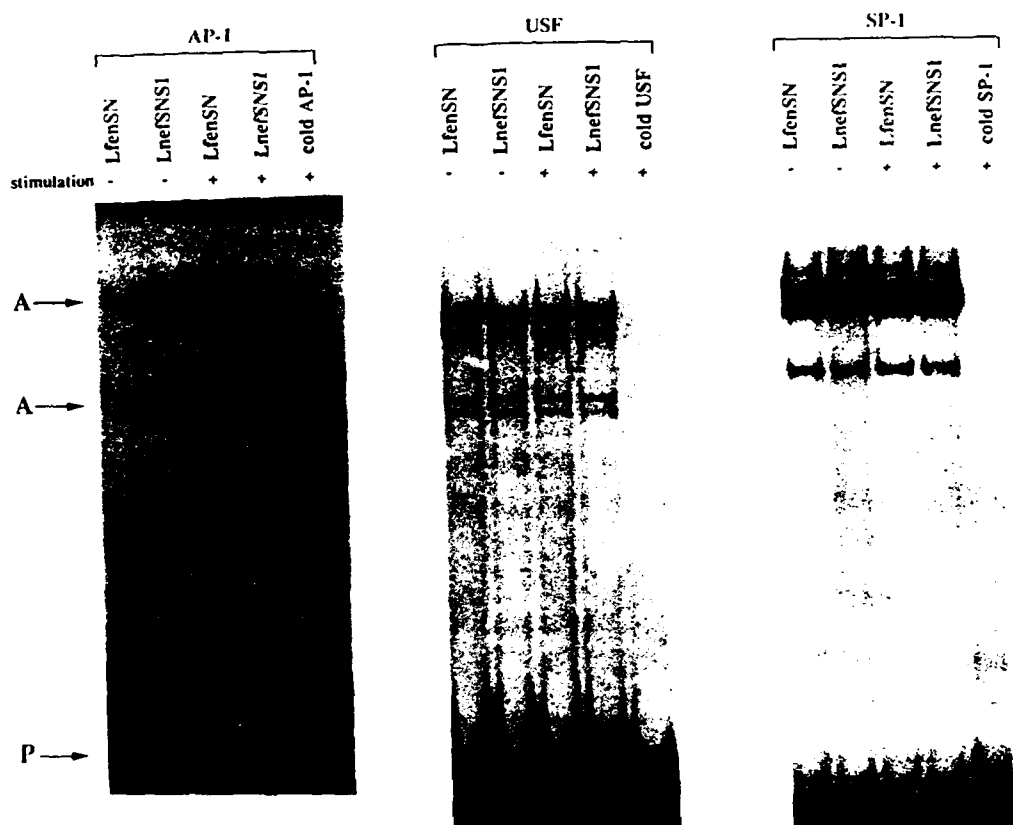


FIG. 2. Gel shift analysis of nuclear extracts prepared from HPB-ALL cells that were not stimulated (-) or were stimulated with (+) with PHA (13 μ g/ml) and PMA (75 ng/ml) for 4 hr. The labeled oligonucleotide probe used is indicated above each panel. The A's indicate inducible AP-1/DNA complexes and P represents free probe. Methods: Nuclear extract preparations and DNA-binding reactions were performed as described in Fig. 1. For the USF probe, we used an oligonucleotide corresponding to nucleotides -159 to -173 of the HIV-1 LTR (40), GCCGCTAGCATTTCATCA-CGTGGCCCGAGAGCTGC. Experiments were repeated three times with similar results.

Previous studies indicated that c-fos expression is induced by PHA, the calcium ionophore A23187, and PMA. In order to determine the signalling pathway required to induce AP-1 DNA binding activity, we assessed the role of PHA, PMA, and the calcium ionophore, ionomycin, alone or in combination (Fig. 27a). Interestingly, the induction of AP-1 activity was maximal with PHA treatment alone and addition of PMA did not significantly increase AP-1/DNA complex formation. The level of inducible AP-1 activity was 18-fold higher in the 22F6 cells compared to the Nef expressing 133 cells with PHA alone (Fig. 27a). PMA alone only slightly induced AP-1 activity in the 22F6 cells, however, no detectable AP-1 activity was observed in the 133 cells treated with PMA alone (Fig. 27a). Ionomycin alone was not sufficient to elicit AP-1 recruitment in either cell line (Fig. 27a).

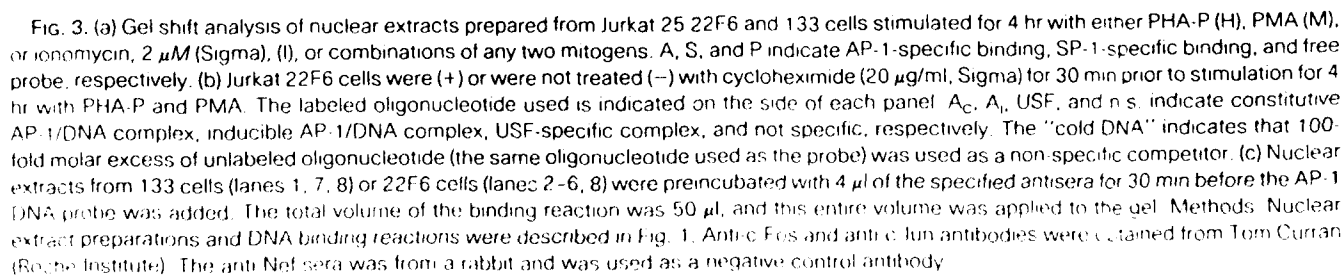
T-cell activation is mediated by increased Ca^{2+} influx and PKC activation which both occur as a consequence of phospholipase-C activation by the T-cell receptor (TCR) complex. Treatment of the Jurkat cells with a combination of ionomycin and PMA, which both bypass the TCR complex, led to significant induction of AP-1 activity, albeit 2.5-fold less efficiently than PHA alone. Whereas there was an 18-fold higher level of induced AP-1 DNA-binding activity in the 22F6 cells compared to the 133 cells using PHA alone, there was only a 3-fold difference using the combination of ionomycin and PMA. Since PHA mimics the normal activation signal (i.e. antigen binding to TCR) of T cells, it appeared that Nef exerted its effects primarily (although not exclusively) on TCR initiated signalling, as has been suggested previously.

To determine whether the induction of AP-1 activity required the activation of pre-existing complexes or new protein synthesis, cycloheximide was added 30 min. before mitogen treatment. That cycloheximide treatment inhibited the recruitment of AP-1 activity, suggests that de novo protein synthesis must be involved (Fig. 27b). This result was consistent with the observation that two hours of stimulation were required before significant induction of AP-1 DNA binding activity (Fig. 25).

To identify the polypeptides present in the inducible AP-1 complex, we incubated nuclear extracts derived from the 22F6 cells with anti-c-Fos and anti-c-Jun antibodies, prior to the addition of labeled oligonucleotides (Fig. 27c). Antisera to both c-Fos and c-Jun inhibited complex formation approximately 3-fold, suggesting the presence of c-Fos and c-Jun in the complex. However, these antibodies did not cause a super-shift, presumably because antibody binding to c-Fos and c-Jun caused conformational changes which are not permissive for DNA binding activity. In these experiments, normal rabbit serum and anti-Nef antibodies were used as negative controls.

Previous studies indicated that the binding of AP-1 to the HIV-1-LTR AP-1 recognition sites play little, if any, role in affecting transcriptional activity. Zeichner and coworkers generated several HIV-1-LTR-CAT linker-scanning mutants in the region of the AP-1 recognition sites and transfected the mutant plasmids into Jurkat cells. There were no significant differences in CAT activity between the wild-type HIV-1-LTR-CAT plasmid and the AP-1 mutant plasmids in cells that were or

Fig
27



However, the intragenic AP-1 recognition sites were capable of mediating transcriptional activation following phorbol ester treatment. Therefore, we cloned a synthetic oligonucleotide, corresponding to the two adjacent AP-1 sites with the pol gene, or an oligonucleotide which contained three nucleotide substitutions in these AP-1 consensus sites, into the polylinker of the enhancer-less pCAT promoter plasmid (Promega). These plasmids were called pCAT-IG-AP1 and pCAT-MIG-AP1, respectively. The pCAT promoter construct, in the absence of the AP-1 sites, contains the SV40 core promoter, afforded low basal chloramphenicol acetyltransferase (CAT) activity in T-cells, and was not inducible in T-cells following treatment with T-cell mitogens (data not shown).

The pCAT-IG-AP1 and pCAT-MIG-AP1 constructs were transiently transfected into the Jurkat 22F6 and 133 cells, as well as Jurkat 25 clone 22D8 cells. The 22D8 cells represent a distinct clonal cell line which, like the 133 cells, also stably express the nef gene from HIV-1 isolate NL43. Transiently transfected cells were either not stimulated or were stimulated with PHA and PMA for 18 hr and CAT activity was then measured. CAT activity in transfected cells was relatively low, between 1-3% conversion to acetylated products. However, we found an average fold induction in CAT activity of 3.6 ± 0.4 in the 22F6 cells transfected with the pCAT-IG-AP1 plasmid, compared to an average fold induction of 1.4 ± 0.2 in the 133 cells and no induction in the 22D8 cells (Fig. 28). Transfection efficiencies were higher in the Nef expressing cells and were determined by parallel transfection with non-Nef responsive promoters including Rous sarcoma virus-CAT, cytomegalovirus-CAT, and simian polyoma virus 40-CAT (data not shown). These determinations were statistically significant, with 95% confidence intervals, with respect to fold-induction, of 2.8-4.4 for the 22F6 cells and the 133 and 22D8 cells is 1 in 1000. CAT activity was not induced in cells transfected with the pCAT-MIG-AP1 construct, indicating that the integrity of the AP-1 site in the inserted oligonucleotide was essential. Thus, Nef-mediated inhibition of AP-1 DNA-binding activity prevented AP-1-mediated transcriptional activation.

What role AP-1 plays with respect to HIV-1 regulation is unclear. Nef could inhibit AP-1-mediated activation of HIV-1 directly, by preventing the interaction of AP-1 with the intragenic enhancer in the pol gene. In addition, by inhibiting AP-1 induction during T-cell activation, Nef may affect the regulation of AP-1 activated cellular genes. Effects on such cellular genes may alter the cellular environment, positively or negatively, which may indirectly affect HIV-1 replication. For example, the finding that c-Fos and c-Jun are early response mediators of T-cell activation, coupled with the observation that HIV-1 cannot replicate in resting, unactivated T-cells, presents a scenario for indirect effects of Nef on HIV-1 expression.

In addition to mediating the suppression of AP-1 induction, we found that Nef also inhibited the mitogen-mediated induction of NF-kB. NF-kB, like AP-1, is an early response effector of T-cell activation and has been shown to be an important activation of HIV-1 replication in stimulated T-cells. Thus, Nef mediated inhibition of recruitment of both AP-1 and NF-kB may intensify the negative effects on HIV-1 replication in T-cells. By inhibiting virus replication directly, and/or

by blocking T-cell activation, Nef may provide a reservoir of persistently infected cells which may ultimately contribute to HIV-1 clinical latency, HIV-1 mediated T-cell depletion, and AIDS.

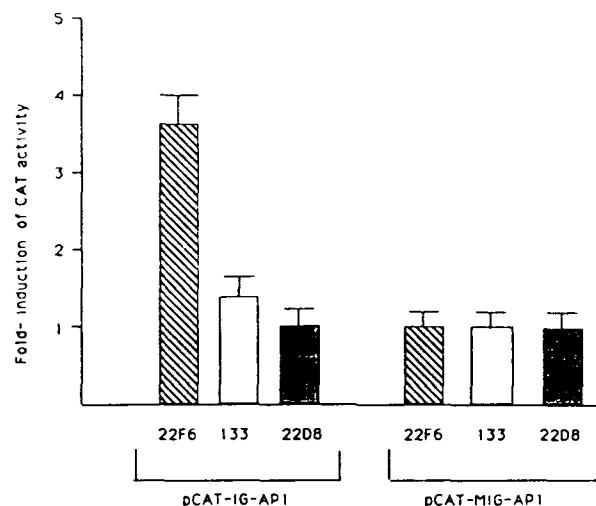


Fig. 4. Chloramphenicol acetyltransferase (CAT) assays extracts prepared from Jurkat 25 cells transfected with the pCAT-IG-AP1 and pCAT-MIG-AP1 plasmids. The data are presented as the mean ratio of the level of CAT activity present in cells stimulated for 18 hr with PHA-P and PMA compared to the level present in unstimulated cells. The error bars represent the standard deviation of the mean. Methods: Jurkat cells were transfected with 40 μ g of the indicated plasmid using DEAE-dextran. Briefly, 10^7 cells were incubated with plasmid DNA suspended in 10 ml of serum-free RPMI 1640, 0.25 M Tris (pH 7.3), and 125 μ g/ml DEAE-dextran (Sigma) at 37° for 40 min. Following centrifugation at 2000 g for 7 min, cells were maintained in growth media containing 10% fetal calf serum for 24 hr. Cells were or were not treated with PHA-P (13 μ g/ml) and PMA (75 ng/ml) and incubated an additional 18–24 hr. Cell extracts were prepared and CAT activity was measured by standard methods (41). Extract equivalent to 3×10^6 cells, as determined by Bradford reagent analysis (Bio-Rad), was used for each 18-hr reaction. CAT activity was in the linear range of analysis with respect to extract amount and incubation time. The amount of CAT activity was quantitated by excising the spots corresponding to the unacetylated and acetylated forms of [¹⁴C]chloramphenicol and measuring radioactivity in a scintillation counter. The plasmid pCAT-IG-AP1 was generated by cloning a double-stranded oligonucleotide corresponding to the two adjacent intragenic AP-1 recognition sites (2) and containing a *Bam*HI sticky end on the 5' end, GATCTCAAAGTGAATCAGAGTTAGTCAATCAAA-TAAT, and a *Sal*I sticky end on the 5' end of the complementary oligonucleotide, TCGAATTATTTGATTGACTAACCAGCTGAT-TCACTTTGA, into the *Bam*HI and *Sal*I sites in the enhancerless pCAT-promoter plasmid (Promega). Plasmid pCAT-MIG-AP1 was made in the same way except that the AP-1 recognition sites in the oligonucleotide used for cloning were disrupted by substitutions at the following, underlined positions; GATCTCAAAGCGGATATCAGC-TGGTTAATCAAATAAT. Cells were transfected 4 to 6 times with each plasmid, a mean-fold induction was calculated, and the standard deviation of the mean was determined. The average-fold induction and standard deviations were 3.6 ± 0.4 , 1.4 ± 0.2 , and 0.9 ± 0.1 for the 22F6, 133, and 22D8 cells, respectively.

The mechanism underlying Nef's negative transcriptional effects on viral transcription may be its ability to inhibit NF- κ B activity in T-cells and NF- κ B-like activity in non-lymphoid cells, such as COS cells. This conclusion is based upon results obtained from Jurkat and COS cells transfected with HIV-1-LTR CAT constructs containing mutations in both of the NF- κ B sites. Basal CAT activity in these cells was significantly lower compared to cells transfected with constructs bearing intact NF- κ B sites. The effect of Nef on the NF- κ B-like factors present in COS cells may be identified by incubating nuclear extracts from Nef-expressing and parental COS cells with an NF- κ B oligonucleotide probe. In these experiments, we will co-transfect a plasmid expressing a chimeric version of NF- κ B fusing the p65 and p50 subunits. It is expected that this assay system will have a low background, and thus will be amenable to a transient transfection assay for Nef. This will provide a useful system for analyzing the effect of various mutations in Nef.

That Nef inhibits the recruitment of NF- κ B in response to the T-cell mitogen, PHA, which acts presumably through the T-cell receptor (TCR) complex, coupled with the results of Luria and colleagues, which indicate that Nef inhibits IL-2 mRNA induction, following treatment with anti-TCR and anti-CD3 antibodies suggests that Nef inhibits signals emanating from the TCR complex. However, since Nef also inhibits, although to a less extent, NF- κ B and AP-1 induction by PMA together with ionomycin, which bypasses the TCR, Nef may also affect signalling that occurs downstream of the TCR complex or through alternative pathways.

To evaluate the effects of Nef protein on activation of transcriptional factors through protein kinase C-independent mechanisms, Jurkat cells carrying the nef gene (133) and the parental cell line (22F6) were stimulated with either TNF or LPS, and the results were compared with those from stimulation with PMA and PHA (Fig 29). A noninducible factor, SP-1 was used to control for protein concentration and quality of the extracts (Fig 29A). TNF or LPS induction of NF- κ B (Fig 29B) and AP-1 (Fig. 29C) was not affected by the presence or absence of Nef protein in 133 and 22F6 cells, respectively. In contrast, the level of induction of both transcription factors was decreased by 6-fold in the case of NF- κ B and by 14-fold in the case of AP-1, when the same cells were stimulated with PMA and PHA.

Similar results were obtained when the comparison was made between the stimulation with IL-1 and that with PMA or PHA (Fig 30). Noninducible transcription factor USF was used as a control (Fig 30A). NF- κ B (Fig 30B) and AP-1 (Fig 30C) activation by IL-1 was not significantly affected by the presence or absence of Nef protein in 133 and 22F6 cells, respectively. Stimulation with PMA or PHA resulted in down regulation of NF- κ B by 5-fold and AP-1 by 15-fold in the presence of Nef protein in this experiment.

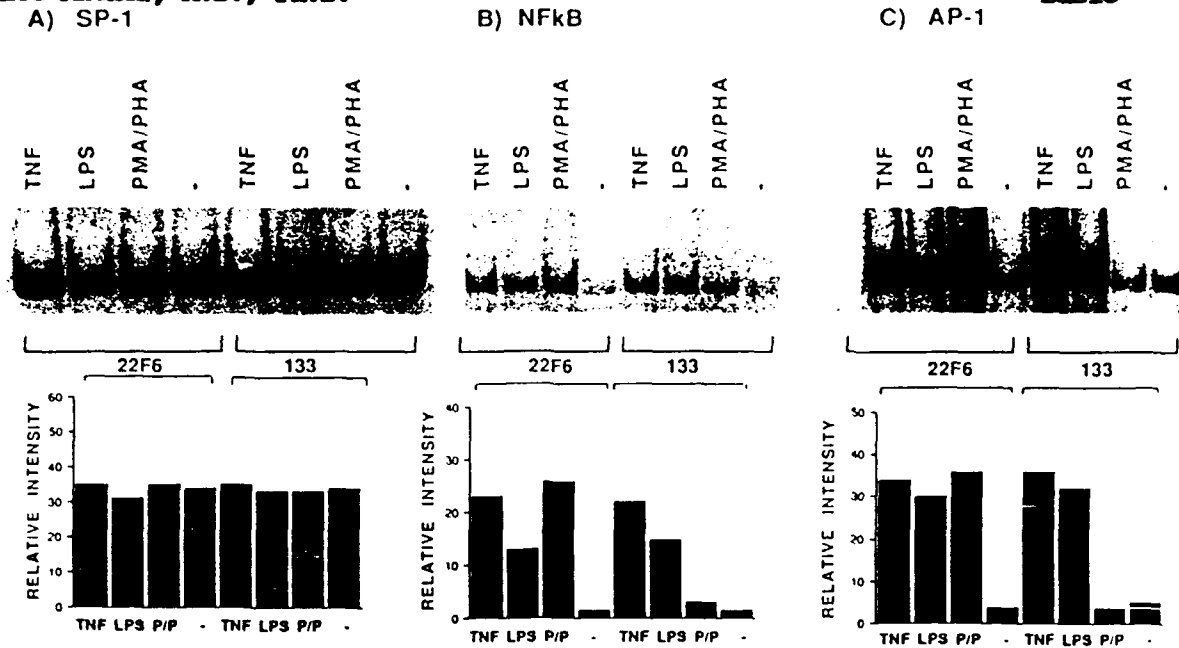


FIG. 1. Effect of Nef protein on induction of transcriptional factors AP-1 and NF-κB in T cells stimulated with TNF, LPS, or PMA and PHA. Gel shift analysis shows induction of transcriptional factors SP-1, NF-κB, and AP-1 in Jurkat T cells (22F6 is the parental cell line, and 133 is the Nef protein-expressing line). Cells were incubated for 4 h with saline (-), TNF, LPS, or PMA and PHA (P/P). Retarded DNA-protein complexes are shown; free DNA complexes are not shown but were equivalent in each lane. The experiments were performed three times with similar results. The relative intensity of the bands was evaluated by laser densitometry.

Fig 29

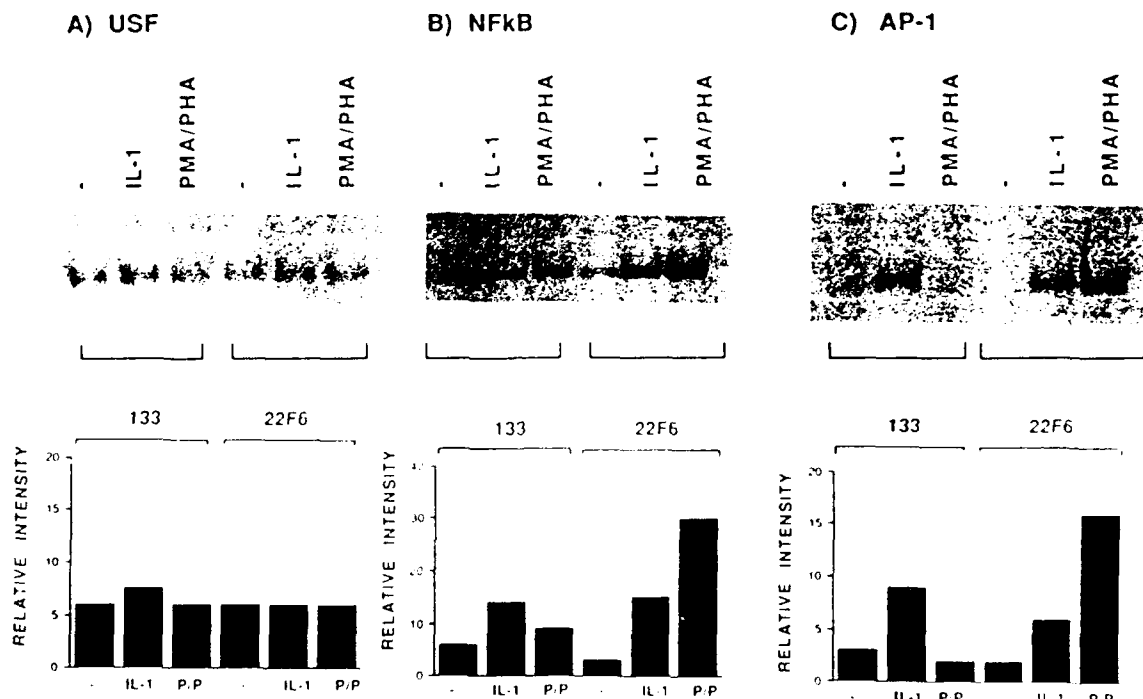


FIG. 2. Effect of Nef protein on induction of transcriptional factors AP-1 and NF-κB in T cells stimulated with recombinant human IL-1 or PMA and PHA. Gel shift analysis shows induction of transcriptional factors USF, NF-κB, and AP-1 in Jurkat T cells (22F6 is the parental cell line, and 133 is the Nef protein-expressing line). Cells were incubated for 4 h with IL-1, PMA and PHA (P/P), or sterile saline (-). Retarded DNA-protein complexes are shown; free DNA complexes are not shown but were equivalent in each lane. The experiments were performed three times with similar results. The relative intensity of the bands was evaluated by laser densitometry.

Fig 30

To determine if induction of NF- κ B and AP-1 correlated with transcriptional activity, cells were transfected with DNA plasmids which use the HIV-1 long terminal repeat to direct expression of a heterologous gene product, CAT. Cells were stimulated with TNF or IL-1 (Fig 31). No difference in acetylation between the cells expressing the nef gene, 133, and the parental cell line, 22F6, was found when both cell lines were stimulated with either IL-1 or TNF (Fig 31A). Because Nef protein also has been reported to suppress the induction of CAT activity directed by the IL-2 CAT plasmid, both 133 and 22F6 cells containing this plasmid were stimulated with TNF or IL-1 (Fig 31B). The results paralleled those obtained with HIV-1-CAT. These data indicate that Nef protein does not affect the induction of transcription factors by the pathway(s) of T-cell activation originating through TNF or IL-1 receptors.

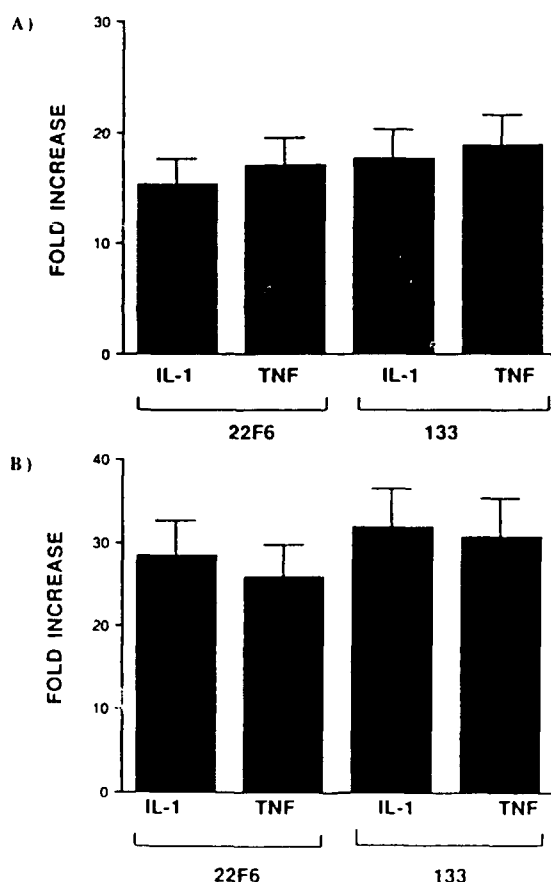


FIG. 3. CAT assay showing the effect of Nef protein on HIV and IL-2 transcription. Jurkat T cells (22F6 is the parental cell line, and 133 is the Nef protein-expressing cell line) were transfected with HIV-1 long terminal repeat-CAT (A) and incubated for 4 h with recombinant human IL-1 or TNF. Similar experiments with IL-2-CAT (B) were performed with 22F6 and 133 cells. Cells were transfected four times with each plasmid, a mean fold induction was calculated, and the standard deviation of the mean was determined. The percentages of acetylation of HIV-1-CAT were 4.6 ± 0.7 (IL-1) and 4.4 ± 0.4 (TNF) for 22F6 cells and 3.9 ± 0.6 (IL-1) and 4.7 ± 0.3 (TNF) for 133 cells. The percentages of acetylation for IL-2-CAT were 14.9 ± 0.9 (IL-1) and 17 ± 0.7 (TNF) for 22F6 cells and 12.7 ± 0.6 (IL-1) and 12.9 ± 0.3 (TNF) for 133 cells.

To further evaluate the effects of Nef protein on signal transduction after PMA or PHA stimulation, the effect of addition of a protein kinase inhibitor, H-7 was examined (Fig 32). The noninducible factor USF was used as a control (Fig 32A). PMA or PHA induction of NF- κ B (Fig 32B) was 10-fold higher in the 22F6 cells than in the 133 cells. The use of H-7 resulted in a significant decrease in NF- κ B induction in the cells that did not express Nef protein. Similarly, PMA and PHA resulted in the induction of AP-1 (Fig 32C) to a level that was 15 times higher in the cells not expressing Nef protein than in the cells expressing Nef protein. H-7 blocked the induction of AP-1 in the 22F6 cells. In both cases, the addition of H-7 to the Nef protein-expressing cells did not cause any further decrease in the already low level of expression of the respective transcription factors.

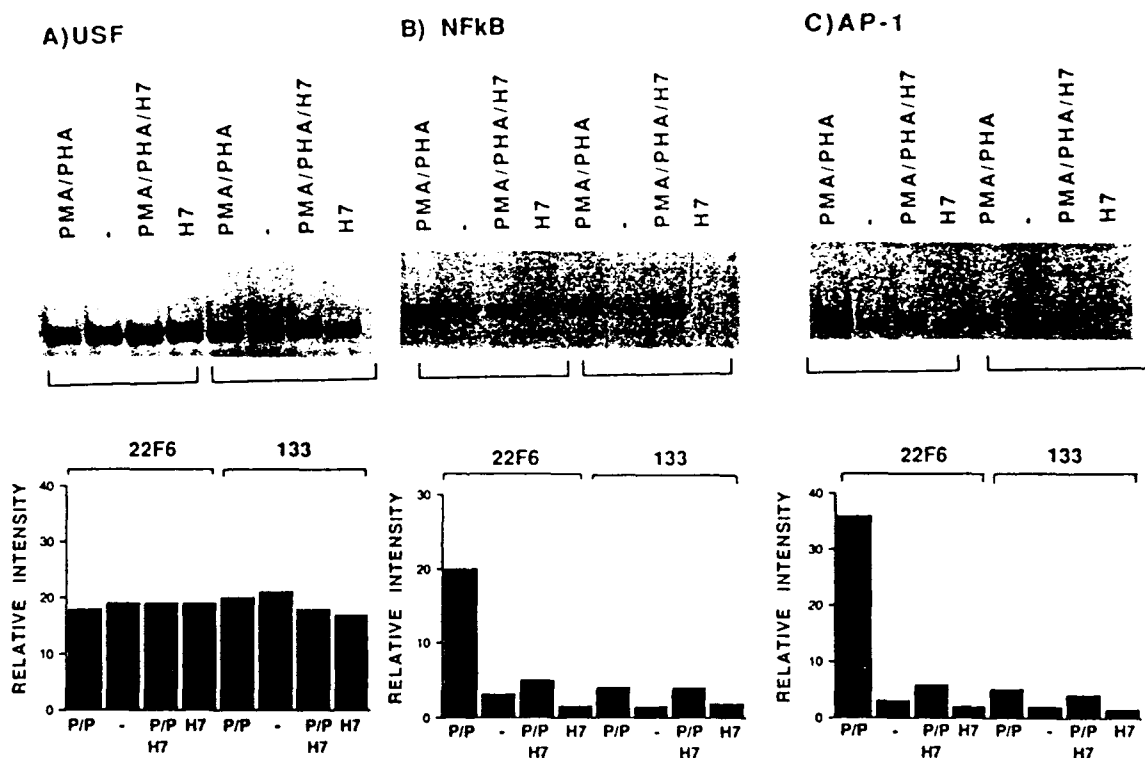


FIG. 4. Effect of Nef protein on induction of transcriptional factors AP-1 and NF- κ B in T cells stimulated with PMA and PHA in the presence or absence of H-7. Gel shift analysis shows induction of transcriptional factors USF, NF- κ B, and AP-1. Jurkat T cells (22F6 is the parental cell line, and 133 is the Nef protein-expressing cell line) were incubated for 4 h with PHA and PMA (P/P) or sterile water (-). H-7 was added 30 min prior to the incubation. Retarded DNA-protein complexes are shown; free DNA complexes are not shown but were equivalent in each lane. The experiments were performed three times with similar results. The relative intensity of the bands was evaluated by laser densitometry.

Fig. 32

To further establish that the effects of Nef protein were related to stimulation through the TCR-CD3 complex, both Jurkat 22F6 and 133 cells were stimulated by anti-CD3 cross-linking in the presence or absence of H7 (Fig 33). Noninducible transcription factor USF was used as a control (Fig 33A). NF- κ B induction (Fig 33B) in 22F6 was increased fivefold by the addition of the antibodies to the TCR-CD3 complex. The presence of H-7 attenuated the induction to a level comparable to that achieved in the 133 cells. Again, induction was not further

decreased by H-7 in the 133 cells, because levels were already fivefold lower for the cells stimulated with anti-CD3 than for the Nef protein-expressing cells. When the oligonucleotide for AP-1 was used (Fig 33C), similar results were obtained, with differences of eightfold for the anti-CD3 antibody stimulation of 22F6 cells compared with the 133 cells.

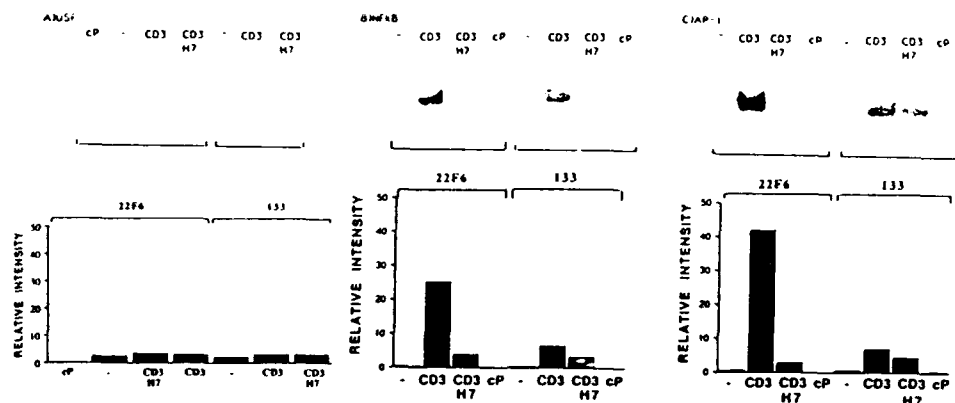


FIG. 5. Effect of Nef protein on induction of transcriptional factors AP-1 and NF-κB in T cells stimulated with cross-linked antibody to CD3 (CD3) or soluble CD3 in the absence of immobilized anti-mouse IgG (-). Gel shift analysis shows induction of transcriptional factors USF, NF-κB, and AP-1. H-7 was added 30 min prior to the incubation. cP, cold probe. Retarded DNA-protein complexes are shown; free DNA complexes are not shown but were equivalent in each lane. The experiments were performed twice with similar results. The relative intensity of the bands was evaluated by laser densitometry.

Fig 33.

To corroborate that the effects on the regulation of transcription factors were correlated with transcriptional activity, CAT assays were performed (Fig 35). The percentage of acetylation was decreased by sixfold with the use of H-7 in the 22F6 cells stimulated with anti-CD3 for HIV-1-CAT (Fig 35A). The difference between the percentage of acetylation in 22F6 and 133 cells (Fig 35B) in the absence of H-7 was 5.5-fold when cells were stimulated with anti-CD3. The results with the IL-2-CAT plasmid with both 22F6 (Fig 35C) and 133 (Fig 35D) cells again paralleled those of the HIV-1 CAT plasmid, except for the greater differences found between the Nef protein-expressing cells and the parental cell lines. Furthermore, the findings with IL-2-CAT reflect previously decreased Nef protein effects on endogenous IL-2 expression. The results presented above indicate that Nef protein down regulates the induction of NF-κB and AP-1 by interreacting with one of the steps involved in T cell activation the TCR-CD3-CD4 complex.

c) To characterize the mechanism of transcriptional suppression by Nef

i) Gel retardation experiments

These experiments are discussed in depth in the preceding section. In addition, to the experiments to be performed with COS cell nuclear extracts, we will also performed assays with a variety of different NF-κB binding sites, in light of recent data of significant differences in the binding ability of different related proteins to each oligonucleotide sequence.

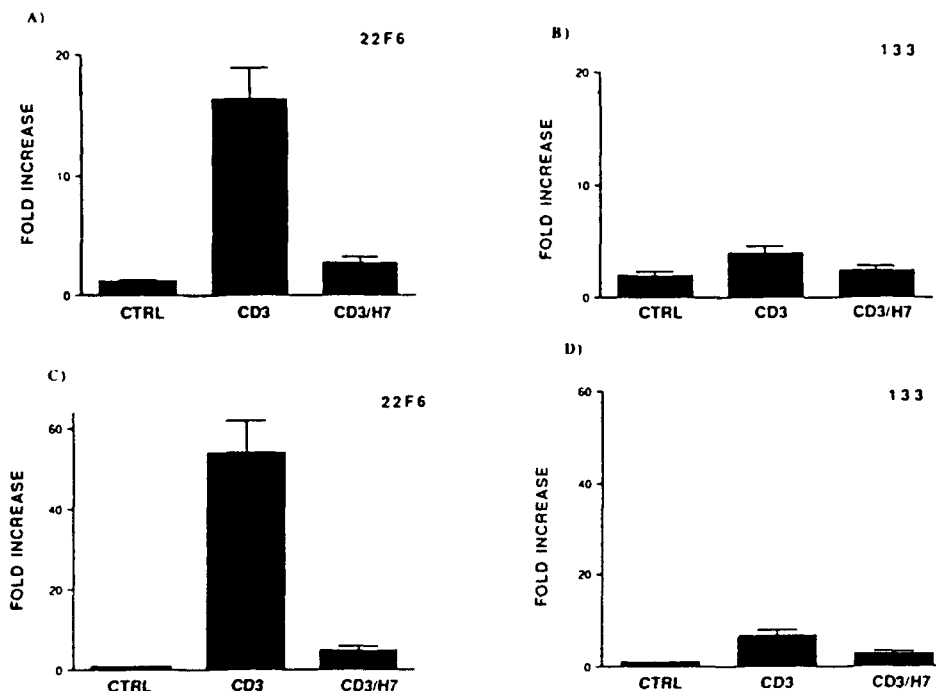


FIG. 6. CAT assay showing the effect of Nef protein on HIV and IL-2 transcription. Jurkat T cells (22F6 [A] is the parental cell line, and 133 [B] is the Nef protein-expressing cell line) were transfected with HIV-1-long terminal repeat-CAT and stimulated with cross-linked antibody to CD3 (CD3) or soluble CD3 in the absence of immobilized anti-mouse IgG (CTRL). H-7 was added 30 min prior to the incubation. Similar experiments with IL-2-CAT were performed with 22F6 cells (C) and 133 cells (D). Cells were transfected four times with each plasmid, a mean fold induction was calculated, and the standard deviation of the mean was determined. The percentages of acetylation for HIV-1-CAT were 0.3 ± 0.02 (CTRL), 4.1 ± 0.45 (CD3), and 0.75 ± 0.2 (CD3/H7) for 22F6 cells and 0.3 ± 0.06 (CTRL), 0.7 ± 0.1 (CD3), and 0.4 ± 0.06 (CD3/H7) for 133 cells. The percentages of acetylation for IL-2-CAT were 0.2 ± 0.03 (CTRL), 16.2 ± 0.8 (CD3), and 1.5 ± 0.25 (CD3/H7) for 22F6 cells and 0.4 ± 0.04 (CTRL), 2.1 ± 0.35 (CD3), and 0.9 ± 0.25 for 133 cells.

Fig 34

ii) DNA footprinting studies

DNA footprinting studies proved unnecessary since it was found that Nef modulated the activity of known transcription factors.

iii) In vitro transcription studies

Insufficient funds were available to complete this task due to severe budgetary cuts during the last six months of the project.

d) To determine the role of phosphorylation, GTP binding, GTPase activity, and myristoylation acceptor activity on Nef activity

Structural studies of Nef have shown that this protein is myristoylated at the N terminus, and acylation has been suggested to be important for its association with cell membranes. In addition, a potential protein kinase C (PKC) phosphorylation site at threonine 15 of HIV-1 Nef and serine 10 of HIV-2 Nef have been identified. These potential phosphorylation sites are homologous to those present in p60^c and epidermal growth factor receptor. Different Nef variants have an alanine residue at position 15 (Nef 1) or a threonine (Nef 2). Conversion of threonine 15 to an alanine residue results in the loss of Nef phosphorylation. Though other Nef phosphorylation sites have been proposed, there is no evidence that they are utilized. We therefore examined the importance of the threonine 15 phosphorylation site with regards to the ability of Nef to downregulate transcription factors.

Human Jurkat J25 T-cell clonal cell lines were selected after transfection with plasmids containing the gene for either Nef 1 (133, 22D8) or Nef 2 (10H10, 1F8) under the control of the simian virus 40 enhancer and human T-cell leukemia virus promoter as previously described. The Nef 1 and Nef 2 proteins differ at amino acid positions 15, 29, and 33 (Fig 35). Jurkat cell clones were also made with the plasmid with the Nef 1 sequence mutated at position 15 from threonine to alanine (Nef 1 clones 18 and 19) or with the plasmid with the Nef 2 sequence mutated at position 15 from alanine to threonine (Nef 2 clones 13 and 16). All these clones have been shown previously to show, in the absence of stimulation, minimal LTR-driven activity as well as recruitment of transcriptional factor NF- κ B and AP-1 (defined as the increase in the nuclear fraction at the active forms of these factors). These characteristics are not unique to these cell clones and have also been observed with other Jurkat cell lines (E6-1) and HP-BALL cells. In addition, these cell lines respond appropriately to T-cell stimulants including PMA, PHA, antibodies to CD3, antibodies to CD2, as well as antibodies to the TNF and IL-1 receptors, indicating that their signal transduction pathways are functional.

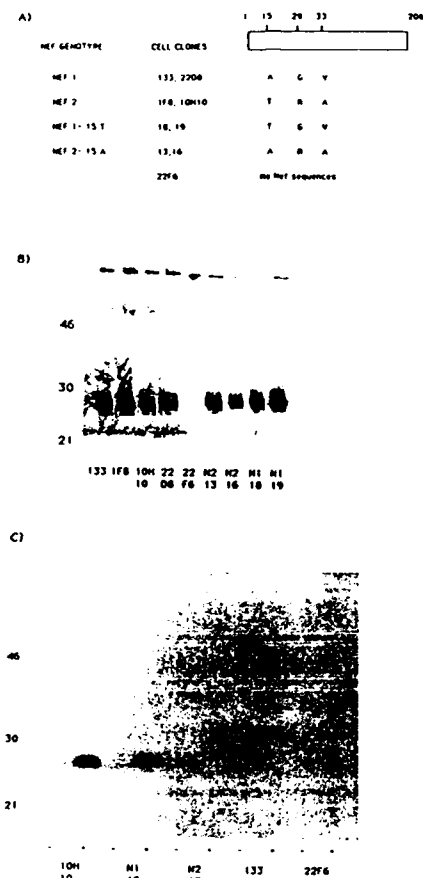


FIG. 1. (A) Structure of Nef expression plasmids. Numbers on top show Nef protein amino acid residues, with number 1 indicating the initiator methionine. Differences in residues between Nef 1 and Nef 2 for the specified positions are indicated for each clone. (B) Western blot analysis of Jurkat cell clone extracts immunoprecipitated with rabbit anti-Nef antiserum (5). These include parental cell line (22F6), Nef 1 expressing clones (133, 22D8), Nef 2 expressing clones (1F8, 10H10), Nef 1 mutants (18, 19), and Nef 2 mutants (13, 16). Positions of molecular weight markers are indicated on the left. (C) Jurkat cell clone extracts after [32 P]orthophosphate labeling and immunoprecipitation with rabbit anti-Nef antiserum. Positions of molecular weight markers (kd) are indicated on the left.

Fig 35B shows the Western blot analysis of all the cell line including the parental cell line 22F6. For this study, cells were kept in log phase growth and immunoprecipitation and immunoblot analysis was performed with a rabbit antiserum as previously described. Nef was detected by the rabbit antiserum in all clones except 22F6, and to a similar level.

In order to examine which Nef proteins can be phosphorylated, ^{32}P -orthophosphate labeling was performed. Briefly, 10^7 cells were grown in phosphate-free media for 4 hr and then $^{32}\text{P}\text{-H}_2\text{PO}_4$ was added at 0.2 mCi/ml. Cells were then stimulated with 50 ng/ml PMA and 13 ug/ml PHA for 4 hr, or with sterile water as a control. Immunoprecipitation was carried out as above except that phosphatase inhibitors (50 mM NaF, 10 mM Na_3VO_4 , and 50 mM beta-glycerolphosphate) were added to the RIPA buffer. Immunoprecipitates were then analyzed by SDS-PAGE, followed by autoradiography. The results are shown in Fig. 35C. Jurkat cells expressing Nef variants carrying a threonine at position 15 (Nef 2 clone 10H10 and mutant Nef 1 clone 18) showed phosphorylation after stimulation with PMA and PHA while neither of the clones with an alanine at position 15 (Nef 1 clone 133, mutant Nef clone 13) showed a significant amount of phosphorylation. No phosphorylation was detected in the absence of PMA and PHA treatment.

To examine the effect of each Nef variant on the recruitment into the nucleus of active transcription factors, electrophoretic mobility shift assays (EMSA) were performed with nuclear extracts prepared from the different Jurkat cell clones, after stimulation with PMA and PHA for 4 hr or after stimulation for the same period of time with sterile saline, as previously described. For EMSA, double-stranded ^{32}P -labeled oligonucleotides were used which include the binding sites of transcription factors SP-1, NF-kB, and AP-1. Nuclear extracts were normalized for protein concentration with the Bradford reagent using bovine serum albumin as a standard. EMSA was performed using the probe for noninducible transcriptional factor SP-1 to control for the quality of the extracts (Fig 36A). Recruitment of transcription factors NF-kB and AP-1 in the absence of PMA and PHA stimulation was negligible (data not shown). Figure 36B shows the downregulation of NF-kB in Jurkat T cells expressing Nef 1 (22D8, 133) as compared with the parental cell line 22F6. On the contrary, cell clones expressing Nef 2 (1F8, 10H10) showed no difference in NF-kB induction from that of 22F6 cells. Results for AP-1 recruitment are shown in Fig 36C and were similar to those for NF-kB. AP-1 was downregulated in cells expressing Nef 1 but not in those expressing Nef 2.

Fig 37 shows mobility shift assays in which the comparison is made between parental cell clone 22F6, Nef 1 producing cell clone 22D8, and clones 18 and 19 in which the Nef 1 protein has been modified with a threonine instead of an alanine at position 15. SP-1 activity from these cell clones is shown in Fig 36A. NF-kB (Fig 37B) and AP-1 (Fig 37B) induction was downregulated in the cells expressing Nef 1 when compared with that of the 22F6 cells. Strikingly, both cell clones 18 and 19 show no effect on NF-kB and AP-1 recruitment when compared with the parental cell clone 22F6.

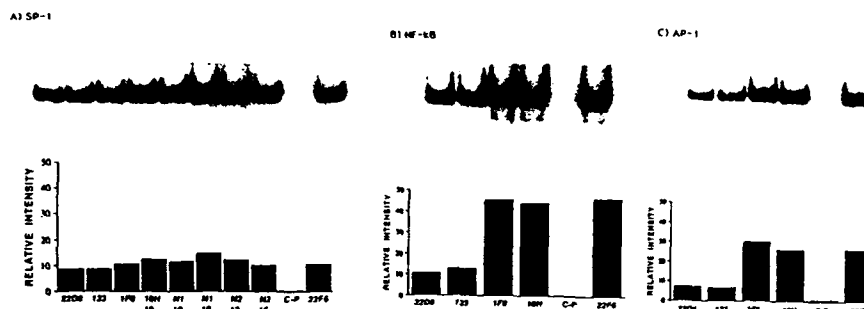


Fig. 2. Electrophoretic mobility shift assays performed from nuclear extracts with 32 P-labeled oligonucleotide probes for binding sites of (A) SP-1, (B) NF-kB, and (C) AP-1. Cell clones: 22F6 (parental cell line), 133 and 22D8 (Nef 1 expressing clone), 1F8 and 10H10 (Nef 2 expressing clone), 18 and 19 (mutant Nef 1 clones), 13 and 16 (mutant Nef 2 clones). C-P, competition by cold probe. The relative intensity of the bands, showing only DNA-protein complexes, was evaluated by laser densitometry (bar graphs). The free probe at the bottom of the gels is not shown. Experiments were performed in duplicate with similar results.

Fig 36

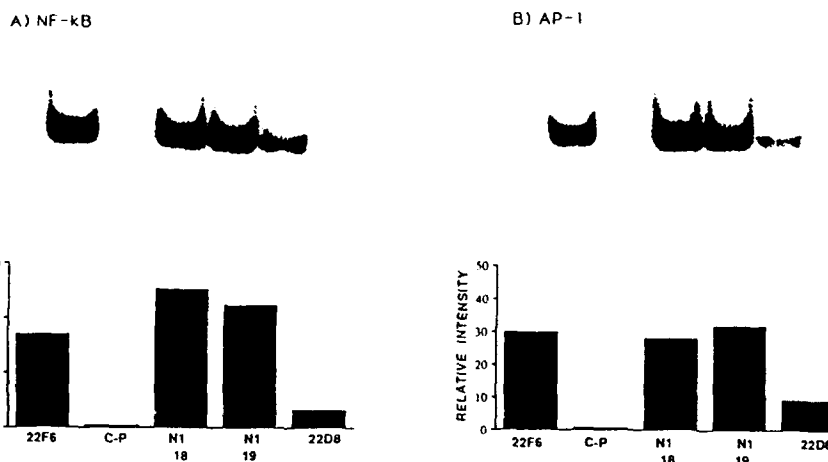


Fig. 3. Electrophoretic mobility shift assays performed from nuclear extracts with 32 P-labeled oligonucleotide probes for binding sites of (A) NF-kB and (B) AP-1. Cell clones: 22F6 (parental cell line), 22D8 (Nef 1 expressing clone), 18 and 19 (Nef 1 mutants). C-P, competition by cold probe. The relative intensity of the bands, showing only DNA-protein complexes, was evaluated by laser densitometry (bar graph). The free probe at the bottom of the gels is not shown. Experiments were performed in duplicate with similar results.

Fig 37

Fig 38 shows the comparison between parental cell clone 22F6, Nef 2 producing cell clone 1F8, Nef 1 producing clone 133, and clones 13 and 16 in which the Nef 2 protein has been modified with an alanine instead of a threonine at position 15. SP-1 activity for these cell clones is shown in Fig 36B. NF-kB (Fig 38A) and AP-1 (Fig 38B) are both downregulated in the cells expressing Nef 1 (133), while no effect is seen in those expressing Nef 2 (1F8). Clones 13 and 16 showed an intermediate phenotype between that exhibited by Nef 1 and Nef 2. The fact that both clones 13 and 16 showed this intermediate phenotype suggest that other determinants in Nef besides phosphorylation at position 15 are important for Nef-dependent downregulation of transcription factors.

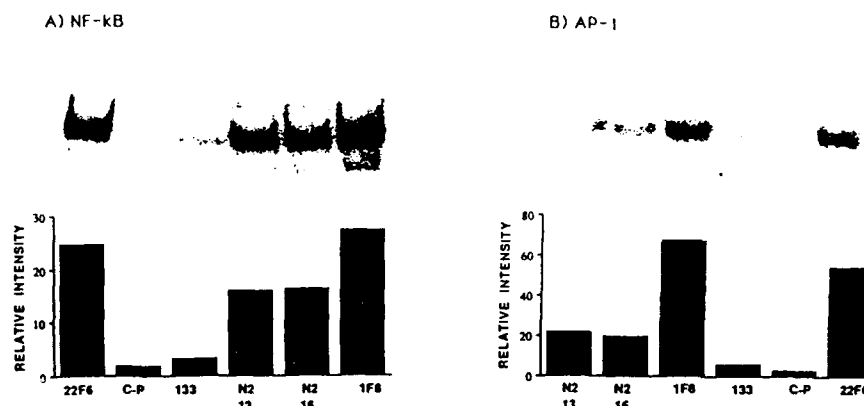


Fig. 4. Electrophoretic mobility shift assays performed from nuclear extracts with 32 P-labeled oligonucleotide probes for binding sites of (A) NF-kB and (B) AP-1. Cell clones: 22F6 (parental cell line), 133 (Nef 1 expressing clone), 1F8 (Nef 2 expressing clone), 13 and 16 (Nef 2 mutants). c-P, competition by cold probe. The relative intensity of the bands, showing only DNA-protein complexes, was evaluated by laser densitometry (bar graph). The free probe at the bottom of the gels is not shown. Experiments were performed in duplicate with similar results.

Fig 38

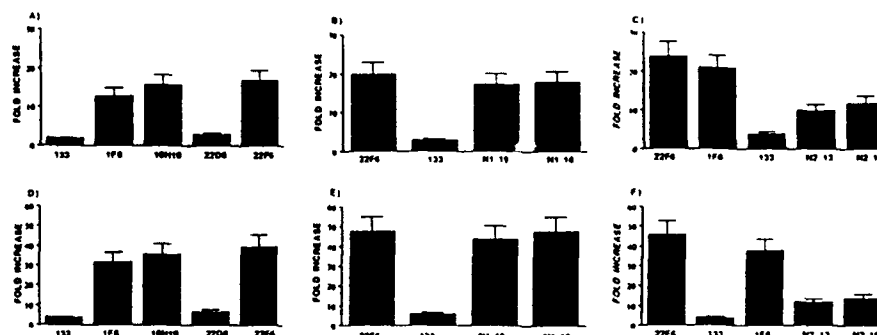


Fig. 5. Chloramphenicol acetyltransferase (CAT) assays for HIV and IL-2 transcription. Extracts were prepared from Jurkat cell clones transfected with HIV-1-CAT (A-C) or IL-2-CAT (D-F). The data are presented as the mean ratio of the level of CAT activity present in the cells stimulated with PMA and PHA for 4 hr compared to the level present in unstimulated cells. The mean values for percentage of acetylation in stimulated cells were 10.2 (22F6), 1.4 (133), 8.7 (N1 19), 9 (N1 18), 8.6 (1F8), 8 (10H10), 5.3 (N2 13), 5.9 (N2 16) for HIV-1-CAT and 22.3 (22F6), 2.6 (133), 22.2 (N1 19), 23.7 (N1 18), 17.5 (1F8), 18.4 (10H10), 3.5 (22D8), 6.3 (N2 13), 7.2 (N2 16) for IL-2-CAT. Experiments were performed in triplicate and error bars represent standard deviation of the mean. Cell clones: 22F6 (parental cell line), 133, 22D8 (Nef 1 expressing clones), 1F8, 10H10 (Nef 2 expressing clones), 13 and 16 (Nef 2 mutants), 18 and 19 (Nef 1 mutants).

Fig 39

To determine if the effects of the changes of amino acid 15 in Nef on transcription factor regulation correlated with transcriptional activity, experiments were performed in which cells were transfected by the DEAE dextran method with plasmid which use the long terminal repeat of HIV (HIV-1-CAT) or the IL-2 promoter (IL-2-CAT) to direct expression of the chloramphenicol acetyl transferase (CAT) gene. After stimulation of the cells with PMA and PHA or sterile saline for 4 hr, cell extracts were prepared and CAT activity was assessed by standard methods. Samples for the CAT assays were normalized to equal protein concentration by Bradford reagent analysis using bovine serum albumin as a standard. CAT assays from different cell lines were also normalized to a noninducible control plasmid RSV-CAT,

which as transfected in parallel with the HIV-1-CAT and the IL-2-CAT. Fig 39 shows the results of these experiments. The CAT activity measurements closely paralleled the EMSA findings. Unstimulated cells showed almost no CAT activity (data not shown). Fig 39A shows decreased CAT activity in cell clones transfected with HIV-1-CAT in the presence of Nef 1 (22D8, 133), when compared with the parental cell line 22F6. On the other hand, clones expressing Nef 2 (1F8, 10H10) showed no difference in HIV-1-CAT activity as compared with parental cell line 22F6. Fig 39B compares the CAT activity in clones transfected with the HIV-1-CAT expressing Nef 1 (133) and the parental cell line (22F6) as well as clones 18 and 19 in which Nef 1 protein has been modified to include a threonine at position 15 instead of an alanine. CAT activity was decreased in cells expressing Nef 1 when compared with the parental cell line. Once again, clones 18 and 19 showed no difference in CAT activity when compared with the parental cell line. Fig 39C shows the comparison between clones transfected with HIV-1-CAT expressing Nef 1 (133), Nef 2 (1F8), and the parental cell line 22F6, as well as clones 13 and 16 in which Nef 2 protein was modified to include an alanine at position 15 instead of a threonine. CAT activity was not significantly different between Jurak cell clones expressing Nef 2 and the parental cell line, while it was clearly decreased in those expressing Nef 1. Clones 13 and 16 expressed an intermediate phenotype. Figures 39D, 39E, and 39F shows the results of similar experiments except that the cells were transfected with IL-2-CAT. IL-2-CAT induction was decreased in clones expressing Nef 1, when compared with the parental cell line, while those expressing Nef 2 showed no significant effect on CAT activity. Clones 13 and 16 also showed an intermediate phenotype with regards to IL-2 expression.

HIV-1 Nef protein has been shown to be phosphorylated by PKC at threonine 15. The mutation from threonine to alanine results in loss of this phosphorylation site. This change has no effect on N-terminal myristoylation of Nef, thus is not likely to affect Nef membrane binding. It also has no effect on downregulation of CD4 expression in T cells. The results of this study show that, as in the case of p60^c, phosphorylation of Nef results in loss of one of the functions of this protein. Also, the results show that, even though other potential phosphorylation sites have been identified in Nef, the predominant site of Nef phosphorylation upon stimulation of T cells is the threonine at position 15. We have shown elsewhere that downregulation of transcription factor NF- κ B by Nef occurs through a PKC-dependent mechanism. The combination of these data presents a model for a unique system by which a protein acts through a pathway that use a protein kinase as an intermediate for its function, and the same protein kinase regulates the presence of the active form of the protein. Furthermore, it has also been shown that Nef associated with the cytoskeleton (see below), and may also localize in specific "channels" in the nucleus (see below). Whether the localization of Nef and its availability for phosphorylation by PKC are related is so far unknown. However, it is intriguing that the PKC phosphorylation site lies within the potential bipartite nuclear localization signal, and therefore, may alter its activity.

Several studies have examined the cellular localization of Nef, but with differing results. The current studies utilized cell fractionation methods to demonstrate localization of a portion of Nef in the cytoskeletal matrix of T lymphocytes. This is a detergent insoluble framework of proteins which includes the cytoskeleton and membrane skeletal fractions. Furthermore, we have developed a novel binding assay to examine the dependence of myristoylation for Nef binding to the cell skeletal matrix.

In order to examine the cellular localization of Nef, we used a Jurkat 25 cell clone resulting from stable transfection of a plasmid (SRalpha) expressing nef from HIV-1 strain NL4-3, using a human T-lymphotropic virus type 1 (HTLV1) promoter and an SV40 enhancer (133 cells). Control Jurkat 25 cells (22F6 or 22 cells) do not express Nef. In addition, we used HPBALL cells infected with a recombinant retrovirus expressing nef from HIV-1 strain SF2 using the MoMuLV promoter (NEF cells) and control HPBALL cells not bearing nef sequences (IN cells). Both unstimulated cells and cells stimulated for 4 hrs with PMA and PHA were used. Cells were lysed in hypotonic lysis buffer (10 mM Hepes, pH 7.9, 10 mM KCl) by Dounce homogenization, and unbroken cells and nuclei were removed by centrifugation at 1500 rpm at 4° in an Eppendorf centrifuge. The postnuclear supernatant was supplemented with NaCl to a final concentration of 150 mM and was then separated by ultracentrifugation at 38,000 rpm in a 70.1 Ti rotor at 4° for 1 hr into a supernatant fraction (cytosol, C) and a pellet. The pellet was resuspended in NTEB buffer (150 mM NaCl, 10 mM Tris-Cl, pH 8.0, 1 mM EDTA, pH 8.0, 3 ul/ml aprotinin, 0.1 mM PMSF, 0.1 mM sodium vanadate, 10 mM NaF, 50 mM glycerol phosphate, 1% Triton X-100, 1% NP-40) and resedimented under the same ultracentrifugation conditions into a supernatant fraction (membrane, M) and a pellet (skeleton, K).

Under these fractionation conditions, 15-50% of the Nef protein was found in the cytosolic fraction, 32-48% in the membrane fraction, and 16-42% in the skeletal fraction (Fig 40). No significant differences were seen between unstimulated or stimulated HPBALL cells (Fig 40a) or Jurkat cells (Fig 40b). Similar results were obtained in fractionation studies using ³H-myristate-labeled Nef (not shown). The skeletal fraction had no significant contaminating membrane or cytosolic proteins, as evidenced by the lack of significant amounts of 5'nucleotidase (5'NT, membrane marker protein) or lactate dehydrogenase (LDH, cytosolic marker protein). Tubulin was used as a marker protein for the skeletal fraction, and 51-59% of this protein was present in the skeletal fraction, 38% in the cytosolic fraction, and only 3-11% in the membrane fraction (Fig 40a). Thus, there is very little contamination of the membrane fraction with skeletal protein.

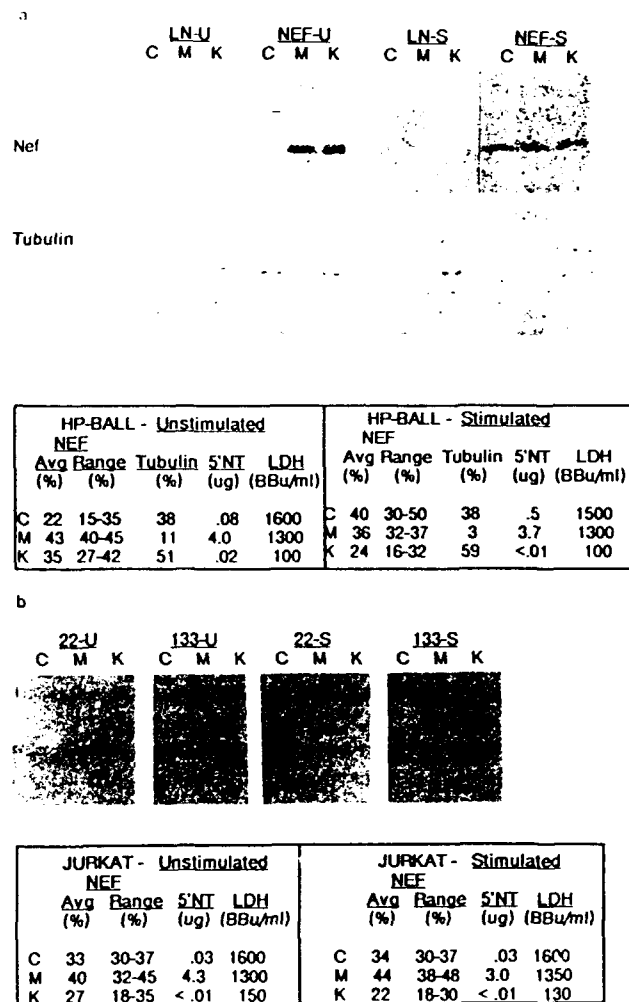


FIG. 1. Nef is associated with skeletal, membrane, and cytoplasmic cellular fractions. (a) HPBALL and (b) JURKAT cells were fractionated by ultracentrifugation into cytoplasmic (C), membrane (M), and skeletal fractions (K). HPBALL-LnefSNS1 cells (NEF-U and NEF-S) express the *nef* gene derived from the HIV-1 isolate SF2 whereas the HPBALL-LN cells (LN-U and LN-S) do not express *nef*. Cells were maintained at logarithmic growth in RPMI-1640 medium supplemented with 10% fetal bovine serum and 2 mM glutamine. Four hours prior to harvest, 7×10^7 cells were either not stimulated (U) or were stimulated (S) with 13 μ g/ml PHA (Sigma) and 50 ng/ml PMA (Sigma). Cells were harvested at 1500 rpm for 5 min and were washed twice with phosphate-buffered saline (PBS). Cell pellets were resuspended in hypotonic lysis buffer and allowed to swell on ice for 15 min. Cells were then dounced 20 times, nuclei and unbroken cells removed at 1500 rpm, and post-nuclear supernatants fractionated by ultracentrifugation into cytoplasmic (C), membrane (M), and skeletal fractions (K) as described in the text. Fraction equivalents were analyzed by 10% SDS-PAGE and immunoblot analysis. The primary antibody was a rabbit anti-Nef antiserum or a mouse anti-tubulin antiserum (Boehringer-Mannheim), and the secondary antibody was a horseradish peroxidase conjugated goat-anti-rabbit IgG (Clontech) or alkaline phosphatase conjugated goat anti-mouse IgG (Promega). Proteins were visualized following the addition of ECL reagent (Amersham) or NBT/BCIP (Promega) and were quantitated by laser densitometry of Kodak XAR films. All bands were in the linear range of analysis as determined by a standard curve. LDH and 5'NT assays (Sigma) were performed using equivalent amounts of each fraction as described by the manufacturer. These results are representative of three separate experiments.

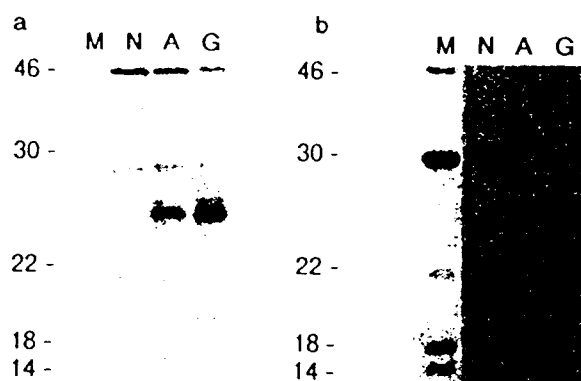


Fig. 2. Myristoylation of Nef in *E. coli*. Bacteria (strain JM101) were transformed with the NMT expression plasmid alone (N) or together with plasmids expressing the myristoylation acceptor mutant Nef (A) or the wild-type Nef (G) (22). Bacteria (2 ml) were grown to mid-log phase ($A_{600} = 0.5-0.6$) and induced with 20 μ l of 100 mM IPTG to induce NMT expression and 2 μ l 50 mg/ml nalidixic acid to induce Nef expression for an additional 2-4 hr in the presence of 400 μ Ci [3 H]myristate (56 Ci/mmol, Amersham). Bacteria were sedimented at 6000 rpm for 15 min in a JA20 rotor at 4°, washed twice with PBS, and lysed by boiling in 100 μ l of 2X sample buffer. Equivalent volumes (5 μ l) were analyzed by SDS-PAGE and (a) immunoblot as described in Fig. 1 or (b) autoradiography (22). Molecular weight markers are shown in lane M.

Fig 41

In order to further assess the nature of binding of Nef to the skeletal matrix, recombinant proteins expressed in *E. coli* were utilized. To obtain myristoylated bacterial Nef proteins, we transformed bacteria with a nef expression plasmid and a plasmid expressing the yeast N-myristoyl transferase. In this experiment, the nef gene was derived from a recombinant of two closely related HIV-1 strains, HXB2 and HXB3. A clone with a glycine to alanine mutation in the myristoylation acceptor site was utilized to generate a nonmyristoylatable form of Nef (A). In addition, expression of yeast N-myristoyl transferase alone (N) was used as a negative control. A 25-kDa protein was detected from both A and G expression system, as detected by a polyclonal rabbit antiserum (Fig 41a). The form of nef with glycine codon 2 could generate a product labeled with 3 H-myristate and detected by SDS-PAGE and autoradiography. In contrast, no 3 H-myristate incorporation occurred into the mutated Nef (A) or into *E. coli* protein (N). Also identified in the A and G Nef expressing bacteria, but not those expressing NMT alone, were small amounts of 19 and 26-kDa proteins, which did not incorporate 3 H-myristate (even with a longer exposure of the autoradiogram shown in Fig 41b).

Recombinant G and A Nef proteins were partially purified from *E. coli* after lysozyme treatment and sonication in NTENT buffer supplemented with 0.5% SDS and 0.5 M NaCl. Insoluble debris was removed by ultracentrifugation at 45,000 rpm for 3 hr at 4° in a 70 Ti rotor before and after dialysis overnight against NTENT buffer.

For in vitro binding reactions, skeletal matrix was prepared from HPBALL (IN) cells as previously described. Binding reactions were performed with 300 ug of partially purified bacterial proteins in 20 ul in a reaction volume of 100 ul in NTEMT buffer at 18° for 30 min. Similar results were obtained in reactions performed for 5-120 min. The reaction mixtures were then treated by ultracentrifugation at 38,000 rpm for 30 min at 4° in a 70 Ti rotor. The supernatant was transferred to 100 ul of 4 x sample buffer (0.25 M Tris-Cl, pH 6.8, 8% SDS, 40% glycerol, 20% 2-mercaptoethanol, 0.02% bromophenol blue), and the pellet was resuspended in 200 ul of 2x sample buffer. Twenty microliters of each sample was then analyzed on a 10% SDS-PAGE and analyzed with the anti-Nef antiserum using the ECL system. The relative proportions of protein in each fraction were determined by densitometric analysis.

Representative results of a binding experiment are shown in Fig 42a. Between 30 and 50% of the Nef G protein (average 34%) was found associated specifically with the skeletal matrix, whereas only 5-15% of the Nef A protein (average 8%) was in the pellet fraction. When expressed in the absence of N-myristoyl transferase, Nef G and Nef A showed no significant differences in cytoskeletal binding (not shown). The results presented in the table represent 12 independent experiments with 6 different preparations of Nef proteins and 6 different preparations of skeletal matrix.

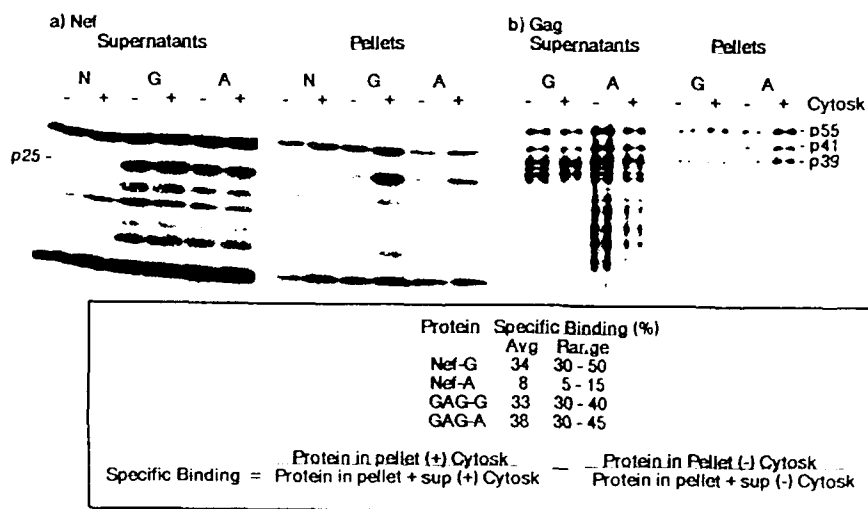


FIG. 3. Binding of Nef and Gag proteins to skeletal matrix. Bacteria (50 ml) were grown to mid-log phase, and induced with 0.5 ml 100 mM IPTG and 50 μ l 50 mg/ml nalidixic acid for an additional 2-4 hr. Extracts were prepared as described in the text from bacteria expressing NMT alone (N) or together with (a) Nef-G or Nef-A proteins or (b) Gag-G or Gag-A proteins. Binding was performed with 300 μ g of recombinant bacterial protein and 300 μ g HPBALL (IN) lymphoid skeletal proteins as described in the text at 18-20° for 30 min. The reaction mixture was separated by ultracentrifugation into a supernatant and pellet fraction, and 20 μ l of each sample was analyzed by 10% SDS-PAGE and immunoblot with the anti-Nef antibody or an anti-Gag p24 antibody as described in the legend to Fig. 1. The Nef bands were in the linear range of analysis as determined by a standard curve. Specific binding of recombinant bacterial proteins to lymphoid skeletal proteins are described at the bottom.

Fig 42.

To determine the specificity of the myristoylation-enhanced Nef binding to skeletal matrix, binding of HIV-1 Gag proteins was also analyzed (Fig 42b). The Gag E coli expression system, was similar to the Nef expression system, and used the gag and pol genes of HIV-1, which were detected with a rabbit anti-p24 polyclonal antiserum. The predominant protein was 55 kDa representing the full Gag precursor, and smaller amounts of 41- and 39-kDa proteins were also expressed which were derived from HIV-1 protease-specific scission at the p17/p24 and p24/p15 cleavage sites. In this system, 30-40% of the Gag G protein (average 33%) bound specifically to the skeletal matrix, and 30-45% of the Gag-A protein bound the pellet components (average 38%). Thus, myristoylation did not enhance Gag association with the skeletal matrix, as it did in the case of Nef.

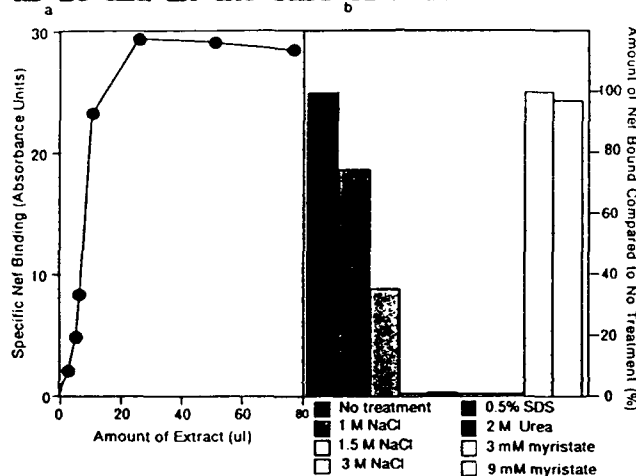


Fig. 4. Saturation binding and inhibition studies of the Nef interaction with the skeletal matrix. (a) Protein extracts from Nef-G bacteria (0-75 μ l, 0-1100 μ g) were incubated with 500 μ g HPBALL-LN skeletal proteins in 140 μ l total NTENT as described in Fig. 3 and the text. (b) Extracts from Nef-G bacteria (300 μ g) were incubated with 300 μ g HPBALL-LN skeletal proteins that were not pretreated, or were pretreated for 5 min with the specific reagents, in a total volume of 100 μ l NTENT, and fractionated as described in the legend to Fig. 3 and the text. The amount of Nef specific binding to the skeletal matrix was determined by SDS-PAGE, immunoblot analysis, and densitometry as described in the legend to Fig. 3. All Nef-specific bands were quantitated in the linear range of analysis as determined by a standard curve. The residual protein contents of the cytoskeletal preparations, as determined with the Bradford reagent, after treatment with specific reagents, compared to the untreated samples were as follows: 65% after 1 M NaCl, 58% after 1.5 M NaCl, 52% after 3 M NaCl, 35% after 0.5% SDS, 72% after 2 M urea, 95% after 3 mM myristic acid, and 97% after 9 mM myristic acid treatment. These experiments were repeated on three separate occasions with similar results.

Fig 43

The nature of the skeletal matrix binding site for the myristoylated Nef protein was analyzed by saturation binding experiments and studies of reagents that prevented Nef association with the insoluble matrix (Fig 43). With increasing amounts of Nef-G protein extract, incubated with a constant amount of skeletal proteins, saturation of binding was achieved with approximately 25 ul (300 ug) of

Nef protein extract (Fig 43a). The amount of Nef protein in this volume of extract was 20 ug as determined by comparing the intensity of the Nef-specific band in the bacterial extract to a standard curve using purified Nef protein (provided by the AIDS Repository). Using 25 kDa as the molecular mass of Nef, this corresponds to 5×10^4 molecules of Nef required to saturate 500 ug of skeletal proteins. Thus, the calculated number of skeletal binding sites for Nef is approximately 2×10^7 sites/cell.

The association of Nef with the skeletal matrix could be inhibited with progressively increasing concentrations of NaCl from 1-3 M (Fig 43b). That 35-40% of Nef bound to the skeletal matrix in the presence of 1.5 M NaCl suggests tight interaction; however, binding was almost completely inhibited with 3 M NaCl. This may suggest that ionic interactions may be critical for Nef-cytoskeletal interaction. Protein denaturants, SDS and urea, could completely prevent the binding of Nef to the cytoskeletal matrix, suggesting that the ternary structure of either Nef, the cytoskeletal binding site, or both is important for binding (Fig 43b). It should be noted that the size or nature of the cytoskeletal pellet in these experiments was not significantly altered in the presence of NaCl, SDS, or urea. Though protein contents of the cytoskeleton were diminished to some extent by these treatments (Fig 43 legend), the effects on Nef binding were significantly larger than those on the protein content. Finally, inclusion of 3 or 9 mM myristic acid did not affect the association of Nef with the skeletal fraction, suggesting that the Nef binding factor is not merely a myristic acid binding receptor. This is in agreement with the observation that myristoylated Gag did not associate with the cytoskeletal fraction to a greater extent than its nonmyristoylated counterpart (Fig 42).

The data presented here suggests that Nef protein derived from three different HIV-1 isolates is capable of associating with the T-cell cytoskeletal matrix, and that the interaction is facilitated by myristoylation. It is possible that Nef binds directly to a cytoskeletal protein such as actin or tubulin, or it is possible that Nef interacts with a protein that binds directly to a cytoskeleton. Additionally, it is possible that myristoylated Nef may bind to one cytoskeletal binding site, while nonmyristoylated Nef may bind to a distinct site. This may explain the different binding patterns of these two forms of Nef. Alternatively, both forms of Nef may bind to the same site, and myristoylation serves to promote or stabilize this interaction. The results that 50-85% of Nef associated with either the membrane or cytoskeletal fraction may reflect the fact that only 50-85% of Nef proteins within the cells are myristoylated. Within intact cells, there may be a dynamic state such that Nef may localize and translocate within cells depending upon differences in post-translational modifications, such as myristoylation, phosphorylation, or glycosylation.

Previous studies regarding the localization of Nef have reported that Nef is primarily extranuclear and that myristoylation is required for membrane association. However, these experiments do not exclude the possibility that myristoylated Nef associated with the cytoskeletal matrix as well. Other studies utilizing

immunohistochemical methods suggest that Nef is present throughout the cytoplasm, but large amounts of Nef are located in a perinuclear location as well. Additionally, Ovod et al report that Nef was also present in elongated cytoplasmic processes, or pseudopods. Interestingly, perinuclear concentration, and the presence of Nef in pseudopods may be consistent with the possibility that Nef is associated with cytoskeletal elements in that the microtubule organizing center is in a perinuclear location, and cytoskeletal components are present in pseudopods, and are important for their formation. The results presented in the current study are consistent with the previous studies in which cytoskeletal association of Nef was not addressed.

The cell matrix includes the cytoskeleton and the membrane matrix. It is composed of a framework of fibers that maintain the structural integrity of the cell, and allow the interaction of cell surface receptors with membrane matrix and cytoskeleton.

There are several interesting parallels between Nef and two other myristoylated proteins, MARKCS and Src. MARKCS (myristoylated alanine-rich C-kinase substrate) is one member of a family of myristoylated proteins in macrophages and neutrophils. It binds calmodulin and regulates cell activation and mitogenesis. MARKCS colocalizes with vinculin, talin, and protein kinase C in focal contracts where the actin cytoskeleton abuts the substrate-adherent plasma membrane. Furthermore, MARKCS can bind and cross-link actin and this binding is regulated by phosphorylation, calcium, and calmodulin. The first 14 amino acids of MARKCS, including the myristoylation acceptor site, are critical for its cytoskeletal binding.

Myristoylation-dependent binding has also been shown for the oncoprotein, Src. In this case, a specific membrane protein of 32 kDa was found to bind myristoylated but not nonmyristoylated Src. Myristoylated peptides corresponding to the amino-terminal sequence of Src were capable of inhibiting binding to the receptor, whereas myristoylated peptides based on sequences of other proteins had no inhibitory effects. Myristoylation is critical for Src-mediated transformation and previous work suggests that myristoylation may be critical for Nef effects as well.

The significance of skeletal matrix binding of Nef remains to be determined. However, recent findings have suggested that Nef disrupts signal transduction in T lymphocytes, inhibiting both NF- κ B and AP-1 generation by PMA and PHA exposure. This may be due to an effect on the T cell receptor-CD3-protein tyrosine kinase-G protein complex, or an effect on protein kinase C activation. Cytoskeletal interaction of one or more of these components or other important cell regulators may be altered by Nef. This may account for the ability of Nef to downregulate HIV-1 transcription and to inhibit T cell activation, which may result in a reservoir or persistently infected cells with repressed virus expression.

Several recent studies strongly suggest that Nef lacks GTP and GTPase activities, and therefore, the proposed studies on these determinants were not carried out.

e) To determine effects of Nef on cellular proteins including those which may modulate HIV-1 infectivity or replication

First, we investigated the importance of the myristoyl group at the N-terminus of Nef for the downregulation of surface CD4. To do so, we used the following constructs: Nef M⁺ (Nef from a chimera of HXB2 and HXB3), and two mutants created by site directed mutagenesis. In the first mutant, Nef M⁻, an alanine codon replaces the glycine codon at position 2 that has been shown to be essential for myristoylation of the Nef protein. The second mutant, Nef ATG⁻, expresses a 25 kD form of Nef that is the product of translation from the second methionine at position 20 and is not myristoylated. All three constructs were transfected by the DEAE dextran method into Jurkat J25 cells and the production of Nef proteins demonstrated by Western blot analysis using a rabbit polyclonal anti-Nef antibody (Fig 44A). To examine the effect of the production of these proteins on CD4 expression, the following DNAs were co-transfected with the Nef DNAs: a fusion protein consisting of the extracellular domain of the G glycoprotein of vesicular stomatitis virus (VSV) and 23 amino acids from the extracellular domain and the entire transmembrane and cytoplasmic domains of CD4 (G-CD4), and the complete G glycoprotein of VSV (VSV-G) (Fig 44B). The results are shown in Fig 44C with a tabulation of the mean channel number and FACS tracings of the fluorescence profiles. Surface expression of VSV-G was used to control for transfection efficiency. Only three cells carrying the Nef M⁺ gene efficiently downregulated G-CD4 as compared with the control cells not producing Nef (Nef⁻). Surface expression of G-CD4 in the cells carrying the Nef M⁻ and Nef ATG⁻ constructs was equivalent to that in the Nef⁻ cells. These experiments show that Nef myristoylation is required for downregulation of CD4.

The G-CD4 construct was also used to study the relevance of the phosphorylation of Nef at position 15. We have previously shown that this is the predominant phosphorylation site upon T-cell stimulation by phorbol esters, and that phosphorylation at this site results in the abrogation of Nef effects on transcription factors. Cell clones carrying the Nef-1 gene (133) with a non-phosphorylatable alanine codon at position 15, or carrying the Nef 2 gene (10H10) with a phosphorylatable threonine codon at position 15, or carrying no Nef sequences (22F6) were transfected with G-CD4 or VSV-G. FACS analysis was performed to examine the effect of the different forms of Nef on CD4 surface expression (Fig 45). Both Nef 1 (133 cells) and Nef 2 (10H10 cells) expressing cells downregulated surface CD4 to a similar extent when compared with the non-Nef expressing cells (22F6). These results show that the effect of Nef on CD4 regulation can be reproduced in stably transfected cells and that this effect is not altered by the presence or absence of the phosphorylation acceptor threonine at position 15 of Nef.

The previous findings, in agreement with those of Anderson and colleagues, and Aiken and colleagues, demonstrate that most of the extracellular domain of CD4 is not required for downregulation by Nef. Experiments were next performed to study the importance of the cytoplasmic tail of CD4 in the regulation of its surface expression by Nef. Jurkat cell clone 22F6 (not expressing Nef) and 133 (expressing Nef) were transfected with DNAs encoding the following proteins: VSV-G, G-CD4, the

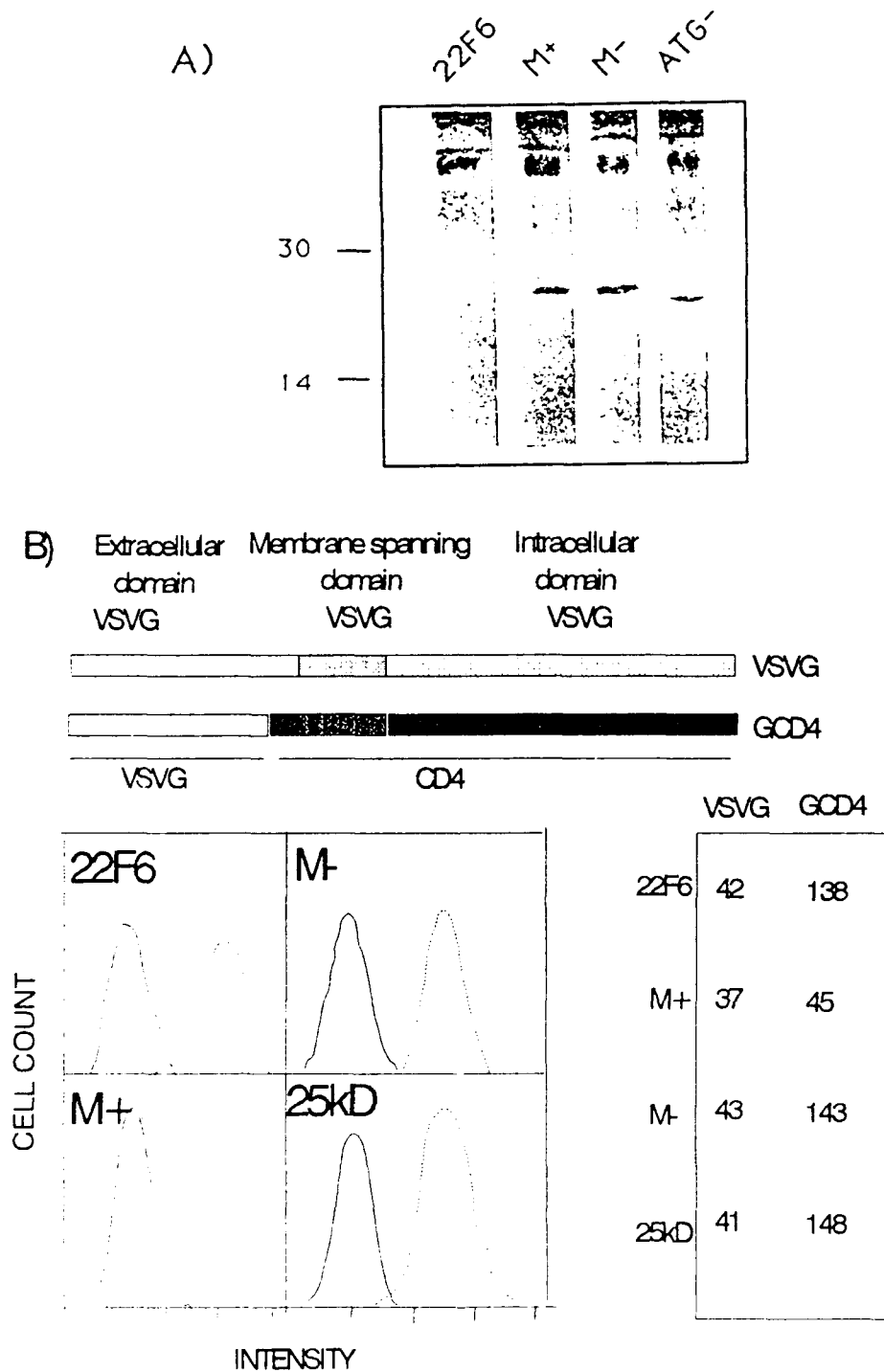


Fig 44.

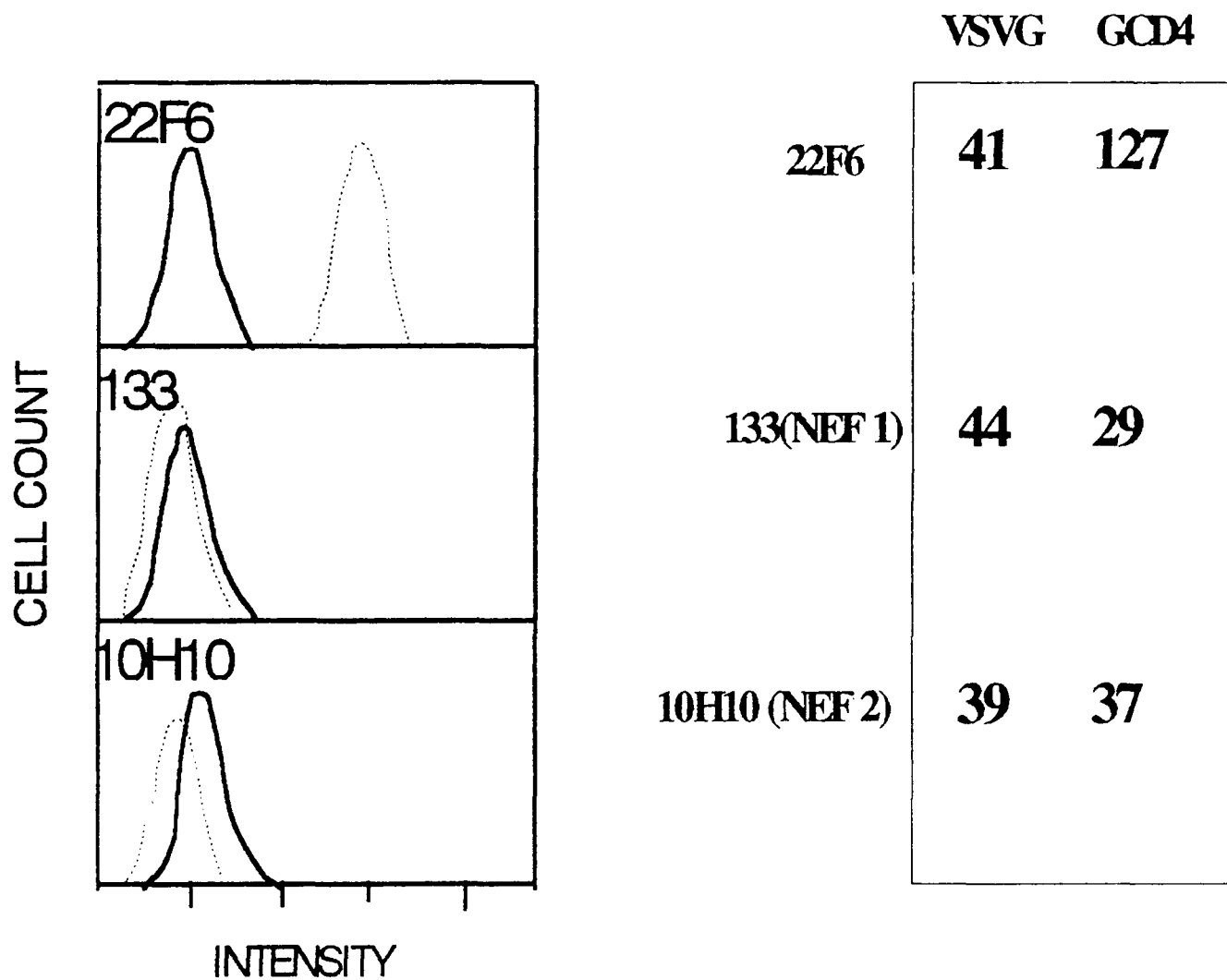


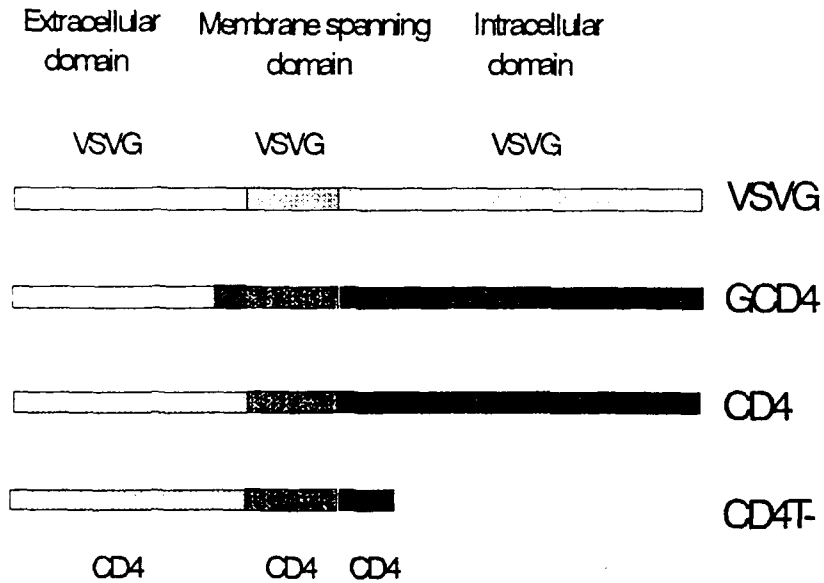
Fig 45

entire CD4 molecule (CD4) and a construct expressing the extracellular domain, the transmembrane domain and only the first 9 amino acids of the cytoplasmic domain of CD4 (CD4T-) (Fig 46A). The endogenous level of CD4 expression on these cell clones was first evaluated and found to be very low (data not shown), has been found for other Jurkat cells. Thus, endogenous CD4 levels were taken into account as background, and further CD4 surface expression was considered to be the result of the transfection of the different DNAs. The results are shown in Fig 46B. VSV-G expression was used to control for transfection efficiency. G-CD4 surface expression was downregulated in the Nef expressing cells as compared with cells that did not express Nef, and to a similar level (about 7-fold) as compared to the downregulation of CD4 in these same clones. In contrast, CD4T- surface expression was not affected by the presence of Nef and similar levels were found on the 22F6 and 133 clones. These results indicate that the cytoplasmic tail of CD4 is required for Nef downregulation, and that the last 23 amino acids of the extracellular domain plus the transmembrane and cytoplasmic domains of CD4 are sufficient for downregulation by Nef.

To define the specific sequences within the CD4 molecule relevant for the interaction of Nef with CD4, DNAs encoding the following constructs were cotransfected into Nef expressing cells (133) and cells not expressing Nef (22F6): VSV-G or G-CD4 as negative and positive controls plus CD4, which has the entire 38 amino acid cytoplasmic CD4 tail, a construct expressing on the first 30 amino acids of the cytoplasmic tail of CD4 (CD4-425), a construct expressing only the first 23 amino acids of the cytoplasmic tail of CD4 (CD4-418), and a construct expressing only the first 19 amino acids of the cytoplasmic tail of CD4 (CD4-414) (Fig 47A). The results are shown in Fig 47B. Only those cells expressing the entire CD4 molecule or the construct that included 30 of the 38 amino acids of the cytoplasmic tail of CD4 showed downregulation of surface expression in the presence of Nef. On the other hand, in the large majority of cells, both the levels of surface CD4-418 or CD4-414 were similar when comparing the 133 and the 22F6 clones. These results indicate that the first 30 amino acids of the cytoplasmic tail of CD4 are critical for Nef downregulation of CD4 and that the sequence between amino acids 419 and 425 of the CD4 molecule contain amino acids relevant for the interaction of Nef with CD4. These results were particularly interesting because these same amino acids have been shown to be critical for the binding of p56lck to CD4.

In order to further explore the role of the lck-binding region of CD4 for Nef mediated downregulation, site specific mutants of CD4 were utilized. Using the same methodology cotransfections were performed now with VSV-G and G-CD4 plus CD4 constructs that included the substitution of cysteines with serines at positions 421 and 423, critical for lck binding to CD4. As a control a construct was used with a substitution of the proline at position 424 for a glycine. The results indicate that amino acid substitutions that affect the binding of CD4 to p56lck also affect the downregulation of CD4 by Nef in lck-bearing cells (Fig 48), again suggesting that the interaction between Nef and CD4 could be mediated, at least in part, by the effects of Nef on p56lck.

A) CD4 CONSTRUCTS



B)

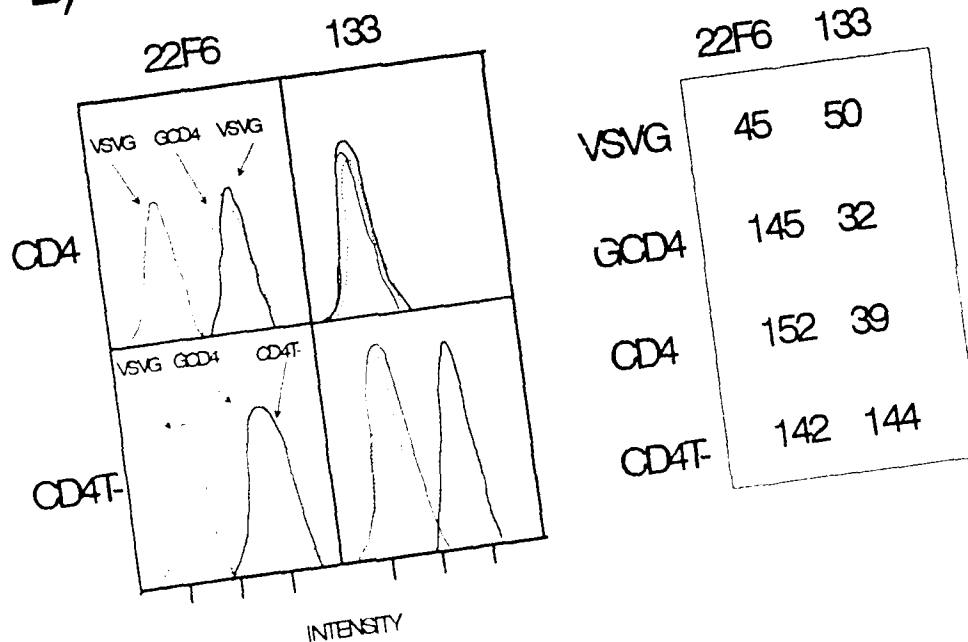


Fig 46

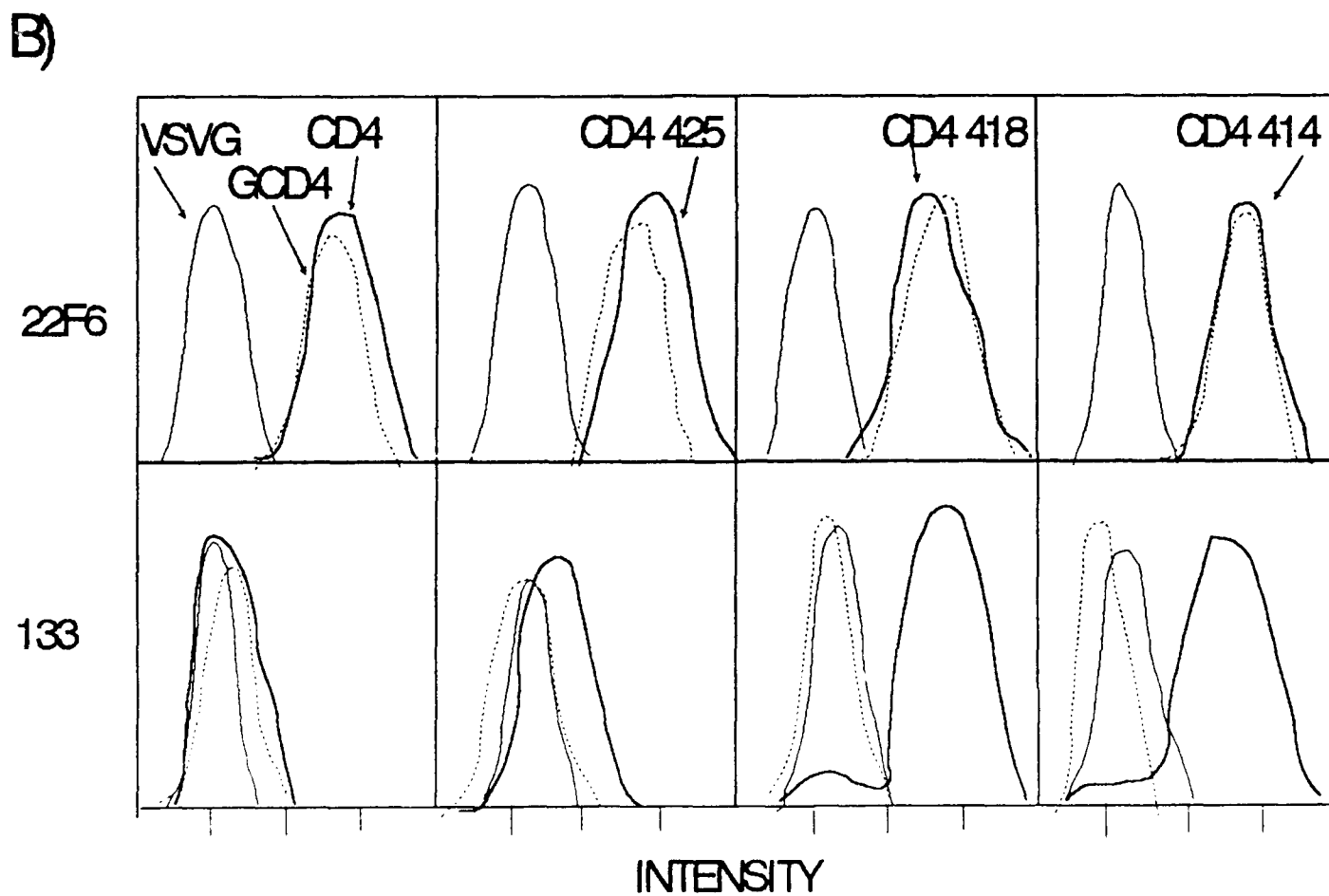
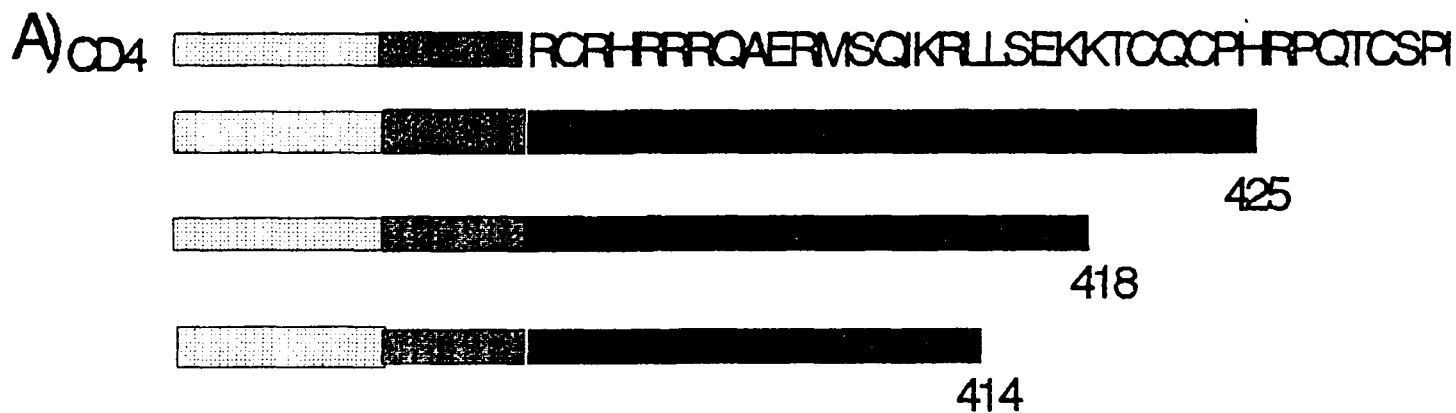


Fig 47

Because it has been shown before that Nef downregulation of CD4 is not restricted only to lck-bearing cells, we next examined the effects of Nef on CD4 surface expression in the presence or absence of p56lck. To do so, we used non-lymphoid U937 cells expressing Nef or a frame-shifted form of Nef, and cotransfected these cells with a DNA encoding for p56lck or an irrelevant DNA (IL2-CAT) plus DNAs encoding for constructs G-CD4 or VSV-G. p56lck expression was confirmed by immunoprecipitation with a polyclonal anti-lck antibody (data not shown). The results are shown in Fig 48. In the absence of lck, Nef resulted in the downregulation of G-CD4 in U937 cells, but when lck was added downregulation of CD4 was increased by one log in repeated experiments indicating that Nef interaction with p56lck results in a more efficient downregulation of CD4.

To further demonstrate the interaction of Nef with p56lck, the following experiments were performed. Using the Jurkat T-cells expressing (133) or not expressing Nef (22F6), and transfected with CD4, we examined if the presence of Nef results in a difference in the binding of p56lck to Thy-1. Normally, p56lck will bind in a majority to CD4, but when CD4 is internalized or in the absence of CD4, most of p56lck remains at the surface membrane bound to other proteins like Thy-1. First, we confirmed that both clones 22F6 and 133 contained the same amount of Thy-1 by immunoprecipitation with an anti-Thy-1 antibody (Fig 50A), and then that both cell lines also contained the same amount of p56lck by immunoprecipitation with an anti-lck antibody (Fig 50B). Then, we examined the amount of p56lck in the immunoprecipitates with anti-Thy-1. As can be seen in Fig. 50C, in the presence of Nef (clone 133), the amount of lck bound to Thy-1 was increased at least 4-fold when compared to the cells that did not express Nef (clone 22F6). This serves as further proof that Nef has a direct effect on the binding of p56lck with membrane molecules like CD4 although the exact nature of this interaction is still unknown.

Finally, because it is well documented that the interaction between p56lck and CD4 is related to the internalization of CD4, we examined the possibility that Nef could also affect the surface expression of CD4 by this mechanism. Lymphocytic cell lines show very low levels of CD4 endocytosis and the steady-state levels of intracellular CD4 are also decreased when compared with non-lymphoid cells. A ten-fold lower rate of CD4 endocytosis is found in lymphoid cells, as compared to non-lymphoid CD4 expressing cells, due to the effect of p56lck binding to CD4. This effect requires the cytoplasmic domain of CD4. We used a flow cytometric method to measure CD4 internalization in the presence or absence of Nef. The results are shown in Fig 50D. The presence of Nef resulted in an increase of internalized CD4 by 2-3-fold when a steady state level was reached (30 min), and an increase in the rate of CD4 internalization in the first 10 min from 0.15%/min to 0.8%/min.

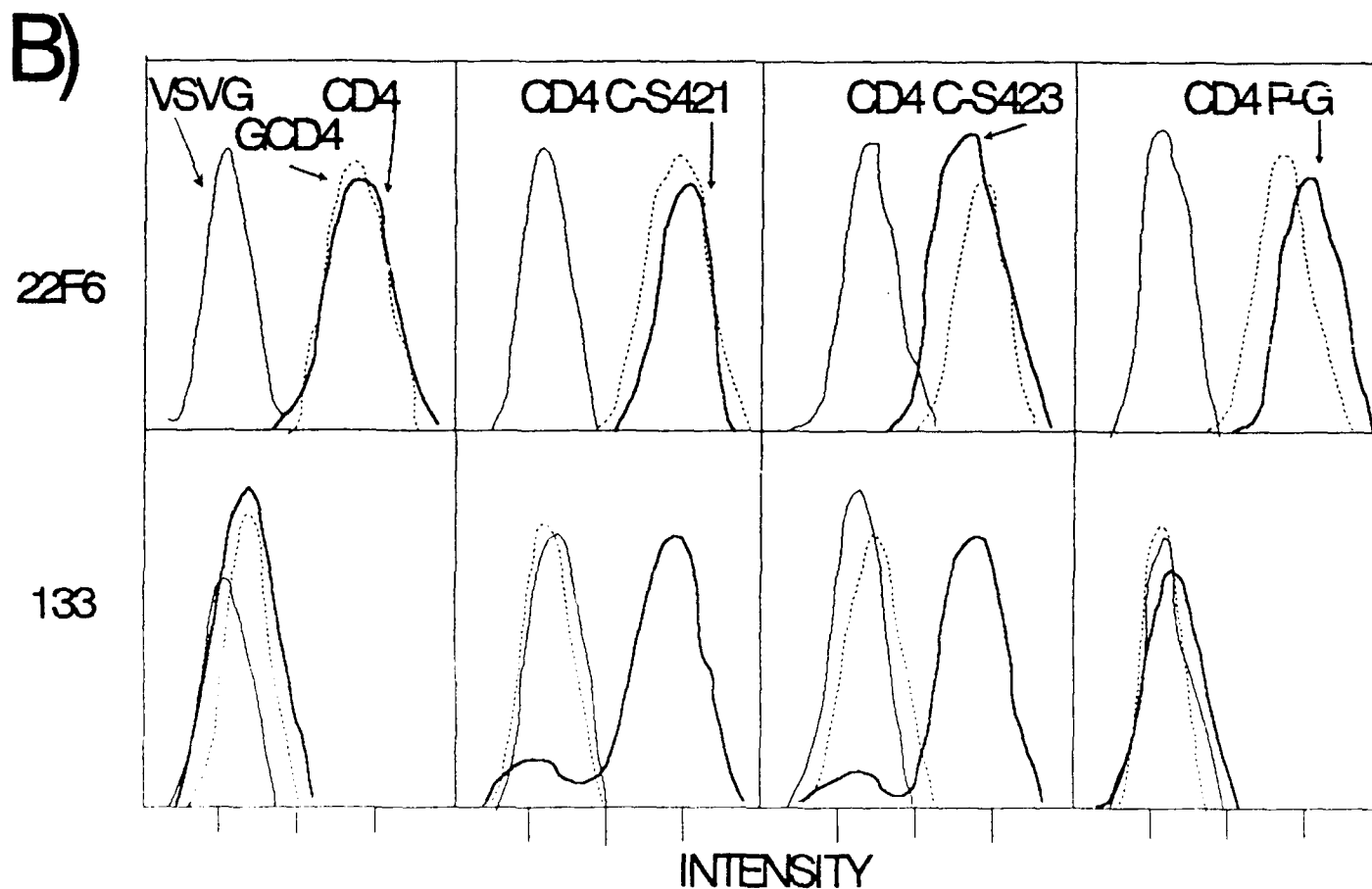
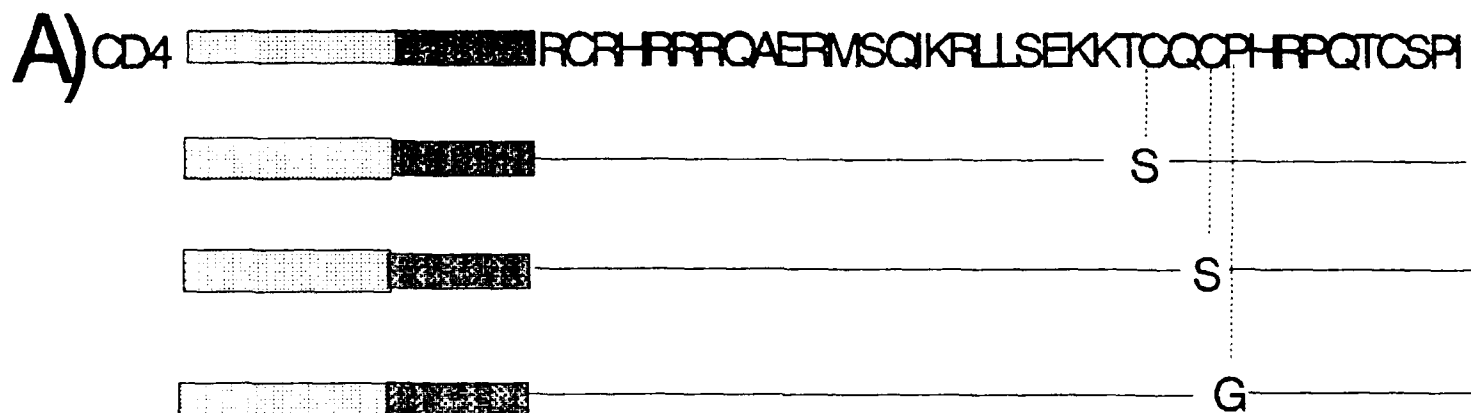


Fig 48

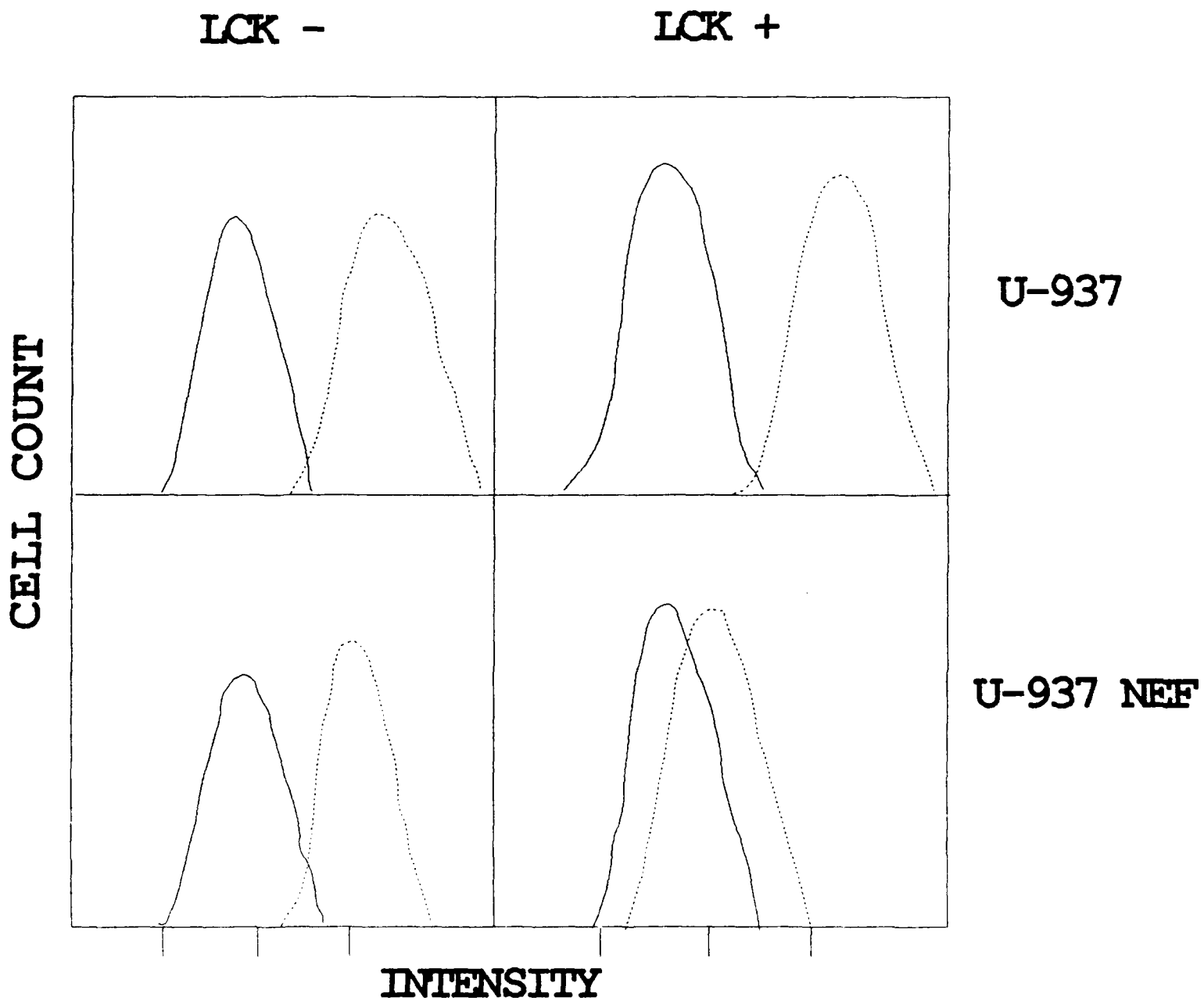




Fig 49.


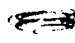
A) 22F6 133

  ←Thy-1

B)

  ←lck

C)

  ←lck

drawing to represent data

	15 min	30 min
133	30%	32%
22F6	12%	15%

Fig 50.

Table 1. Percentage of internalized CD4 in Jurkat human T-cells expressing Nef (clone 133) or not expressing Nef (clone 22F6).

We have also performed immunogold/electron microscopy studies to map the subcellular localization of Nef. As a prelude to these studies, we first performed immunofluorescence studies with a polyclonal anti-Nef antiserum on nef- (HPBALL/LN) and nef+ (NPBALL/LnefSN-S1) cells. As shown in Fig 50, the cells are generally round and contained a large kidney-shaped nucleus that filled most of the volume of the cell. The cytoplasm was polar and was most abundant near an indentation of the nucleus, typically seen in T cells. In nef+ cells, the anti-Nef antibody revealed a homogenous labeling of the cytoplasm (Fig 50A). In general, the distribution of Nef seems polar, but this is evidently due to the polar distribution of the cytoplasm; the thin ring of the cytoplasm surrounding the nucleus, when visible, also showed labeling. The nuclei, in general, showed little or no fluorescence (Fig 50A). However, focusing of the nuclei at different planes revealed narrow bands of fluorescence in some nuclei (Fig 50B). These bands were seen in 8 of the 89 nuclei examined and each nucleus showed only one band. The bands are very faint and required long exposure to photograph them. No fluorescence was observed in nef- cells incubated with the anti-Nef serum (Fig 50C) or in nef+ cell incubated with normal rabbit serum (Fig 50D), although several hundred of these cells were examined.

The technique used for immunogold labeling was the post-embedding method. Fixed and dehydrated cells are embedded in a water-soluble embedding resin (LR White) and sectioned, and sections are incubated with primary and secondary (gold-conjugated antibodies). We have maintained three sets of controls to ensure the specificity of the antibodies used. First, we performed the immunogold labeling with anti-Nef antibodies using sections of HPBALL/LN control cells (nef-). As shown in Fig 51A, the nonspecific binding of the anti-Nef antibodies in these cells was negligible. Second, as a control for nonspecific binding of primary and gold-conjugated secondary antibodies, we performed immunogold labeling on nef+ (HPBALL/LnefSN-S1) cells using normal rabbit antiserum followed by gold-conjugated anti-rabbit antibody. The results illustrated in Fig 51B show that neither the rabbit serum proteins, nor the secondary antibodies bind nonspecifically to nef+ cells. Finally, to check for the specificity of labeling of subcellular structures by immunogold labeling method used here, nef+ cells were labeled with anti-vimentin (intermediate filament) specific antibody. The intermediate filaments are readily identifiable cytoplasmic structures that provide convenient markers to test the resolution and specificity of immunogold labeling. The results illustrated in Fig 51C show the exclusive distribution of label over the 10-nm intermediate filaments. Little or no labeling in the nucleus was observed in any of these controls. These studies suggest that the immunogold technique use here provides specific labeling of subcellular structures.

When T cells expressing Nef (HPBALL/LnefSN-S1) were examined by the immunogold labeling method, the results were as follows. In a few sections of the nuclei, the label due to Nef was detected in highly localized tracks that extend between the nuclear envelope and the nucleoplasm. Fig 53 illustrates these tracks in sections of three different nuclei (A-C). The longest of the tracks measured about 7 μ m (Fig 53A) and the tracks appeared to commence/terminate at the cytoplasmic side of the nuclear envelope (Fig 53B). The tracks were seen in only 4 nuclei among 100

examined, and serial sections revealed only one track per nucleus. It is possible that these tracks may occur with greater frequency than that observed but that they are not detectable due to technical reasons. The tracks occur in thin bands and occupy a fraction of the total nuclear volume and, therefore, their detection would depend on their perfect alignment to the plane of sectioning. In addition to the tracks, a small amount of label is also found in the nucleoplasm but the nucleoli are totally free from the label. These tracks may correspond to the fluorescence bands observed in a few nuclei by the immunofluorescence method (Fig 51B). A thorough examination of sections of hundreds of nuclei of nef- cells incubated with anti-nef serum and nef+ cells incubated with normal serum has failed to reveal any nuclear labeling. In fact there is only one other instance in published literature concerning a nuclear protein that forms tracks in the nucleus. A study by Meier and Blobel has shown that a nucleolar phosphoprotein (Nopp140) of rat liver cells shuttles on tracks that extend between the nucleolus and nuclear pore complexes. The Nef tracks are different from the Nopp140 tracks in that they traverse the nucleoplasm with no relationship to the nucleolus.

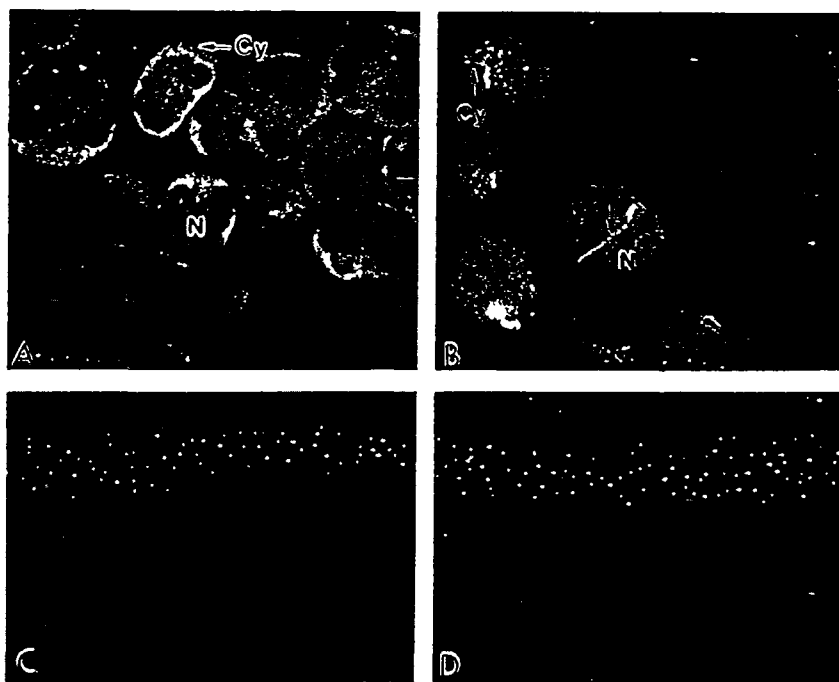


FIG. 2. Immunofluorescence analysis of Nef⁺ (HPBALL/Lnef/SN-S1) and Nef⁻ (HPBALL/LN) cells with antiserum against Nef. (A) Nef⁺ cells labeled with the anti-Nef antiserum show label in the cytoplasm. (B) The Nef⁺ cells labeled as in A were focused on the interior of the nucleus. Note a fluorescent band across the nucleus. (C) Nef⁻ cells labeled with the anti-Nef antiserum were not labeled. (D) Nef⁺ cells labeled with normal rabbit serum were also not labeled. (×800.)

Fig 51.

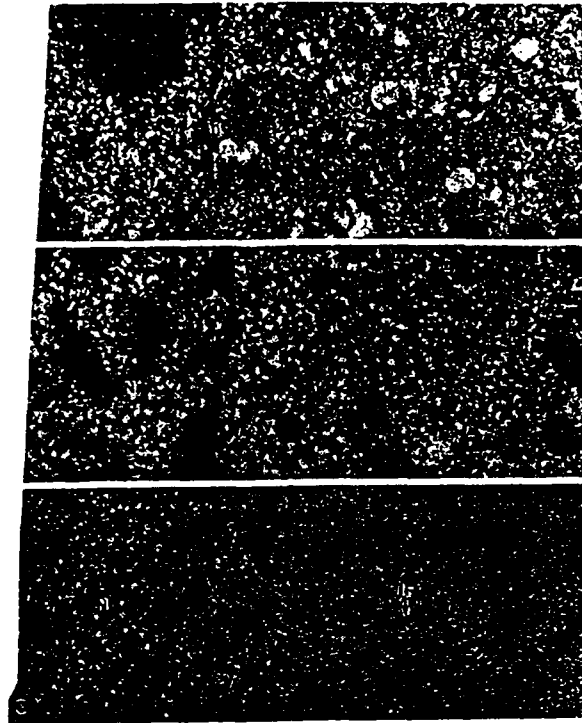


FIG. 3. Electron micrographs of controls for the immunogold labeling technique. (A) Nef⁻ cells were incubated with polyclonal anti-Nef antiserum followed by gold-conjugated anti-rabbit antibody. Labeling of cytoplasmic and nuclear components is negligible. (B) Nef⁺ cells were incubated with normal rabbit antiserum followed by goat anti-rabbit antibody conjugated with gold particles. No nonspecific labeling of either cytoplasm or nucleus is evident. (C) Nef⁺ cells were incubated with a monoclonal anti-intermediate filament (vimentin) antibody followed by gold-conjugated (anti-mouse) second antibodies. The label is seen over intermediate filaments (IF). M, mitochondrion; C, centriole; N, nucleus; Cy, cytoplasm. (A, $\times 8100$; B, $\times 8550$; C, $\times 19,800$.)

Fig 52.

In the cytoplasm (data not shown) the label due to Nef was most abundant near the indentation of the nucleus as was the case with cells processed by immunofluorescence (see Fig 51A); this region contained most of the cell organelles, including the microtubule organizing center, Golgi complex, and vesicles.

It has been hypothesized that the transport of RNA and proteins occurs on specific tracks in the nucleus, and these tracks may be composed of cytoskeletal filaments (e.g. microfilaments, microtubules, or intermediate filaments). To determine if any of these filaments form tracks within the nucleus of T cells, we have conducted immunogold labeling studies with anti-tubulin, anti-vimentin, and anti-actin antibodies. The nuclei remained largely unlabeled with either anti-vimentin (Fig 51C) or anti-tubulin antibodies (data not shown). However, anti-actin antibodies showed some labeling of the nuclei (Fig 54). Although not as clear as Nef tracks, the label due to actin showed a preferential alignment in the nucleus. Additionally, short tracks of actin were seen extending between the nuclear envelope and the nucleoplasm (Fig 54). These results are consistent with previous

biochemical evidence for the presence of actin in the nucleus and its proposed role in the shuttling of proteins between the nucleus and cytoplasm.

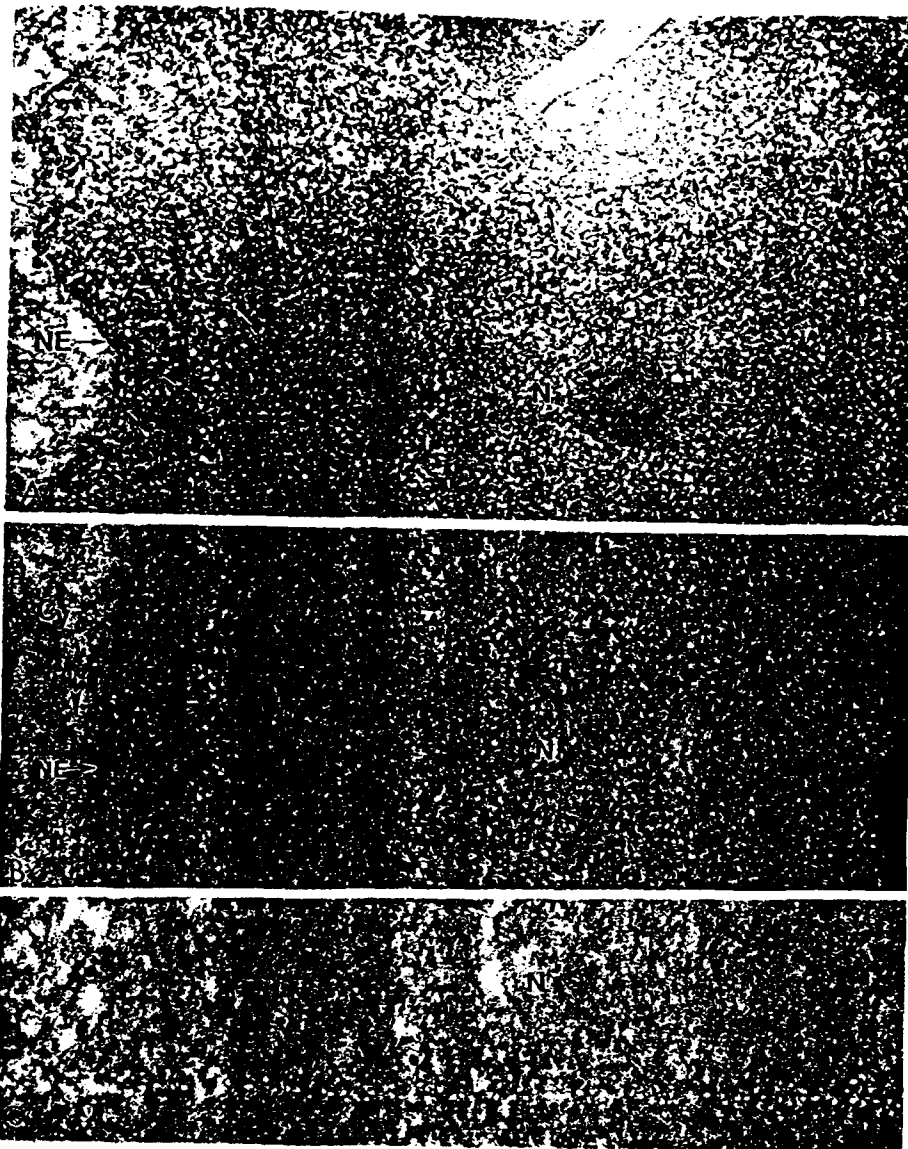


Fig 53.

FIG. 4. Electron micrograph showing immunogold labeling of the nuclei of three different Nef⁺ cells. Note the tracks of gold particles extending from the nuclear envelope to the nucleoplasm in A and B. (A) Arrows mark the track of Nef label. (B) The tracks of Nef appear to originate in the cytoplasm (arrowhead). (C) Part of the Nef track at high magnification. NE, nuclear envelope; Cy, cytoplasm. (A, $\times 23,800$; B, $\times 30,800$; C, $\times 56,700$.)

The localization of Nef in the nucleus also led us to search for a nuclear localization signal in the nef sequence. Since Nef is found in the nucleoplasm and not in the nucleolus, we focused on localization sequences on nucleoplasmic proteins. Previous studies with *Xenopus* oocyte nuclear proteins (nucleoplasmin and N1) have shown that these proteins share a bipartite nuclear targeting motif. The motif consists a 16-amino acid sequence with two basic residues at the amino terminal end, 10 "spacer" residues, and a cluster of 4 basic residues at the carboxyl-terminal end (see below). Amino acids in both basic domains are required

for nuclear targeting and the transport defect of a mutation in one domain is amplified by a simultaneous mutation in the other. In addition to *Xenopus* proteins, a number of eukaryotic and viral nuclear proteins contain this motif. The SF2 clone of Nef used here also shares this motif:

Nucleoplasmin	KRpaatkkgap	KKKK
Thyroid alpha1	KRvakkklieqn	ReRRR
Mef-SF2	KRsmggwsaire	RmRRR

The presence of the nuclear targeting sequence may be required but not sufficient for the nuclear localization of Nef. Indeed, a substantial fraction of Nef appears to be cytoplasmic associated with organelles and cytoskeletal elements, suggesting that it may disrupt host cytoplasmic activities. It is still possible that a fraction of Nef has a nuclear function that is yet to be identified.

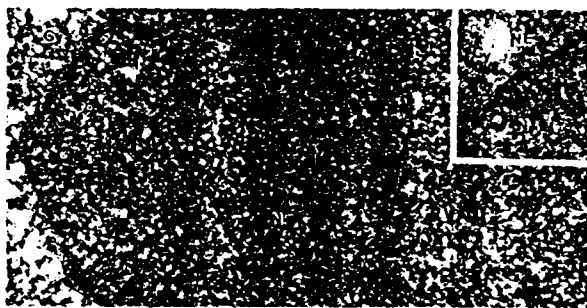


FIG. 5. Electron micrograph showing immunogold labeling of the nucleus of Nef⁺ cells with a monoclonal anti-actin antibody. In the nucleus the actin label shows preferential alignment along tracks. (Inset) Short track of actin label near the nuclear envelope (NE). ($\times 27,000$; Inset, $\times 46,800$.)

Fig 54

f) To determine the role of Nef in HIV-2 and SIV replication

Experiments on the replication of SIVmac102 and SIVmac239 Nef⁺ and Nef⁻ clones have been completed.

g) To determine the role of Nef in vivo with animal model systems

The SIVmac239 clones used for our analysis of Nef have already been studied by Desrosiers and colleagues in rhesus macaques, and these investigators demonstrated that Nef was critical for pathogenicity. Our studies in vitro with those virus strains and with the HIV-2 strains should provide important information in explaining this finding. One possibility is that Nef is required for establishment of a state of "latency" in vivo, and that in the absence of Nef, infected cells are rapidly lost due to lysis or immune clearance.

Studies in scid-hu mice with the HIV-1 clones were performed after the initial studies outlined in 1.i. However, insufficient funds were available to complete this task due to severe budgetary cuts in the last six months of the project.

h) To determine the role of Nef in modulating manifestations of HIV-1 infection

Blood samples from 48 patients were analyzed for immunological markers. CD4+ lymphocyte counts ranged from 0 to 1280/mm³ (mean 352/mm³; normal range 1000-1500/mm³); CD4 percentage ranged from 0 to 52% (mean 20%); CD8+ percentage ranged from 22 to 85 (mean, 55%); and CD4/CD8 ratio ranged from 0 to 1.81 (mean 0.21). The subjects are listed in Fig 55 according to increasing CD4+ lymphocyte counts.

As shown in Fig 56, HIV RNAs were detected with nested sets of PCR primers. The locations of primers within the HIV genome and relative to each other are shown in Fig 56B-D. Primer pairs for gag and pol were designed to amplify unspliced RNAs (Fig 56B), and primer pairs for env-spliced (Fig 56C), tat (Fig 56D), nef (Fig 56D) and nef-sequence (using primers S7B and NefAS in the first round and primers 8306 and 9134 in the second round, Fig 56E) were designed to amplify spliced mRNA. Whereas primers for env-genomic are capable of amplifying both unspliced and single-spliced transcripts, primers for env-spliced amplify only spliced env mRNA. Two different sets of primers were utilized for nef mRNA which amplify products of 108 bp (nef) or 828 bp (nef-sequence). For RNA preparations in which HIV-specific transcripts were not detected, the quality of the RNA was confirmed by RT-PCR with beta-actin primers (Fig 56E).

The results of the nested PCR assays for HIV RNA with seven different sets of primers are shown in Fig 55. Of the 48 patient samples that were analyzed with all 7 sets of nested primers, 45 (93.8%) were positive with at least 1 set of HIV-specific primers. The three samples in which no HIV-1 transcripts were detected were obtained from patients with CD4 cell counts of 383, 587, and 902/mm³, respectively. None of the latter patients had received antiretroviral therapy.

When nested primers were used for the detection of unspliced RNAs, the gag primer set yielded 29 of 48 (60%) positive results, the pol nested primer set yielded 30 of 48 (63%) positive results, and the env-genomic nested primer set yielded 31 of 48 (65%) positive. All of these primer sets should detect unspliced RNA, whereas the env-genomic primer set should also detect spliced env RNA species. There was good correlation between the results with gag and pol primer sets, with 23 samples yielding positive results with both primer sets, 6 samples yielding positive results with the gag primer set but not the pol primer set, and 7 samples yielding positive results with pol primer set but not the gag primer set. Discordances may be due to sequence variation at sites of binding of individual primers. Twenty-two samples were positive with env-genomic primers as well as both gag and pol primer sets, 5 samples were positive with env-genomic primers and gag or pol primer sets, 4 samples were positive with env-genomic primers, but neither gag nor pol primers, and 11 samples negative with env-genomic primers were positive with gag and/or pol primers.

TABLE 1. IMMUNOLOGICAL MEASUREMENTS AND POLYMERASE CHAIN REACTION RESULTS ON PATIENT COHORT

Patient No.	CDC class	Immunological						PCR results						
		CD4 ⁺ (No.)	CD4 (%)	CD8 (No.)	CD8 (%)	T4/T8	AVT ^a	gag	pol	env (genomic)	env (spliced)	tat	nef	nef-seq
1	C3	0	0	223	62	0.0	Yes	+	+	+	-	-	-	-
2	C3	0	0	529	55	0.0	Yes	+	+	+	+	-	-	-
3	C3	6	7	37	41	0.16	Yes	+	+	+	-	-	-	-
4	B3	8	1	424	51	0.02	Yes	+	+	+	+	-	+	-
5	C3	8	1	178	22	0.04	Yes	+	+	+	+	-	-	-
6	C3	10	5	119	57	0.08		+	+	+	-	-	-	-
7	C3	23	2	897	79	0.03		-	+	+	+	-	-	+
8	B3	24	2	722	59	0.03	Yes	+	-	-	-	-	-	-
9	B3	32	5	486	76	0.07	Yes	+	+	+	-	-	+	-
10	B3	62	4	1287	83	0.05		+	+	+	-	+	+	-
11	B3	86	8	713	66	0.12		+	-	-	-	-	-	-
12	B3	105	5	990	47	0.11	Yes	+	-	-	-	-	+	-
13	A3	137	6	1938	85	0.07		-	-	-	-	-	+	+
14	A3	177	12	854	58	0.21	Yes	-	+	+	-	-	+	-
15	B3	185	19	614	63	0.30		-	-	+	+	-	+	+
16	B3	191	11	1180	68	0.16		+	+	+	+	-	-	+
17	B3	195	21	492	53	0.40		+	+	+	-	+	+	-
18	A2	255	16	894	56	0.29		-	-	-	+	-	+	+
19	B2	259	16	875	54	0.30		+	+	+	-	-	+	-
20	A2	281	15	1161	62	0.24		+	+	+	+	-	+	-
21	A2	297	25	654	55	0.45		-	+	+	-	-	-	-
22	B1	306	29	444	42	0.69		-	-	+	+	-	-	-
23	B2	333	17	1420	58	0.29		-	+	-	+	-	+	-
24	B2	336	28	576	43	0.65		+	+	-	-	-	+	-
25	A2	358	23	935	60	0.38		+	+	+	-	-	+	-
26	B2	365	28	770	59	0.47		+	-	+	+	-	+	+
27	A2	370	22	959	57	0.39		+	+	+	+	-	-	-
28	B2	370	14	1614	61	0.23		+	+	+	+	-	-	-
29	B2	383	25	826	54	0.46		-	-	-	-	-	-	-
30	A2	390	29	685	51	0.57		-	-	-	-	-	+	-
31	A2	392	30	626	48	0.63		-	-	-	+	-	-	-
32	A2	408	17	1392	58	0.29	Yes	+	+	+	+	+	+	-
33	A2	421	20	1221	58	0.34		-	-	+	+	-	-	-
34	A2	424	16	1962	74	0.22		+	+	-	-	+	+	+
35	C2	426	36	463	39	0.92		+	+	-	-	-	-	-
36	A2	434	29	763	51	0.57		+	+	+	+	-	+	-
37	A2	460	31	728	49	0.63		+	-	-	-	-	-	-
38	A2	490	28	998	57	0.49		+	+	-	+	-	+	+
39	A1	535	25	1214	59	0.44		+	+	+	-	-	+	+
40	A1	560	32	980	56	0.57		-	-	-	+	-	-	-
41	B1	564	18	1942	62	0.29		+	+	-	-	-	+	-
42	A1	569	19	2065	69	0.28		-	+	+	+	-	-	-
43	B1	587	26	1331	59	0.44		-	-	-	-	-	-	-
44	B1	647	33	902	46	0.72		+	-	-	-	-	-	-
45	A1	686	26	1399	53	0.49	Yes	-	+	+	-	-	+	-
46	A1	822	31	1405	53	0.59		-	+	-	+	-	+	+
47	A1	902	52	520	30	1.73		-	-	-	-	-	-	-
48	A1	1280	49	706	27	1.81		-	-	+	-	-	-	-

^aAVT, antiviral therapy; yes, patients were known to have been on therapy within the previous 6 months; blanks indicate patient had not been on therapy.

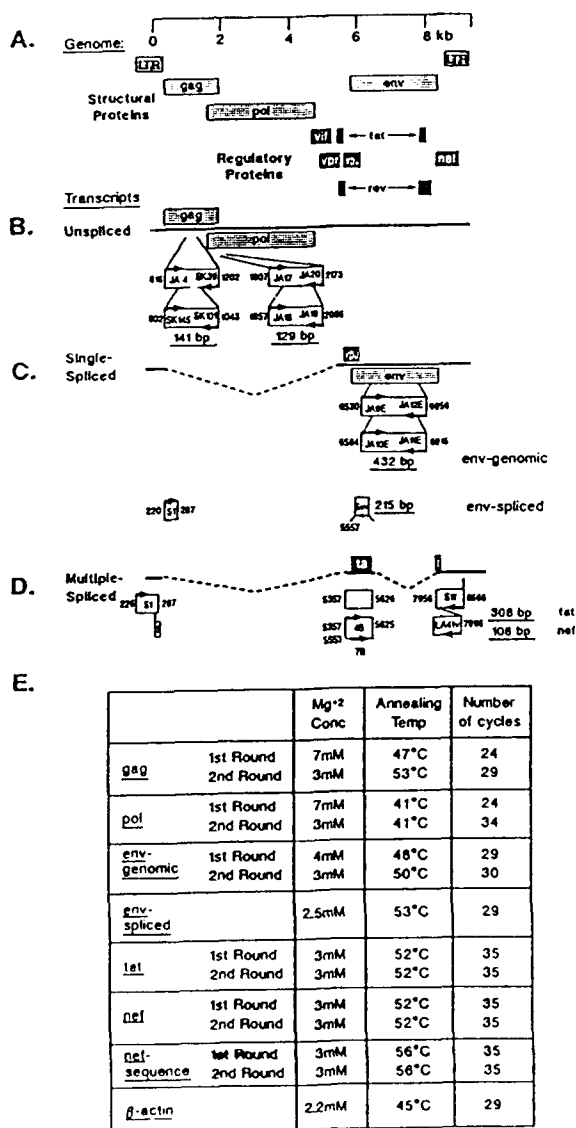


FIG. 1. HIV-1 RNA RT-PCR analysis. (A) The schematic drawing of the HIV-1 genome is shown with the nucleotide positions relative to the RNA initiation site indicated above. Genes encoding structural proteins and regulatory proteins are indicated separately. (B) The unspliced transcript that encodes Gag and Pol proteins is indicated as well as the positions of the nested primer sets in each gene. Arrows indicate positions of the primers, and the designation for each primer is shown in the box above or below the arrow. Nucleotide positions of the primers are indicated outside the boxes. The predicted sizes of the products of the nested PCR reactions are underlined and indicated below the boxes. In the case of *env*-genomic products, the actual product size was 22 bp larger than the genome locations would indicate because of the addition of 11 bp on each primer, including an *EcoRI* restriction enzyme site. (C) The single-spliced transcript encoding *Env* and *Vpu* products is indicated with the dotted line indicating the intron that is removed by splicing. The nested *env*-genomic primers are indicated, as well as the *env*-spliced primers. (D) The multiple-spliced transcripts are represented by a schematic showing one of the *tat* mRNAs. In each case, the first round of PCR was performed with primers S1 and S11 shown in the 5'- and 3'-most exons. The second round of PCR was performed with primers S4B (for *tat* mRNAs) or S7B (for *nef* mRNAs), both of which span the first splice site, and with primer LA41, found in the 3'-most exon. The predicted nested PCR product sizes for *tat* and *nef* transcripts are underlined and indicated to the right. (E) Reaction conditions for PCR are listed.

Fig 56

When nested sets of primers were used for the detection of spliced RNAs, the *env* spliced primer set yielded 21 or 48 (44%) positive results, the *tat* set yielded 3 or 48 (6.2%) positive results, *nef* primers yielded 28 of 53 (53%) positive results, and the *nef*-sequence primer set yielded 9 of 48 (19%) positive results.

Discrepancies between the two different nef primer sets may be due to sequence heterogeneity, as well as to the lower sensitivity of the nef sequence primer set compared to the nef primer set.

TABLE 2. KENDALL TAU b CORRELATION ANALYSIS BETWEEN PRESENCE OF HIV-1 RNA TRANSCRIPTS AND IMMUNOLOGICAL PARAMETERS

Gene	Correlation coefficient (P)					CDC ^a clin	CDC ^b clin/CD4
	CD4	CD4 (%)	CD8	CD8 (%)	CD4/CD8		
<i>gag</i>	-0.25 (0.03)	-0.24 (0.05)	-0.18 (0.13)	-0.02 (0.90)	-0.21 (0.08)	0.36 (0.01)	0.38 (0.003)
<i>pol</i>	-0.17 (0.16)	-0.25 (0.04)	0.02 (0.88)	0.09 (0.47)	-0.22 (0.06)	0.16 (0.25)	0.16 (0.22)
<i>env-gen</i>	-0.22 (0.06)	-0.29 (0.02)	-0.07 (0.56)	0.20 (0.11)	-0.27 (0.02)	0.12 (0.40)	0.13 (0.31)
<i>nef</i>	0.09 (0.94)	0.006 (0.96)	0.20 (0.09)	0.10 (0.43)	0.009 (0.94)	-0.27 (0.05)	-0.15 (0.24)
<i>nef-seq</i>	-0.08 (0.95)	-0.02 (0.87)	0.21 (0.08)	0.28 (0.02)	-0.04 (0.72)	-0.09 (0.53)	-0.05 (0.71)

^aCDC classification of HIV infection based on clinical status. Categories are (1) asymptomatic, (2) symptomatic, non-AIDS, and (3) AIDS-indication illness.

^bCDC classification of HIV infection based on clinical status and CD4 cell count. Above categories are subdivided into three groups: CD4 count >500/mm³, 200-499/mm³, and <200/mm³.^{17a}

Fig 57

Kendall Tau b correlation coefficient and p values of significant inverse correlations were determined between results of transcript detection and immunological parameters and clinical parameters. Fig 57 shows the results of these calculations for transcripts that either approaches or attained statistical significance when correlated with various immunological parameters. Statistical significance (at the level of $p < 0.05$) was achieved in the correlation of *gag* transcripts with CD4 cell count, CDC clinical stage, and CDC clinical/CD4 stage, *pol* transcripts with CD4%, *env-genomic* transcripts with CD4% and *nef-sequence* transcripts with CD8%.

Sequences from *nef* transcripts from 7 patients have been determined and a single expression clone from each patient derived for functional studies. In addition, we examined the evolution of the *nef* gene in sequentially derived samples of adults infected with HIV-1. Since the *nef* protein is partially encoded by sequences within the U3 region of the 3'LTR, and the dual functions of these overlapping sequence may place additional constraints on *nef* evolution, the current analysis examined sequences from the entire U3 region as well. The current study is novel in that sequences are derived from early as well as late stages of disease, unlike several previous studies of *nef* and LTR evolution.

Four subjects (S1-S4) were identified from whom peripheral blood mononuclear cells (PBMCs) were obtained over a 2.5-4.5 yr period. The first time point (A or D) was selected at the earliest time after seroconversion when the CD4+ lymphocyte count was $>900/\text{mm}^3$. The intermediate time points (B) were selected when the CD4+ lymphocyte count was $400-800/\text{mm}^3$. The last time point (C or G) was selected at a time when the CD4+ lymphocyte count was $<400/\text{mm}^3$. The same samples were used in an earlier study examining sequence variation in the V3 coding domain of env.

DNA was isolated from the uncultivated PBMCs, and PCR was performed with a nested set of primers. PCR products were digested with Hind III, and cloned into pUC9. Eight independent clones were selected and complete sequence analysis performed on both DNA strands of the plasmids by the dideoxy sequencing method. Taq polymerase induced errors or other cloning associated errors contributed minimally to the sequence diversity noted in this study, based on control experiments measuring the nucleotide misincorporation and recombination rates generated under our PCR amplification conditions, in agreement with previous studies.

Predicted amino acid sequences for Nef are shown for each of the four subjects in Fig 58. The first sequence obtained from each subject at the earliest available time point is shown, and differences in other clones from the same subject are indicated below.

Levels of nucleotide and amino acid sequence diversity are shown in Fig 59. In addition to the level of sequence diversity in the entire nef gene, tabulations were performed separately for the 5' portion of nef which does not overlap the LTR, and the 3' portion of nef which overlaps the LTR. Intrapatient, interpatient, and interperiod diversity were also determined.

At the earliest time point, 0-1.3% nef nucleotide and 0-3.2% amino acid diversity was noted for subjects S1, S2, and S4 (Fig 59). No early time point samples were available for S3. At later time points, 0.4-3.5% nucleotide and 0.6-6.3% amino acid sequence variation was noted. Though subjects S1 and S4 demonstrated higher levels of sequence variation at late points compared to the earliest time points, sequences for subject S2 showed comparable level of diversity at time points A and C.

Interperiod diversity was higher than intrapatient diversity, with 1.2-6.5% nef nucleotide and 2.7-13.8% amino acid variation (Fig 59). Intrapatient diversity was generally higher than intrapatient diversity, with 5.8-10.8% nef nucleotide and 10.7-20.3% amino acid diversity.

Sequence diversity within Nef was not uniform over the length of the predicted protein product. The initiator methionine codon was conserved in all sequences described in Fig. 58, and all previously reported sequences except one. Glutamic acid residues at positions 62-65 were well conserved, as previously reported, but substitutions with glycine, lysine, or aspartic acid residues are noted in clones 49-50, and 53-80. A tetrad repeat of proline residues at residues 69-78 were

altered in only a few instances (clones 10 and 36), and were noted previously to be conserved. A Gly-Pro-Gly sequence at residues 130-132, similar to that in the V3 loop of the HIV-1 envelope and predicted to form a beta-turn, were also well conserved (except clone 25), as previously noted.

Many of the Nef amino acid alterations arising over time in each subject were similar to those described in comparisons between different infected subjects (Fig. 58). A protein kinase C phosphorylation site at Thr-15 was frequently altered to Ala (clones 9-19, 21-25, 29-37), Lys (clones 49-50 and 70), or Arg (clones 64, 65, 68, 69, 71-80), as previously reported. The presence of Thr at this position abrogates transcriptional effects of Nef, but does not affect the ability to downregulate cell surface CD4 expression. This residue is located within a highly polymorphic region of Nef, including amino acids 8-15 (clones 5-11, 16, 18, 53-57, 60-80) (21, 68), which has also been implicated as a nuclear localization signal. A potential protein kinase phosphorylation site has also been described at Thr-80, within conserved residues 77-82 (except clones 63-66, 68-72, and 74-80) but it remains to be demonstrated that this residue is actually phosphorylated. The potential casein kinase II phosphorylation site noted at residues 157-160 in 24 of 54 sequences reported by Shugars et al, is altered in all clones described in Fig. 58. The potential tyrosine kinase recognition site at positions 94-102 noted in 36 of 54 sequences of Shugars et al. and 7 of 60 sequences of Delassus et al. is present in 29 of the 63 Nef protein sequences in Fig. 1. Gly-99, previously shown to be important for Nef stability was altered to Arg in clones 5-8 and 10-11.

Met-20, which may serve as an internal initiator codon, was well conserved, altered to Ile in only clones 16 and 18. A variable duplication has been described for residues 23-25 and is noted in clones 1-8. Cys-142 was previously shown to be important for Nef stability and was completely conserved in the sequences analyzed here and previously. In contrast, Cys-168, shown by Zazopoulos and Haseltine to be important for Nef activity was present only in clone 53, and in none of the 60 clones analyzed by Delassus et al. Cys-55, which was not found to be required for Nef activity was well conserved, altered only in clone 8. Asn-127, a potential glycosylation site noted by Guy et al, but not thought to be critical for Nef activity was conserved in all sequences except clone 36, and all 60 sequences reported by Delassus et al.

Several novel and potentially important amino acid changes, which were not previously reported, were noted in this study. Alteration of Gly-2 to Cys in predicted Nef products from clones 61 and 62 alter the myristylation acceptor signal of Nef. These alterations should prevent myristylation, which is important for Nef membrane and cytoskeletal association, cell surface CD4 downregulation, and suppression of HIV transcription. Other novel amino acid substitutions were noted at positions 12 (Arg in clones 16 and 18), 19 (Gly in clones 1-4), 21 (Asn in clones 9, 12-19, 21-25, 29-37), 38 (Gly in clones 21, 22, 24, 25 and 33-36), 85 (Phe in clone 5-8 and 10-11), 86 (Tyr in clones 6-7), 92 (Asn in clone 19), 102 (Trp in clones 1-8 and 11), 120 (His in clones 1-4, Phe in clones 5-8 and 11), 128 (Ala in clone 31 and Ser in clones 53-65, 67, and 69), 139 (Cys in clones 53-72 and 77-80), 159 (Arg in clone 8, Glu in clone 21-25), and 201 (Lys in clones 1-4, 16, and 18)

Premature stop codons have been noted frequently at position 124 in previous studies, including 6 of 54 sequences described by Shugars et al. Though premature stop codons were not identified at position 124 in the current study, a premature stop codon was noted in clone 24 at position 141, and premature stop codons arose at positions 92 (clone 35) and 100 (clones 73-76) as a result of frameshift

mutations. Premature stop codons were noted at positions 22, 57, 84, and 104 in HIV-1 Nef and at position 93 of SIVmac239 *nef*. Premature stop codons have also been reported within the open reading frames of HIV-1 sequences for *tat*, *rev*, *pol*, and *env*.

The analysis of Nef sequence variation in this study and V3 envelope sequence variation from the same patient samples allows a direct comparison of the results. In both cases, inpatient intraperiod diversity was generally lower than inpatient interperiod and interpatient diversity. Furthermore, higher levels of intraperiod diversity were generally identified at later time points as compared to the earliest time point for each subject. Similar results were obtained when Nef sequences from adults with primary HIV-1 infection were compared to those obtained from their HIV-1 infected sexual partners, and when Nef sequences derived from HIV-1 infected PBMC transcripts from individuals with >450 CD4 lymphocytes/ mm^3 were compared to those from individuals with <450 CD4 lymphocytes/ mm^3 .

Studies of V3 envelope diversity have consistently shown increasing levels of sequence diversity from early times of infection to later stages of disease. Moreover, V3 sequence heterogeneity was found to be lower in infected neonates compared to that in their infected mothers and in adults with primary infection compared to their infected sexual partners. In addition, several studies have shown lower levels of interpatient V3 envelope sequence diversity among HIV-1 clones obtained early after infection, compared to that found at later times of disease. Sequences obtained within a few months after infection were highly homologous with the North American consensus V3 envelope sequence and sequences determined to be important for regulation of HIV-1 infection of macrophages. In contrast, intraperiod Nef sequence variation did not always increase in magnitude over the course of disease *in vivo*, as shown by the results with subject 2 of this study. Moreover, interpatient Nef sequence diversity at the earliest time points was comparable to that identified at later time points (not shown).

Nucleotide sequences are provided in Fig. 60 for a portion of the 3'LTR (nucleotides -228 to +79, numbered relative to the RNA initiation site) from all 80 clones of the four subjects. This includes sequences downstream of the *nef* termination codon at positions -124 to -122, NFkB binding sites at -104 to -95 and -90 to -81, SP1 binding sites at -77 to -68, -65 to -57, and -54 to -46, TATA sequence at -27 to -24, the TAR stem 1 at +1 to +29, the TAR loop at +30 to +35, the TAR stem 2 at +36 to +58, and the polyadenylation signal at +74 to +79.

Sequence diversity in the portion of the LTR following *nef* is comparable to the portion of the LTR overlapping *nef*, as well as the portion of *nef* preceding the LTR (Fig 59). At the earliest time points, inpatient intraperiod diversity for the portion of the LTR following *nef* was 0-1.9%. At the later time points, inpatient intraperiod diversity was 0.3-2.9%. Inpatient interperiod diversity for this portion of the LTR was 0.4-3.7%, lower than that found for *nef*. Interpatient diversity was 3.1-6.7%, lower than that found for *nef*.

The cellular transcription factor, NF-kappa B, recognizes the motif GGGGACTTC, which occurs twice in the HIV-1 LTR. Pettersson and Schaffner have demonstrated synergistic activation of transcription by multiple binding sites compared to that found with a single binding site. These sites mediate responses to T-cell and macrophage activation signals, as well as viral gene products from herpesviruses, and other retroviruses. Substitution of C at position 6 with A (clone 61) is predicted to have no effect since this matches the NF-kappa B-binding site in the beta interferon gene promoter. However, substitutions at position 3 (clone 68), and position 7 (clones 14 and 68) are more likely to disrupt NF-kappa B binding. Naturally occurring HIV-1 isolates with deletions and/or duplications in the NF-kappa B binding site have been described previously.

The cellular transcription factor, Sp1, recognizes an assymmetric decanucleotide sequence, (G/T)GGGCGPuPuPy. The affinity of binding of Sp1 to this site is determined by the match of the given sequence to the consensus sequence. A single Sp1 site can activate transcription, and although site III (distal site) has the highest affinity for binding Sp1, it is clear that sites I and II are important in activation of transcription from the HIV-1 promoter. Transversions at specific nucleotides may or may not have significant effects on transcription. Single G to C transversion mutations at positions 4, 6, 7, or 8 reduce the binding of Sp1, although a G to T transversion at position 7 is acceptable, as seen in site III with clones 9 and 10 from subject 1, and all clones from subject 2. Guanines at positions 3, 4, 6, and 9 are highly preferred, but purines at positions 2 and 8 are equivalent. Positions 1 and 10 within each binding site have the greatest flexibility, and multiple mutations are found at these positions in site III in clones from subject 4.

The TATA sequence at nucleotides -27 to -24 is required for correct viral RNA initiation and serves as a binding site for several cellular factors. In addition it mediates transactivation by a cytomegalovirus immediate early protein. Mutation of the highly conserved T at position 3 in this motif as is found in clones 1-8, 11, 43-48, 78, and 80 is predicted to significantly reduce the binding activity of this motif.

TAR is a *cis*-acting RNA element localized to nucleotides +18 to +44. Tat function requires direct interaction with TAR. The TAR element is a stem-loop structure with a 6 nucleotide loop, and a bulge in the stem below the loop. The loop is not required for Tat binding, but is essential for Tat function, and is conserved in all the clones shown in Fig. 60. The bulge structure in TAR ($U_{21}CU$) is essential for Tat binding, and deletion of the bulge markedly reduces Tat binding *in vitro*.

Specific nucleotides are required for optimal Tat-TAR recognition, and these include U_{21} , as well as nucleotides 17, 28, 32, and 34. The $G_{28}-C_{32}$ and $A_{27}-U_{34}$ base pairs, located just above the bulge, are extremely important for binding and function, and are generally highly conserved. Subjects 1 and 3 in the present study have a conserved UCU bulge and 26-39 and 27-38 base pairs except in clone 9, which

has a C to T transversion in the middle of the bulge, as is found in several other HIV-1 isolates previously described. TAR bulge sequences in clones from subject 2 exhibit the same C to T transversion with the exception of clone 20, and clone 15 which has a CUU bulge sequence. Subject 4 has conserved sequences throughout the TAR structure, except in the lower part of the stem, with G to A transversions at site 15 in clones 71 and 72. A previous study of Tat and TAR from sequential patient samples found no consistent alteration in activity with disease progression.

The AAUAAA polyadenylation signal at nucleotides +74 to +79 is important for viral RNA processing. The U residue at position 3 of this motif is completely conserved among eukaryotic polyadenylation signals, and thus deletion or transversion to C as seen in several clones is likely to abrogate its function. However, the presence of cryptic polyadenylation sites elsewhere in the 3'LTR can not be excluded.

In contrast to several previous studies, large deletions, insertions, and rearrangements were found in several clones (Fig. 60). Clones 73-76 had deletions of nucleotides -228 to -5, and clones 77-80 had deletions of nucleotides -228 to -39. Clones 51 and 52 exhibited an insertion of novel sequences in place of those at positions -129 to +20 and -278 to +25, respectively. The inserted sequences did not closely match each other, any other HIV-1 sequences, or any sequences available in Genbank. In contrast, clones 43-48 exhibited a novel rearrangement in which the LTR sequences have been replaced by a repeated sequence corresponding to R-U5 sequences. These LTR alterations are not likely to be a consequence of an artifact related to PCR or cloning, since very similar deletions, insertions, and rearrangements were noted when different PCR primers were utilized with these same patient samples, but not other patient samples. It should be noted that these alterations were only noted in last time point from two of the four subjects, and in none of the earlier time points. Delassus et al also noted deletions in 2 of 60 clones. It is unclear whether such gross sequence alterations in *nef*/LTR relate directly to disease progression or longer duration of disease *in vivo*. If so, this could represent a selection for more disparate, perhaps non-functional *nef*/LTR sequences during the course of disease. Alternatively, these sequences may have arisen from a lack of selective forces which may have been present at earlier stages of disease for preservation of *nef*/LTR function.

The plasticity of the HIV-1 genome has been extensively described and is due to reverse transcriptase miscopying, duplication, deletion, recombination, and hypermutation. These effects provide the virus the ability to respond to selection pressures and adapt to the local environments. The pattern of sequence evolution in *nef* and LTR sequences is clearly different from that previously characterized for the portion of *env* encoding the V3 loop. Detailed sequence analysis of both regions of the HIV-1 genome using the same patient samples provides a useful comparison. Though progressive sequence heterogeneity was identified in V3 encoding *env* sequences for all three subjects, progressive sequence diversity in the *nef*/LTR region was noted for only two of the three subjects for whom these data were available. Furthermore, V3 encoding *env* sequences at the earliest time points from different subjects exhibited very similar predicted amino acid sequences within the

Mechanisms of Cytotoxicity of the AIDS Virus
P.I.: Lee Ratner, M.D., Ph.D.

Contract No. DAMD17-90-C-0125
Basic

V3 loop, similar to those previously defined as the North American consensus sequence and also demonstrated to be important for defining non-syncytia-inducing, macrophage-tropic isolates. In contrast, interpatient comparisons of *nef*/LTR sequences from the earliest time points resulted in no greater global or regional similarities than interpatient comparisons of sequences from later time points. These findings suggest independent sequence evolution for the *env* V3 domain and the *nef*/LTR region, most likely reflect different selective forces.

10/7

Subj

Time

Clone

Myristylation
Site

Phosphor-
ylation Site

2nd
Initiator
Methionine

PKC
Phosphor-
ylation Site

Acidic
Charged

(Pxx)

PKC
Phosphor-
ylation Site

Protein
Homology

G

150

1

D

1

MGGKSKrIgdGVstVREGhrqAEpatepAAeGVAVSRDLeKHGAIITSSNTattNaacAWLEAQEEEEVGFPvRPQVPLRPMTYKGAldLSHFLKEKGGLeglIWSQKRADlILDWVYHTGghFPDWNYPGPGtrYPPLTFGWCfKLVpVep

2

3

4

E

5

6

7

8

F

9

G

10

11

2

A

12

13

14

15

16

17

18

19

B

21

22

23

24

25

26

27

C

29

30

31

32

33

34

35

36

37

96

FIG 58- UPPER LEFT

1	D	1	160	170	180	190	200
2		2	DKVEEANGENNSLLHPMSQHGHMDPEKVLQKFD	SRLAFHHMARELHPKTYKNC			
3		3					
4		4					
5	E	5					EY
6		6					E
7		7					E
8		8	R		G		E
9	F	9	K				EY D
10	G	10		L	R	E	R
11		11					E
12	A	12	160	170	180	190	200
13		13	DQVEEANGENNSLLHPMSQHGHMDPEKEVLQKFD	SRLAFHHMARELHPKTYKNC			
14		14	S				
15		15	S				N
16		16	S	C	I		K
17	E	17	S			R	
18		18	S	I			K
19		19	S				
20		20					
21	B	21	E	S			
22		22	E	S	Y		
23		23	E	S		S	
24		24	E				
25		25	E	S			
26		26					
27		27					
28		28					
29	C	29	E	S			
30		30	E	S			
31		31	E	S		G	
32		32	E	S	L		
33		33	E	S			
34		34	E	S			
35		35					
36		36	SS			C	
37		37	E	S			

FIG 18 - UPPER RIGHT

	160	170	180	190	200
3 C	DKVEEAVGENNSLLHPMSQHGDDPPEKEVLMNKFD SKLAFHHVARELHPDYK N				
		M			
4 A	EqvEKANE Genns LLHPMcLHGMeDSEKEVLMNKFD SRLAFHmAKELHPEYKDC				
53					
54	S				
55	S				
56	S				
57	S				
58	S				
59	S				
60	S				
61	S				
62	S				
B					
63	S	D	V		
64	S	D	I	V	
65	S	D	I	V	
66	S	D	V		
C					
67	S				
68	S	D	I	V	
69	S				
70	S	D	V	V	
71	S	D	V	V	
72	S	D	V E	V	
73					
74					
75					
76					
77	RCCI*				
78	RCCIGAAAFCLFWSLVRPDL SIGALWAGEPTA*				
79	RCCI*				
80	A				
	A	RCCIGAAAFCLFWSLVRPDL SIGALWAGEPTA*			

FIG 13- LOWER RIGHT

Fig 59

Table - Genetic Diversity

Subject Period		5'nef (289 nt)				3'nef (329 nt)				Nucleotide Diversity (%) ref (618 nt)				LIR (194 nt)				Total (812 nt)				N-Term Nef (96 aa)				Amino Acid Diversity (%) C-Term Nef (110 aa)				Nef (206 aa)						
		Range		Average		Range		Average		Range		Average		Range		Average		Range		Average		Range		Average		Range		Average		Range		Average				
		D	0	0	0	0	0	0	0	0	0	0	0	0	0	0	0	0	0	0	0	0	0	0	0	0	0	0	0	0	0					
<u>Intrapatient Diversity</u>		S1	E	0	-4.1	0.4	0	-1.2	0.7	0	-0.9	0.6	0	-1.0	1.2	0	-0.9	4.7	0	-1.0	0.7	0	-0.9	0.5	0	-0.9	0.6	0	-1.0	0.7	0	-0.9	0.5	0	-0.9	0.6
		G	-	-	2.1	-	-	4.3	-	-	3.2	-	-	2.5	-	-	3.0	-	-	5.2	-	-	8.2	-	-	6.8	-	-	5.2	-	-	8.2	-	-	6.8	
		S2	A	0	-3.1	1.5	0	-2.1	1.1	0.3	-2.9	1.3	0	-2.6	1.2	0.6	-2.3	1.3	0	-1.0	3.2	0.9	-0.6	3.2	0.9	-0.6	3.2	0	-1.0	3.2	0.9	-0.6	3.2	0.9	-0.6	3.2
		B	0	-0.7	0.3	0.4	-0.8	0.5	0.2	-0.6	0.4	0	-1.0	0.3	0.1	-0.5	0.4	0	-1.0	0.1	0	-1.8	1.8	0.5	-1.5	1.0	0	-1.0	0.1	0	-1.8	1.8	0.5	-1.5	1.0	
		C	0.3	-2.1	1.2	0.8	-3.6	1.7	0.6	-2.9	1.5	0	-2.6	1.0	0.6	-2.1	1.3	0	-2.6	1.5	0.9	-9.0	4.1	0.9	-0.8	2.9	0	-4.2	1.5	0.9	-9.0	4.1	0.9	-0.8	2.9	
		S3	-	-	1.4	-	-	0.6	-	1.0	-	1.0	-	1.0	-	1.0	-	1.0	-	-	-	-	-	-	-	-	-	-	-	-	-	-	-	-	-	
		S4	A	0	-1.0	0.5	0	-1.8	1.0	0	-1.5	0.8	0	-3.6	1.9	0.3	-1.7	1.0	0	-2.1	0.8	0	-4.5	2.2	0	-2.9	1.5	0	-2.1	0.8	0	-4.5	2.2	0	-2.9	1.5
		B	0	-5.2	3.4	0	-3.6	2.4	0	-4.2	2.9	1.0	-2.1	1.5	0.3	-3.7	2.5	1.0	-2.1	6.8	0	-4.5	3.0	0	-6.8	4.8	0	-10.4	6.8	0	-4.5	3.0	0	-6.8	4.8	
		C	0	-4.8	3.2	0.6	-5.8	4.0	0.3	-5.3	3.5	0	-5.1	2.9	0.3	-4.7	3.3	0	-5.1	5.9	0	-11.8	6.6	1.4	-11.1	6.3	2.0	-11.5	5.9	0	-11.8	6.6	1.4	-11.1	6.3	
<u>Interpatient Diversity</u>		S1	D/E	1.0	-1.4	1.3	1.5	-2.4	1.9	1.5	-1.9	1.6	0	-1.0	0.4	1.1	-1.6	1.3	0	-1.0	3.6	3.6	4.5	3.9	3.4	3.9	3.7	3.1	-4.1	3.6	3.6	4.5	3.9	3.4	3.9	3.7
		D/F	-	-	7.3	-	-	5.8	-	6.5	-	6.5	-	3.6	-	5.8	-	5.8	-	13.5	-	-	10.9	-	-	12.1	-	-	13.5	-	-	10.9	-	-	12.1	-
		D/G	4.4	-5.9	5.2	1.8	-4.9	3.3	3.7	-4.7	4.2	0.5	-2.6	1.5	3.0	-4.2	5.9	0.5	-2.6	13.0	4.5	-10.0	7.2	9.0	-10.7	9.9	11.4	-14.5	13.0	4.5	-10.0	7.2	9.0	-10.7	9.9	
		E/F	6.9	-7.3	7.0	5.5	-7.0	6.2	6.1	-7.1	6.6	3.6	-4.1	3.7	5.5	-6.4	5.9	3.6	-4.1	14.3	12.7	-13.6	13.4	13.1	-14.1	13.8	13.5	-14.5	14.3	12.7	-13.6	13.4	13.1	-14.1	13.8	
		E/G	3.5	-5.2	4.4	0.3	-5.5	2.8	2.6	-4.7	3.6	0.5	-3.1	1.9	2.2	-4.3	3.2	0.5	-3.1	12.7	9.0	-10.0	5.2	7.3	-10.2	8.7	10.4	-14.5	12.7	9.0	-10.0	5.2	7.3	-10.2	8.7	
		F/G	5.5	-5.9	5.7	6.4	-8.2	7.3	6.0	-7.1	6.6	2.1	-3.1	2.6	5.3	-5.9	5.6	2.1	-3.1	7.3	12.7	-16.4	14.5	10.2	-12.1	11.1	7.3	-7.3	7.3	12.7	-16.4	14.5	10.2	-12.1	11.1	
		S2	A/B	0	-2.8	1.2	0.3	-1.5	1.2	0.6	-2.1	1.2	0	-2.1	0.8	0.6	-2.1	1.2	0	-2.1	2.3	0.9	-4.5	3.1	1.5	-5.3	2.7	0	-6.3	2.3	0.9	-4.5	3.1	1.5	-5.3	2.7
		B/C	0.3	-2.1	1.1	0.3	-2.1	1.7	0.6	-2.1	1.4	0	-3.1	0.9	0.5	-1.8	1.2	0	-3.1	2.4	0.9	-9.1	4.4	1.5	-8.2	3.5	0	-7.3	2.4	0.9	-9.1	4.4	1.5	-8.2	3.5	
		A/C	0.3	-3.8	1.7	0.6	-3.0	1.8	0.8	-3.1	1.7	0	-3.6	1.1	0.9	-3.2	1.6	0	-3.6	1.1	0.9	-5.4	3.8	1.5	-8.2	2.5	0	-3.1	1.1	0.9	-5.4	3.8	1.5	-8.2	2.5	
		S4	A/B	3.6	-	3.6	2.4	-4.8	3.8	2.7	-4.5	3.7	1.5	-4.6	3.1	2.7	-4.6	3.6	1.5	-4.6	9.2	5.4	-10.9	7.7	6.8	-10.2	8.4	8.3	-10.4	9.2	5.4	-10.9	7.7	6.8	-10.2	8.4
		B/C	1.4	-5.9	3.6	1.2	-4.3	3.3	1.1	-4.7	3.4	1.0	-4.1	2.8	0.9	-5.0	3.6	1.0	-4.1	7.9	1.8	-14.5	7.7	2.4	-11.2	6.9	2.1	-11.5	7.9	1.8	-14.5	7.7	2.4	-11.2	6.9	
		A/C	0	-5.5	3.7	0.3	-6.1	3.9	0.8	-5.3	3.8	0.5	-4.1	3.2	1.1	-5.3	3.7	0.5	-4.1	6.7	0	-8.2	4.5	1.9	-8.3	5.5	4.3	-10.4	6.7	0	-8.2	4.5	1.9	-8.3	5.5	
<u>Interpatient Diversity</u>		S1/S2		6.6	-	6.6	5.2	-	5.2	5.8	-	5.8	3.1	-	3.1	5.2	-	5.2	10.4	10.9	-	10.9	10.7	-	10.7	10.4	10.7		10.4	10.9	-	10.9	10.7		10.7	
		S1/S3		9.7	-	9.7	7.9	-	7.9	8.7	-	8.7	5.7	-	5.7	8.0	-	8.0	15.6	11.8	-	11.8	13.6	-	13.6	15.6	13.6		15.6	11.8	-	11.8	13.6	-	13.6	
		S1/S4		5.9	-	5.9	9.1	-	9.1	7.6	-	7.6	6.7	-	6.7	7.4	-	7.4	16.6	18.1	-	18.1	17.5	-	17.5	16.6	17.5		16.6	18.1	-	18.1	17.5	-	17.5	
		S2/S3		10.0	-	10.0	9.7	-	9.7	9.9	-	9.9	5.7	-	5.7	8.9	-	8.9	16.6	17.3	-	17.3	15.6	-	15.6	16.6	16.6		16.6	17.3	-	17.3	15.6	-	15.6	
		S2/S4		5.5	-	5.5	7.9	-	7.9	6.6	-	6.6	6.7	-	6.7	6.7	-	6.7	13.5	17.3	-	17.3	13.5	-	13.5	13.5	15.5		13.5	17.3	-	17.3	15.5	-	15.5	
		S3/S4		9.7	-	9.7	11.9	-	11.9	10.8	-	10.8	5.1	-	5.1	9.5	-	9.5	20.8	20.0	-	20.0	20.3	-	20.3	20.8	20.3		20.8	20.0	-	20.0	20.3	-	20.3	

— **1999** —

102

FIG 20- LOWER LEFT

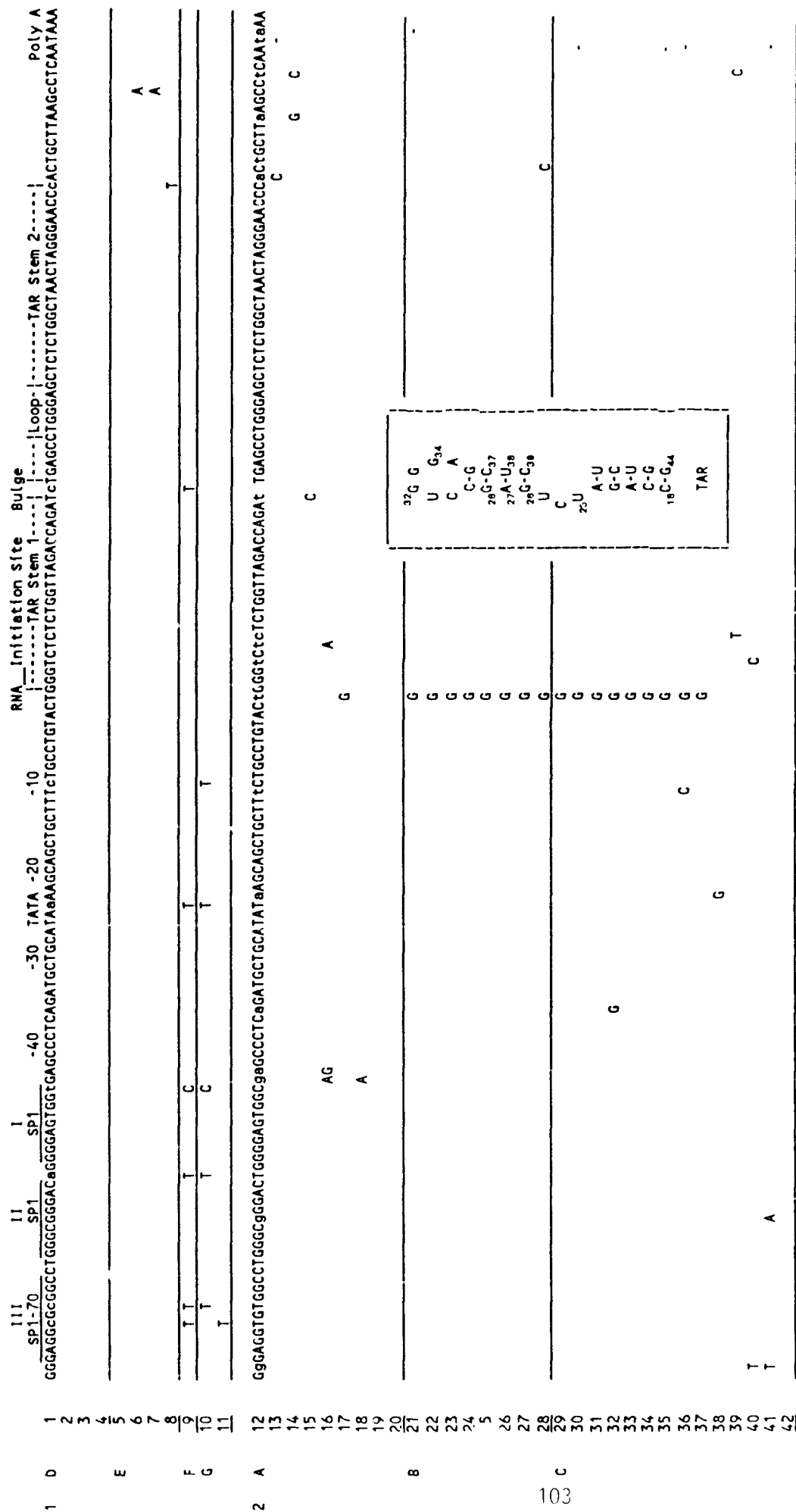


FIG 2C- UPPER RIGHT

3	B	AAGCTTGTAGAGCTATTCCGGCTGTACTGGGTCTCTCTGGTTAGACCAGATCTGAGCCTGGGAGCTCTCTGGCTAaCTAGGGAACCCAL .JTTAAaCCctCAATAAA									
43										G	
44										G	
45										G	
46										G	
47										G	
48										G	
49	C	AGG	CGCGGCTGGG	CGG	ACTGGG	GAGTGGCGAGCCCTCAGATGCTGCATATAAGCAGCT	T	T			
50		AGG	TCCGGCTGGG	CGG	ACTGGG	GAGTGGCGAGCCCTCAGATGCTGCATATAAGCAGCT	T	T			
51		CGGTAGTGTATGTCAC	TGTCAGCATCCCTCCCTAGCCCTGATAACCTTCAAAAGTCAAAACTGGCTCTCAATTGGTCTGAGGTTGACTCATTTGGTTT						T		
52		TCTATAAATGAGGACACAGCT	CTGCCCCCTGTGAGCGGTGTGACTCTGGTAACTAGAGATCCCTCTAGACCCCTACCAACCAAGGTGATGTGACTGTCTCTCTTTT								
53	4	AGGgaG-	CGTGGCTGGGGCGGGACTgGGGgGtGGCGAGCCTCAGATGCTGCATATAAGCAGCTGCTTTTtGGCTGTTCCGGGTCTCTCTAGTTAgCCAGATCTGAGCCTGGGAGCTCTCTGGCTAaCTAgggAAACCCACTGCTTAAGCCtG, .T	AA							
54		G									
55											
56		TG									
57											
58		TG									
59											
60											
61											
62		G									
63	B	G	C	-	C	C					
64		G	C	-	C	C					
65											
66		C	C								
67	C	G	C		C	C					
68											
69											
70		AG									
71		AG									
72		AG									
73											
74											
75											
76											
77											
78											
79											
80											

FIG 20- LOWER RIGHT

i) To determine the therapeutic role of Nef in down-regulating HIV-1

Since Nef has been shown to be a pathogenic factor in SIVmac in rhesus macaques, our goal in this regard is altered. Insufficient funds were available to further pursue this task, due to drastic budgetary cuts in the last six months of the project.

(7) CONCLUSIONS

The studies of Vpr have shown that this protein is critically important for productive infection in monocytes. In addition, Vpu may functionally complement the activity of Vpr. The mechanisms of action of Vpr and the domains critical for this activity were defined.

The studies of Vpx have focused on the mechanism of packaging of Vpx into virus particles. This has led to the very interesting observation of an association of Vpx with gag p24. This provides specific ideas about the mechanism of Vpx activity.

The studies of Nef have clearly demonstrated an effect on NF- κ B and AP1 activity. The effects are shown to be specific by the lack effect on other transcriptional factors, including SP1, URS, and USF. Moreover, we have found that these effects are functionally important with regards to HIV-1 transcription and IL2 expression. It is likely that a common mediator in signal transduction is affected by Nef.

We have also found that Nef interacts with the cellular cytoskeleton and that this interaction depends upon Nef myristoylation. This may provide specific clues to the way Nef interrupts signal transduction and down-regulates cell surface CD4 expression.

Studies of nef sequences from patients at different stages of disease have shown no major alterations in the gene early during HIV-1 infection, but frequent insertions, deletions, or rearrangements at late stages of disease. This may have important implications concerning the role of Nef in disease progression.

(8) REFERENCES

- Ahmad and Venketessan 1988. *Science* 241:1487.
Allan et al., 1985, *Science* 230:810
Ameisen et al., 1989a *N. Engl. J. Med.* 320:251.
Ameisen et al., 1989b, *AIDS Res. & Hum. Retrovir.* 5:87.
Arya et al., 1986. *Proc. Natl. Acad. Sci.* 83:2209.
Chakrabarti et al., 1987, *Nature* 333:457
Chengsong-Popov et al., 1989, 5th International AIDS Conf, WCP 124
Dedera et al., 1989, *J. Virol.* 63:3;205
Felber et al., 1989, 5th International AIDS Conf
Franchini et al., 1986, *Proc. Natl. Acad. Sci.* 83:5282.
Franchini et al., 1987, *Blood* 69:437.
Fukasawa et al., 1988, *Nature* 333:457.
Guy et al., 1987, *Nature* 330:266.
Guyader et al., 1987, *Nature* 326:662.
Guyader et al., 1989. *EMBO J.* 8:1169.
Haas et al., 1985, *Nature* 322:130.
Haseltine et al., 1988. *J. AIDS* 1:217.
Henderson et al., 1988, *Science* 241:199.
Hirsch et al., 1989, *Nature* 339:389.
Hu et al., 1989, *Virol.*
Issel et al., 1986 In Salzman, *Animal Models of Retrovirus Infection and their Relationship to AIDS*, pp. 95.
Kappes et al., 1988, *J. Virol.* 65:3501.
Kim and Baltimore, 1989, 5th International Conference on AIDS, W0035
Klotman et al., 1989
Lange et al., 1989, 5th International Conference on AIDS
Laure et al., 1989, 5th International Conference on AIDS
Levy et al., 1989, 5th International Conference on AIDS
Luciw et al., 1989, *Proc. Natl. Acad. Sci.* 84:1434.
Myers et al., 1989, *Human Retroviruses and AIDS*.
Narayan and Cork, 1985, *Rev. Infect. Dis.* 7:89.
Niederman et al., 1989, *Proc. Natl. Acad. Sci.* 86:1128.
Pederson et al., 1987, *Science* 235:790.
Ratner et al., 1985, *Nature* 313:277.
Reiss et al., 1989, *AIDS* 3:227
Ronde et al., 1989, *Lancet* 2:574.
Sabatier et al., 1989, *AIDS* 3:215.
Samuel et al., 1987, *FEBS Lett.* 81:218.
Sonigo et al., 1985, *Cell* 42:369.
Terwilliger et al., 1986, *J. Virol.* 60:754.
Tsujimoto et al., 1989, 5th International Conference on AIDS
Wong-Staal et al., 1987, *AIDS Res. & Hum. Retovir* 3:33
Yu et al., 1988, *Nature* 335:262.
Yu et al., 1989, 5th International Conference on AIDS, T0017
Yu et al., 1991, *J. Virol.*

(9) APPENDIX

Manuscripts and Abstracts

Cumulative List of Manuscripts Submitted to Peer-Review Journals Supported by this Contract:

1. Westervelt P, Gendelman HE, Li Y, and Ratner L. A determinant within the HIV-1 gp120 envelope protein critical for infection of primary monocytes. *Vaccines* 91, Cold Spring Harbor Laboratory Press, p. 71-76.
2. Niederman TMJ, Hu W, and Ratner L. Simian immunodeficiency virus negative factor (NEF) suppresses viral mRNA accumulation in COS cells. *J. Virol.* 65:3538-3546, 1991.
3. Westervelt P, Gendelman HE, and Ratner L. Identification of a determinant within the HIV-1 surface envelope glycoprotein critical for productive infection of cultured primary monocytes. *Proc. Natl. Acad. Sci.* 88:3097-3101, 1991.
4. Bryant ML, Ratner L, Duronio RJ, Kishore NS, Adams SP, and Gordon JI. Incorporation of 12-methoxydodecanoate into the gag polyprotein precursor of HIV-1 inhibits its proteolytic processing as well as virus production in a chronically infected human lymphoid cell line. *Proc. Natl. Acad. Sci.* 88:2055-2059, 1991.
5. Westervelt P, Trowbridge DB, Henkel T, Gendelman HE, Orenstein J, and Ratner L. Dual regulation of silent and productive infection in monocytes by distinct human immunodeficiency virus type 1 determinants. *J. Virol.* 66:3925-3931, 1992.
6. Niederman TMJ, Garcia JV, Hastings WR, Luria S, and Ratner L. HIV-1 Nef protein inhibits NF- κ B induction in human T cells, *J. Virol.*, 62:6213-6219, 1992.
7. Niederman TMJ, Hastings WR, Luria S, and Ratner L. HIV-1 nef protein inhibits the induction of AP-1 DNA binding activity in human T cells. *Virol.*, 194:338-344, 1993.
8. Vander Heyden N, Wang JJ, and Ratner L. HIV-2 vpx incorporation into viral particles and effect on virus infectivity. In preparation
9. Horton R and Ratner L. HIV-2 viral protein X association with Gag p27 and incorporation into virus particles. Submitted, *Virol.* 199:453-457, 1994.
10. Niederman TMJ, Hastings, WR, Bryant M, and Ratner L. Myristoylation-enhanced binding of the HIV-1 nef protein to T cell skeletal matrix. *Virol.* 197:420-425, 1993.

11. Lu Y-L, Spearman P, and Ratner L. HIV-1 viral protein R localization and incorporation into virus particles, *J. Virol*, 67:6542-6550, 1993.
12. Bandres J and Ratner L. HIV-1 NEF protein down-regulates transcription factor NF-kB and AP-1 in human T-cells in vitro after T cell receptor stimulation. *J Virol* 68: , 1994.
13. Murti KG, Brown PS, Ratner L, and Garcia JV. Highly localized tracts of HIV-1 Nef in the nucleus of a human CD4+ T cell line. *Proc. Natl. Acad. Sci. U.S.A.*, 90:11895-11899, 1993.
14. McNearney T, Birdwell A, Arens M, Markham R, and Ratner L. Nef and LTR sequence variation from sequentially derived human immunodeficiency virus type 1 isolates. *J AIDS*, Submitted.
15. Bandres J and Ratner L. Regulation of human immunodeficiency virus nef protein by phosphorylation, *Virol*, 1994.
16. Wang JJ, Lu Y-L, and Ratner L. Viral assembly and expression of Vpr in human immunodeficiency virus type 1 demonstrated by electron microscopy. In preparation for *J. Gen. Virol*, In press.
17. Arens M, Joseph T, Nag S, Miller JP, Powderly WG, and Ratner L. Alterations in spliced and unspliced HIV-1 specific RNA detection in peripheral blood mononuclear cells of individuals with varying CD4-positive lymphocyte counts. *AIDS Res. Hum. Retrovir.*, 9:1251-1257, 1993.
18. Heinzinger N, Bukrinsky M, Haggerty S, Ragland A, Lee M-A, Kewalramani V, Gendelman H, Ratner L, Stevenson M, and Emerman M. The HIV-1 vpr protein is a component of the viral preintegration complex which influences nuclear targeting of viral nucleic acids in non-dividing host cells. *Proc Natl Acad Sci USA*, In press.
19. Bandres JC, Shaw AS, Ratner L. HIV-1 nef protein downregulation of CD4 surface expression is mediated by the lck binding domain of CD4. *J Virol*, Submitted.

Cumulative List of Reviews Supported by this Contract

1. Ratner L, Niederman TMJ, Lozeron H, and Bryant M. Structure and function of the negative factor (NEF) of HIV and SIV. In Kumar A, ed. *Advances in Molecular Biology and Targetted Treatment of AIDS*. Plenum Press, 1991.
2. Ratner L, Niederman TJ, Lozeron H, and Bryant M. Structure and function of the HIV and SIV nef products. In Haseltine W and Wong-Staal F, eds. *The Genetic Structure and Regulation of HIV*, Raven Press, New York, 1991.
3. Niederman T and Ratner L. Functional analysis of HIV-1 and SIV nef proteins. *Research in Virology* 143:43-46, 1992.

4. Bryant M and Ratner. The biology and molecular biology of HIV-1. *Ped. Infect. Dis. J.*, 11:390-400, 1992.
5. Ratner L. Nef. In: Srinivasan A and Koprowski H, eds., *Role of HIV Accessory Genes in AIDS Pathogenesis, Current Topics in Microbiology and Immunology Series*, Springer-Verlag Press, In press.
6. Ratner L. Molecular biology and pathogenesis of HIV. In Burke, D. *HIV Infections and AIDS, Current Opinion in Infectious Diseases*, vol. 6, no. 2, 6:181-190, 1993.
7. Ratner L. Viral life cycle and genetic approaches. *Perspective in Drug Discovery and Design*, 1:3-22, 1993.

Cumulative List of Abstracts Supported by this Contract

1. Westervelt P and Ratner L. An HIV-1 gp120 envelope protein determinant critical for infection of primary monocytes. *Cold Spring Harbor Vaccine/AIDS Meeting*, 1990.
2. Westervelt P, Gendelman HE, and Ratner L. An HIV-1 gp120 envelope protein determinant critical for infection of primary monocytes. *Clin. Res.*, 1990.
3. Ratner L, Niederman TMJ, Lozeron H, and Bryant M. Structure and function of HIV and SIV Nef products. *Structure and Regulation of HIV, Harvard AIDS Institute Symposium*, 1990.
4. Westervelt P, Trowbridge DB, Gendelman HE, and Ratner L. Regulation of silent and productive HIV-1 infection in primary monocytes by two distinct genetic determinants. *Clin. Res.* 1991.
5. Westervelt P, Trowbridge DB, Gendelman HE, and Ratner L. Regulation of silent and productive HIV-1 infection in primary monocytes by two distinct genetic determinants. *Proceedings for the 7th International Conference on AIDS, Florence, Italy*, 1991.
6. Niederman TMJ and Ratner L. Nef mediated transcriptional suppression and its cellular release. *Cold Spring Harbor Symposium on RNA Tumor Viruses*, 1991.
7. Ratner L, Westervelt P, Trowbridge DB, and Gendelman HE. Regulation of silent and productive HIV-1 infection in primary monocytes by two distinct genetic determinants. *Am. Soc. Virol.*, 1991.
8. Westervelt P, Trowbridge DB, Gendelman HE, and Ratner L. Regulation of silent and productive HIV-1 infection in primary monocytes by two distinct genetic determinants. *Cold Spring Harbor Symposium on RNA Tumor Viruses*, 1991.

9. Ratner L and Westervelt P. Molecular basis for HIV1 tropism for monocytes: interaction of envelope, vpr, and vpu proteins. Am. Soc. Hematol., 1991.
10. Ratner L and Westervelt P. Regulation of HIV1 tropism for monocytes. National Cooperative Drug Discovery Group Meeting, San Diego, 1991.
11. Henkel TJ, Westervelt P, and Ratner L. HIV infection of primary monocytes is regulated by multiple genetic determinants. UCLA Symposium, AIDS, 1992.
12. Niederman TMJ and Ratner L. HIV-1 nef protein inhibits the induction of NF-kB and AP-1 in human T cell lines. Am. Soc. Virol., 1992.
13. Niederman TMJ and Ratner L. HIV-1 nef inhibits the induction of NF-kB and AP-1 in human T cell lines. VIII International Conference on AIDS, Amsterdam, 1992.
14. Niederman TMJ and Ratner L. HIV-1 nef inhibits the induction of NF-kB and AP-1 in human T cell lines. Cold Spring Harbor Symposium on RNA Tumor Viruses, 1992.
15. Niederman TMJ and Ratner L. HIV-1 nef inhibits the induction of NF-kB and AP-1 in human T cell lines. Annual Meeting of the Laboratory of Tumor Cell Biology, 1992.
16. Bandres J, Niederman T, and Ratner L. Analysis of HIV-1 Nef inhibition of NF-kB and AP-1 activation. UCLA Symposium: Frontiers in HIV Pathogenesis, 1993.
17. McNearney T, Hornickova Z, Birdwell A, Kulczykcki A, Arens, M, Markham R, and Ratner L. Sequentially derived HIV-1 isolates display progressive heterogeneity in the nef gene. UCLA Symposium: Frontiers in HIV Pathogenesis, 1993.
18. Ratner L, Lu Y-L, Lindenbach B, and Horton R. Localization of vpr & vpx of HIV-1 & 2 in virions and infected cells. IXth International Conference on AIDS, Berlin, 1993.
19. McNearney T, Hornickova Z, Birdwell A, Kulczykcki A, Arens M, Markham R, and Ratner L. Sequentially derived HIV-1 isolates display progressive heterogeneity in the nef gene. IXth International Conference on AIDS, Berlin, 1993.
20. Ratner L. Interaction of HIV-1 regulatory and envelope proteins with macrophage tropism determinants. Genetic Resistance to HIV-1, Bethesda, Maryland, 1993.
21. Horton R, Spearman P, and Ratner L. HIV-2 VPX association with GAG p27 capsid protein and incorporation into virus particles. Cold Spring Harbor Retroviruses Meeting, 1993.

22. Lu Y-L, Spearman P, and Ratner L. Cellular localization and packaging of HIV-1 VPR. Cold Spring Harbor Retroviruses Meeting, 1993.
23. Ratner L. Nef, The Role of Accessory Genes in HIV Pathogenesis, Am Soc for Microbiol, 1993.
24. Bandres JC and Ratner L. HIV-1 Nef downregulates the induction of NF-kB and AP-1 through a protein kinase C dependent mechanism. Inf Dis Soc of America, 1993.
25. Ratner L, Lu Y-L, Lindenbach B, and Horton R. Localization of VPR and PVX products of HIV-1 & 2 in virions and infected cells. Annual Meeting of the Laboratory of Tumor Cell Biology, 1993.
26. Ratner L and Bandres J. HIV-1 nef suppresses transcription through NF-kB and AP-1 in T-cells through a protein kinase C-dependent mechanism. 1st National Conf on Human Retroviruses and Related Infections, Washington DC, 1993.
27. Joseph T, Ratner L, and Arens M. RT-PCR detection and sequence analysis of nef mRNA during HIV-1 disease. 1st National Conference on Human Retroviruses and Related Infections, Washington DC, 1993.
28. Bukrinsky M, Lee M-A, Heinzinger N, Haggerty S, Ratner L, and Stevenson M. Nuclear targeting of HIV-1 genetic material: Vpr supplements MA NLS for the efficient transportation of the preintegration complex to the nucleus of macrophages. Xth International Conference on AIS, Yokohama, 1994.
29. Bandres JC and Ratner L. Regulation of nef function by myristylation and phosphorylation. Cold Spring Harbor Retroviruses Meeting, 1994.
30. Ratner L, McNearney T, Joseph T, and Arens M. Nef and LTR sequence variation from sequentially derived HIV-1 isolates. ColdSpring Harbor Retroviruses Meeting, 1994.
31. Bandres JC, Shaw AS, and Ratner L. HIV-1 nef protein downregulation of CD4 surface expression is mediated by the 1ck binding domain of CD4. Cold Spring Harbor Retroviruses Meeting, 1994.
32. Bandres JC and Ratner L. Regulation of nef function by myristylation and phosphorylation. ICAAC, 1994.

A Determinant within the HIV-1 gp120 Envelope Protein Critical for Infection of Primary Monocytes

Peter Westervelt and Lee Ratner

Departments of Medicine and Molecular Microbiology, Washington University School of Medicine, St. Louis, Missouri 63110

Howard E. Gendelman

*Department of Cellular Immunology
HIV Immunopathogenesis Program
Walter Reed Army Institute of Research
Rockville, Maryland 20850*

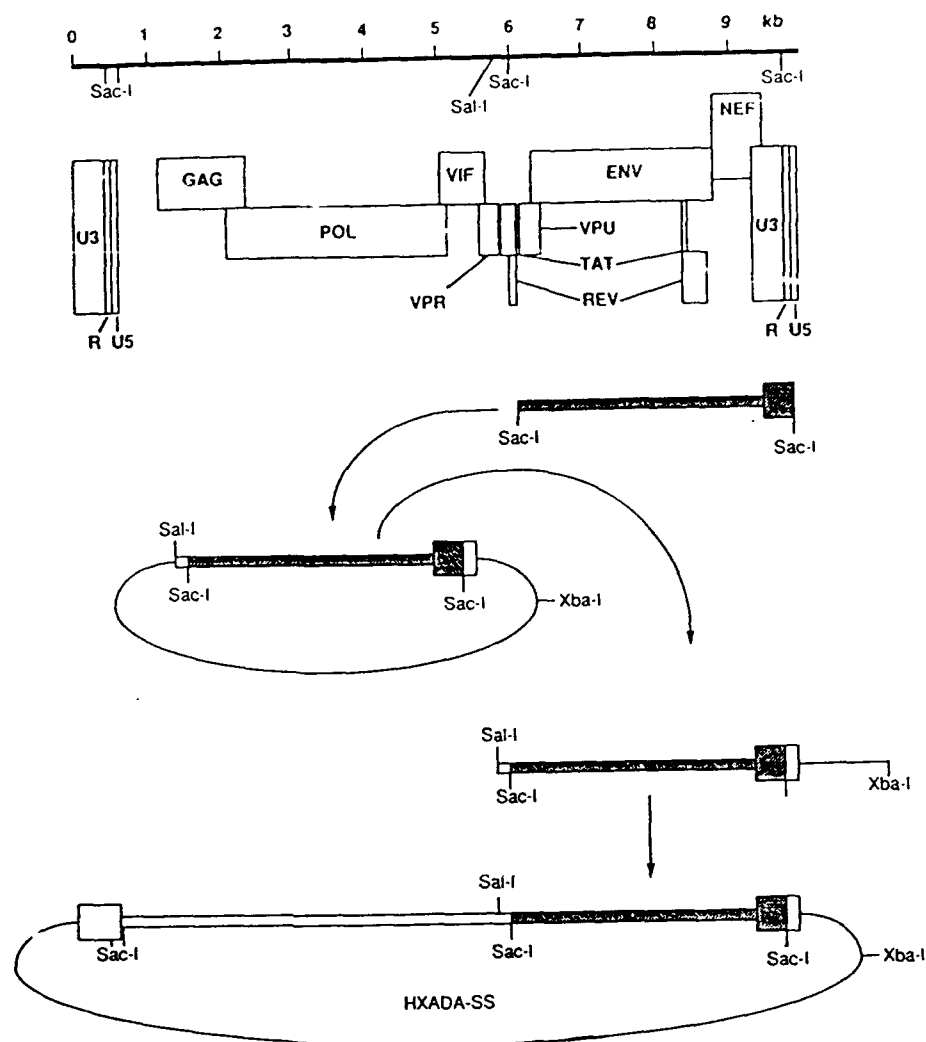
Yuexia Li

*Human Retrovirology Laboratory
University of Alabama
Birmingham, Alabama 35294*

Monocytes and tissue macrophages present a target for human immunodeficiency virus type 1 (HIV-1) infection in vivo in diverse tissues, including brain, spinal cord, lung, and lymph node, as documented by electron microscopy, immunohistochemistry, and in situ RNA hybridization methods (Gendelman et al. 1989). The potential importance of macrophage infection in AIDS is supported by the central role of infected macrophages in the pathogenesis of other lentivirus infections (e.g., visna-maedi and equine infectious anemia virus), in which the macrophage is believed to act as a silent reservoir of virus throughout the course of subclinical infection and disease (Narayan and Clements 1989). Despite these observations, however, profound differences have been observed in the abilities of various HIV-1 isolates to infect and replicate in primary monocytes cultured in vitro (Gartner et al. 1986; Koyanagi et al. 1987; Gendelman et al. 1988). The focus of this work therefore has been to identify molecular determinant(s) within the HIV-1 genome that control its ability to utilize primary monocytes as a host cell in vitro.

For these studies, we have employed the ADA HIV-1 isolate (Gendelman et al. 1988), which replicates to high levels in primary monocytes; the HXB2 proviral clone (Fisher et al. 1985), which is incapable of monocyte infection in vitro; and a full-length molecular HIV-1 clone, Yu2, isolated from infected brain tissue without prior passage in vitro (Y. Li et al., in prep.). DNA derived from an ADA-infected monocyte culture was used to isolate a partial molecular ADA-M clone, consisting of a 3.5-kb *SacI-SacI* fragment spanning *env*, *nef*, and *vpu*, and portions of *tat*, *rev*, and the 3' long terminal repeat (LTR) (Fig. 1). Sequence analysis demonstrated that each of these ADA-M open reading frames was intact and of full length, with 80–92% predicted amino acid sequence homology relative to HXB2 (not shown).

To study the biological properties of the ADA-M-encoded genes, all or portions of the 3.5-kb clone were exchanged for analogous HXB2 sequences to generate a panel of full-length, recombinant HXADA clones (Figs. 1 and 3). Virus stocks generated from these clones by transfection of SW480 or COS-7 monolayers were used to infect primary peripheral blood lymphocyte (PBL) or monocyte cultures. Virus replication was monitored by serial determination of reverse transcriptase (RT) activity in culture super-

**Figure 1**

ADA-M molecular cloning and recombinant construction. Hirt supernatant DNA was isolated from an ADA-infected primary monocyte culture, digested with *Sac*I, ligated into *Sac*I-digested λ -ZAP arms, and packaged to generate a phage library. Plaques (2.5×10^5) were screened with a labeled 3.5-kb *Sac*I-*Sac*I fragment from HIV-1 clone HXB2, spanning *env*, *nef*, and *vpu*, and portions of *tat*, *rev*, and the 3' LTR as diagramed. A single positive plaque was isolated, from which a phagemid was excised and shown to contain a 3.5-kb *Sac*I-*Sac*I insert (shaded box). The ADA-M clone was subcloned into a plasmid containing HXB2-derived *Sal*I-*Sac*I and *Sac*I-*Xba*I adaptor sequences (open box). The *Sal*I-*Xba*I fragment containing the ADA-M partial clone was then subcloned into an HXB2gpt2 plasmid lacking these sequences to generate a full-length recombinant clone, HXADA-SS. The 3.5-kb ADA-M clone was subdivided further to generate the panel of recombinant HXADA clones shown in Fig. 3.

natants. "Silent infection" of monocyte cultures that failed to generate levels of progeny virion release detectable by RT assay was determined ultimately by virus recovery following cocultivation with fresh, uninfected PBLs at 24 days postinfection.

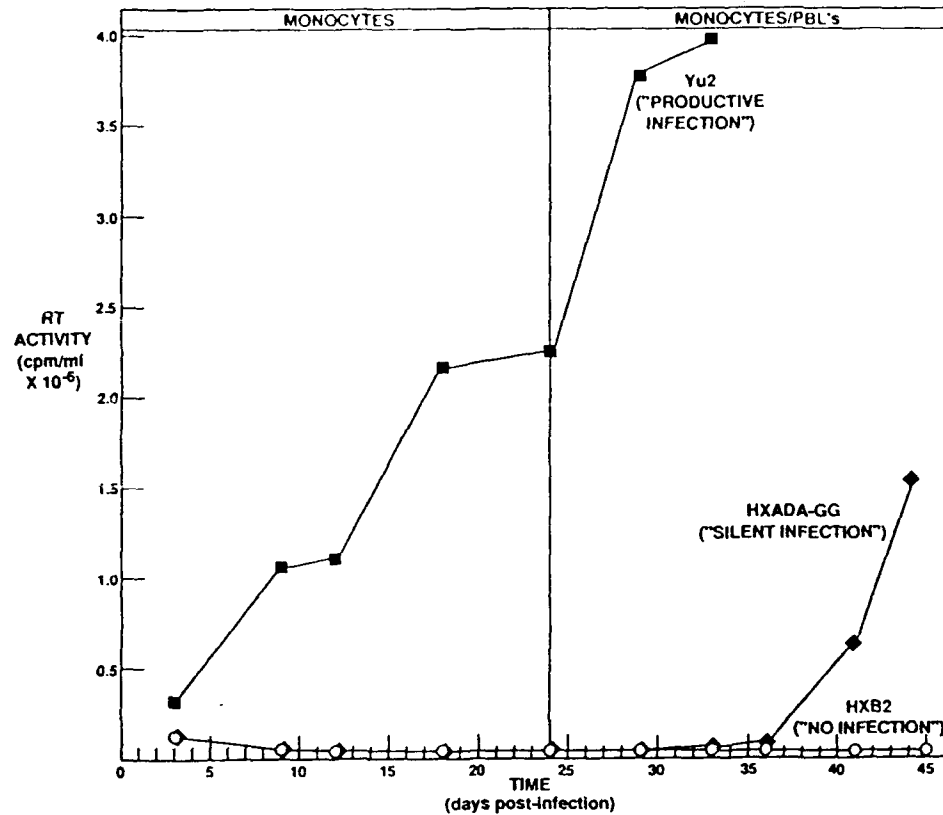
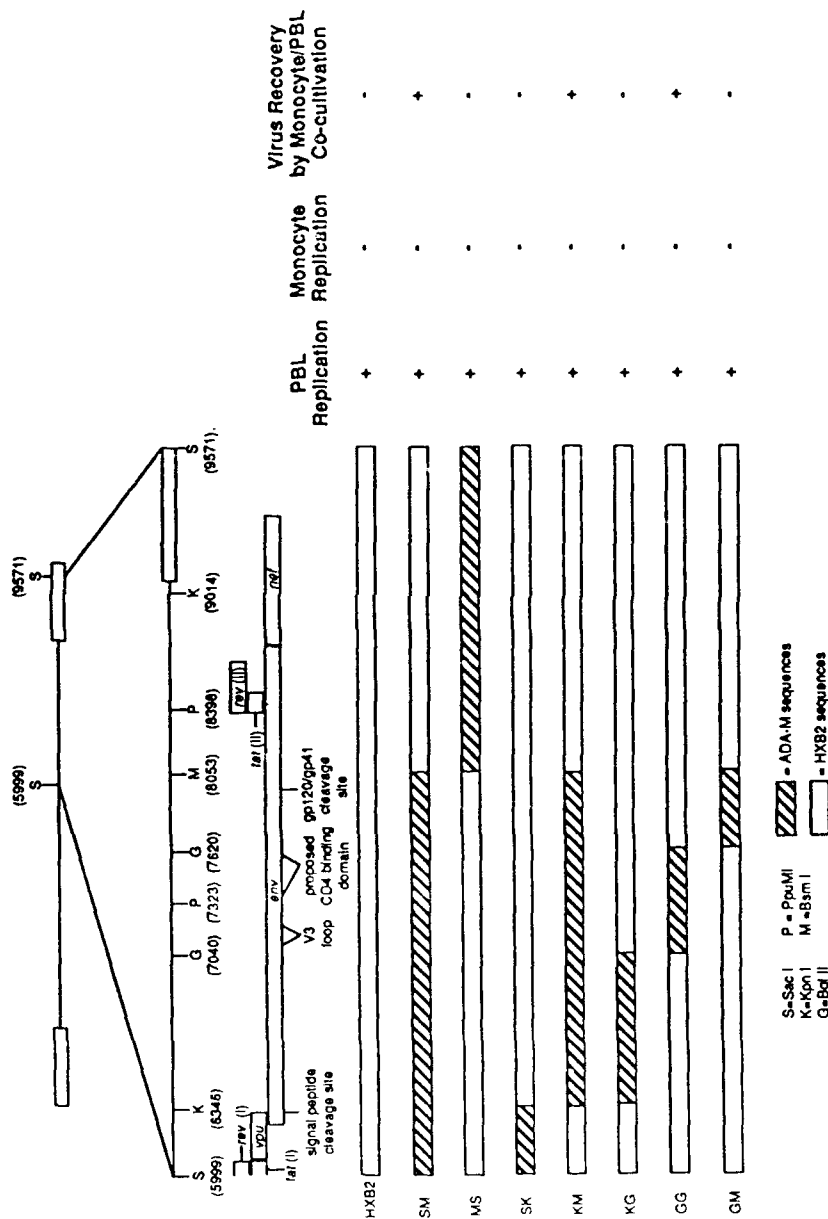


Figure 2

Replication of HIV-1 molecular clones in primary monocytes and virus recovery by PBL cocultivation. Data from three representative clones (Yu2, HXADA-GG, and HXB2), each of which demonstrated a distinct replication phenotype in primary monocytes, are shown. Virus stocks were prepared by transfection of 50% confluent SW480 or COS-7 cells with 10 μ g of proviral DNA by the calcium phosphate method. Filtered 1.0-ml culture supernatant aliquots harvested at 60 hr post-transfection were used to inoculate primary monocyte monolayers. Monocytes were purified by elutriation of leukaphoresis preparations obtained from normal donors and plated 7 days prior to infection in 24-well plates at a density of 200,000 cells per well. Monocytes were maintained in AIM-V medium (GIBCO) supplemented with 10% heat-inactivated normal human serum and 1000 cfu/ml rM-CSF. Virus replication was monitored by serial determination of RT activity in culture supernatants. At 24 days postinfection, cells were washed three times with phosphate-buffered saline (PBS) prior to the addition of 1 million fresh uninfected PBLs, which were purified by centrifugation onto Ficoll, stimulated with PHA (14 μ g/ml), and grown in RPMI medium supplemented with 10% heat-inactivated fetal calf serum, 4 mM glutamine, and 50 units/ml rIL2 for 4 days prior to cocultivation. Following 2 days of monocyte/PBL cocultivation, nonadherent cells were removed by vigorous pipetting and maintained in PBL growth medium for an additional 14–21 days. Virus recovery onto PBLs was determined by measurement of RT activity in culture supernatants.

HXB2, Yu2, and each of the HXADA clones generated high levels of replication in PBLs (more than 1 million cpm/ml RT activity; not shown). However, three distinct replication phenotypes were observed in primary monocytes (Fig. 2). Virus derived from the Yu2 clone rapidly achieved high levels of replication that were sustained throughout



Flaure 3

Figure 3
Summary of the replication properties of HXADA constructs in PBLs and monocytes. A panel of recombinant clones generated by reciprocal exchange of restriction fragments between HXB2 and the ADA-M clone is diagrammed above. The 3.5-kb *SacI-SacI* fragment of each clone is aligned with the relevant HIV-1 open reading frames and restriction sites. Each recombinant clone is identified on the left by letters assigned to the restriction sites that mark the borders between HXB2- and ADA-M-derived sequences. The ability of each clone to replicate in PBLs or monocytes and virus rescue from monocytes by PBL cocultivation as described in Fig. 2 are indicated on the right. + indicates at least two successive time points with RT activity tenfold higher than background

Figure 3
Summary of the replication properties of HXADA constructs in PBLs and monocytes. A panel of recombinant clones generated by reciprocal exchange of restriction fragments between HXB2 and the ADA-M clone is displayed above. The 3.5-kb *Sac*-*Sac* fragment of each clone is aligned with the relevant 1 open reading frame and restriction sites. Each recombinant clone is identified on the left by letters assigned to the restriction sites that mark the borders between HXB2- and ADA-M-derived sequences. The ability of each clone to replicate in PBLs or monocytes and virus rescue from monocytes by PBL cocultivation as described in Fig. 2 are indicated on the right. + indicates at least two successive time points with RT activity tenfold higher than background.

the 24-day culture period in monocytes, a phenotype designated productive infection. In contrast, neither HXB2 nor the recombinant HXADA clones generated detectable levels of virus replication in monocyte cultures. However, virus was recovered consistently following PBL cocultivation with monocyte cultures infected with HXADA clones that shared a 580-bp ADA-M-derived *env* sequence encoding amino acids 240–435 of the mature gp120 protein. The phenotype of monocyte infection without subsequent virus replication detectable by RT assay has been designated silent infection. Virus was never recovered from monocyte cultures infected with clones in which this *env* element was derived from HXB2 sequences, despite the inclusion of flanking ADA-M-derived sequences encoding *nef*, *vpr*, or the U3 portion of the 3' LTR. This phenotype has been designated no infection, although the possibility of a noninducible latent infection by these clones has not been excluded rigorously at present. These data are summarized in Figure 3.

On the basis of these experiments, it is apparent that three distinct phenotypes of virus replication are observed in primary monocytes using molecularly defined HIV-1 clones. A productive infection leads to rapid generation of high levels of virus replication, as seen with the Yu2 clone, as well as with the original ADA isolate and other primary HIV-1 isolates. Silent infection of monocytes, similar to that described by other investigators using primary isolates (Valentin et al. 1990), is observed with certain recombinant HXADA clones and is characterized by a lack of detectable replication, despite consistent virus recovery from monocytes after extended periods in culture by cocultivation with a sensitive target cell type.

Finally, HIV-1 clones such as HXB2 appear incapable of infecting primary monocytes, as indicated by our inability to rescue virus from these cells by cocultivation with PBLs. A 580-bp *env* sequence derived from the ADA-M clone, encoding the V3 loop and CD4-binding domain of gp120, is both necessary and sufficient to convert the no infection phenotype of HXB2 to that of silent infection.

Although these data clearly implicate *env* as a critical determinant for HIV-1 infection of primary monocytes, an obvious discrepancy exists between the productive infection phenotype of the ADA isolate and that of the HXADA clones that contain *env* sequences derived from that isolate but fail to replicate to high levels in monocytes. To account for this discrepancy, we propose two alternative models. According to the first model, *env* would be sufficient for infection of primary monocytes, but additional genetic elements would be required to attain high levels of virus replication. Since the ADA-M clone utilized in these studies comprised less than half of the HIV-1 genome, it is reasonable to speculate that other viral genes, such as *vpr* or *vif*, could act in concert with *env* to regulate the virus life cycle in primary monocytes. Alternatively, it is possible that *env* acts as the sole determinant of HIV-1 infection and replication in monocytes. In this scenario, differences in replication phenotype would reflect various degrees of adaptation to monocytes encoded in the critical *env* determinant of various clones, with the Yu2 and HXB2 clones situated at opposite ends of a continuous spectrum. The inability of specific HXADA clones to generate high replication levels in monocytes could be explained by this model if the virus from which the molecular clone was derived, a component of a presumably heterogeneous primary isolate, is postulated to have been only "moderately adapted" to monocyte replication.

Additional studies, including the construction of recombinants from the Yu2 clone, are under way to address these possibilities and to identify the steps in the HIV-1 life cycle that are regulated in the expression of these replication phenotypes in primary monocytes. An understanding of the molecular basis of both silent and productive HIV-1 infection of monocytes in vitro, facilitated by the use of molecularly defined clones, will provide valuable insight into the viral components of such complex and poorly understood phenomena in vivo as disease latency and progression to AIDS.

ACKNOWLEDGMENTS

We thank Brad Trowbridge and Nancy Vander Heyden for technical assistance; Eric Brown and Max Arens for gifts of primary monocytes and PBLs; Cetus for gifts of rIL2 and rM-CSF; the Walter Reed Retroviral Research Group for continued support; and Charlie Rice and John Majors for their advice and critical review. This work was supported by National Institutes of Health grant AI-24745, Department of the Army Medical Research and Development Command contract 17-90C-0125, the Washington University Medical Scientist Training Program grant (P.W.), and training grant 5T32AI07172 (P.W.). H.E.G. is a Carter-Wallace Fellow of the Johns Hopkins University School of Public Health and Hygiene. L.R. is an American Cancer Society Research Professor.

REFERENCES

- Fisher, A.G., E. Collalti, L. Ratner, R.C. Gallo, and F. Wong-Staal. 1985. A molecular clone of HTLVIII-B with biological activity. *Nature* 316: 262.
- Gartner, S., P. Markovits, D.M. Markovitz, M.H. Kaplan, R.C. Gallo, and M. Popovic. The role of mononuclear phagocytes in HTLV-III/LAV infection. 1986. *Science* 233: 215.
- Gendelman, H.E., J.M. Orenstein, L.M. Baca, B. Weiser, H. Burger, D.C. Kalter, and M.S. Meltzer. 1989. Review: The macrophage in the persistence and pathogenesis of HIV infection. *AIDS* 3: 475.
- Gendelman, H.E., J.M. Orenstein, M.A. Martin, C. Ferrua, R. Mitra, T. Phipps, L.M. Wahl, H.C. Lane, A.S. Fauci, D.S. Burke, D. Skillman, and M.S. Meltzer. 1988. Efficient isolation and propagation of human immunodeficiency virus onto CSF-1 stimulated human monocytes. *J. Exp. Med.* 167: 1428.
- Koyanagi, Y., S. Miles, R.T. Mitsuyasu, J.E. Merrill, H.V. Vinters, and I.S.Y. Chen. 1987. Dual infection of the central nervous system by AIDS viruses with distinct cellular tropisms. *Science* 236: 819.
- Narayan, O. and J.E. Clements. 1989. Review: Biology and pathogenesis of lentiviruses. *J. Gen. Virol.* 70: 1617.
- Valentin, A., J. Albert, E.M. Fenyo, and B. Asjo. 1990. HIV-1 infection of normal human macrophage cultures: Implication for silent infection. *Virology* 177: 790.

Simian Immunodeficiency Virus Negative Factor Suppresses the Level of Viral mRNA in COS Cells

THOMAS M. J. NIEDERMAN, WEN HU, AND LEE RATNER*

Departments of Medicine and Molecular Microbiology, Washington University School of Medicine,
Box 8125, 660 South Euclid, St. Louis, Missouri 63110

Received 20 August 1990/Accepted 29 March 1991

The *nef* gene is conserved among all human and simian lentiviruses. However, the amino acid similarity between simian immunodeficiency virus (SIV) and human immunodeficiency virus type 1 NEF is only 38%. To assess the role of SIV NEF on virus replication and compare its activity with that of its human immunodeficiency virus type 1 counterpart, we examined the activity of an intact *nef* gene from proviral clone pSIV 102, an isolate from SIV-MAC-251-infected cells. Proviral clone pSIV BA was constructed by introducing a premature termination codon at codon 40 of the *nef* gene without altering the predicted amino acid sequence of the overlapping *env* gene. These two clones were transfected into CD4⁺ COS cells, and virus replication was monitored by p27 enzyme-linked immunosorbent assay kits. In seven independent experiments, clone pSIV BA afforded two- to sixfold greater levels of viral antigen compared with those in clone pSIV 102 and two- to sixfold-increased levels of viral mRNAs as indicated with Northern (RNA) blot and S1 nuclease protection analyses. Nuclear run-on assays demonstrated a two- to threefold increased rate of RNA synthesis with nuclei isolated from cells transfected with pSIV BA compared with that from cells transfected with pSIV 102. In contrast, there was no apparent destabilization of SIV mRNAs by NEF, as measured in dactinomycin-treated cells. This study demonstrates that SIV NEF is a negative regulator of virus replication and acts by suppressing the level of mRNA synthesis and accumulation in COS cells.

Simian immunodeficiency virus (SIV) is closely related to human immunodeficiency virus types 1 (HIV-1) and 2 (HIV-2) (5, 25). Both SIV and HIV include an open reading frame at the 3' end of their genomes, the protein product of which has been named negative factor (NEF) (8). There is considerable amino acid sequence polymorphism, up to 17%, among the *nef* gene products of different HIV-1 strains (22, 26). However, there is a 62% amino acid sequence difference between the NEF proteins of SIV and those of HIV-1 (Fig. 1). Moreover, SIV NEF contains 250 amino acids, whereas HIV-1 NEF contains only 206 amino acids. Although *nef* is not required for virus replication or cytopathic effects in cultured cells (6), the gene has been conserved within all HIV and SIV genomes, which suggests that NEF serves an important function.

We and others have found that HIV-1 NEF suppresses virus replication (1, 2, 9, 16, 20, 24, 28). NEF mediates this suppression at the level of viral transcription (1, 24). However, others have been unable to demonstrate this negative effect (15, 19), indicating that NEF effects may be extremely sensitive to experimental conditions.

In this study, the role of SIV NEF on the replication of SIV MAC was examined in the CD4⁺ COS cell line. Although SIV and HIV-1 NEF proteins have only 38% sequence similarity, the two proteins mediate downregulation of virus production by suppressing the rate of viral transcription and mRNA accumulation. SIV *nef*-positive and -negative proviral clones will be useful in assessing the physiologic role of NEF in macaques infected with virus derived from these clones. This animal model may then contribute to our understanding of viral latency in vivo.

MATERIALS AND METHODS

DNA clones. Clone PK102 (kindly provided by B. Hahn, University of Alabama at Birmingham School of Medicine) contains a full-length SIV genome cloned into bacteriophage lambda gt10 (14). Lambda PK102 DNA was digested with *Eco*RI and cloned into the *Eco*RI site of the plasmid expression vector pSV2gpt (21) to produce clone pSIV 102 ERL. This clone has four *Sac*I sites, two in the SIV genome (nucleotides [nt] 5731 and 9208) and two in the cellular flanking sequences. Clone pSIV 102 SDS was obtained from pSIV 102 ERL by removing the 3.5-kb *Sac*I fragment and destroying the two *Sac*I sites in the flanking sequence by excising the 0.3-kb sequence between the two sites and annealing a *Sac*I-*Sac*I adapter that destroys the *Sac*I site. A full-length, proviral clone with an intact *nef* gene, pSIV 102, was constructed by returning the 3.5-kb *Sac*I fragment to clone pSIV 102 SDS.

To generate a *nef* mutant proviral clone that is otherwise isogenic, the 3.5-kb *Sac*I fragment was subcloned into the plasmid vector pUC19 (Pharmacia) to form pUC19-SIV 3.5. Polymerase chain reaction mutagenesis was performed with a primer overlapping the *Bgl*II site (nt 9100) and a mutant primer overlapping the *Avr*II site (nt 9184), GGTTGGAAGATGGATCTTAGCAATCCCTAGGAGG, which contains a C-to-T transition and a C-to-A transversion, which introduce a termination codon at *nef* amino acid position 40 without altering the amino acid sequence of the overlapping *env* gene (Fig. 2). The nucleotide changes also eliminated the *Bam*HI site at nt 9170 by converting the sequence GGATCC to GGATCT. The mutation was confirmed by restriction enzyme digestion and sequence analysis. In addition, sequence analysis of the entire *nef* gene of clones pSIV 102 and pSIV BA confirmed that no additional cloning artifacts had occurred. The mutant *Bgl*II-*Avr*II fragment was substituted into the corresponding sites in pUC SIV 3.5. The mutant 3.5-kb *Sac*I fragment from pUC SIV 3.5 was inserted into

* Corresponding author.

	Site of Myristoylation	PKC Phosphorylation Site	
HIV-1	MGG...KWSKSSVIGWPTV-RERMRAEPAAD-----CVC--AASRDLEKH		40
SIVmac	MGGATSMRRSKPAGDLRQKLLRARCETCYGRLLGEVEDCSQSLGGLKGLSSRSCEGQ		58
HIV-1	GATTS--NTAANNAACAVLEAQ-----EEEKVGFPVTHQVPLRPMTYKAA		84
SIVmac	KYNQOQYHNTPWNRPAEEKEKLAYRKQNMDDIDEEDDLVGVSVRPKVPLRAMTYKLA		117
HIV-1	VDSLHFLKEK GGLEGLIHSQRRQD LD LWIWHTQCYFPDQWNYTPGPGIRYPLTFG		140
SIVmac	IDMSHFIEK GGLEGLIYSARRRR LD MYLEKEEGIIIPDQDYTSQPGIRYKPTFG		172
HIV-1	WRYKLVPVEPEKLEEAANKGENTSLLHPVSLHCHDDPEREVLG-WRFDRLAFHHVARE		198
SIVmac	WLWKLVPVNVSDAEQEDERHYLMQPAQTSKV--DDPWCEVLLAWKSQPTLAYTYEAYV		231
HIV-1	LHPEYFKNC		206
SIVmac	RYPEELEASQACQKRILEEG		250

FIG. 1. Amino acid alignment of the NEF proteins derived from HIV-1 (HXB2/3gpt [24, 26]) and SIV isolate 102 (derived from SIV MAC-251 [22]). Based on this alignment, there is a 38% sequence similarity between HIV-1 NEF and SIV NEF. Both forms of NEF may be myristoylated and share sequence similarity to the nucleotide binding domain of G proteins (boxed sequences).

clone pSIV 102 SDS to generate the *nef*-negative clone pSIV BA.

The chloramphenicol acetyltransferase (CAT) expression plasmid pSV2CAT was described previously (10). The actin cDNA clone was kindly provided by J. Milbrandt (4). The *AluI* probe was derived from a *c-sis* genomic clone, pL33M (17). The neomycin resistance gene (*neo*) expression clone pCB6 utilizes the simian virus 40 early promoter to express *neo* mRNA and was kindly provided by Evan Sadler, Howard Hughes Medical Institute.

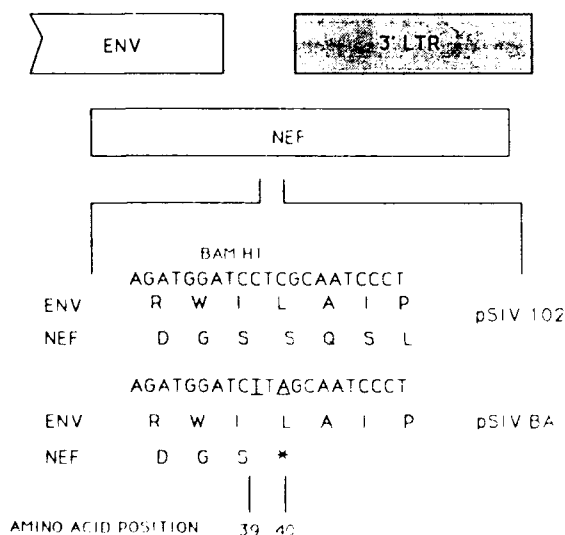


FIG. 2. Construction of *nef* mutant clone pSIV BA from wild-type clone pSIV 102. A premature termination codon was engineered at codon 40 of the *nef* gene by using polymerase chain reaction site-directed mutagenesis with a synthetic oligonucleotide spanning the mutated region. The truncated NEF protein contains only the first 39 amino acids, but the ENV protein is unaffected by the mutation since *env* and *nef* lie in different reading frames.

DNA transfection and cells. COS-7 cells are derived from African green monkey kidney cells, which do not express CD4 molecules at the cell surface and therefore cannot be infected by SIV. These cells were used because they are easily transfected and provide a system for examining the role of *nef* in a system not complicated by the possibility of multiple rounds of reinfection by viruses generated during transfection.

Proximal DNAs for transfections were purified twice by cesium chloride density centrifugation. DNA concentration was determined by optical absorption measurements and confirmed by using agarose gel electrophoresis with ethidium bromide staining. DNA clones were transfected by diluting the DNA in 4.5 ml of Dulbecco modified Eagle medium (DME) and adding 0.5 ml of a DEAE-dextran solution containing 70 ml of DME, 25 ml of 1 M Tris (pH 7.3), and 5 ml of 25-mg/ml DEAE-dextran (Sigma Chemical Co.). After the DNA solution was mixed, it was added to 60 to 80% confluent COS-7 cells on 100-mm tissue culture plates. After 4 h, the DNA solution was replaced by 5 ml of 100 μ M chloroquine (Sigma) in DME supplemented with 10% fetal calf serum, 50 U of penicillin per ml, 50 μ g of streptomycin per ml, and 1 mM pyruvate (DME-S). After 2 h, the cells were shocked for 2.5 min at room temperature with 2 ml of 10% dimethyl sulfoxide in DME-S, washed with phosphate-buffered saline (PBS), and cultured with DME-S at 37°C in a 5% CO₂ atmosphere.

Detection of p27^{gag} core protein. Cell-free supernatants of transfected COS cells were analyzed according to the protocols of the manufacturers with a SIV p27 enzyme-linked immunosorbent assay (ELISA) kit (Coulter) or an HIV-1 p24 kit (Abbott) with significant immunological cross-reactivity for SIV-MAC p27^{gag} antigen.

Detection of SIV proteins. At 60 h posttransfection, COS cells were metabolically labeled for 6 h with 500 μ Ci of [³⁵S]methionine and [³⁵S]cysteine (ICN; specific activity, >1,000 Ci/mmol) in 3 ml of methionine- and cysteine-free DME supplemented with 5% dialyzed fetal calf serum. Cells were washed and harvested by scraping in PBS, and the cell pellet was solubilized in 750 μ l of protein-solubilizing buffer (0.1% SDS, 0.5% deoxycholate, 1.0% Triton X-100 [Sigma] in PBS). A 200- μ l aliquot of solubilized cells was precleared with uninfected macaque serum and then immunoprecipitated with 2 μ l of serum from an SIV-infected macaque (kindly provided by R. Desrosiers, New England Primate Research Center). Immunoprecipitates were washed and subjected to 7.5 to 20% gradient sodium dodecyl sulfate (SDS)-polyacrylamide gel electrophoresis (PAGE). The gels were fixed, enhanced with Amplify (Amersham), dried, and exposed to Kodak XAR-5 film at -90°C.

RNA analyses. (i) **Northern blot analysis.** COS cells were washed with PBS and harvested by scraping, and RNA was isolated as described previously (3). RNA was denatured at 65°C for 10 min, electrophoresed on a 1.3% agarose formaldehyde gel, and transferred to a Nitroplus 2000 hybridization membrane (Micron Separations Inc.). Filters were baked in vacuo at 80°C for 90 min and prehybridized for 2 h in 50% formamide-5 \times SSC (1 \times SSC is 0.15 M NaCl plus 0.015 M sodium citrate)-1% SDS-50 mM NaPO₄ (pH 7.5)-5 \times Denhardt medium-200 μ g of yeast tRNA per ml-50 μ g of sheared salmon sperm DNA per ml. Filters were probed for 18 h at 37°C with random hexamer primer-labeled fragments generated from the internal 3.5-kb *SacI* fragment from clone pSIV 102 or from the 2.0-kb *HindIII* fragment of the actin cDNA clone. Filters were washed three times at 65°C in 0.5 \times SSC-0.1% SDS and exposed to Kodak XAR-5

film at -90°C . Ten percent of the cells were saved for CAT activity analysis.

(ii) **S1 nuclease protection assay.** DNA probes were constructed by digesting clone pSIV 102 with *Stu*I, isolating the 590-bp fragment extending from nt 369 to 959, and end labeling with $[\gamma\text{-}^{32}\text{P}]\text{ATP}$ (ICN; specific activity, 3,000 Ci/mmol [1 mCi = 37 mBq]) or by digesting clone pSIV 102 with *Ava*I (nt 1494), end labeling, digesting with *Bsu*36I, and isolating the 1.4-kb *Bsu*36I-to-*Ava*I fragment extending from nt 95 to 1494. A probe for *neo*-specific mRNA was generated by end labeling the 0.65-kb *Ava*II-to-*Pvu*II fragment, which is contained exclusively in the *neo* gene, from the *neo* expression clone. Total cellular RNA (12 or 18 μg) from transfected COS cells was hybridized to either probe at 56°C for 90 min and then at 53°C for 90 min in 80% formamide–40 mM PIPES [piperazine-*N,N'*-bis(2-ethanesulfonic acid)] (pH 6.4)–1 mM EDTA–0.4 M NaCl. Samples were cooled to 16°C and digested for 30 min by adding 0.3 ml of ice-cold S1 buffer (0.28 M NaCl, 0.05 M sodium acetate [pH 4.6], 4.5 mM ZnSO_4 , 20 μg of sheared salmon sperm DNA per ml) containing 1,000 U of S1 nuclease (Pharmacia) per ml. Reactions were stopped by adding 50 μl of 4.0 M ammonium acetate–0.1 M EDTA. Then 10 μg of yeast tRNA was added, and the nucleic acids were precipitated with ethanol. Precipitates were dried, suspended in 20 μl of loading buffer (38% formamide, 8 mM EDTA, 0.002% bromophenol blue, 0.002% xylene cyanol FF), and subjected to denaturing PAGE (5% polyacrylamide) with 50% urea. Gels were dried and exposed to Kodak XAR-5 film for 3 days at -90°C . Ten percent of the cells were saved for CAT activity analysis.

Nuclear run-on assays. Nuclear run-on assays were performed as described (24) with the exception that 1.0- μg samples of plasmids pL33M, pSV2gpt, and pSIV 102 were used as the cold DNA targets immobilized on the nitrocellulose filters.

Dactinomycin analysis. COS cells (70% confluent) in 75-cm flasks were transfected with 12 μg of either pSIV 102 or pSIV BA. At 24 h posttransfection, cells were trypsinized and the pSIV 102 and pSIV BA flasks were separately pooled and seeded onto 150-mm plates. At 24 h after reseeding, media was replaced with DME-S containing 5 μg of dactinomycin (Sigma) per ml, and cells were harvested for RNA at 0, 12, 24, 36, and 48 h posttransfection. Isolated RNA was subjected to Northern blot analysis and probed with hexamer primer-labeled fragments derived from the 3.5-kb *Sac*I fragment or to labeled actin sequences.

CAT assays. The pSV2CAT expression vector and the assay protocol were described previously (10).

RESULTS

pSIV 102 and pSIV BA direct the synthesis of SIV proteins. A functional SIV proviral clone with an intact *nef* gene, pSIV 102, was used to generate an otherwise isogenic *nef* mutant, pSIV BA, by polymerase chain reaction site-directed mutagenesis (Fig. 2). The predicted length of the mutant NEF protein is truncated from 250 to 39 amino acids. Proviral clones pSIV 102 and pSIV BA and negative control plasmid pSV2gpt were transfected into COS cells, which were then metabolically labeled with $[\text{S}]\text{methionine}$ and $[\text{S}]\text{cysteine}$ and immunoprecipitated with antiserum from an infected macaque. The cells transfected with the proviral clones demonstrate the presence of precursor and processed *gag* proteins, whereas the cells transfected with the negative control do not (Fig. 3). Equal volumes of cell lysate were applied to the gel; however, Bradford protein analysis and

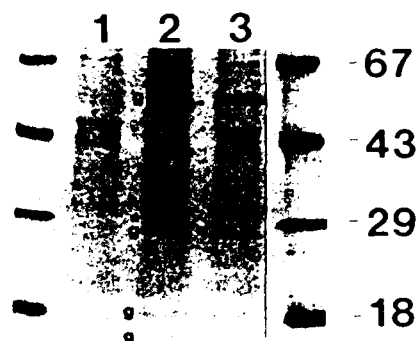


FIG. 3. Expression of SIV NEF and GAG proteins. COS cells were transfected with 10 μg of pSV2gpt (lane 1), pSIV 102 (lane 2), or pSIV BA (lane 3). At 48 h posttransfection, cells were labeled with $[\text{S}]\text{methionine}$ and $[\text{S}]\text{cysteine}$ and immunoprecipitated with serum from an infected macaque. Immunoprecipitated samples were then denatured and subjected to SDS-PAGE in a 7.5 to 20% gradient. *, NEF protein expressed in pSIV 102-transfected cells; g, precursor and processed *gag* proteins in pSIV 102- and pSIV BA-transfected cells.

densitometric scanning of background bands indicate that protein concentration was 3.5-fold greater in the pSIV 102 sample than in the pSIV BA sample. Additionally, densitometric analysis indicates that the intensity of the p27 *gag* band was 1.5-fold greater in the pSIV 102 lane than in the pSIV BA lane. Therefore, in this experiment, there was a 2.3-fold suppression of p27 with clone pSIV 102 compared with that for pSIV BA. As expected, NEF protein was identified only in cells transfected with clone pSIV 102 (Fig. 3, lane 2). The apparent molecular mass of NEF protein, calculated by using the size markers indicated, was 29.5 kDa, which agrees well with the predicted molecular mass of 29 kDa.

NEF downregulates SIV replication in COS cells. To assess the role of *nef* on the replication of SIV, COS cells were transfected with proviral clones pSIV 102 and pSIV BA. Supernatants from transfected cells were solubilized and screened for viral antigens by using a p27 SIV ELISA kit (Fig. 4A) or a p24 HIV ELISA kit (Fig. 4B). In seven independent experiments with different DNA preparations and cell stocks, the clone lacking *nef* pSIV BA, consistently afforded two- to sixfold-higher levels of virus particles in the supernatant compared with those in pSIV 102. Transfection efficiency was measured by cotransfecting with pSV2CAT and measuring CAT activity in cellular protein extracts. This analysis indicated that the mean values of CAT activity were $6.1\% \pm 3.0\%$, $4.9\% \pm 3.0\%$, and $4.7\% \pm 1.8\%$ for the pSV2gpt-, pSIV 102-, and pSIV BA-transfected cells, respectively. These values represent the percentage conversion to acetylated products and were in the linear range of analysis.

NEF decreases the level of SIV mRNA accumulation. To assess the step in the virus life cycle that was downregulated by NEF, Northern blot analysis was performed. COS cells were transfected with pSIV 102 or pSIV BA; at 72 h posttransfection, cells were harvested, and total cellular RNA was prepared and subjected to Northern blot analysis (Fig. 5). The level of SIV 9.0-kb mRNA was on the average 4.5-fold greater from the cells transfected with clone pSIV BA than from cells transfected with pSIV 102. Similarly, the level of the SIV 4.5-kb single-spliced *env* mRNA was threefold higher in the absence of NEF protein with pSIV BA

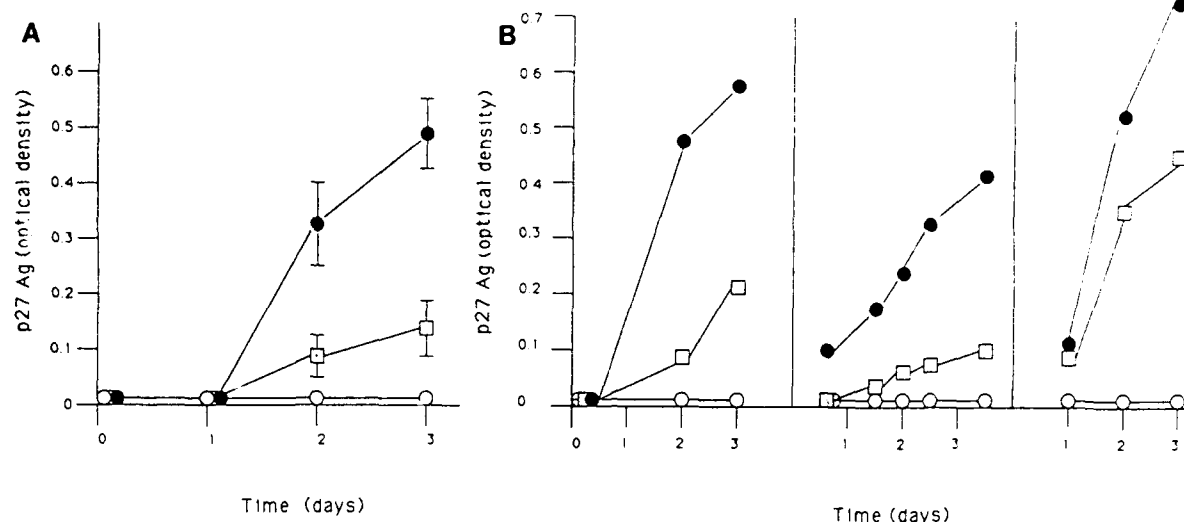


FIG. 4. NEF downregulates SIV replication in transfected COS cells. In seven independent experiments, 10 μ g of either pSV2gpt, pSIV 102, or pSIV BA was transiently transfected into COS cells. An aliquot of the overlying medium was removed at the indicated times after transfection and assessed for solubilized p27^{K_{KK}} core protein with (A) a Coulter SIV p27 ELISA kit or (B) an Abbott p24 HIV ELISA kit. (A) Averages of four experiments with error bars indicating 1 standard deviation from the mean. (B) Three different experiments. Transfection efficiency was monitored by cotransfecting pSV2CAT and measuring CAT activity; however, this parameter did not vary by more than 10% in any given experiment. For panel A, 1 optical density unit is approximately equal to an antigen concentration of 15 ng/ml. Symbols: ○, pSV2gpt; □, pSIV 102; ●, pSIV BA.

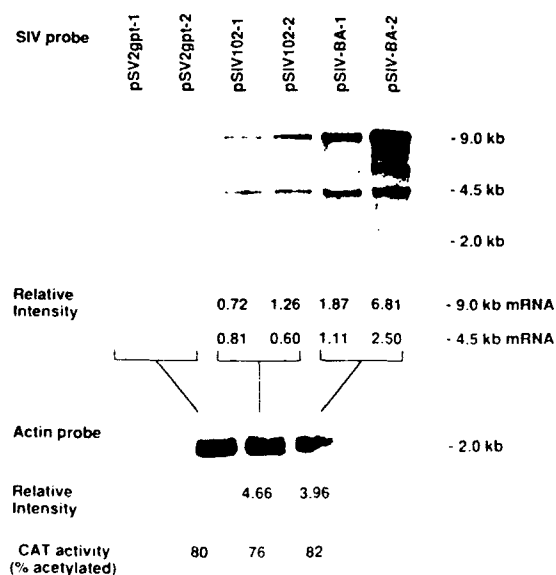


FIG. 5. SIV NEF decreases viral mRNA accumulation. COS cells were transfected with 10 μ g of either pSV2gpt, pSIV 102, or pSIV BA and cotransfected with clone pSV2CAT to control for transfection efficiency. Total cellular RNA was isolated 3 days after transfection from 90% of the cells and subjected to Northern blot analysis. Protein extracts were prepared from the remaining 10% of the cells for CAT analysis. Hybridization was performed with hexamer-primed probes generated from the 3.5-kb *SacI* fragment from clone pSIV 102. In this experiment, duplicate transfections were performed. RNAs from experiments 1 and 2 were combined equally, subjected to Northern blot analysis, and hybridized to actin sequences that demonstrated that similar amounts of RNA were applied to the gel. CAT activities were similar within the linear range of analysis.

than in the presence of NEF with pSIV 102 based on densitometry analysis of the bands. All three major viral RNA species were detected, and the presence or absence of NEF protein did not appear to alter their relative abundance. The probe used in this analysis, derived from the 3.5-kb *SacI* fragment, hybridized weakly to the 2.0-kb double-spliced mRNAs. Hybridization of the same RNA samples to actin sequences was used to correct for differences in RNA extraction and concentration determinations. Transfection efficiency was assessed by cotransfecting the cells with pSV2CAT and was similar in all samples (Fig. 5). This analysis was repeated twice with comparable results.

S1 nuclease protection assays provided further evidence that SIV mRNA accumulation is depressed in cells transfected with the NEF-expressing proviral clone (Fig. 6). Total cellular RNA from transfected cells was hybridized with end-labeled DNA probes extending from nt 95 to 1494 (Fig. 6A) or nt 369 to 959 (Fig. 6B), where the RNA initiation (CAP) site is at nucleotide position 507. In addition to the SIV probe in Fig. 6B, an end-labeled DNA probe for *neo* mRNA was also added to the hybridization reactions (Fig. 6C). The mRNAs presented in Fig. 6C were isolated from cells cotransfected with 5 μ g of the *neo* expression vector pCB6. With the longer SIV probe, in experiments 1 and 2, respectively, there were 6.6- and 4.7-fold increases in the level of the protected, correctly initiated viral RNA from cells transfected with clone pSIV BA compared with that from cells transfected with pSIV 102 (Fig. 6A). There was also a significant increase in the level of a spliced RNA species, recently described by Viglianti and coworkers (29), in cells transfected with pSIV BA compared with that in cells transfected with pSIV 102. With the shorter probe, there was a 4.4-fold increase in protected RNA of the expected size from the cells transfected with pSIV BA compared with that in cells transfected with pSIV 102 (Fig. 6B). There was also an increase in protected spliced RNA with proviral clone pSIV BA compared with that with pSIV 102. With the

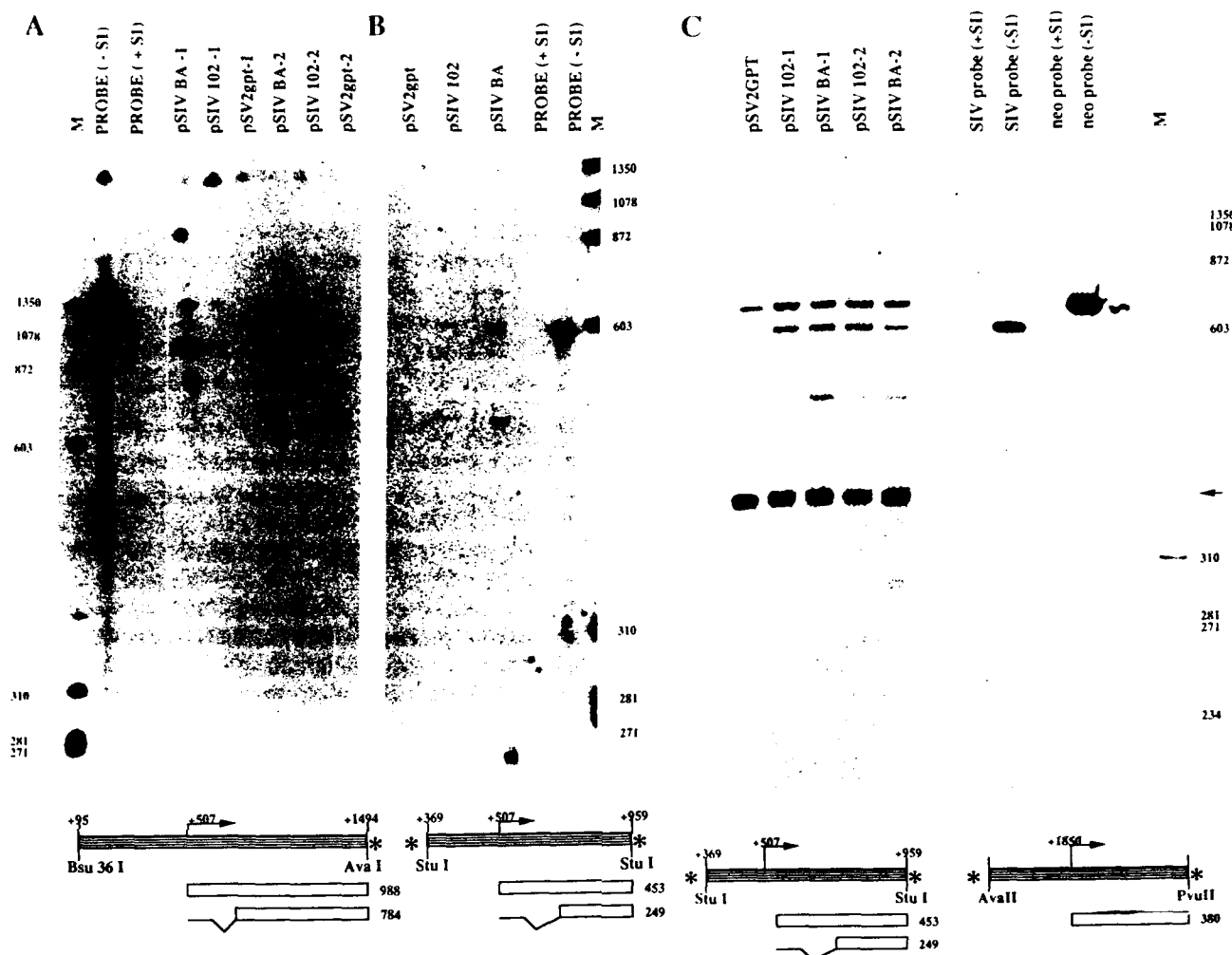


FIG. 6. SIV NEF decreases steady-state levels of SIV mRNA and does not affect the transcription start position. COS cells were transfected with proviral clones pSIV 102 and pSIV BA, and total cellular RNA was isolated 72 h later. RNA was annealed to either the *Bsu36I* (nt 94)-to-*AvaI* (nt 1494) fragment (A) or the 590-nt *StuI* fragment (B). RNA was annealed to the 590-nt *StuI* probe and the 655-nt *AvaII*-to-*PvuII* *neo* probe in panel C. Samples were then digested with S1 nuclease, and the protected, labeled DNA fragments were separated on denaturing PAGE (5% polyacrylamide). Symbols: \blacksquare , length of the probe; \square , region of protection; *, labeled sites. The numbers next to the empty boxes indicate the lengths of the protected fragments of the unspliced and spliced transcripts (29). The arrow over the striped box at nt 507 indicates the RNA CAP site. Panel A represents two independent experiments (1 and 2), panel B represents a third experiment, and panel C represents two additional independent experiments. Transfection efficiency, measured by cotransfecting pSV2CAT and assaying CAT activity (percent acetylation), was determined for all transfections. In part A, the mean CAT activity was $3.0\% \pm 0.4\%$ and $3.9\% \pm 0.7\%$; in part B, the activity was 3.9% and 3.4% ; and in part C, the mean activity was $70\% \pm 6\%$ and $69\% \pm 6\%$ for pSIV 102- and pSIV BA-transfected cells, respectively. In addition, the intensity of the protected *neo* probe (band indicated by arrow on right) was determined, and the value was used to adjust the relative concentration of viral mRNAs from transfected cells.

shorter SIV probe in the experiments presented in Fig. 6C, there was a mean 2.3-fold decrease in the unspliced mRNA from pSIV 102 compared with that in mRNA from pSIV BA and a 2.1-fold decrease in the spliced mRNA species. Hybridization to the *neo* probe demonstrated similar transfection and RNA extraction efficiencies and was used to calculate the ratio of SIV to *neo* mRNAs from pSIV 102- and pSIV BA-transfected cells. Transfection efficiency, measured by cotransfection of pSV2CAT, was similar in all transfections. In the experiments shown in Fig. 6A, B, and C, the mean CAT activities were 3.0 and 3.9%, 3.9 and 3.4%, and 70 and 68% for pSIV 102 and pSIV BA, respectively. Hybridization of the RNAs to actin sequences was performed to confirm that extraction efficiency and concentra-

tion determinations were similar in all RNA preparations. The increased level of full-length protected probe in the lanes with RNA from pSIV BA-transfected cells compared with those from the pSV2gpt- or pSIV 102-transfected cells in Fig. 6 may represent effects on an aberrantly initiated transcript.

NEF suppresses the rate of SIV mRNA transcription. To determine whether the effects of NEF protein on mRNA accumulation could be accounted for at the level of RNA synthesis, nuclear run-on assays were performed. COS cells were transfected, nuclei were isolated, and preinitiated mRNA transcripts were labeled *in vitro* with [α - 32 P]UTP. The ratio of hybridization of labeled RNAs to SIV sequences to that of *AluI* sequences was twofold higher with nuclei

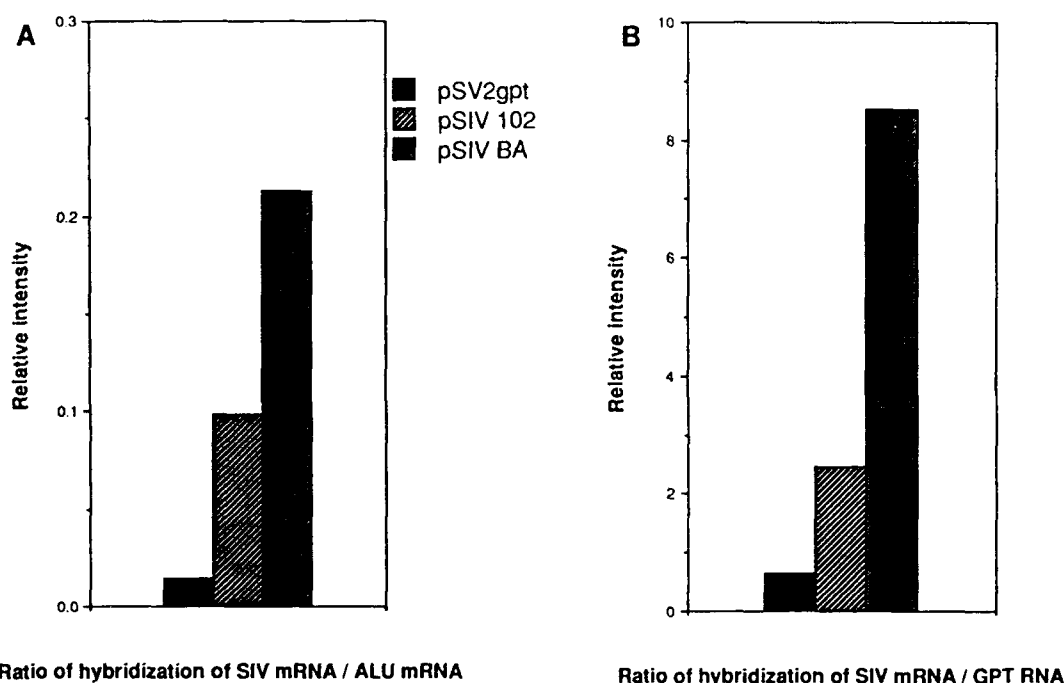


FIG. 7. SIV NEF decreases the rate of viral RNA synthesis. Nuclear run-on assays were performed with [α - 32 P]UTP (specific activity, 3,000 Ci/mmol) to label nuclei isolated from COS cells transfected with 10 μ g of pSV2gpt, pSIV 102, or pSIV BA. The nascent, labeled transcripts were hybridized to SIV sequences (pSIV 102), *AluI* repetitive sequences (pL33M), or *gpt* sequences (pSV2gpt) to control for the efficiency of labeling, RNA yield, and transfection efficiency. Hybridization intensity was measured by densitometry and is expressed as the ratio of hybridization to SIV sequences to that to *AluI* (A) or *gpt* (B) sequences.

isolated from pSIV BA-transfected cells than with nuclei from pSIV 102-transfected cells (Fig. 7A). The ratio of hybridization of labeled transcripts to SIV sequences to that of xanthine-guanine phosphoribosyl transferase (*gpt*) sequences was threefold greater with nuclei from pSIV BA transfected cells than with nuclei from pSIV 102-transfected cells (Fig. 7B). Hybridization to *AluI* sequences corrects for labeling efficiency, RNA extraction, and concentration of RNA used for hybridization. Hybridization to *gpt* sequences corrects for transfection efficiency, since proviral clones pSIV 102, pSIV BA, and pSV2gpt express *gpt* mRNA at the same level. This experiment was repeated twice with similar results.

NEF does not destabilize SIV mRNA. To assess whether NEF-induced RNA degradation contributes to decreased steady-state levels of mRNAs, viral mRNA stability was measured. COS cells transfected with pSIV 102 or pSIV BA were treated with the RNA synthesis inhibitor dactinomycin and harvested 0, 12, 24, 36, and 48 h later. RNAs were subjected to Northern blot analysis, which revealed a relatively intense signal for the 4.5-kb single-spliced *env* transcript compared with that of the 9.0-kb unspliced transcript (Fig. 8); therefore, RNA measurements were performed on the *env* transcript. There was no apparent difference in the kinetics of RNA degradation in the presence (pSIV 102) or absence (pSIV BA) of an intact *nef* gene. Cells transfected with either clone displayed an RNA half-life of approximately 9 h. Hybridization of RNA to actin sequences was used to correct for RNA extraction efficiency and concentration determinations. Hybridization to *c-myc* sequences indicated that dactinomycin treatment of cells was effective in halting RNA synthesis (data not shown). The observation that the single-spliced mRNA species was more intense in

this experiment than in the Northern blot in Fig. 5 may be due to the fact that these mRNAs were harvested at 48 h rather than 72 h posttransfection. Furthermore, the cells in this experiment were scraped at 24 h posttransfection and replated. It is also possible that the RNA blotting process was less efficient in this experiment than in the experiment of Fig. 5 in that the larger unspliced species failed to transfer as well. This experiment was repeated with comparable results.

DISCUSSION

Conservation of the *nef* gene in both simian and human immunosuppressive viruses suggests that the gene plays an important role in the biology of these lentiviruses. To define this role, a *nef*-positive SIV proviral clone (pSIV 102) and a *nef*-negative clone (pSIV BA) were compared. The *nef* gene product was found to suppress the rate of transcription and level of viral RNAs.

The initial comparison of the *nef*-positive and -negative proviral clones involved transfecting them into COS cells and assaying the overlying culture medium for the SIV p27 core protein. The level of p27 in the media of cells transfected with proviral clone pSIV BA was two- to sixfold higher than that of cells transfected with clone pSIV 102 (Fig. 4). This result is consistent with the role of NEF as a negative factor with respect to virus replication.

We found previously that the HIV-1 *nef* gene product did not affect the infectivity of virus particles (24). This is consistent with the data in the current study indicating that SIV NEF suppressed virus replication in cells that were unable to be infected by virus particles generated during transfections. Thus, the steps involved with the first half of the virus life cycle, i.e., virus binding, uptake, uncoating,

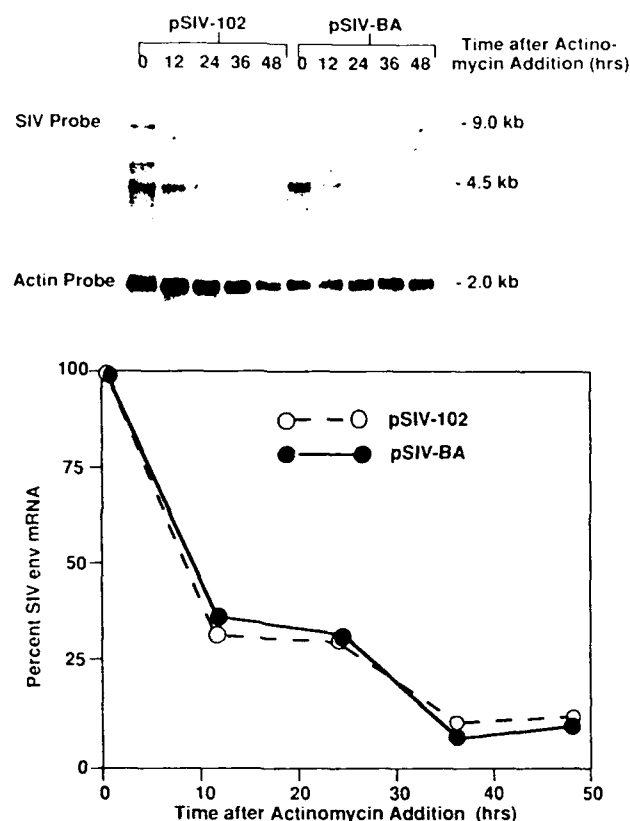


FIG. 8. SIV NEF does not destabilize SIV mRNAs. COS cells (in eight 75-mm flasks) were transfected with either clone pSIV 102 or pSIV BA. At 24 h after transfection, the COS cells were harvested and pooled with similarly transfected cells and replated onto 150-mm plates. At 24 h after replating, the cells were incubated with dactinomycin for 0 to 48 h. At the indicated times, total cellular RNA was isolated and subjected to Northern blot analysis. The blot was first hybridized with the SIV probe as in the experiment shown in Fig. 4, exposed to film, stripped of RNA, and rehybridized to an actin probe as a control for the amount of RNA loaded on the gel. In this analysis, the stability of the 4.5-kb *env* mRNA was measured because it was the predominant species. At each time point, the calculated amount of SIV mRNA was determined by densitometry and the level of *env* mRNA was adjusted to the amount of actin mRNA.

reverse transcription, and integration, are not the primary target for NEF-mediated suppression. Instead, we found that NEF was active during the second half of the virus life cycle, i.e., during transcription, RNA processing and translocation, and translation. Northern blot analysis with RNA extracted from COS cells transfected with the proviral clones showed that the steady-state levels of viral RNAs were three- to fourfold lower in the *nef*-positive clone than in the *nef*-negative clone (Fig. 5). Similar results were found with analyses of cytoplasmic or nuclear RNAs (data not shown). S1 nuclease protection analysis demonstrated a four- to sixfold suppression of correctly initiated viral mRNAs in the cells transfected with the *nef*-positive clone relative to that in the cells transfected with the *nef*-negative clone (Fig. 6).

A collection of 17 independent comparisons from 10 different experiments of viral mRNAs from pSIV 102- and pSIV BA-transfected cells is presented in Table 1. The mean suppression of viral mRNA mediated by NEF was 3.2-fold \pm

TABLE 1. SIV NEF downregulates viral mRNA levels^a

Expt	Proviral pSIV clone	Ratio ^b	mRNA suppression			CAT activity ^c (%)	Analysis
			SIV	Actin	<i>neo</i>		
1	102	2.7	0.9	1.8	8.9	64	Slot blot
	BA		2.1	1.4	6.1	74	
	102		1.3	2.3	7.2	77	
	BA		2.5	1.8	9.1	63	
2	102	1.9	2.1	1.1	7.2	44	Slot blot
	BA		2.9	1.3	9.7	50	
	102		2.4	1.5	12	49	
	BA		2.6	0.7	8.8	50	
	102		2.2	1.8	7.7	39	
3	102	2.6	1.8	2.7	ND ^d	ND	Slot blot
	BA		3.6	2.8	ND	ND	
	102		3.0	1.6	ND	ND	
	BA		8.8	1.4	ND	ND	
4	102	1.7	1.4	5.3	ND	ND	Slot blot
	BA		2.3	4.8	ND	ND	
5	102	4.0	0.8	4.7	ND	76	Northern
	BA		1.5	4.0	ND	82	
	102		0.9	4.7	ND	76	
	BA		4.7	4.0	ND	82	
6	102	5.8	1.4	5.1	ND	3.4	S1 nuclease
	BA		6.2	3.9	ND	3.2	
	102		1.0	4.2	ND	2.5	
	BA		6.3	4.7	ND	4.6	
	102		0.6	5.1	ND	3.9	
7	102	3.5	3.5	5.0	ND	ND	Northern
	BA		7.1	2.9	ND	ND	
8	102	1.9	2.4	6.7	ND	ND	Northern
	BA		2.2	3.3	ND	ND	
9	102	2.7	1.0	0.9 ^e	ND	ND	Run-on
	BA		2.9	1.0 ^e	ND	ND	
10	102	2.6	1.5	1.4 ^e	ND	ND	Run-on
	BA		2.0	0.7 ^e	ND	ND	

^a This table summarizes the data from 10 separate experiments and includes 17 different matched pairs of densitometry scans of SIV, actin, or *neo* mRNAs (expressed as relative areas under each curve) from pSIV 102- and pSIV BA-transfected COS cells. In all cases, COS cells were transfected with 10 μ g of proviral DNA per 100-mm plates. These data include mRNAs that were analyzed by slot blot and Northern blot hybridization, S1 nuclease protection assays, and nuclear run-on assays. We calculated the level of viral mRNA suppression for each of the 17 matched pairs of pSIV 102 and pSIV BA values in order of the pairs from the top of the table downward. We found that the mean suppression of NEF on viral mRNA levels was 3.2-fold \pm 1.6-fold, where 1.6 represents the standard deviation. In addition, the 95% confidence intervals (2.4 and 4.0) indicate that the mean of 17 random matched pairs will lie between 2.4- and 4.0-fold 95% of the time.

^b Average ratio of the SIV densitometry values of pSIV BA divided by those of pSIV 102 multiplied by the ratio of actin densitometry values of pSIV 102 divided by those of pSIV BA-transfected cells.

^c CAT activity (measured as percent conversion to acetylated products) of a pSV2CAT plasmid that was cotransfected with the SIV proviral clones.

^d ND, Not done.

^e In the nuclear run-on assays, hybridization to *Ahd* sequences served as a control for viral RNA concentration determinations instead of actin sequences.

1.6-fold, where 1.6 is the standard deviation. Ninety-five percent confidence intervals indicate that the mean suppression in any 17 matched pairs of viral mRNAs from pSIV 102 and pSIV BA-transfected cells is intermediate between 2.4- and 4.0-fold.

The observation that steady-state viral mRNA levels were decreased in the presence of *nef* suggests that *nef* either suppresses the rate of RNA synthesis or enhances the rate of RNA degradation. Therefore, nuclear run-on and dactinomycin stability studies were performed. Nuclear run-on analysis of COS cells transfected with either pSIV 102 or pSIV BA indicated that the rate of RNA synthesis was suppressed two- to threefold in the *nef*-positive clone relative to that in the *nef*-negative clone (Fig. 7). This level of transcriptional suppression could account for the differences in the steady-state level of viral mRNA in the presence or absence of NEF in that differences in the magnitude of suppression could reflect differences in experimental approaches. Analysis of viral RNA levels after dactinomycin treatment indicated that NEF did not significantly alter the rate of degradation of viral mRNA (Fig. 8).

We conclude from these experiments that SIV NEF suppresses virus replication in COS cells and that this suppression occurs at the level of viral mRNA synthesis. This study of SIV NEF parallels our previous analysis of the HIV-1 *nef* gene product (24) and the results of other investigators (1). However, others have not demonstrated a suppressive role for HIV-1 NEF on virus replication (15, 19). The discrepancy may lie in the fact that the experiments were not conducted with similar reagents in the same context. That is, Kim et al. (19) used a proviral clone that was different from that used by Ahmad and Venkatesan (1) or in our laboratory (24). Perhaps more significantly, the multiplicity of infection (MOI) varied greatly between our experiments and those of Kim et al.; we used very low MOIs whereas Kim et al. used high MOIs. It is likely that the subtle effects of NEF may be masked by the high MOI used by Kim et al. The proviral clone studied by Hammes et al. was HXB3, which contains a *nef* gene similar to the clone used in our previous experiments except that clone HXB3 contains an alanine instead of a threonine residue at amino acid position 15. Guy et al. (12) demonstrated that protein kinase C requires a threonine residue for phosphorylation at amino acid residue 15 and that this phosphorylation event may be critical for NEF activity. Currently, we are studying the role of the MOI on NEF activity with different proviral clones in an attempt to explain the discrepancies that have arisen with respect to the role of NEF on virus replication.

The precise mechanism by which NEF mediates transcriptional suppression is not known. HIV-1 NEF has not yet been found in the nucleus; however, HIV-1 NEF (12, 15, 18) and SIV NEF (13) are myristoylated (Fig. 1) and can associate with the plasma or other cellular membranes, which may be essential for their activity (7, 15). HIV-1 and SIV NEF bear amino acid sequence similarity to the nucleotide binding domain of p21^{src}, p60^{src}, cyclic AMP-dependent protein kinase, and epidermal growth factor and insulin receptors (12, 27) (Fig. 1). With respect to HIV-1 NEF, GTP-binding and GTP-cleaving activities have been reported (12, 13); however, others have been unable to detect these activities (18). HIV-1 NEF has been reported to exhibit autophosphorylation activities (12), which indicates that NEF may be able to phosphorylate other regulatory proteins in a signal pathway into the nucleus. Recently, it was found that HIV-1 NEF can downregulate the binding of a proliferation-associated DNA binding protein in nontransformed

human T lymphocytes (11). Thus, NEF may act as a signal transducer to either facilitate the binding of negative cellular factors or inhibit the binding of positive cellular factors of transcription.

We have begun to examine the replication of SIV NEF⁺ and SIV NEF⁻ viruses in rhesus macaque primary lymphocytes; preliminary results indicate downregulatory effects exerted by NEF early after infection, which is consistent with the data presented in this manuscript. However, the role of NEF in vivo has yet to be examined. It is possible that NEF may be contributing significantly to the establishment and maintenance of viral latency exhibited by infected humans and macaques. However, downregulation of viral expression may actually contribute to disease progression in that NEF may be required for persistent infection. That is, if *nef*-negative viruses replicate unchecked, heavily infected cells may die and a swift, immune response may clear circulating virus. However, cells infected with *nef*-positive viruses may persist because virus replication is suppressed and thereby provide a virus reservoir. It should be noted that the subtle effects of NEF on transcription were determined in cell culture and that the ability of NEF to downregulate virus expression in living organisms may be more substantial. Studies of macaques infected with SIV *nef*-positive and *nef*-negative viruses will be crucial for determining the physiologic role of NEF in virus expression and disease progression (23).

ACKNOWLEDGMENTS

We thank Jeffrey Milbrandt for experimental advice on nuclear run-on assays and critical review of the manuscript, Lisa Westfield and Evan Sadler (Howard Hughes Medical Institution) for oligonucleotides, and G. Viglianti for sharing unpublished data.

This work was supported by contracts DAMD-87C-7107 and DAMD-90C-0125 from the U.S. Army Medical Research Acquisition Activity, Public Health Service grant AI24745, and training grant HL 07088-15 (to T.M.J.N.) from the National Institutes of Health. Lee Ratner is an American Cancer Society Research Professor.

REFERENCES

1. Ahmad, N., and S. Venkatesan. 1988. Nef protein of HIV-1 is a transcriptional repressor of HIV-1 LTR. *Science* 241:1481-1485.
2. Cheng-Mayer, C., P. Lannello, K. Shaw, P. A. Luciw, and J. A. Levy. 1989. Differential effects of *nef* on HIV replication: implications for viral pathogenesis in the host. *Science* 246:1629-1632.
3. Chirgwin, J. B., A. E. Przybyla, R. J. MacDonald, and W. J. Rutter. 1979. Isolation of biologically active ribonucleic acid from sources enriched in ribonuclease. *Biochemistry* 18:5294-5299.
4. Cleveland, D. W., M. A. Lopata, R. J. MacDonald, N. J. Cowan, W. J. Rutter, and M. W. Kirschner. 1980. Number and evolutionary conservation of alpha- and beta-tubulin and cytoplasmic beta- and gamma-actin genes using specific cloned cDNA probes. *Cell* 20:95-105.
5. Daniel, M. D., N. L. Letvin, N. W. King, M. Kannagi, P. K. Sehgal, R. D. Hunt, P. J. Kanki, M. Essex, and R. C. Desrosiers. 1985. Isolation of T-cell tropic HTLV-III like retrovirus from macaques. *Science* 228:1201-1204.
6. Fisher, A. G., E. Collalti, L. Ratner, R. C. Gallo, and F. Wong-Staal. 1985. A molecular clone of HTLV-III with biological activity. *Nature (London)* 316:262-265.
7. Franchini, G., M. Robert-Guroff, J. Ghayeb, N. Chang, and F. Wong-Staal. 1986. Cytoplasmic localization of the HTLV-III 3'orf protein in cultured T cells. *Virology* 155:593-599.
8. Gallo, R. C., F. Wong-Staal, L. Montagnier, W. A. Haseltine, and M. Yoshida. 1988. HIV/HTLV gene nomenclature. *Nature*

- (London) 333:504.
9. Gama Sosa, M. A., R. DeGasperi, L. D. Bernard, J. Hall, F. Fazely, and R. M. Ruprecht. 1990. VI International Conference on AIDS (San Francisco), abstr. FA227.
 10. Gorman, C. M., L. F. Moffat, and B. H. Howard. 1982. Recombinant genomes which express chloramphenicol acetyltransferase in mammalian cells. *Mol. Cell. Biol.* 2:1044-1051.
 11. Guy, B., R. B. Acres, M. P. Kieny, and J.-P. Lecocq. 1990. DNA binding factors that bind to the negative regulatory element of the human immunodeficiency virus type 1: regulation by nef. *J. Acquired Immune Defic. Syndr.* 3:797-809.
 12. Guy, B., M. P. Kieny, Y. Riviere, C. LePeuch, K. Dott, M. Girard, L. Montagnier, and J. P. Lecocq. 1987. HIV F/3'orf encodes a phosphorylated GTP-binding protein resembling an oncogene product. *Nature (London)* 330:266-269.
 13. Guy, B., Y. Riviere, K. Dott, A. Regnault, and M. P. Kieny. 1990. Mutational analysis of the HIV nef protein. *Virology* 176:413-425.
 14. Hahn, B. H., L. I. Kong, S.-W. Lee, P. Kumar, M. E. Taylor, S. K. Arya, and G. M. Shaw. 1987. Relation of HTLV-4 to simian and human immunodeficiency-associated viruses. *Nature (London)* 330:184-186.
 15. Hammes, S. R., E. P. Dixon, M. H. Malim, B. R. Cullen, and W. C. Greene. 1989. Nef protein of human immunodeficiency virus type 1: evidence against its role as a transcriptional inhibitor. *Proc. Natl. Acad. Sci. USA* 86:9549-9553.
 16. Hermann, R., A. Ludwigsen, M. Chuah, R. Brack-Werner, B. Kohleisen, A. Kleinschmidt, and V. Erfle. 1990. VI International Conference on AIDS (San Francisco), abstr. FA302.
 17. Josephs, S. F., G. Chan, L. Ratner, and F. Wong-Staal. 1984. Human proto-oncogene nucleotide sequences corresponding to the transforming region of simian sarcoma virus. *Science* 223:487-490.
 18. Kaminchik, J., N. Bashan, D. Pinchasi, B. Amit, N. Sarver, M. I. Johnston, M. Fischer, Z. Yavin, M. Gorecki, and A. Panet. 1990. Expression and biochemical characterization of human immunodeficiency virus type 1 *nef* gene product. *J. Virol.* 64:3447-3454.
 19. Kim, S., R. Ikeuchi, R. Byrn, J. Groopman, and D. Baltimore. 1989. Lack of a negative influence on viral growth by the *nef* gene of human immunodeficiency virus type 1. *Proc. Natl. Acad. Sci. USA* 86:9544-9548.
 20. Luciw, P. A., C. Cheng-Mayer, and J. A. Levy. 1987. Mutational analysis of the human immunodeficiency virus: the *orf-B* region down-regulates virus replication. *Proc. Natl. Acad. Sci. USA* 84:1434-1438.
 21. Mulligan, R. C., and P. Berg. 1980. Expression of a bacterial gene in mammalian cells. *Science* 209:1422-1427.
 22. Myers, G., A. B. Rabson, J. A. Berzofsky, T. F. Smith, and F. Wong-Staal (ed.). 1990. Theoretical biology and biophysics, p. 1169-1170. Los Alamos Laboratory, Los Alamos, N.Mex.
 23. Naidu, Y. M., H. S. Kestler III, Y. Li, C. V. Butler, D. P. Silva, D. K. Schmidt, C. D. Troup, P. K. Sehgal, P. Sonigo, M. D. Daniel, and R. C. Desrosiers. 1988. Characterization of infectious molecular clones of simian immunodeficiency virus (SIV-MAC) and human immunodeficiency virus type 2: persistent infection of rhesus monkeys with molecularly cloned SIV-MAC. *J. Virol.* 62:4691-4696.
 24. Niederman, T. M. J., B. J. Thielan, and L. Ratner. 1989. Human immunodeficiency virus type 1 negative factor is a transcriptional silencer. *Proc. Natl. Acad. Sci. USA* 86:1128-1132.
 25. Ratner, L., W. Haseltine, R. Patarca, K. J. Livak, B. Starcich, S. F. Josephs, E. R. Doran, J. A. Rafalski, E. A. Whitehorn, K. Baumeister, L. Ivanoff, S. R. Petteway, Jr., M. L. Pearson, J. A. Lautenberger, T. S. Papas, J. Ghayeb, N. T. Chang, R. C. Gallo, and F. Wong-Staal. 1985. Complete nucleotide sequence of the AIDS virus, HTLV-III. *Nature (London)* 313:277-284.
 26. Ratner, L., B. Starcich, S. F. Josephs, B. H. Hahn, E. P. Reddy, K. J. Livak, S. R. Petteway, Jr., M. L. Pearson, W. A. Haseltine, S. K. Arya, and F. W. Staal. 1985. Polymorphism of the 3' open reading frame of the virus associated with the acquired immune deficiency syndrome, human T-lymphotropic virus type III. *Nucleic Acids Res.* 13:8219-8229.
 27. Samuel, K. P., A. Seth, A. Konopka, J. A. Lautenberger, and T. S. Papas. 1987. The 3' *orf* protein of human immunodeficiency virus shows structural homology with the phosphorylation domain of human interleukin-2 receptor and the ATP-binding site of the protein kinase family. *FEBS Lett.* 218:81-86.
 28. Terwilliger, E., J. G. Sodroski, C. A. Rosen, and W. A. Haseltine. 1986. Effects of mutations within the 3' *orf* open reading frame region of human T-cell lymphotropic virus type III (HTLV-III/LAV) on replication and cytopathogenicity. *J. Virol.* 60:754-760.
 29. Viglianti, G. A., P. L. Sharma, and J. I. Mullins. 1990. Simian immunodeficiency virus displays complex patterns of RNA splicing. *J. Virol.* 64:4207-4216.

Identification of a determinant within the human immunodeficiency virus 1 surface envelope glycoprotein critical for productive infection of primary monocytes

(macrophage/tropism/third variable domain of gp120/CD4)

PETER WESTERVELT*, HOWARD E. GENDELMAN[†], AND LEE RATNER*[‡]

*Departments of Medicine and Molecular Microbiology, Washington University School of Medicine, St. Louis, MO 63110; and [†]Department of Cellular Immunology, HIV Immunopathogenesis Program, Walter Reed Army Institute of Research and the Henry M. Jackson Foundation for the Advancement of Military Medicine, Rockville, MD 20850

Communicated by Stuart Kornfeld, January 4, 1991

ABSTRACT Profound differences exist in the replicative capacities of various human immunodeficiency virus 1 isolates in primary human monocytes. To investigate the molecular basis for these differences, recombinant full-length clones were constructed by reciprocal DNA fragment exchange between a molecular clone derived from a monocyte-tropic isolate (ADA) and portions of two full-length clones incapable of infection or replication in primary monocyte cultures (HXB2 and NL4-3). Virions derived from proviral clones that contained ADA sequences encoding *vpu* and the N and C termini of the surface envelope glycoprotein (gp120) were incapable of replication in monocytes. However, a 283-base-pair ADA sequence encoding amino acids 240–333 of the mature gp120 protein conferred the capacity for high-level virus replication in primary monocytes. The predicted amino acid sequence of this ADA clone differed from NL4-3 and HXB2 at 22 of 94 residues in this portion of gp120, which includes the entire third variable domain. Only 2 of 11 residues implicated in CD4 binding are located in this region of gp120 and are identical in HXB2, NL4-3, and ADA. Alignment of the ADA sequence with published amino acid sequences of three additional monocyte-replicative and three monocyte-nonreplicative clones indicates 6 discrete residues with potential involvement in conferring productive human immunodeficiency virus 1 infection of primary monocytes.

Cells of monocyte-macrophage lineage present targets for infection by the human immunodeficiency virus 1 (HIV-1) in widely diverse tissues *in vivo*, including brain, spinal cord, lung, lymph node, and skin (1). These observations are based on extensive documentation by several different investigators utilizing electron microscopy, *in situ* RNA hybridization, and immunohistochemistry. The potential importance of macrophage infection in AIDS is underscored by the central role of infected macrophages in the pathogenesis of other lentivirus infections, such as visna maedi and equine infectious anemia virus, in which the macrophage serves as a reservoir of virus throughout the course of subclinical infection and disease (2).

Despite these observations, however, profound differences exist in the abilities of various HIV-1 isolates to infect and replicate in primary monocytes cultured *in vitro*. Many primary isolates, derived from peripheral blood, in which CD4⁺ T cells represent the predominant infected cell type, have demonstrated a limited capacity for replication in monocytes, despite highly efficient replication in peripheral blood mononuclear cells (PBMCs; primarily lymphocytes) (3–6). However, several groups have reported productive infection of both monocytes and PBMCs by using primary isolates

derived from brain and lung, tissues in which HIV-1 infection of macrophages predominates (1, 5–7). In the present study, we sought to determine the molecular basis for HIV-1 infection and replication in primary monocytes by constructing chimeric full-length proviral clones from a molecular clone derived from a monocyte-replicative isolate (ADA) and two monocyte-nonreplicative functional clones (NL4-3 and HXB2) (8–10). Our results indicate that a discrete portion of the HIV-1 surface envelope glycoprotein (gp120) confers the capacity for productive infection of primary monocytes.

MATERIALS AND METHODS

Cells. COS-7 cells were obtained from the American Type Culture Collection and maintained as monolayer cultures in Duibecco's modified Eagle's medium (DMEM) supplemented with 10% heat-inactivated (56°C; 30 min) fetal calf serum (Hazelton Biologics, Denver, PA) and 1 mM sodium pyruvate. PBMCs were purified from normal human leukocytes (American Red Cross) by centrifugation onto Ficoll. After 3 days of stimulation with phytohemagglutinin (15 µg/ml; Sigma), PBMCs were maintained in RPMI 1640 medium supplemented with 10% heat-inactivated fetal calf serum, 4 mM glutamine, and recombinant interleukin 2 (50 units/ml; Cetus). Primary monocytes were isolated by counter-current centrifugal elutriation of mononuclear leukocyte-rich cell preparations obtained from normal donors by leukapheresis (11). Cell suspensions were routinely >95% monocytes by the criteria of size (by Coulter analysis) and nonspecific esterase staining. Elutriated monocytes were cultured as adherent cell monolayers at a density of 200,000 cells per well in 24-well plates in AIM-V medium (GIBCO) supplemented with 10% heat-inactivated normal human serum (Pel-Freez Biologicals), 4 mM glutamine, and recombinant monocyte-colony-stimulating factor (1000 units/ml; Cetus).

Molecular Cloning and Recombinant Provirus Construction. The isolation and functional characterization of the full-length HIV-1 proviral clones HXB2 and NL4-3 have been described (9, 10). The HIV-1 isolate ADA was obtained by cocultivation of PBMCs freshly obtained from a HIV-1-infected individual with uninfected primary monocytes as described (8). Hirt supernatant DNA (12) from an ADA-infected monocyte culture was digested with *Sac* I, ligated into *Sac* I-cut Lambda ZAP phage arms (Stratagene), and packaged (Gigapack Plus, Stratagene) to generate a phage

Abbreviations: HIV-1, human immunodeficiency virus 1; V3, third variable domain of gp120; PBMC, peripheral blood mononuclear cell; RT, reverse transcriptase.

[‡]To whom reprint requests should be addressed at: Department of Medicine, Washington University School of Medicine, 660 South Euclid Avenue, St. Louis, MO 63110.

The publication costs of this article were defrayed in part by page charge payment. This article must therefore be hereby marked "advertisement" in accordance with 18 U.S.C. §1734 solely to indicate this fact.

library (13); 250,000 plaques were screened with a random hexamer-labeled *Sac* I/*Sac* I probe derived from HXB2 [nucleotides 5999–9571; according to Myers *et al.* (14)]. Phage from a single positive plaque was isolated, from which phagemid was excised and demonstrated to contain a 3.6-kilobase (kb) insert by restriction enzyme mapping. To facilitate the construction of full-length recombinant clones containing ADA-derived sequences, the 3.6-kb *Sac* I/*Sac* I clone was subcloned in the proper orientation into a pSVL-based vector (Pharmacia) containing *Sal* I/*Sac* I (nucleotides 5785–5999) and *Sac* I/*Xba* I (nucleotide 9571–3' polylinker) adaptor sequences from the clone HXB2gpt2. The ADA clone was then subdivided by reciprocal fragment exchanges between the chimeric subclone and a similar subclone containing the entire HXB2gpt2-derived *Sal* I/*Xba* I sequence. The resultant recombinant subclones were then used to generate recombinant full-length clones by exchange of *Sal* I/*Bam*HI fragments (nucleotides 5785–8474) with clone NL4-3. The structure of the clones was confirmed by restriction enzyme and nucleotide sequence analysis.[§]

DNA Sequence Analysis. DNA sequencing was performed by a modification of the dideoxynucleotide method using Sequenase 2.0 according to the manufacturer's protocols (United States Biochemical) and a panel of oligonucleotide primers spanning the 3' portion of the HIV-1 genome in both orientations (15).

Virus Infection. Virus stocks were generated by transfection of 50% confluent 10-cm COS-7 plates with 10 μ g of proviral DNA and 2 μ g of pCV-1 (*lat* expression vector) (16) by the calcium phosphate method (13) followed by dimethyl sulfoxide shock (2-min wash with 10% dimethyl sulfoxide in DMEM 12 hr posttransfection) before refeding with fresh medium. Culture supernatants were harvested 36 hr posttransfection, filtered (pore size, 0.2 μ m), and titered by determination of reverse transcriptase (RT) activity (17). Viral inocula consisting of 50,000 cpm of RT activity in 1 ml were used to infect 200,000 primary monocytes 7 days after plating or 500,000 PBMCs 4 days after plating. Virus replication was monitored by serial determinations of RT activity in culture supernatants.

RESULTS

ADA Molecular Clone. A 3569-base-pair (bp) *Sac* I/*Sac* I molecular clone was isolated from unintegrated DNA prepared from a monocyte culture productively infected with the ADA isolate. The ADA clone spanned the entire *env*, *vpu*, and *nef* genes, as well as portions of *tat*, *rev*, and the 3' long terminal repeat (Fig. 1). DNA sequence analysis of the clone demonstrated 92% overall nucleotide homology with HXB2, which is within the range expected for unrelated HIV-1 isolates (14). Similarly, predicted amino acid homologies with HXB2 ranged from 80% to 93% in the encoded open reading frames (data not shown). The regions within *env* of greatest amino acid homology and divergence between the two clones corresponded to previously identified conserved and variable domains, respectively (data not shown) (18). Each of the ADA-encoded open reading frames was intact and full length, in contrast to HXB2, in which *vpu* lacks an initiator methionine codon and *nef* is truncated at 123 amino acids (19). Furthermore, the ADA-encoded *tat* second exon extended an additional 14 amino acids beyond the termination codon observed in HXB2.

Mapping the Monocyte Tropism Determinant. A panel of chimeric full-length clones was constructed to assess the ability of various ADA sequences to confer the capacity for

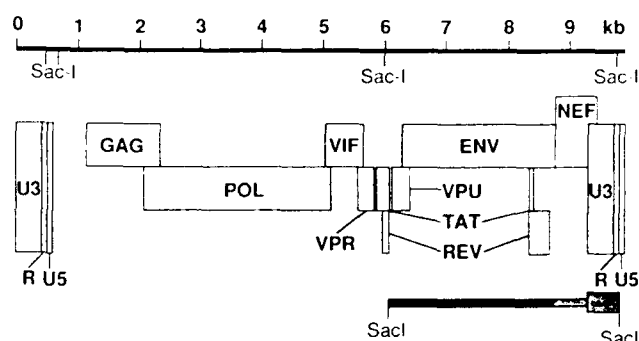


FIG. 1. Structure of the ADA molecular clone. The 3569-bp ADA molecular clone (shaded box) is aligned with the open reading frames and long terminal repeats of the HIV-1 genome above (open boxes).

replication in primary monocytes upon a recombinant construct derived from the monocyte-nonreplicative clones NL4-3 and HXB2 (Fig. 2). The NLHXADA chimeras were used to evaluate the ADA-encoded *vpu* and discrete fractions of the gp120 portion of *env*, both separately and together, for their potential roles in conferring the ability to replicate in monocytes. All the chimeric NLHXADA clones, as well as NL4-3 and HXB2, generated virions capable of high repli-

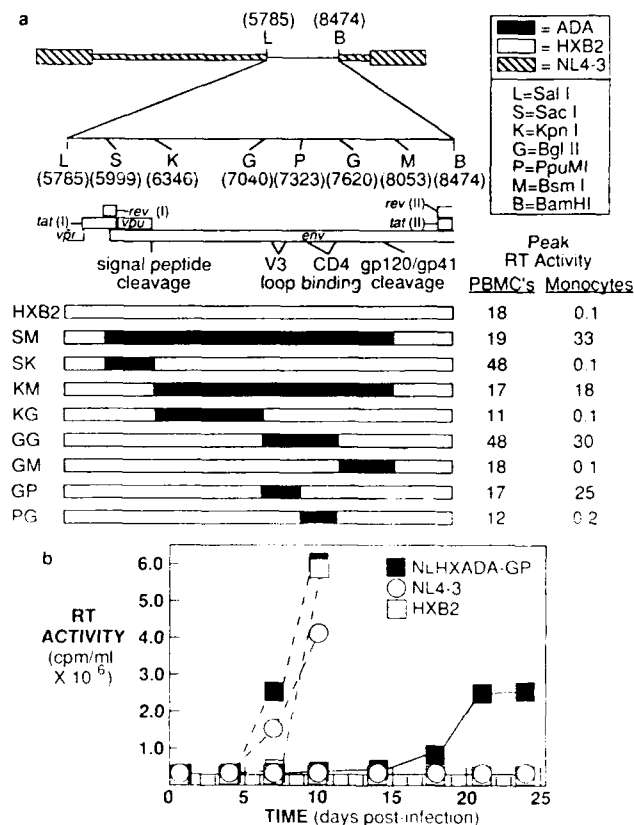


FIG. 2. Replication of NLHXADA recombinant clones in PBMCs and primary monocytes. (a) A panel of recombinant clones generated by exchange of restriction fragments between the ADA, HXB2, and NL4-3 clones is represented diagrammatically on the left. The 2.7-kb *Sal* I/*Bam*HI fragment of each clone has been expanded to demonstrate the relative positions of ADA-derived sequences and HXB2-derived sequences with respect to the open reading frames and restriction enzyme sites shown above. Peak RT activities ($\times 10^5$) generated by virions derived from each clone in PBMCs (days 12–18) and primary monocytes (days 18–24) are indicated on the right. (b) The replication kinetics of NL4-3, HXB2, and NLHXADA-GP in PBMCs (dashed lines) and primary monocytes (solid lines) are shown. Similar results were obtained in two to five replicate experiments.

[§]The complete nucleotide sequence of the ADA clone from which the amino acid sequence reported in this paper was derived has been deposited in the GenBank data base (accession no. M60472).

cation levels in PBMCs. In contrast, only a subset of NLHX-ADA clones, designated -SM, -KM, -GG, and -GP, generated virus capable of replication levels detectable by RT assay in primary monocytes (typically 180- to 500-fold higher than background). Each of these clones shared in common a 283-bp *Bgl* II/*Ppu*MI ADA-derived sequence. Virus from NLHXADA constructs lacking this element consistently failed to generate RT levels detectable above background.

The 283-bp ADA-derived element encodes amino acids 240–333 of the mature ADA surface envelope glycoprotein (Fig. 3). This portion of gp120 encompasses the entire third variable domain of gp120 (V3 loop) (20) but includes only 2 of 11 amino acid residues previously demonstrated to participate in or impact on binding to CD4 (21–24). The amino acid sequence predicted by the *Bgl* II/*Ppu*MI element differs from those of HXB2 and NL4-3 at 22 of 94 positions. To identify amino acids potentially involved in controlling HIV-1 replication in monocytes, predicted amino acid sequences from three monocyte-replicative clones (ADA, SF162, Yu2) and three monocyte-nonreplicative clones (HXB2, NL4-3, SF2) were aligned (9, 19, 25, 26). In addition, the sequence of

a molecular clone derived from a monocyte-replicative isolate in our laboratory (JF-L) was included with the former group, although no data on the functional properties of this clone yet exist (6) (Fig. 4). Based on the alignment, six amino acid residues were identified (ADA gp120 residues 242, 275, 283, 287, 302, and 313), which were different in every case between the monocyte-replicative and -nonreplicative clones and could potentially account for the observed phenotypic difference. Of particular note was the presence of a tyrosine residue at position 283 in each monocyte-replicative clone, and the presence of an acidic residue at position 287 in each monocyte-replicative clone, in contrast to the monocyte-nonreplicative clones, which each contained a basic residue at this position.

DISCUSSION

Through the use of chimeric HIV-1 molecular clones, we have demonstrated a discrete region of gp120 to be critical for productive infection of primary monocytes. Our results are consistent with data obtained in other retroviral systems,

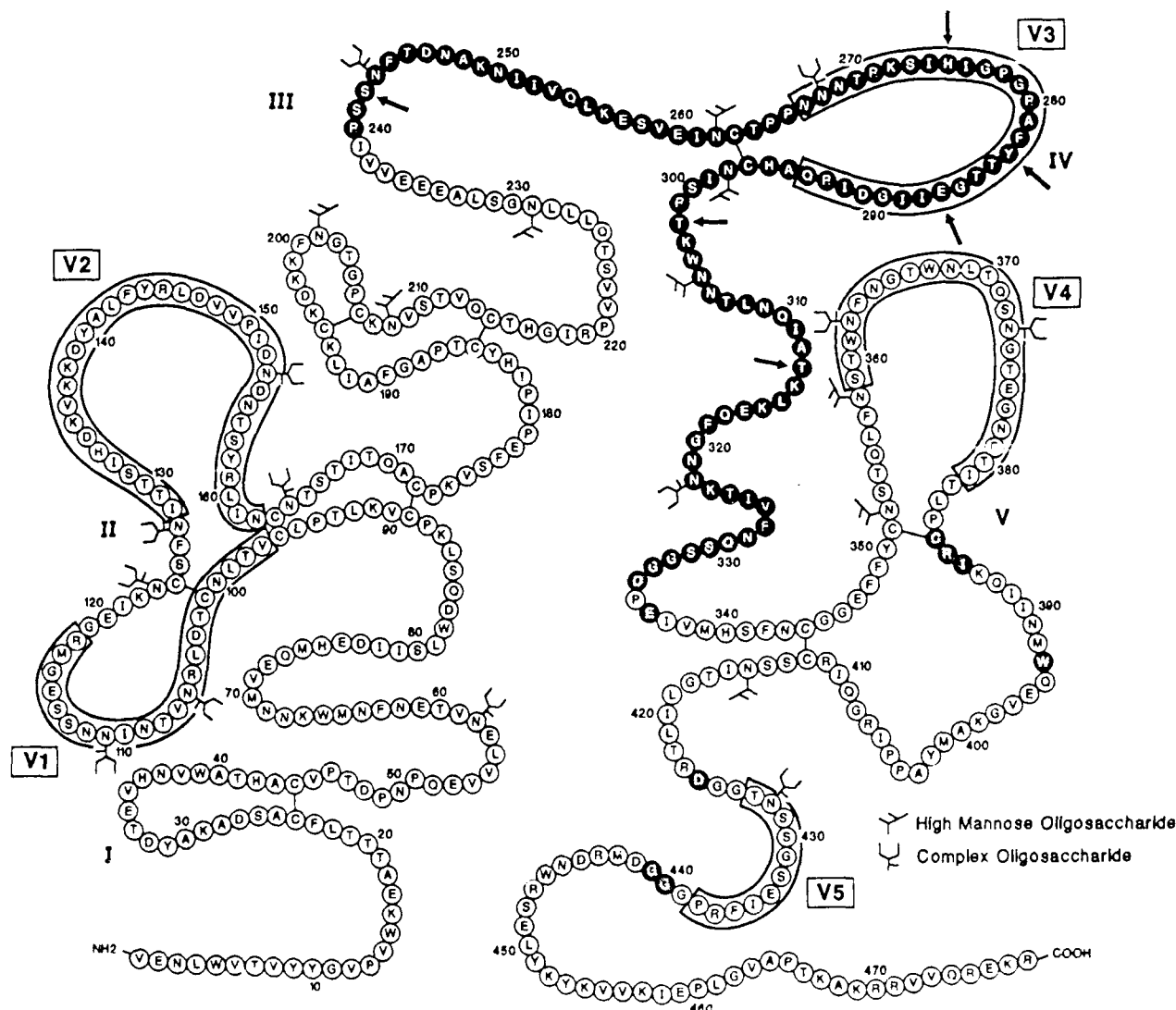


FIG. 3. Diagram of the ADA-encoded surface envelope glycoprotein. The primary structure of the mature gp120 protein predicted by the ADA clone is shown superimposed on the secondary structure determination of the HXB2 gp120 [modified with permission (20); copyright The American Society for Biochemistry and Molecular Biology 1990]. Residues encoded by the monocyte tropism determinant (residues 240–333) are represented as shaded circles; residues implicated in CD4 binding are represented as partially shaded circles; the remaining residues are represented as open circles. Residues located within variable domains are enclosed in boxes. Arrows designate residues identified by sequence alignment (see Fig. 4) as potentially involved in conferring the ability to establish productive infection of primary monocytes.

cated well in primary monocytes, suggests that *vpu* function is not an absolute requirement for HIV-1 replication in monocytes since the HXB2 *vpu* gene lacks an initiator methionine codon (19). Further studies involving, for instance, mutagenesis of the various accessory genes will address the intriguing possibility that additional genetic element(s), acting independently or in concert with the *env* determinant, play a role in mediating HIV-1 tropism for primary monocytes.

Note. After this work was completed, O'Brien *et al.* (43) and Liu *et al.* (44) published similar reports, which are consistent with these findings.

We are grateful to N. Vander Heyden and B. Trowbridge for technical assistance; E. Brown and M. Arens for primary monocytes and PBMCs, respectively; Cetus for recombinant interleukin 2 and recombinant monocyte-colony-stimulating factor; and M. Meltzer for helpful discussions. This work was supported by National Institutes of Health Grant AI 24745, U.S. Army Medical Research and Development Command Contract 17-90C-0125, the Military Medical Consortium, the Washington University Medical Scientist Training Program grant, and Training Grant 5T32AI07172 (P.W.). H.E.G. is a Carter-Wallace Fellow. L.R. is an American Cancer Society Research Professor.

- Gendelman, H. E., Orenstein, J. M., Baca, L. M., Weiser, B., Burger, H., Kalter, D. C. & Meltzer, M. S. (1989) *AIDS* **3**, 475-495.
- Narayan, O. & Clements, J. E. (1989) *J. Gen. Virol.* **70**, 1617-1639.
- Schnittman, S. M., Psallidopoulos, M. C., Lane, H. C., Thompson, L., Baseler, M., Massari, F., Fox, C. H., Salzman, N. P. & Fauci, A. S. (1989) *Science* **245**, 305-308.
- Valentin, A., Albert, J., Fenyo, E. M. & Asjo, B. (1990) *Virology* **177**, 790-794.
- Gartner, S., Markovits, P., Markovitz, D. M., Kaplan, M. H., Gallo, R. C. & Popovic, M. (1986) *Science* **233**, 215-219.
- McNearney, T., Westervelt, P., Thielan, B. J., Trowbridge, D. B., Garcia, J., Whittier, R. & Ratner, L. (1990) *Proc. Natl. Acad. Sci. USA* **87**, 1917-1921.
- Koyanagi, Y., Miles, S., Mitsuyasu, R. T., Merrill, J. E., Vinters, H. V. & Chen, I. S. Y. (1987) *Science* **236**, 819-822.
- Gendelman, H. E., Orenstein, J. M., Martin, M. A., Ferrua, C., Mitra, R., Phipps, T., Wahl, L. M., Lane, H. C., Fauci, A. S., Burke, D. S., Skillman, D. & Meltzer, M. S. (1988) *J. Exp. Med.* **167**, 1428-1441.
- Adachi, A., Gendelman, H. E., Koenig, S., Folks, T., Willey, R., Rabson, A. & Martin, M. A. (1986) *J. Virol.* **59**, 284-291.
- Fisher, A. G., Collalti, E., Ratner, L., Gallo, R. C. & Wong-Staal, F. (1985) *Nature (London)* **316**, 262-265.
- Wahl, L. M., Katona, I. M., Wilder, R. L., Winter, C. C., Haraoui, B., Scher, I. & Wahl, S. M. (1984) *Cell. Immunol.* **85**, 373-383.
- Hirt, B. (1967) *J. Mol. Biol.* **26**, 365-367.
- Sambrook, J., Fritsch, E. F. & Maniatis, T. (1989) *Molecular Cloning: A Laboratory Manual* (Cold Spring Harbor Lab., Cold Spring Harbor, NY).
- Myers, G., Rabson, A. B., Berzofsky, J. A., Smith, T. F. & Wong-Staal, F. (1990) *Human Retroviruses and AIDS, 1990* (Los Alamos Natl. Lab., Los Alamos, NM).
- Sanger, F., Nicklen, S. & Coulson, A. R. (1977) *Proc. Natl. Acad. Sci. USA* **74**, 5463-5467.
- Arva, S. K., Guo, C., Josephs, S. F. & Wong-Staal, F. (1985) *Science* **229**, 69-73.
- Poiesz, B. J., Ruscetti, F. W., Gazdar, A. F., Bunn, P. A., Minna, J. D. & Gallo, R. C. (1980) *Proc. Natl. Acad. Sci. USA* **77**, 7415-7419.
- Modrow, S., Hahn, B. H., Shaw, G. M., Gallo, R. C., Wong-Staal, F. & Wolf, H. (1987) *J. Virol.* **61**, 570-578.
- Ratner, L., Haseltine, W., Patarca, R., Livak, K. J., Starcich, B., Josephs, S. F., Doran, E. R., Rafalski, J. A., Whitehorn, E. A., Baumeister, K., Ivanoff, L., Petteway, S. R., Jr., Pearson, M. L., Lautenberger, J. A., Papas, T. S., Ghrayeb, J., Chang, N. T., Gallo, R. C. & Wong-Staal, F. (1985) *Nature (London)* **313**, 277-284.
- Leonard, C. K., Spellman, M. W., Riddle, L., Harris, R. J., Thomas, J. N. & Gregory, T. J. (1990) *J. Biol. Chem.* **265**, 10373-10382.
- Kowalski, M., Potz, J., Basiripour, L., Dorman, T., Goh, W. C., Terwilliger, S., Dayton, A., Rosen, C., Haseltine, W. & Sodroski, J. (1987) *Science* **237**, 1351-1355.
- Lasky, L. A., Nakamura, G., Smith, D. H., Fennie, C., Shimasaki, C., Patzer, E., Borman, P., Gregory, T. & Capon, D. J. (1987) *Cell* **50**, 975-985.
- Cordonnier, A., Montagnier, L. & Emerman, M. (1989) *Nature (London)* **340**, 571-574.
- Olshovsky, U., Helseth, E., Furman, C., Li, J., Haseltine, W. & Sodroski, J. (1990) *J. Virol.* **64**, 5701-5707.
- Cheng-Mayer, C., Quiroga, M., Tung, J. W., Dina, D. & Levy, J. A. (1990) *J. Virol.* **64**, 4390-4398.
- Li, Y., Kappes, J. C., Conway, J. A., Price, R. W., Hahn, B. H. & Shaw, G. S. (1990) *J. Virol.* in press.
- Dorner, A. J. & Coffin, J. M. (1986) *Cell* **45**, 365-374.
- Tsichlis, P. N., Conklin, K. F. & Coffin, J. M. (1980) *Proc. Natl. Acad. Sci. USA* **77**, 536-540.
- Brown, D. W. & Robinson, H. L. (1988) *J. Virol.* **62**, 4828-4831.
- Vogt, M., Hagblom, C., Swift, S. & Haas, M. (1985) *J. Virol.* **55**, 184-192.
- Dalgleish, A. G., Beverly, P. C. L., Clapham, P. R., Crawford, D. H., Greaves, M. F. & Weiss, R. A. (1984) *Nature (London)* **312**, 763-766.
- Maddon, P. J., Dalgleish, A. G., McDougal, J. S., Clapham, P. R., Weiss, R. A. & Axel, R. (1986) *Cell* **47**, 333-348.
- Gomatos, P. J., Stamatou, N. M., Gendelman, H. E., Fowler, A., Hoover, D. L., Kalter, D. C., Burke, D. S., Tramont, E. C. & Meltzer, M. S. (1990) *J. Immunol.* **144**, 4183-4188.
- Collman, R., Godfrey, B., Cutilli, J., Rhodes, A., Hassan, N. F., Sweet, R., Douglas, S. D., Friedman, H., Nathanson, N. & Gonzalez-Scarano, F. (1990) *J. Virol.* **64**, 4468-4476.
- Daar, E. S., Li, X. L., Moudgil, T. & Ho, D. D. (1990) *Proc. Natl. Acad. Sci. USA* **87**, 6574-6578.
- Ivey-Hovle, M., Culp, J. S., Chaikin, M. A., Hellmig, E. D., Matthews, J. J., Sweet, R. W. & Rosenberg, M. (1991) *Proc. Natl. Acad. Sci. USA* **88**, 512-516.
- Rusche, J. R., Javaherian, K., McDanal, C., Petro, J., Lynn, D. L., Grimaldi, R., Langlois, A., Gallo, R. C., Arthur, L. O., Fischinger, P. J., Bolognesi, D. P., Putney, S. D. & Matthews, T. J. (1988) *Proc. Natl. Acad. Sci. USA* **85**, 3198-3202.
- LaRosa, G. J., Davide, J. P., Weinhold, K., Waterbury, J. A., Profy, A. T., Lewis, J. A., Langlois, A. J., Dreesman, G. R., Boswell, R. N., Shaddock, P., Holley, L. H., Karplus, M., Bolognesi, D. P., Matthews, T. J., Emini, E. A. & Putney, S. D. (1990) *Science* **249**, 932-935.
- Stephens, P. E., Clements, G., Yarranton, G. T. & Moore, J. (1990) *Nature (London)* **343**, 219.
- Hattori, T., Kito, K., Takatsuki, K., Kido, H. & Katanuma, N. (1989) *FEBS Lett.* **248**, 48-52.
- Clements, G. J., Price-Jones, M. J., Stephens, P. E., Sutton, C., Schulz, T. F., Clapham, P. R., McKeating, J. A., McClure, M. O., Thomson, S., Marsh, M., Kay, J., Weiss, R. A. & Moore, J. P. (1991) *AIDS Rev. Hum. Retroviruses* **7**, 3-16.
- Hattori, N., Michaels, F., Fargnoli, K., Marcon, L., Gallo, R. C. & Franchini, G. (1990) *Proc. Natl. Acad. Sci. USA* **87**, 8080-8084.
- O'Brien, W. A., Koyanagi, Y., Namazie, A., Zhao, J.-Q., Diagne, A., Idler, K., Zack, J. A. & Chen, I. S. Y. (1990) *Nature (London)* **348**, 69-73.
- Liu, Z.-Q., Wood, C., Levy, J. A. & Cheng-Mayer, C. (1990) *J. Virol.* **64**, 6148-6153.

Incorporation of 12-methoxydodecanoate into the human immunodeficiency virus 1 gag polyprotein precursor inhibits its proteolytic processing and virus production in a chronically infected human lymphoid cell line

(protein N-myristoylation/AIDS/fatty acid analogs)

MARTIN L. BRYANT*, LEE RATNER^{†‡}, ROBERT J. DURONIO[§], NANDINI S. KISHORE[¶], BALEKUDRU DEVADAS^{||}, STEVEN P. ADAMS^{||}, AND JEFFREY I. GORDON^{†§}

Departments of *Pediatrics, [†]Medicine, [‡]Molecular Microbiology, and [§]Molecular Biology and Pharmacology, Washington University School of Medicine, St. Louis, MO 63110; [¶]Molecular and Cell Biology Department, G. D. Searle, St. Louis, MO 63198; and ^{||}Corporate Research Department, Monsanto Company, St. Louis, MO 63198

Communicated by Howard A. Schneiderman**, November 21, 1990 (received for review September 4, 1990)

ABSTRACT Covalent linkage of myristate (tetradecanoate; 14:0) to the NH₂-terminal glycine residue of the human immunodeficiency virus 1 (HIV-1) 55-kDa gag polyprotein precursor (Pr55^{gag}) is necessary for its proteolytic processing and viral assembly. We have shown recently that several analogs of myristate in which a methylene group is replaced by a single oxygen or sulfur atom are substrates for *Saccharomyces cerevisiae* and mammalian myristoyl-CoA:protein N-myristoyltransferase (EC 2.3.1.97; NMT) despite their reduced hydrophobicity. Some inhibit HIV-1 replication in acutely infected CD4⁺ H9 cells without accompanying cellular toxicity. To examine the mechanism of their antiviral effects, we performed labeling studies with two analogs, 12-methoxydodecanoate (13-oxamyristate; 13-OxaMyr) and 5-octyloxypentanoate (6-oxamyristate; 6-OxaMyr), the former being much more effective than the latter in blocking virus production. [³H]Myristate and [³H]13-OxaMyr were incorporated into Pr55^{gag} with comparable efficiency when it was coexpressed with *S. cerevisiae* NMT in *Escherichia coli*. [³H]6-OxaMyr was not incorporated, even though its substrate properties *in vitro* were similar to those of 13-OxaMyr and myristate. [³H]13-OxaMyr, but not [³H]6-OxaMyr, was also efficiently incorporated into HIV-1 Pr55^{gag} and nef (negative factor) in chronically infected H9 cells. Analog incorporation produced a redistribution of Pr55^{gag} from membrane to cytosolic fractions and markedly decreased its proteolytic processing by viral protease. 13-OxaMyr and 3'-azido-3'-deoxythymidine (AZT) act synergistically to reduce virus production in acutely infected H9 cells. Unlike AZT, the analog is able to inhibit virus production (up to 70%) in chronically infected H9 cells. Moreover, the inhibitory effect lasts 6–8 days. These results suggest that (i) its mechanism of action is distinct from that of AZT and involves a late step in virus assembly; (ii) the analog may allow reduction in the dose of AZT required to affect viral replication; and (iii) combinations of analog and HIV-1 protease inhibitors may have synergistic effects on the processing of Pr55^{gag}.

Myristic acid (14:0) is covalently linked via an amide bond to the NH₂-terminal glycine residues of several proteins encoded by the human immunodeficiency virus 1 (HIV-1) genome—the 55-kDa gag polyprotein precursor (Pr55^{gag}), the 180-kDa gag-pol fusion protein, and a 27-kDa protein termed “negative factor” (nef), whose precise role in regulating virus replication remains uncertain (1, 2). Attachment of this rare

fatty acid to Pr55^{gag} is required for HIV-1 replication: transfection of HeLa, COS, or Jurkat cells with a functional provirus clone of HIV-1 containing a Gly-2 → Ala mutation in Pr55^{gag} eliminates virus production (3, 4). The nonmyristoylated mutant protein appears to undergo redistribution from the membrane to the cytosolic fraction (4). Blockade of myristoylation is also associated with a dramatic reduction in the rate of proteolytic processing of the polyprotein precursor by viral protease (4).

We have shown (5) that heteroatom-substituted analogs of myristate inhibit HIV-1 replication in acutely infected CD4⁺ H9 cells. In these analogs, a methylene group is replaced by a single oxygen or sulfur atom. Such replacements produce a reduction in hydrophobicity comparable to the loss of two to four methylene groups without significant alterations in chain length or stereochemistry (6). Metabolic labeling studies (7) using several cultured cell lines indicated that these analogs enter mammalian cells and are substrates for acyl-CoA synthetase and myristoyl-CoA:protein N-myristoyltransferase (NMT). Analog incorporation is very selective: only a subset of cellular N-myristoylated proteins incorporate a given analog, and a given protein may incorporate one but not another analog depending on the site of heteroatom substitution (7). This probably reflects the cooperative interactions that occur between the acyl-CoA and peptide binding sites of NMT: *in vitro* studies with purified *Saccharomyces cerevisiae* NMT indicate that binding of analog-CoA species can produce changes in the catalytic efficiencies (V_m/K_m) of some but not all octapeptide substrates (6, 8). These studies (7) also revealed that analog incorporation had very selective effects on protein targeting. Only a small subset of analog-substituted proteins underwent redistribution from the membrane to cytosolic fractions. An even smaller subset of proteins displayed analog-specific redistribution—i.e., one analog affected targeting while another analog, containing an oxygen-for-methylene substitution at a different position, produced no detectable change in protein compartmentalization (7).

Exploiting cellular NMT activity to deliver analogs of myristate with altered physicochemical properties provides an opportunity to examine (*in vivo*) structural features of the acyl moiety that affects the functional properties of individual

Abbreviations: HIV-1, human immunodeficiency virus 1; NMT, myristoyl-CoA:protein N-myristoyltransferase (EC 2.3.1.97); AZT, 3'-azido-3'-deoxythymidine; 13-OxaMyr, 13-oxamyristate (12-methoxydodecanoate); 6-OxaMyr, 6-oxamyristate (5-octyloxypentanoic acid); RT, reverse transcriptase; Pr55^{gag}, 55-kDa gag polyprotein precursor; nef, negative factor.

**Deceased December 5, 1990.

The publication costs of this article were defrayed in part by page charge payment. This article must therefore be hereby marked “advertisement” in accordance with 18 U.S.C. §1734 solely to indicate this fact.

N-myristoylated proteins. In this report, we used radiolabeled analogs to begin to define the mechanism of their inhibitory effects on HIV-1 assembly in acutely and chronically infected lymphoid cell lines. The results are consistent with the notion that these compounds function in a manner that is distinct from 3'-azido-3'-deoxythymidine (AZT).

MATERIALS AND METHODS

Vectors for Expression of gag, gag-pol, or nef in *Escherichia coli*. pGG1 contains a functional clone of HIV-1 (HXB2gpt2 in ref. 9). pGA1 was produced by mutagenesis of the codon encoding Gly-2 in the gag gene of pGG1 to a codon-encoding alanine (4). Oligonucleotide-directed mutagenesis was used to introduce a new *Nco* I restriction site at the initiator methionine (ATG) codon contained in the 5.3-kilobase (kb) *Sac* I fragment of pGG1 or pGA1. pMGG1 and pMGA1 are gag expression vectors created by subcloning the *Nco* I-EcoRI "subfragments" from each of the above plasmids into pMON5840 (10). pMGGP1 and pMGPA1 are gag-pol expression vectors with codons encoding Gly-2 and Ala-1, respectively. They were constructed by subcloning the *Nco* I-Nco I fragments from pGG1 and pGA1 into pMON5840.

The polymerase chain reaction was used to introduce simultaneously a new *Nco* I site at the initiator methionine (ATG) codon and a unique *Hind*III site 3' to the termination codon of the nef gene, in p2/3MBNG1 (11) and in p2/3MBNA1 (which contains a Gly-2 → Ala mutation). The 627-base-pair (bp) *Nco* I-*Hind*III fragment from each plasmid was subcloned into pMON5840, yielding the nef expression vectors pMNG1 and pMNA1, respectively.

Metabolic Labeling Studies in Human Lymphoid Cells. Uninfected CD4⁺ H9 cells or those chronically producing HIV-1 (H9IIIB; ref. 9) were grown in RPMI 1640 medium containing 10% (vol/vol) fetal bovine serum, 100 units of penicillin per ml, 100 µg of streptomycin per ml, and 2 mM glutamine. Cells (10⁷) were "starved" overnight in RPMI 1640/5% delipidated fetal bovine serum and then incubated for 8 hr with fresh medium supplemented with 1 mCi (1 Ci = 37 GBq) of [³H]myristate or tritiated analog (final specific activity, 32 Ci/mmol) per ml and 5 mM pyruvate. Cells were washed twice with phosphate-buffered saline (PBS) at 4°C, scraped into ice-cold PBS, pelleted by centrifugation at 250 × g for 10 min, and lysed in radioimmunoprecipitation assay buffer (4). For immunoblot analyses, 50 µg of reduced and denatured lysate protein was separated by SDS/PAGE (12) and electroblotted onto nitrocellulose membranes. Virus-specific proteins were identified by sequential incubation of the blot with (i) pooled sera of AIDS patients or a monospecific rabbit polyclonal anti-nef serum; (ii) biotin-conjugated goat anti-human (or anti-rabbit) IgG; (iii) avidin-conjugated horseradish peroxidase (HRP); and (iv) the HRP substrate 4-chloro-1-naphthol.

Chronic Virus Replication Assay. H9IIIB cells were dispensed at 2 × 10⁵ cells per ml of RPMI 1640 medium into each well of 48-well culture plates. An equal volume of serum-free RPMI 1640 medium with or without analog (or AZT) was immediately added. After 48 hr, the cells were washed with serum-free medium to remove residual virus, refed with complete medium with or without analog, and maintained in culture for an additional 48 hr. The cell culture supernatant was subsequently collected, filtered through a 0.22-µm Millipore filter, and assayed for reverse transcriptase activity (13) or p24 virus antigen (Du Pont, ELISA).

Toxicity Studies. Cell viability was measured at the end of the treatment period in both acute (4) and chronic replication assays by (i) metabolic labeling studies with [³H]leucine or [³H]thymidine (5) and (ii) determination of the number of viable cells based on trypan blue exclusion (5).

RESULTS

Heteroatom-Containing Analogs of Myristate Serve as Alternative Substrates for *S. cerevisiae* NMT and Are Linked to the gag and nef Proteins of HIV-1 Expressed in *E. coli*. HIV-1 Pr55^{gag} is efficiently N-myristoylated when expressed in *S. cerevisiae* (14). Therefore, we first compared the substrate properties of myristate with the oxygen-substituted analogs in a coupled *in vitro* assay (6) that contained purified *S. cerevisiae* NMT (8) and a radiolabeled octapeptide (Gly-Ala-Arg-[³H]Ala-Ser-Val-Leu-Ser-NH₂) representing residues 2–9 of Pr55^{gag}. The results (Table 1) indicated that when converted to CoA thioesters, the three fatty acids have quite similar kinetic properties.

A second and more "physiologic" assay for analog incorporation involved the use of a dual plasmid expression system (Fig. 1A) that allows us to recreate this eukaryotic protein modification in *E. coli*, a bacterium that contains no endogenous NMT activity (10). *S. cerevisiae* NMT can be efficiently synthesized (~1% of total *E. coli* proteins) when its gene is placed under the control of the isopropyl β-D-thiogalactoside-inducible *tac* promoter in the plasmid pBB131 (10). Moreover, the fatty acid and peptide substrate specificities of *E. coli*-derived *S. cerevisiae* NMT are indistinguishable from those of the authentic yeast enzyme (8, 10). A second plasmid containing the nalidixic acid-inducible *recA* promoter can be used to direct production of a protein that is a known or potential substrate for the enzyme. Sequential induction of each promoter (NMT first) allows N-myristoylation to occur "in vivo" (10). When NMT and either wild-type (Gly-2) gag-pol (pMGGP1) or gag (pGG1) sequences were coexpressed in *E. coli*, a prominent radiolabeled 41-kDa band was recovered from [³H]myristate-labeled lysates by using anti-HIV-1 serum (Fig. 1B, lanes 1 and 3). Since synthesis of the 180-kDa gag-pol polyprotein in eukaryotic cells occurs by an inefficient translational frameshifting mechanism (15), we did not expect to find a labeled product of this size in *E. coli*. However, only trace quantities of the intact [³H]myristate-labeled Pr55^{gag} polypeptide were noted after immunoprecipitation of *E. coli* lysates even though this species could be easily detected in immunoblots (Western blots) of the same lysates (compare Fig. 1B Left and Right). [Previous studies in *E. coli* (16, 17) and *S. cerevisiae* (14) indicated that Pr55^{gag} undergoes proteolytic processing to a 41-kDa form even in the absence of HIV protease.]

The [³H]myristate 41-kDa labeled band was not present in lysates prepared from (i) strains producing NMT and mutant (Ala-2-containing) gag-pol (pMGPA1) or gag (pGA1) polypeptides and (ii) strains that contained pBB131 and pMON5840, the expression vector lacking HIV-1 sequences (Fig. 1B, lanes 2, 6, and 9). Western blot analysis revealed

Table 1. *In vitro* characterization of fatty acid analogs using an octapeptide (GARASVLS NH₂) derived from the NH₂ terminus of HIV-1 Pr55^{gag}

Fatty acid	Peptide			Fatty acid	
	K _m	V _{max}	V _{max} /K _m	K _m	V _{max}
CH ₃ (CH ₂) ₁₂ COOH	9	100	12	2	100
CH ₃ O(CH ₂) ₁₂ COOH	8	100	12	1	370
CH ₃ (CH ₂) ₈ O(CH ₂) ₄ COOH	14	118	8	2	99

As in previous reports (e.g., ref. 6), the apparent peptide K_m and V_{max} was first determined by using saturating concentrations of analog (15 µM). The acyl-CoA K_m and V_{max} was then measured by using the peptide substrate (specific activity, 0.8 Ci/mmol) at its K_m. The kinetic properties of each analog CoA were determined in parallel with myristoyl-CoA. All experiments were performed three times, and the data were averaged. Direct measurements of acyl-CoA production by *Pseudomonas* acyl-CoA synthetase (6) indicate that each of the three tritiated fatty acids has similar substrate properties: efficiency of conversion to their CoA thioesters ~60–70%.

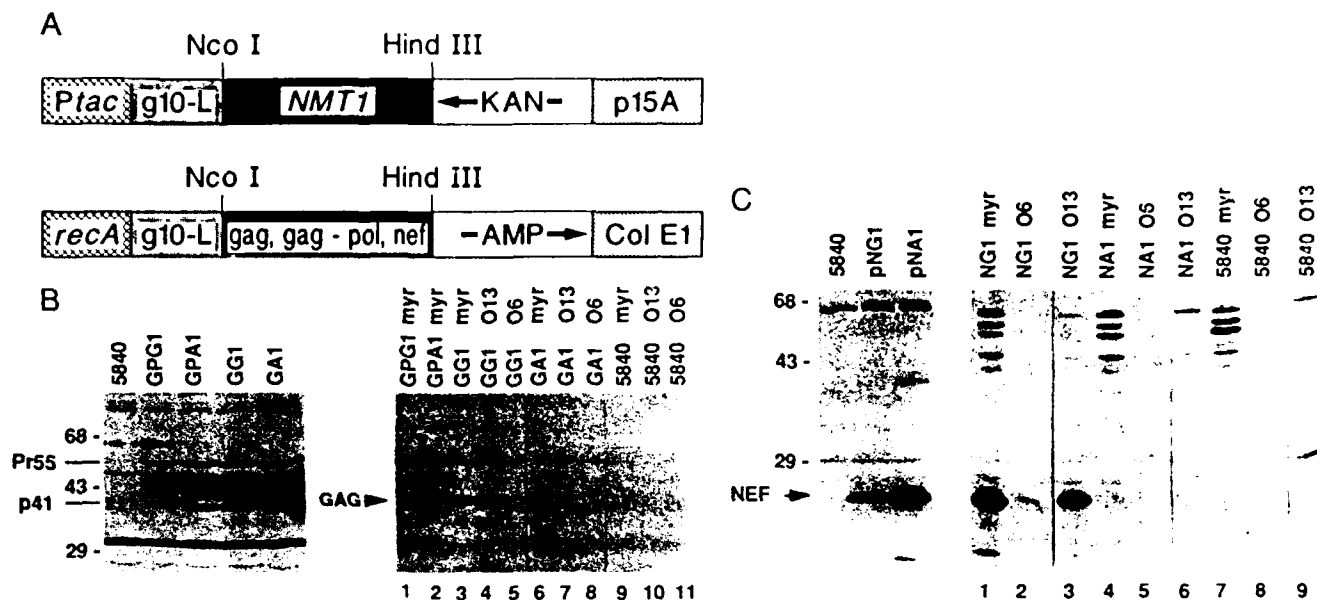


FIG. 1. Coexpression of *S. cerevisiae* NMT and HIV-1 gag, gag-pol, or nef in *E. coli*. Dual plasmid expression system. (B) Coexpression of NMT and HIV gag, or gag-pol, in midlogarithmic phase *E. coli* metabolically labeled (9) with [3 H]myristic acid (myr) or tritiated analog (ref. 7; final specific activity = 32 Ci/mmol; 100 μ Ci/ml of culture). (B Left) Immunodetection of HIV gag in the *E. coli* lysates (50 μ g of total protein) after reduction, denaturation, and electrophoresis through 7.5–20% polyacrylamide gels. Anti-HIV-1 sera were used to probe the Western blot. (B Right) Immunoprecipitation of the [3 H]myristic acid- or tritiated analog-labeled HIV-1 gag protein with the same antiserum. (C) Coexpression of NMT and HIV-1 nef in *E. coli* (50 μ g of total protein) labeled with [3 H]myristate or tritiated analog and detected by immunoblot (Left) or immunoprecipitation (Right) with rabbit anti-nef sera. O6, 6-OxaMyr; O13, 13-OxaMyr; g10-L, bacteriophage T7 gene 10 leader.

that the steady-state levels of the 55- and 41-kDa wild-type and mutant gag polypeptides were identical in all *E. coli* gag transformants and that neither species was present in bacteria containing pBB131 and pMON5840 (Fig. 1B Left). Control experiments also established that strains containing wild-type gag or gag-pol recombinant plasmids alone or either of the plasmids with pMON5839 (pBB131 without the NMT1 insert) failed to incorporate [3 H]myristate (data not shown).

Parallel studies revealed that tritiated 12-methoxydodecanoate [13-oxamyristate (13-OxaMyr)] was as efficiently incorporated into the wild-type gag as myristate (compare lanes 3 and 4 in Fig. 1B). Incorporation was blocked with the Gly-2 \rightarrow Ala mutation and required simultaneous expression of both NMT and gag (or gag-pol) (Fig. 1B, lanes 7 and 10). Interestingly, tritiated 5-octyloxypentanoate [6-oxamyristate (6-OxaMyr)] produced no detectable labeling of the wild-type gag proteins (Fig. 1B, lanes 5, 8, and 11). This finding, together with the *in vitro* data presented in Table 1 and the fact that treatment with the radiolabeled analog had no effect on the steady-state levels of the HIV-1 proteins in *E. coli* (as determined by Western blots), suggested that the efficiency of import of [3 H]6-OxaMyr by the *E. coli* fatty acid transporter (18) may be poor. Subsequent analyses showed that after a 30-min incubation period, uptake of [3 H]6-OxaMyr into logarithmically growing *E. coli* strain JM101 is 1/10th that of [3 H]13-OxaMyr, allowing us to postulate that the position of heteroatom substitution may effect interactions with this inner membrane-associated protein (18).

Similar labeling patterns were seen with nef (Fig. 1C). Myristate and 13-OxaMyr were incorporated into this protein with comparable efficiency (compare lanes 1 and 3 in Fig. 1C Right). Even though the wild-type (Gly-2) and mutant (Ala-2) nef proteins achieved comparable steady-state levels (Fig. 1C Left), only the Gly-2-containing species was labeled (Fig. 1C Right, compare lane 1 with 4 and 3 with 6). Incorporation of [3 H]myristate or the analog required simultaneous expression of NMT and nef (Fig. 1C Right, lanes 1 and 7); [3 H]6-OxaMyr labeled this protein poorly (lanes 2 and 5).

13-OxaMyr Inhibits Proteolytic Processing of HIV-1 Pr55^{gag} in Chronically Infected Human Lymphoid Cells. H9/IIIB cells

chronically produce HIV-1. Labeling studies indicated that [3 H]myristate-labeled gag proteins (55 and 41 kDa) are almost equally distributed between cytosolic (S100) and membrane (P100) fractions prepared (4) from these cells (cytosolic/membrane ratio = 1; Fig. 2B). The p17 matrix antigen of HIV-1 contains the NH₂-terminal myristoyl moiety and is cleaved by the virus-specific protease from Pr55^{gag} at the plasma membrane during virus assembly. Fig. 2B shows that this [3 H]myristate-labeled protein is almost exclusively associated with the P100 fraction. The additional 27- and 25-kDa labeled bands seen in these lanes represent incorporation of myristate into nef species (these were immunoprecipitated with a monospecific rabbit anti-nef serum) (Fig. 2C). Detection of two N-myristoylated forms of nef is not surprising because the H9/IIIB isolate is a mixture of at least three viral strains and produces several nef species including the intact 27-kDa protein as well as a species that is truncated at the COOH terminus (refs. 9, 11, and 12 and our unpublished observations).

13-OxaMyr was incorporated into the 27- and 25-kDa nef proteins but did not affect their predominant cytosolic distribution (Fig. 2C). By contrast, 13-OxaMyr incorporation into Pr55^{gag} was associated with a redistribution from the membrane to the cytosolic fraction (cytosolic/membrane ratio = 3; Fig. 2B). Moreover, there was a marked reduction in the intensity of labeling of p17 (compare the myristate- and 13-OxaMyr-labeled pellet fractions in Fig. 2B), suggesting that the analog inhibited proteolytic processing of Pr55^{gag}. Incubation of H9/IIIB cells with [3 H]6-OxaMyr for 8 hr resulted in very poor labeling of nef (Fig. 2C) and virtually undetectable labeling of the gag proteins (Fig. 2B).

To examine the specificity of the analog's effect on proteolytic processing, we incubated H9/IIIB cells for 48 hr with 40 μ M 13-OxaMyr, 40 μ M decanoate (10:0) (the hydrophobicities of 13-OxaMyr and decanoate are equivalent; ref. 6), 0.1% ethanol (the solvent used to dissolve the analog), or 5 μ M AZT. Western blots of total cellular proteins were then probed with a mouse monoclonal anti-p24 antiserum (4). Pr55^{gag} and its specific cleavage product p24 were readily identified in each of the lysates (Fig. 2A). A marked decrease

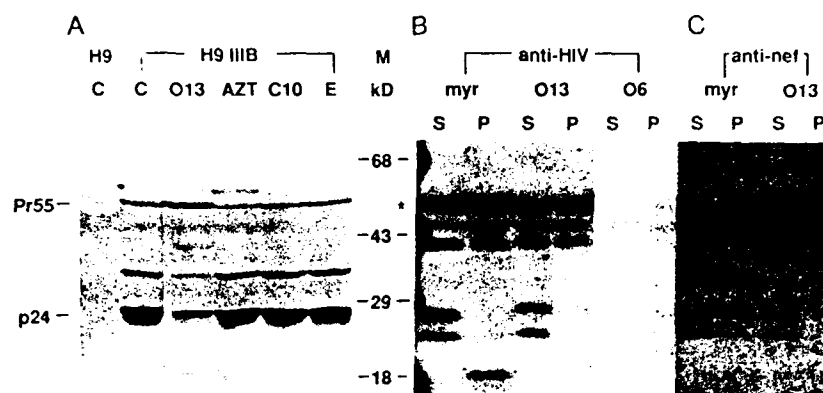


FIG. 2. 13-OxaMyr blocks proteolytic processing of HIV-1 Pr55^{gag} in chronically infected human lymphoid cells. (A) Immunoblot detection of HIV Pr55^{gag} and p24 in H9 IIB cells after incubation with medium alone (lanes C), 0.1% ethanol (lane E), 40 μ M decanoic acid (lane C10), 40 μ M 13-OxaMyr (lane O13), or 5 μ M AZT (lane AZT). A monoclonal anti-p24 antibody (4) was used. (B) Immunoprecipitation of HIV-1 proteins in 100,000 \times g soluble (lanes S) or pellet (lanes P) fractions of H9 IIB cells metabolically labeled (4) with [³H]myristate (lanes myr), [³H]13-OxaMyr (lanes O13), or [³H]6-OxaMyr (lanes O6). The intact Pr55^{gag} is indicated by an asterisk. (C) Immunoprecipitation of HIV nef species from the same fractions as in B. The results shown in A–C are representative of those obtained in three independent experiments.

in proteolytic processing of Pr55^{gag} to p24 was noted only with analog treatment.

[³H]13-OxaMyr Reduces the Concentration of AZT Required to Inhibit HIV-1 Replication in an Acute Replication Assay. 13-OxaMyr produces a dose-dependent reduction in HIV-1 production in acutely infected CD4⁺ H9 cells without accompanying cellular toxicity: the \approx 90% reduction in cell-free reverse transcriptase (RT) and p24 antigen levels achieved with 20–40 μ M analog is comparable to that produced by 5 μ M AZT (5). We examined the combined effect of 13-OxaMyr and AZT because (i) the data presented in Fig. 2 suggested that 13-OxaMyr may affect a step that occurs late in virus replication (i.e., assembly at the membrane and/or proteolytic processing of gag polypeptide precursors), and (ii) AZT blocks proviral DNA synthesis by inhibiting RT—an early step in virus infectivity. We determined in preliminary experiments (data not shown) that 0.03 μ M AZT produced a 50% reduction in virus-associated RT activity. At concentrations where neither analog nor AZT alone produced significant (>10%) reductions in virus production, the combination of the two compounds produced a moderate but reproducible synergistic effect (0.01 or 0.02 μ M AZT plus 0.1 or 1.0 μ M analog in Fig. 3A). When the concentration of analog exceeded 10 μ M or when AZT was added at 0.05 μ M or more, the advantage of combining drugs was obscured by the significant effect of each alone.

[³H]13-OxaMyr Inhibits Chronic HIV-1 Production in H9/IIB Cells. Chronically infected cells in human hosts could play a significant role in HIV-1 persistence and latency. Virus production from such cells would not be affected by treatment with AZT. However, compounds that disrupt late steps in virus replication could decrease virus load and interrupt the replicative cycle. Therefore, the effects of 40 μ M 13-OxaMyr, 40 μ M decanoate, 5 μ M AZT, and 0.1% ethanol were compared in chronically infected cells. A 60% reduction in p24 antigen and RT activity was documented 2 days after treatment with analog; AZT, decanoate, or ethanol had no effect on these measures of virus production (Fig. 3B). Furthermore, analog treatment had no demonstrable toxic effects on the host H9 cells as measured by cell number and protein synthesis (Fig. 3B).

The long-term effect of this analog (50 μ M) on virus production was tested by extending the treatment period to 12 days (Fig. 3C). RT activity was reduced \approx 70% by day 6 of treatment and was maintained at this level until removal of 13-OxaMyr from the culture medium. Analog withdrawal resulted in a progressive rise in RT activity. However, no

increases were noted for 48 hr, and levels had not fully returned to pretreatment or control (0.1% ethanol) values 8 days later (Fig. 3C). (Note that the number of viable cells in each of the test groups was comparable at the end of the test period.) The long-lived antiviral effect suggests that the analog is able to avoid metabolic processing and/or that the intracellular levels of drug that are required to inhibit HIV-1 replication may be very low.

DISCUSSION

We have explored the mechanism by which myristic acid analogs can selectively inhibit HIV-1 replication and assembly. A dual plasmid expression system that reconstitutes protein N-myristoylation in *E. coli* was initially used to determine whether two fatty acid analogs—differing only in the site of the oxygen-for-methylene substitution—could be converted to their CoA thioesters and incorporated into HIV-1 Pr55^{gag} and nef proteins. [³H]13-OxaMyr worked as well as myristate in this assay system and also was incorporated into these two proteins in H9 cells. This analog causes Pr55^{gag} to redistribute from membrane to cytosolic fractions and markedly reduces its proteolytic processing by viral protease. These results have implications not only about the function of the myristoyl moiety in Pr55^{gag} but also about potential therapeutic strategies for the treatment of AIDS.

The metabolic labeling studies carried out in HIV-1-infected H9 cells confirmed our earlier hypothesis (5) that 13-OxaMyr serves as an alternative substrate for human lymphocyte acyl-CoA synthetase and NMT. The poor incorporation of [³H]6-OxaMyr into gag and nef was part of a general failure to label H9 cellular proteins compared with [³H]myristate and [³H]13-OxaMyr (data not shown). Studies with a murine myocyte cell line (BC₃H1) and rat fibroblasts have indicated that 6-OxaMyr is incorporated into a much smaller subset of cellular proteins than is 13-OxaMyr (7). This may reflect differences in their uptake, conversion to acyl-CoAs, susceptibility to metabolic processing, and/or interactions with NMT.

The two observed consequences of incorporating 13-OxaMyr into Pr55^{gag} (redistribution from membrane to cytosolic fractions and inhibition of proteolytic processing) may be interrelated. Gly-2 \rightarrow Ala mutagenesis of Pr55^{gag} blocks N-myristoylation and proteolytic processing in HeLa cells (4). However, the Myr⁻-Pr55^{gag} can be processed by purified HIV protease *in vitro* (4). The myristoyl moiety may be required for intermolecular association of the larger gag-pol precursor and autocatalytic release/activation of viral pro-

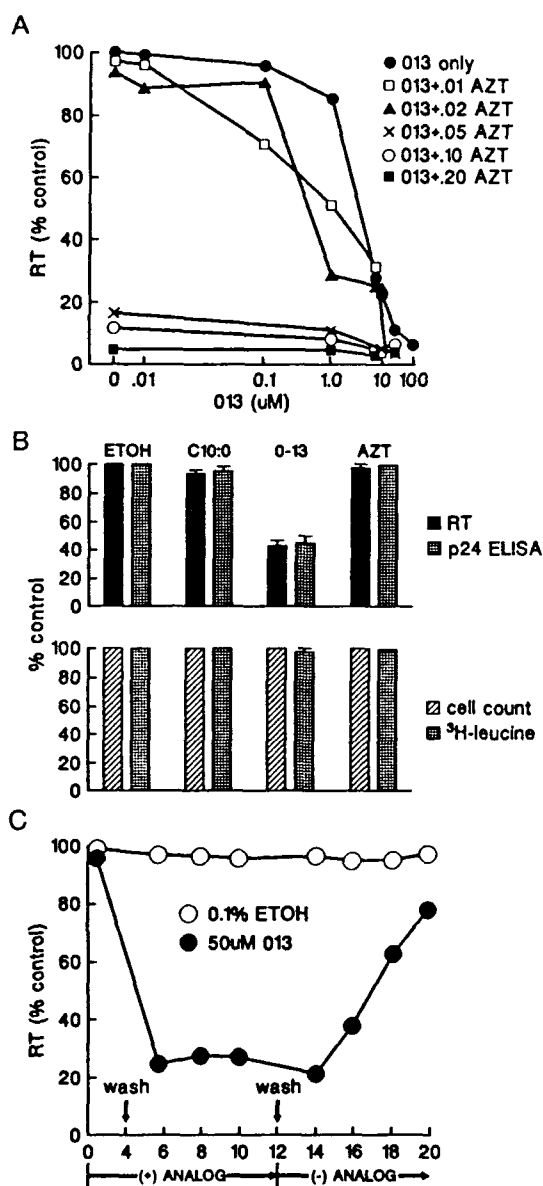


FIG. 3. Effect of 13-OxaMyr (O13) on the propagation of HIV-1 in acute and chronic replication assays. (A) Combined effect of 13-OxaMyr and AZT on virus replication in an acute infectivity assay (5). HIV-1-infected H9 cells were treated with 13-OxaMyr, AZT, or both for 10 days (5), and virus replication was measured by RT activity and compared to untreated or ethanol (0.1%)-treated infected cells. The SEM at each point varied no more than 10% ($n = 2$ experiments, each assay done in triplicate). (B) The effect of 40 μ M 13-OxaMyr (bars O-13), 5 μ M AZT, 40 μ M decanoate (bars C10:0), and 0.1% ethanol on virus production and cell viability in chronically infected H9/IIIB cells is expressed as a percentage of untreated virus-producing cells. (C) The long-term effect of 50 μ M 13-OxaMyr on HIV-1 replication in chronically infected H9/IIIB cells. The virus-producing cells were treated with 50 μ M 13-OxaMyr (O13) or 0.1% ethanol for 48 hr, washed to remove residual virus, and refed every other day with medium containing either 13-OxaMyr or ethanol. On day 12, the cells were washed and refed with medium alone.

tease (19) or it may exert its effects by stabilizing association with the plasma membrane where such protein-protein interactions could become more likely, and autocatalytic cleavage, more efficient. Although the precise mechanism is unclear, our data suggest that treatment of H9 cells with combinations of HIV protease inhibitors and heteroatom-

containing analogs may produce even greater (synergistic?) inhibition of gag polyprotein precursor processing. Additional experiments with radiolabeled analogs containing other structural perturbations may provide further insights about the physical-chemical features of the acyl chain that are required for targeting and processing of HIV-1 gag proteins.

The results obtained in the chronic virus replication assay are consistent with the hypothesis that 13-OxaMyr affects a late step in the virus life-cycle. However, it is premature to conclude that the analog exerts its antiviral effects only as a result of its incorporation into gag, gag-pol, or nef. It may perturb the biological function of other cellular N-myristoylated proteins that could modulate the course of viral infection. For example, the NH₂-terminal region of the src-like protein tyrosine kinase, p56^{lck}, interacts with the cytoplasmic domain of the cell-surface glycoproteins CD4/CD8 on the inner aspect of the plasma membrane (20, 21). Such interactions appear to be important in T-lymphocyte proliferation and activation (21). Analog incorporation into p56^{lck} may disrupt these events. Our results do raise the possibility that combination chemotherapy with these analogs and AZT not only may allow reduction in the dose of AZT, but also may provide a therapeutic strategy that is useful for both acute and chronic aspects of viral infection.

This work was supported by grants from the National Institutes of Health, the Monsanto Company, and the American Foundation for AIDS Research.

- Veronese, F. D., Copeland, T. D., Oroszlan, S., Gallo, R. C. & Sarngadharan, M. G. (1988) *J. Virol.* **62**, 795-801.
- Guy, B., Kieny, M. P., Riviere, Y., Lepeuch, C., Dott, K., Girard, M., Montagnier, L. & Lecocq, J. P. (1987) *Nature (London)* **330**, 266-269.
- Gottlinger, H. G., Sodroski, J. G. & Haseltine, W. A. (1989) *Proc. Natl. Acad. Sci. USA* **86**, 5781-5785.
- Bryant, M. L. & Ratner, L. (1990) *Proc. Natl. Acad. Sci. USA* **87**, 523-527.
- Bryant, M. L., Heuckeroth, R. O., Kimata, J. T., Ratner, L. & Gordon, J. I. (1989) *Proc. Natl. Acad. Sci. USA* **86**, 8655-8659.
- Heuckeroth, R. O., Glaser, L. & Gordon, J. I. (1988) *Proc. Natl. Acad. Sci. USA* **85**, 8795-8799.
- Johnson, D. R., Cox, A. D., Solski, P. A., Devadas, B., Adams, S. P., Leimgruber, R. M., Heuckeroth, R. O., Buss, J. E. & Gordon, J. I. (1990) *Proc. Natl. Acad. Sci. USA* **87**, 8511-8515.
- Rudnick, D. A., McWherter, C. A., Adams, S. P., Ropson, I. J., Duronio, R. J. & Gordon, J. I. (1990) *J. Biol. Chem.* **265**, 13370-13378.
- Fisher, A. G., Ratner, L., Mitsuya, H., Marselle, L. M., Harper, M. E., Broder, S., Gallo, R. C. & Wong-Staal, F. (1986) *Science* **233**, 655-659.
- Duronio, R. J., Jackson-Machelski, E., Heuckeroth, R. O., Olins, P. O., Devine, C. S., Yonemoto, W., Slice, L. W., Taylor, S. S. & Gordon, J. I. (1990) *Proc. Natl. Acad. Sci. USA* **87**, 1506-1510.
- Ratner, L., Fisher, A., Jagodzinski, L. L., Mitsuya, H., Liou, R.-S., Gallo, R. C. & Wong-Staal, F. (1987) *AIDS Res. Hum. Retroviruses* **3**, 57-69.
- Laemmli, U. K. (1970) *Nature (London)* **227**, 680-685.
- Poiesz, B. J., Ruscetti, F. W., Gazdar, A. F., Bunn, P. A., Minna, J. D. & Gallo, R. C. (1980) *Proc. Natl. Acad. Sci. USA* **77**, 7415-7419.
- Bathurst, I. C., Chester, N., Gibson, H. L., Dennis, A. F., Steimer, K. S. & Barr, P. (1989) *J. Virol.* **63**, 3176-3179.
- Jacks, T., Power, M. D., Masiarz, F. R., Luciw, P. A., Barr, P. J. & Varmus, H. E. (1988) *Nature (London)* **331**, 280-283.
- Debouck, C., Gorniale, J. G., Strickler, J. E., Meek, T. D., Metcalf, B. W. & Rosenberg, M. (1987) *Proc. Natl. Acad. Sci. USA* **84**, 8903-8906.
- Komiyama, N., Hattori, N., Inoue, J.-I., Sakuma, S., Kurimura, T. & Yoshida, M. (1989) *AIDS Res. Hum. Retroviruses* **5**, 411-419.
- Nunn, W. D., Colburn, R. W. & Black, P. N. (1986) *J. Biol. Chem.* **261**, 167-171.
- Navia, M. A., Fitzgerald, P. M. D., McKeever, B. M., Leu, C., Heimbach, J. L., Herber, W. K., Sigal, I. S., Darke, P. L. & Springer, J. P. (1989) *Nature (London)* **337**, 615-620.
- Veillette, A., Bookman, M. A., Horak, E. M., Samelson, L. E. & Bolen, J. B. (1989) *Nature (London)* **338**, 257-259.
- Turner, J. M., Brodsky, M. H., Irving, B. A., Levin, S. O., Perlmutter, R. M. & Littman, D. R. (1990) *Cell* **60**, 755-765.

Dual Regulation of Silent and Productive Infection in Monocytes by Distinct Human Immunodeficiency Virus Type 1 Determinants

PETER WESTERVELT,¹ TIMOTHY HENKEL,¹ DAVID B. TROWBRIDGE,¹ JAN ORENSTEIN,² JOHN HEUSER,¹ HOWARD E. GENDELMAN,⁴ AND LEE RATNER^{1*}

Departments of Medicine and Molecular Microbiology¹ and Cell Biology,³ Washington University School of Medicine, St. Louis, Missouri 63110; Department of Pathology, George Washington University, Washington D.C. 20037²; and Henry M. Jackson Foundation for the Advancement of Military Medicine and the Department of Cellular Immunology, HIV Immunopathogenesis Program, Walter Reed Army Institute of Research, Rockville, Maryland 20850⁴

Received 23 December 1991/Accepted 16 March 1992

The regulation of human immunodeficiency virus type 1 infection and replication in primary monocytes was investigated by mutagenesis of recombinant proviral clones containing an *env* determinant required for the infectivity of monocytes. Virus replication was assayed by determination of reverse transcriptase activity in culture fluids and by recovery of virus from monocytes following cocultivation with uninfected peripheral blood mononuclear cells. Three virus replication phenotypes were observed in monocytes: productive infection, silent infection, and no infection. Incorporation of the monocyctotropic *env* determinant in a full-length clone incapable of infection or replication in primary monocytes (no infection) conferred the capacity for highly efficient virus replication in monocytes (productive infection). Clones with the *env* determinant but lacking either functional *vpr* or *vpu* genes generated lower replication levels in monocytes. Mutation of both *vpr* and *vpu*, however, resulted in nearly complete attenuation of virus replication in monocytes, despite subsequent virus recovery from infected monocytes by cocultivation with uninfected peripheral blood mononuclear cells (silent infection). These findings indicate a central role for the "accessory" genes *vpu* and *vpr* in productive human immunodeficiency virus type 1 replication in monocytes and indicate that *vpu* and *vpr* may be capable of functional complementation.

Human immunodeficiency virus type 1 (HIV-1) infection of macrophages has been demonstrated in brain, spinal cord, lung, lymph node, and skin during subclinical infection and disease and is postulated to underlie important clinical manifestations of HIV-1 infection, including disease latency and development of a spectrum of AIDS-related central nervous system disorders (2, 4, 11, 14, 15, 19, 33, 37). However, detailed molecular analysis of virus-host cell interactions involving monocytes was limited until recently by the restricted tropism of the earliest and most widely studied HIV-1 genetic clones for primary monocytes cultured *in vitro* (14, 15). Previously, we and others have demonstrated that a discrete *env* determinant, including the V3 loop but not the CD4-binding domain, is necessary and sufficient for HIV-1 infection of monocytes (23, 29, 36). Additionally, we have identified three virus replication phenotypes in monocytes *in vitro*, using molecularly defined proviral clones (35). These include productive infection, with the generation of high virus replication levels; silent infection, with low to undetectable virus replication in monocytes, despite ultimate virus recovery from infected monocytes following cocultivation with uninfected, phytohemagglutinin-stimulated peripheral blood mononuclear cells (PBMCs [lymphoblasts]); and no infection, with neither virus replication in nor virus recovery from monocytes observed. In the present study, we investigated the roles of the HIV-1 "accessory" genes *vpr* and *vpu*, which are dispensable for virus replication in primary and immortalized CD4⁺ T lymphocytes. We demonstrate that *vpr* and *vpu* are central to the regulation of virus replication in primary

monocytes and together mediate the expression of silent versus productive infection.

To study viral regulation of monocyte infection, we utilized a panel of chimeric HIV-1 clones, constructed from the nonmonocyctotropic clone HXB2 and the monocyctotropic clone ADA, as previously described (16, 26, 35, 36). To correct a *vpr* defect in each of these clones, the result of a single base insertion in HXB2, 2.7-kb *Sall*-*Bam*HI HXADA DNA fragments (nucleotides 5785 to 8474) were subcloned into the full-length proviral clone NL4-3, in which the *vpr* open reading frame is intact (1). The resultant NLHXADA clones contained the ADA-derived *env* determinant previously localized to nucleotides 7040 to 7323, flanked by additional ADA- or HXB2-derived sequences encoding other portions of *env* and *vpu* and small portions of *tat* and *rev*. A clone in which the entire 5785-to-8474 sequence was HXB2 derived (thus lacking a monocyctotropic *env* determinant) was used as a negative control for these experiments. Because HXB2 lacks a *vpu* initiator methionine codon, clones in which *vpu* was HXB2 derived were defective for that product, in contrast to clones with an ADA-encoded *vpu*. Finally, a *vpr* mutant corresponding to each NLHXADA clone was generated by introducing a frameshift mutation at codon 63.

Virions from the recombinant clones, generated by transfection, were assayed for their ability to infect and replicate in primary monocytes by the presence of reverse transcriptase (RT) activity in culture supernatants (25) and by the ultimate recovery of virus following cocultivation of monocytes with uninfected PBMCs. The results are summarized in Fig. 1. All clones containing the ADA-derived *env* determinants and an intact *vpr* gene generated high virus replication levels in monocytes. Inactivation of *vpr* in these

* Corresponding author.

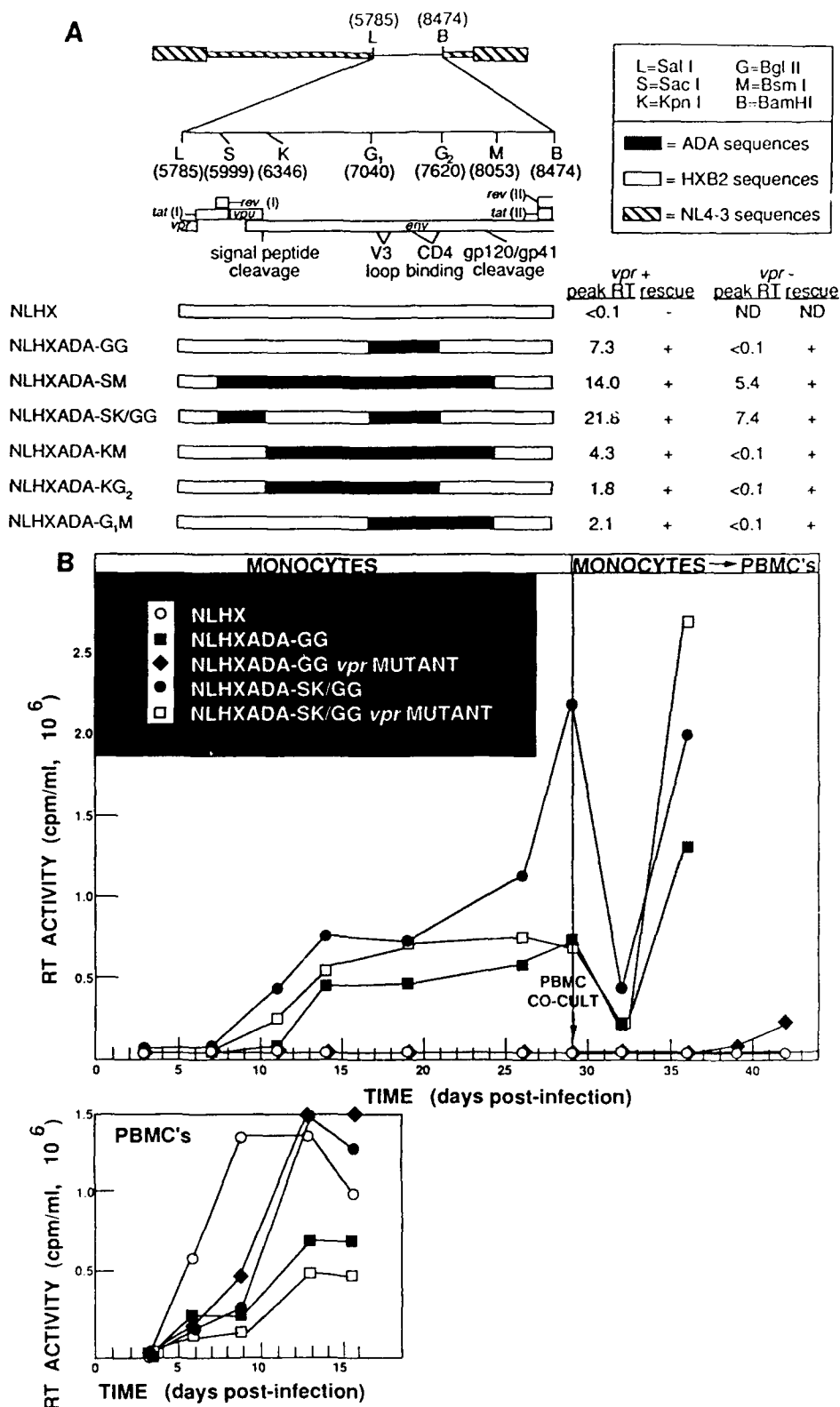


FIG. 1. Replication of recombinant HIV-1 clones with both wild-type and mutant *vpr* genes. (A) The panel of recombinant NLHXADA clones is represented diagrammatically. The region of the genome corresponding to the HXB2- and ADA-derived sequences (nucleotides 5785 to 8474) is expanded to highlight the relative positions of HXB2- and ADA-derived sequences. The open reading frames in this portion of the genome are represented above. Recombinant clones were generated by reciprocal DNA fragment exchanges of ADA- and HXB2-derived sequences into a *SalI*-*BamHI* fragment (5785 to 8474) from HXB2 subcloned into an intermediate shuttle vector, utilizing the restriction enzyme sites indicated on top. The resultant chimeric *SalI*-*BamHI* fragments were then subcloned into the clone NL4-3 to generate

clones, however, generated divergent results, depending upon the derivation of nucleotide sequences 5999 to 6345 (SK fragment). Clones in which this portion of the genome was ADA derived generated lower (but readily detectable) virus replication levels than did their wild-type *vpr* counterparts. However, *vpr* mutants in which SK was HXB2 derived typically failed to generate virus replication levels detectable above background in monocytes, despite subsequent virus recovery from these cultures onto uninfected PBMCs. The negative control clone, which carried a wild-type *vpr* but lacked the monocytotropic *env* determinant, generated virions which neither replicated in nor were recovered from monocytes, as previously demonstrated. No significant differences were seen in the replication of each virus strain on PBMCs obtained from several different donors.

Monocytes were infected with recombinant HIV-1 clones containing a functional *vpr* gene, stained with toluidine blue, and examined by light microscopy (1- μ m-thick plastic sections). Cultures infected with a nonmonocytotropic virus, NLHXADA-SK, which contains a functional *vpu* gene, were indistinguishable from uninfected cells, with rare, small multinucleated cells (Fig. 2A). Cultures productively infected with virus containing the monocytotropic *env* determinant and a functional (NLHXADA-SM [Fig. 2B]) or nonfunctional (NLHXADA-GG [Fig. 2C]) *vpu* gene showed characteristic cytopathic effects (15). These consisted of the formation of multinucleated giant cells, often containing 10 or more nuclei per cell, and cell lysis. The frequencies and sizes of these cells were comparable in the NLHXADA-SM- and NLHXADA-GG-infected monocyte cultures. Virus production and cellular degeneration and necrosis were primarily confined to the multinucleated cells. Transmission electron microscopy examination demonstrated typical budding and mature virions in intracellular vacuoles that were associated with the plasma membrane, in both the presence and absence of *vpu*, but not in the NLHXADA-SK-infected cells (Fig. 2D). Freeze fracture scanning electron microscopy demonstrated budding of virion particles from the plasma membrane of monocytes infected with virus which lacked a functional *vpu* (Fig. 2E). No virus could be detected in monocytes infected with recombinant clones lacking both *vpr* and *vpu* (data not shown).

The SK fragment encodes the entire *vpu* gene product, 14 amino acids at the C termini of both the *tat* and the *rev* first exons, and the N-terminal 41 amino acids of *env* (Fig. 3). Although the absence of a *vpu* initiator methionine codon in HXB2 is the most obvious difference between the SK portions of HXB2 and ADA, a role for *tat*, *rev*, or *env* could not be ruled out. The *env* sequences differ at 7 of 41 predicted amino acid positions, not including the nonaligned insertion of 3 residues and deletion of 4 residues in ADA. All but three of these differences are confined to the signal peptide, which varies by up to 30% between different clones

(20). Furthermore, *tat* and *rev* both differ at 3 of 14 amino acid positions between the ADA and HXB2 SK fragments, with four of these six changes being conservative in nature. Therefore, it is unlikely that these alterations in *env*, *tat*, or *rev* alter their function. However, to formally determine the specific requirement for *vpu* during HIV-1 infection of monocytes, the *vpu* initiator methionine codon of the silent infection clone NLHXADA-GG (*vpr* mutant) was restored by site-directed mutagenesis. The resultant clone was found to generate virus capable of productive infection of monocytes (data not shown).

HIV-1 and related lentiviruses are distinct from most other retroviruses in that besides the structural *gag*, *pol*, and *env* genes common to all retroviruses, they also encode a number of genes whose functions have been shown or are speculated to be regulatory in nature. In HIV-1, these genes include *tat*, *rev*, *vif*, *nef*, *vpu*, and *vpr* (6-8, 26, 32, 38). While *tat*, *rev*, and *vif* are essential for viral gene expression or virion infectivity, the precise role and overall importance of *vpr*, *vpu*, and *nef* are unclear, since these genes are dispensable for virus infection and replication in CD4⁺ lymphocytes in vitro (8-10, 12, 13, 22, 24, 30, 32). The availability of molecular HIV-1 clones which infect and replicate in monocytes at levels comparable to those observed with many monocytotropic virus isolates has facilitated investigation of the role that these viral genes may play in regulating the virus life cycle in monocytes. In the present study, we observed moderately decreased levels of virus replication in the absence of either *vpr* or *vpu*, whereas in the absence of both genes, virus replication in monocytes dropped to levels barely at or below the level of detection by the RT assay, such that infection of these cells usually could be detected only by virus rescue onto PBMCs.

The *vpr* open reading frame encodes a protein of 96 amino acids in most HIV-1 clones and is conserved in other lentiviruses, including visna-maedi virus (20, 31). Previous studies have shown that *vpr* is not required for HIV-1 infection or replication in CD4⁺ lymphocytic cell lines in vitro, although its inactivation led to slower replication kinetics and delayed cytopathogenicity in these cells (6, 10, 24). A recent study involving HIV type 2 (HIV-2) has shown that *vpr* is likewise dispensable during infection of PBMCs and T-cell lines but essential for productive infection of monocytes (17). The *vpr* protein has been demonstrated by radioimmunoprecipitation to be virion associated, and thus it is speculated to function either late in the virus life cycle, during particle assembly or maturation, or early, during the initial stages of infection (6). The *vpu* gene encodes an 80-to-82-amino-acid protein. It has not been reported whether the *vpu* protein is found in virion particles. *vpu* has been shown to augment virion particle release from infected cells without affecting levels of viral RNA or protein synthesis (8, 32). In the absence of *vpu*, a higher ratio of immature to mature particles has been seen, with a shift in capsid

recombinant NLHXADA clones. To inactivate *vpr*, clones were digested with *EcoRI* (nucleotide 5745), treated with Klenow fragment, and religated to generate a 4-bp insertion, as previously described (24). The replication levels of these clones in monocytes are summarized to the right of each clone. Monocytes were infected as previously described (36) by using filtered virus stocks generated by transection of proviral DNA onto SW480 cell monolayers, and titers were determined by measuring RT activity. Infections were done at low multiplicities of infection (10 to 100 tissue culture infective doses per well) with monocytes plated at an initial density of 2×10^5 cells per well. Virus replication was monitored by serial determinations of RT activity in culture supernatants (25). Peak RT activities (days 26 to 29) are expressed as 10^3 counts per minute per milliliter. To determine virus rescue, fresh, uninfected PBMCs were added to monocyte cultures at 29 days postinfection, cocultivated (co-cult) for 2 days, and maintained separately for up to 12 additional days, while RT activity was monitored. Rescue was scored as positive with two successive RT results that were more than fivefold above background level. (B) The replication kinetics of representative NLHXADA clones is graphed. Similar results were obtained in three to five replicate experiments.

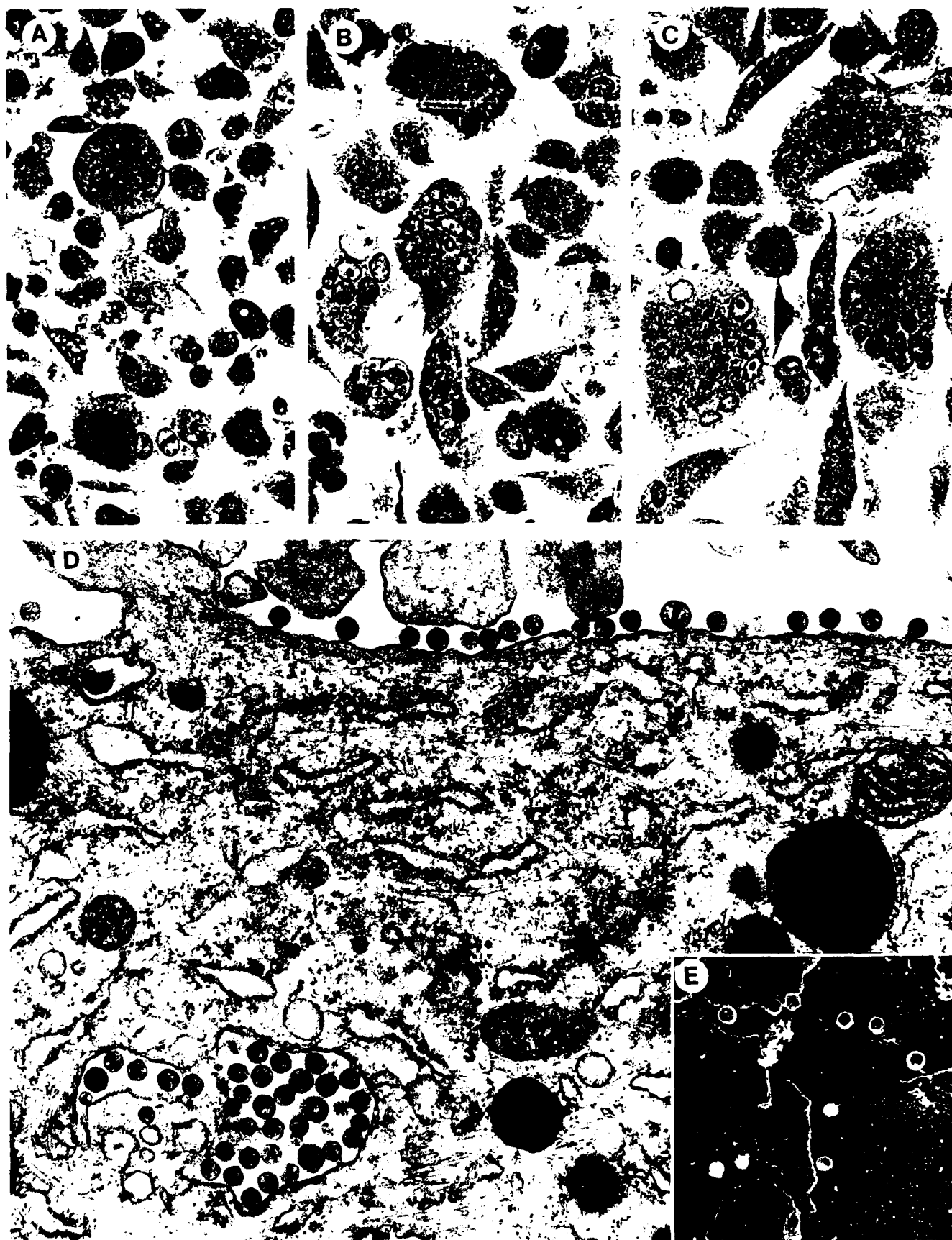


FIG. 2. Light, transmission, and freeze fracture scanning electron microscopy of infected monocytes. Light micrographs of toluidine blue-stained semithin plastic sections showing typical fields of primary monocytes infected by nonmonocytotropic clone NLHXADA-SK (35) (A) and monocytotropic clones NLHXADA-SM (B) and NLHXADA-GG (C) are shown (15). The multinucleated giant cells were fewer and smaller in panel A than in panels B and C. Magnification, $\times 480$. Infected adherent cultured cells were carefully washed twice with phosphate-buffered saline (PBS), fixed in situ with 2% glutaraldehyde (pH 7.2) in PBS, scraped free with a rubber policeman, transferred to a 15-ml plastic conical tube, and pelleted for 10 min at $600 \times g$ centrifugation. The cells were mixed with warm agar, repelleted in the Microfuge for 1 min, and refrigerated overnight to form a firm agar block. The agar block was divided into small pieces and processed into Spurr's plastic, after osmification and block uranyl acetate staining (15). Sections (1 μ m thick) were stained with toluidine blue for light microscopy, while thin sections (600 Å [60.0 nm]) were stained with uranyl acetate and lead citrate for transmission electron microscopy. (D) Transmission electron micrograph of a small portion of a multinucleated cell from NLHXADA-GG-infected monocytes showing a cytoplasmic vacuole (lower left) containing immature and mature virions and numerous typical mature particles associated with a stretch of plasma membrane. Magnification, $\times 34,000$. (E) Transmission electron microscopy view of NLHXADA-GG-infected monocytes, stabilized by formaldehyde fixation before quick-freezing, freeze-drying, and platinum replication (18). Budding from the convoluted surface are several 50-nm-diameter brightly outlined spherical virus particles. At higher magnification (not shown), these display characteristic surface coats of gp120 "pegs."

formation from the plasma membrane to intracellular membranes (8). In monocytes, however, particle assembly and release occur both at the plasma membrane and in intracellular vacuoles in the presence or absence of *vpu*, as shown in Fig. 2D.

It is intriguing that HIV-2 and simian immunodeficiency virus lack a *vpu* open reading frame but instead carry a gene designated *vpx*, which encodes a protein of 114 to 118 amino acids in these viruses (20). *vpu* and *vpx* occupy similar positions in their respective viral genomes, between *pol* and *env*, but have only distant amino acid homology. Recently, it has been suggested that *vpx* and *vpr* arose by duplication from a common progenitor in HIV-2 and simian immunodeficiency virus, on the basis of predicted amino acid sequence homology between the genes (34). To investigate the possibility of a similar link between *vpr* and *vpu* in HIV-1, the predicted amino acid sequences of both *vpu* and *vpr* were aligned with that of *vpr* (Fig. 4). Although less compelling than the homology between *vpr* and *vpx*, a 38% identity was observed between *vpr* and *vpu* over a 24-residue overlap at the C terminus of *vpu* and the N terminus of *vpr*. These sequences were particularly rich in acidic residues. Similarity in the hydrophilicity profiles of these portions of the *vpu*, *vpr*, and *vpx* products was also noted. The striking effect on virus replication levels in monocytes observed only when both genes were defective suggests that their gene products may perform similar roles and thus provide partial functional complementation. Alternatively, since lower replication lev-

els were observed in the absence of either gene, the nearly complete attenuation observed in the absence of both may result from a compound effect of the loss of two relatively important but functionally unrelated genes. More detailed studies to determine the precise mechanisms of action of the *vpr* and *vpu* gene products will be required to address these alternatives. In either case, our data indicate that together, *vpr* and a second determinant, *vpu*, are more important for efficient HIV-1 infection and replication in primary monocytes than was observed previously in lymphocytes. These observations provide a rationale for designing potential antiviral therapies to block the action of these gene products during HIV-1 infection of monocytes.

Persistent infection of tissue macrophages plays an important role in the pathogenic effects of other lentiviruses, including equine infectious anemia virus, visna-maedi virus, and caprine arthritis-encephalitis virus, providing a sanctuary for continuous virus replication in the face of a vigorous host immune response (15, 21). The onset of increased virus replication has been correlated with the onset of clinical disease manifestations, such as encephalitis, pneumonitis, arthritis, and hemolytic anemia. Similarly, HIV-1 infection of macrophages generates a reservoir of virus which is present throughout the course of subclinical infection and clinical disease. The existence of poorly replicative HIV-1 variants may be essential for establishment of persistent macrophage infection during the early, asymptomatic stage of disease. Several studies have suggested a relationship

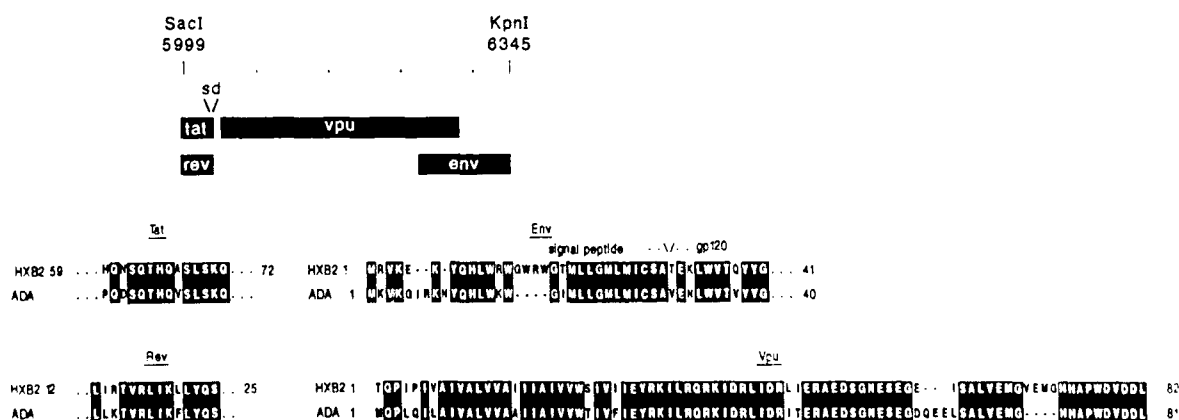


FIG. 3. Comparison of SK virus replication determinant from HXB2 and ADA. The predicted amino acid sequences of *vpu* and the portions of *tat*, *rev*, and *env* which are encoded by nucleotides 5999 to 6345 (SK fragment) from HXB2 and ADA are aligned by using single-letter amino acid designations. Identical residues are indicated within boxes.

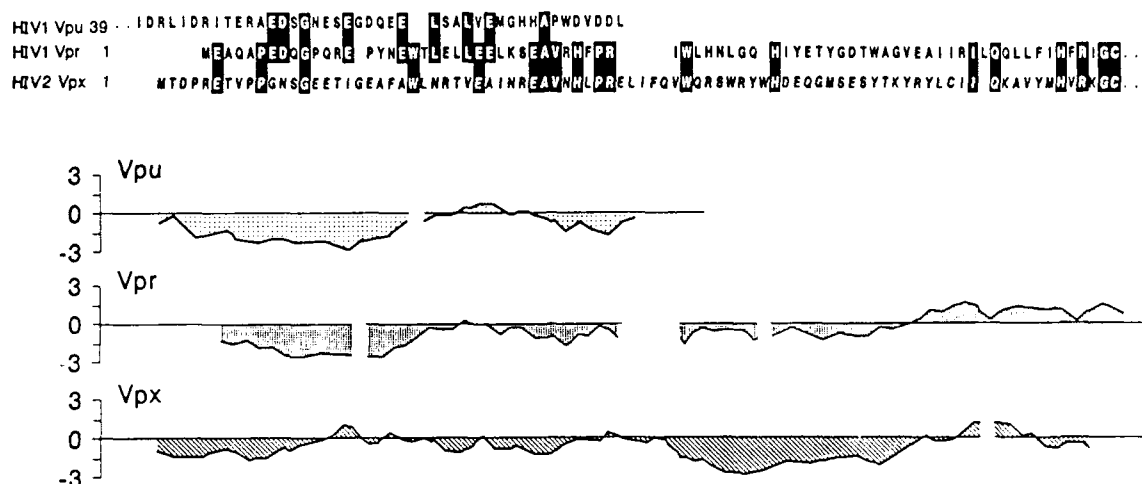


FIG. 4. Predicted amino acid homology between *vpr*, *vpu*, and *vpx*. The predicted amino acid sequence of the NL4-3-derived *vpr* gene is aligned with homologous regions of the ADA-derived *vpu* gene and the *vpx* gene encoded by the HIV-2_{ROD} clone, with single-letter amino acid designations. Identical residues are indicated within boxes. Hydrophilicity profiles for the corresponding segments of each protein are shown at the bottom.

between the *in vitro* replicative properties of HIV-1 isolates in T lymphocytes and clinical-disease stage, with earlier isolates tending to replicate more slowly and to lower levels ("slow, low") than isolates from later stages of disease ("rapid, high") (3, 5, 27). Nonessential regulatory genes are ideally suited to act as "molecular switches" for control of replication phenotypes by their activation or inactivation, particularly in viruses such as HIV-1, which characteristically generate high levels of sequence diversity. We demonstrate here that discrete genetic alterations in such accessory genes result in profoundly different replication rates in monocytes *in vitro*, which suggests a mechanism for transition from subclinical to clinical disease *in vivo*. These findings thus provide a rationale for addressing on a wider scale whether functional status of *vpr* and/or *vpu* correlates with disease stage or serves as a potential prognostic indicator of disease progression and outcome.

We are grateful to Nancy Vander Heyden for expert technical assistance; Eric Brown and Max Arens for gifts of primary monocytes and PBMCs, respectively; Cetus Corp. and Immunex for gifts of recombinant interleukin-2 and recombinant macrophage colony-stimulating factor, respectively; and the Military Medical Consortium for Applied Retroviral Research for continued support.

This work was also supported by NIH grant AI 24745, DAMD contract 17-90C-0125, the Washington University Medical Scientist Training Program (P.W.), and training grant 5T32AI07172 (P.W.). H. E. Gendelman is a Carter-Wallace Fellow of the Johns Hopkins University School of Public Health and Hygiene. L. Ratner is an American Cancer Society Research Professor.

REFERENCES

- Adachi, A., H. E. Gendelman, S. Koenig, T. Folks, R. Willey, A. Rabson, and M. A. Martin. 1986. Production of acquired immunodeficiency syndrome-associated retrovirus in human and non-human cells transfected with an infectious molecular clone. *J. Virol.* **59**:284-291.
- Armstrong, J. A., and K. Horne. 1984. Follicular dendritic cells and virus-like particles in AIDS-related lymphadenopathy. *Lancet* **ii**:370-372.
- Asjo, B., L. Manson-Morfeldt, J. Albert, G. Biberfeld, A. Karlsson, K. Ludman, and E. M. Fenyo. 1986. Replicative capacity of human immunodeficiency virus from patients with varying severity of HIV infection. *Lancet* **ii**:660-662.
- Chayt, K. J., M. E. Harper, L. M. Marselle, E. B. Lewin, R. M. Rlose, J. M. Oleske, L. G. Epstein, F. Wong-Staal, and R. C. Gallo. 1986. Detection of HTLV-III RNA in lungs of patients with AIDS and pulmonary involvement. *JAMA* **256**:2356-2359.
- Cheng-Mayer, C., D. Seto, M. Tateno, and J. A. Levy. 1988. Biologic features of HIV-1 that correlate with virulence in the host. *Science* **240**:80-82.
- Cohen, E. A., G. Dehni, J. G. Sodroski, and W. A. Haseltine. 1990. Human immunodeficiency virus *vpr* product is a virion-associated regulatory protein. *J. Virol.* **64**:3097-3099.
- Cohen, E. A., Y. Lu, H. Gottlinger, G. Dehni, Y. Jalinoos, J. G. Sodroski, and W. A. Haseltine. 1990. The T open reading frame of human immunodeficiency virus type 1. *J. AIDS* **3**:601-608.
- Cohen, E. A., E. F. Terwilliger, J. G. Sodroski, and W. A. Haseltine. 1988. Identification of a protein encoded by the *vpu* gene of HIV-1. *Nature (London)* **334**:532-534.
- Dayton, A. L., J. G. Sodroski, C. A. Rosen, W. C. Hoh, and W. A. Haseltine. 1986. The trans-activator gene of the human T cell lymphotropic virus type III is required for replication. *Cell* **44**:941-947.
- Dedera, D. A., W. Hu, N. Vander Heyden, and L. Ratner. 1989. Viral protein R of human immunodeficiency virus types 1 and 2 is dispensable for replication and cytopathogenicity in lymphoid cells. *J. Virol.* **63**:3205-3208.
- Eilbott, D. J., N. Peress, H. Burger, D. LaNeve, J. Orenstein, H. E. Gendelman, R. Seidman, and B. Weiser. 1989. Human immunodeficiency virus type 1 in spinal cords of acquired immunodeficiency syndrome patients with myelopathy: expression and replication in macrophages. *Proc. Natl. Acad. Sci. USA* **86**:3337-3341.
- Fisher, A. G., B. Ensoli, L. Ivanoff, M. Chamberlain, S. Pette-way, L. Ratner, R. C. Gallo, and F. Wong-Staal. 1987. The *src* gene of HTLV-III-LAV modulates virus propagation *in vitro*. *Science* **237**:888-893.
- Fisher, A. G., M. B. Feinberg, S. F. Josephs, M. E. Harper, L. M. Marselle, G. Reyes, M. A. Gonda, A. Aldovini, C. Debouk, R. C. Gallo, and F. Wong-Staal. 1986. The trans-activator gene of HTLV-III is essential for virus replication. *Nature (London)* **320**:367-371.
- Gartner, S., P. Markovits, D. M. Markovitz, M. H. Kaplan, R. C. Gallo, and M. Popovic. 1986. The role of mononuclear phagocytes in HTLV-III LAV infection. *Science* **233**:215-219.
- Gendelman, H., J. M. Orenstein, L. M. Baca, B. Weiser, H. Burger, D. C. Kalter, and M. S. Meltzer. 1990. The macrophage in the persistence and pathogenesis of HIV-1 infection. *AIDS*

- 3:475-495.
16. Gendelman, H. E., J. M. Orenstein, M. A. Martin, C. Ferrua, R. Mitra, T. Phipps, L. A. Wahl, C. H. Lane, A. S. Fauci, and D. S. Burke. 1988. Efficient isolation and propagation of human immunodeficiency virus on recombinant colony-stimulating factor 1-treated monocytes. *J. Exp. Med.* **167**:1478-1481.
17. Hattori, T., F. Michaels, K. Fargnoli, L. Marcon, R. C. Gallo, and G. Franchini. 1990. The human immunodeficiency virus type 2 *vpr* gene is essential for productive infection of human macrophages. *Proc. Natl. Acad. Sci. USA* **87**:8080-8084.
18. Heuser, J. E. 1989. Effects of cytoplasmic acidification on clathrin lattice morphology. *J. Cell Biol.* **108**:401-411.
19. Koenig, S., H. E. Gendelman, J. M. Orenstein, M. C. Dal Canto, G. H. Pezeshkpour, M. Yungbluth, F. Janotta, A. Aksamit, M. A. Martin, and A. S. Fauci. 1986. Detection of AIDS virus in macrophages in brain tissue from AIDS patients with encephalopathy. *Science* **233**:1089-1093.
20. Myers, G., A. B. Rabson, J. A. Berzofsky, T. F. Smith, and F. Wong-Staal (ed.). 1990. Human retroviruses and AIDS, 1990. Los Alamos National Laboratory, Los Alamos, N.M.
21. Narayan, O., and J. E. Clements. 1989. The biology and pathogenesis of lentiviruses. *J. Gen. Virol.* **70**:1617-1639.
22. Niederman, T. M. J., B. J. Thielan, and L. Ratner. 1989. Human immunodeficiency virus type 1 negative factor is a transcriptional silencer. *Proc. Natl. Acad. Sci. USA* **86**:1128-1132.
23. O'Brien, W. A., Y. Koyanagai, A. Namazie, J. Zhao, A. Diagne, K. Idler, J. A. Zack, and I. S. Y. Chen. 1990. HIV-1 tropism for mononuclear phagocytes can be determined by regions of gp120 outside the CD4 binding domain. *Nature (London)* **348**:69-73.
24. Ogawa, K., R. Shibata, T. Kiyomasu, I. Higuchi, Y. Kishida, A. Ishimoto, and A. Adachi. 1989. Mutational analysis of the human immunodeficiency virus *vpr* open reading frame. *J. Virol.* **63**:4110-4114.
25. Poiesz, B. J., F. W. Ruscetti, A. F. Gazdar, P. A. Bunn, J. D. Minna, and R. C. Gallo. 1980. Detection and isolation of type C retrovirus particles from fresh and cultured lymphocytes of a patient with cutaneous T-cell lymphoma. *Proc. Natl. Acad. Sci. USA* **77**:7415-7419.
26. Ratner, L., W. Haseltine, R. Patarca, K. J. Livak, B. Starcich, S. F. Josephs, E. R. Doran, J. A. Rafalski, E. A. Whitehorn, K. Baumeister, L. Ivanoff, S. R. Petteway, Jr., M. L. Pearson, J. A. Lautenberger, T. S. Papas, J. Ghayeb, N. T. Chang, R. C. Gallo, and F. Wong-Staal. 1985. Complete nucleotide sequence of the AIDS virus, HTLV-III. *Nature (London)* **313**:277-284.
27. Schuitemaker, H., N. A. Kootstra, R. E. de Goede, F. de Wolf, F. Miedema, and M. Tersmette. 1991. Monocytotropic human immunodeficiency virus type 1 (HIV-1) variants detectable in all stages of HIV-1 infection lack T-cell line tropism and syncytium-inducing ability in primary T-cell culture. *J. Virol.* **65**:356-363.
28. Schwartz, S., B. K. Felber, E. M. Fenyo, and G. N. Pavlakis. 1989. Rapidly and slowly replicating human immunodeficiency virus type 1 isolates can be distinguished according to target cell tropism and monocyte cell lines. *Proc. Natl. Acad. Sci. USA* **86**:7200-7203.
29. Shioda, T., J. A. Levy, and C. Cheng-Mayer. 1991. Macrophage and T cell-line tropisms of HIV-1 are determined by specific regions of the envelope gp120 gene. *Nature (London)* **349**:167-169.
30. Sodroski, J. G., W. C. Goh, C. Rosen, A. Dayton, E. Terwilliger, and W. Haseltine. 1986. A second post-transcriptional *trans*-activation gene required for HTLV-III replication. *Nature (London)* **321**:412-417.
31. Sonigo, P., M. Alizon, K. Staskus, D. Klatzmann, S. Cole, O. Danos, E. Retzel, P. Tiollais, A. Haase, and S. Wain-Hobson. 1987. Nucleotide sequence of the visna lentivirus: relationship to the AIDS virus. *Cell* **42**:369-382.
32. Strebel, K., T. Klimkait, and M. A. Martin. 1988. A novel gene of HIV-1, *vpu*, and its 16-kilodalton product. *Science* **241**:1221-1223.
33. Tschachler, E., V. Groh, M. Popovic, D. L. Mann, K. Konrad, B. Safai, L. Eron, F. diMarzo-Veronese, K. Wolff, and G. Stingl. 1987. Epidermal Langerhans cells—a target for HTLV-III/LAV infection. *J. Invest. Dermatol.* **88**:233-237.
34. Tristen, M., C. Marshall, A. Karpas, J. Petrik, and F. Hill. 1990. Origin of *vpx* in lentiviruses. *Nature (London)* **347**:341-342.
35. Westervelt, P., H. E. Gendelman, Y. Li, and L. Ratner. 1990. A determinant within the HIV-1 gp120 envelope protein critical for infection of primary monocytes, p. 71-76. In R. M. Chanock, H. S. Ginsberg, F. Brown, and R. A. Lerner (ed.), *Vaccines 91*. Cold Spring Harbor Laboratory Press, Cold Spring Harbor, N.Y.
36. Westervelt, P., H. E. Gendelman, and L. Ratner. 1991. Identification of a determinant within the HIV-1 surface envelope glycoprotein critical for productive infection of cultured primary monocytes. *Proc. Natl. Acad. Sci. USA* **88**:3097-3101.
37. Wiley, C. A., R. D. Schrier, J. A. Nelson, P. W. Lampert, and M. B. Oldstone. 1986. Cellular localization of human immunodeficiency virus infection within the brains of acquired immune deficiency syndrome patients. *Proc. Natl. Acad. Sci. USA* **83**:7089-7093.
38. Wong-Staal, F., P. K. Chanda, and J. Ghayeb. 1987. Human immunodeficiency virus: the eighth gene. *AIDS Res. Hum. Retroviruses* **3**:33-39.

Human Immunodeficiency Virus Type 1 Nef Protein Inhibits NF- κ B Induction in Human T Cells

THOMAS M. J. NIEDERMAN,¹ J. VICTOR GARCIA,² W. RANDALL HASTINGS,¹
SYLVIE LURIA,³ AND LEE RATNER^{1*}

Departments of Medicine and Molecular Microbiology, Washington University School of Medicine, St. Louis, Missouri 63110¹; Department of Virology and Molecular Biology, Saint Jude Children's Research Hospital, Memphis, Tennessee 38101²; and Department of Biochemistry, Beckman Center, Stanford University Medical Center, Stanford, California 94305³

Received 30 April 1992/Accepted 21 July 1992

Human immunodeficiency virus type 1 (HIV-1) can establish a persistent and latent infection in CD4⁺ T lymphocytes (W. C. Greene, *N. Engl. J. Med.* 324:308-317, 1991; S. M. Schnittman, M. C. Psallidopoulos, H. C. Lane, L. Thompson, M. Baseler, F. Massari, C. H. Fox, N. P. Salzman, and A. S. Fauci, *Science* 245:305-308, 1989). Production of HIV-1 from latently infected cells requires host cell activation by T-cell mitogens (T. Folks, D. M. Powell, M. M. Lightfoote, S. Benn, M. A. Martin, and A. S. Fauci, *Science* 231:600-602, 1986; D. Zagury, J. Bernard, R. Leonard, R. Cheynier, M. Feldman, P. S. Sarin, and R. C. Gallo, *Science* 231:850-853, 1986). This activation is mediated by the host transcription factor NF- κ B [C. Nabel and D. Baltimore, *Nature (London)* 326:711-717, 1987]. We report here that the HIV-1-encoded Nef protein inhibits the induction of NF- κ B DNA-binding activity by T-cell mitogens. However, Nef does not affect the DNA binding activity of other transcription factors implicated in HIV-1 regulation, including SP-1, USF, URS, and NF-AT1. Additionally, Nef inhibits the induction of HIV-1- and interleukin 2-directed gene expression, and the effect on HIV-1 transcription depends on an intact NF- κ B-binding site. These results indicate that defective recruitment of NF- κ B may underlie Nef's negative transcriptional effects on the HIV-1 and interleukin 2 promoters. Further evidence suggests that Nef inhibits NF- κ B induction by interfering with a signal derived from the T-cell receptor complex.

Human immunodeficiency virus type 1 (HIV-1) can establish a latent infection in CD4⁺ T cells (14, 29). Production of HIV-1 from latently infected cells requires host cell stimulation by T-cell mitogens (9, 34). Stimulation of T cells by T-cell-specific stimuli (e.g., antigen or antibody to CD2 or CD3) or nonspecific mitogens (e.g., phytohemagglutinin [PHA] and phorbol 12-myristate 13-acetate [PMA]) results in the induction of the DNA-binding activity of the host transcription factor NF- κ B (14). The NF- κ B family of proteins normally regulates the expression of genes involved in T-cell activation and proliferation, such as interleukin 2 (IL-2) and the alpha subunit of the IL-2 receptor (14). The HIV-1 promoter possesses two adjacent NF- κ B-binding sites which allow the virus to subvert the normal activity of NF- κ B to enhance its own replication (23).

Previous work suggests that the HIV-1-encoded Nef protein is a negative regulator of HIV-1 replication (1, 7, 20, 25, 31). Furthermore, we and others have found that Nef may suppress both HIV-1 and IL-2 transcription (1, 21, 25). To investigate whether Nef affects the DNA binding activity of NF- κ B or other transcription factors implicated in HIV-1 regulation, we used human T-cell lines stably transfected with the *nef* gene. Jurkat (J25) human T-cell clone 133 constitutively expresses the NL43 *nef* gene. 22F6 cells represent another antibiotic-resistant clone of J25 cells; however, these cells do not contain *nef* sequences and do not express Nef (21). Additionally, we used oligoclonal Jurkat E6-1 and HPB-ALL cells expressing the SF2 *nef* gene either in the correct orientation (Jurkat/LnefSN and HPB-ALL/LnefSNS1 cells) or in the reverse orientation (Jurkat/

LfenSN and HPB-ALL/LfenSN cells) with respect to the Moloney murine leukemia virus promoter (10). These cells represent a mixed population of cells expressing Nef to various degrees and were used to exclude the possibility that clonal selection accounts for Nef effects observed in the J25 clones.

To determine the impact of T-cell activation on the expression of Nef, the human T-cell lines were stimulated with PHA and PMA. Cells were maintained in logarithmic growth in RPMI 1640 medium supplemented with 10% fetal bovine serum and 2 mM glutamine. J25 and Jurkat E6-1 cells (5×10^6 each) and HPB-ALL cells (1.5×10^7) were either not stimulated or stimulated with 13 μ g of PHA-P (Sigma) and 75 ng of PMA (Sigma) per ml for 4 h. The cells were lysed in RIPA buffer, and lysates were immunoprecipitated with rabbit anti-Nef polyclonal serum (6). The immunoprecipitates were subjected to sodium dodecyl sulfate-polyacrylamide gel electrophoresis (12% polyacrylamide), and the proteins were transferred to nitrocellulose for Western immunoblot analysis. The primary antibody was the rabbit anti-Nef serum, and the secondary antibody was alkaline phosphatase-conjugated goat anti-rabbit immunoglobulin, specific for the heavy chain (Promega). The proteins were visualized by color development with nitroblue tetrazolium and 5-bromo-4-chloro-3-indolylphosphate toluidinium (Promega). Band intensity was determined by laser densitometry scanning of the Western blot and was in the linear range of analysis as established by a standard curve. Jurkat E6-1 cells were obtained from the AIDS Repository, American Type Culture Collection (Arthur Weiss) (32), and were stably transduced with the SF2 *nef* gene as previously described (10).

Immunoblot analysis with anti-Nef antibodies showed that

* Corresponding author.

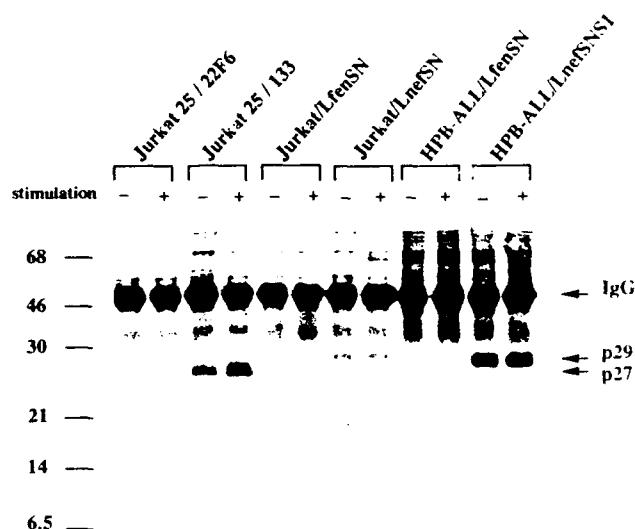


FIG. 1. Immunoblot analysis of the HIV-1 Nef protein in stably transfected and transduced human T-cell lines. Cell lysates were immunoprecipitated with rabbit anti-Nef polyclonal serum, electrophoresed, transferred to nitrocellulose, and immunoblotted with the same anti-Nef serum. The cells were either unstimulated (–) or stimulated (+) with PHA and PMA before cell harvesting. Prestained protein size markers are indicated on the left in kilodaltons. Nef protein in the 133 cells (21) was expressed from the *nef* gene of isolate pNL432 and had an apparent molecular mass of 27 kDa, whereas the Nef proteins expressed in the Jurkat E6-1 and HPB-ALL cells were encoded by the *nef* gene of isolate SF2 and demonstrated an apparent molecular mass of 29 kDa. Immunoglobulin G (IgG) heavy chain, which was present in the antiserum used for the immunoprecipitation step, is indicated at the right.

stimulation caused a two- to threefold increase in Nef expression in clone 133 cells (Fig. 1). This increase was probably due to the inducibility of the chimeric simian virus 40 (SV40)–human T-cell leukemia virus type I promoter used to direct Nef expression. However, Nef expression was not induced in the Jurkat E6-1 or HPB-ALL cells (Fig. 1). The level of Nef expressed in these cells is comparable to the amount of Nef generated by HIV-1 in productively infected CEM human T cells (data not shown). The difference in the apparent molecular weight of the Nef produced in clone 133 cells and those produced in the Jurkat/LnefSN and HPB-ALL/LnefSNS1 cells is due to the presence of an alanine at amino acid position 54 in the NL43 Nef gene compared with the presence of an aspartic acid at that position in the SF2 Nef gene (26). The amount of lysate equivalents loaded in the HPB-ALL/LnefSNS1 lanes was threefold larger than that in the Jurkat/LnefSN lanes. Nevertheless, the amount of Nef expressed in the HPB-ALL/LnefSNS1 cells was approximately fourfold larger than the amount produced in the Jurkat/LnefSN cells (Fig. 1). Nef did not appear to be toxic, in that the Nef-producing cells exhibited the same doubling time and morphology as the control cells.

Gel shift assays were performed with nuclear extracts prepared from stimulated and unstimulated cells. Nuclear extracts were prepared from 5×10^7 cells with a modified version of the method of Dignam et al. (8) as adapted by Montminy and Bilezikjian (22). Following ammonium sulfate precipitation, nuclear proteins were resuspended in 100 μ l of a solution containing 20 mM HEPES (*N*-2-hydroxyethylpi-

perazine-*N*'-2-ethanesulfonic acid; pH 7.9), 20 mM KCl, 1 mM MgCl₂, 2 mM dithiothreitol, and 17% glycerol (33) with the addition of 10 mM NaF, 0.1 mM sodium vanadate, and 50 mM beta-glycerol-phosphate. Cytoplasmic extracts consisted of the supernatant resulting from the lysis of cells in hypotonic lysis solution, Dounce homogenization, and low-speed centrifugation to pellet nuclei. Binding reaction mixtures contained 2 μ l (2 μ g) of nuclear extract (Fig. 2a through d) or 6 μ l (7 μ g) of cytoplasmic extract (Fig. 2e), 2 μ g of poly(dI-dC) (Pharmacia), 100-fold molar excess of unlabeled NF- κ B mutant oligonucleotide (ACAACTCACTTTCCGCTGCTCACTTTCCAGGGA), and 20,000 cpm of end-labeled oligonucleotide probe, in DNA binding buffer (27), in a final volume of 22 μ l. Reactions were performed at 30°C for 25 min, immediately loaded on a 4.5% polyacrylamide gel with 0.5 \times Tris-borate-EDTA, and run at 200 V. Oligonucleotides used were as follows: NF- κ B, ACAAGGGACTTTCCGC TGGGACTTTCCAGGGA; SP-1, CAGGGAGGCGTGGCC TGGGCGGGACTGGGGAGTGGCGTCC. All DNA probes were gel purified and end labeled with [γ -³²P]ATP. The intensity of the indicated bands was determined by laser densitometry and by measuring the radioactivity of excised bands in a liquid scintillation counter. There was a linear relationship between the amount of extract used and DNA-binding activity (data not shown). There was no NF- κ B DNA-binding activity with the cytoplasmic extracts in the absence of deoxycholic acid (data not shown). Protein concentration was determined with the Bradford reagent (Bio-Rad) with bovine serum albumin as a standard. Nuclear extract preparations and binding reactions were repeated on three separate occasions with similar results.

The induction of NF- κ B activity in stimulated 133 cells was suppressed five- to sevenfold compared with that in the 22F6 cells. This inhibition was evident 40 min poststimulation and was sustained throughout the 4-h stimulation period (Fig. 2a). J25 clone 22D8 cells represent a distinct clonal cell line which, like the 133 cells, also stably express Nef (21). NF- κ B induction was suppressed four- to fivefold in the 22D8 cells compared with that in the 22F6 cells (Fig. 2b). NF- κ B suppression was more profound in the 133 cells than in the 22D8 cells, which correlates with the observation that Nef expression was higher in the 133 cells (21). Similarly to the Nef-expressing J25 clones, Nef inhibited NF- κ B induction three- to fourfold in the Jurkat/LnefSN and HPB-ALL/LnefSNS1 cells compared with their non-Nef-expressing counterparts (Fig. 2c and d). Nef-mediated NF- κ B suppression was more profound in the Jurkat/LnefSN cells than in the HPB-ALL/LnefSNS1 cells, even though the HPB-ALL/LnefSNS1 cells expressed severalfold higher levels of Nef. This result is likely due to the biological differences that exist between the two cell lines. That is, Jurkat cells may be more sensitive to the effects of Nef than HPB-ALL cells because of differential expression of proteins involved in signal transduction. That Nef-mediated NF- κ B suppression in the 133 and 22D8 cells was greater than in the Jurkat/LnefSN and HPB-ALL/LnefSNS1 cells may be due to the expression of a different *nef* allele in the 133 and 22D8 cells. Alternatively, this result could be due to the fact that every cell in the culture of 133 and 22D8 cells produced a relatively high level of Nef, whereas the Jurkat/LnefSN and HPB-ALL/LnefSNS1 cells represent a mixed population of cells expressing low and high levels of Nef or no Nef at all.

NF- κ B activity in nuclei from unstimulated cells was extremely low but detectable, and no differences between the Nef-expressing and control cells were observed (data not shown). Additionally, when cytoplasmic extracts from un-

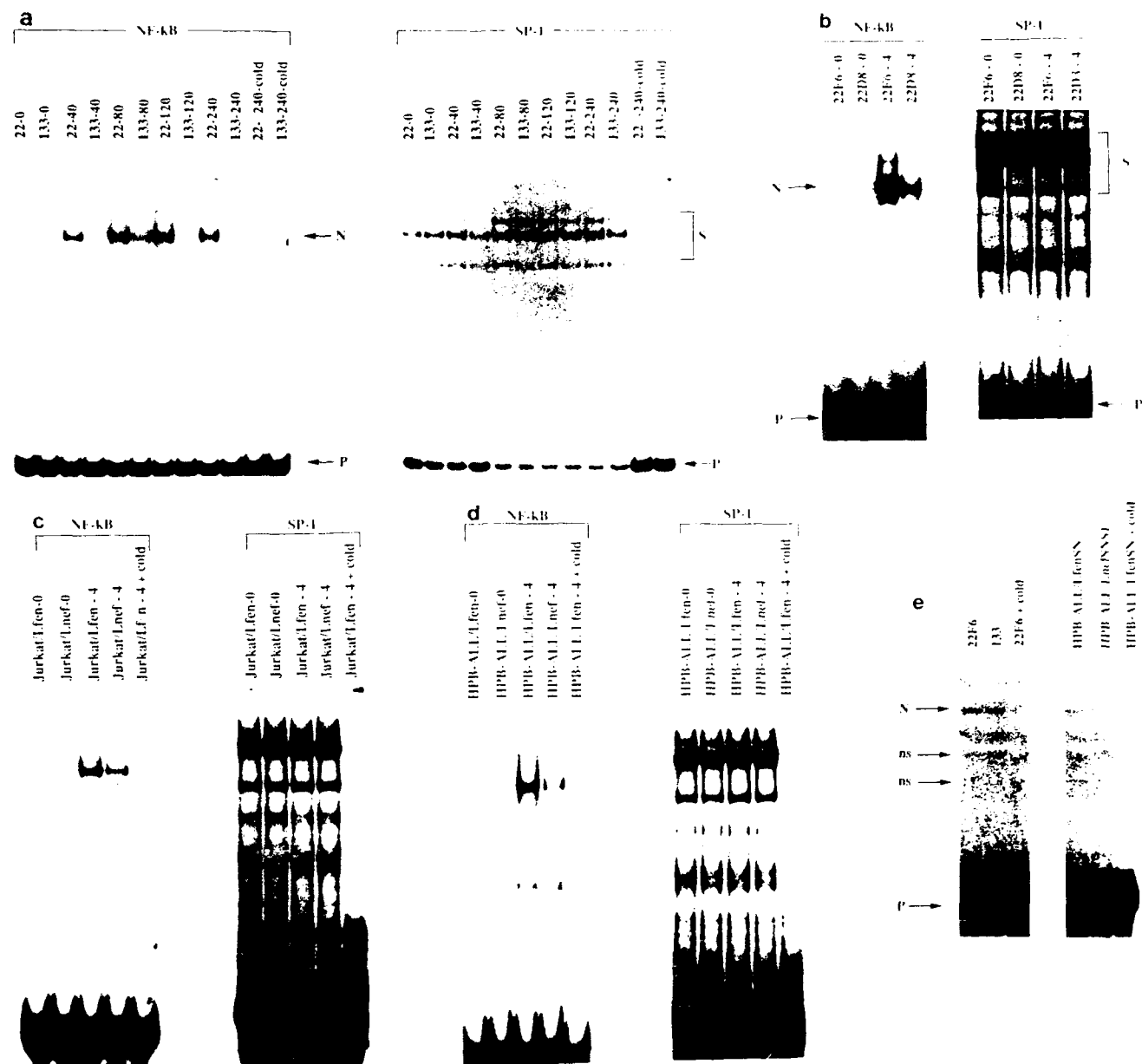


FIG. 2. Gel shift analysis of NF- κ B activity in nuclear extracts prepared from J25 (a and b), Jurkat E6-1 (c), or HPB-ALL (d) cells. (a) 22F6 and 133 cells were stimulated with PHA (13 μ g/ml) and PMA (75 ng/ml) for 0, 40, 80, 120, or 240 min; 22F6 and 22D8 (b), Jurkat E6-1 (c), or HPB-ALL (d) cells were not stimulated (0) or were stimulated with PHA and PMA as described above for 4 h (4). DNA probes used for binding are specified on the top of each panel. (e) Cytoplasmic protein extracts (7 μ g each) from the indicated cells were incubated with the NF- κ B DNA probe as described in the text, in the presence of 0.6% deoxycholic acid (Sigma). N, S, and P, NF- κ B-specific binding, SP-1-specific binding, and free probe, respectively. SP-1 binding served as a control for extract quality and specificity of Nef effects. Cold indicates that 100-fold molar excess of unlabeled DNA was added for competition. ns, nonspecific binding. Data represent at least three independent experiments.

stimulated cells were treated with deoxycholic acid (which releases NF- κ B from its cytoplasmic inhibitor, I κ B [3]), they exhibited NF- κ B activity independent of Nef expression (Fig. 2e). Finally, that Nef suppressed the level of NF- κ B induction after only 40 min of stimulation suggests that Nef does not suppress p110 or p65 NF- κ B mRNA expression. These observations indicate that Nef affects the recruitment and not the cytoplasmic concentration of NF- κ B. The binding of SP-1 was independent of Nef expression and stimula-

tion, and the amount of SP-1 probe used in these gel shift assays was not limiting (Fig. 2a through d). In addition, no differences in binding to NF-AT γ , USF γ , and URS-specific probes between the 22F6 and 133 cells were observed (data not shown). These data suggest that Nef specifically inhibited the induction of NF- κ B activity.

To further demonstrate Nef's suppressive effect on NF- κ B recruitment, 22F6 cells were transiently transfected with DNA plasmids expressing Nef from the SV40 early pro-

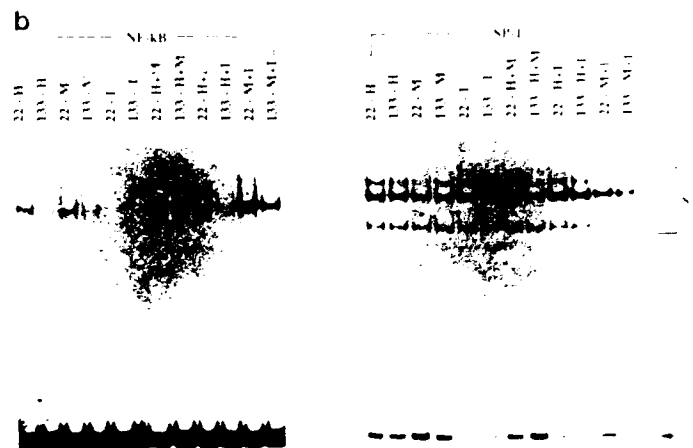
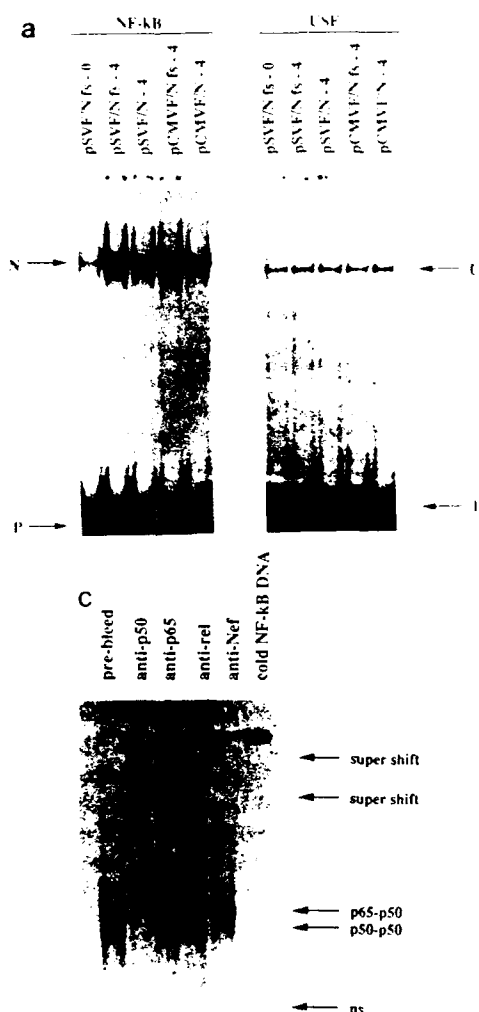


FIG. 3. Gel shift analysis of nuclear extracts prepared from 22F6 cells (a) transiently transfected with the indicated DNA plasmids that were not stimulated (0) or were stimulated for 4 h (4) with PHA-P and PMA and 22F6 and 133 cells (b) stimulated for 4 h with PHA-P (H), PMA (M), or ionomycin (I) (2 μ M) or combinations of any two mitogens. N, U, S, and P, NF- κ B-specific binding, USF-specific binding, SP-1-specific binding, and free probe, respectively. (c) Nuclear extract 22F6 H+M from panel b was preincubated with the specified antiserum for 15 min before the NF- κ B DNA probe was added. NF- κ B p65-p50 heterodimer- and p50-p50 homodimer-DNA complexes and supershifted heterodimer- and homodimer-DNA-antibody complexes are indicated at the right. Data represent at least three independent experiments.

moer, pSVF/N, or the cytomegalovirus immediate-early promoter, pCMVF/N, or with plasmids containing frame-shift mutations in the *nef* gene (pSVF/N fs and pCMVF/N fs, respectively). Nuclear extract preparation and DNA-binding reactions were as described above. 22F6 cells (2×10^7) (Fig. 3a) were transfected with 30 μ g of the indicated plasmid DNA by using DEAE-dextran. Briefly, cells (10^7) were incubated with plasmid DNA suspended in a solution containing 10 ml of serum-free RPMI 1640, 0.25 M Tris (pH 7.3), and 125 μ g of DEAE-dextran (Sigma) per ml at 37°C for 40 min. Following centrifugation at $2,000 \times g$ for 7 min, the cells were maintained in growth medium for 60 h prior to stimulation and cell harvesting. Plasmid pSVF/N is similar to plasmid pSVF (25), except that HIV-1 nucleotides 8994 to 9213 (including the NF- κ B recognition sites) and 3' flanking cellular sequences were deleted. Plasmid pSVF/N was digested at the unique *Bgl*III site at codon 88 of the *nef* gene, the sticky ends were filled in with the Klenow fragment of DNA polymerase I, and the plasmid was religated with T4 DNA ligase. This plasmid was called pSVF/N fs to indicate the introduction of a frameshift in the *nef* gene. The *Bam*HI

fragment from pSVF/N and pSVF/N fs, which includes the entire length of the HIV-1 sequences present in these clones, was inserted into the vector pCB6 (24) in the correct orientation with respect to the cytomegalovirus immediate-early promoter to generate clones pCMVF/N and pCMVF/N fs, respectively. Cells transfected with plasmids pSVF/N and pCMVF/N express Nef protein, but cells transfected with pSVF/N fs and pCMVF/N fs do not, as determined by Western blot and immunoprecipitation analysis (data not shown). Transfection efficiency was determined by cotransfection with 2 μ g of pSV2-CAT. Chloramphenicol acetyltransferase (CAT) activity (reported as the percent conversion to acetylated products) was determined as described below, and the values for the pSVF/N fs-0, pSVF/N fs-4, pSVF/N-4, pCMVF/N fs-4, and pCMVF/N-4-transfected cells were 51, 60, 61, 58, and 61%, respectively. A USF-specific DNA probe (corresponding to nucleotides -159 to -173 of the HIV-1 long terminal repeat, GCCGCTAG CATITCATCACGTGGCCCGAGAGCTGC) was used as a control for the specificity of Nef effects and extract integrity.

NF- κ B induction was consistently inhibited at least two-fold in cells transfected with either pSVF/N or pCMVF/N compared with cells transfected with their *nef* mutant counterparts (Fig. 3a). Transfection efficiencies in these experiments were determined by cotransfecting cells with the pSV2-CAT plasmid and measuring CAT activity. No significant differences in transfection efficiency between the *nef*-expressing and the *nef* mutant plasmids were observed (Fig. 3a). The suppressive effect of Nef in these transiently transfected cells was not as dramatic as the effects observed in the stably transfected and transduced cells. The more subtle effect of Nef in this experiment may be due to the expression of a *nef* allele which was derived from an HIV-1 isolate distinct from either the NL-43 or the SF2 isolates

(25). In addition, cells which did not receive the *nef* expression plasmid during the transient-transfection process were not eliminated (by antibiotic selection) from the total cell population.

To explore the relative contributions of individual mitogens to the recruitment of Nef-inhibitable complexes, cells were stimulated with PHA, PMA, or ionomycin alone or in combination. The maximal induction of NF- κ B activity occurred when PHA was combined with PMA (Fig. 3b). This result, coupled with the observation that PHA mimics the effects of the natural ligand for the T-cell receptor (TCR) complex (32), suggests that Nef may inhibit signal transduction emanating from the TCR complex. The addition of the Ca^{2+} ionophore, ionomycin, when coupled with PMA treatment, partially substituted for the absence of PHA with respect to NF- κ B induction (Fig. 3b). However, ionomycin treatment did not significantly reduce Nef's inhibitory effects, suggesting that events other than Ca^{2+} mobilization may be disrupted by Nef.

Using antibodies against the p50 and p65 NF- κ B subunits, we found that Nef-inhibitable complexes included both p50-p50 homodimers and p50-p65 heterodimers (Fig. 3c). Anti-p50, anti-p65, anti-*v-rel*, and prebleed sera (Fig. 3c) were kindly provided by Mark Hannink (University of Missouri, Columbia, Mo.). Because the gels in Fig. 3a and b and Fig. 2 were run for a shorter length of time, the two bands indicated in Fig. 3c appear as one band in Fig. 3a and b and Fig. 2.

To determine whether Nef-mediated inhibition of NF- κ B-binding activity correlated with a decrease in transcriptional activity, cells were transfected with DNA plasmids which use the HIV-1 long terminal repeat to direct expression of a heterologous gene product, CAT. Jurkat cells were transfected, as described above, with 15 μ g of the CAT constructs indicated in Fig. 4. Following transfection, the cells were maintained in growth medium for 24 h. Cells were or were not treated with PHA-P (13 μ g/ml) and PMA (75 ng/ml) and incubated for an additional 18 h. Cell extracts were prepared, and CAT activity was assessed by standard methods (13). Extract equivalent to 3×10^6 cells was used for each 18-h reaction. CAT activity was in the linear range of analysis with respect to extract amount and incubation time (data not shown). CAT assays were normalized to a noninducible control plasmid, RSV-CAT (12) (2 μ g), which was transfected in parallel with the HIV-1-CAT plasmids as described above. Assays were also normalized to protein concentrations as determined by Bradford reagent analysis (Bio-Rad). The amount of CAT activity was quantitated by excising the spots corresponding to the unacetylated and acetylated forms of [14 C]chloramphenicol and measuring radioactivity in a liquid scintillation counter. CAT activity is expressed as the percentage of radioactivity in the acetylated forms compared with the sum of that of the acetylated and unacetylated forms. The wild-type HIV-1-CAT (CD12-CAT was derived by a small deletion in the *nef* coding sequence upstream of the long terminal repeat start site of clone C15-CAT [2]), and mutant NF- κ B HIV-1-CAT (23) and IL-2-CAT (30) plasmids were generously provided by Steven Josephs, Gary Nabel, and Gerald Crabtree, respectively. δ NRE-HIV-1-CAT was generated by excising the *Ava*I-*Ava*I fragment from C15-CAT (2) and therefore lacks the negative regulatory element sequences present in C15-CAT.

CAT activity correlated well with DNA-binding activity in that 133 cells exhibited a capacity to induce CAT activity that was fivefold less than that of 22F6 cells (Fig. 4a). Similarly, CAT activity induction was suppressed twofold in

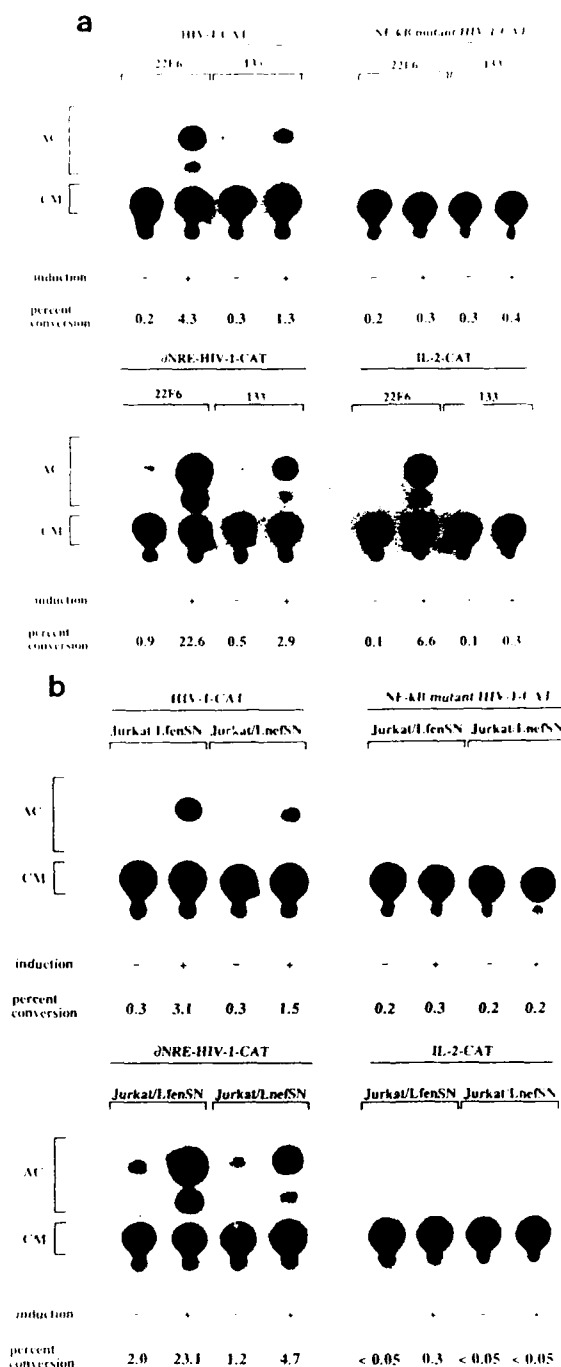


FIG. 4. CAT assays of extracts from cells transiently transfected with HIV-1-CAT and IL-2-CAT DNA plasmids. J25 (a) and Jurkat E6-1 (b) cells were transfected with the CAT constructs as indicated above each panel. Cells were not induced (-) or were induced (+) with PHA and PMA. CAT activity was determined by conversion of unacetylated [14 C]chloramphenicol (CM) to monoacetylated forms (AC). These data represent at least three independent experiments.

the Jurkat/LnefSN cells compared with that in the Jurkat/L.fenSN cells (Fig. 4b). This inhibition was demonstrated with both wild-type HIV-1-CAT and the negative regulatory element deletion clone, δ NRE-HIV-1-CAT, which lacks nucleotides -453 to -156 of the HIV-1 long terminal repeat

(Fig. 4a and b). This result suggests that negative regulatory element sequences are not primary targets of Nef regulation in stimulated T cells. An HIV-1-CAT plasmid containing mutated NF- κ B sequences (23) was induced, at most, only twofold above basal levels, and induction was independent of cell type and Nef expression (Fig. 4a and b).

The importance of NF- κ B with respect to the induction of IL-2 by T-cell mitogens was demonstrated by Hoyos et al. (17). These authors showed that the induction of CAT activity was prevented up to 80% with IL-2-CAT constructs bearing mutations in the NF- κ B site compared with that of IL-2-CAT constructs containing wild-type NF- κ B recognition sequences (17). As previously reported (21), we found that Nef profoundly suppressed the induction of CAT activity directed by the IL-2-CAT plasmid in the 133 cells (Fig. 4a). Whereas there was a 50- to 60-fold induction of CAT activity in the 22F6 cells, there was only a 2- to 3-fold induction in the 133 cells (Fig. 4a). Although NF- κ B appears to play an important role in IL-2 induction, it is possible that Nef blocks other factors in addition to NF- κ B which may be required for the efficient induction of IL-2 gene expression. This possibility may explain the dramatic suppressive effect of Nef on IL-2 induction compared with the results of Hoyos et al. (17). CAT activity generated by the IL-2-CAT construct was induced to a much lower extent in the Jurkat E6-1 cells. This result is likely due to differences that exist between Jurkat E6-1 and J25 cells. Despite the low level of induction of the IL-2 promoter in the Jurkat E6-1 cells, CAT activity was higher in the Jurkat/LnfSN cells than in the Jurkat/LnfSN cells (Fig. 4b). Nef did not affect CAT activity driven by the SV40 early promoter or the promoters from Rous sarcoma virus, cytomegalovirus, or Mason-Pfizer monkey virus, indicating that Nef specifically suppressed the HIV-1 and IL-2 promoters (data not shown). The Jurkat E6-1 cells were transfected with equivalent efficiency; however, the Nef-expressing 133 cells were more easily transfected than were the control cells (22F6 cells). Therefore, CAT activity generated by an RSV-CAT plasmid that was transfected in parallel was used to assess the transfection efficiency and to normalize the CAT activity derived from the HIV-1-CAT and IL-2-CAT constructs.

The observation that Nef prevents IL-2 induction (Fig. 4a) (21), coupled with the demonstrations that IL-2 induction requires CD4 and p56^{lck} (11) and NF- κ B recruitment (17), provides additional evidence to suggest that Nef uncouples signals originating from the TCR complex. Furthermore, the TCR complex induces NF- κ B activity after treatment with antibodies to either CD2 or CD3 (5). Nef inhibits the induction of IL-2 by both of these stimuli (21).

Interestingly, Nef has been reported to down-modulate the surface expression of CD4 (10, 15). Although Nef did not affect the rate of CD4 transcription or translation (10), the mechanism by which Nef mediates the down-modulation of CD4 at the cell surface remains unclear. The connection between Nef-mediated negative effects on CD4 cell surface expression and HIV-1 and IL-2 regulation has not yet been established.

Previously, we and others reported that HIV-1 Nef mediated HIV-1 transcriptional suppression (1, 25). Some investigators were unable to confirm this effect (16, 19); however, differences in experimental approaches may explain the apparent discrepancy. For the first time, the data presented here suggest that the primary underlying event in Nef-mediated transcriptional repression in activated T cells is the inhibition of induction of NF- κ B activity. In vivo, this suppression may limit the production and cell surface

expression of viral gene products in infected cells, thereby allowing the cells to evade clearance by the cellular and humoral arms of the immune response. This model for Nef-mediated viral persistence in vivo may be consistent with the results of Kestler et al., which demonstrated that the presence of an intact *nef* gene was required to prolong simian immunodeficiency virus infection and induce pathogenesis in infected macaques (18). Furthermore, we and others demonstrated that simian immunodeficiency virus Nef inhibited simian immunodeficiency virus replication in vitro in a way that was analogous to the way in which HIV-1 Nef inhibited HIV-1 (4, 24). It is possible that high-level Nef expression early after infection (28) is sufficient to maintain HIV-1 in a relatively latent state, which may be critical for establishing a reservoir of HIV-1-infected cells and the eventual development of AIDS.

We thank Lisa Westfield and Evan Sadler for oligonucleotides, Jason Kimata for helpful discussions, and Alec Cheng for excellent technical advice.

This work was supported by Public Health Service grant A124745 and U.S. Army grant DAMD-17-90C-0125 to L.R., National Institute of Health training grant HL-07088-17 to T.M.J.N., American Federation for AIDS Research grant 1405 to J.V.G., and the Washington University Medical Scientist Training Program to T.M.J.N. L.R. is an American Cancer Society research professor.

REFERENCES

1. Ahmad, N., and S. Venkatesan. 1988. Nef protein of HIV-1 is a transcriptional repressor of HIV-1 LTR. *Science* **241**:1481-1485.
2. Arya, S. K., G. Chan, S. F. Josephs, and F. Wong-Staal. 1985. Trans-activator gene of human T-lymphotropic virus type III (HTLV-III). *Science* **229**:69-73.
3. Baeuerle, P., and D. Baltimore. 1988. Activation of DNA-binding activity in an apparently cytoplasmic precursor of the NF- κ B transcription factor. *Cell* **53**:211-217.
4. Binninger, D., J. Ennen, D. Bonn, S. G. Norley, and R. Kurth. 1991. Mutational analysis of the simian immunodeficiency virus SIVmac *nef* gene. *J. Virol.* **65**:5237-5243.
5. Bressler, P., G. Pantaleo, A. Demaria, and A. S. Fauci. 1991. Anti-CD2 receptor antibodies activate the HIV long terminal repeat in T lymphocytes. *J. Immunol.* **147**:2290-2294.
6. Bryant, M. L., L. Ratner, R. J. Dronio, N. S. Kishore, B. Devadas, S. P. Adams, and J. I. Gordon. 1991. Incorporation of 12-methoxydodecanoate into the human immunodeficiency virus 1 gag polyprotein precursor inhibits its proteolytic processing and virus production in a chronically infected human lymphoid cell line. *Proc. Natl. Acad. Sci. USA* **88**:2055-2059.
7. Cheng-Mayer, C., P. Ianello, K. Shaw, P. A. Luciw, and J. A. Levy. 1989. Differential effects of *nef* on HIV replication: implications for viral pathogenesis in the host. *Science* **246**:1629-1632.
8. Dignam, J. D., R. M. Lebowitz, and R. G. Roeder. 1983. Accurate transcription by RNA polymerase II in a soluble extract from isolated mammalian nuclei. *Nucleic Acids Res.* **11**:1475-1489.
9. Folks, T., D. M. Powell, M. M. Lightfoote, S. Benn, M. A. Martin, and A. S. Fauci. 1986. Induction of HTLV-III_{AV} from a nonvirus-producing T-cell line: implications for latency. *Science* **231**:600-602.
10. Garcia, J. V., and A. D. Miller. 1991. Serine phosphorylation-independent downregulation of cell-surface CD4 by *nef*. *Nature (London)* **350**:508-511.
11. Gleichenhaus, N., N. Shastri, D. Littman, and J. M. Turner. 1991. Requirement for association of p56^{lck} with CD4 in antigen-specific signal transduction in T cells. *Cell* **64**:511-520.
12. Gorman, C. M., G. T. Merlino, M. C. Willingham, I. Pastan, and B. H. Howard. 1982. The Rous sarcoma virus long terminal repeat is a strong promoter when introduced into a variety of eukaryotic cells by DNA-mediated transfection. *Proc. Natl.*

- Acad. Sci. USA 79:6777-6781.
13. Gorman, C. M., L. F. Moffat, and B. H. Howard. 1982. Recombinant genomes which express chloramphenicol acetyltransferase in mammalian cells. *Mol. Cell. Biol.* 2:1044-1051.
14. Greene, W. C. 1991. The molecular biology of human immunodeficiency virus type 1 infection. *N. Engl. J. Med.* 324:308-317.
15. Guy, B., M. P. Kieny, Y. Riviere, C. LePeuch, K. Dott, M. Girard, L. Montagnier, and J. P. Lecocq. 1987. HIV F/3' orf encodes a phosphorylated GTP-binding protein resembling an oncogene product. *Nature (London)* 330:266-269.
16. Hammes, S. R., E. P. Dixon, M. H. Malim, B. R. Cullen, and W. C. Greene. 1989. Nef protein of human immunodeficiency virus type 1: evidence against its role as a transcriptional inhibitor. *Proc. Natl. Acad. Sci. USA* 86:9549-9553.
17. Hoyos, B., D. W. Ballard, E. Bohnlein, M. Siekevitz, and W. C. Greene. 1989. Kappa B-specific DNA binding proteins: role in the regulation of the human interleukin 2 gene expression. *Science* 244:457-460.
18. Kestler, H. W., D. J. Ringler, K. Mori, D. L. Panicali, P. K. Sehgal, M. D. Daniel, and R. C. Desrosiers. 1991. Importance of the nef gene for maintenance of high virus loads and for development of AIDS. *Cell* 65:651-662.
19. Kim, S., R. Ikeuchi, R. Byrn, J. Groopman, and D. Baltimore. 1989. Lack of a negative influence on viral growth by the nef gene of human immunodeficiency virus type 1. *Proc. Natl. Acad. Sci. USA* 86:9544-9548.
20. Luciw, P. A., C. Cheng-Mayer, and J. A. Levy. 1987. Mutational analysis of the human immunodeficiency virus: the orf-B region down-regulates virus replication. *Proc. Natl. Acad. Sci. USA* 84:1434-1438.
21. Luria, S., I. Chambers, and P. Berg. 1991. Expression of the type 1 human immunodeficiency virus nef protein in T cells prevents antigen receptor-mediated induction of interleukin 2 mRNA. *Proc. Natl. Acad. Sci. USA* 88:5326-5330.
22. Montminy, M. R., and L. M. Bilezikjian. 1987. Binding of a nuclear protein to the cyclic-AMP response element of the somatostatin gene. *Nature (London)* 328:175-178.
23. Nabel, G., and D. Baltimore. 1987. An inducible transcription factor activates expression of human immunodeficiency virus in T cells. *Nature (London)* 326:711-713.
24. Niederman, T. M. J., W. Hu, and L. Ratner. 1991. Simian immunodeficiency virus negative factor suppresses the level of viral mRNA in COS cells. *J. Virol.* 65:3538-3546.
25. Niederman, T. M. J., B. J. Thielan, and L. Ratner. 1989. Human immunodeficiency virus type 1 negative factor is a transcriptional silencer. *Proc. Natl. Acad. Sci. USA* 86:1128-1132.
26. Obaru, K., J. E. DeClue, and W. A. Haseltine. 1992. An amino-terminal amino acid affects the electrophoretic mobility of the HIV-1 Nef protein. *J. Acquired Immune Defic. Syndr.* 5:308-312.
27. Piette, J., M. H. Kryszke, and M. Yaniv. 1985. Specific interaction of cellular factors with the B enhancer of polyoma virus. *EMBO J.* 4:2675-2685.
28. Robert-Guroff, M., M. Popovic, S. Gartner, P. Markham, R. C. Gallo, and M. S. Reitz. 1990. Structure and expression of *tat*-, *rev*-, and *nef*-specific transcripts of human immunodeficiency virus type 1 infected lymphocytes and macrophages. *J. Virol.* 64:3391-3398.
29. Schnittman, S. M., M. C. Psallidopoulos, H. C. Lane, L. Thompson, M. Baseler, F. Massari, C. H. Fox, N. P. Salzman, and A. S. Fauci. 1989. The reservoir for HIV-1 in human peripheral blood is a T cell that maintains expression of CD4. *Science* 245:305-308.
30. Siebenlist, U., D. B. Durand, P. Bressler, N. J. Holbrook, C. A. Norris, M. Kamoun, J. A. Kant, and G. Crabtree. 1986. Promoter region of interleukin-2 gene undergoes chromatin structure changes and confers inducibility on chloramphenicol acetyltransferase gene during activation of T cells. *Mol. Cell. Biol.* 6:3042-3049.
31. Terwilliger, E., J. G. Sodroski, C. A. Rosen, and W. A. Haseltine. 1986. Effects of mutations within the 3' *orf* open reading frame region of human T-cell lymphotropic virus type III (HTLV-III/LAV) on replication and cytopathogenicity. *J. Virol.* 60:754-760.
32. Weiss, A., R. L. Wiskocil, and J. D. Stobo. 1984. The role of T3 surface molecules in the activation of human T cells: a two-stimulus requirement for IL-2 production reflects events occurring at a pre-translational level. *J. Immunol.* 133:123-128.
33. Wildeman, A. G., P. Sassone-Corsi, T. Grundstrom, M. Zenke, and P. Chambon. 1984. Stimulation of in vitro transcription from the SV40 early promoter by the enhancer involves a specific trans-acting factor. *EMBO J.* 3:3129-3133.
34. Zagury, D., J. Bernard, R. Leonard, R. Cheynier, M. Feldman, P. S. Sarin, and R. C. Gallo. 1986. Long-term cultures of HTLV-III-infected T cells: a model of cytopathology of T-cell depletion in AIDS. *Science* 231:850-853.

HIV-1 Nef Protein Inhibits the Recruitment of AP-1 DNA-Binding Activity in Human T-Cells

THOMAS M. J. NIEDERMAN,* W. RANDALL HASTINGS,* SYLVIE LURIA,† JUAN C. BANDRES,* AND LEE RATNER*,¹

*Departments of Medicine and Molecular Microbiology, Washington University School of Medicine, St. Louis, Missouri 63110; and

†Department of Biochemistry, Beckman Center, Stanford University Medical Center, Stanford, California 94305

Received July 21, 1992; accepted January 11, 1993

The human immunodeficiency virus type 1 long terminal repeat, HIV-1-LTR, contains binding sites for several cellular transcription factors which contribute to HIV-1 gene expression. Our previous studies on the function of the HIV-1-encoded Nef protein suggested that Nef may be an inhibitor HIV-1 transcription. To determine whether Nef affects the binding of cellular factors implicated in HIV-1 regulation, ³²P-labeled oligonucleotides corresponding to the binding sites were incubated with nuclear extracts prepared from Nef-expressing T-cell lines that were not stimulated or were stimulated with T-cell mitogens. We found that Nef inhibited the recruitment of AP-1 DNA-binding activity in mitogen-stimulated human T-cells. Additionally, Nef expressing cells were transiently transfected with a plasmid in which HIV-1 AP-1 DNA recognition sequences were cloned downstream of the chloramphenicol acetyltransferase (CAT) gene. Mitogen-mediated transcriptional activation of the CAT gene in this construct was inhibited in Nef-expressing cells but not in control cells. These studies suggest that, by inhibiting AP-1 activation, Nef may play a role in regulating HIV-1 gene expression in infected T-cells. © 1993 Academic Press, Inc.

The human immunodeficiency virus type 1 long terminal repeat, HIV-1-LTR, contains two adjacent AP-1 binding sites and three intragenic AP-1 sites are located within the *pol* gene (1, 2). The AP-1 DNA-binding complex is composed of homo- and heterodimers of the *c-fos* and *c-jun* family of transcription factors (3) which dimerize by interdigitation of hydrophobic α -helices, called 'leucine-zippers' (4). The consensus DNA recognition site for AP-1 is TGACTCA (5-7) and this sequence has also been shown to confer phorbol ester inducibility (8). *c-fos* and *c-jun* mRNAs are induced in T-cells by the lectin phytohemagglutinin (9) (PHA), the calcium ionophore A23187 (10), and the phorbol ester, phorbol-12-myristate-13-acetate (PMA) (8). AP-1 can serve as both a positive and a negative regulator with respect to the expression of a variety of genes under different conditions (11-15).

It has been reported that the product of the *nef* gene of HIV-1 and SIV could function as a negative regulator of virus replication (16-22). Furthermore, we found that Nef could function as a viral transcriptional inhibitor (16, 17). This result was confirmed by other investigators (18, 19) although, not by all investigators (23, 24). Recently, Luria *et al.* showed that Nef, stably expressed in Jurkat human T-cell clones, prevented the transcriptional activation of the interleukin-2 (IL-2) gene (25). IL-2 is a critical T-cell proliferation factor and serves as a marker for T-cell activation. Interestingly,

the HIV-1-LTR and the IL-2 promoter contain binding sites for the T-cell activation-associated transcription factors, AP-1 and NF- κ B.

In order to elucidate the mechanism underlying Nef's negative effects on HIV-1 and IL-2 transcription in T-cells, we examined the binding of cellular transcription factors with recognition sites in the HIV-1-LTR in the presence and absence of Nef. In these studies, we used the Jurkat (J25) human T-cell clone 133, which stably expresses the Nef protein derived from the HIV-1 isolate NL-43 (25). As a control, we used a G418-resistant, Jurkat 25 clone, 22F6, which does not contain any HIV-1 sequences and does not express Nef (25). Additionally, we used oligoclonal HPB-ALL human T-cells stably transduced with a recombinant retrovirus expressing the *nef* gene, derived from the HIV-1 isolate SF-2, either in the correct orientation, HPB-ALL/LnefSNS1 cells, or the reverse orientation, HPB-ALL/LfenSN cells, with respect to the Moloney murine leukemia virus promoter (26). Nef was expressed to a high degree in the Jurkat 133 cells and the HPB-ALL/LnefSNS1 cells, but was not produced in the Jurkat 22F6 cells or the HPB-ALL/LfenSN cells as determined by Western blot and immunoprecipitation analysis (Ref. 33 and data not shown). The HPB-ALL cells, in contrast to the Jurkat cells, represent a mixed population of cells expressing Nef and thus do not suffer from the potential limitation that Nef-mediated effects observed in the Jurkat cells are a result of cloning. However, the advantage of the clonal Jurkat 133 cells is that Nef is expressed in every cell, possibly magnifying the effects exerted by Nef. It is noteworthy that the

¹ To whom reprint requests should be addressed at Washington University School of Medicine, 660 S. Euclid Ave., Box 8125, St. Louis, MO 63110.

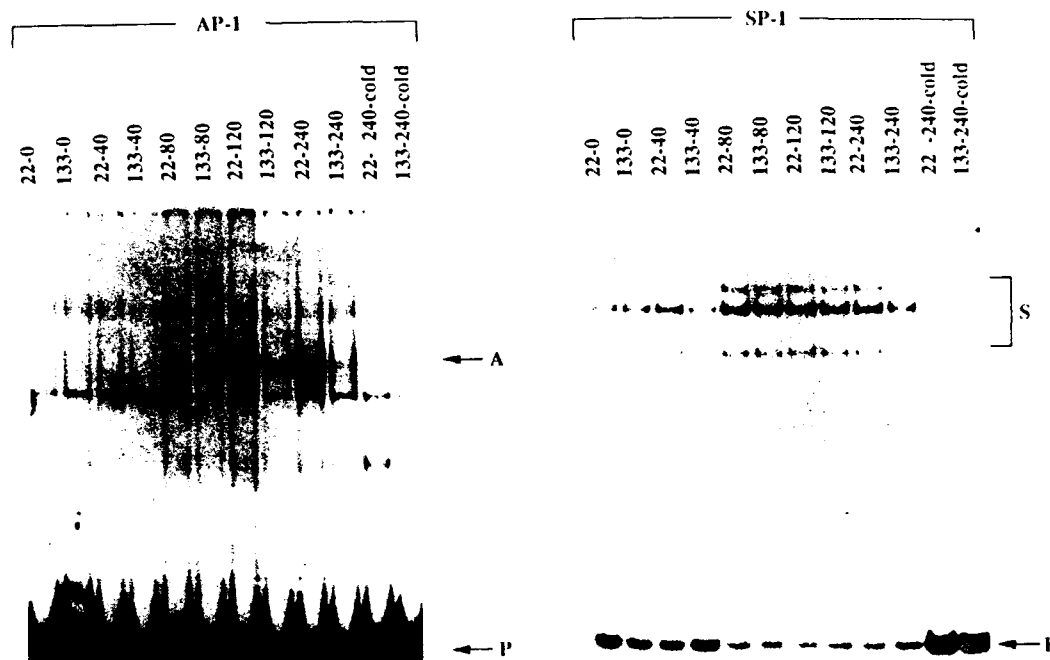


Fig. 1. Gel shift analysis of AP-1 DNA binding activity in extracts prepared from Jurkat 25 cells. Cells were stimulated with PHA-P (13 μ g/ml, [SIGMA]) and PMA (75 ng/ml, Sigma) for 0, 40, 80, 120, or 240 min. Oligonucleotide probes used for binding are specified on the top of each panel. A indicates the inducible AP-1/DNA complexes. S and P represent SP-1-specific binding and free probe, respectively. SP-1 binding served as a control for extract quality and specificity of Nef-mediated effects. Cold indicates that 100-fold molar excess of unlabeled DNA was added for competition. Methods: Cells were maintained in logarithmic growth in RPMI 1640 medium supplemented with 10% fetal calf serum and 2 mM glutamine. Nuclear extracts were prepared from 5×10^7 cells using a modified version of the method of Dignam *et al.* (36) as adapted by Montminy and Bilezikian (37). Following ammonium sulfate precipitation, nuclear proteins were resuspended in 100 μ l of 20 mM HEPES (pH 7.9), 20 mM KCl, 1 mM MgCl₂, 2 mM DTT, and 17% glycerol (38) with the addition of 10 mM NaF, 0.1 mM sodium vanadate, and 50 mM β -glycerol-phosphate. Binding reactions contained 2 μ l (2 μ g) of nuclear extract, 2 μ g poly(dI-dC) (Pharmacia), 100-fold molar excess of unlabeled intragenic AP-1 mutant oligonucleotide (GATCTCAAAGCGGATATCAGCTGGTTAATCAAATAAT), and 20–40,000 cpm of end-labeled oligonucleotide probe, in DNA binding buffer (39), in a final volume of 22 μ l. Reactions were performed at 30° for 30 min, immediately loaded onto a 4.5% polyacrylamide gel using 0.5 \times TBE, and run at 200 V. Oligonucleotides used were as follows: AP-1, CAGGGCCAGGAGTCAGATATCCACTGACCTTTGGATGGTGCT; SP-1, CAGGGAGGCGTGGCCTGGGCGGGAGTGGGGAGTGGCGTCC. All DNA probes were gel purified and end-labeled with [γ -³²P]ATP. The intensity of indicated bands was determined by laser densitometry scanning. There was a linear relationship between the amount of extract used and the DNA binding activity. Nuclear extract preparations and binding reactions were repeated on three separate occasions with similar results.

doubling times for the Nef expressing and the control cells were indistinguishable and no gross morphologic differences between the cells were noted either prior to or post-stimulation.

Gel shift analyses were performed with nuclear extracts prepared from cells that were not stimulated, or were stimulated, with the T-cell mitogen, phytohemagglutinin (PHA-P) and the protein kinase C (PKC) activator, PMA. Nuclear extracts were incubated with a ³²P-labeled oligonucleotide corresponding to the HIV 1 AP-1 DNA recognition sites (7). In the parental 22F6 Jurkat cells, an induced AP-1/DNA complex, which was not present in unstimulated cells, was detected between 1 and 2 hr post-stimulation and was abundant 4 hr post-stimulation (Fig. 1). In contrast, the recruitment of the same AP-1/DNA complex was inhibited fivefold at 2 hr and ninefold at 4 hr in the Nef expressing 133 cells compared to the 22F6 cells (Fig. 1). The addition of 100-fold molar excess of unlabeled AP-1-specific oligonucleotide inhibited the appearance of

the major inducible complex (Fig. 1). However, an oligonucleotide with three nucleotide substitutions in the AP-1 recognition site did not compete away the inducible complex, and we included a 100-fold excess of the unlabeled mutant AP-1 oligonucleotide in all binding reactions as a non-specific inhibitor.

The presence of the constitutive AP-1/DNA complex (the slowest migrating complex in Fig. 1) was minimally, if at all, affected by Nef and may be due to the constant presence of serum in the cell growth media (27). Moreover, this complex was not inducible (Fig. 3b). In addition, the constitutively active transcription factor SP-1 was not affected by the presence or absence of Nef and was used as a control for extract quality (Fig. 1). Therefore, Nef inhibited the inducible AP-1/DNA complexes specifically.

Gel shift analysis with extracts prepared from stimulated and unstimulated HPB ALL cells afforded results similar to those obtained with the Jurkat cells (Fig. 2). However, in contrast to the Jurkat cells, the mitogen-in

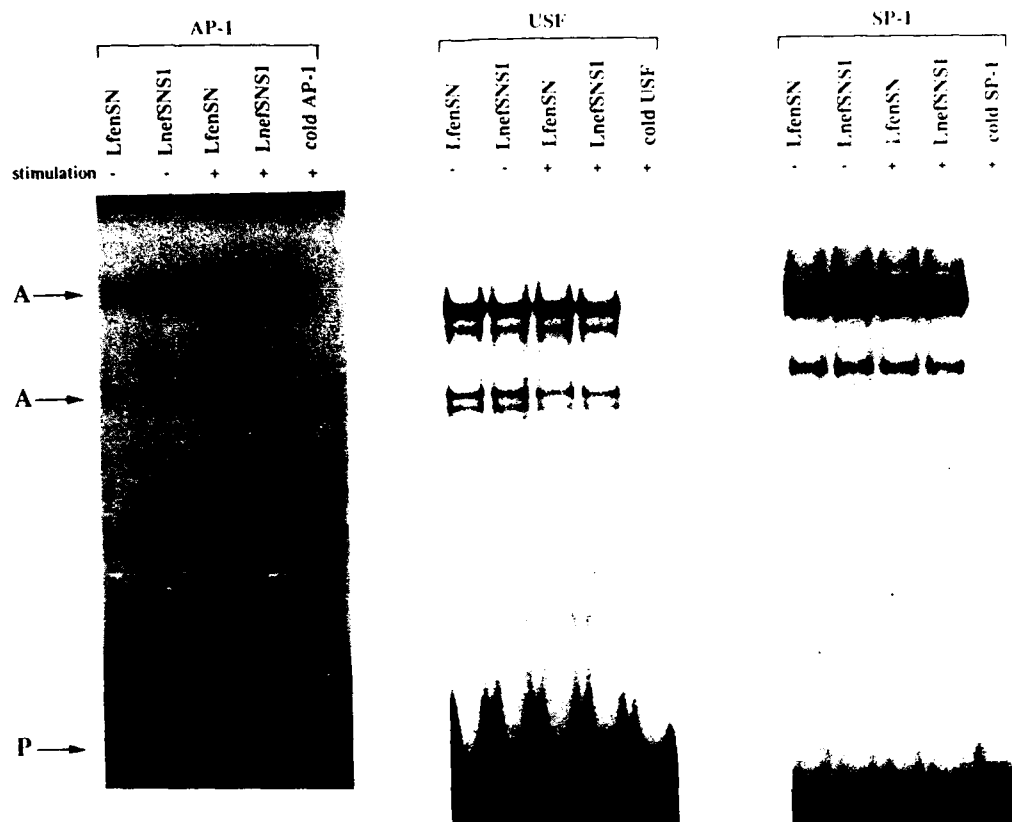


FIG. 2. Gel shift analysis of nuclear extracts prepared from HPB-ALL cells that were not stimulated (–) or were stimulated with (+) with PHA (13 μ g/ml) and PMA (75 ng/ml) for 4 hr. The labeled oligonucleotide probe used is indicated above each panel. The A's indicate inducible AP-1/DNA complexes and P represents free probe. Methods: Nuclear extract preparations and DNA-binding reactions were performed as described in Fig. 1. For the USF probe, we used an oligonucleotide corresponding to nucleotides -159 to -173 of the HIV-1 LTR (40), GCCGCTAGCATTTTCATCA-CGTGGCCCGAGAGCTGC. Experiments were repeated three times with similar results.

ducible AP-1/DNA complexes were present in the unstimulated cells as well as in the stimulated cells. Whereas the stimutable AP-1/DNA complexes in the HPB-ALL/LfenSN cells were induced approximately fivefold after 4 hr of PHA and PMA treatment, there was no significant induction of these complexes in the HPB-ALL/LnefSNS1 cells (Fig. 2). In this experiment, the amount of AP-1 activity in unstimulated HPB-ALL/LfenSN cells was lower than the HPB-ALL/LnefSNS1 cells; however, this was not a consistent finding (unpublished results). In this experiment, we included another Nef non-responsive transcription factor, USF, to demonstrate the specificity of Nef action and the integrity of the extract. The apparent difference in migration of the major inducible AP-1/DNA complexes between the HPB-ALL and the Jurkat cells probably reflects differences that exist between the different T-cell lines.

Previous studies indicated that *c-fos* expression is induced by PHA (9), the calcium ionophore A23187 (10), and PMA (8). In order to determine the signaling pathway required to recruit AP-1 DNA-binding activity, we assessed the role of PHA, PMA, and the calcium ionophore, ionomycin, alone or in combination (Fig. 3a). Interestingly, the recruitment of AP-1 activity was

maximal with PHA treatment alone and the addition of PMA did not significantly increase AP-1/DNA complex formation. The level of inducible AP-1 activity was 18-fold higher in the 22F6 cells compared to the Nef-expressing 133 cells with PHA alone (Fig. 3a). PMA alone only slightly induced AP-1 activity in the 22F6 cells; however, no detectable AP-1 activity was observed in the 133 cells treated with PMA alone (Fig. 3a). Ionomycin alone was not sufficient to elicit AP-1 recruitment in either cell line (Fig. 3a).

T-cell activation is mediated by increased Ca^{2+} influx and PKC activation which both occur as a consequence of phospholipase-C activation by the T-cell receptor (TCR) complex (28). Treatment of the Jurkat cells with a combination of ionomycin and PMA, which both bypass the TCR complex, led to significant recruitment of AP-1 activity, albeit 2.5-fold less efficiently than PHA alone. Whereas there was an 18-fold higher level of induced AP-1 DNA-binding activity in the 22F6 cells compared to the 133 cells using PHA alone, there was only a 3-fold difference using the combination of ionomycin and PMA. Since PHA mimics the normal activation signal (i.e., antigen binding to the TCR) of T-cells (29), it appeared that Nef exerted its effects pri-

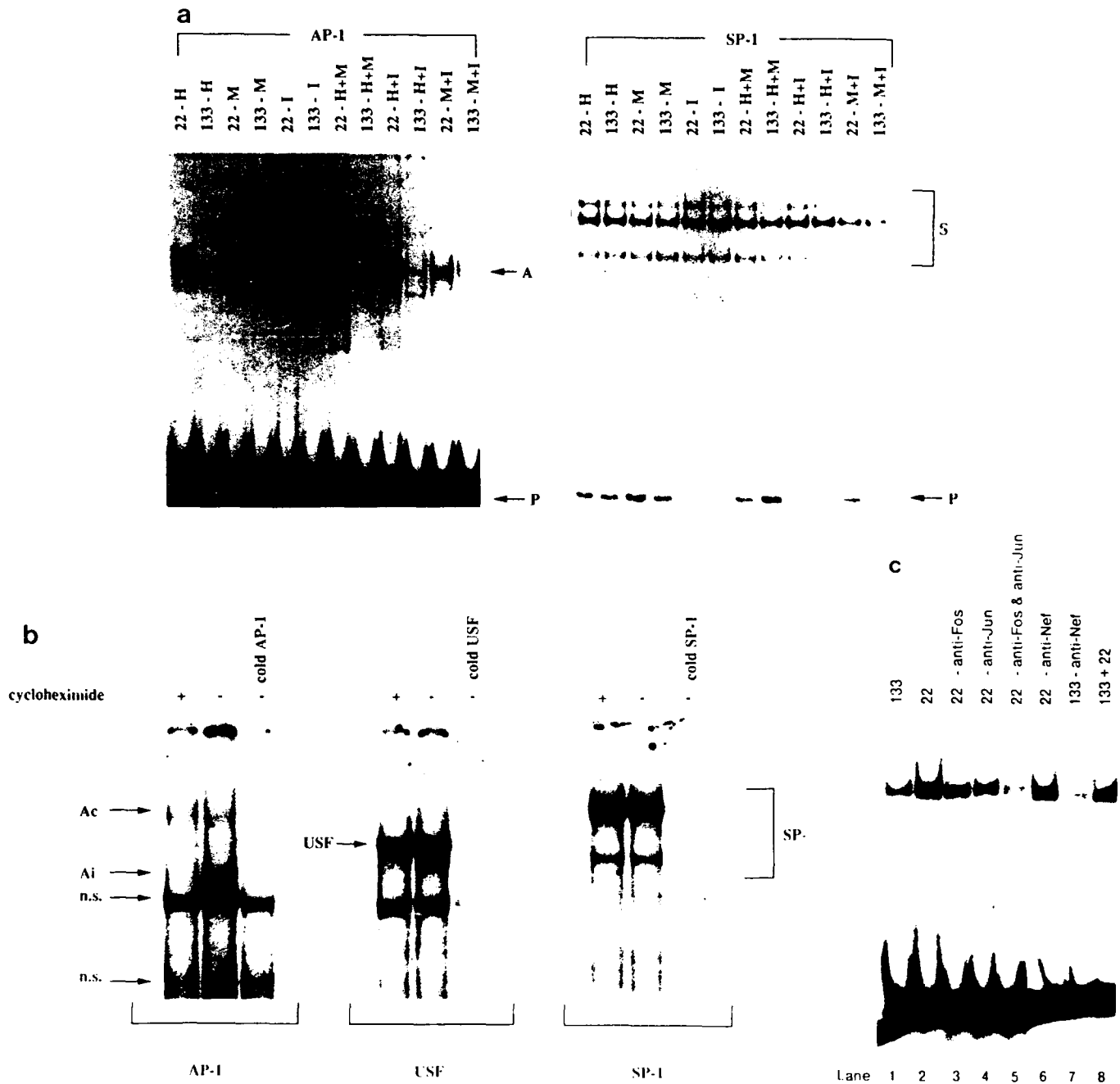


FIG. 3. (a) Gel shift analysis of nuclear extracts prepared from Jurkat 25 22F6 and 133 cells stimulated for 4 hr with either PHA-P (H), PMA (M), or ionomycin, 2 μ M (Sigma), (I), or combinations of any two mitogens. A, S, and P indicate AP-1 specific binding, SP-1 specific binding, and free probe, respectively. (b) Jurkat 22F6 cells were (+) or were not treated (-) with cycloheximide (20 μ g/ml, Sigma) for 30 min prior to stimulation for 4 hr with PHA-P and PMA. The labeled oligonucleotide used is indicated on the side of each panel. Ac, Ai, USF, and n.s. indicate constitutive AP-1/DNA complex, inducible AP-1/DNA complex, USF-specific complex, and not specific, respectively. The "cold DNA" indicates that 100-fold molar excess of unlabeled oligonucleotide (the same oligonucleotide used as the probe) was used as a non-specific competitor. (c) Nuclear extracts from 133 cells (lanes 1, 7, 8) or 22F6 cells (lanes 2, 6, 8) were preincubated with 4 μ l of the specified antisera for 30 min before the AP-1 DNA probe was added. The total volume of the binding reaction was 50 μ l, and this entire volume was applied to the gel. Methods: Nuclear extract preparations and DNA binding reactions were described in Fig. 1. Anti c-Fos and anti c-Jun antisera were obtained from Tom Curran (Roche Institute). The anti-Nef sera was from a rabbit and was used as a negative control antibody.

marily (although not exclusively) on TCR-initiated signalling, as has been suggested previously (25).

To determine whether the recruitment of AP-1 activity required the activation of preexisting complexes or

new protein synthesis, cycloheximide was added 30 min before mitogen treatment. That cycloheximide treatment inhibited the recruitment of AP-1 activity suggests that *de novo* protein synthesis must be in

volved (Fig. 3b). This result was consistent with the observation that 2 hr of stimulation were required before significant recruitment of AP-1 DNA-binding activity (Fig. 1). Thus, it is conceivable that Nef inhibits *c-fos* and/or *c-jun* transcription. Alternatively, Nef may affect the expression of another factor which inhibits AP-1 activity.

To identify the polypeptides present in the inducible AP-1 complex, we incubated nuclear extracts derived from the 22F6 cells with an anti-c-Fos and anti-c-Jun antibody, individually or in combination, prior to the addition of labeled oligonucleotides (Fig. 3c). Antisera to c-Fos or c-Jun inhibited complex formation approximately 3-fold (lanes 3 and 4 compared to lane 2) and, in combination, inhibited complex formation 7-fold (lane 5 compared to lane 2), suggesting the presence of c-Fos and c-Jun in the complex. However, these antibodies did not cause a supershift, presumably because antibody binding to c-Fos and c-Jun caused conformational changes which are not permissive for DNA binding activity. In these experiments, an anti-Nef antibody was used as a negative control (lane 6 compared to lane 2).

Additional experiments were performed to exclude the possibility that Nef directly inhibits AP-1 binding to DNA, or that Nef induces a secondary component that interferes with complex formation (Fig. 3c). An antibody to Nef did not relieve the inhibition of AP-1 recruitment in 133 cells (compare lane 7 to lane 1). Moreover, mixing nuclear extracts from 133 and 22F6 cells did not result in inhibition of AP-1 activity compared to that seen in extracts from 22F6 cells alone (compare lane 8 to lane 2).

Previous studies indicated that the binding of AP-1 to the HIV-1-LTR AP-1 recognition sites plays little, if any, role in affecting transcriptional activity (2, 30). Zeichner and co-workers generated several HIV-1-LTR-CAT linker-scanning mutants in the region of the AP-1 recognition sites and transfected the mutant plasmids into Jurkat cells (30). There were no significant differences in CAT activity between the wild-type HIV-1-LTR-CAT plasmid and the AP-1 mutant plasmids in cells that were or were not stimulated with PHA and PMA (30).

However, the intragenic AP-1 recognition sites were capable of mediating transcriptional activation following phorbol ester treatment (2). Therefore, we cloned a synthetic oligonucleotide, corresponding to the two adjacent AP-1 sites within the *pol* gene (2) or an oligonucleotide which contained three nucleotide substitutions in these AP-1 consensus sites, into the polylinker of the enhancerless pCAT promoter plasmid (Promega). These plasmids were called pCAT-IG-AP1 and pCAT-MIG-AP1, respectively. The pCAT promoter construct, in the absence of the AP-1 sites, contains the SV40 core promoter, afforded low basal chlorampheni-

col acetyltransferase (CAT) activity in T-cells, and was not inducible in T-cells following treatment with T-cell mitogens (data not shown).

The pCAT-IG-AP1 and pCAT-MIG-AP1 constructs were transiently transfected into the Jurkat 22F6 and 133 cells, as well as Jurkat 25 clone 22D8 cells. The 22D8 cells represent a distinct clonal cell line which, like the 133 cells, also stably express the *nef* gene from HIV-1 isolate NL-43 (25). Transiently transfected cells were either not stimulated or were stimulated with PHA and PMA for 18 hr and CAT activity was then measured. CAT activity in transfected cells was relatively low, between 1 and 3% conversion to acetylated products. However, we found an average-fold induction in CAT activity of 3.6 ± 0.4 in the 22F6 cells transfected with the pCAT-IG-AP1 plasmid, compared to an average-fold induction of 1.4 ± 0.2 in the 133 cells and no induction in the 22D8 cells (Fig. 4). Transfection efficiencies were higher in the Nef-expressing cells and were determined by parallel transfections with non-Nef responsive promoters including Rous sarcoma virus-CAT, cytomegalovirus-CAT, and simian polyoma virus 40-CAT (data not shown). These determinations were statistically significant, with 95% confidence intervals, with respect to fold induction, of 2.8–4.4 for the 22F6 cells, 1.0–1.8 for the 133 cells, and 0.9–1.1 for the 22D8 cells. Using a Mann-Whitney U test analysis, the probability that there is no difference in the fold induction between the 22F6 cells and the 133 and 22D8 cells is 1 in a 1000. CAT activity was not induced in cells transfected with the pCAT-MIG-AP1 construct, indicating that the integrity of the AP-1 site in the inserted oligonucleotide was essential. Thus, Nef-mediated inhibition of AP-1 DNA-binding activity prevented AP-1-mediated transcriptional activation.

What role AP-1 plays with respect to HIV-1 regulation is unclear. Nef could inhibit AP-1-mediated activation of HIV-1 directly, by preventing the interaction of AP-1 with the intragenic enhancer in the *pol* gene. In addition, by inhibiting AP-1 recruitment during T-cell activation, Nef may affect the regulation of AP-1-activated cellular genes. Effects on such cellular genes may alter the cellular environment, positively or negatively, which may indirectly affect HIV-1 replication. For example, the finding that c-Fos and c-Jun are early response mediators of T-cell activation (9), coupled with the observation that HIV-1 cannot replicate in resting, unactivated T-cells (31, 32), presents a scenario for indirect effects of Nef on HIV-1 expression.

In addition to mediating the suppression of AP-1 recruitment, we found that Nef also inhibited the mitogen-mediated induction of NF- κ B (33). NF- κ B, like AP-1, is an early response effector of T-cell activation (34) and has been shown to be an important activator of HIV-1 replication in stimulated T cells (35). Thus, Nef-

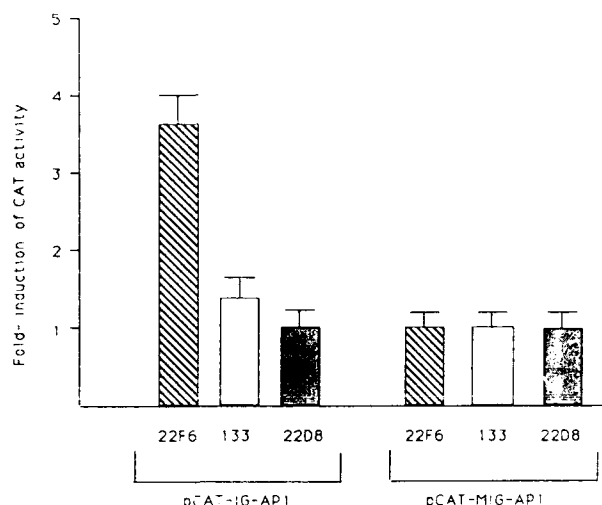


FIG. 4. Chloramphenicol acetyltransferase (CAT) assays extracts prepared from Jurkat 25 cells transfected with the pCAT-IG-AP1 and pCAT-MIG-AP1 plasmids. The data are presented as the mean ratio of the level of CAT activity present in cells stimulated for 18 hr with PHA-P and PMA compared to the level present in unstimulated cells. The error bars represent the standard deviation of the mean. Methods: Jurkat cells were transfected with 40 μ g of the indicated plasmid using DEAE-dextran. Briefly, 10^7 cells were incubated with plasmid DNA suspended in 10 ml of serum-free RPMI 1640, 0.25 M Tris (pH 7.3), and 125 μ g/ml DEAE-dextran (Sigma) at 37° for 40 min. Following centrifugation at 2000 g for 7 min, cells were maintained in growth media containing 10% fetal calf serum for 24 hr. Cells were or were not treated with PHA-P (13 μ g/ml) and PMA (75 ng/ml) and incubated an additional 18–24 hr. Cell extracts were prepared and CAT activity was measured by standard methods (41). Extract equivalent to 3×10^6 cells, as determined by Bradford reagent analysis (Bio-Rad), was used for each 18-hr reaction. CAT activity was in the linear range of analysis with respect to extract amount and incubation time. The amount of CAT activity was quantitated by excising the spots corresponding to the unacetylated and acetylated forms of [14 C]chloramphenicol and measuring radioactivity in a scintillation counter. The plasmid pCAT-IG-AP1 was generated by cloning a double-stranded oligonucleotide corresponding to the two adjacent intragenic AP-1 recognition sites (2) and containing a *Bam*HI sticky end on the 5' end, GATCTCAAAGTGAATCAGAGTTAGTCAATCAAA-TAAT, and a *Sal*I sticky end on the 5' end of the complementary oligonucleotide, TCGAATTATTTGATTGACTAACCAGCTGAT-TCACTTTGA, into the *Bam*HI and *Sal*I sites in the enhancerless pCAT-promoter plasmid (Promega). Plasmid pCAT-MIG-AP1 was made in the same way except that the AP-1 recognition sites in the oligonucleotide used for cloning were disrupted by substitutions at the following, underlined positions; GATCTCAAAGCGGATATCAGC-TGGTTAATCAAATAAT. Cells were transfected 4 to 6 times with each plasmid, a mean-fold induction was calculated, and the standard deviation of the mean was determined. The average-fold induction and standard deviations were 3.6 ± 0.4 , 1.4 ± 0.2 , and 0.9 ± 0.1 for the 22F6, 133, and 22D8 cells, respectively.

mediated inhibition of recruitment of both AP-1 and NF- κ B may intensify the negative effects on HIV-1 replication in T-cells. By inhibiting virus replication directly and/or by blocking T-cell activation, Nef may provide a reservoir of persistently infected cells which may ultimately contribute to HIV-1 clinical latency, HIV-1-mediated CD4 T-cell depletion, and AIDS.

ACKNOWLEDGMENTS

We thank Dr. J. Victor Garcia for providing the HPB-ALL/LfensN and the HPB-ALL/LfensNS1 cells, Dr. Tom Curran for the anti-c-Fos and anti-c-Jun antibodies, and Lisa Westfield and Dr. Evan Sadler for oligonucleotide synthesis. This work was supported by Public Health Service Grant A124745 and U.S. Army Grant DAMD-17-90C-0125 to L.R., National Institute of Health training Grant HL-07088-17 to T.M.J.N. and the Washington University MSTP (T.M.J.N.). L.R. is an American Cancer Society research professor.

REFERENCES

1. FRANZA, B. R., RAUSCHER, F. J., JOSEPHS, S. F., and CURRAN, T., *Science* **239**, 1150–1153 (1988).
2. VAN LINT, C., BURNY, A., and VERDIN, E., *J. Virol.* **65**, 7066–7072 (1991).
3. CURRAN, T., and FRANZA, B. R., *Cell* **55**, 395–397 (1988).
4. LANDSCHULTZ, W. H., JOHNSON, P. F., and MCKNIGHT, S. L., *Science* **240**, 1759–1764 (1988).
5. BOHMANN, D., BOS, T. J., ADMON, A., NISHIMURA, T., and VOGT, P. K., *Science* **238**, 1386–1392 (1987).
6. BOS, T. J., BOHMANN, D., TSUCHIE, H., TJAN, R., and VOGT, P. K., *Cell* **52**, 705–712 (1988).
7. ANGEL, P., ALLEGRETO, E., OKINO, S., HASTTORI, K., BOYLE, W., HUNTER, T., and KARIN, M., *Nature* **332**, 166–171 (1988).
8. ANGEL, P., IMAGAWA, M., CHIU, R., STEIN, B., IMBRA, R. J., RHAMSDORF, H. J., JONAT, C., HERRLICH, P., and KARIN, M., *Cell* **54**, 541–552 (1987).
9. REED, J. C., ALPERS, J. D., NOWELL, P. C., and HOOVER, R. G., *Proc. Natl. Acad. Sci. USA* **83**, 3982–3986 (1986).
10. RAUSCHER, F. J., COHEN, D. R., CURRAN, T., BOS, T. J., VOGT, P. K., BOHMANN, D., TJAN, R., and FRANZA, B. R., *Science* **240**, 1010–1016 (1988).
11. SETOYAMA, C., FRUNZIO, L., LIAU, G., MUDRYI, M., and DE CROMBRUGHE, B., *Proc. Natl. Acad. Sci. USA* **83**, 3213–3217 (1986).
12. SCHONTHAL, A., HERRLICH, P., RAHMSDORF, H. J., and PONTA, H., *Cell* **54**, 325–334 (1988).
13. CHIU, R., BOYLE, W. J., MEEK, J., SMEAL, T., HUNTER, T., and KARIN, M., *Cell* **54**, 541–552 (1988).
14. SASSONE-CORSI, P., SISSON, J. P., and VERMA, I. M., *Nature* **334**, 314–319 (1988).
15. SASSONE-CORSI, P., LAMPH, W. W., KAMPS, M., and VERMA, I. M., *Cell* **54**, 553–560 (1988).
16. NIEDERMAN, T. M. J., THIELAN, B. J., and RATNER, L., *Proc. Natl. Acad. Sci. USA* **86**, 1128–1132 (1989).
17. NIEDERMAN, T. M. J., HU, W., and RATNER, L., *J. Virol.* **65**, 3538–3546 (1991).
18. AHMAD, N., and VENKATESAN, S., *Science* **241**, 1481–1485 (1988).
19. MAITRA, R., AHMAD, N., HOLLAND, S. M., and VENKATESAN, S., *Virology* **182**, 522–533 (1991).
20. TERWILLIGER, E., SODROSKI, J. G., ROSEN, C. A., and HASFLTINE, W. A., *J. Virol.* **60**, 754–760 (1986).
21. LUCIW, P. A., CHENG-MAYER, C., and LEVY, J. A., *Proc. Natl. Acad. Sci. USA* **84**, 1434–1438 (1987).
22. CHENG-MAYER, C., IANELLO, P., SHAW, K., LUCIW, P. A., and LEVY, J. A., *Science* **246**, 1629–1632 (1989).
23. KIM, S., IKEUCHI, R., BYRN, R., GROOPMAN, J., and BALTIMORE, D., *Proc. Natl. Acad. Sci. USA* **86**, 9544–9548 (1989).
24. HAMMES, S. R., DIXON, E. P., MALIM, M. H., CULLEN, B. R., and GREENE, W. C., *Proc. Natl. Acad. Sci. USA* **86**, 9549–9553 (1989).

25. LURIA, S., CHAMBERS, I., and BERG, P., *Proc. Natl. Acad. Sci. USA* **88**, 5326-5330 (1991).
26. GARCIA, J. V., and MILLER, A. D., *Nature* **350**, 508-511 (1991).
27. RYDER, K., and NATHANS, D., *Proc. Natl. Acad. Sci. USA* **85**, 8464-8467 (1988).
28. WEISS, A., In "Fundamental Immunology" (W. E. Paul, Ed.), pp. 359-384 Raven Press, New York, 1989.
29. WEISS, A., WISKOCIL, R. L., and STOBO, J. D., *J. Immunol.* **133**, 123-128 (1984).
30. ZEICHNER, S. L., KIM, J. Y. H., and ALWINE, J. C., *J. Virol.* **65**, 2436-2444 (1991).
31. ZAGURY, D., BERNARD, J., LEONARD, R., CHEYNIER, R., FELDMAN, M., SARIN, P. S., and GALLO, R. C., *Science* **231**, 850-853 (1986).
32. FOLKS, T., POWELL, D. M., LIGHTFOOTE, M. M., BENN, S., MARTIN, M. A., and FAUCI, A. S., *Science* **231**, 600-602 (1986).
33. NIEDERMAN, T. M. J., GARCIA, J. V., HASTINGS, W. R., LURIA, S., and RATNER, L., *J. Virol.* **66**, 6213-6219 (1992).
34. GREENE, W. C., *N. Engl. J. Med.* **324**, 308-317 (1991).
35. NABEL, G., and BALTIMORE, D., *Nature* **326**, 711-713 (1987).
36. DIGNAM, J. D., LEBOWITZ, R. M., and ROEDER, R. G., *Nucleic Acids Res.* **11**, 1475-1489 (1983).
37. MONTMINY, M. R., and BILEZIKIAN, L. M., *Nature* **328**, 175-178 (1987).
38. WILDEMAN, A. G., SASSONE-CORSI, P., GRUNDSTROM, T., ZENKE, M., and CHAMBON, P., *EMBO J.* **3**, 3129-3133 (1984).
39. PIETTE, J., KRYSZKE, M. H., and YANIV, M., *EMBO J.* **4**, 2675-2685 (1985).
40. SMITH, M. R., and GREENE, W. C., *Proc. Natl. Acad. Sci. USA* **86**, 8526-8530 (1989).
41. GORMAN, C. M., MOFFAT, L. F., and HOWARD, B. H., *Mol. Cell Biol.* **2**, 1044-1051 (1982).

HIV-2 Viral Protein X Association with the Gag p27 Capsid Protein

ROBERT HORTON, PAUL SPEARMAN, AND LEE RATNER¹*Departments of Medicine and Molecular Microbiology, Washington University School of Medicine, St. Louis, Missouri 63110**Received July 9, 1993; accepted December 3, 1993*

VPX is a 16 kDa accessory protein expressed in cells infected with HIV-2 and most SIV strains and is packaged into virus particles. In order to define the requirements for incorporation of VPX into virions, VPX and HIV-2 GAG-POL were expressed independently from a vaccinia virus-based transient expression system. Under these conditions, VPX was exported from transfected cells only when coexpressed with the HIV-2 GAG-POL plasmid. A 27 kDa protein coprecipitating with VPX was found to have an identical electrophoretic mobility as the GAG capsid protein, and reacted with an anti-GAG antiserum. Coexpression of VPX and GAG-POL resulted in virus-like particles containing both proteins, as determined by sucrose gradient analyses. Expression of VPX and HIV-2 GAG without POL gave similar results. VPX association with HIV-2 GAG p27 capsid protein was specific, since no association was found with the HIV-1 GAG p25/p24 capsid protein. © 1994 Academic Press, Inc.

Vpx and *vpr* are homologous genes found in human and simian immunodeficiency viruses (SIV) (1). The *vpr* gene is found in all of these lentiviruses, while the *vpx* gene is only found in HIV-2, SIV_{mac}, SIV_{mac}, and SIV_{smm}. The protein products (VPR and VPX) are similar in molecular mass (14–16 kDa, 96–112 amino acids) and demonstrate 26–39% amino acid sequence identity.

The function of the *vpx* protein product is unknown. Though *vpx* is dispensable for virus replication in T lymphoid cell lines, replication is accelerated by the presence of *vpx* (2–4). The magnitude of enhancement of virus replication appears to be greatest in primary lymphocytes and macrophages (5, 6). The *vpx* product appears to act at an early step in virus replication prior to reverse transcription (7).

The *vpx* gene product is packaged in the virion, resulting in a 1:1 stoichiometry with the GAG p27 protein (8). Moreover, VPX may be an RNA binding protein (8). However, the mechanism of virion packaging of VPX and the localization of VPX within the virion have not been defined and are the focus of the current study.

To examine the requirements for VPX and GAG-POL association, we expressed the protein products separately or together in a vaccinia virus expression system. For this purpose, the HIV-2 *vpx* gene was amplified by the polymerase chain amplification reaction (PCR) and cloned between the *Nco*I and *Sac*I sites of pTM3 (9), and the resultant plasmid was designated pTMX. This plasmid includes a T7 polymerase pro-

moter and an encephalomyocarditis 5' untranslated sequence to enhance CAP-independent protein synthesis. The *gag* and *pol* genes of HIV-2 were cloned between the *Nco*I and *Sac*I sites of pTM3 to produce clone pTMGP2. These plasmids were then transfected into an African green monkey kidney cell line (BSC40) which had first been infected with a vaccinia virus expressing the T7 polymerase (VTF7-3) (9). The transfected cells were labeled with Trans[³⁵S]label (ICN) and the labeled cell-associated (Fig. 1A) and conditioned media-associated proteins (Fig. 1B) were immunoprecipitated with anti-VPX (odd-numbered lanes) and anti-HIV2 GAG antisera (even-numbered lanes).

Cells transfected with pTMX contained a labeled product of 16 kDa (Fig. 1A, lane 3) that was not found in pTM3 or pTMGP2 transfected cells (lanes 1 and 5, respectively). Cells transfected with pTMGP2 contained protein products of 44, 27, and 25 kDa (lane 6). The 44- and 25-kDa proteins were not detected in cells transfected with pTM3 (lanes 1 and 2) or pTMX (lanes 3 and 4), while a cellular protein reacting nonspecifically with the anti-GAG and anti-VPX antisera and coelectrophoresing with the 27-kDa protein is evident in the control samples (lanes 1–5). The 44-kDa product is most likely a partially cleaved GAG product which includes the N-terminal p17 matrix residues and the p27 sequences. The 27- and 25-kDa products are probably two isoforms of the HIV-2 capsid protein, as has been previously reported (10–12). Two isoforms of the HIV1 capsid protein have also been described which have electrophoretic mobilities equivalent to 25- and 24-kDa proteins (13). It is also notable that the anti-VPX and anti-GAG antisera show no evidence of serological cross-reactivity (lanes 4 and 5). Cotransfection of

¹ To whom correspondence and reprint requests should be addressed at: Box 8125, 660 S. Euclid, Washington University, St. Louis, Missouri 63110. Telephone: 314 362-8836. Teletax: 314-362 8826.

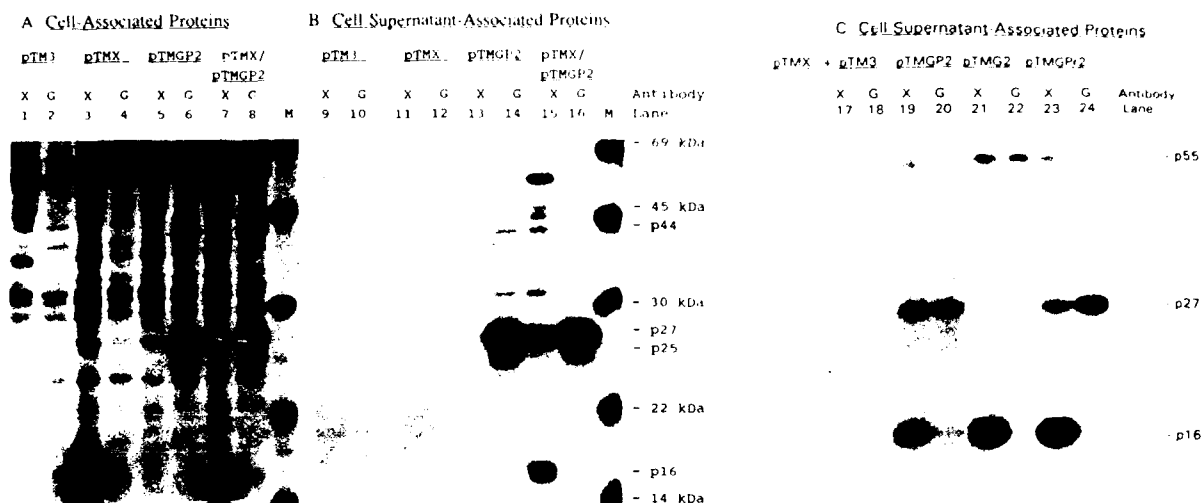


FIG. 1. Association of recombinant vaccinia virus expressed VPX with GAG p27. BSC40 cells were cotransfected 1 hr after infection with VTF7-3 with 20 μ g of pTM3 (lanes 1, 2, 9, 10), pTMX (lanes 3, 4, 11, 12, 17, 18), pTMGP2 (lanes 5, 6, 13, 14), pTMX and pTMGP2 (lanes 7, 8, 15, 16, 19, 20), pTMX and pTMG2 (lanes 21, 22), or pTMX and pTMGPr2 (lanes 23, 24). The calcium phosphate precipitation method was used for transfection (A) and (B) and the lipofectin transfection method for (C), and equivalent amounts of DNA were transfected in each case (with the addition of pTM3). After 3 hr of cultivation in DMEM supplemented with 10% fetal calf serum, 50 μ /ml penicillin, and 50 μ g/ml streptomycin the cells were placed in medium lacking methionine and cysteine, and labeled for 16 hr with 100 μ Ci/ml Trans³⁵S]label (ICN). Samples of conditioned medium (lanes 9–24) were cleared of cellular debris by centrifugation at 1000 rpm for 5 min and then 0.1 vol of 10 \times lysis buffer was added. Cells were washed with PBS and then PBS was added to the plates during scraping with a rubber policeman. 0.1 vol of 10 \times lysis buffer was added and the cells were vortexed at 4 $^{\circ}$ for 1 min. Nuclei were removed by centrifugation at 2000 rpm for 10 min. Immunoprecipitation was performed with a rabbit anti-VPX antiserum (odd-numbered lanes) or a mouse monoclonal anti-HIV-2 GAG antiserum (even-numbered lanes; provided by Dr. Paul Yoshihara through the NIH AIDS Reagent Repository). Immunoprecipitates were washed with 1 \times lysis buffer three times and then 30 μ l of 2 \times sample buffer was added. Samples were treated at 100 $^{\circ}$ for 5 min and analyzed on 12% PAGE. Molecular weight markers are indicated (M) and the sizes are listed on the right of the figure in kDa.

BSC40 cells with pTMX and pTMGP2 resulted in the expression of both the 16-kDa VPX product (Fig. 1A, lane 7) and the 44-, 27-, and 25-kDa GAG products (lane 8).

Analysis of the conditioned media from the vaccinia virus infected and transfected BSC40 cells demonstrated no detectable VPX protein when pTMX was transfected alone (lane 11). However, expression of pTMGP2 resulted in expression in the medium of the 27- and 25-kDa GAG proteins (lane 14). These proteins showed no reactivity with the anti-VPX antiserum (lane 13). When cells were cotransfected with pTMX and pTMGP2, VPX was detectable in the medium (lane 15). This suggests that expression of GAG and/or POL proteins are required for the export of VPX from transfected cells. Furthermore, exposure of the conditioned media to the anti-VPX antiserum resulted in coprecipitation of the GAG p27 protein (lane 15). This provides evidence for association of the p27 GAG protein and p16 VPX protein. However, very little 16 kDa protein coprecipitated with the 27 kDa protein when anti GAG antiserum was used (lane 16). Differences in the ability of the anti-VPX and anti GAG antisera in precipitating the GAG-VPX complex may be due to masking of the anti GAG epitope by VPX.

To determine if *pol* products are required for VPX export, pTMX was cotransfected with either pTM3

(Fig. 1C, lanes 17 and 18), pTMGP2 (lanes 19 and 20), or an expression clone for HIV-2 *gag* only, pTMG2 (lanes 21 and 22). Alternatively, pTMX was cotransfected with an expression clone for HIV-2 *gag* and protease products only, pTMGPr2 (lanes 23 and 24). pTMG2 and pTMGPr2 were constructed from PCR products of HIV-2 nucleotides 540–2113 and 540–2669, respectively, and cloned between the *Nco*I and *Eco*RI sites of pTM3.

As in the previous experiments (Fig. 1B), expression of pTMX without *gag* products did not result in the release of VPX into the conditioned media (Fig. 1C, lane 17). Coexpression of pTMX with pTMGP2 resulted in release from the cell of GAG p27, a smaller amount of GAG p55, and VPX (p16, Fig. 1C, lanes 19 and 20). Coexpression of pTMX with pTMG2 resulted in the release from the cell of GAG p55, but not GAG p27 (Fig. 1C, lane 22), as expected, since the viral protease was deleted from this expression clone. VPX was exported with GAG p55 in this experiment (Fig. 1C, lane 21). Coexpression of pTMX with pTMGPr2 resulted in the release from the cell of GAG p27, a smaller amount of GAG p55, and VPX (Fig. 1C, lanes 23 and 24). In each case in which VPX was released from the cell, immunoprecipitation of VPX with the anti-VPX antiserum resulted in coprecipitation of proteins with identical electrophoretic mobilities to those of the

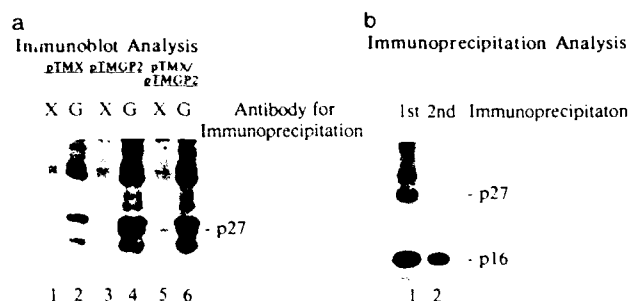


Fig. 2. Immunological characterization of the 27-kDa protein coprecipitating with VPX. (a) Anti-VPX (lanes 1, 3, 5) and anti-GAG immunoprecipitates (lanes 2, 4, 6) of conditioned media from cells transfected with pTMX (lanes 1, 2), pTMGP2 (lanes 3, 4), or both plasmids (lanes 5, 6) were analyzed by SDS-PAGE and immunoblotted with the anti-GAG antiserum. Detection was with the horseradish peroxidase-coupled anti-mouse antibody, followed by enhanced chemiluminescence detection (ECL, Amersham). The specific 27-kDa protein is indicated to the right. (b) Anti-VPX immunoprecipitates from Trans^[35S]labeled cells cotransfected with pTMX and pTMGP2 were analyzed by immunoprecipitation with the anti-VPX antiserum with (lane 2) or without (lane 1) solubilization in 2× sample buffer, dilution in 1 ml lysis buffer, and repeat immunoprecipitation with the anti-VPX antiserum.

GAG protein products (p27 or p55, Fig. 1C, lanes 19, 21, and 23). Thus, *pol* products are dispensable for VPX export from the cell in the presence of *gag* products.

To prove that the 27-kDa protein coprecipitating with VPX is the HIV-2 capsid protein, we performed immunoblots with the immunoprecipitated proteins (Fig. 2a). Immunoprecipitates obtained with the rabbit anti-VPX antiserum (lanes 1, 3, and 5) or the mouse anti-GAG antiserum (lanes 2, 4, and 6) were analyzed by SDS-PAGE, transferred to nitrocellulose, and blotted with the anti-GAG monoclonal antibody. Although background bands due to immunoglobulins are noted, a specific band of 27 kDa is recognized in the anti-VPX immunoprecipitate of conditioned medium from cells transfected with pTMGP2 and pTMX (lane 5) and anti-GAG immunoprecipitates of conditioned media from cells transfected with pTMGP2 alone (lane 4) or cells transfected with pTMGP2 and pTMX (lane 6). This protein was not detected in the negative control lanes (lanes 1–3).

Kappes *et al.* have recently described a 30-kDa protein in HIV-2 particles reacting with anti-VPX antiserum (7). They suggested that this may represent a protein with VPX sequences fused to other viral sequences. To exclude the possibility that the p27 protein expressed in the vaccinia expression system described here is such a fusion protein, experiments were performed to dissociate the p27-p16 complex. The anti-VPX immunoprecipitate from conditioned media of cells cotransfected with pTMGP2 and pTMX was solubilized by heating at 100° for 5 min in sample buffer (62.5 mM Tris, Cl, pH 6.8, 2% SDS, 5% 2-mercaptoethanol), di-

luted in lysis buffer, and reimmunoprecipitated with the anti-VPX antiserum (Fig. 2b). The products of the first immunoprecipitation included both the 16- and 27-kDa proteins (lane 1), whereas after dissociation of the complex, only the 16-kDa protein was immunoprecipitated (lane 2). This provided evidence that the 27-kDa protein lacks an epitope reactive with the anti-VPX antiserum, in agreement with the previous findings (Fig. 1). Thus, immunoprecipitation of the 27-kDa protein with the anti-VPX antiserum (Fig. 2b, lane 1) must be a result of an association with VPX.

In order to determine if the VPX and GAG proteins exported from transfected cells were associated with virus-like particles, sucrose gradient analyses were undertaken (Fig. 3). Proteins released from metabolically labeled VTF7-3 infected cells transfected with pTMX, pTMGP2, or both plasmids were sedimented through a 20% sucrose cushion and analyzed on 20–60% (w/v) sucrose gradients. Each fraction was concentrated with 10% (w/v) trichloroacetic acid and analyzed by SDS-PAGE (Fig. 3). Fraction 9 represented the peak fraction, at density 1.142, for both the 16- and 27-kDa proteins (Figs. 3b and 3c). Immunoprecipitation of fraction 9 from pTMGP2 transfected cells revealed no products reactive with anti-VPX antiserum and only the 27-kDa capsid protein reactive with the anti-GAG antiserum (not shown). Analysis of fraction 9 from cells cotransfected with pTMGP2 and pTMX demonstrated the 16- and 27-kDa proteins after immunoprecipitation with the anti-VPX antiserum and the 27-kDa protein after immunoprecipitation with the anti-GAG antiserum (not shown). Immunoprecipitation of fraction 9 of sucrose gradients of particulate material from pTMX transfected cells (Fig. 3a) using either the anti-VPX antiserum or the anti-GAG antiserum revealed no particle-associated viral proteins. This is consistent with the previous finding (Fig. 1) that VPX is exported from transfected cells only in the presence of GAG protein expression.

Immunogold electron microscopy using anti-VPX antiserum confirmed the presence of VPX in particles released from BSC40 cells cotransfected with pTMX and pTMGP2. In these studies, gold particles were also seen overlying budding particles at the plasma membrane (not shown). No labelling of the plasma membrane was seen in cells that were transfected with pTMX alone, or pTMGP2 alone.

In order to examine the specificity of the interaction of the HIV2 p27 GAG protein and VPX, an experiment was performed to ask whether HIV1 GAG protein associates with VPX (Fig. 4). For this purpose, we cloned both the *gag* and *pol* genes of HIV1 into pTM3 at the *NcoI* site in the polylinker in clone pTMGP1. A plasmid capable of expressing only the HIV 1 *gag* product was constructed from pTMGP1 by introducing a frameshift

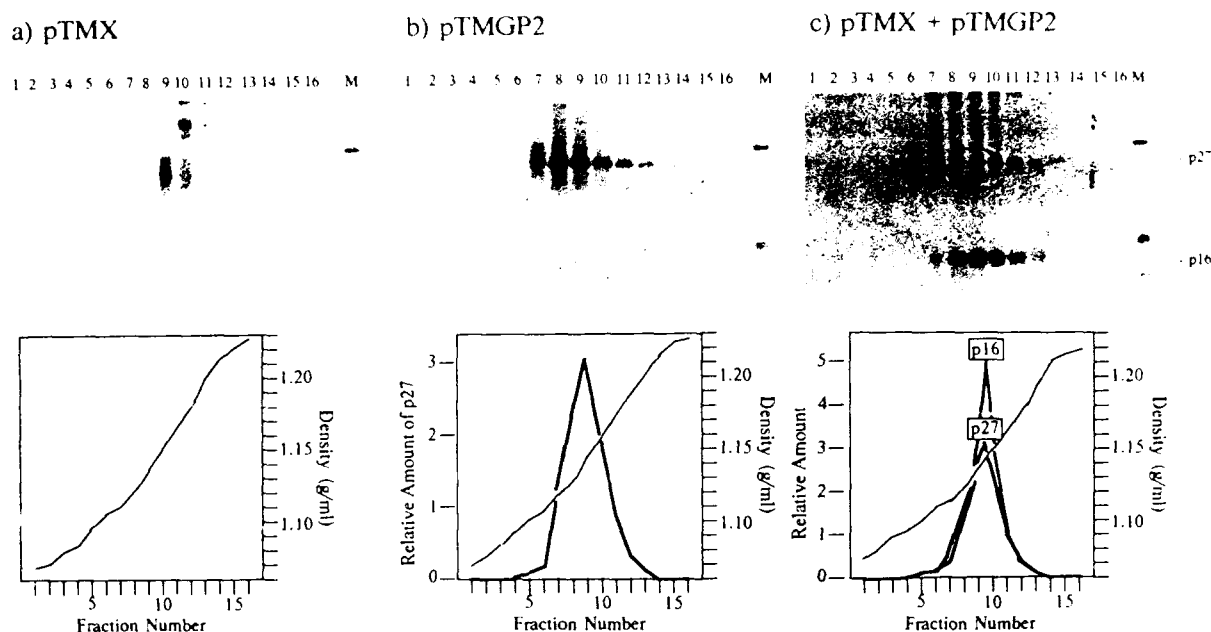


FIG. 3. Sucrose gradient analysis of particles expressed from recombinant vaccinia virus infected cells. BSC40 cells were infected, transfected, and labeled with Trans^[35S]label as described in Fig. 1 legend. Cellular debris was removed from the conditioned media by centrifugation at 2000 rpm for 10 min at 4°. Particles were concentrated by sedimentation through a 20% sucrose cushion prepared in PBS at 28,000 rpm for 90 min at 4° in a SW 28.1 rotor. Particles were resuspended in 200 μ l PBS, layered on linear 20–60% sucrose gradients in PBS, and centrifugation was performed in a SW28.1 rotor at 20,000 rpm for 16 hr at 4°. Fractions were removed from the bottom of the tube. (a) Sucrose gradient fractions from cells transfected with (a) pTMX, (b) pTMGP2, or (c) pTMX and pTMGP2 were precipitated with 10% trichloroacetic acid and analyzed by 12% SDS-PAGE. The densitometric analysis of the sucrose gradients is shown below each autoradiogram with the densities of each fraction as determined by refractive indices. M indicates molecular weight markers, which are 30, 22, and 14 kDa in size.

mutation at the *Bcl*I site in the 5' portion of the *pol* gene and designated pTMG1. BSC40 cells transfected with pTMX with or without the GAG expression clones were labeled with Trans^[35S]label and proteins in the cell lysate (not shown) and conditioned media (Fig. 4) were immunoprecipitated with anti-VPX or anti-GAG antisera. Cells transfected with pTMX alone or pTMX with pTMGP1, pTMGP2, or pTMG1 expressed similar amounts of VPX protein in the cell lysates (not shown).

Examination of the conditioned media demonstrated no VPX protein from cells transfected with pTMX alone (Fig. 4, lane 6). Conditioned media from cells transfected with pTMGP1 alone show a predominant 25-kDa product and smaller amounts of 24- and 41-kDa products (lane 7). Conditioned media from cells transfected with pTMGP2 alone show a 27-kDa product and a smaller amount of the 25-kDa product (lane 9), as previously demonstrated (Fig. 1). Conditioned media from cells transfected with pTMG1 included a 55-kDa product (lane 11), representing the GAG precursor protein which is not cleaved due to the absence of viral protease expression from this plasmid.

Coexpression of pTMX and pTMGP2 results in VPX export into the conditioned media (Fig. 4, lane 16) as well as GAG p27 expression (lane 15). Furthermore, GAG p27 coprecipitates with VPX using the anti-VPX antiserum (lane 16), and to a lesser degree VPX coprecipitates with GAG with the anti-GAG antiserum (lane

15). In contrast, coexpression of pTMX with pTMGP1 (lane 14) or pTMG1 (lane 18) did not result in VPX export or coprecipitation with GAG (lanes 13 and 17). These data suggest that VPX associates specifically with HIV2 GAG products and not HIV1 GAG products.

The current study has examined the viral determinants required for VPX packaging. This work demonstrates an association between GAG p27 and VPX. This may represent a direct interaction of the viral capsid protein and VPX. Alternatively, an indirect association through another factor is possible. Such a factor could be RNA, in light of the previous report that VPX binds RNA (8). HIV-2-specific viral RNA would not be expected in the particles produced with the vaccinia virus vector since the presumed viral packaging sequence is not included in the expression plasmid. Some RNA species is present in the particle, as demonstrated by [³H]uridine labeling experiments and sucrose gradient analysis, but attempts to coprecipitate RNA with VPX using anti-VPX antiserum were unsuccessful (not shown). This suggests that there is not a tight association of VPX with RNA in particles produced in this expression system. The current data also do not exclude the presence of additional viral GAG proteins in the complex with VPX. This must be examined with additional specific antisera.

The current findings demonstrate that expression of *gag* is sufficient for incorporation of VPX into virus like

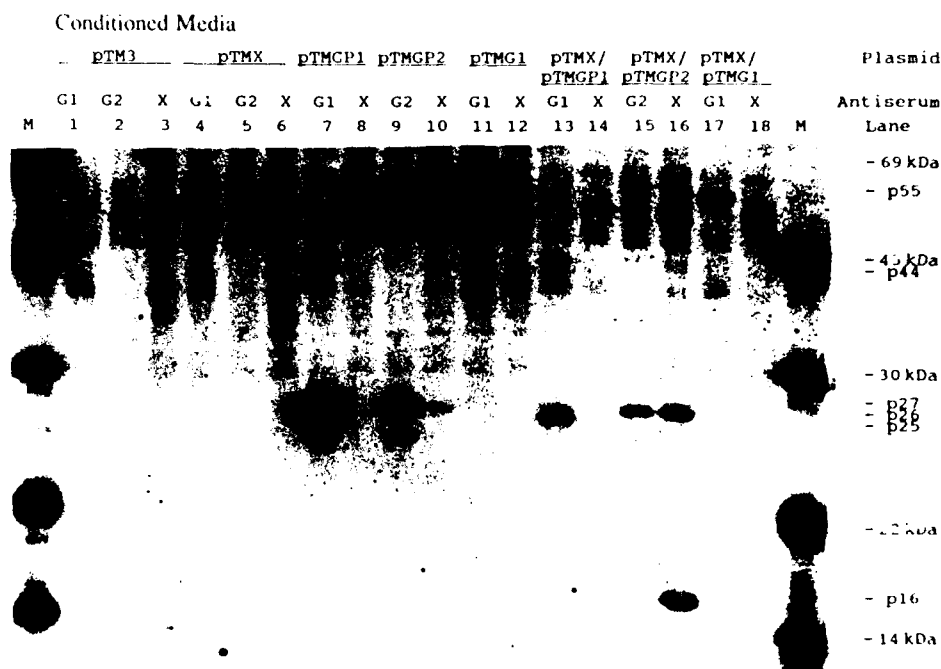


FIG. 4. Specificity of VPX for association with HIV-2 GAG but not HIV-1 GAG protein. BSC40 cells were transfected with pTM3 (lanes 1-3), pTMX (lanes 4-6), pTMGP1 (lanes 7, 8), pTMGP2 (lanes 9, 10), pTMGP1 (lanes 11, 12), pTMX and pTMGP1 (lanes 13, 14), pTMX and pTMGP2 (lanes 15, 16), or pTMX and pTMGP1 (lanes 17, 18). Cells were transfected with equivalent amounts of DNA and labeled with Trans[³⁵S]label, as described in Fig. 1 legend. Samples of conditioned media were immunoprecipitated with an anti-HIV-1 GAG antiserum (lanes 1, 4, 7, 11, 13, 17, produced in rabbits with a recombinant protein provided by the NIH AIDS Reagent Repository through American Biotech), the anti-HIV-2 p24 antiserum (lanes 2, 5, 9, 15), or the anti-VPX antiserum (lanes 3, 6, 8, 10, 12, 14, 16, 18). Samples were electrophoresed on SDS-PAGE and molecular weight standards (M) are shown on the right.

particles. Neither the envelope protein nor *pol*-encoded proteins are required for VPX packaging.

The association of VPX and the GAG p27 protein and the incorporation of VPX in the virus particles suggest a role early in the virus life cycle for VPX. VPX may facilitate the dissolution of the viral core in order for reverse transcription to occur. The exact mechanism of VPX function remains to be defined.

ACKNOWLEDGMENTS

We thank Brett Lindenbach for assistance with these experiments and Jaang Jing Wang for the immunogold electron microscopy results. The anti HIV2 GAG antiserum and the recombinant VPX and HIV1 GAG p24 proteins used to produce antiserum were provided by the AIDS Reagent Repository Program. This work was supported by contract DAMD17-90C-0125. P.S. was supported by PHS Grant 5T32AI07172. T.R. is an American Cancer Society Research professor.

REFERENCES

1. TRISTEM, M., MARSHALL, C., KARPAS, A., and HILL, E., *EMBO J* **11**, 3405-3412 (1992).
2. HU, W., VANDERHEYDEN, N., and RATNER, L., *Virology* **173**, 624-630 (1989).
3. KAPPEL, J. C., CONWAY, J. A., LEE, S.-W., SHAW, G. M., and HAHN, B. H., *Virology* **184**, 197-209 (1991).
4. MARCON, L., MICHAEL, F., HATTORI, N., FARGNOLI, K., GALLO, R. C., and FRANCHINI, G., *J. Virol.* **65**, 3938-3942 (1991).
5. GUYADER, M., EMDERMAN, M., MONTAGNIER, L., and PÉDINI, K., *EMBO J* **8**, 1169-1175 (1989).
6. YU, X.-F., YU, Q.-C., ESSEX, M., and LEE, T.-H., *J. Virol.* **65**, 5088-5091 (1991).
7. KAPPEL, J. C., PARKIN, J. S., CONWAY, J. A., KIM, J., BROUILLETTE, C. G., SHAW, G. M., and HAHN, B. H., *Virology* **193**, 222-233, (1993).
8. HENDERSON, L. E., SOWDER, R. C., COPELAND, C. D., BENVENISTE, R. E., and OROZCO, S., *Science* **241**, 199-201 (1988).
9. MOSS, B., ELROY-STEIN, O., MIZUKAMI, T., ALEXANDER, W. A., and FUELL, T. R., *Nature* **348**, 91-92 (1990).
10. ESPINO, R. T., and URBEL, P., *J. Clin. Microbiol.* **28**, 2107-2110 (1990).
11. FRANCHINI, G., FARGNOLI, K. A., GIOMBINI, F., JAGODZINSKI, E., DE ROSSI, A., BOSCHI, M., BIBERFELD, G., FENYO, E. M., ALBERT, J., GALLO, R. C., and WONG STAAI, F., *Proc. Natl. Acad. Sci. USA* **86**, 2455-2457 (1989).
12. KJØNE, E., VON BRIESEN, H., DIETRICH, U., ADAMSKI, M., MIE, D., BASER, E., KREUTZ, R., IMMELMANN, A., HENCO, K., MICHOSKE, G., ANDERSEN, R., GILDERBLOM, H., and RUSAMEN WAGMANN, H., *Proc. Natl. Acad. Sci. USA* **86**, 2383-2387 (1989).
13. LAURENT, A. G., KREIB, B., REY, M. A., MONTAGNIER, L., and EL VANDERHART, A. G., *J. Virol.* **63**, 4074-4078 (1989).

Myristoylation-Enhanced Binding of the HIV-1 Nef Protein to T Cell Skeletal Matrix

THOMAS M. J. NIEDERMAN, W. RANDALL HASTINGS, AND LEE RATNER¹

Departments of Medicine and Molecular Microbiology, Washington University School of Medicine, St. Louis, Missouri 63110

Received February 11, 1993; accepted July 14, 1993

The negative factor, Nef, of HIV-1 was found to associate to an extent of 16–42% with the detergent insoluble cytoskeletal fraction of T lymphocytes. Furthermore, *Escherichia coli* expressed Nef protein was found to bind during *in vitro* reactions with the cytoskeletal matrix to an extent of 30–50%. Cytoskeletal association of Nef was significantly enhanced by myristoylation. The specificity of the myristoylation-enhanced binding was demonstrated by the lack of an effect of myristoylation on binding of the HIV-1 Gag protein to the cytoskeleton. Cytoskeletal binding was saturable, and inhibited by high concentrations of sodium chloride, or with SDS or urea. Binding of Nef to the cytoskeletal matrix may be important in mediating its effects on HIV-1 replication. © 1993 Academic Press, Inc.

The *negative factor* gene, *nef*, is present in all human and simian immunodeficiency viruses (1). The *nef* gene product of HIV-1 is generally 25–27 kDa and 197–210 amino acid long, whereas the *nef* gene products of HIV-2 and SIVs are generally 32 kDa and 240–264 amino acids in length (1). Though there is only 38% sequence homology between HIV-1 and SIV_{mac} Nef proteins, there is a much higher level of conservation of the central region of the proteins which have homology to G proteins (2). In addition, a myristoylation acceptor glycine codon at the penultimate codon position is present in all *nef* genes (1). Though the role of the myristoyl modification of Nef is not clear, it has been suggested to be critical for its cellular localization and its activity (3, 4).

In vivo, Nef is important for the pathogenicity of SIV_{mac} in rhesus macaques (5). Several *in vitro* studies have suggested that both HIV-1 and SIV_{mac} Nef proteins function to depress virus replication (6–10) at the level of viral transcription (2, 3, 8, 11), but not all authors have reached similar conclusions (12–14). In addition, Nef appears to depress cell surface expression of CD4 and induction of IL2 expression in T lymphocytes (15, 16). The relationship between the *in vitro* and *in vivo* activities of Nef remains to be defined.

Several studies have also examined the cellular localization of Nef, but with differing results (4, 13, 17–19). The current studies utilized cell fractionation methods to demonstrate localization of a portion of Nef in the cytoskeletal matrix of T lymphocytes. This is a detergent insoluble framework of proteins which includes the cytoskeleton and membrane skeletal fractions. Furthermore, we have developed a novel binding assay to

examine the dependence of myristoylation for Nef binding to the cell skeletal matrix.

In order to examine the cellular localization of Nef, we used a JURKAT 25 cell clone resulting from stable transfection of a plasmid (SRalpha) expressing *nef* from HIV-1 strain NL4-3, using a human T-lymphotropic virus type 1 (HTLV1) promoter and an SV40 enhancer (133 cells) (15, 20, 21). Control JURKAT 25 cells (22F6 or 22 cells) do not express Nef. In addition, we used HPBALL cells infected with a recombinant retrovirus expressing *nef* from HIV-1 strain SF2 using the Mo-MuLV promoter (NEF cells), and control HPBALL cells not bearing *nef* sequences (LN cells) (16, 20, 21). Both unstimulated cells and cells stimulated for 4 hr with phorbol-12-myristate-13-acetate and phytohemagglutinin were used. Cells were lysed in hypotonic lysis buffer (10 mM HEPES, pH 7.9, 10 mM KCl) by Dounce homogenization, and unbroken cells and nuclei were removed by centrifugation at 1500 rpm at 4° in an Eppendorf centrifuge. The postnuclear supernatant was supplemented with NaCl to a final concentration of 150 mM and was then separated by ultracentrifugation at 38,000 rpm in a 70.1 Ti rotor at 4° for 1 hr into a supernatant fraction (cytosol, C) and a pellet. The pellet was resuspended in NTENT buffer (150 mM NaCl, 10 mM Tris-Cl, pH 8.0, 1 mM EDTA, pH 8.0, 3 µl/ml aprotinin, 0.1 mM PMSF, 0.1 mM sodium vanadate, 10 mM NaF, 50 mM glycerol phosphate, 1% Triton X-100, 1% NP-40) and resedimented under the same ultracentrifugation conditions into a supernatant fraction (membrane, M) and a pellet (skeleton, K).

Under these fractionation conditions, 15–40% of the Nef protein was found in the cytosol fraction, 3–12% in the membrane fraction, and 4–17% in the skeletal fraction (Fig. 1). No significant differences were

¹ To whom all reprint requests should be addressed.

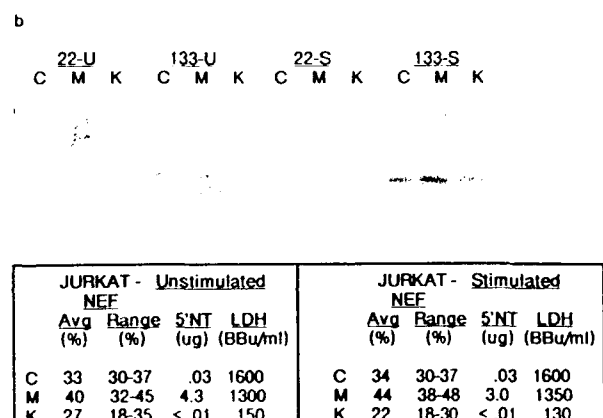
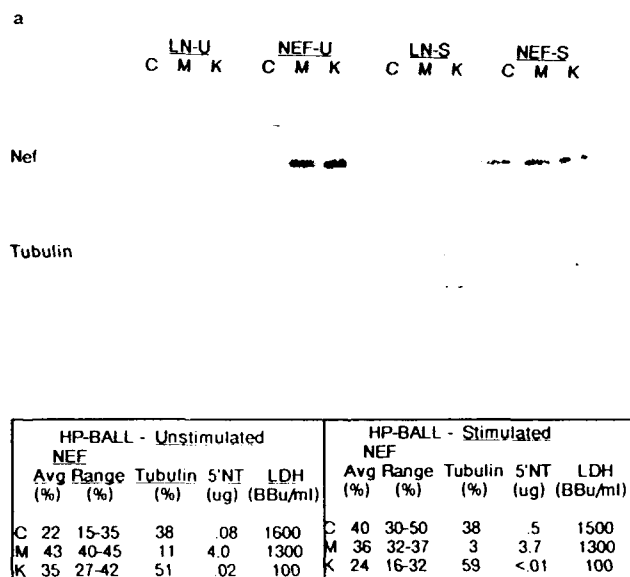


FIG. 1. Nef is associated with skeletal, membrane, and cytoplasmic cellular fractions. (a) HPBALL and (b) JURKAT cells were fractionated by ultracentrifugation into cytoplasmic (C), membrane (M), and skeletal fractions (K). HPBALL-LnefSNS1 cells (NEF-U and NEF-S) express the *nef* gene derived from the HIV-1 isolate SF2 whereas the HPBALL-LN cells (LN-U and LN-S) do not express *nef*. Cells were maintained at logarithmic growth in RPMI-1640 medium supplemented with 10% fetal bovine serum and 2 mM glutamine. Four hours prior to harvest, 7×10^7 cells were either not stimulated (U) or were stimulated (S) with $13 \mu\text{g/ml}$ PHA (Sigma) and 50 ng/ml PMA (Sigma). Cells were harvested at 1500 rpm for 5 min and were washed twice with phosphate buffered saline (PBS). Cell pellets were resuspended in hypotonic lysis buffer and allowed to swell on ice for 15 min. Cells were then dounced 20 times; nuclei and unbroken cells removed at 1500 rpm, and post nuclear supernatants fractionated by ultracentrifugation into cytoplasmic (C), membrane (M), and skeletal fractions (K) as described in the text. Fraction equivalents were analyzed by 10% SDS-PAGE and immunoblot analysis. The primary antibody was a rabbit anti Nef antiserum or a mouse anti tubulin antiserum (Boehringer Mannheim), and the secondary antibody was a horseradish peroxidase conjugated goat anti rabbit IgG (Pierce and Warriner) or alkaline phosphatase conjugated goat anti mouse IgG (Pierce and Warriner). Proteins were visualized following the addition of ECL (Amersham) or NBT/BCIP (Promega) and were quantitated by densitometry of Kodak XAR films. All bands were in the same fraction of analysis as determined by a standard curve. LDH and 5'NT assays (Sigma) were performed using equivalent amounts of each fraction as described by the manufacturer. These results are representative of three separate experiments.

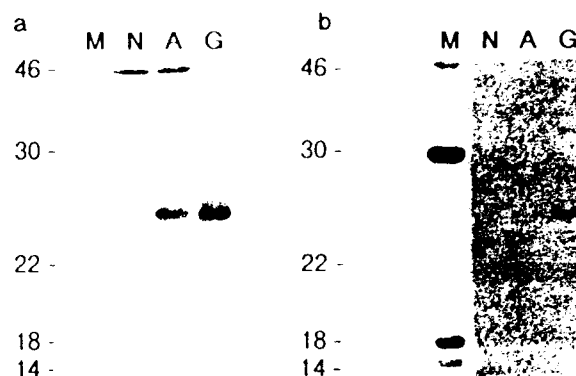


FIG. 2. Myristoylation of Nef in *E. coli*. Bacteria (strain JM101) were transformed with the NMT expression plasmid alone (N) or together with plasmids expressing the myristoylation acceptor mutant Nef (A) or the wild-type Nef (G) (22). Bacteria (2 ml) were grown to mid log phase ($A_{600} = 0.5-0.6$) and induced with $20 \mu\text{l}$ of 100 mM IPTG to induce NMT expression and $2 \mu\text{l}$ 50 mg/ml nalidixic acid to induce Nef expression for an additional 2-4 hr in the presence of $400 \mu\text{Ci}$ [^3H]myristate (56 Ci/mmol, Amersham). Bacteria were sedimented at 6000 rpm for 15 min in a JA20 rotor at 4° , washed twice with PBS, and lysed by boiling in $100 \mu\text{l}$ of 2 \times sample buffer. Equivalent volumes ($5 \mu\text{l}$) were analyzed by SDS-PAGE and (a) immunoblot as described in Fig. 1 or (b) autoradiography (22). Molecular weight markers are shown in lane M.

seen between unstimulated or stimulated HPBALL cells (Fig. 1a) or JURKAT cells (Fig. 1b). Similar results were obtained in fractionation studies using [^3H]myristate-labeled Nef (not shown). The skeletal fraction had no significant contaminating membrane or cytosolic proteins, as evidenced by the lack of significant amounts of 5' nucleotidase (5'NT, membrane marker protein) or lactate dehydrogenase (LDH, cytosolic marker protein). Tubulin was used as a marker protein for the skeletal fraction, and 51-59% of this protein was present in the skeletal fraction, 38% in the cytosolic fraction, and only 3-11% in the membrane fraction (Fig. 1a). Thus, there is very little contamination of the membrane fraction with skeletal protein.

In order to further assess the nature of the binding of Nef to the skeletal matrix, recombinant proteins expressed in *Escherichia coli* were utilized (22). To obtain myristoylated bacterial Nef proteins, we transformed bacteria with a *nef* expression plasmid and a plasmid expressing the yeast *N* myristoyl transferase (Fig. 2a, G). In this experiment, the *nef* gene was derived from a recombinant of two closely related HIV-1 strains, HXB2 and HXB3 (22). A clone with a glycine to alanine mutation in the myristoylation acceptor site was utilized to generate a nonmyristoylatable form of Nef (A). In addition, expression of yeast *N* myristoyl transferase alone (N) was used as a negative control. A 25 kDa protein was detected from both A and G expression systems, as detected by a polyclonal rabbit antiserum to Nef (Fig. 2a). The form of *nef* with glycine codon could generate a product labeled with [^3H]myristate in *E. coli*.

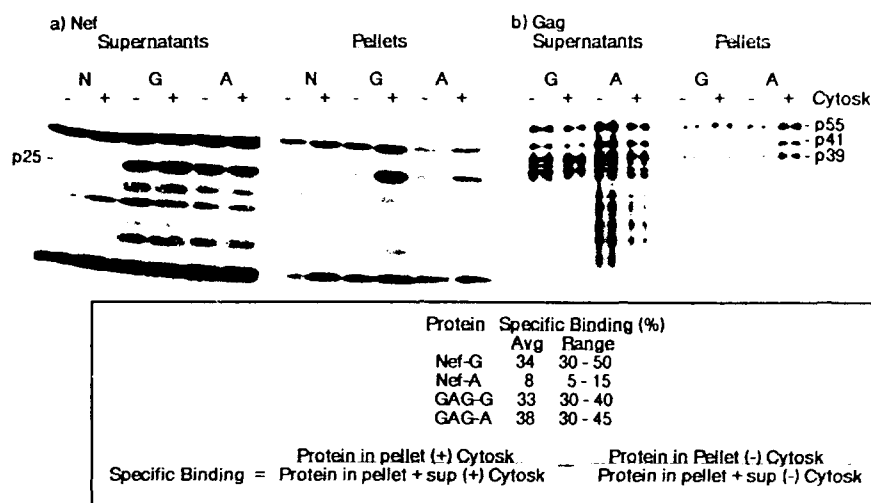


FIG. 3. Binding of Nef and Gag proteins to skeletal matrix. Bacteria (50 ml) were grown to mid-log phase, and induced with 0.5 ml 100 mM IPTG and 50 μ l 50 mg/ml nalidixic acid for an additional 2-4 hr. Extracts were prepared as described in the text from bacteria expressing NMT alone (N) or together with (a) Nef-G or Nef-A proteins or (b) Gag-G or Gag-A proteins. Binding was performed with 300 μ g of recombinant bacterial protein and 300 μ g HPBALL (LN) lymphoid skeletal proteins as described in the text at 18-20° for 30 min. The reaction mixture was separated by ultracentrifugation into a supernatant and pellet fraction, and 20 μ l of each sample was analyzed by 10% SDS-PAGE and immunoblot with the anti-Nef antibody or an anti-Gag p24 antibody as described in the legend to Fig. 1. The Nef bands were in the linear range of analysis as determined by a standard curve. Specific binding of recombinant bacterial proteins to lymphoid skeletal proteins are described at the bottom.

tected by SDS-PAGE and autoradiography. In contrast, no [3 H]myristate incorporation occurred into the mutated Nef (A) or into *E. coli* proteins (N). Also identified in the A and G Nef expressing bacteria, but not those expressing NMT alone, were small amounts of 19 and 26-kDa proteins which did not incorporate [3 H]myristate (even with a longer exposure of the autoradiogram shown in Fig. 2b).

Recombinant G and A Nef proteins were partially purified from *E. coli* after lysozyme treatment and sonication in NTENT buffer supplemented with 0.5% SDS and 0.5 M NaCl. Insoluble debris was removed by ultracentrifugation at 45,000 rpm for 3 hr at 4° in a 70 Ti rotor before and after dialysis overnight against NTENT buffer. For *in vitro* binding reactions, skeletal matrix was prepared from HPBALL (LN) cells as previously described. Binding reactions were performed with 300 μ g of partially purified bacterial proteins (in 20 μ l) and 300 μ g of insoluble skeletal proteins (in 20 μ l) in a reaction volume of 100 μ l in NTENT buffer at 18° for 30 min. Similar results were obtained in reactions performed for 5-120 min. The reaction mixtures were then treated by ultracentrifugation at 38,000 rpm for 30 min at 4° in a 70 Ti rotor. The supernatant was transferred to 100 μ l of 4 \times sample buffer (0.25 M Tris-Cl, pH 6.8, 8% SDS, 40% glycerol, 20% 2-mercaptoethanol, 0.02% bromophenol blue), and the pellet was resuspended in 200 μ l of 2 \times sample buffer. Twenty microliters of each sample was then analyzed on a 10% SDS-PAGE and analyzed with the anti-Nef antiserum using the ECL system (Amersham). The relative proportions of protein in each fraction were determined by densitometric analysis.

Representative results of a binding experiment are shown in Fig. 3a. Between 30 and 50% of the Nef-G protein (average 34%) was found associated specifically with the skeletal matrix, whereas only 5-15% of the Nef-A protein (average 8%) was in the pellet fraction. When expressed in the absence of *N*-myristoyl transferase, Nef-G and Nef-A showed no significant differences in cytoskeletal binding (not shown). The results presented in the table represent 12 independent experiments with 6 different preparations of Nef proteins and 6 different preparations of skeletal matrix.

To determine the specificity of the myristoylation-enhanced Nef binding to skeletal matrix, binding of HIV-1 Gag proteins was also analyzed (Fig. 3b). The Gag *E. coli* expression system, was similar in the Nef expression system, and used the *gag* and *pol* genes of HIV-1, which were detected with a rabbit anti-p24 polyclonal antiserum, as previously described (22). The predominant protein was 55 kDa, representing the full Gag precursor, and smaller amounts of 41- and 39-kDa proteins were also expressed which were derived from HIV-1 protease-specific scission at the p17/p24 and p24/p15 cleavage sites. In this system, 30-40% of the Gag-G protein (average 33%) bound specifically to the skeletal matrix, and 30-45% of the Gag-A protein bound the pellet components (average 38%). Thus, myristoylation did not enhance Gag association with the skeletal matrix, as it did in the case of Nef.

The nature of the skeletal matrix binding site for the myristoylated Nef protein was analyzed by saturation binding experiments and studies of reagents that prevented Nef association with the insoluble matrix (Fig. 4). With increasing amounts of Nef-G protein extract,

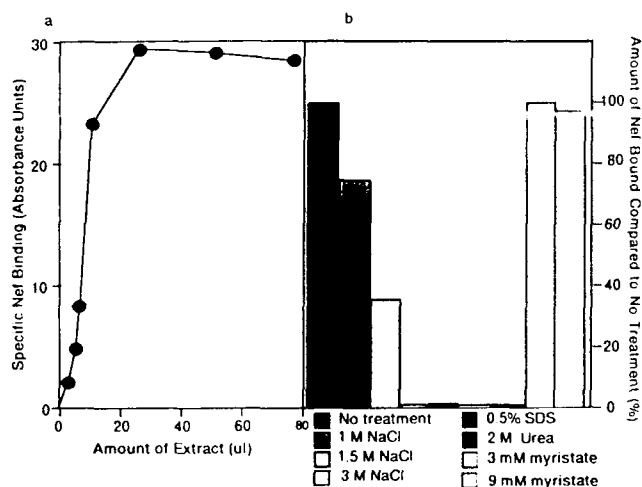


FIG. 4. Saturation binding and inhibition studies of the Nef interaction with the skeletal matrix. (a) Protein extracts from Nef-G bacteria (0–75 μ l, 0–1100 μ g) were incubated with 500 μ g HPBALL-LN skeletal proteins in 140 μ l total NTENT as described in Fig. 3 and the text. (b) Extracts from Nef-G bacteria (300 μ g) were incubated with 300 μ g HPBALL-LN skeletal proteins that were not pretreated, or were pretreated for 5 min with the specific reagents, in a total volume of 100 μ l NTENT, and fractionated as described in the legend to Fig. 3 and the text. The amount of Nef specific binding to the skeletal matrix was determined by SDS PAGE, immunoblot analysis, and densitometry as described in the legend to Fig. 3. All Nef-specific bands were quantitated in the linear range of analysis as determined by a standard curve. The residual protein contents of the cytoskeletal preparations, as determined with the Bradford reagent, after treatment with specific reagents, compared to the untreated samples were as follows: 65% after 1 M NaCl, 58% after 1.5 M NaCl, 52% after 3 M NaCl, 35% after 0.5% SDS, 72% after 2 M urea, 95% after 3 mM myristic acid, and 97% after 9 mM myristic acid treatment. These experiments were repeated on three separate occasions with similar results.

incubated with a constant amount of skeletal proteins, saturation of binding was achieved with approximately 25 μ l (300 μ g) of Nef protein extract (Fig. 4a). The amount of Nef protein in this volume of extract was 20 μ g as determined by comparing the intensity of the Nef-specific band in the bacterial extract to a standard curve using purified Nef protein (provided by the AIDS Repository). Using 25 kDa as the molecular mass of Nef, this corresponds to 5×10^{14} molecules of Nef required to saturate 500 μ g of skeletal proteins. Thus, the calculated number of skeletal binding sites for Nef is approximately 2×10^7 sites/cell.

The association of Nef with the skeletal matrix could be inhibited with progressively increasing concentrations of NaCl from 1 to 3 M (Fig. 4b). That 35–40% of Nef bound to the skeletal matrix in the presence of 1.5 M NaCl suggests a tight interaction; however, binding was almost completely inhibited with 3 M NaCl. This may suggest that ionic interactions may be critical for Nef-cytoskeletal interaction. Protein denaturants, SDS and urea, could completely prevent the binding of Nef to the cytoskeletal matrix, suggesting that the tertiary

structure of either Nef, the cytoskeletal binding site, or both is important for binding (Fig. 4b). It should be noted that the size or nature of the cytoskeletal pellet in these experiments was not significantly altered in the presence of NaCl, SDS, or urea. Though protein contents of the cytoskeleton were diminished to some extent by these treatments (Fig. 4 legend), the effects on Nef binding were significantly larger than those on the protein content. Finally, inclusion of 3 or 9 mM myristic acid did not affect the association of Nef with the skeletal fraction, suggesting that the Nef binding factor is not merely a myristic acid binding receptor. This is in agreement with the observation that myristoylated Gag did not associate with the cytoskeletal fraction to a greater extent than its nonmyristoylated counterpart (Fig. 3).

The data presented here suggests that Nef protein derived from three different HIV-1 isolates is capable of associating with the T-cell cytoskeletal matrix and that the interaction is facilitated by myristoylation. It is possible that Nef binds directly to a cytoskeletal protein such as actin or tubulin, or it is possible that Nef interacts with a protein that binds directly to the cytoskeleton. Additionally, it is possible that myristoylated Nef may bind to one cytoskeletal binding site, while nonmyristoylated Nef may bind to a distinct site. This may explain the different binding patterns of these two forms of Nef. Alternatively, both forms of Nef may bind to the same site, and myristoylation serves to promote or stabilize the interaction. The result that 50–85% of Nef associates with either the membrane or cytoskeletal fraction (Fig. 1) may reflect the fact that only 50–85% of Nef proteins within the cell are myristoylated. Within intact cells, there may be a dynamic state such that Nef may localize and translocate within cells depending upon differences in post-translational modifications, such as myristoylation, phosphorylation, or glycosylation.

Previous studies regarding the localization of Nef have reported that Nef is primarily extranuclear (13, 17) and that myristoylation is required for membrane association (4). However, these experiments do not exclude the possibility that myristoylated Nef associated with the cytoskeletal matrix as well. Other studies utilizing immunohistochemical methods suggest that Nef is present throughout the cytoplasm, but large amounts of Nef are located in a perinuclear location as well (18, 19). Additionally, Oved *et al.* report that Nef was also present in elongated cytoplasmic processes, or pseudopods (18). Interestingly, perinuclear concentration, and the presence of Nef in pseudopods may be consistent with the possibility that Nef is associated with cytoskeletal elements in that the microtubule organizing center is in a perinuclear location, and cytoskeletal components are present in pseudopods, and are important for their formation. The results presented in the

current study are consistent with the previous studies in which cytoskeletal association of Nef was not addressed.

The cell matrix includes the cytoskeleton and the membrane matrix. It is composed of a framework of fibers that maintain the structural integrity of the cell, and allow the interaction of cell surface receptors with membrane matrix and cytoskeleton.

There are several interesting parallels between Nef and two other myristoylated proteins, MARCKS and Src. MARCKS (myristoylated alanine-rich C-kinase substrate) is one member of a family of myristoylated proteins in macrophages and neutrophils (23). It binds calmodulin and regulates cell activation and mitogenesis. MARCKS colocalizes with vinculin, talin, and protein kinase C in focal contacts where the actin cytoskeleton abuts the substrate-adherent plasma membrane. Furthermore, MARCKS can bind and cross-link actin, and this binding is regulated by phosphorylation, calcium, and calmodulin. The first 14 amino acids of MARCKS, including the myristoylation acceptor site, are critical for its cytoskeletal binding.

Myristoylation-dependent binding has also been shown for the oncoprotein Src (24). In this case, a specific membrane protein of 32 kDa was found to bind myristoylated but not nonmyristoylated Src. Myristoylated peptides corresponding to the amino-terminal sequence of Src were capable of inhibiting binding to the receptor, whereas myristoylated peptides based on sequences of other proteins had no inhibitory effects. Myristoylation is critical for Src-mediated transformation, and previous work suggests that myristoylation may be critical for Nef effects as well (3).

Cytoskeletal binding has also been found for several members of the G protein family, including G α , rab 5, M α , and a homologous protein in *Dictyostelium* (25-28). Other cytoskeletal binding proteins in lymphocytes include ezrin, intercellular adhesion molecule 1 (ICAM-1), CD11a/CD18, and LSP-1 which may be phosphorylated and utilize a basic domain for cytoskeletal binding (29-32). In several cases, cytoskeletal binding has been implicated in the regulation of cell activation. Another interesting example of a cytoskeletal binding protein is the Epstein-Barr virus latent membrane protein which is important for the ability of the virus to immortalize B lymphocytes (33). Thus, Nef may have similar properties to these proteins in that it has homology to G proteins (though GTP does not bind well if at all to Nef), it is phosphorylated by protein kinase C, and it can modulate T cell activation (34).

The significance of skeletal matrix binding of Nef remains to be determined. However, recent findings have suggested that Nef disrupts signal transduction in T lymphocytes, inhibiting both NF- κ B and AP1 generation by PMA and PHA exposure (20, 21). This may be due to an effect on the T cell receptor/CD3 protein

tyrosine kinase-G protein complex, or an effect on protein kinase C activation. Cytoskeletal interaction of one or more of these components or other important cell regulators may be altered by Nef. This may account for the ability of Nef to downregulate HIV-1 transcription and to inhibit T cell activation, which may result in a reservoir of persistently infected cells with repressed virus expression.

ACKNOWLEDGMENTS

We thank Drs. Victor Garcia and Sylvie Luna for the gift of the Nef expressing eukaryotic cells, Dr. Martin Bryant for the nef expression clones, and Dr. Jeffrey Gordon for the yeast *N* myristoyl transferase expression plasmid. The recombinant Nef protein used to generate antiserum was provided by the NIAID AIDS Reagent Repository. This work was supported by contract DAMD 90-C-0125 T.M.J.N. was supported by Washington University MSTP and PHS Grant T32-HL07088-17. L.R. is an American Cancer Society Research Professor.

REFERENCES

- MYERS, G., BERZOFKY, J. A., RABSON, A. B., SMITH, T. F., and WONG STAAL, F. (Eds.). "Human Retroviruses and AIDS." Los Alamos National Laboratory, Los Alamos, NM, 1990.
- NIEDERMAN, T. M. J., HU, W., and RATNER, L. *J. Virol.* **65**, 3538-3546 (1991).
- YU, G., and FELSTED, R. L. *Virology* **187**, 46-55 (1992).
- KAMINCHIK, J., BASHAN, N., ITACH, A., SARVER, N., GORECKI, M., and PANET, A. *J. Virol.* **65**, 583-588 (1991).
- KESTLER, H. W., RINGLER, D. J., MORI, K., PANICALI, D. L., SEHGAL, P. K., DANIEL, M. D., and DESROSIERS, R. C. *Cell* **65**, 651-662 (1991).
- TERWILLIGER, E. F., SODROSKI, J. G., ROSEN, C. A., and HASELTINE, W. A. *J. Virol.* **60**, 754-760 (1986).
- LUCIW, P. A., CHENG-MAYER, C., and LEVY, J. A. *Proc. Natl. Acad. Sci. USA* **84**, 1434-1438 (1987).
- NIEDERMAN, T. M. J., THIELAN, B. J., and RATNER, L. *Proc. Natl. Acad. Sci. USA* **86**, 1128-1132 (1989).
- CHENG-MAYER, C., IANNELLO, P., SHAW, K., LUCIW, P. A., and LEVY, J. A. *Science* **246**, 1636-1637 (1989).
- TSUNETSUGU YOKOTA, Y., MATSUDA, S., MAEKAWA, M., SAITO, T., TAKEMORI, T., and TAKEBE, Y. *Virology* **191**, 960-963 (1992).
- AHMAD, N., and VENKATESAN, S. *Science* **241**, 1481-1485 (1988).
- BACHERIELE, E., ALLAMET, I., HAZAN, U., ISRAEL, B., GOUD, F., ARIZANNA-SEREDOS, and VIGNATZ, J. *J. Virol.* **64**, 3059-3067 (1990).
- HAMMES, G. P., DIXON, E. P., MAHMOUD, M., GILLEN, R. B., and GREENE, W. C. *Proc. Natl. Acad. Sci. USA* **86**, 9544-9555 (1989).
- KIM, S., DELUCHE, K., BYRN, R., GOODMAN, J., and BALTIMORE, D. *Proc. Natl. Acad. Sci. USA* **86**, 9544-9548 (1989).
- LUNA, S., CHAMBERS, J., and BURR, P. *Proc. Natl. Acad. Sci. USA* **88**, 5329-5330 (1991).
- GARCIA, J. V., and MILLER, A. D. *Virol.* **350**, 206-211 (1991).
- FRANCHINI, G., ROBERT-GUROFF, M., GORRABER, J., CHANG, N. J., and WONG STAAL, F. *Virology* **155**, 104-108 (1988).
- OYON, V., LAFRANCOIS, A., RANDE, A., FLEMMING, J. O., SHERIN, D., TAJEMER, M., JUNG, G., and FROST, A. *J. Virol.* **6**, 15-24 (1992).

19. KIENZLE, N., BACHMANN, M., MULLER, W. E. G., and MULLER-LANTZSCH, N., *Arch. Virol.* **124**, 123-132 (1992).
20. NIEDERMAN, T. M. J., GARCIA, J. V., HASTINGS, W. R., LURIA, S., and RATNER, L., *J. Virol.* **66**, 6213-6219 (1992).
21. NIEDERMAN, T. M. J., HASTINGS, W. R., LURIA, S., and RATNER, L., *Virology* **194**, 338-345 (1993).
22. BRYANT, M. L., RATNER, L., DURONIO, R. J., KISHORE, N. S., ADAMS, S. P., and GORDON, J. I., *Proc. Natl. Acad. Sci. USA* **88**, 2055-2059 (1991).
23. LI, J., and ADEREM, A., *Cell* **70**, 791-801 (1992).
24. RESH, M. D., and LING, H., *Nature* **346**, 84-86 (1990).
25. SARNDahl, E., BOKOCH, G. M., SPICHER, K., STENDAHL, O., and ANDERSSON, T., *Biochem. Soc. Trans.* **19**, 1127-1129 (1991).
26. KURZCHALIA, T. V., GORVEL, J. P., DUPREE, P., PARTON, R., KELLNER, R., HOUTHAEVE, T., GRUENBERG, J., and SIMONS, K., *J. Biol. Chem.* **267**, 18419-18423 (1992).
27. HORISBERGER, M. A., *J. Virol.* **66**, 4705-4709 (1992).
28. DE HOSTOS, E. L., BRADTKE, B., LOTTSPREICH, F., GUGGENHEIM, R., and GERISCH, G., *EMBO J.* **10**, 4097-4104 (1991).
29. CARPEN, O., PALLAI, P., SAUNTON, D. E., and SPRINGER, T. A., *J. Cell Biol.* **118**, 1223-1234 (1992).
30. PARDI, R., INVERARDI, L., RUGARLI, C., and BENDER, J. R., *J. Cell Biol.* **116**, 1211-1220 (1992).
31. EGERTON, M., BURGESS, W. H., CHEN, D., DRUKER, B. J., BRETSCHER, A., and SAMELSON, L. E., *J. Immunol.* **149**, 1847-1852 (1992).
32. JONGSTRA-BILEN, J., JANMEY, P. A., HARTWIG, J. H., GALEA, S., and JONGSTRA, J., *J. Cell Biol.* **118**, 1443-1453 (1992).
33. MARTIN, J., and SUGDEN, B., *J. Virol.* **65**, 3246-3258 (1991).
34. RATNER, L., and NIEDERMAN, T. M. J., (1993) In Srinivasan, A. and Koprowski, H., (Eds.), "Role of HIV Accessory Genes in AIDS Pathogenesis: Current Topics in Microbiology and Immunology." A. Srinivasan and Springer-Verlag, in press.

Human Immunodeficiency Virus Type 1 Viral Protein R Localization in Infected Cells and Virions

YUH-LING LU, PAUL SPEARMAN, AND LEE RATNER*

Departments of Medicine and Molecular Microbiology, Washington University School of Medicine,
St. Louis, Missouri 63110

Received 19 April 1993/Accepted 26 July 1993

The subcellular localization of human immunodeficiency virus type 1 (HIV-1) viral protein R (Vpr) was examined by subcellular fractionation. In HIV-1-infected peripheral blood mononuclear cells, Vpr was found in the nuclear and membrane fractions as well as the conditioned medium. Expression of Vpr without other HIV-1 proteins, in two different eukaryotic expression systems, demonstrated a predominant localization of Vpr in the nuclear matrix and chromatin extract fractions. Deletion of the carboxyl-terminal 19-amino-acid arginine-rich sequence impaired Vpr nuclear localization. Indirect immunofluorescence confirmed the nuclear localization of Vpr and also indicated a perinuclear location. Expression of Vpr alone did not result in export of the protein from the cell, but when coexpressed with the Gag protein, Vpr was exported and found in virus-like particles. A truncated Gag protein, missing the p6 sequence and a portion of the p9 sequence, was incapable of exporting Vpr from the cell. Regulation of Vpr localization may be important in the influence of this protein on virus replication.

The human immunodeficiency virus type 1 (HIV-1) genome is more complex than those of murine and avian retroviruses. In addition to the basic functions encoded by *gag*, *pol*, and *env*, the HIV-1 genome includes at least six additional genes with distinct regulatory roles (see references 31 and 39 for reviews). Two of these regulatory genes, *tat* and *rev*, are essential for virus gene expression. The remaining genes, *vpr*, *vpr*, *vif*, and *nef* are dispensable for virus replication in tissue culture, but mutations of these genes alter the replication properties of the virus.

HIV-1 *vpr* encodes a protein (viral protein R [Vpr]) of 96 amino acids (27). Previous studies have shown that the *vpr* products can increase the rate of replication of the virus and accelerate its cytopathic effects in T-cell lines and in peripheral blood mononuclear cells (PBMCs) (6, 8, 28, 29). Cohen and colleagues suggested that *vpr* increased gene expression from the HIV-1 promoter, as well as a wide range of other promoters, but the mechanism of this effect remains to be determined (7). *vpr* is also found in the genomes of HIV-2 and several strains of simian immunodeficiency virus (SIV) (5, 14). The activity of the HIV-2 and SIV *vpr* gene products appears to be similar to that of HIV-1 *vpr* (16, 35). Furthermore, SIV_{mac} *vpr* is important for the development of an AIDS-like disease in rhesus macaques (22).

HIV-1, HIV-2, and SIV *vpr* gene products have 26 to 36% amino acid identity (40). Certain features of the Vpr proteins among different HIV isolates are highly conserved, including the presence of a single cysteine residue at amino acid position 76 of HIV-1 Vpr, a predicted amphipathic alpha-helical loop in the N-terminal portion of the protein, and the presence of an arginine-rich carboxyl-terminal tail.

Vpr is packaged within the HIV-1 virion (6, 45). Similar findings have been reported for SIV_{mac} Vpr (44). The Vpr protein is the only regulatory product of HIV-1 found in virus particles, though the homologous *vpr* gene products of HIV-2 and SIV_{mac} are also associated with virus particles (17, 19). However, the subcellular distribution of Vpr and the mecha-

nism of incorporation into virus particles are unclear. In this study, the subcellular localization of Vpr in HIV-1-infected PBMCs and in two different *vpr* expression systems in mammalian cells was examined by subcellular fractionation and indirect immunofluorescence techniques. The role in cellular localization of the carboxyl-terminal arginine-rich sequence of Vpr was specifically studied. Lastly, the effects of Gag coexpression on Vpr export and incorporation into virus particles were examined.

MATERIALS AND METHODS

Cell lines and culture. COS-7 cells were obtained from the American Type Culture Collection and maintained in Dulbecco's modified Eagle's medium (DMEM) supplemented with 10% heat-inactivated fetal calf serum, 1 mM pyruvate, 100 U of penicillin per ml, and 100 µg of streptomycin per ml. BSC40 cells were maintained in the same medium. PBMCs were purified from normal human leukocytes by centrifugation onto Ficoll. After 3 days of stimulation with phytohemagglutinin (15 µg/ml; Sigma), PBMCs were maintained in RPMI 1640 medium supplemented with 10% heat-inactivated fetal calf serum, 4 mM glutamine, 50 U of recombinant interleukin 2 (Cetus) per ml, 100 U of penicillin per ml, and 100 µg of streptomycin per ml.

Vpr and Gag expression plasmids. HIV-1 nucleotides 5558 to 5869 (numbered according to reference 27) encompassing the pNL4-3 *vpr* gene was obtained by the polymerase chain amplification reaction, using primers AATACCAATGGAA CAAGCCCCAGAGA and GATGCTTCCAGGGATCCGCTCAGGATCTACTG. The reaction product was digested with *Nco*I and *Bam*HI and cloned into pTM3 (designated here pTM) (12, 26), to produce pTM-VPR. The *Nco*I-*Bam*HI fragment of pTM-VPR was cloned between the *Sall* and *Sac*I sites of pSRalpha (25) after blunt ending with T4 DNA polymerase, in the correct orientation (pSR-VPRs) and in the incorrect or antisense orientation (pSR-VPRa) (see Fig. 2A). The CRSE mutant clone was constructed by digestion of pNL4-3 with *Sall*, at nucleotide 5786, and blunt ending with the Klenow fragment of DNA polymerase I. It was then cloned

* Corresponding author.

into the pTM vector by the strategy used to construct pTM-VPR.

An *NcoI*-*NcoI* fragment from plasmid pGG1 (3, 32), containing nucleotides 789 to 5674, was cloned into the *NcoI* site of plasmid pTM3, to produce plasmid pTM-GAG-POL. This clone contains the *gag* and *pol* open reading frames. Expression of the *pol* gene was abrogated by frameshift mutation at the *BclI* site at nucleotide 2428 in the 5' portion of *pol* to produce pTM-GAG. Plasmid pTM-GAG(p41) was constructed from pTM-GAG-POL by frameshift mutation at the *ApaI* site at nucleotide 2005, using T4 DNA polymerase I. This results in a termination codon at nucleotide 2058 after the first Cys-His box coding region of p9.

Vpr and Gag p24 antisera. A New Zealand White rabbit was inoculated with complete Freund's adjuvant containing 200 µg of Vpr protein, synthesized according to the sequence of HIV-1 strain LAI and kindly provided by H. Gras-Masse (13). Booster doses of 200 µg of Vpr in incomplete Freund's adjuvant were given at 3, 6, 9, and 18 weeks after the initial inoculation. A New Zealand White rabbit was inoculated with complete Freund's adjuvant containing 100 µg of recombinant p24 protein (provided by American Biotechnology through the NIH AIDS Research and Reference Reagent Program), and 100-µg booster doses were given 2 and 4 weeks later.

Virus infection. HIV-1 virus stocks were generated by transfection of 60% confluent 10-cm-diameter COS-7 plates with 10 µg of recombinant proviral clone NLHADA(GG) (41) and 2 µg of pCV1 (*tat* expression vector [1]) by the calcium phosphate precipitation method, followed 5 h later by 10% dimethyl sulfoxide shock for 2 min. The cells were washed twice with phosphate-buffered saline (PBS) before refeeding with 10 ml of fresh medium. Culture supernatants were harvested after 48 h and filtered (0.2-µm-pore-size Millipore filter). Five milliliters of culture supernatant was used to infect 5×10^7 PBMCs. Virus replication was monitored by determination of reverse transcriptase activity (30). PBMCs (10^7) were labeled for 20 h in 2 ml of leucine-free RPMI 1640 medium containing 200 µCi of [4,5- 3 H]leucine and fractionated as described below. Mock-infected cultures were exposed to 5 ml of filtered culture supernatants from untransfected COS-7 cells.

Transfection and radiolabeling of COS-7 cells. COS-7 cells were grown to 60% confluence on 10-cm-diameter culture dishes and transfected with 15 µg of pSR-VPRs or pSR-VPRa by lipofection as recommended by GIBCO. Briefly, 15 µl of Lipofectin (GIBCO) was mixed with 3 ml of Opti-MEM 1 reduced-serum medium (GIBCO), and then 15 µg of DNA was added. The mixture was allowed to incubate at room temperature for 10 min before addition of the cells. Forty-eight hours after transfection, the cells were labeled with 4 ml of leucine-free DMEM containing 100 µCi of [4,5- 3 H]leucine per ml for 40 h.

Infection-transfection protocol for the vaccinia virus expression system. BSC40 cells were grown to 90% confluence on 10-cm-diameter plates, infected for 1 h at 37°C with vH7-3 (12, 26) at a multiplicity of infection of 10, and transfected with pTM vectors by the lipofectin transfection method. Four hours after transfection, the cells were labeled for 20 h with 3 ml of leucine-free DMEM containing 100 µCi of [4,5- 3 H]leucine per ml.

Subcellular fractionation. Labeled cells were fractionated into membrane, cytosolic, postnuclear, and nuclear fractions as previously described (23), with minor modifications. Nuclei were further fractionated into nucleoplasm, chromatin extract, and nuclear matrix as described by Staufenbiel and Deppert (37). Cells were washed with ice-cold PBS and scraped in PBS.

The cell pellet volume was measured and resuspended in 10 volumes of Dounce buffer (10 mM Tris-HCl [pH 7.5], 1.5 mM MgCl₂, 10 mM KCl, 0.2 mM phenylmethylsulfonyl fluoride [PMSF], 0.5 mM dithiothreitol). The cells were allowed to swell on ice for 10 min before disruption with 20 to 25 strokes of a Dounce homogenizer. A small aliquot was saved and mixed with an equal volume of 0.4% (wt/vol) trypan blue in PBS to examine cell disruption under phase microscopy. Dounce homogenization was continued until >99% cells were disrupted. The homogenate was centrifuged at 1,500 rpm for 10 min in a Beckman GS-6 rotor to generate the supernatant containing both the membrane and cytosolic fractions and the nuclear pellet.

The nuclear pellet was subsequently extracted by four steps. First, the nuclear pellet was resuspended in buffer A (10 mM *N*-2-hydroxyethylpiperazine-*N'*-2-ethanesulfonic acid [HEPES-KOH; pH 7.4], 0.25 M sucrose, 0.2 mM PMSF, 0.5 mM dithiothreitol) supplemented with 0.1% (vol/vol) Triton X-100 and then incubated for 15 min on ice. The nuclei were pelleted at 1,500 rpm for 10 min, and the supernatant was designated the postnuclear wash fraction. Second, the pellet was resuspended in buffer A supplemented with 0.5% Nonidet P-40 and incubated for 30 min on ice. The nuclei were pelleted again at 1,500 rpm for 10 min, and the supernatant was designated the nucleoplasmic fraction. The latter procedure was repeated twice, and the supernatants were pooled. Third, the Nonidet P-40-extracted nuclear pellet was subjected to DNase I digestion (1% [vol/vol] Triton X-100, 1.5 mM MgCl₂, 0.2 mM PMSF, and 50 µg of DNase I [Sigma] per ml in PBS) for 15 min at 37°C. Then an equal volume of 4 M NaCl was added, and incubation was continued for 30 min at 4°C. The sample was then subjected to centrifugation at 2,500 rpm for 10 min. The supernatant was designated the chromatin extract, and the pellet was resuspended in radioimmunoprecipitation assay (RIPA) buffer (1% [vol/vol] Triton X-100, 0.5% [wt/vol] deoxycholate, 0.1% [wt/vol] sodium dodecyl sulfate [SDS], and 0.2 mM PMSF in PBS) for 30 min on ice. The insoluble portion was removed by centrifugation at 1,000 rpm for 15 min. The supernatant was designated the nuclear matrix. The purity of the nuclei was examined by using a control cytosolic protein, β-galactosidase, expressed in the same cells by transfection of a cDNA expression clone. More than 98% of the β-galactosidase activity was found in the cytosol, as measured by enzymatic assay. Only 1.4% of the β-galactosidase activity was detected in the postnuclear wash fraction. No detectable activity was found in the purified nuclei.

For the membrane and cytosolic fractions, the salt concentration was adjusted to 0.15 M NaCl and then the preparations were fractionated by ultracentrifugation at 100,000 × *g* for 30 min. The supernatant was designated the cytosolic fraction. The pellet was washed with 1 M NaCl in PBS for 30 min on ice, and ultracentrifugation was repeated. The supernatant was designated the membrane wash fraction, and the membrane pellet was resuspended in RIPA buffer.

Immunoprecipitation. Equivalent proportions (volume/volume) of each of the subcellular fractions were precipitated overnight with 10% trichloroacetic acid at 4°C. The resulting pellets were washed in 70% ethanol, solubilized in sample buffer (0.125 M Tris-HCl [pH 6.8], 20% glycerol, 10% [vol/vol] 2-mercaptoethanol, 4% [wt/vol] SDS). An aliquot was taken for scintillation counting to determine relative labeled protein content.

Equivalent proportions (volume/volume) of each of the subcellular fractions were adjusted to 500 µl of RIPA buffer. Immunoprecipitation was performed by the addition to 500 µl of each fraction > µl of anti-Vpr antiserum or 5 µl of anti-Gag

antiserum. Incubation was continued overnight at 4°C. Twenty microliters of protein A-Sepharose beads (50% [vol/vol] in PBS) was added, and the mixture was incubated for 120 min at 4°C. Immunoprecipitates were collected at 500 × g for 3 min at room temperature and washed three times with RIPA buffer. The beads were resuspended in 30 µl of sample buffer. Samples were treated at 100°C for 10 min before SDS-12% polyacrylamide gel electrophoresis (PAGE), fixation for 30 min in 25% isopropanol-10% acetic acid, treatment with Amplify (Amersham), and autoradiography were performed. Band intensities were determined by densitometry.

Immunofluorescence. BSC40 cells (10⁴) were plated on eight-well Lab-Tek chamber slides overnight. The cells were infected with vTF7-3 and transfected as described above. The cells were fixed with 2.5% (wt/vol) glutaraldehyde for 15 min and permeabilized with 0.2% (vol/vol) Triton X-100 for 6 min at room temperature. The cells were then blocked for nonspecific binding of immunoglobulin by incubation for 30 min with PBS containing 5% (wt/vol) nonfat dry milk and 0.1% (vol/vol) Tween 20. Slides were then incubated with rabbit anti-Vpr antibody (1:100 in Tween buffer [PBS with 0.5% Tween 20 and 1% bovine serum albumin]) and mouse monoclonal antihistone antibody (1:500 in Tween buffer; Chemicon) for 1 h at room temperature. The cells were washed several times with 0.3% (vol/vol) Triton X-100 in PBS and incubated at 4°C for 60 min with fluorescein isothiocyanate (FITC)-conjugated goat anti-rabbit immunoglobulin G to detect Vpr and rhodamine-conjugated goat anti-mouse immunoglobulin G to detect histones. The slides were washed extensively with PBS and mounted in Aqua mount solution (Lerner Lab) containing 2.5% 1,4-diazobicyclo-[2,2,2]-octane (Sigma) to prevent photobleaching of the FITC signal. Slide preparations were examined on a Nikon fluorescence microscope equipped with appropriate filters and a microflex UFX camera system. Photographs were prepared by using Kodak T-MAX film, push processed to ASA 3200.

Sucrose gradients. BSC40 cells were infected, transfected, and labeled with [³H]leucine as described above. Cellular debris was removed from the conditioned medium by centrifugation at 2,500 rpm for 15 min in a Beckman GS-6 rotor. Particles were concentrated by sedimentation through a 20% sucrose cushion prepared in PBS at 28,000 rpm for 90 min at 4°C in an SW28.1 rotor. Particles were resuspended in 200 µl of PBS, layered on a linear 20 to 60% sucrose gradient in PBS, and centrifuged in an SW28.1 rotor at 20,000 rpm for 16 h at 4°C. Fractions were collected from the top of the tube.

RESULTS

Localization of Vpr in HIV-1-infected PBMCs. To examine the intracellular localization of Vpr, PBMCs, a natural target cell population, were chosen for HIV-1 infection. HIV-1 strain NLHX ADA(GG) was chosen since it encodes a functional 96-amino-acid form of Vpr identical in amino acid sequence to that encoded by NL4-3 (27, 29, 42). Nine days after infection, the cells were labeled for 20 h with [³H]leucine, lysed by Dounce homogenization, and then fractionated into nuclear, cytosolic, and membrane fractions by differential centrifugation. Each fraction was immunoprecipitated with a polyclonal rabbit anti-Vpr antiserum and subjected to SDS-PAGE (Fig. 1). A Vpr-specific protein of 14 kDa was detected in NLHX ADA(GG)-infected cells and conditioned medium but not in mock-infected cultures. This protein was not immunoprecipitated with a control antiserum obtained from the prebleed serum of the same rabbit prior to inoculation with the synthetic

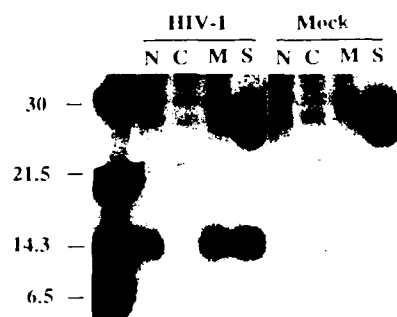


FIG. 1. Localization in PBMCs of Vpr expressed from infectious virus. PBMCs were infected for 9 days with HIV-1 strain NLHX ADA(GG) or were mock infected. The cells were labeled with [³H]leucine, the medium was harvested (S), and the cells were fractionated into nuclear (N), cytosolic (C), and membrane (M) fractions as described in Materials and Methods. Equivalent portions of each fraction were immunoprecipitated with the anti-Vpr antiserum and analyzed by SDS-PAGE. Molecular mass markers are shown at the left in kilodaltons.

Vpr used for production of the anti-Vpr antiserum (not shown).

The majority of Vpr was found in the culture supernatant, consistent with previous reports that Vpr is virion associated (6, 45). Intracellular Vpr was found in both nuclear (26%) and membrane (20%) fractions. Vpr in the nuclear fraction was not due to contamination with unbroken cells, which made up <1% of the total cell population used in the fractionation experiments. Less than 4% of the Vpr was found in the cytosolic fraction. Approximately 50% of the labeled Vpr was found in the conditioned medium.

Expression and localization of Vpr in mammalian cells. To study the cellular localization of Vpr without the effect of other HIV-1 components, the NLHXADA(GG) *vpr* gene was cloned into a simian virus 40 (SV40)-based vector system, pSRalpha, in both the correct (pSR-VPRs) and incorrect or antisense (pSR-VPRa) orientations (Fig. 2A). The expression plasmid contains both the SV40 early enhancer (SV40-ori) and a human T-cell leukemia virus type I (HTLV-I) promoter with R and U5 elements of the HTLV-I long terminal repeat. This expression plasmid has previously been reported to achieve high levels of expression of a number of different lymphokine cDNAs in a variety of cell types (38) and to facilitate the expression of HIV-2 *vpr* in COS-1 cells (21).

pSR-VPRs and pSR-VPRa were transfected into COS-7 cells, and the cells were labeled with [³H]leucine and separated into membrane, membrane wash, cytosolic, and nuclear fractions. Membranes loosely associated with nuclei were removed by a wash with 0.1% Triton X-100 and were designated the postnuclear wash. Soluble nucleoplasmic proteins were extracted with two successive washes in 0.5% Nonidet P-40, which permeabilizes the nuclear membrane (2). This method has previously been demonstrated to preserve overall nuclear and nucleolar architecture (33). The chromatin fraction was obtained by digestion of the resultant insoluble nuclear fraction with DNase I and by a subsequent wash in a high salt buffer. This fraction contained all of the major histone proteins found in intact nuclei (not shown). The salt- and detergent-insoluble fraction was pelleted to yield the nuclear matrix fraction, which was solubilized in RIPA buffer.

The partition of Vpr during fractionation was examined by immunoprecipitation with the anti-Vpr antibody, SDS-PAGE, and densitometric quantitation (Fig. 2B). The chromatin frac-

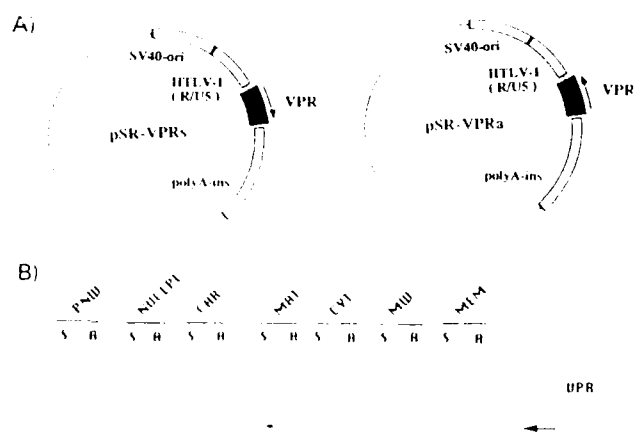


FIG. 2. Localization in COS-7 cells of Vpr expressed from pSR. (A) Vpr sense (pSR-VPRs) and antisense (pSR-VPRa) expression plasmids, which include a transcriptional enhancer (SV40-ori), a transcriptional promoter (HTLV-I long terminal repeat [R-U5]), and a polyadenylation insertion sequence (polyA-ins). (B) Subcellular fractionation of Vpr expressed in transfected and [3 H]leucine-labeled COS-7 cells from pSV-VPRs (S) and pSR-VPRa (A) in postnuclear wash (PNW), nucleoplasm (NUCLPL), chromatin (CHR), nuclear matrix (MAT), cytosol (CYT), membrane wash (MW), and membranes (MEM). Equivalent amounts of each fraction were immunoprecipitated with the anti-Vpr antiserum and analyzed by SDS-PAGE. The electrophoretic position of Vpr is shown by an arrow at the right.

tion included 17% of the intracellular labeled proteins and 44% of the total Vpr. The nuclear matrix included 1% of the intracellular labeled proteins and 56% of the total Vpr. Less than 1% of the total Vpr was found in the other cellular fractions.

Truncation of the C terminus of Vpr impairs nuclear localization. Most nuclear localization signals consist of a short stretch of positively charged amino acids (15). Interestingly, the C terminus of Vpr contains a high proportion of positively charged amino acids, including 7 arginine residues among the C-terminal 20 amino acids (Fig. 3A). To characterize the role of this C-terminal sequence, a vaccinia virus expression system was used to achieve high-level and rapid expression of Vpr. The NLHXADA(GG) *vpr* gene was cloned into pTM3, a plasmid utilizing a T7 promoter for heterologous gene expression. This plasmid was designated pTM-VPR. A carboxyl-terminal truncation mutant of pTM-VPR, pTM-CRST, was constructed by frameshift mutation at the *SaII* site. A recombinant vaccinia virus, vTF7-3, which encodes T7 RNA polymerase was used for expression in mammalian cells.

BSC40 cells were infected with vTF7-3 and transfected with pTM-VPR or pTM-CRST. Cells were labeled with [3 H]leucine, cell supernatants were harvested, and disrupted cells were fractionated into membrane, membrane wash, cytosolic, and postnuclear wash fractions and various nuclear fractions (nucleoplasmic proteins, chromatin, and nuclear matrix). Equivalent amounts of each fraction were immunoprecipitated with the anti-Vpr antiserum and analyzed by SDS-PAGE (Fig. 3B), and band intensities were quantitated by laser densitometry (Fig. 3C). The predominant Vpr product expressed from pTM-VPR had an electrophoretic mobility of a 14-kDa protein, with a minor band with a mobility of a 13-kDa protein. Vpr expressed from pTM-CRST electrophoresed as a 12-kDa

protein, consistent with the removal of 17 amino acids from the carboxyl terminus.

Eighty-four percent of pTM-VPR-expressed Vpr was found in nuclear fractions, primarily the nuclear matrix and chromatin fractions (Fig. 3B [left] and C). This result is in agreement with the fractionation data with pSR-VPR-expressed Vpr (Fig. 2). Eight percent of pTM-VPR-expressed Vpr was tightly associated with the membrane fraction (Fig. 3B and C, MEM). The possible discrepancy in the amount of membrane association of Vpr expressed with the vaccinia virus expression system compared with the data obtained with pSR-VPR (Fig. 2) may be related to the significantly higher level of expression of Vpr with the vaccinia virus expression system than with the SV40 plasmid expression system. Only 4% of Vpr was found in the cytosol (Fig. 3B and C, CYT), and no detectable Vpr was released from cells into the cell supernatant.

Deletion of the arginine-rich C terminus of Vpr resulted in a dramatic shift of Vpr cellular localization (Fig. 3B [right] and C). Only 25% of the truncated Vpr was retained in the nuclear fraction. Furthermore, the distribution in nuclear fractions of pTM-CRST product was distinctly different from that of pTM-VPR, with the majority of the truncated protein in the nucleoplasm. Twenty-four percent of the pTM-CRST protein was in the postnuclear wash, compared with 3% of the pTM-VPR product. Thirty-eight percent of the mutant Vpr was found in the cytosol, compared with 4% of the parental Vpr. Similar amounts of pTM-CRST and pTM-VPR products were bound to membranes.

Indirect immunofluorescence localization of Vpr. Subcellular fractionation experiments indicated predominant localization of Vpr in the nucleus. To confirm these results, indirect immunofluorescence was performed with fixed cells. BSC40 cells were infected with vTF7-3 and then transfected with pTM-VPR or pTM. Vpr was detected by anti-Vpr rabbit antibody and visualized with FITC-conjugated anti-rabbit antibody. Intense immunofluorescence was observed in the majority of cells transfected with pTM-VPR (Fig. 4A, left), but no fluorescence was observed in cells transfected with the vector pTM alone (Fig. 4A, right) or if preimmune serum was used (not shown).

Four types of staining patterns were observed in four independent experiments in which 50 cells were randomly selected and enumerated. Sixty-two percent of the cells showed a diffuse nuclear and focal perinuclear staining pattern (Fig. 4B, middle). The nucleus is visualized by phase-contrast microscopy (Fig. 4B, left) and mouse antihistone and rhodamine-conjugated anti-mouse antibody (Fig. 4B, right). Twenty-seven percent of the cells showed focal perinuclear staining only. Six percent of the cells had diffuse perinuclear staining with intense immunofluorescence surrounding the nucleus. Four percent of the cells showed only diffuse nuclear staining.

Influence of Gag protein on Vpr export and virion incorporation. In HIV-1-infected cells, Vpr was found to be exported into the medium in virus particles (Fig. 1) (6, 45), though no export was found when Vpr was expressed in the absence of other virion components (Fig. 3). To assess the requirements for export, Vpr was coexpressed with the HIV-1 Gag p55 precursor protein by using plasmid pTM-GAG. BSC40 cells were infected with vTF7-3 and transfected with pTM-VPR alone, pTM-GAG alone, or both plasmids. No differences were noted in the electrophoretic mobility or quantity of the 14-kDa product in the cell lysates with pTM-VPR expressed in the presence or absence of pTM-GAG (Fig. 5A, left). The pTM-GAG product was primarily a 55-kDa protein, with smaller amounts of 43- and 41-kDa products. The latter proteins were found to be Gag proteins, since they did not react with a

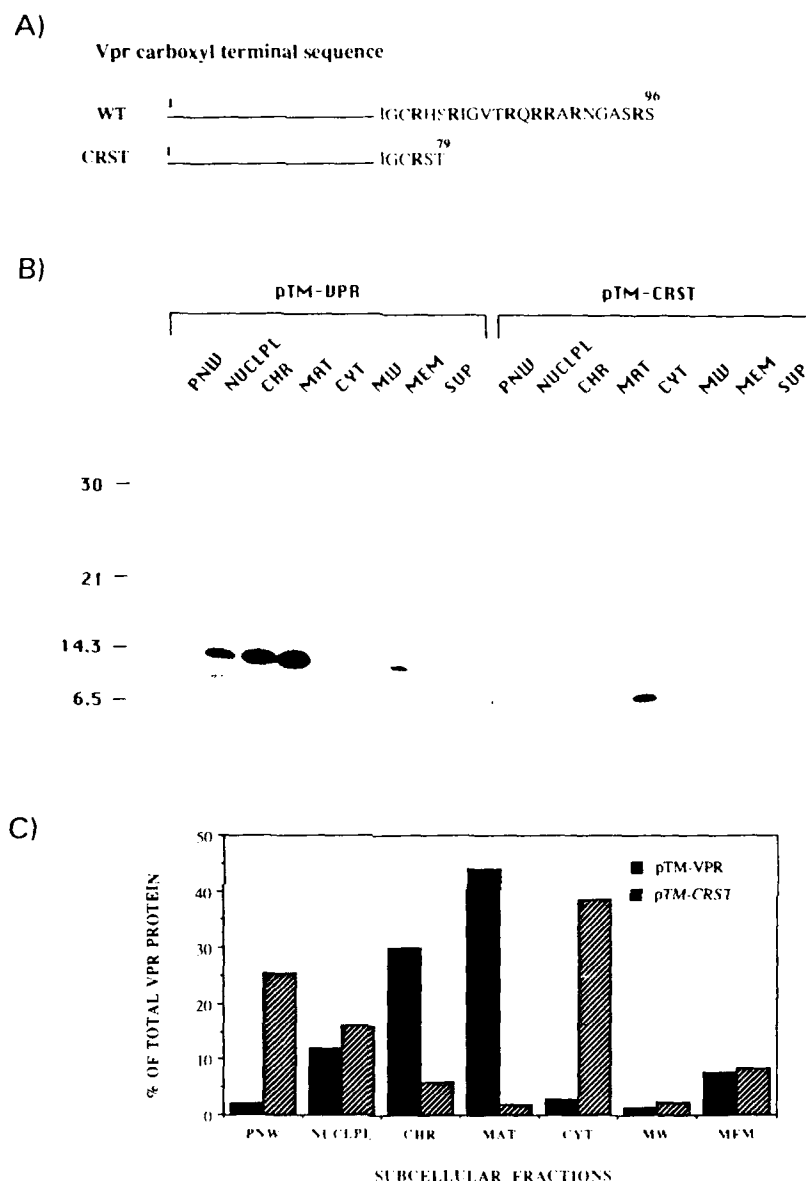


FIG. 3. Subcellular distribution of vaccinia virus-expressed parental Vpr and carboxyl-terminal truncation mutant CRST in BSC40 cells. (A) Schematic drawing of the Vpr protein, indicating the carboxyl-terminal arginine-rich sequence of the wild type (WT) and of the truncation mutant, CRST. (B) Vpr expressed from pTM3 in vTF7-3-infected cells. Cells were labeled with [3 H]leucine and fractionated into postnuclear wash (PNW), nucleoplasm (NUCLEPL), chromatin (CHR), nuclear matrix (MAT), cytosol (CYT), membrane wash (MW), membranes (MEM), and cellular supernatant (SUP). Molecular mass markers are shown at the left in kilodaltons. (C) Proportion of VPR in each subcellular fraction as determined by laser densitometry from pTM-VPR (solid bars) or pTM-CRST (hatched bars)-transfected cells.

preimmune serum or the anti-Vpr antibody (not shown). These smaller proteins may represent nonspecific cleavage products, products from initiation at a downstream AUG codon, or premature translational termination. No effects on Gag protein expression were noted with coexpression of Vpr.

Expression of pTM-VPR alone did not result in export in the cell supernatant (Fig. 5A, right). Expression of pTM-GAG resulted in the 55-kDa product in the cell supernatant. Coexpression of pTM-GAG with pTM-VPR promoted the export of Vpr into the cell supernatant.

To determine whether the viral proteins released into the cell supernatant were associated with particles, sucrose gradient analysis was performed (Fig. 6). Particles were first con-

centrated from the cell supernatant samples by centrifugation through a 20% sucrose cushion. The resultant particulate material was resuspended and analyzed on a linear 20 to 60% sucrose gradient. Each fraction was concentrated with 10% trichloroacetic acid and analyzed by SDS-PAGE. No particle-associated protein was found from cells transfected with pTM-VPR alone (Fig. 6A). Expression of pTM-GAG alone resulted in particle-associated Gag protein banding in fractions 10 and 11, at a density of 1.16 to 1.17 g/ml (Fig. 6B). Expression of pTM-GAG together with pTM-VPR resulted in cosedimentation of both Vpr and Gag in fractions 11 and 12, at a density of 1.16 to 1.17 g/ml (Fig. 6C).

Vpr packaging was also assessed with a clone expressing a

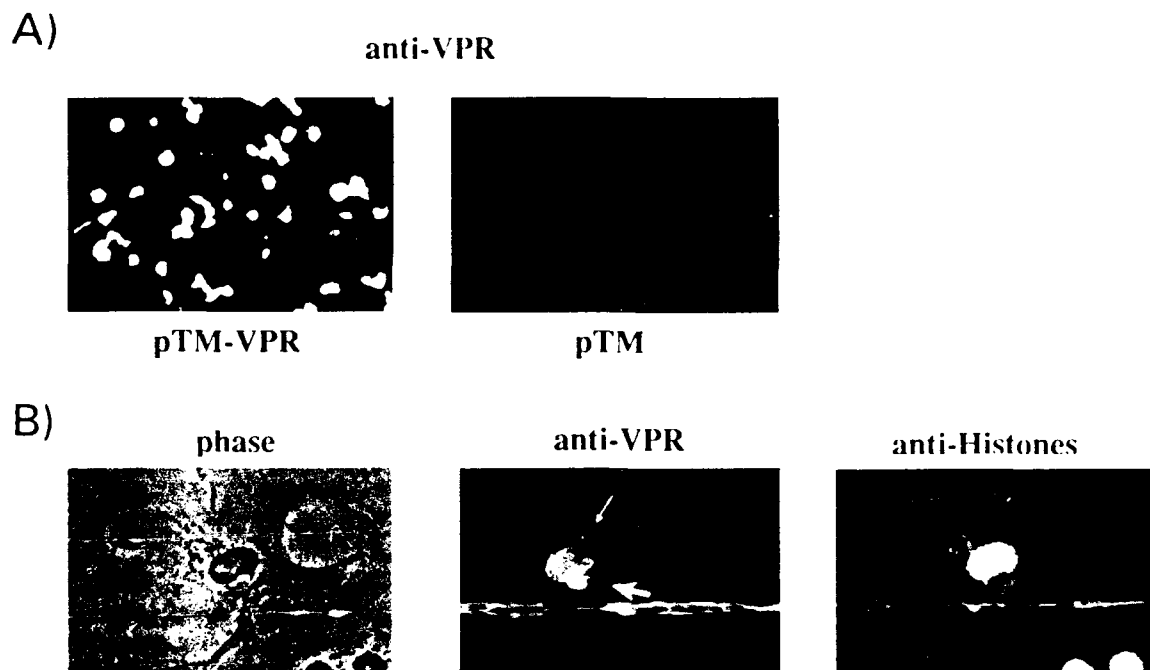


FIG. 4. Immunofluorescence localization of Vpr in BSC40 cells. (A) pTM-VPR (left)- or pTM (right)-transfected vTI 7-3 infected cells were incubated with the anti-Vpr antiserum and an FITC-conjugated goat anti-rabbit immunoglobulin. Magnification, $\times 188$. (B) Higher magnification ($\times 752$) by phase-contrast microscopy (left) and fluorescence microscopy (middle and right) of a representative cell incubated with anti-Vpr antiserum and FITC-conjugated goat anti-rabbit immunoglobulin (middle; filter with excitation range of 450 to 490 nm and emission range of 520 to 560 nm) and antihistone antiserum and rhodamine-conjugated goat anti-mouse immunoglobulin (right; filter with excitation range of 510 to 560 nm and emission range of >590 nm). Diffuse nuclear (thin arrow) and focal perinuclear staining (thick arrow) are indicated in the middle panel.

truncated form of the Gag precursor protein, pTM-GAG(p41), in which all of the amino acids following the first Cys-His box of NC as well as the C-terminal p6 coding sequence were removed. This construct has been shown to produce virus-like particles in the vaccinia virus infection-transfection system in a manner similar to that of pTM-GAG (not shown). When coexpressed with pTM-VPR, p41 appeared in the supernatant but did not result in the export of Vpr from the cells (Fig. 5B). The failure to detect Vpr in the cell supernatant was due to the absence of Vpr export rather than to the lower quantity of p41 Gag particles produced, since no Vpr was detected, even after overexposure of the autoradiogram shown in Fig. 5B. In contrast, in the same experiment, production of p55 from pTM-GAG resulted in significant export of Vpr.

DISCUSSION

Localization of Vpr in the nucleus. In this study, we used three different expression systems to provide evidence for the localization of a significant proportion of Vpr in the nucleus, as demonstrated by subcellular fractionation techniques. In HIV-1-infected PBMCs, 26% of the expressed Vpr was found in the nucleus (Fig. 1). In contrast, when Vpr was expressed in the absence of other viral components by using an SV40 expression plasmid, almost all of the protein was found in the nucleus (Fig. 2). Similar results were obtained with the vaccinia virus expression system, in which case 84% of the Vpr was found in the nucleus (Fig. 3). Results of the indirect immunofluorescence experiments support the results obtained by using subcellular fractionation techniques, indicating nuclear staining in 66% of Vpr-expressing cells (Fig. 4; see Results).

Further fractionation of the isolated nuclei provides additional evidence for Vpr localization in the nucleus rather than

in membranes loosely associated with the nuclear membranes. These experiments identified the predominant association of Vpr with the chromatin and nuclear matrix fractions (Fig. 2 and 3). The association of Vpr with the nuclear matrix is unlikely to be spurious, since it is resistant to Nonidet P-40, DNase, and high-salt extraction procedures. Although the role of the nuclear matrix in transcriptional regulation is unclear, several studies have indicated that it may play an important role. The nuclear matrix has been reported to have a role in mRNA transcription and processing via its involvement in attachment and/or association with newly transcribed mRNA (20), ribonucleoprotein particles (11), and pre-mRNA splicing machinery (36, 46). Several gene products, characterized for their ability to promote oncogenic transformation, are also associated with the nuclear matrix. These include the large T antigen of polyomavirus (4), *myc* gene products (9), the adenovirus E1A protein (10), and the Tax protein of HTLV-I (43). The presence of Vpr in the nuclear matrix might indicate a role in *trans* activation of viral gene expression or RNA processing. This is consistent with a report by Cohen and colleagues suggested that Vpr may serve as a *trans* activator of HIV-1 gene expression as well as a *trans* activator of other genes (7). However, the mechanism of this effect and its relevance to Vpr action during virus replication remain unclear. Alternatively, Vpr association with the nuclear matrix may affect host cell gene expression. This view is consistent with a recent report that Vpr induces muscle cell differentiation (24).

Though Vpr lacks a classical nuclear localization signal (15), the carboxyl terminal portion of the protein is rich in basic amino acids. A truncation mutation which removes the carboxyl terminal 19 amino acids was found to impair Vpr localiza-

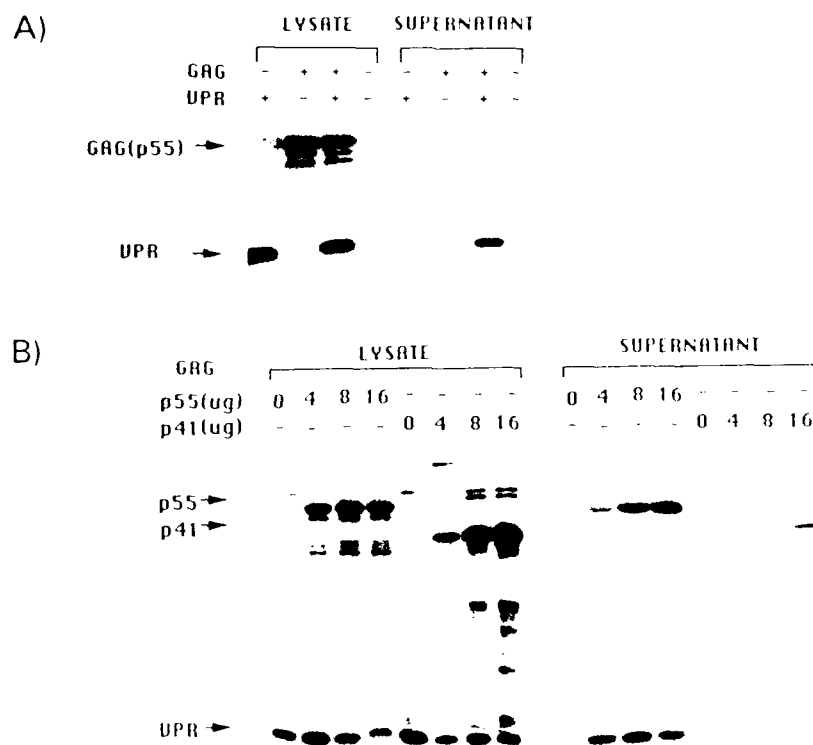


FIG. 5. Influence of Gag expression on Vpr localization. (A) BSC40 cells (10^6) were grown on 60-mm-diameter plates overnight and then infected with vTF7-3 and transfected with 7.5 μ g of pTM-VPR (VPR) and/or 7.5 μ g of pTM-GAG (GAG). The negative control cells were transfected with 15 μ g of pTM vector. The cells were labeled with 100 μ Ci of [3 H]leucine per ml for 16 h, scraped in PBS, and resuspended in RIPA buffer. The cell lysates and cell supernatant fractions were immunoprecipitated with both the anti-Vpr and anti-Gag antisera and analyzed by SDS-PAGE. The electrophoretic positions of Gag and Vpr are shown at the left. (B) BSC40 cells (0.3×10^6) on 35-mm-diameter plates were infected and transfected with 2 μ g of pTM-VPR and 0, 4, 8, or 16 μ g of pTM-GAG(p55) or pTM-GAG(p41), as indicated at the top. The cells were labeled and analyzed as described above.

tion in the nucleus (Fig. 3). Furthermore, the distribution of the small proportion of truncated Vpr found in the nucleus was distinctly different from that of full-length Vpr, with the truncated Vpr localized predominantly in the nucleoplasm and very little Vpr in the nuclear matrix or chromatin fractions. It is possible that truncation of the carboxyl-terminal portion of Vpr alters the conformation of the molecule. Alternatively, it is possible that the carboxyl-terminal arginine-rich sequence serves as at least part of a nuclear localization signal. This view is supported by our preliminary observations that attachment of the C-terminal 19 amino-acid Vpr sequence onto β -galactosidase directed this protein to the nucleus (not shown).

Previous studies with lymphoid cells had indicated an important functional role for the C-terminal Vpr sequence (29). Therefore, these findings are consistent with an important role for Vpr localization in the nucleus for HIV-1 replication.

Membrane-associated Vpr. Though very little Vpr could be identified in the cytosol, a small proportion was consistently associated with the membrane fraction. This observation is in agreement with findings of Sato and colleagues (34). In HIV-1-infected PBMCs, 20% of Vpr was found in the membrane fraction (Fig. 1), whereas with the vaccinia virus expression form of the protein, 8% was found in the membrane (Fig. 3B and C). The indirect immunofluorescence experiments also suggested that some Vpr is found at an extranuclear site, but

closely associated with the nucleus (Fig. 4; see Results). The latter site may represent intracellular membranes, possibly with either the endoplasmic reticulum or Golgi apparatus. However, a Golgi location for Vpr is unlikely, since brefeldin A treatment did not change Vpr localization (not shown). The nature and significance of membrane localization of VPR require further analysis.

VPR export from cells and incorporation into virus particles. Several previous studies have demonstrated that HIV- and SIV-expressed Vpr is incorporated into virus particles (6, 44, 45). This finding is in agreement with our observation that 50% of Vpr expressed in HIV-1-infected PBMCs is exported from the cells (Fig. 1). Vpr expression in the absence of other viral components resulted in no detectable export (Fig. 3 and 5). However, coexpression with the Gag p55 precursor protein resulted in export of VPR from the transfected cells (Fig. 5) and incorporation into virus-like particles (Fig. 6). Thus, Vpr incorporation into virus particles is independent of viral envelope incorporation. This finding suggests that Vpr associates directly or indirectly with a portion of the Gag precursor protein. The finding that the p41 truncation form of Gag is unable to package Vpr suggests the possibility of an interaction between either the p9 nucleocapsid protein or the p6/p7/p8/p9 protein and Vpr.

Although the significance of Vpr incorporation into viruses

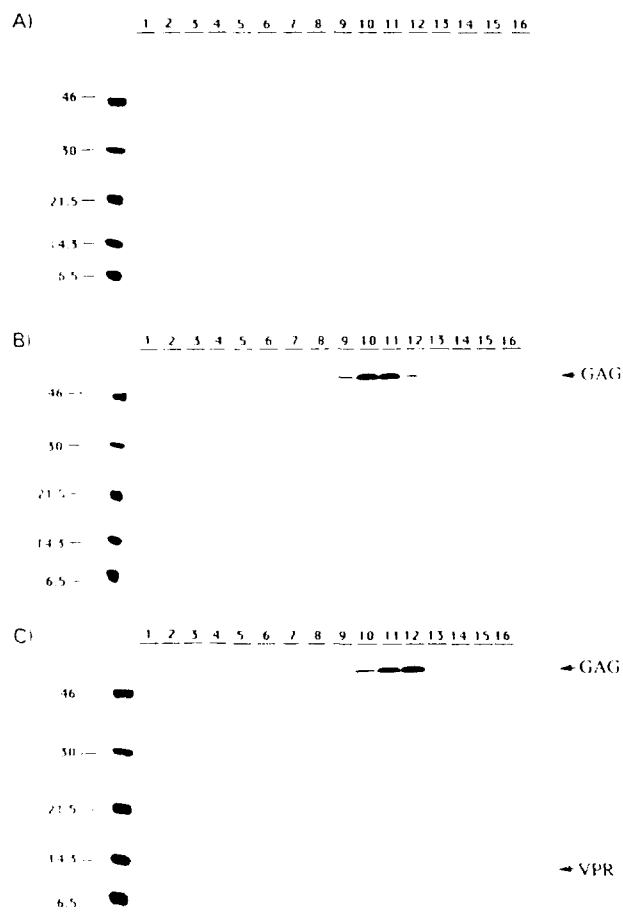


FIG. 6. Sucrose gradient analysis of particles released from BSC40 cells transfected with pTM-VPR (A), pTM-GAG (B), pTM-VPR and pTM-GAG (C). Fractions were pre-precipitated with 10% (wt/vol) trichloroacetic acid and analyzed by SDS-PAGE. Fraction 1 is from the bottom and fraction 16 from the top of each gradient. Molecular mass markers are shown at the left in kilodaltons.

is unclear, it is likely that this protein plays an important role in early events in the virus life cycle. It is tempting to speculate that the nuclear localization domain of Vpr allows targeting of the viral preintegration complex to the nucleus. Further studies on this important regulatory protein will be required to fully elucidate its role in the HIV life cycle.

ACKNOWLEDGMENTS

We thank Mike Aron for the pRRC, Lisa Westfield and Lynn Sallier (Howard Hughes Medical Institute) for the oligonucleotides, Charles Rice and Bernard Moss for pTM-GAG and pTM-VPR, and psRalpha, and Cetus Corporation for the linker. The recombinant Vpr and Gag proteins used for localization of rabbits for virus production were provided by H. Gras-Masse and the NIH AIDS Reagent Repository, respectively.

This work was supported by the DAMD1700-01-0-1055 (P.S.) cooperative program (USA/CHN). Y.H. was supported by the Wissenschaften Universität Gießen, D. and the Bundesgesundheitsministerium, Bonn, Germany. S.R. is a member of the American Cancer Society Research Program.

REFERENCES

1. Arya, S. K., C. Guo, S. L. Josephs, and F. Wong-Staal. 1990. Identification of a nuclear localization signal in the HIV-1 p17 protein. *J. Biol. Chem.* **265**:11111-11114.

2. Boyle, W. J., M. A. Lampert, A. C. Li, and M. A. Baluda. 1985. Nuclear compartmentation of the *v-myc* oncogene product. *Mol. Cell Biol.* **5**:3017-3023.
3. Bryant, M. L., and L. Ratner. 1990. Myristoylation-dependent replication and assembly of HIV-1. *Proc. Natl. Acad. Sci. USA* **87**:523-527.
4. Buckler-White, A. J., G. W. Humphrey, and V. Pigiet. 1980. Association of polyoma T antigen and DNA with the nuclear matrix from lytically infected 3T6 cells. *Cell* **22**:37-46.
5. Chakrabarti, L., M. Guyader, M. Alizon, M. D. Daniel, R. C. Desrosiers, P. Tiollais, and P. Sonigo. 1987. Sequence of simian immunodeficiency virus from macaque and its relationship to other human and simian retroviruses. *Nature (London)* **328**:543-547.
6. Cohen, E. A., G. Dehni, J. G. Sodroski, and W. A. Haseltine. 1990. Human immunodeficiency virus *vpr* product is a virion-associated regulatory protein. *J. Virol.* **64**:3097-3099.
7. Cohen, E. A., E. F. Terwilliger, Y. Jalinos, J. Proulx, J. G. Sodroski, and W. A. Haseltine. 1990. Identification of HIV-1 *vpr* product and function. *J. Acquired Immune Defic. Syndr.* **3**:11-18.
8. Dedera, D., W. Hu, N. Vander Heyden, and L. Ratner. 1989. Viral protein R of human immunodeficiency virus types 1 and 2 is dispensable for replication cytopathogenicity in lymphoid cells. *J. Virol.* **63**:3205-3208.
9. Eisenman, R. N., C. Y. Tachibana, H. D. Abrams, and S. R. Hann. 1985. *v-myc*- and *c-myc*-encoded proteins are associated with the nuclear matrix. *Mol. Cell Biol.* **5**:114-126.
10. Feldman, L. T., and J. R. Nevins. 1983. Localization of the adenovirus E1A protein, a positive-acting transcriptional factor in infected cells. *Mol. Cell Biol.* **3**:829-838.
11. Fey, E. G., G. Krochmalnic, and S. Penman. 1986. The nonchromatin substructures of the nucleus: the ribonucleoprotein (RNP)-containing and RNP-depleted matrices analyzed by sequential fractionation and resinless section electron microscopy. *J. Cell Biol.* **102**:1654-1665.
12. Fuerst, T. R., E. G. Niles, F. W. Studier, and B. Moss. 1986. Eukaryotic transient-expression system based on recombinant vaccinia virus that synthesizes bacteriophage T7 RNA polymerase. *Proc. Natl. Acad. Sci. USA* **83**:8122-8126.
13. Gras-Masse, H., J. C. Ameisen, C. Bouteillon, J. C. Gesquiere, S. Vian, J. L. Neyrinck, H. Drobecq, A. Capron, and A. Tartar. 1990. A synthetic peptide corresponding to the entire *vpr* gene product from the human immunodeficiency virus HIV-1 is recognized by antibodies from HIV infected patients. *Int. J. Peptide Protein Res.* **36**:219-226.
14. Guyader, M., M. Emerman, P. Sonigo, F. Clavel, L. Montagnier, and M. Alizon. 1987. Genome organization and transactivation of the human immunodeficiency virus type 2. *Nature (London)* **326**:662-666.
15. Hanover, J. A. 1992. The nuclear pore: at the crossroads. *FASEB J.* **6**:2288-2295.
16. Hattori, N., E. Michaels, K. Fargnoli, I. Marcon, R. C. Gallo, and G. Franchini. 1990. The human immunodeficiency virus type 2 *vpr* gene is essential for productive infection of human macrophages. *Proc. Natl. Acad. Sci. USA* **87**:8080-8084.
17. Henderson, L. L., R. C. Sowder, L. D. Copeland, R. Z. Benevise, and S. Oroszlan. 1988. Isolation and characterization of a novel protein (X-ORF) product from HIV-1. *Science* **241**:199-201.
18. Horton, R., P. Spearman, and L. Ratner. 1990. *Basic Principles of HIV-1*. New York: Academic Press.
19. Hu, W., N. Vander Heyden, and L. Ratner. 1990. A *vpr* gene product that is essential for productive infection of HIV-1. *Virology* **174**:61-69.
20. Jackson, D. A., S. J. McCready, and P. R. Cook. 1985. RNA synthesis in the nucleus. *Nature (London)* **316**:227-230.
21. Kappes, J. C., J. S. Parkin, J. A. Conway, J. Kim, C. G. Brouillette, G. M. Shaw, and B. H. Hann. 1989. Effects of transcriptional activation on the expression of HIV-1. *J. Virol.* **63**:1937-1945.
22. Lang, S., M. Weeger, C. Stahl-Henning, C. Conibaly, G. Hunsmann, J. Mutter, H. Mutter-Hermelink, D. Fuchs, H. Wachter, M. M. Daniel, R. C. Desrosiers, and B. Herrkenstein. 1990. The HIV-1 *vpr* gene product is a nuclear matrix-associated protein. *J. Virol.* **64**:3097-3099.

- immunodeficiency virus. *J. Virol.* **67**:902-912.
23. Lejbkowitz, F., C. Goyer, A. Darveau, S. Neron, and R. Lemieux. 1992. A fraction of mRNA 5' cap-binding protein, eukaryotic initiation factor 4E, localizes to the nucleus. *Proc. Natl. Acad. Sci. USA* **89**:9612-9616.
24. Levy, D. N., L. S. Fernandes, W. V. Williams, and D. B. Weiner. 1993. Induction of cell differentiation by human immunodeficiency virus 1 *vpr*. *Cell* **72**:541-550.
25. Luria, S., I. Chambers, and P. Berg. 1991. Expression of the type 1 human immunodeficiency virus Nef protein in T cells prevents antigen receptor-mediated induction of interleukin 2 mRNA. *Proc. Natl. Acad. Sci. USA* **88**:5326-5330.
26. Moss, B. E., T. Mizukami, W. A. Alexander, and T. R. Fuerst. 1990. New mammalian expression vectors. *Nature (London)* **348**:91-92.
27. Myers, G., B. Korber, J. A. Berzofsky, R. F. Smith, and G. N. Pavlakis. 1992. Human retroviruses and AIDS, 1992. Theoretical Biology and Biophysics Group T-10. Los Alamos National Laboratory, Los Alamos, N.Mex.
28. Nishino, Y., M. Kishi, M. Sumiya, K. Ogawa, A. Adachi, K. Maotani-Imai, S. Kato, K. Hirai, and K. Ikuta. 1991. Human immunodeficiency virus type 1 *vif*, *vpr*, and *nef* mutants can produce persistently infected cells. *Arch. Virol.* **120**:181-192.
29. Ogawa, K., R. Shibata, T. Kiyosau, I. Higuchi, Y. Kishida, A. Ishimoto, and A. Adachi. 1989. Mutational analysis of the human immunodeficiency virus *vpr* open reading frame. *J. Virol.* **63**:4110-4114.
30. Poiesz, B. J., F. W. Ruscetti, A. F. Gazdar, P. A. Bunn, J. M. Minna, and R. C. Gallo. 1990. Detection and isolation of type C retrovirus particles from fresh and cultured lymphocytes of a patient with cutaneous T-cell lymphoma. *Proc. Natl. Acad. Sci. USA* **77**:7415-7419.
31. Ratner, L. *Viral life cycle and genetic approaches. In Perspectives in drug discovery and design*, in press.
32. Ratner, L., A. Fisher, L. L. Jagodzinski, H. Mitsuya, R.-S. Liou, R. C. Gallo, and F. Wong-Staal. 1987. Complete nucleotide sequences of functional clones of the AIDS virus. *AIDS Res. Hum. Retroviruses* **3**:57-67.
33. Slamon, D. J., W. J. Boyle, D. E. Keith, M. F. Press, D. W. Golde, and L. M. Souza. 1988. Subcellular localization of the *trans*-activation protein of human T-cell leukemia virus type I. *J. Virol.* **62**:680-686.
34. Sato, A., H. Igarashi, A. Adachi, and M. Hayami. 1990. Identification and localization of *vpr* gene product of human immunodeficiency virus type 1. *Virus Genes* **4**:303-312.
35. Shibata, R., T. Miura, M. Hayami, K. Ogawa, H. Sakai, T. Kiyomasu, A. Ishimoto, and A. Adachi. 1990. Mutational analysis of the human immunodeficiency virus type 2 (HIV-2) genome in relation to HIV-1 and simian immunodeficiency virus SIV_{AGM}. *J. Virol.* **64**:742-747.
36. Smith, H. C., S. G. Harris, M. Zillman, and S. M. Berget. 1989. Evidence that a nuclear matrix protein participates in pre-messenger RNA splicing. *Exp. Cell Res.* **182**:521-533.
37. Staufenbiel, M., and W. Deppert. 1983. Different structural systems of the nucleus are targets for SV40 large T antigen. *Cell* **33**:173-181.
38. Takebe, Y., M. Seiki, J. I. Fujisawa, P. Hov, F. Yokota, K. I. Aria, M. Yoshida, and N. Aria. 1988. SR alpha promoter: an efficient and versatile mammalian cDNA expression system composed of the simian virus 40 early promoter and the R-U5 segment of human T-cell leukemia virus type 1 long terminal repeat. *Mol. Cell. Biol.* **8**:466-472.
39. Teitz, J., and E. 1992. The accessory gene functions of the primate immunodeficiency viruses, p. 3-27. *In* W. C. Koff, E. Wong-Staal, and R. C. Kennedy (ed.), *AIDS research reviews*. Marcel Dekker, Inc., New York.
40. Tristem, M., C. Marshall, A. Karpas, and F. Hill. 1992. Evolution of the primate lentiviruses: evidence from *vpr* and *vpr*. *EMBO J.* **11**:3405-3412.
41. Westervelt, P., H. E. Gendelman, and L. Ratner. 1991. Identification of a determinant within the human immunodeficiency virus 1 surface envelope glycoprotein critical for productive infection of primary monocytes. *Proc. Natl. Acad. Sci. USA* **88**:3097-3101.
42. Westervelt, P., T. Henkel, D. B. Trowbridge, J. Orenstein, J. Heuser, H. E. Gendelman, and L. Ratner. 1992. Dual regulation of silent and productive infection in monocytes by distinct human immunodeficiency virus type 1 determinants. *J. Virol.* **66**:3925-3931.
43. Wu, L.-C., C. T.-H. Tan, and S. I. Shahied. 1992. Expression and characterization of the transactivating protein Tax of human T-cell leukemia virus type 1 in *Saccharomyces cerevisiae*. *J. Virol.* **66**:7253-7261.
44. Yu, X.-F., M. Matsuda, M. Essex, and T.-H. Lee. 1990. Open reading frame of *vpr* of simian immunodeficiency virus encodes a virion-associated protein. *J. Virol.* **64**:5688-5693.
45. Yuan, X., Z. Matsuda, M. Matsuda, M. Essex, and T.-H. Lee. 1990. Human immunodeficiency virus *vpr* gene encodes a virion-associated protein. *AIDS Res. Hum. Retroviruses* **6**:1265-1271.
46. Zeitlin, S., A. Parent, S. Silberstein, and A. Efstratiadis. 1987. Pre-mRNA splicing and the nuclear matrix. *Mol. Cell. Biol.* **7**:111-120.

Human Immunodeficiency Virus Type 1 Nef Protein Down-Regulates Transcription Factors NF- κ B and AP-1 in Human T Cells In Vitro after T-Cell Receptor Stimulation

JUAN C. BANDRES AND LEE RATNER*

*Departments of Medicine and Molecular Microbiology, Washington University
School of Medicine, St. Louis, Missouri 63110*

Received 12 November 1993 Accepted 16 February 1994

Human immunodeficiency virus type 1 (HIV-1) negative factor (Nef) has been shown to down-regulate the transcription factors NF- κ B and AP-1 in vitro. To define the mechanism of action of the Nef protein, the signal transduction pathways which may be affected in T cells by constitutive expression of the *nef* gene were examined. Stimulation of T cells with tumor necrosis factor, interleukin-1, or lipopolysaccharide resulted in the recruitment of transcriptional factors to a similar level whether or not the cells expressed the *nef* gene. On the other hand, stimulation of T cells by mitogens or antibodies to the T-cell receptor (TCR)-CD3 complex resulted in the down-regulation of transcriptional factors NF- κ B and AP-1 in cells expressing the *nef* gene compared with cells not expressing the *nef* gene. Because the Nef protein does not affect the surface expression of the CD3-TCR complex, we conclude that the Nef protein down-regulates the transcriptional factors NF- κ B and AP-1 in T cells in vitro through an effect on the TCR-dependent signal transduction pathway.

Human immunodeficiency virus type 1 (HIV-1) negative factor (Nef) is dispensable for virus replication in vitro (10, 44) but is essential for the pathogenicity of the closely related simian immunodeficiency virus (6, 22). We have previously reported that HIV-1 and simian immunodeficiency virus Nef proteins affect virus replication in vitro (33, 34) and that this effect is related to down-regulation of transcriptional factors NF- κ B and AP-1 (30, 31). These transcriptional factors normally regulate the expression of genes involved in T-cell activation and proliferation (16). The HIV-1 promoter possesses multiple binding sites for both NF- κ B and AP-1 which allow the virus to subvert the normal activity of these factors to enhance its own replication (29).

The mechanism by which HIV-1 Nef protein affects signal transduction is unknown. Although HIV-1 Nef protein also down-regulates the cell surface expression of CD4 (13), the mechanism for this effect is also unknown. However, this function requires the cytoplasmic domain of CD4 (12). Because Nef protein localizes preferentially in the cytoplasm, membranes, and cytoskeleton (11, 32), its effects on nuclear factors must be mediated by a physical interaction or enzymatic regulation of one or more factors involved in signal transduction.

Several pathways of signal transduction for activation of T cells have been described. Antigenic stimulation of the T-cell receptor (TCR)-CD3-CD4 complex results in translocation of NF- κ B into the nucleus. The mechanism of NF- κ B activation in T cells is not completely understood, but it may involve dissociation of NF- κ B from I κ B as a result of phosphorylation and/or proteolysis of I κ B (3, 8, 11, 19, 21, 28, 40). Alternatively, T cells can be activated by cytokines and other surface receptors (tumor necrosis factor [TNF], interleukin 1 [IL-1], lipopolysaccharide [LPS]), also resulting in activation of transcriptional factors (4, 9, 35, 36, 39).

In this report, we describe the signal transduction path-

way(s) affected in T cells by constitutive expression of the *nef* gene. We found that stimulation of these cells through pathways originating from the TNF or IL-1 receptors is not affected by Nef protein, whereas stimulation of these cells through the TCR-CD3-CD4 complex resulted in down-regulation of NF- κ B and AP-1 in the presence of Nef protein compared with the parental cell line not expressing the *nef* gene.

MATERIALS AND METHODS

Cell lines and nuclear extract preparation. The cell lines used included Jurkat (J25) human T-cell clone 133, which stably expresses the Nef protein derived from the HIV-1 isolate NL-43, and its parental counterpart, clone 22F6, which does not express Nef protein (26). Confirmation of Nef protein production was performed by immunoprecipitation with rabbit anti-Nef serum and Western blot (immunoblot) analysis as reported previously (30). Cells were maintained in the logarithmic growth phase in RPMI 1640 medium supplemented with 10% fetal calf serum, 2 mM L-glutamine, 100 U of penicillin per ml, and 100 μ g of streptomycin per ml.

Cells were stimulated with different combinations of 50 to 75 ng of phorbol 12-myristate 13-acetate (PMA) per ml (Sigma, St. Louis, Mo.), 13 μ g of phytohemagglutinin (PHA) per ml (Sigma), 1,000 U of TNF per ml (Genentech Inc., San Francisco, Calif.), 15 ng of recombinant human IL-1 per ml (generously provided by D. Chaplin, Washington University, St. Louis, Mo.), or 10 μ g of lipopolysaccharide (LPS) per ml (Sigma). Antibody cross-linking was performed as described previously (17). Briefly, sheep anti-mouse immunoglobulin G (IgG) antibody (Becton Dickinson, San Jose, Calif.) diluted 1:100 in 0.1 M Tris buffer (pH 9.5) was immobilized onto plastic microtiter plates by incubation at room temperature for 1 h and then washed with phosphate buffered saline three times. One microgram of monoclonal antibody to CD3 per ml (clone 4, Becton Dickinson) was added to the Jurkat cells, and the cells were incubated for 4 h at 37°C in the microtiter plates in the presence or absence of sheep anti-mouse IgG. The protein kinase inhibitor isouquinolinesulfonyl fluoride (N-ethylmaleimide) was added to the cells at the end of the incubation period.

*Corresponding author. Mailing address: Washington University School of Medicine, 660 S. Euclid Ave., Box 8110, St. Louis, MO 63110. Phone: (314) 772-5886; Fax: (314) 367-8876.

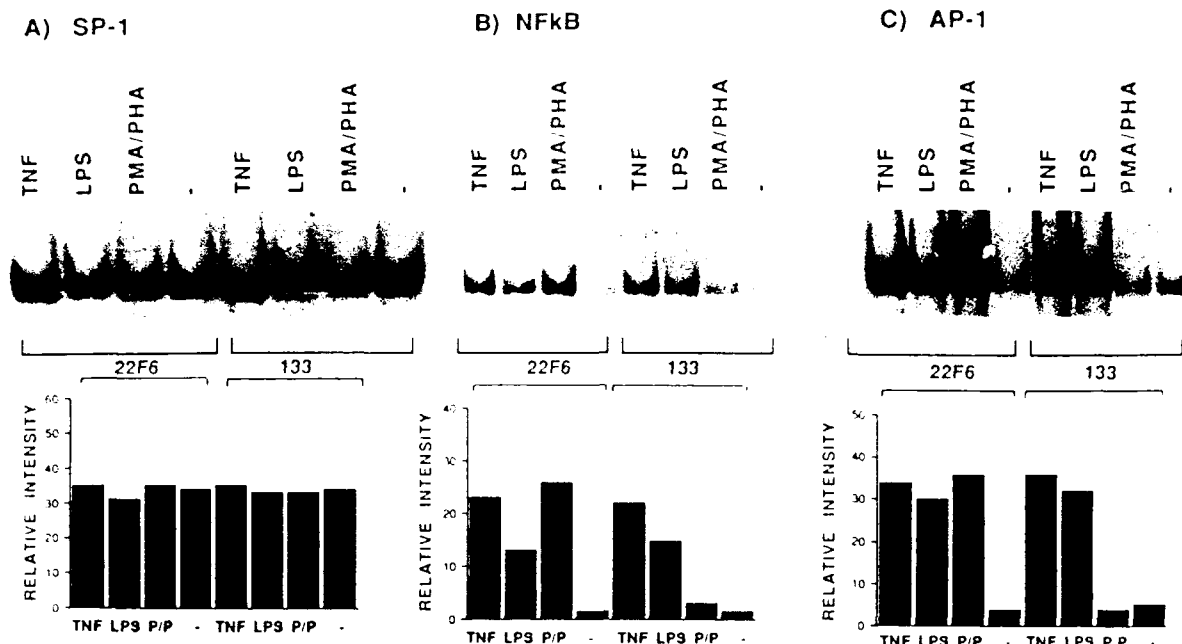


FIG. 1. Effect of Nef protein on induction of transcriptional factors AP-1 and NF- κ B in T cells stimulated with TNF, LPS, or PMA and PHA. Gel shift analysis shows induction of transcriptional factors SP-1, NF- κ B, and AP-1 in Jurkat T cells (22F6 is the parental cell line, and 133 is the Nef protein-expressing line). Cells were incubated for 4 h with saline (-), TNF, LPS, or PMA and PHA (P/P). Retarded DNA-protein complexes are shown; free DNA complexes are not shown but were equivalent in each lane. The experiments were performed three times with similar results. The relative intensity of the bands was evaluated by laser densitometry.

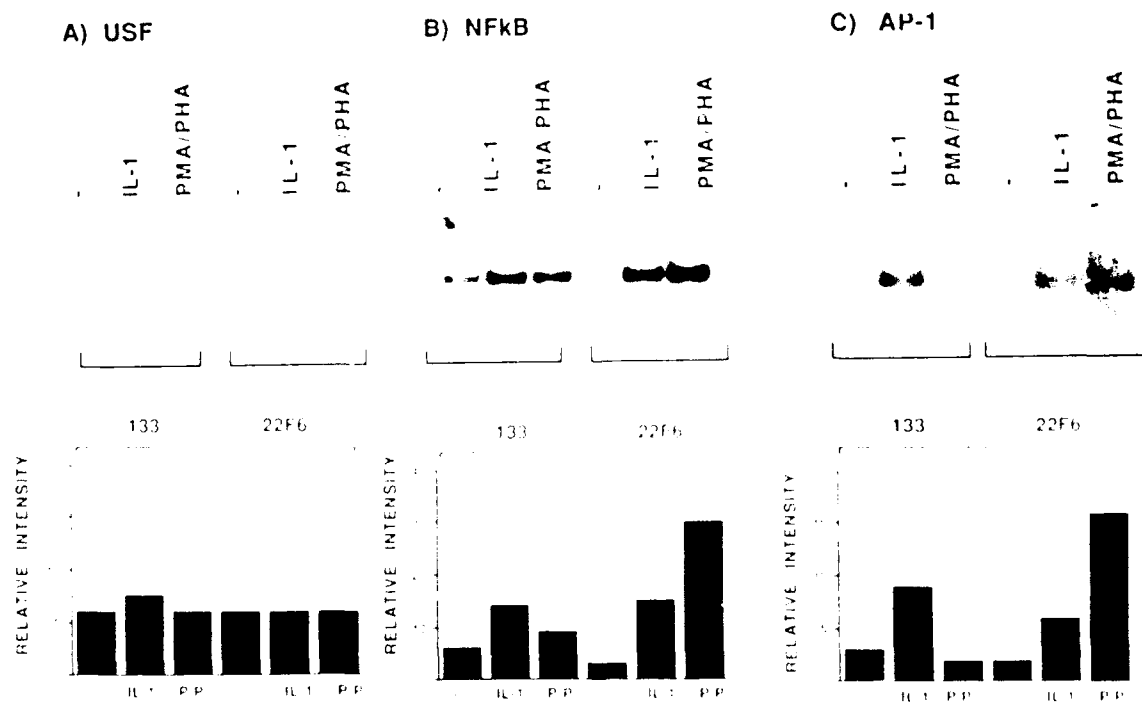


FIG. 2. Effect of Nef protein on induction of transcriptional factors AP-1 and NF- κ B in T cells stimulated with recombinant human IL-1 or PMA and PHA. Gel shift analysis shows induction of transcriptional factors USF, NF- κ B, and AP-1 in Jurkat T cells (22F6 is the parental cell line, and 133 is the Nef protein-expressing line). Cells were incubated for 4 h with IL-1, PMA, and PHA (P/P) or stimulated with IL-1. Retarded DNA-protein complexes are shown; free DNA complexes are not shown but were equivalent in each lane. The experiments were performed three times with similar results. The relative intensity of the bands was evaluated by laser densitometry.

(Sigma), when used, was added to the cells 30 min prior to the stimulants to a final concentration of 100 μ M. Nuclear extracts were prepared from 5×10^7 cells as previously described (30, 31) with the following modifications: after ammonium sulfate precipitation, nuclear proteins were resuspended in 100 μ l of 20 mM HEPES (*N*-2-hydroxyethylpiperazine-*N'*-2-ethanesulfonic acid [pH 7.9])–20 mM KCl–1 mM $MgCl_2$ –2 mM dithiothreitol–17% glycerol, with the addition of 10 mM sodium fluoride, 0.1 mM sodium vanadate, and 50 mM β -glycerol-phosphate. Binding reaction mixtures contained 2 μ g of nuclear extract, 2 μ g of poly(dI-dC) (Pharmacia, Milwaukee, Wis.), 20,000 to 40,000 cpm of end-labeled oligonucleotide probe and the equivalent amount of labeled probe in each assay for a given experiment, with or without a 100-fold molar excess of unlabeled oligonucleotide, in DNA binding buffer at a final volume of 30 to 40 μ l. Reactions were performed at 30°C for 25 min.

Gel retardation assays. For the gel retardation assays, the following double-stranded oligonucleotides were used: NF- κ B, ACAAGGGACTTTCCGCTGGGACTTTCAGGGA; SP-1, CAGGGAGGCGTGGCCTGGCGGGAGCTGGGGAGTGGCGTCC; AP-1, CAGGCCAGGAGTCAGATATCCA CTGACCTTTGGATGGTGCT; and USF, GCCGCTAGCA TTTTCATCACGTGGCCCGAGAGCTGC.

All DNA probes were gel purified and end labeled with [γ - 32 P]ATP. Gel retardation assays were performed as previously described (30) by using the radiolabeled probes, with DNA-protein complexes being separated from the free DNA probe by electrophoresis through low-ionic-strength 4.5% polyacrylamide gels and run at 200 V with Tris-borate-EDTA (3.7 g of Na EDTA, 54 g of Tris, and 27.5 g of boric acid per liter). The intensity of indicated bands for DNA-protein complexes was determined by laser densitometry scanning.

CAT assay. Chloramphenicol acetyltransferase (CAT) assays were performed as described previously (15) with samples with the same protein concentration as determined by the method of Bradford (Biorad, Hercules, Calif.). Transfections were performed in parallel with previously described reporter plasmids Rous sarcoma virus-CAT, HIV-1-CAT, and IL-2-CAT (1, 41) in both cell lines, and the results were normalized to the values obtained in parallel from the noninducible Rous sarcoma virus-CAT to control for transfection efficiency. Reaction products were analyzed by thin-layer chromatography followed by autoradiography and liquid scintillation counting. CAT activity was expressed as fold increases in the percentage of radioactivity in the acetylated forms compared with the sum of that of the acetylated and unacetylated forms.

RESULTS

To evaluate the effects of Nef protein on activation of transcriptional factors through protein kinase C-independent mechanisms, Jurkat cells carrying the *nef* gene (133) and the parental cell line (22F6) were stimulated with either TNF or LPS, and the results were compared with those from stimulation with PMA and PHA (Fig. 1). A noninducible factor, SP-1, was used to control for protein concentration and quality of the extracts (Fig. 1A). TNF or LPS induction of NF- κ B (Fig. 1B) and AP-1 (Fig. 1C) was not affected by the presence or absence of Nef protein in 133 and 22F6 cells, respectively. In contrast, the level of induction of both transcription factors was decreased by 6-fold in the case of NF- κ B and by 14-fold in the case of AP-1, when the same cells were stimulated with PMA and PHA.

Similar results were obtained when the comparison was made between the stimulation with IL-1 and that with PMA or

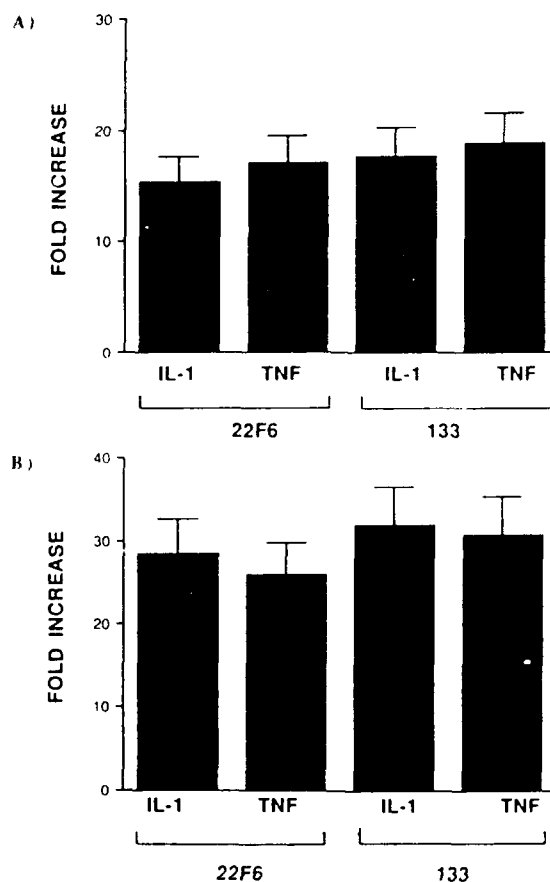


FIG. 3. CAT assay showing the effect of Nef protein on HIV and IL-2 transcription. Jurkat T cells (22F6 is the parental cell line, and 133 is the Nef protein-expressing cell line) were transfected with HIV-1 long terminal repeat-CAT (A) and incubated for 4 h with recombinant human IL-1 or TNF. Similar experiments with IL-2-CAT (B) were performed with 22F6 and 133 cells. Cells were transfected four times with each plasmid, a mean fold induction was calculated, and the standard deviation of the mean was determined. The percentages of acetylation of HIV-1-CAT were 4.6 ± 0.7 (IL-1) and 4.4 ± 0.4 (TNF) for 22F6 cells and 3.9 ± 0.6 (IL-1) and 4.7 ± 0.3 (TNF) for 133 cells. The percentages of acetylation for IL-2-CAT were 14.9 ± 0.9 (IL-1) and 17 ± 0.7 (TNF) for 22F6 cells and 12.7 ± 0.6 (IL-1) and 12.9 ± 0.3 (TNF) for 133 cells.

PHA (Fig. 2). Noninducible transcription factor USF was used as a control (Fig. 2A). NF- κ B (Fig. 2B) and AP-1 (Fig. 2C) activation by IL-1 was not significantly affected by the presence or absence of Nef protein in 133 and 22F6 cells, respectively. Stimulation with PMA or PHA resulted in down-regulation of NF- κ B by 5-fold and AP-1 by 15-fold in the presence of Nef protein in this experiment.

To determine if induction of NF- κ B and AP-1 correlated with transcriptional activity, cells were transfected with DNA plasmids which use the HIV-1 long terminal repeat to direct expression of a heterologous gene product, CAT. Cells were stimulated with TNF or IL-1 (Fig. 3). No difference in acetylation between the cells expressing the *nef* gene (133) and the parental cell line, 22F6, was found when both cell lines were stimulated with either IL-1 or TNF (Fig. 3A). Because Nef protein also has been reported to suppress the induction of CAT activity directed by the IL-2-CAT plasmid (26), 133 cells and 22F6 cells containing this plasmid were stimulated

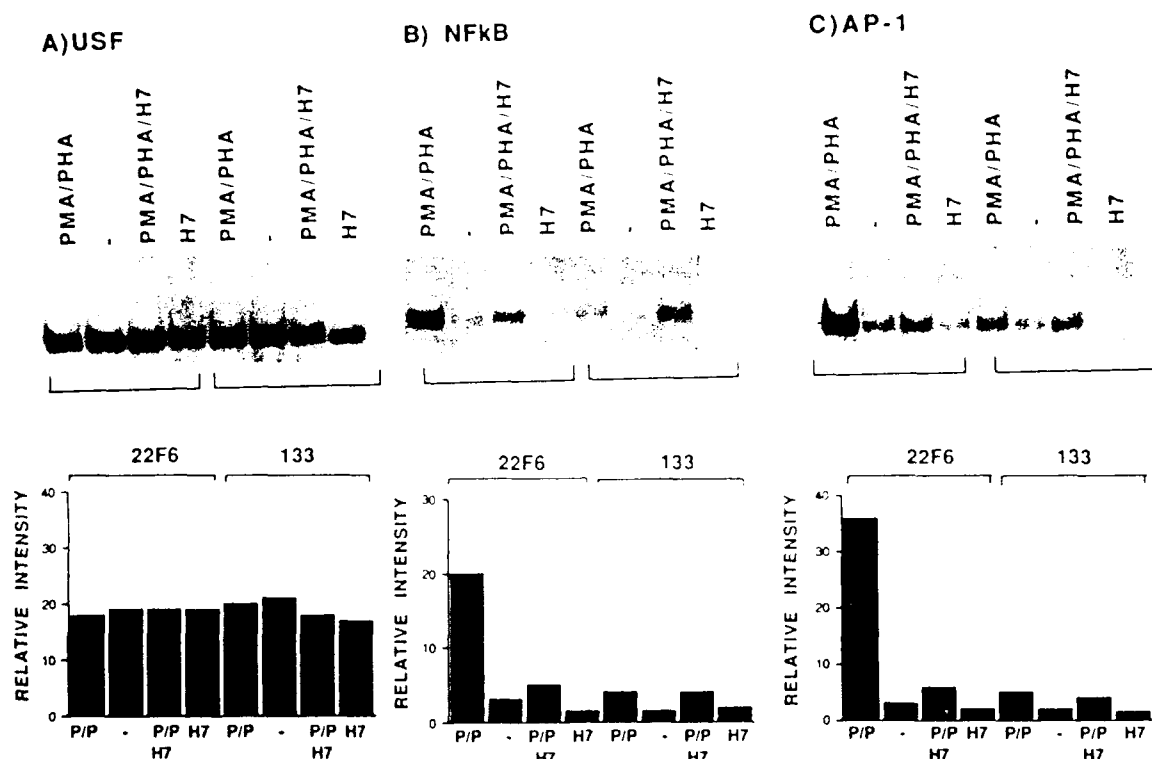


FIG. 4. Effect of Nef protein on induction of transcriptional factors AP-1 and NF- κ B in T cells stimulated with PMA and PHA in the presence or absence of H-7. Gel shift analysis shows induction of transcriptional factors USF, NF- κ B, and AP-1. Jurkat T cells (22F6 is the parental cell line, and 133 is the Nef protein-expressing cell line) were incubated for 4 h with PHA and PMA (P/P) or sterile water (-). H-7 was added 30 min prior to the incubation. Retarded DNA-protein complexes are shown; free DNA complexes are not shown but were equivalent in each lane. The experiments were performed three times with similar results. The relative intensity of the bands was evaluated by laser densitometry.

with TNF or IL-1 (Fig. 3B). The results paralleled those obtained with HIV-1-CAT. These data indicate that Nef protein does not affect the induction of transcription factors by the pathway(s) of T-cell activation originating from the TNF or IL-1 receptors.

To further evaluate the effects of Nef protein on signal transduction after PMA or PHA stimulation, the effect of addition of a protein kinase inhibitor, H-7, was examined (Fig. 4). The noninducible factor USF was used as a control (Fig. 4A). PMA or PHA induction of NF- κ B (Fig. 4B) was 10-fold higher in the 22F6 cells than in the 133 cells. The use of H-7 resulted in a significant decrease in NF- κ B induction in the cells that did not express Nef protein. Similarly, PMA and PHA resulted in the induction of AP-1 (Fig. 4C) to a level that was 15 times higher in the cells not expressing Nef protein than in the cells expressing Nef protein. H-7 blocked the induction of AP-1 in the 22F6 cells. In both cases, the addition of H-7 to the Nef protein-expressing cells did not cause any further decrease in the already low level of expression of the respective transcription factors.

To further establish that the effects of Nef protein were related to stimulation through the TCR-CD3 complex, both Jurkat 22F6 and 133 cells were stimulated by anti-CD3 cross-linking in the presence or absence of H-7 (Fig. 5). Noninducible transcription factor USF was used as a control (Fig. 5A). NF- κ B induction (Fig. 5B) in 22F6 cells was increased fivefold by the addition of the antibodies to the TCR-CD3 complex. The presence of H-7 attenuated the induction to a level comparable to that achieved in the 133 cells. Again, induction was not further decreased by H-7 in the 133 cells, because

levels were already fivefold lower for the cells stimulated with anti-CD3 than for the cells stimulated with PMA and PHA. When the oligonucleotide for AP-1 was used (Fig. 5C), similar results were obtained, with differences of eightfold for the anti-CD3 antibody stimulation of 22F6 cells compared with the 133 cells.

To corroborate that the effects on the regulation of the transcription factors were correlated with transcriptional activity, CAT assays were performed (Fig. 6). The percentage of acetylation was decreased by sixfold with the use of H-7 in 22F6 cells stimulated with anti-CD3 for HIV-1-CAT (Fig. 6A). The difference between the percentage of acetylation in 22F6 and 133 cells (Fig. 6B) in the absence of H-7 was 5.5-fold when cells were stimulated with anti-CD3. The results with the IL-2-CAT plasmid with both 22F6 (Fig. 6C) and 133 (Fig. 6D) cells again paralleled those of the HIV-1-CAT plasmid, except for the greater differences found between the Nef protein-expressing cells and the parental cell lines. Furthermore, the findings with IL-2-CAT reflect previously described Nef protein effects on endogenous IL-2 expression (26). The results presented above indicate that Nef protein down-regulates the induction of NF- κ B and AP-1 by interacting with one of the steps involved in T-cell activation from the TCR-CD3-CD4 complex.

DISCUSSION

The function of HIV-1 Nef protein remains unclear. Whether the results of the experiments *in vitro* correlate with an *in vivo* situation is, at this point, impossible to ascertain. The only available animal data from the experiments with simian

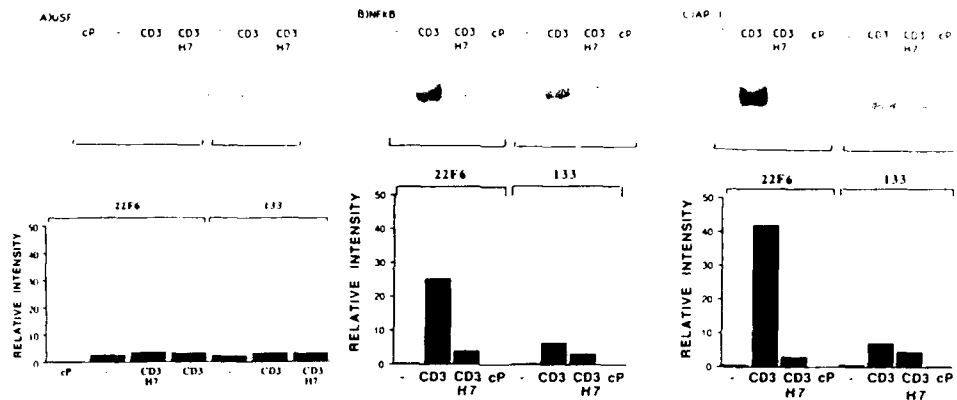


FIG. 5. Effect of Nef protein on induction of transcriptional factors AP-1 and NF-κB in T cells stimulated with cross-linked antibody to CD3 (CD3) or soluble CD3 in the absence of immobilized anti-mouse IgG (-). Gel shift analysis shows induction of transcriptional factors AP-1, NF-κB, and AP-1. H-7 was added 30 min prior to the incubation. cP, cold probe. Retarded DNA-protein complexes are shown; free DNA complexes are not shown but were equivalent in each lane. The experiments were performed twice with similar results. The relative intensity of the bands was evaluated by laser densitometry.

immunodeficiency virus may indicate the importance of the gene for the pathogenicity of the virus (6, 22) *in vivo*. Differences in the results of the *in vitro* experiments among various groups may be due to the use of different *nef* alleles (18, 43, 48), the conditions of the experiment (23), or the use of peripheral blood lymphocytes (7) versus stable cell lines. In our *in vitro* system, Nef protein has been shown to down-regulate

both NF-κB (30) and AP-1 (31) after PMA and PHA stimulation.

The current work aimed at clarifying the mechanism of action of Nef protein by examining the pathways of signal transduction affected by this protein in T cells. Several signaling pathways have been described, although further clarification is still required. Multiple stimuli, including IL-1 (4, 9, 38),

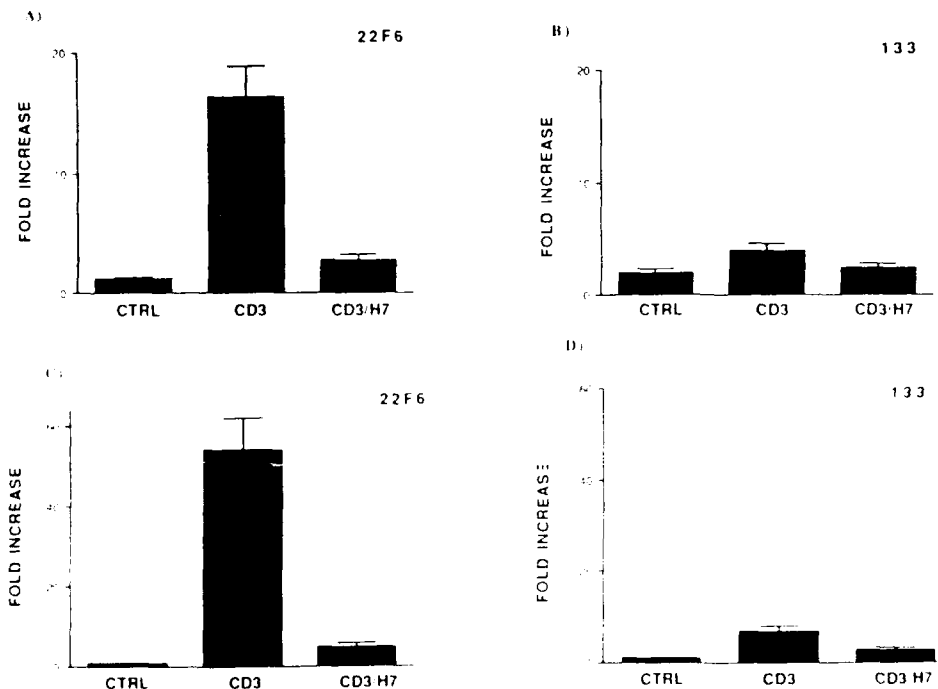


FIG. 6. CAT assay showing the effect of Nef protein on HIV and IL-2 transcription. Jurkat T cells (22F6 [A] is the parental cell line, and 133 [B] is the Nef protein expressing cell line) were transfected with HIV-1 long terminal repeat CAT and stimulated with cross-linked antibody to CD3 (CD3) or soluble CD3 in the absence of immobilized anti-mouse IgG (CTRL). H-7 was added 30 min prior to the incubation. Similar experiments with IL-2 CAT were performed with 22F6 cells (C) and 133 cells (D). Cells were transfected four times with each plasmid, a mean fold induction was calculated, and the standard deviation of the mean was determined. The percentages of acetylation for HIV-1 CAT were 0.5 ± 0.02 (CTRL), 1.1 ± 0.48 (CD3), and 0.78 ± 0.2 (CD3 H7) for 22F6 cells and 0.3 ± 0.06 (CTRL), 0.7 ± 0.1 (CD3), and 0.4 ± 0.06 (CD3 H7) for 133 cells. The percentages of acetylation for IL-2 CAT were 0.2 ± 0.03 (CTRL), 1.2 ± 0.8 (CD3), and 1.8 ± 0.28 (CD3 H7) for 22F6 cells and 0.4 ± 0.04 (CTRL), 2.1 ± 0.38 (CD3), and 0.9 ± 0.5 for 133 cells.

CD28 (46), CD45 (24), TNF (25, 38, 39, 47), gamma interferon (47), LPS (4), PMA and PHA (4, 25, 38), human T-cell lymphotropic virus Tax protein (38), and the antigenic stimulation of the TCR-CD3-CD4 complex, have been shown to induce expression of cellular genes, including IL-2 and IL-8 and surrogate HIV genes. The diverse mechanisms by which this stimulation is achieved include direct stimulation of the hydrolysis of inositol phospholipids by CD45 (24), activation of protein kinase C (as with PMA and PHA), and phosphorylation of I- κ B through breakdown of sphingomyelin products to ceramide (as with TNF) (2, 27, 37, 42, 45). The current work indicates that Nef protein affects the T-cell signal transduction pathway originating from TCR-CD3 complex stimulation. Nef protein has been shown to down-regulate CD4, but it does not affect the expression of CD3 (12) or TCR (data not shown) at the cell surface. Therefore, Nef protein probably affects one of the downstream steps resulting from stimulation of the TCR-CD3 complex. Whether this is due to physical interaction with a component or components of this pathway, like the ζ subunit of the TCR, or whether it is due to enzymatic regulation of pathway intermediates like tyrosine kinases (*lek*) or tyrosine phosphatases remains to be determined. It is interesting that the effect of Nef protein on CD4 expression requires the cytoplasmic domain of CD4 (12), which includes two sites that bind to p56^{lck} (5). Whether Nef affects CD4 expression and signal transduction by the same molecular interaction or through a different mechanism needs to be clarified.

To determine if the effects in vitro on transcriptional regulation correlate with the in vivo effects of Nef protein requires first an understanding of the molecular mechanisms of its action in vitro. It needs to be kept in mind that our in vitro system does not take into account circumstances that could be important in an in vivo situation and could be affected by Nef protein, such as reinfection of T cells. Therefore, we are unable to ascertain the relative importance of diverse activities of Nef protein. This report indicates that Nef protein interacts with the signal transduction pathway originating from the TCR-CD3 complex and does not affect the stimulation of T cells with the cytokines IL-1 and TNF. The complete definition of this system is required to determine if Nef protein is involved in the cellular latency of HIV and, if so, through which mechanism.

ACKNOWLEDGMENTS

We thank Lisa Westfield and Evan Sadler for oligonucleotide synthesis, William R. Hastings for technical assistance, and Sylvie Luria for providing the cell lines.

This work was supported by U.S. Army grant DAMD-17-90C-0125 to L.R. and ACS grant FRA373.

REFERENCES

1. Arya, S. K., G. Chan, S. F. Josephs, and F. Wong-Staal. 1985. Transactivator gene of human T-lymphotropic virus type III (HTLV-III). *Science* **229**:69-73.
2. Atluru, D., S. Polam, S. Atluru, and G. E. Woloschak. 1990. Regulation of mitogen-stimulated human T-cell proliferation, IL-2 production and IL-2 receptor expression by protein kinase C inhibitor H7. *Cell. Immunol.* **129**:310-320.
3. Baeuerle, P. A., and D. Baltimore. 1988. I- κ B: a specific inhibitor of the NF- κ B transcription factor. *Science* **242**:530-536.
4. Bomsztyk, K., J. W. Rooney, E. Iwaski, N. A. Rachic, S. K. Dower, and C. Hopkins Sibley. 1991. Evidence that interleukin 1 and phorbol esters activate NF- κ B by different pathways: role of protein kinase C. *Cell. Regul.* **2**:329-335.
5. Crise, B., and J. K. Rose. 1992. Identification of palmitoylation sites on CD4: the human immunodeficiency virus receptor. *J. Biol. Chem.* **267**:13593-13597.
6. Daniel, M. D., E. Kirchhoff, S. C. Czajak, P. K. Sehgal, and R. C. Desrosiers. 1992. Protective effects of a live attenuated SIV vaccine with a deletion of the nef gene. *Science* **258**:1938-1941.
7. deRonde, A., B. Klaver, W. Keulen, L. Smit, and J. Goudsmit. 1992. Natural HIV nef accelerates virus replication in primary human lymphocytes. *Virology* **188**:391-395.
8. Diaz-Meco, M. T., E. Berra, M. N. Municio, L. Sanz, J. Lozano, I. Dominguez, V. Diaz-Golpe, M. T. Lain de Lera, J. Alcami, C. V. Payá, F. Arenzana-Seisdedos, J.-L. Virelizier, and J. Moscat. 1993. A dominant negative protein kinase C ζ subspecies blocks NF- κ B activation. *Mol. Cell. Biol.* **13**:4770-4775.
9. Edbrooke, M. R., J. Foldi, J. K. Cheshire, F. Li, D. J. Faulkes, and P. Woo. 1991. Constitutive and NF- κ B like proteins in the regulation of the serum amyloid A gene by interleukin 1. *Cytokine* **3**:380-388.
10. Fisher, A. G., L. Ratner, H. Mitsuya, L. M. Marselle, M. E. Harper, S. Broder, R. C. Gallo, and F. Wong-Staal. 1986. Infectious mutants of HTLV-III with changes in the 3' region and markedly reduced cytopathic effects. *Science* **233**:655-659.
11. Franchini, G., M. Robert-Guroff, J. Ghayeb, N. T. Chang, and F. Wong-Staal. 1986. Cytoplasmic localization of the HTLV-III 3' end in cultured human T-cells. *Virology* **155**:593-599.
12. Garcia, J. V., J. Alfano, and A. D. Miller. 1993. The negative effect of human immunodeficiency virus type 1 Nef on cell surface expression is not species specific and requires the cytoplasmic domain of CD4. *J. Virol.* **67**:1511-1516.
13. Garcia, J. V., and A. D. Miller. 1991. Serine phosphorylation-independent down-regulation of cell surface CD4 by nef. *Nature (London)* **350**:508-511.
14. Ghosh, S., and D. Baltimore. 1990. Activation in vitro of NF- κ B by phosphorylation of its inhibitor I- κ B. *Nature (London)* **344**:678-682.
15. Gorman, C. M., G. T. Merlino, M. C. Willingham, I. Pastan, and B. H. Howard. 1982. The Rous sarcoma virus long terminal repeat is a strong promoter when introduced into a variety of eukaryotic cells by DNA-mediated transfection. *Proc. Natl. Acad. Sci. USA* **79**:6777-6781.
16. Greene, W. C. 1991. The molecular biology of human immunodeficiency virus type 1 infection. *N. Engl. J. Med.* **324**:308-317.
17. Gur, H., M. C. Wacholtz, L. S. Davis, T. D. Geppert, and P. E. Lipsky. 1992. Modulatory effect of aggregating the CD3 molecular complex on T cell activation. *Cell. Immunol.* **140**:81-96.
18. Hammes, S. R., E. P. Dixon, M. H. Malim, B. R. Cullen, and W. C. Greene. 1989. Nef protein of human immunodeficiency virus type 1: evidence against its role as a transcriptional inhibitor. *Proc. Natl. Acad. Sci. USA* **86**:9549-9553.
19. Henkel, T., T. Machleidt, I. Alkalay, M. Kronke, Y. Ben-Neriah, and P. A. Baeuerle. 1993. Rapid proteolysis of I- κ B is necessary for activation of transcription factor NF- κ B. *Nature (London)* **365**:182-185.
20. Jamieson, C., P. G. McCaffrey, A. Rao, and R. Sen. 1991. Physiologic activation of T-cells via the T-cell receptor induces NF- κ B. *J. Immunol.* **147**:416-420.
21. June, C. H., M. C. Fletcher, J. A. Ledbetter, G. L. Schieven, J. N. Siegel, A. E. Phillips, and L. E. Samelson. 1990. Inhibition of tyrosine phosphorylation prevents T-cell receptor-mediated signal transduction. *Proc. Natl. Acad. Sci. USA* **87**:7722-7726.
22. Kestler, H. W., D. J. Ringler, K. Mori, D. L. Panicci, P. K. Sehgal, M. D. Daniel, and R. C. Desrosiers. 1991. Importance of the nef gene for maintenance of high virus loads and for the development of AIDS. *Cell* **65**:651-662.
23. Kim, S., K. Ikeuchi, R. Byrn, J. Groopman, and D. Baltimore. 1989. Lack of a negative influence on viral growth by the nef gene of human immunodeficiency virus type 1. *Proc. Natl. Acad. Sci. USA* **86**:9544-9548.
24. Koretzky, G. A., J. Picus, M. L. Thomas, and A. Weiss. 1990. Tyrosine phosphatase CD45 is essential for coupling T-cell antigen receptor to the phosphatidylinositol pathway. *Nature (London)* **346**:66-68.
25. Krasnow, S. W., L. Zhang, K. Leung, L. Osborn, S. Kunkel, and G. J. Nabel. 1991. Tumor necrosis factor alpha, interleukin 1, and phorbol myristate acetate are independent activators of NF- κ B which differentially activate T cells. *Cytokine* **3**:377-379.
26. Luria, S., I. Chambers, and P. Berg. 1991. Expression of the type 1 immunodeficiency virus nef protein in T cells prevents antigen

- receptor-mediated induction of interleukin-2 mRNA. *Proc. Natl. Acad. Sci. USA* **88**:5326-5330.
27. Manger, B., A. Weiss, J. Imboden, T. Laing, and J. D. Stobo. 1987. The role of protein kinase C in transmembrane signaling by the T-cell receptor antigen complex. *J. Immunol.* **139**:2755-2760.
28. Mustelin, T., K. M. Coggeshall, N. Isakov, and A. Altman. 1990. T cell antigen receptor-mediated activation of phospholipase C requires tyrosine phosphorylation. *Science* **247**:1584-1587.
29. Nabel, G., and D. Baltimore. 1987. An inducible transcription factor activates expression of human immunodeficiency virus in T-cells. *Nature (London)* **326**:711-713.
30. Niederman, T. M. J., J. V. Garcia, W. R. Hastings, S. Luria, and L. Ratner. 1992. Human immunodeficiency virus type 1 Nef protein inhibits NF- κ B induction in human T cells. *J. Virol.* **66**:6213-6219.
31. Niederman, T. M. J., W. R. Hastings, S. Luria, J. C. Bandres, and L. Ratner. 1993. HIV-1 Nef protein inhibits the recruitment of AP-1 DNA binding activity in human T-cells. *Virology* **194**:338-344.
32. Niederman, T. M. J., W. R. Hastings, and L. Ratner. 1993. Myristoylation-enhanced binding of the HIV-1 Nef protein to T cell skeletal matrix. *Virology* **197**:420-425.
33. Niederman, T. M. J., W. Hu, and L. Ratner. 1991. Simian immunodeficiency virus negative factor suppresses the level of viral mRNA in COS cells. *J. Virol.* **65**:3538-3546.
34. Niederman, T. M. J., B. J. Thielan, and L. Ratner. 1989. Human immunodeficiency virus type 1 negative factor is a transcriptional silencer. *Proc. Natl. Acad. Sci. USA* **86**:1128-1132.
35. Osborn, L., S. Kunkel, and G. Nabel. 1989. Tumor necrosis factor alpha and interleukin 1 stimulate the human immunodeficiency virus enhancer by activation of the nuclear factor κ B. *Proc. Natl. Acad. Sci. USA* **86**:2336-2340.
36. Pomerantz, R. J., M. B. Feinberg, D. Trono, and D. Baltimore. 1990. LPS is a potent monocyte/macrophage specific stimulator of human immunodeficiency virus type 1 expression. *J. Exp. Med.* **172**:253-261.
37. Rayter, S. I., M. Woodrow, S. C. Lucas, D. A. Cantrell, and J. Downward. 1992. p21ras mediates control of the IL-2 gene promoter function in T-cell activation. *EMBO J.* **11**:4549-4556.
38. Schreck, R., R. Grassmann, B. Fleckenstein, and P. A. Baeuerle. 1992. Antioxidants selectively suppress activation of NF- κ B by human T-cell leukemia virus type I Tax protein. *J. Virol.* **66**:6288-6293.
39. Schutze, S., K. Pothoff, T. Machleidt, D. Berkovic, K. Wiegmann, and M. Kronke. 1992. TNF activates NF- κ B by phosphatidylcholine-specific phospholipase C-induced "acidic" sphingomyelin breakdown. *Cell* **71**:765-776.
40. Shirakawa, F., and S. B. Mizel. 1989. In vitro activation and nuclear translocation of NF- κ B catalyzed by cyclic AMP-dependent protein kinase and protein kinase C. *Mol. Cell. Biol.* **9**:2424-2430.
41. Siebenlist, U., D. B. Durand, P. Bressler, N. J. Holbrook, C. A. Norris, M. Kamoun, J. A. Kant, and G. R. Crabtree. 1986. Promoter region of interleukin-2 gene undergoes chromatin structure changes and confers inducibility on chloramphenicol acetyltransferase gene during activation of T cells. *Mol. Cell. Biol.* **6**:3042-3049.
42. Strahler, J. R., N. Hailat, B. Lamb, K. P. Rogers, J. A. Underhill, R. F. Melhem, D. R. Keins, X. Zhu, R. D. Kuick, D. A. Fox, and S. M. Hanash. 1992. Activation of resting peripheral blood lymphocytes through the T-cell receptor induces rapid phosphorylation of Op 18. *J. Immunol.* **149**:1191-1198.
43. Terwilliger, E., J. G. Sodroski, C. A. Rosen, and W. A. Haseltine. 1986. Effects of mutations within the 3' *orf* open reading frame region of human T-cell lymphotropic virus type III (HTLV-III/LAV) on replication and cytopathogenicity. *J. Virol.* **60**:754-760.
44. Terwilliger, E. F., E. Langhoff, D. Gabuzda, E. Zazopoulos, and W. A. Haseltine. 1991. Allelic variation in the effects of the nef gene on replication of human immunodeficiency virus type 1. *Proc. Natl. Acad. Sci. USA* **88**:10971-10975.
45. Valge, V. E., J. G. P. Wong, D. M. Datlof, A. J. Sinskey, and A. Rao. 1988. Protein kinase C is required for responses to T-cell receptor ligands but not to IL-2 in T-cells. *Cell* **55**:101-112.
46. Verweij, C. L., M. Geerts, and L. A. Aarden. 1991. Activation of interleukin-2 gene transcription via the T-cell surface molecule CD28 is mediated through an NF- κ B-like response element. *J. Biol. Chem.* **266**:14179-14182.
47. Yasumoto, K., S. Okamoto, N. Mukaida, S. Murakai, M. Mai, and K. Matsushima. 1992. Tumor necrosis factor alpha and interferon gamma synergistically induce interleukin 8 production in a human gastric cancer cell line through acting concurrently on AP-1 and NF- κ B like binding sites of the interleukin 8 gene. *J. Biol. Chem.* **267**:22506-22511.
48. Zazopoulos, E., and W. A. Haseltine. 1992. Mutational analysis of the human immunodeficiency virus type 1 Nef function. *Proc. Natl. Acad. Sci. USA* **89**:6634-6638.

Highly localized tracks of human immunodeficiency virus type 1 Nef in the nucleus of cells of a human CD4⁺ T-cell line

K. G. MURTI*†‡, P. S. BROWN*, LEE RATNER§, AND J. VICTOR GARCIA*

*Department of Virology and Molecular Biology, St. Jude Children's Research Hospital, 332 North Lauderdale, P.O. Box 318, Memphis, TN 38101-0318; †Department of Pathology, University of Tennessee, The Health Science Center, 800 Madison Avenue, Memphis, TN 38163; and ‡Division of Hematology-Oncology, Washington University School of Medicine, 660 South Euclid Avenue, St. Louis, MO 63110

Communicated by David M. Prescott, September 7, 1993 (received for review July 6, 1993)

ABSTRACT A human T-cell line constitutively expressing the *nef* gene from the human immunodeficiency virus type 1 SF2 isolate was used to examine the distribution of the Nef protein in the nucleus. High-resolution immunogold labeling/electron microscopic studies with polyclonal anti-Nef antibodies on *nef*⁺ and *nef*⁻ cells revealed that a small fraction of Nef is in the nucleus and it is localized in specific curvilinear tracks that extend between the nuclear envelope and the nucleoplasm. An examination of the sequence of the SF2 *nef* gene revealed a putative nuclear targeting sequence that was previously found in several other eukaryotic nucleoplasmic proteins. The nuclear localization of Nef suggests a potential nuclear function for this protein. The presence of Nef in distinct nuclear tracks suggests that Nef is transported along a specific pathway that extends from the nuclear envelope into the nucleoplasm. A previous study [Meier, U. T. & Blobel, G. (1992) *Cell* 70, 127-138] has shown that the nucleolar protein nucleolin (Nopp140) shuttles from the nucleolus to the nuclear envelope on distinct tracks. The present study has demonstrated that the transport of a nucleoplasmic protein may also occur on distinct nuclear pathways.

The human immunodeficiency virus (HIV) is a complex retrovirus that contains several genes that regulate virus replication and gene expression (1-3). The role of one of these genes, *nef*, has been the subject of a great deal of controversy (4). Nef is encoded by a single open reading frame that overlaps with the 3' long terminal repeat of HIV and simian immunodeficiency virus (SIV) (4-6). Nef is a 27- to 32-kDa protein that is myristoylated at its amino terminus (7-9). In some instances, a 25-kDa product that is not myristoylated has been reported; however, this form of Nef is not always detectable (10). *nef* mRNA is detected along with that coding for *tat* and *rev* early after infection (11). The presence of antibodies reactive with Nef in patients infected with HIV or in macaques infected with SIV is evidence of *nef* expression *in vivo* (12-15). Although Nef is not required for replication (16), it is present in HIV-1, HIV-2, and SIV (4). The expression of this gene in all three viruses can be considered an indication that *nef* might have an effect on virus replication or disease progression. Indeed, experiments conducted using SIV (mac239 isolate) indicate that *nef* plays an important role in the development of disease *in vivo* (16).

A knowledge of the subcellular distribution of Nef may provide clues to its function. Previous light microscopic studies using immunofluorescence or immunoperoxidase techniques have found Nef primarily in the cytoplasm (7, 17, 18) associated with the plasma membrane, Golgi complex, and endoplasmic reticulum. A recent biochemical study has demonstrated that a substantial fraction of Nef of HIV-1 is associated with the cytoskeletal fraction of T lymphocytes

and that the association is enhanced by myristoylation of Nef (20). The distribution of Nef in the nucleus remains controversial. Some recent studies using immunocytochemical techniques at the light microscopic level have described the possible association of Nef with the nuclear envelope and the nucleoplasm (18, 19, 21). In this study we have attempted to resolve the question of the nuclear localization of Nef in human T cells using the high-resolution method of immunogold/electron microscopy. The studies done with a highly specific polyclonal antiserum to Nef have revealed that a fraction of Nef is localized in distinct tracks in the nucleus.

MATERIALS AND METHODS

Cells and Antibodies. HPBALL human CD4⁺ T cells expressing *nef* (HPBALL/LnefSN-S1) or transduced with a control vector (HPBALL/LN) have been described (22). Cells were grown in RPMI medium containing 25 mM Hepes and supplemented with 10% fetal bovine serum, penicillin, and streptomycin. A rabbit anti-Nef polyclonal antiserum (23) whose specificity was established by Western blot analysis (see Fig. 1) was used in immunogold labeling studies. Monoclonal anti-vimentin (no. 814318) and anti-actin (no. 1378996) antibodies were obtained from Boehringer Mannheim. Monoclonal anti-tubulin (no. MAB065) antibodies were purchased from Chemicon. The specificity of three antibodies was established by immunofluorescence and/or Western blot analysis.

Western Blot Analysis. To determine the specificity of the rabbit anti-Nef polyclonal antiserum, HPBALL/LnefSN or LN cells were lysed in 1% Nonidet P-40 buffer and proteins were separated by SDS/PAGE on a 12.5% gel. Proteins were transferred to a nitrocellulose filter, probed with the anti-Nef antiserum (1:500 dilution), and developed with goat anti-rabbit alkaline phosphatase secondary antibody essentially as described (24).

Immunofluorescence and Immunogold Labeling. Immunofluorescence was performed as described (25). Briefly, cells were spun (Cytospin) onto glass slides, fixed with 3.7% paraformaldehyde, and permeabilized with acetone. Cells were then incubated with the primary antibodies [diluted 10- to 20-fold with phosphate-buffered saline (PBS)] at 37°C for 1 hr. After thorough rinsing, cells were incubated as above with fluorescein-conjugated goat anti-rabbit antibodies (ICN; diluted 10-fold with PBS). The slides were viewed and photographed in a Zeiss IM35 microscope.

Immunogold labeling was done as described (26, 27) with slight modifications. Cells were fixed in 2.0% paraformaldehyde/0.05% glutaraldehyde in 0.01 M sodium cacodylate buffer, dehydrated in 15%, 30%, and 50% ethanol for 15 min each, and stained with 2% uranyl acetate in 50% ethanol for 30 min. They were further dehydrated in 70% and 100%

ethanol for 15 min each and immersed in 1:1 ethanol/LR White resin (Polyscience) for 1 hr. Finally, they were embedded in LR White resin for 24 hr at 50°C. Sections were cut with a diamond knife on a Sorvall MT 6000 ultramicrotome and picked up on nickel grids. For antibody labeling, grids bearing sections were floated on drops of primary antibodies (anti-Nef or anti-cytoskeleton) diluted 10- to 20-fold in Tris-buffered saline (TBS, 500 mM NaCl/25 mM Tris, pH 7.6) containing 0.1% fish gelatin and 0.5% bovine serum albumin. Incubation was carried out at 10°C for 16 hr. Grids were rinsed with TBS and floated on gold-conjugated second antibodies (Amersham) diluted 20-fold with TBS containing fish gelatin and bovine serum albumin. Incubation with the gold-conjugated antibody was carried out at 21°C for 3 hr. After thorough rinsing, grids were stained with Reynold's lead citrate before electron microscopic examination. All samples were examined in a Philips EM301 electron microscope operated at 80 kV.

RESULTS

Nef Expression in HPB-ALL Cells. We have established a series of cell populations that constitutively express the *nef* gene of HIV-1 (SF2 isolate; refs. 6 and 22). The human T-cell line HPBALL/*Lnef*SN-S1 was chosen to determine the intracellular distribution of Nef because it is a human CD4⁺ T-cell line susceptible to HIV infection. As shown in Fig. 1, HPBALL/*Lnef*SN-S1 cells express a 27- to 29-kDa protein that reacts specifically with a rabbit anti-Nef antiserum. These cells were originally isolated by fluorescence-activated cell sorting on the basis of their low CD4 cell surface levels (22). A low level of surface CD4 expression correlates with Nef expression and serves as an indicator of the presence of a functional *nef* gene (22, 24).

Localization of Nef by Immunofluorescence. As a prelude to the immunogold/electron microscopy studies to map the subcellular localization of Nef, we performed immunofluorescence studies with a polyclonal anti-Nef antiserum on *nef*⁻ (HPBALL/LN) and *nef*⁺ (HPBALL/*Lnef*SN-S1) cells. As shown in Fig. 2, the cells are generally round and contained a large kidney-shaped nucleus that filled most of the volume of the cell. The cytoplasm was polar and was most abundant near an indentation of the nucleus, typically seen in T cells. In *nef*⁺ cells, the anti-Nef antibody revealed a

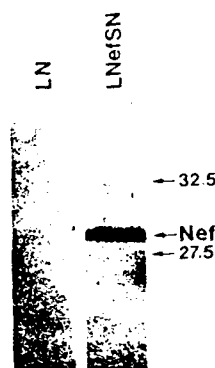


FIG. 1. Specificity of anti-Nef rabbit polyclonal antiserum. Extracts from HPBALL cells transduced with *Lnef*SN or a control vector, LN, were separated by SDS PAGE on 12.5% gels, and Nef was detected by Western blot analysis with a rabbit anti-Nef specific antiserum using alkaline phosphatase-labeled goat anti-rabbit antibodies (heavy chain specific) as described in the text. The position of Nef on the gel is indicated. Positions of prestained molecular mass standards are indicated in kDa.

homogeneous labeling of the cytoplasm (Fig. 2A). In general, the distribution of Nef seems polar but this evidently is due to the polar distribution of the cytoplasm; the thin ring of the cytoplasm surrounding the nucleus, when visible, also showed labeling. The nuclei, in general, showed little or no fluorescence (Fig. 2A). However, focusing of the nuclei at different planes revealed narrow bands of fluorescence in some nuclei (Fig. 2B). These bands were seen in 8 of the 89 nuclei examined and each nucleus showed only one band. The bands are very faint and required long exposures to photograph them. No fluorescence was observed in *nef*⁻ cells incubated with the anti-Nef serum (Fig. 2C) or in *nef*⁺ cells incubated with normal rabbit serum (Fig. 2D), although several hundred of these cells were examined.

Nuclear Localization of Nef by Immunogold Electron Microscopy. The technique used for immunogold labeling was the post-embedding method (27). Fixed and dehydrated cells are embedded in a water-soluble embedding resin (LR White) and sectioned, and sections are incubated with primary and secondary (gold-conjugated) antibodies. We have maintained three sets of controls to ensure the specificity of the antibodies used. First, we performed the immunogold labeling with anti-Nef antibodies using sections of HPBALL/LN control cells (*nef*⁻). As shown in Fig. 3A, the nonspecific binding of the anti-Nef antibodies in these cells was negligible. Second, as a control for nonspecific binding of primary and gold-conjugated secondary antibodies, we performed immunogold labeling on *nef*⁺ (HPBALL/*Lnef*SN-S1) cells using normal

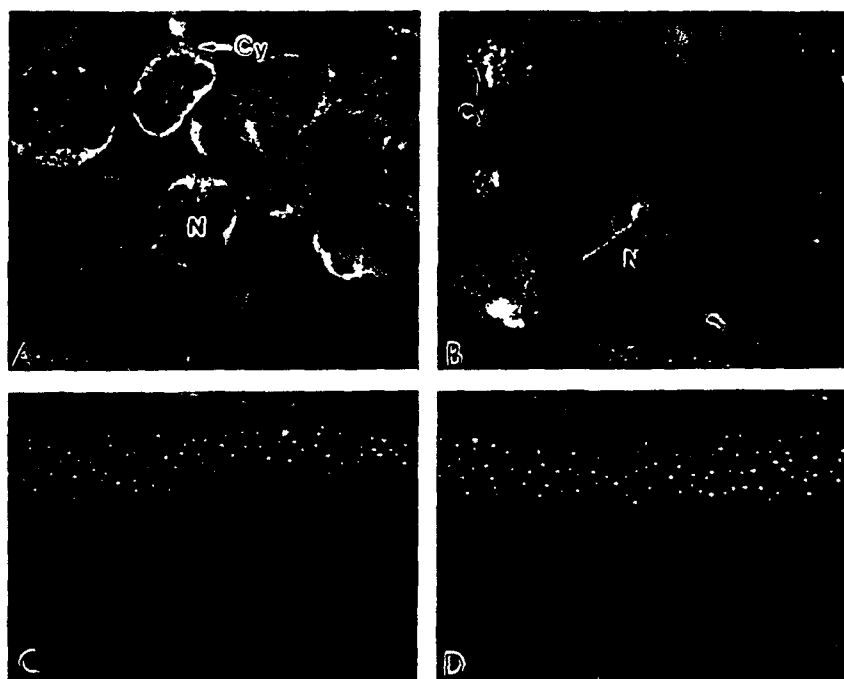


FIG. 2. Immunofluorescence analysis of Nef⁺ (HPBALL/*Lnef*SN-S1) and Nef⁻ (HPBALL/LN) cells with antiserum against Nef. (A) Nef⁺ cells labeled with the anti-Nef antiserum show label in the cytoplasm. (B) The Nef⁺ cells labeled as in A were focused on the interior of the nucleus. Note a fluorescent band across the nucleus. (C) Nef⁻ cells labeled with the anti-Nef antiserum were not labeled. (D) Nef⁺ cells labeled with normal rabbit serum were also not labeled. (×800.)

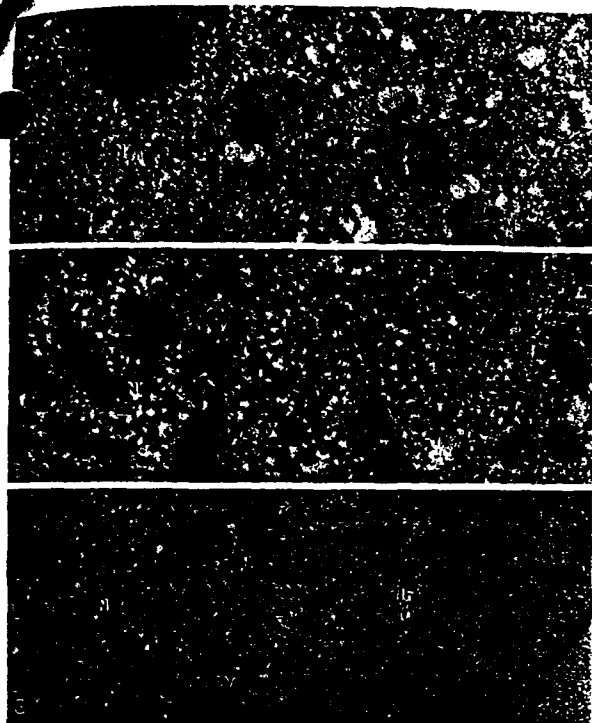


FIG. 3. Electron micrographs of controls for the immunogold labeling technique. (A) *Nef*⁻ cells were incubated with polyclonal anti-Nef antiserum followed by gold-conjugated anti-rabbit antibody. Labeling of cytoplasmic and nuclear components is negligible. (B) *Nef*⁺ cells were incubated with normal rabbit antiserum followed by goat anti-rabbit antibody conjugated with gold particles. No nonspecific labeling of either cytoplasm or nucleus is evident. (C) *Nef*⁺ cells were incubated with a monoclonal anti-intermediate filament (vimentin) antibody followed by gold-conjugated (anti-mouse) second antibodies. The label is seen over intermediate filaments (IF). M, mitochondrion; C, centriole; N, nucleus; Cy, cytoplasm. (A, $\times 8100$; B, $\times 8550$; C, $\times 19,800$.)

rabbit antiserum followed by gold-conjugated anti-rabbit antibody. The results illustrated in Fig. 3B show that neither the rabbit serum proteins nor the secondary antibodies bind nonspecifically to *nef*⁺ cells. Finally, to check for the specificity of labeling of subcellular structures by immunogold labeling method used here, *nef*⁺ cells were labeled with an anti-vimentin (intermediate filament) specific antibody. The intermediate filaments are readily identifiable cytoplasmic structures that provide convenient markers to test the resolution and specificity of immunogold labeling. The results illustrated in Fig. 3C show the exclusive distribution of label over the 10-nm intermediate filaments. Little or no labeling in the nucleus was observed in any of these controls. These studies suggest that the immunogold technique used here provides specific labeling of subcellular structures.

When T cells expressing Nef (HPBALL/L*nef*SN-S1) were examined by the immunogold labeling method, the results were as follows. In a few sections of the nuclei the label due to Nef was detected in highly localized tracks that extended between the nuclear envelope and the nucleoplasm. Fig. 4 illustrates these tracks in sections of three different nuclei (A–C). The longest of the tracks measured about 7 μ m (Fig. 4A) and the tracks appeared to commence/terminate at the cytoplasmic side of the nuclear envelope (Fig. 4B). The tracks were seen in only 4 nuclei among 100 examined and serial sections revealed only one track per nucleus. It is possible that these tracks may occur with greater frequency than that observed but that they are not detectable due to technical reasons. The tracks occur in thin bands and occupy

a fraction of the total nuclear volume and, therefore, their detection would depend on their perfect alignment to the plane of sectioning. In addition to the tracks, a small amount of label is also found in the nucleoplasm but the nucleoli are totally free from the label. These tracks may correspond to the fluorescence bands observed in a few nuclei by the immunofluorescence method (Fig. 2B). A thorough examination of sections of hundreds of nuclei of *nef*⁻ cells incubated with anti-*nef* serum and *nef*⁺ cells incubated with normal serum has failed to reveal any nuclear labeling. In fact there is only one other instance in published literature concerning a nuclear protein that forms tracks in the nucleus. A study by Meier and Blobel (28) has shown that a nucleolar phosphoprotein (Nopp140) of rat liver cells shuttles on tracks that extend between the nucleolus and nuclear pore complexes. The Nef tracks are different from Nopp140 tracks in that they traverse the nucleoplasm with no relationship to the nucleolus.

In the cytoplasm (data not shown) the label due to Nef was most abundant near the indentation of the nucleus as was the case with cells processed by immunofluorescence (see Fig. 2A); this region contained most of the cell organelles, including the microtubule organizing center, Golgi complex, and vesicles.

Do the Nuclear Tracks Represent Cytoskeletal Filaments? It has been hypothesized that the transport of RNA (29, 30) and proteins (28) occurs on specific tracks in the nucleus and that these tracks may be composed of cytoskeletal filaments (e.g., microfilaments, microtubules, or intermediate filaments). To determine if any of these filaments form tracks within the nucleus of T cells, we have conducted immunogold labeling studies with anti-tubulin, anti-vimentin, and anti-actin antibodies. The nuclei remained largely unlabeled with either anti-vimentin (Fig. 3C) or anti-tubulin antibodies (data not shown). However, anti-actin antibodies showed some labeling of the nuclei (Fig. 5). Although not as clear as Nef tracks, the label due to actin showed a preferential alignment in the nucleus. Additionally, short tracks of actin were seen extending between the nuclear envelope and the nucleoplasm (Fig. 5). These results are consistent with previous biochemical evidence for the presence of actin in the nucleus (for references, see ref. 28) and its proposed role in the shuttling of proteins between the nucleus and cytoplasm (28).

DISCUSSION

The *nef* gene is present in HIV and SIV and several functions have been ascribed to it. These functions include a negative effect on HIV replication *in vitro* (31–34), down-regulation of CD4 from the cell surface (8, 22, 24), and binding and hydrolysis of GTP (35). Conflicting reports have also been published questioning the role of Nef in each of the above functions (9, 36). The issue of the biological function of Nef is further complicated by the fact that isoforms of Nef exist that differ either in the primary amino acid sequence or in their posttranslational modification (37) and these isoforms may have different functions.

In an attempt to gain insights into the function of Nef, earlier studies have focused on the intracellular localization of Nef using immunocytochemical studies at the light microscopic level (7, 17–19, 21) and obtained varied results. Initial studies suggested an exclusive cytoplasmic distribution of Nef (7, 17), whereas three recent studies indicated the presence of Nef in the nucleus as well (18, 19, 21). In the present study our objective was to obtain a more precise intracellular localization of Nef using immunogold labeling techniques at the electron microscopic level.

The studies described here have important implications for the function of Nef in HIV-1 life cycle and for the general question of the import of proteins into the nucleus. They have

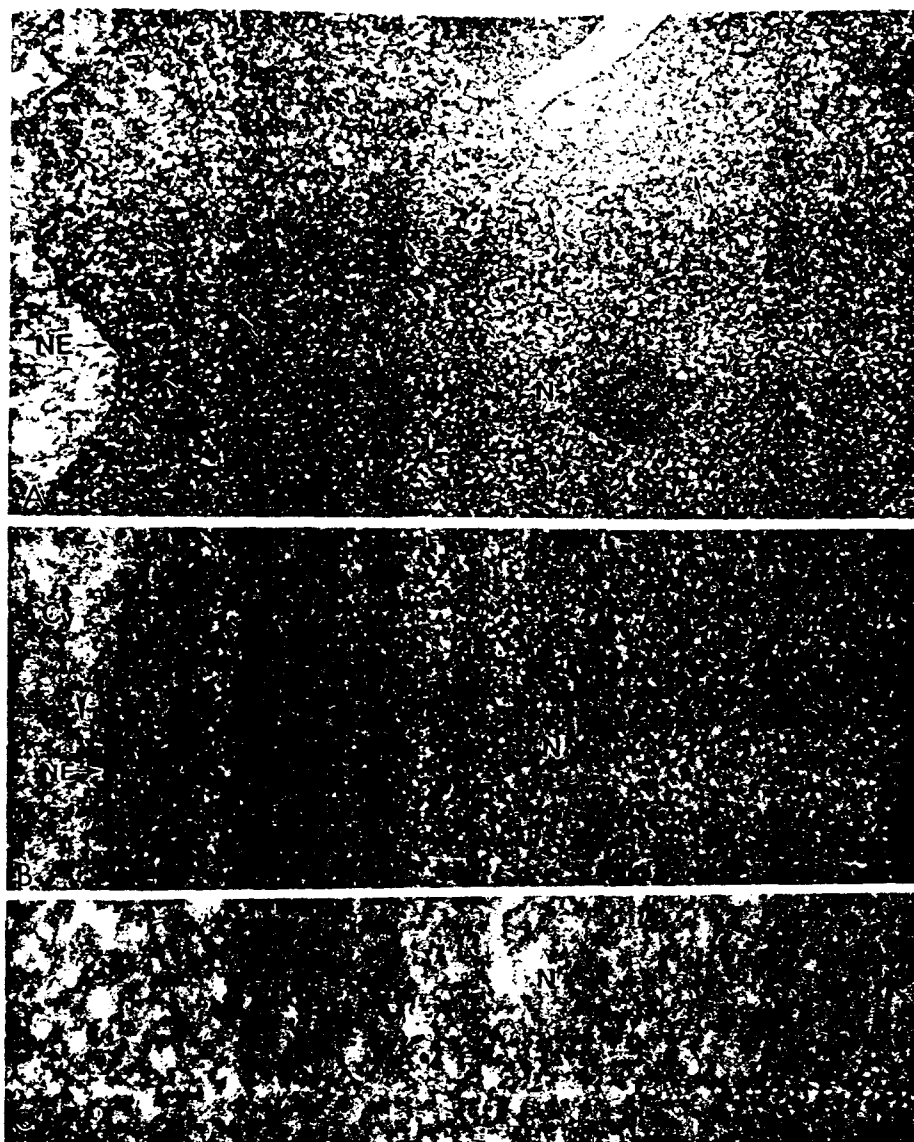


FIG. 4. Electron micrograph showing immunogold labeling of the nuclei of three different *Nef*⁺ cells. Note the tracks of gold particles extending from the nuclear envelope to the nucleoplasm in A and B. (A) Arrows mark the track of *Nef* label. (B) The tracks of *Nef* appear to originate in the cytoplasm (arrowhead). (C) Part of the *Nef* track at high magnification. NE, nuclear envelope; Cy, cytoplasm. (A, $\times 23,800$; B, $\times 30,800$; C, $\times 56,700$.)

shown that a fraction of *Nef* is present in the nucleus and that it occurs in localized tracks within the nucleoplasm. The precise nuclear role of nuclear *Nef* remains unknown but some previous studies have suggested a regulatory role for *Nef* in the HIV gene expression (31–34). The localization of *Nef* in distinct tracks in the nucleoplasm is significant in view of transport of proteins into the nucleus. The first example of a nuclear protein that occurs in tracks is the nucleolar



FIG. 5. Electron micrograph showing immunogold labeling of the nucleus of *Nef*⁺ cells with a monoclonal anti-actin antibody. In the nucleus the actin label shows preferential alignment along tracks. (Inset) Short track of actin label near the nuclear envelope (NE). ($\times 27,000$; Inset, $\times 46,800$.)

phosphoprotein (Nopp140) of rat liver cells (28). Nopp140 binds nuclear localization signal peptides and shuttles between the nucleolus and cytoplasm. Immunogold labeling studies have shown that this protein occurs in tracks that extend from the nuclear envelope to the fibrillar component of the nucleolus. These results led the authors (28) to suggest that Nopp140 shuttles on distinct tracks that may be composed of actin with the motive force for transport being generated by the putative nuclear myosin motors. Although details of the mechanism of nuclear transport remain to be resolved, it appears that most, if not all, macromolecular traffic including that of mRNA molecules (29, 30) proceeds on distinct nuclear pathways. To our knowledge, demonstration of a nucleoplasmic protein on distinct tracks has not been reported previously. The *Nef* tracks in the nucleus remarkably resemble the Nopp140 tracks and, like the latter, may represent nuclear transport pathways. The fact that there is only one *Nef* track per nucleus suggests that *Nef* traverses to the nucleus along a single specific pathway into the nucleoplasm. As has been suggested before for Nopp140 (28), the specificity may reside in the nuclear pore complex to which the protein binds and to which the track is presumably anchored.

Previous studies have shown that the eukaryotic nucleus contains an organized matrix of proteinaceous filament that provides a scaffold for the organization and function of the

nuclear components (for references, see ref. 38). Recent studies have shown that various biochemical reactions, including DNA replication, transcription, and RNA processing, take place on defined regions of the nuclear matrix and the nuclear matrix may also provide tracks for the movement of proteins and RNA transcripts (28–30) in and out of the nucleus. The identity of proteins that compose the nuclear matrix remains to be resolved. Some studies have implicated lamins (proteins of the fibrous lamina beneath the inner nuclear membrane) in forming the nuclear matrix (39); lamins are related to proteins of cytoplasmic intermediate filaments and can form coiled-coil rods, which, in turn, can associate to form higher order structures (40). Another protein that has been detected in the nucleus (for references, see ref. 28) and is believed to compose the matrix is actin. It has also been speculated that actin may provide tracks in the nucleus along which macromolecules move in and out of the nucleus (28). A recent study has demonstrated the affinity of HIV-1 Nef to the cytoskeletal components *in vitro* and *in vivo* (20). All of these findings led us to conduct a preliminary immunogold labeling study to determine if any of the major cytoskeletal proteins occur in tracks within the nucleus. The results suggested that, among the cytoskeletal proteins, actin appears to form short tracks within the nucleus.

The localization of Nef in the nucleus also led us to search for a nuclear localization signal in the *nef* sequence. Since Nef is found in the nucleoplasm and not in the nucleolus, we focused on localization sequences on nucleoplasmic proteins. Previous studies with *Xenopus* oocyte nuclear proteins (nucleoplasmin and N1) have shown that these proteins share a bipartite nuclear targeting motif (41). The motif consists of a 16-amino acid sequence with two basic residues at the amino-terminal end, 10 "spacer" residues, and a cluster of 4 basic residues at the carboxyl-terminal end (see below).

Amino acids in both basic domains are required for nuclear targeting and the transport defect of a mutation in one domain is amplified by a simultaneous mutation in the other. In addition to *Xenopus* proteins, a number of eukaryotic and viral nuclear proteins contain this motif (41). The SF2 clone of Nef used here also shares this motif (24).

Nucleoplasmin	KRpaatkkagqaKKKK
Thyroid α 1	KRvkrklieqnReRRR
Nef-SF2	KRsmgwsaireRmRR

The presence of the nuclear targeting sequence may be required but not sufficient for the nuclear localization of Nef. Indeed, a substantial fraction of Nef appears to be cytoplasmic associating with organelles and cytoskeletal elements, suggesting that it may disrupt host cytoplasmic activities. It is still possible that a fraction of Nef has a nuclear function that is yet to be identified.

We thank Mrs. Glenith Newberry for typing the manuscript. This work was funded in part by Grants CA-59195 from the National Cancer Institute and 1405 and 1559 from the American Foundation for AIDS Research (J.V.G.), Grant FRA-373 from the American Cancer Society and Contract 17-90C-0125 from the U.S. Army (L.R.), Cancer Center Support Grant CA-21765 from the National Institutes of Health to St. Jude Children's Research Hospital, and the American Lebanese Syrian Associated Charities.

1. Cullen, B. R. (1991) *Annu. Rev. Microbiol.* **45**, 219–250.
2. Pavlakakis, G. N. & Felber, B. K. (1990) *New Biol.* **2**, 20–31.
3. Vaishnav, Y. N. & Wong-Staal, F. (1991) *Annu. Rev. Biochem.* **60**, 577–630.
4. Hovanessian, A. G. (1992) *Res. Virol.* **143**, 31–81.
5. Ratner, L., Haseltine, W. A., Patarca, R., Livak, K. J., Starcich, B., Josephs, S. F., Doran, E. A., Rafalski, J. A., Whitehorn, E. A., Baumeister, K., Ivanoff, L., Petteway, S. R., Jr., Pearson, M. L., Lautenberger, J. A., Papas, T. S., Ghayeb, J., Chang, N., Gallo, R. C. & Wong-Staal, F. (1985) *Nature (London)* **313**, 277–284.
6. Sanchez-Pescador, R., Power, M. D., Barr, P. J., Steimer, K. S., Stempien, M. M., Brown-Shimer, S. L., Gee, W. W., Renard, A., Randolph, A., Levy, J. A., Dina, D. & Luciw, P. (1985) *Science* **227**, 484–492.
7. Franchini, G., Robert-Guroff, M., Ghayeb, J., Chang, N. & Wong-Staal, F. (1986) *Virology* **155**, 593–599.
8. Guy, B., Kieny, M. P., Riviere, Y., LePeuch, C., Dott, K., Girard, M., Montagnier, L. & Lecocq, J.-P. (1987) *Nature (London)* **330**, 266–269.
9. Hammes, S., Dixon, E., Malim, M., Cullen, B. & Greene, W. C. (1989) *Proc. Natl. Acad. Sci. USA* **86**, 9549–9553.
10. Kaminski, J., Bashan, N., Itach, A., Sarver, N., Gorecki, M. & Panet, A. (1991) *J. Virol.* **65**, 583–588.
11. Robert-Guroff, M., Popovic, M., Gartner, S., Markham, P., Gallo, R. C. & Reitz, M. S. (1990) *J. Virol.* **64**, 3391–3398.
12. Ameisen, J. C., Guy, B., Chamaret, S., Loche, M., Mouton, Y., Neyrinck, J. L., Khalife, J., Leprevost, C., Beaucaire, G., Boutillon, C., Gras-Masse, H., Maniez, M., Kieny, M. P., Laustriat, D., Berthier, A., Mach, B., Montagnier, L., Lecocq, J. P. & Capron, A. (1989) *AIDS Res. Hum. Retroviruses* **5**, 279–291.
13. Gombert, F. O., Blecha, W., Tähtinen, M., Ranki, A., Pfeifer, S., Troger, W., Braun, R., Müller-Lantzsch, N., Jung, G., Rubsamen-Waigman, H. & Krohn, K. (1990) *Virology* **176**, 458–466.
14. Kirchhoff, F., Vos, G., Nick, S., Stahl-Hennig, C., Coulbaly, C., Frank, R., Jentsch, K. D. & Hunsmann, G. (1991) *Virology* **183**, 267–272.
15. Sabatier, J. M., Clerget-Raslain, B., Fontan, G., Fenouillet, E., Rochat, H., Granier, C., Gluckman, J. C., Van Rietschoten, J., Montagnier, L. & Bahraoui, E. (1989) *AIDS* **3**, 215–220.
16. Kestler, H. W., Ringler, D. J., Mori, K., Panicali, D. L., Shegal, P. K., Daniel, M. D. & Desrosiers, R. C. (1991) *Cell* **65**, 651–662.
17. Hammes, S. R., Dixon, E. P., Malim, M. H., Cullen, B. R. & Greene, W. C. (1989) *Proc. Natl. Acad. Sci. USA* **86**, 9549–9553.
18. Ovod, V., Lagerstedt, A., Ranki, A., Gombert, F. O., Spohn, R., Tähtinen, M., Jung, G. & Krohn, K. J. E. (1991) *AIDS* **6**, 25–34.
19. Kohlisen, B., Neumann, M., Herrman, R., Brack-Werner, R., Krohn, K. J. E., Ovod, V., Ranki, A. & Erfle, V. (1992) *AIDS* **6**, 1427–1436.
20. Neiderman, T. M. J., Hastings, W. R. & Ratner, L. (1993) *Virology* **197**, 420–425.
21. Kienle, N., Bachmann, M., Müller, W. E. G. & Müller-Lantzsch, N. (1992) *Arch. Virol.* **124**, 123–132.
22. Garcia, J. V. & Miller, A. D. (1991) *Nature (London)* **350**, 508–511.
23. Neiderman, T. M. J., Garcia, J. V., Hastings, W. R., Luria, S. & Ratner, L. (1992) *J. Virol.* **66**, 6213–6219.
24. Anderson, S., Shugars, D. C., Swanson, R. & Garcia, J. V., J. *Virol.* **67**, 4923–4931.
25. Murti, K. G., Kaur, K. & Goorha, R. (1992) *Exp. Cell Res.* **202**, 36–44.
26. Murti, K. G., Brown, P. S., Bean, W. J., Jr., & Webster, R. G. (1992) *Virology* **186**, 294–299.
27. Murti, K. G., Davis, D. S. & Kitchingman, G. (1990) *J. Gen. Virol.* **71**, 2847–2857.
28. Meier, U. T. & Blobel, G. (1992) *Cell* **70**, 127–138.
29. Lawrence, J. B., Singer, R. H. & Marselle, L. M. (1989) *Cell* **57**, 493–502.
30. Huang, S. & Spector, D. L. (1991) *Genes Dev.* **5**, 2288–2302.
31. Neiderman, T., Thielan, B. & Ratner, L. (1989) *Proc. Natl. Acad. Sci. USA* **86**, 1128–1132.
32. Ahmad, N. & Venkatesan, S. (1988) *Science* **241**, 1481–1485.
33. Cheng-Mayer, C., Iannello, P., Shaw, K., Luciw, P. & Levy, J. (1989) *Science* **246**, 1629–1632.
34. Luciw, P. A., Cheng-Mayer, C. & Levy, J. A. (1987) *Proc. Natl. Acad. Sci. USA* **84**, 1434–1438.
35. Nebreda, A. R., Bryan, T., Segade, F., Wingfield, P., Venkatesan, S. & Santos, E. (1991) *Virology* **183**, 151–159.
36. Kim, S., Ikeuchi, K., Byrn, R., Groopman, J. & Baltimore, D. (1989) *Proc. Natl. Acad. Sci. USA* **86**, 9544–9548.
37. Ratner, L., Starcich, B., Josephs, S. F., Hahn, B. H., Reddy, E. P., Livak, K. J., Petteway, S. R., Jr., Pearson, M. L., Haseltine, W. A., Arya, S. K. & Wong-Staal, F. (1985) *Nucleic Acids Res.* **13**, 8219–8229.
38. Mirzayan, C., Copeland, C. S. & Snyder, M. (1992) *J. Cell Biol.* **110**, 1319–1332.
39. Gerace, L., Blum, A. & Blobel, G. (1978) *J. Cell Biol.* **79**, 546–566.
40. Aebi, V., Cohn, J., Buhle, L. & Gerace, L. (1986) *Nature (London)* **323**, 560–564.
41. Robbins, J., Dilworth, S. M., Laskey, R. A. & Dingwall, C. (1991) *Cell* **64**, 615–623.

Regulation of Human Immunodeficiency Virus Nef Protein by Phosphorylation

J. C. BANDRES,* S. LURIA,† AND L. RATNER*¹

*Departments of Medicine and Molecular Microbiology, Washington University School of Medicine, St. Louis, Missouri, and

†Department of Biochemistry, Beckman Center, Stanford University Medical Center, Stanford, California

Received November 12, 1993, accepted February 11, 1994

Human immunodeficiency virus isolates express a Nef protein with either an alanine or a threonine at amino acid residue 15. The threonine residue is a site for phosphorylation by protein kinase C. Jurkat T cells constitutively expressing the alanine variant of Nef exhibit the ability to downregulate the induction of transcription factors NF- κ B and AP-1. In contrast, Jurkat cells with the threonine variant of Nef are at least partially restored in their ability to recruit NF- κ B and AP-1. © 1994

Academic Press, Inc.

Human immunodeficiency virus (HIV) "negative factor" (Nef) protein is the product of the *nef* gene, a regulatory gene shown to be dispensable for virus replication *in vitro* (1) but essential for virus pathogenicity *in vivo* in an animal model with simian immunodeficiency virus (2). The mechanism by which Nef affects HIV infection/disease is still poorly understood. Nef has been shown to downregulate surface expression of CD4 in T cells (3, 4). It has also been shown to downregulate transcription factors NF- κ B and AP-1 *in vitro* (5, 6).

Structural studies of Nef have shown that this protein is myristoylated at the N terminus (7), and acylation has been suggested to be important for its association with cell membranes (8, 9). In addition, a potential protein kinase C (PKC) phosphorylation site at threonine 15 of HIV-1 Nef and serine 10 of HIV-2 Nef have been identified (3, 10). These potential phosphorylation sites are homologous to those present in p60^{src} and epidermal growth factor receptor (11). Different Nef variants have an alanine residue at position 15 (Nef 1) or a threonine (Nef 2) (12). Conversion of threonine 15 to an alanine residue results in the loss of Nef phosphorylation (3). Though other Nef phosphorylation sites have been proposed, there is no evidence that they are utilized (12). The current study was undertaken to determine the importance of the threonine 15 phosphorylation site with regards to the ability of Nef to downregulate transcription factors.

Human Jurkat J25 T-cell clonal cell lines were selected after transfection with plasmids containing the gene for either Nef 1 (133, 22D8) or Nef 2 (10H10, 1F8) under the control of the simian virus 40 enhancer and human T-cell leukemia virus promoter as previously described (13). The products Nef 1 and Nef 2 proteins differ at

amino acid positions 15, 29, and 33 (Fig. 1A). Jurkat cell clones were also made with the plasmid with the Nef 1 sequence mutated at position 15 from threonine to alanine [Nef 1 clones 18 and 19], or with the plasmid with the Nef 2 sequence mutated at position 15 from alanine to threonine [Nef 2 clones 13 and 16]. All these clones have been shown previously to show, in the absence of stimulation, minimal LTR-driven activity as well as recruitment of transcriptional factors NF- κ B and AP-1 (defined as the increase in the nuclear fraction of the active forms of these factors). These characteristics are not unique to these cell clones and have also been observed with other Jurkat cell lines (E6-1) and HP-BALL cells (5, 13). In addition, these cell lines respond appropriately to T-cell stimulants including phorbol myristate (PMA), phytohemagglutinin (PHA), antibodies to CD3, antibodies to CD2, as well as antibodies to the T-cell receptor, TNF and IL-1, indicating that their signal transduction pathways are functional.

Figure 1B shows the Western blot analysis of all the cell lines, including the parental cell line 22F6. For this study, cells were kept in log phase growth and immunoprecipitation and immunoblot analysis was performed with a rabbit antiserum as previously described (5). Nef was detected by the rabbit antiserum in all clones except 22F6 and to a similar level.

In order to examine which Nef proteins can be phosphorylated, [³²P]orthophosphate labeling was performed as described (14). Briefly, 10⁷ cells were grown in phosphate-free media for 4 hr and then [³²P]H₂PO₄ (ICN Biochemicals, Irvine, CA) was added at 0.2 mCi/ml. Cells were then stimulated with 50 ng/ml PMA and 13 μ g/ml PHA for 4 hr, or with sterile water as a control. Immunoprecipitation was carried out as above except that phosphatase inhibitors (50 mM NaF, 10 mM Na₂VO₄, and 50 mM β -glycerolphosphate) were added to the RIPA buffer.

¹ To whom correspondence and reprint requests should be addressed.

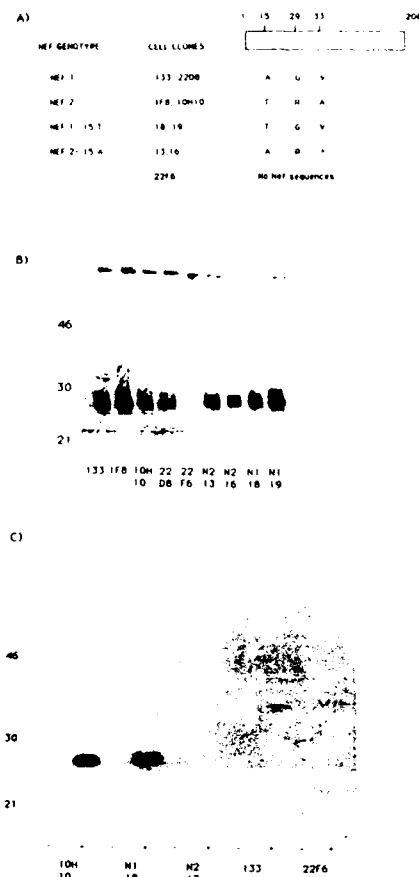


Fig. 1. (A) Structure of Nef expression plasmids. Numbers on top show Nef protein amino acid residues, with number 1 indicating the initiator methionine. Differences in residues between Nef 1 and Nef 2 for the specified positions are indicated for each clone. (B) Western blot analysis of Jurkat cell clone extracts immunoprecipitated with rabbit anti-Nef antiserum (5). These include parental cell line (22F6), Nef 1 expressing clones (133, 22D8), Nef 2 expressing clones (1F8, 10H10), Nef 1 mutants (18, 19), and Nef 2 mutants (13, 16). Positions of molecular weight markers are indicated on the left. (C) Jurkat cell clone extracts after [32 P]orthophosphate labeling and immunoprecipitation with rabbit anti-Nef antiserum. Positions of molecular weight markers (kd) are indicated on the left.

Immunoprecipitates were then analyzed by SDS-PAGE followed by autoradiography. The results are shown in Fig. 1C. Jurkat cells expressing Nef variants carrying a threonine at position 15 (Nef 2 clone 10H10 and mutant Nef 1 clone 18) showed phosphorylation after stimulation with PMA and PHA while neither of the clones with an alanine at position 15 (Nef 1 clone 133, mutant Nef 2 clone 13) showed a significant amount of phosphorylation. No phosphorylation was detected in the absence of PMA and PHA treatment.

To examine the effect of each Nef variant on the recruitment into the nucleus of active transcription factors, electrophoretic mobility shift assays (EMSA) were performed with nuclear extracts prepared from the different Jurkat cell clones, after stimulation with PMA and PHA for 4 hr or after stimulation for the same period of time with sterile saline, as previously described (15, 16). For EMSA double stranded 32 P-labeled oligonucleotides were used which include the binding sites of transcription factors SP-1, NF-kB, and AP-1 (5). Nuclear extracts were normalized for protein concentration with the Bradford reagent (Bio-Rad) using bovine serum albumin as a standard. EMSA was performed using the probe for noninducible transcriptional factor SP-1 to control for the quality of the extracts (Fig. 2A). Recruitment of transcription factors NF-kB and AP-1 in the absence of PMA and PHA stimulation was negligible (data not shown). Figure 2B shows downregulation of NF-kB in Jurkat T cells expressing Nef 1 (22D8, 133) as compared with the parental cell line 22F6. On the contrary, cell clones expressing Nef 2 (1F8, 10H10) showed no difference in NF-kB induction from that of 22F6 cells. Results for AP-1 recruitment are shown in Fig. 2C and were similar to those for NF-kB. AP-1 was downregulated in cells expressing Nef 1 but not in those expressing Nef 2.

Figure 3 shows mobility shift assays in which the comparison is made between parental cell line 22F6, Nef 1 producing cell clone 22D8, and clones 18 and 19 in which the Nef 1 protein has been modified with a threonine instead of an alanine at position 15. SP-1 activity from

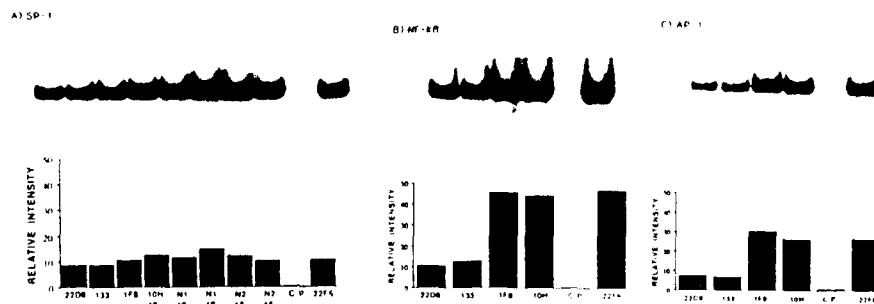


Fig. 2. Electrophoretic mobility shift assays performed from nuclear extracts with 32 P-labeled oligonucleotide probes for binding sites of (A) SP-1, (B) NF-kB, and (C) AP-1. Cell clones: 22F6 (parental cell line), 133 and 22D8 (Nef 1 expressing clone), 1F8 and 10H10 (Nef 2 expressing clone), 18 and 19 (mutant Nef 1 clones), 13 and 16 (mutant Nef 2 clones). C-P, competition by cold probe. The relative intensity of the bands, showing only DNA-protein complexes, was evaluated by laser densitometry (bar graphs). The free probe at the bottom of the gels is not shown. Experiments were performed in duplicate with similar results.

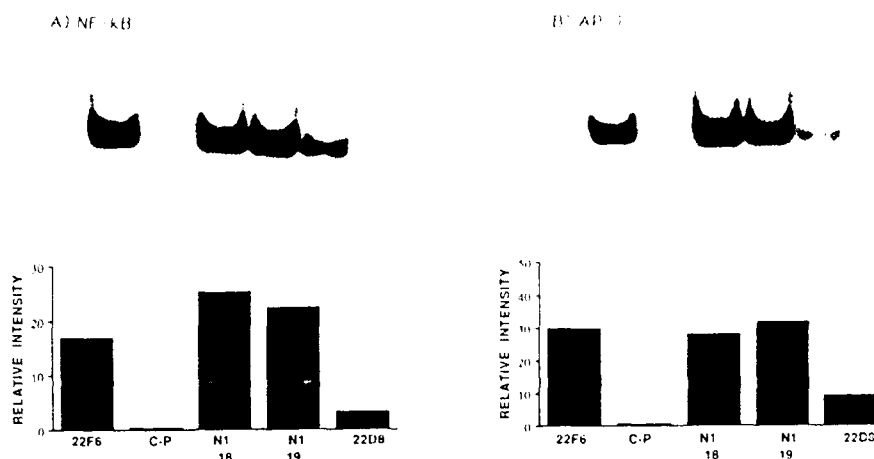


Fig. 3. Electrophoretic mobility shift assays performed from nuclear extracts with 32 P-labeled oligonucleotide probes for binding sites of (A) NF-kB and (B) AP-1. Cell clones: 22F6 (parental cell line), 22D8 (Nef 1 expressing clone), 18 and 19 (Nef 1 mutants). c-P, competition by cold probe. The relative intensity of the bands, showing only DNA-protein complexes, was evaluated by laser densitometry (bar graph). The free probe at the bottom of the gels is not shown. Experiments were performed in duplicate with similar results.

these cell clones is shown in Fig. 2A. NF-kB (Fig. 3A) and AP-1 (Fig. 3B) induction was downregulated in the cells expressing Nef 1 when compared with that of the 22F6 cells. Strikingly, both cell clones 18 and 19 show no effect on NF-kB and AP-1 recruitment when compared with that of the parental cell line 22F6.

Figure 4 shows the comparison between parental cell line 22F6, Nef 2 producing cell clone 1F8, Nef 1 producing clone 133, and clones 13 and 16 in which the Nef 2 protein has been modified with an alanine instead of a threonine at position 15. SP-1 activity for these cell clones is shown in Fig. 2A. NF-kB (Fig. 4A) and AP-1 (Fig. 4B) are both downregulated in the cells expressing Nef 1 (133), while no effect is seen in those expressing Nef 2 (1F8). Clones 13 and 16 showed an intermediate phenotype between that exhibited by Nef 1 and Nef 2. The fact that both clones 13 and 16 showed this intermediate phenotype suggests that other determinants in Nef be-

sides phosphorylation at position 15 are important for Nef-dependent downregulation of transcriptional factors.

To determine if the effects of the changes of amino acid 15 in Nef on transcription factor regulation correlated with transcriptional activity, experiments were performed in which cells were transfected by the DEAE Dextran method (6) with plasmids, which use the long terminal repeat of HIV (HIV-1-CAT) or the IL-2 promoter (IL-2-CAT) to direct expression of the chloramphenicol acetyl transferase (CAT) gene. After stimulation of the cells with PMA and PHA or sterile saline for 4 hr, cell extracts were prepared and CAT activity was assessed by standard methods (17). Samples for the CAT assays were normalized to equal protein concentration by Bradford reagent analysis (Bio-Rad) using bovine serum albumin as a standard. CAT assays from different cell lines were also normalized to a nonirreducible control plasmid RSV-CAT (18) which was transfected in parallel with the HIV-1-CAT

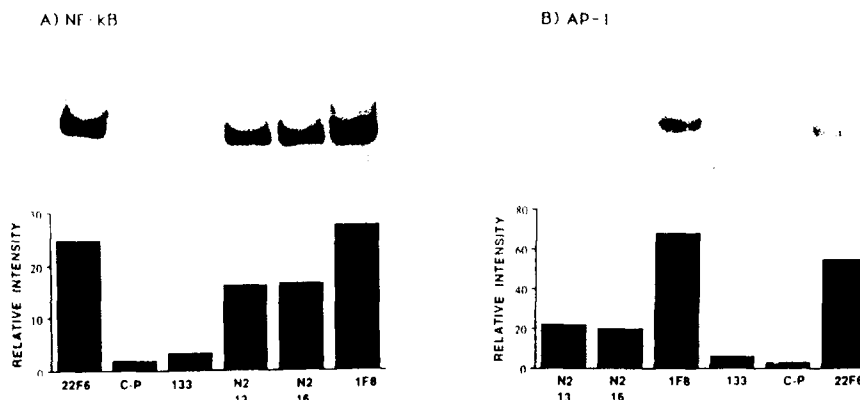


Fig. 4. Electrophoretic mobility shift assays performed from nuclear extracts with 32 P-labeled oligonucleotide probes for binding sites of (A) NF-kB and (B) AP-1. Cell clones: 22F6 (parental cell line), 133 (Nef 1 expressing clone), 1F8 (Nef 2 expressing clone), 13 and 16 (Nef 2 mutants). c-P, competition by cold probe. The relative intensity of the bands, showing only DNA-protein complexes, was evaluated by laser densitometry (bar graph). The free probe at the bottom of the gels is not shown. Experiments were performed in duplicate with similar results.

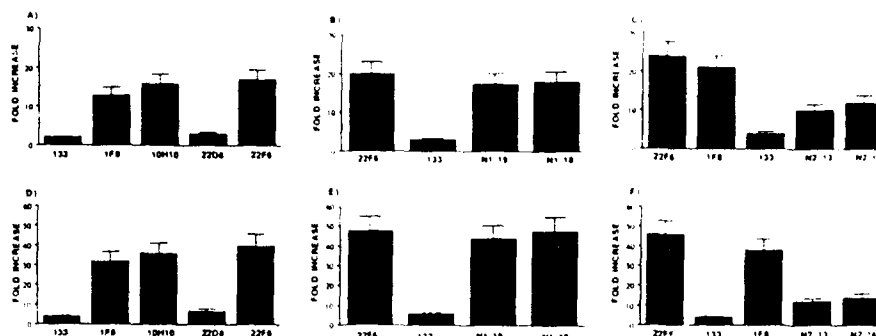


FIG. 5 Chloramphenicol acetyltransferase (CAT) assays for HIV and IL-2 transcription. Extracts were prepared from Jurkat cell clones transfected with HIV-1-CAT (A-C) or IL-2-CAT (D-F). The data are presented as the mean ratio of the level of CAT activity present in the cells stimulated with PMA and PHA for 4 hr compared to the level present in unstimulated cells. The mean values for percentage of acetylation in stimulated cells were 10.2 (22F6), 1.4 (133), 8.7 (N1 19), 9 (N1 18), 8.6 (1F8), 8 (10H10), 5.3 (N2 13), 5.9 (N2 16) for HIV-1-CAT and 22.3 (22F6), 2.6 (133), 22.2 (N1 19), 23.7 (N1 18), 17.5 (1F8), 18.4 (10H10), 3.5 (22D8), 6.3 (N2 13), 7.2 (N2 16) for IL-2-CAT. Experiments were performed in triplicate and error bars represent standard deviation of the mean. Cell clones: 22F6 (parental cell line), 133, 22D8 (Nef 1 expressing clones), 1F8, 10H10 (Nef 2 expressing clones), 13 and 16 (Nef 2 mutants), 18 and 19 (Nef 1 mutants).

and the IL-2-CAT. Figure 5 shows the results of these experiments. The CAT activity measurements closely paralleled the EMSA findings. Unstimulated cells showed almost no CAT activity (data not shown). Figure 5A shows decreased CAT activity in cell clones transfected with HIV-1-CAT in the presence of Nef 1 (22D8, 133) when compared with the parental cell line 22F6. On the other hand, clones expressing Nef 2 (1F8, 10H10) showed no difference in HIV-1-CAT activity as compared with parental cell line 22F6. Figure 5B compares CAT activity in clones transfected with HIV-1-CAT expressing Nef 1 (133) and the parental cell line (22F6) as well as clones 18 and 19 in which Nef 1 protein has been modified to include a threonine at position 15 instead of an alanine. CAT activity was decreased in cells expressing Nef 1 when compared with the parental cell line. Once again, clones 18 and 19 showed no difference in CAT activity when compared with the parental cell line. Figure 5C shows the comparison between clones transfected with HIV-1-CAT expressing Nef 1 (133), Nef 2 (1F8) and the parental cell line 22F6, as well as clones 13 and 16 in which Nef 2 protein was modified to include an alanine at position 15 instead of a threonine. CAT activity was not significantly different between Jurkat cell clones expressing Nef 2 and the parental cell line, while it was clearly decreased in those expressing Nef 1. Clones 13 and 16 expressed an intermediate phenotype. Figures 5D, 5E, and 5F show the results of similar experiments except that the cells were transfected with IL-2-CAT. IL-2-CAT induction was decreased in clones expressing Nef 1, when compared with the parental cell line, while those expressing Nef 2 showed no significant effect on CAT activity. Clones 13 and 16 also showed an intermediate phenotype with regards to IL-2 expression.

HIV-1 Nef protein has been shown to be phosphorylated by PKC at threonine 15 (3). The mutation from threonine to alanine results in loss of this phosphorylation site. This change has no effect on N-terminal myristoylation of

Nef, thus is not likely to affect Nef membrane binding. It also has no effect on downregulation of CD4 expression in T cells (3). The results of our study show that, as in the case of p60^{src}, phosphorylation of Nef results in loss of one of the functions of this protein. Also, the results show that, even though other potential phosphorylation sites have been identified in Nef (12), the predominant site of Nef phosphorylation upon stimulation of T cells is the threonine at position 15. We have shown elsewhere (19) that downregulation of transcription factor NF- κ B by Nef occurs through a PKC-dependent mechanism. The combination of these data presents a model for a unique system by which a protein acts through a pathway that uses a protein kinase as an intermediate for its function, and the same protein kinase regulates the presence of the active form of the protein. Furthermore, it has also recently been shown that Nef associates with the cytoskeleton (20) and may also localize in specific "channels" in the nucleus (21). Whether the localization of Nef and its availability for phosphorylation by PKC are related is so far unknown. However, it is intriguing that the PKC phosphorylation site lies within the potential bipartite nuclear localization signal and, therefore, may alter its activity.

The results of this study provide new insights into structural aspects of Nef, and their importance with respect to one of the functions of Nef *in vitro*.

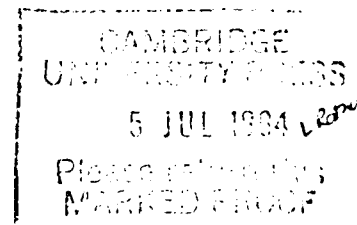
ACKNOWLEDGMENTS

We thank Ms. Lisa Westfield and Dr. Evan Sadler for oligonucleotide synthesis and William R. Hastings for technical assistance. This work was supported by U.S. Army Grant DAMD 17-92-0-0125 to R. and A.C. Grant 554170.

REFERENCES

1. Ewing, A. G., Ratner, L., Musy, R., Maer, J. L., Harker, M. L., Broder, S., Gallo, R. C., and Wong-Staal, F. Science 233, 655-659 (1986).

2. KESTLER, H. W., RINGLER, D. J., MORI, K., PANICELLI, D. L., SEHGAL, P. K., DANIEL, M. H., and DESROSIER, R. C., *Cell* **65**, 651-662 (1991).
3. GUY, B., KIENY, M. P., RIVIERE, Y., LEPEUCH, C., DOTT, K., GIRARD, M., MONTAIGNER, L., and LECOCO, J. P., *Nature* **330**, 266-269 (1987).
4. GARCIA, J. V., and MILLER, A. D., *Nature* **350**, 508-511 (1991).
5. NIEDERMAN, T. M., J., GARCIA, J. V., HASTINGS, W. R., LURIA, S., and RATNER, L., *J. Virol.* **66**, 6213-6219 (1992).
6. NIEDERMAN, T. M. J., HASTINGS, W. R., LURIA, S., BANDRES, J. C., and RATNER, L., *Virology* **194**, 338-344 (1993).
7. ALLAN, J. S., COLIGAN, J. E., LEE, T. H., MCLANE, M. F., KANKI, D. J., GROOPMAN, J. E., and ESSEX, M., *Science* **230**, 810-813 (1985).
8. KAMINCHIK, J., BASHAN, N., ITACH, A., SARVER, N., GORECKI, M., PANET, A., *J. Virol.* **65**, 583-588 (1991).
9. YU, G. and FELSTED, R. L., *Virology* **187**, 156-164 (1992).
10. SAMUEL, K. P., SETH, A., KONOPKA, A., LAUTENBERGER, J. A., and PAPAS, T. S., *FEBS Lett.* **218**, 81-86 (1987).
11. GOULD, K. L., WOODGET, J. R., COOPER, J. A., BUSS, J. E., SHALLOWAY, D., and HUNTER, T., *Cell* **42**, 849-857 (1985).
12. SHUGARS, D. C., SMITH, M. S., GLUECK, D. H., NANETERMET, P. V., SEILLIER-MOISEWISCH, F., and SWANSTROM, R., *J. Virol.* **67**, 4639-4650 (1993).
13. LURIA, S., CHAMBERS, I., and BERG, P., *Proc. Natl. Acad. Sci. USA* **88**, 5326-5330 (1991).
14. BEG, A. A., FINCO, T. S., NANETERMET, P. V., and BALDWIN, A. S., JR., *Mol. Cell. Biol.* **13**, 3301-3310 (1993).
15. DIGNAM, J. D., LEBOWITZ, R. M., and ROEDER, R. G., *Nucleic Acids Res.* **11**, 1475-1489 (1983).
16. MONTMINY, M. R., and BILEZIKJIAN, L. M., *Nature (London)* **328**, 175-178 (1987).
17. GORMAN, C. M., MOFFAT, L. F., and HOWARD, P. H., *Mol. Cell. Biol.* **2**, 1044-1051 (1982).
18. GORMAN, C. M., MERLING, G. T., WILLINGHAM, M. C., PASTAN, I., and HOWARD, B. H., *Proc. Natl. Acad. Sci. USA* **79**, 6777-6781 (1982).
19. BANDRES, J. C., and RATNER, L., *J. Virol.*, in press.
20. NIEDERMAN, T. M. J., HASTINGS, W. R., and RATNER, L., *Virology* **197**, 420-425 (1993).
21. MURTI, K. G., BROWN, P. S., RATNER, L., and GARCIA, J. V., *Proc. Natl. Acad. Sci. USA* **90**, 11895-11899 (1993).



Particle assembly and Vpr expression in human immunodeficiency virus type 1-infected cells demonstrated by immunoelectron microscopy

Jaang J. Wang,^{1,2} Yuh-ling Lu³ and Lee Ratner^{3*}

¹ Department of Biology and Anatomy, National Defense Medical Center, Taipei, ² Institute of Biomedical Sciences, Academia Sinica, Taipei, Taiwan, Republic of China and ³ Departments of Medicine and Molecular Microbiology, Washington University, St Louis, Missouri 63110, U.S.A.

The 96 amino acid viral protein R (Vpr) of human immunodeficiency virus type 1 (HIV-1) was detected during virus assembly in intracellular vacuoles and at the plasma membrane on peripheral blood mononuclear cells. In both immature and mature virus particles, Vpr was located immediately beneath the viral envelope, co-localizing with the core structural protein, Gag p24. Vpr was present in intracellular HIV-1 wild-type virions at 50% of the level found in extracellular HIV-1 particles. Cells infected with HIV-1 strains with C-terminal truncations of Vpr manifested a different pattern of Vpr

expression. A mutant with an alteration of amino acids 79 to 85 exhibited a 23% reduction in total levels of Vpr expression, but a marked accumulation of Vpr in intracellular rather than extracellular virions. A mutant with the last 17 amino acids of Vpr deleted expressed only 10% of wild-type levels of Vpr. These observations indicate that Vpr is incorporated into virions from the cytoplasmic aspect of either the vacuolar or plasma membrane. Furthermore, the proportion of Vpr on intracellular compared to extracellular virions is affected by a specific locus within the protein.

Introduction

Human immunodeficiency virus (HIV) is released from the host cell surface by budding from the plasma membrane (Gelderblom, 1991). The budding process releases immature virus particles containing a non-condensed core of Gag precursor proteins, together with the RNA genome and viral enzymes necessary for initiation of replication, all enclosed within a lipid bilayer containing the envelope proteins. Maturation of the virus particle, associated with viral protease activity, results in condensation of the particle core.

Viral protein R (Vpr) is incorporated into the virion. This involves an association of Vpr with the C terminus of the Gag precursor protein, Pr55^{gag} (Cohen *et al.*, 1990b; Yuan *et al.*, 1990; Lu *et al.*, 1993; Paxton *et al.*, 1993). Vpr is one of seven regulatory proteins expressed by all HIV types and simian immunodeficiency virus (Rosen, 1991). It encodes a 96 amino acid protein that is dispensable for virus replication in T lymphoid cell lines (Dedera *et al.*, 1989). However, Vpr accelerates HIV-1 replication about threefold in a variety of T lymphoid cell lines, and to a significantly greater degree in primary macrophages (Ogawa *et al.*, 1989; Hattori *et al.*, 1990; Westervelt *et al.*, 1992). Vpr has also been shown to increase gene expression non-specifically by threefold from a wide range of transcriptional promoters, by a

mechanism that remains to be defined (Cohen *et al.*, 1990a). The packaging of Vpr into the virions suggests that this protein plays an important role in virus assembly or infectivity (Cohen *et al.*, 1990a; Yuan *et al.*, 1990).

The subcellular localization of Vpr in infected cells has been determined by subcellular fractionation and indirect immunofluorescence microscopy (Lu *et al.*, 1993). These data suggest that Vpr expression in the absence of other viral proteins results in a predominant localization in the nucleus. However, coexpression of Gag Pr55^{gag} results in the release of a portion of the expressed Vpr protein in extracellular virions. In the present study, we defined more carefully the localization of Vpr during virus assembly at both intracellular and extracellular sites using wild-type and mutants forms of Vpr with a double immunogold electron microscopic labelling technique.

Methods

Cell lines and culture. COS-7 cells were obtained from the ATCC and maintained in Dulbecco's modified Eagle's medium supplemented with heat-inactivated fetal calf serum, 1 mM-pyruvate, 100 units/ml penicillin and 100 µg/ml streptomycin. Peripheral blood mononuclear cells (PBMCs) were purified from normal human leukocytes by centrifugation onto Ficoll. After 3 days of stimulation with phytohaemagglutinin (15 µg/ml; Sigma), PBMCs were maintained in RPMI 1640 medium supplemented with 10% heat-inactivated fetal calf serum, 4 mM-glutamine, recombinant interleukin 2 (50 units/ml; Cetus), 100 units/ml penicillin and 100 µg/ml streptomycin.

mutants. HIV-1 mutant SRIG was made from a proviral clone, NLHXADA(GG), which expresses a 96 amino acid form of Vpr (Scherfeld *et al.*, 1992). In this mutant four amino acids of Vpr, residues 79 to 82, numbered according to Myers *et al.*, 1992), Ser-Arg-Gly, were deleted and the Arg at position 85 was changed to Gln. The mutant was made by inserting the sequence 5' TCGACATGTTA-CTCAACAGAGGAGAGCAAGAAACGGAGCCAGTAGATCT-TAG 3' into the *Sa*I site at nucleotide 5785 by linker ligation. The mutant CRST, in which residues 80 to 96 of Vpr were deleted, was constructed by digestion of NLHXADA(GG) with *Sa*I and blunt-ending with the Klenow fragment of *Escherichia coli* DNA polymerase I. The C-terminal amino acid sequence of wild-type Vpr and the mutants, SRIG and CRST, are shown below (the substituted amino acids are shown underlined).

WT HFRIGCRHSR IGVTQ QRRAR NGASRS
 SRIG HFRIGCRH VTQ QRRAR NGASRS
 CRST HFRIGCRST

Place numbers over indicated residues

Put under identical residues on line above

no space

only underline T

Virus infection. HIV-1 stocks were generated by transfection of 60% confluent cos-7 cells in 10 cm-diameter plates with 10 µg of the recombinant proviral clones NLHXADA(GG), SRIG or CRST together with 2 µg of pCV1, a *tat* expression vector (Arya *et al.*, 1985). The calcium phosphate precipitation method was used for transfection, and 5 hours later the cells were treated with 10% DMSO for 2 min before being washed twice with PBS. Cell culture supernatants were harvested after 48 h and filtered (0.2 µm Millipore filter). Culture supernatant (5 ml) was used to infect 1×10^7 PBMCs. The cells were collected as pellets 7 days post-infection. After washing with serum-free culture medium, the cells were fixed in freshly prepared 2.5% glutaraldehyde in PBS for 30 min at room temperature. After fixation, the cells were washed in PBS overnight, dehydrated in graded concentrations of ethanol and then embedded in LR white acrylic resin (Strasny & Gay, 1991).

Post-embedding immunoelectron microscopy. Sections of resin containing the cells, with a thickness of 100 nm, were collected on 270-mesh nickel or gold grids for immunocytochemical analysis (Gelderblom *et al.*, 1987; Gelderblom, 1991). The sections were etched with freshly prepared 5% H_2O_2 for 5 to 10 min in a vacuum chamber. Non-specific binding was blocked with 1% BSA. Vpr rabbit antiserum was prepared as previously described (Lu *et al.*, 1993). The mouse monoclonal antibody C246, which reacts to Gag p24, was kindly provided by T.-W. Chang. The sheep antibody to Env gp120 was obtained from BioCell. For dual labelling, the anti-Vpr antiserum was added first and incubated at 20 °C for 1 h, followed by a wash with PBS, and then the mouse anti-Gag p24 or sheep anti-Env gp120 was applied. The cells were then washed in Tris-buffered saline (TBS) and 15 nm gold particle-conjugated goat anti-rabbit IgG (Auoprobe EM; Amsterdam) and either 5 nm gold particle-conjugated goat anti-mouse IgG (Amersham) or 10 nm gold particle-conjugated donkey anti-sheep IgG (BioCell) were added. Sections were stained with uranyl acetate and lead citrate and examined under a Zeiss electron microscope.

Results

Expression of wild-type and mutant Vpr proteins

HIV-1 strains capable of encoding a full-length Vpr protein, or mutated forms of Vpr with deletions were used in this study. To confirm that the mutations gave rise to proteins of the predicted M_r and with similar stability and antibody reactivity, the wild-type and

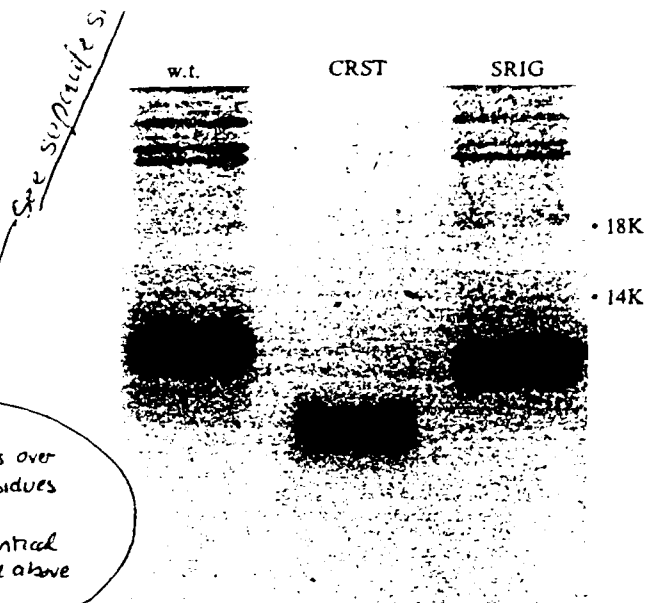


Fig. 1. Expression of wild-type (w.t.) and mutant forms of Vpr protein. Each *vpr* gene was cloned into plasmid pTM3 between *Nco*I and *Sac*I sites downstream of the T7 promoter. The plasmids were transfected into BSC-40 cells infected with vTF7-3, a recombinant vaccinia virus expressing T7 polymerase. After 4 h, the cells were labelled with [3 H]leucine overnight, and cell lysates were immunoprecipitated with the anti-Vpr antiserum. The differences in M_r are consistent with deletion of four amino acids in SRIG and deletion of 17 amino acids in CRST.

mutated (CRST and SRIG) *vpr* genes were cloned into a recombinant vaccinia virus expression system. After expression in BSC-40 cells, the specific Vpr proteins were immunoprecipitated with a rabbit anti-Vpr antiserum and analysed by PAGE (Fig. 1). The electrophoretic mobility of wild-type Vpr was consistent with a protein of 11.4K, slightly larger than that predicted for a 96 amino acid protein, but consistent with other studies of Vpr (Lu *et al.*, 1993; Paxton *et al.*, 1993). Mutant Vpr protein from SRIG has a deletion of four amino acids and an electrophoretic mobility that was consistent with a decrease of 1K in M_r , compared to the wild-type. Mutant Vpr protein from CRST has a deletion of 17 amino acids, and an electrophoretic mobility consistent with a decrease of 3K. All three *vpr* gene products reacted with the rabbit polyclonal anti-Vpr antiserum.

Vpr expression in intracellular and extracellular virions

HIV-1 infection of primary PBMCs was examined by immunogold electron microscopy. Virus particles were found budding at the plasma membrane (Fig. 2a) and within intracellular vacuoles (Fig. 2a, b). Budding virus particles at intracellular membranes were also

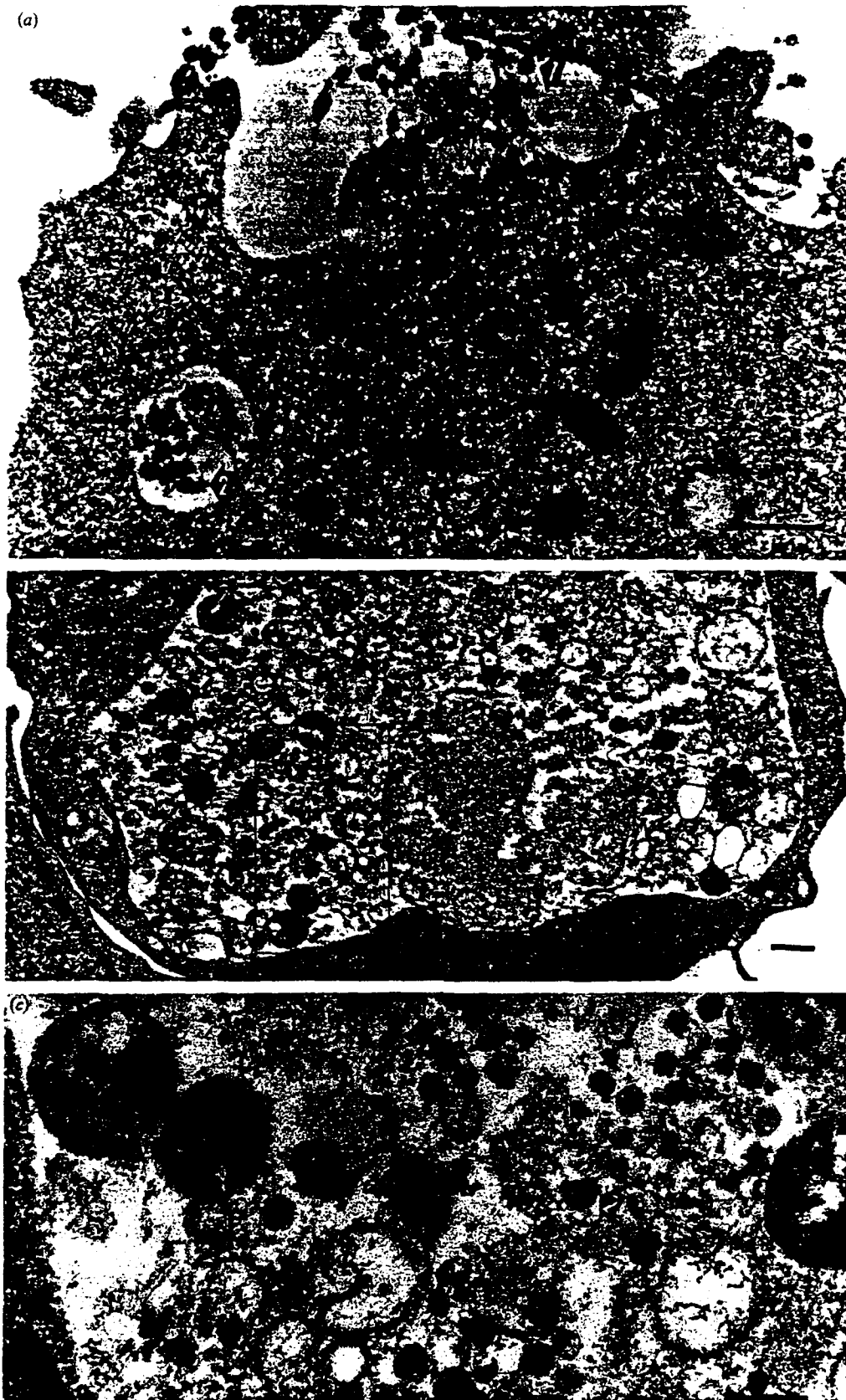


Fig. 2. Immunogold localization of Vpr in virus particles. (a) Vpr-specific gold particles were seen in the wild-type HIV-1 virions in the extracellular region (arrow 1) and in a cytoplasmic vacuole (arrow 2). Labelling was also found at a portion of the vacuolar membrane that showed higher density, consistent with that of a budding virus particle (arrow 3). The bar represents 500 nm. (b) Vpr-specific gold labelled particles (15 nm diameter; arrowhead) were found in a large vacuole of an infected PBMC. N, nucleus. The bar represents 500 nm. (c) An enlarged area of the vacuole (boxed) in (b) is shown (rotated 90°) with Vpr-specific gold particles (15 nm

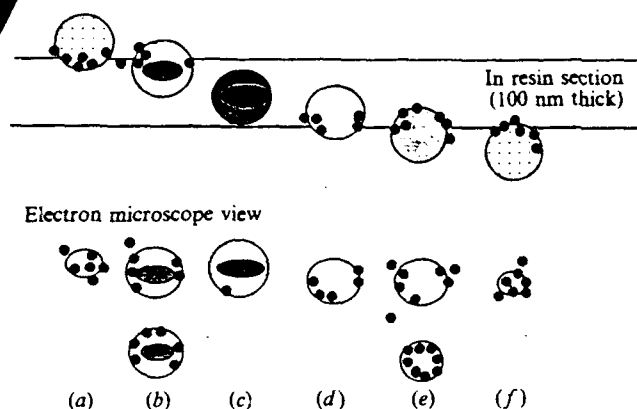


Fig. 3. Schematic representation of possible locations of Vpr-specific gold particles in HIV-1 virions embedded in thin resin sections. HIV-1 virions associated with infected cells were embedded in resin and cut into sections of 100 nm in thickness for post-embedding immunostaining and electron microscopic observations. Virions located at the upper (a) or lower portion of the section (f) would have been cut tangentially and the exposed Vpr antigen could be labelled with the antibody if Vpr was situated near or beneath the viral envelope. These virions would be predicted to appear smaller under the electron microscope and the gold particles would form a cluster. Virions cut through the centre would be predicted to appear larger and gold particles would form a ring-shaped pattern with (b) or without a core (d and e). The diameter of these virions would appear to be similar to that of typical virions. Virions embedded within the resin would not be accessible to H_2O_2 etching and their associated antigens would not be exposed. A typical virion diameter is approximately 100 nm.

immunogold-labelled with the anti-Vpr antiserum (Fig. 2a). Particles at both sites were Vpr-positive, as indicated by indirect immunolabelling with gold particles. No significant background labelling was seen in the absence of HIV-1, or when the Vpr antiserum was omitted or substituted with a Vpx antiserum (data not shown).

The diameter of the virions was about 100 nm. With 100 nm-thick sections, the virus particles may be cut at different levels, as shown schematically in Fig. 3. Sections through the mid-portion of the virion would be predicted to show immunogold labelling in a ring-like pattern if

Vpr was situated primarily just beneath the viral envelope (Fig. 3b, e). With sections near the edge of a virion (Fig. 3a, f), immunogold labelling of protein just beneath the viral envelope would be predicted to cause clusters of gold particles. Several examples of such gold particle distributions are evident in Fig. 2(c).

Vpr expression during virus budding

Vpr gold labelling was also identified on virus particles budding from the plasma membrane (Fig. 4). Immunolabelled Vpr could be identified on the condensed membrane areas of budding (Fig. 4a, b) and beneath the virus envelope of immature virus particles (Fig. 4b to f). In some cases, a ring-shaped distribution of gold-labelled Vpr was evident (Fig. 4d, f). In dual labelling experiments, gold particles (15 nm) specific for Vpr were found beneath the virus envelope, whereas Gag p24-specific gold particles (5 nm) were generally seen in the core of the virion (Fig. 4d to f).

Wild-type and mutant Vpr expression in virions

Virions containing the 96 amino acid wild-type Vpr protein as well as deletion mutants with alterations between amino acids 79 and 85 (SRIG) or a truncation mutant missing the C-terminal 17 amino acids (CRST) were also examined. SRIG virions (Fig. 5b) contained Vpr-specific gold particles in a similar distribution to that of wild-type virions (Fig. 5a). However, CRST virions contained very few Vpr-specific gold particles (Fig. 5c).

Quantification of Vpr-specific gold particles was performed on several hundred electron micrographs and the number of intracellular and extracellular particles per virion determined (Table 1, Fig. 6). Wild-type virions were labelled with an average of 1.5 Vpr-specific gold particles per virion, whereas SRIG virions had an average of 1.1 particles per virion and CRST virions contained only 0.1 particles per virion. Since both Vpr mutants are

Table 1. Distribution of Vpr-specific gold particles on HIV-1 in PBMCs 7 days after infection

Sample (number)*	Number of particles	Number of virions	Average particles per virion	Percentage of wild-type	Particles per virion (extra-cellular)	Particles per virion (intra-cellular)
Wild-type (83)	6683	4467	1.5	100	1.6	0.8
SRIG (33)	1482	1292	1.1	77	0.4	0.9
CRST (12)	65	639	0.1	7	ND†	ND
Control (5)	12	550	0	1	ND	ND

* Number of micrographs examined.

† ND, Not detected.

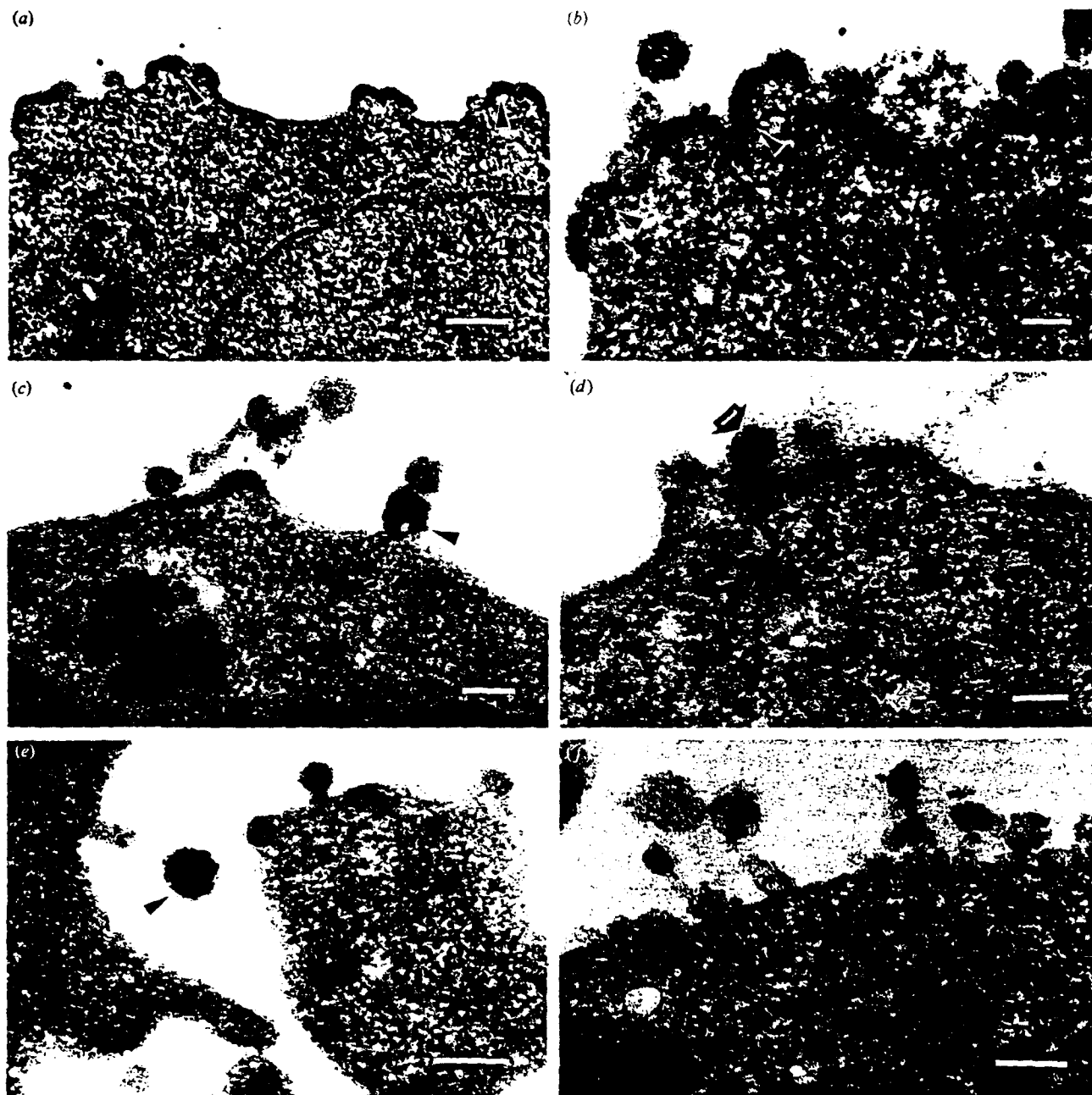


Fig. 4. Vpr localization on budding virus particles. (a) Condensed plasma membrane structures are immunolabelled with Vpr-specific gold particles (arrowheads). The bar represents 200 nm. (b) Virus budding from a condensed area of the cell membrane was labelled with Vpr-specific gold particles (arrowheads). A single extracellular immature virion labelled weakly with these particles (15 nm), but better labelling with Gag p24-specific gold particles (5 nm) was observed. The bar represents 100 nm. (c) Other immature virions immunolabelled with Vpr-specific gold particles (arrowhead). The bar represents 100 nm. (d) Additional immature virions labelled with Vpr-specific gold particles (15 nm, arrow 1) under the virus envelope as well as Gag p24-specific gold particles (5 nm, arrow 2). (e) An immature virion near the cell surface was identified that labelled with Vpr-specific gold particles under the viral envelope (15 nm, arrowhead), whereas Gag p24-specific gold particles (5 nm) were seen in the central area of the virion. The bar represents 200 nm. (f) A ring-shaped distribution of Vpr-specific gold particles (15 nm) was evident on an extracellular virus particle, with Gag p24-specific gold particles (5 nm) localized in the central core of the virion.

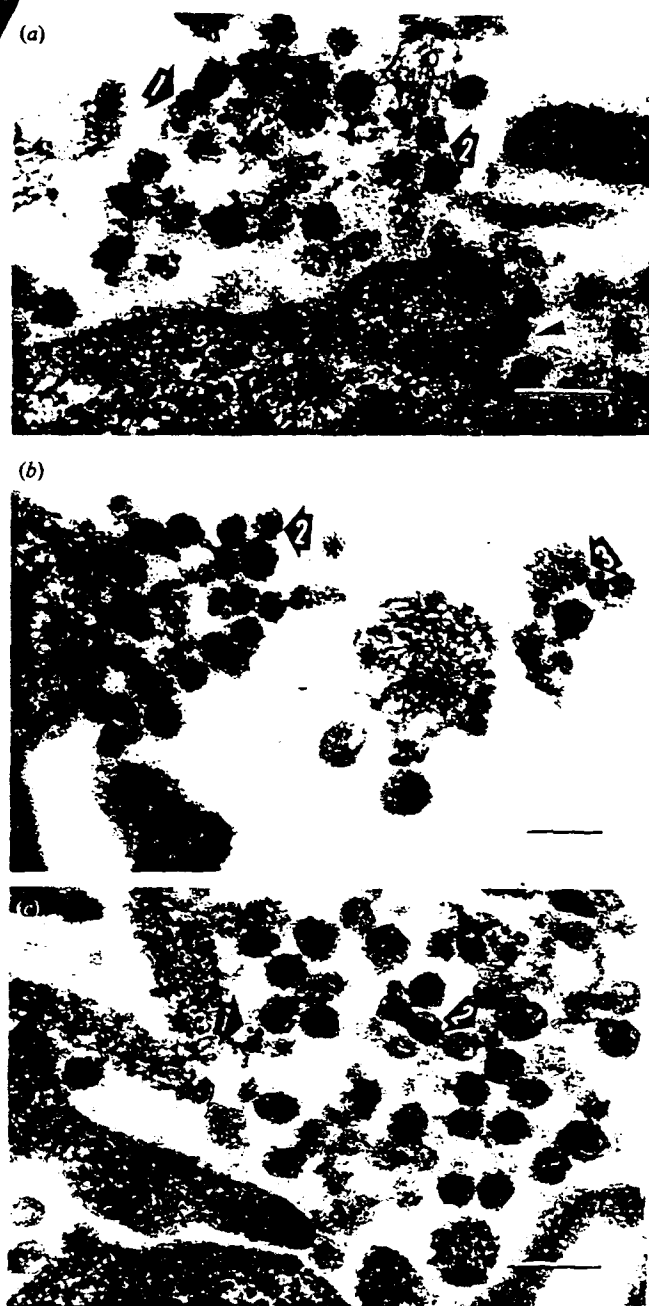


Fig. 5. Immunolabelling of wild-type and mutant forms of Vpr on HIV-1 virions. (a) Vpr-specific gold particles labelled extracellular wild-type virions (15 nm, arrow 1). Gag p24-specific gold particles (5 nm, arrow 2) were also observed in virions. An average of 1.5 Vpr-specific gold particles per virion was found. The bar represents 200 nm. (b) Vpr mutant SRIG virions also labelled with Vpr-specific gold particles (15 nm, arrow 1). Gag p24-specific gold particles (5 nm, arrow 2) and Env gp120-specific gold particles (10 nm, arrow 3) were also identified. An average of 1.1 Vpr-specific gold particles per virion was measured. The bar represents 200 nm. (c) Vpr mutant CRST virions showed very little Vpr-specific labelling (arrow 1), whereas Gag p24-specific gold particles were still observed (5 nm, arrow 2). An average of 0.1 Vpr-specific gold particles per virion was counted. The bar represents 200 nm.

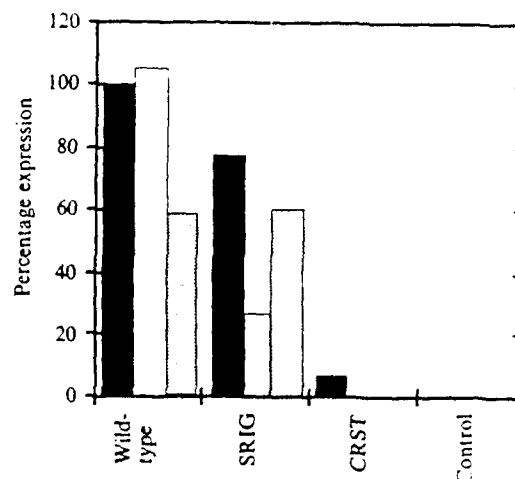


Fig. 6. Wild-type and mutant Vpr expression in virions as a percentage of the total expression in the wild-type in HIV-1-infected PBMCs infected for 7 days. Extracellular (□) and intracellular (■) Vpr expression are shown, together with the average number of Vpr-specific gold particles (on both extracellular and intracellular virions) as a percentage of the wild-type (■).

recognized by the Vpr-antiserum (Fig. 1; J. J. Wang *et al.*, unpublished results), the lower number of Vpr-specific gold particles on CRST virions must be due to lower expression of the mutant protein in the virion, rather than a loss of immunogenicity.

With the wild-type, intracellular virions contained about half the number of Vpr-specific gold particles per virion compared to extracellular virions (Table 1, Fig. 6). In contrast, SRIG intracellular virions were immunolabelled to a greater extent with the Vpr antiserum than SRIG extracellular virions. The primary difference in SRIG virions compared to wild-type virions is a result of the much lower level of Vpr-specific gold particles in extracellular virions (0.4 for SRIG compared to 1.6 for wild-type), whereas no significant differences were seen in the number of these particles in intracellular virions (0.9 for SRIG and 0.8 for wild-type).

Discussion

The current findings demonstrate that HIV-1 virions assemble in infected PBMCs by budding into cytoplasmic vacuoles and by budding from the plasma membrane. Other investigators have also noted HIV-1 virions budding into cytoplasmic vacuoles of infected primary monocytes (Orenstein *et al.*, 1988), the U937 monocytoid cell line (Pautrat *et al.*, 1990) and the JM T lymphoid cell line (Grief *et al.*, 1991). Orenstein *et al.* (1988) and Grief *et al.* (1991) identified these cytoplasmic vacuoles as Golgi saccules. Our observations of HIV-1-infected PBMCs failed to identify virions associated with typical Golgi apparatus. However, it is possible that the

cytoplasmic vacuoles associated with HIV-1 virions in PBMCs are derived from the endoplasmic reticulum or Golgi saccules. Dual-labelling immunogold electron microscopy experiments should be useful in further characterizing the cellular compartment involved.

The Vpr protein was detected by immunogold electron microscopy at sites of virus budding, intracellularly as well as at the plasma membrane, in both immature and mature virions. Our triple immunolabelling studies demonstrated the localization of Vpr, Gag p24 and Env gp120 proteins in virions. Lower levels of Gag immunolabelling than Vpr are a consequence of the use of a monoclonal antibody for Gag p24, whose epitope is more easily lost during fixation than the multiple epitopes recognized by the anti-Vpr antiserum. The low intensity of gp120 labelling in this study is consistent with previous studies and reflects a lower level of gp120 than p24 incorporation into virions (Hausmann *et al.*, 1987; Hart *et al.*, 1993). In virions, Vpr was generally localized beneath the viral envelope. This is consistent with biochemical data suggesting that Vpr packaging into virions is mediated by an interaction with the C-terminal portion of the Gag precursor protein, which is cleaved into the p6 protein (Lu *et al.*, 1993; Paxton *et al.*, 1993). Though the function of the Gag p6 protein is unclear, it has been proposed to make up a core-envelope linker, situated just beneath the virus envelope (Gelderblom *et al.*, 1987).

Mutations in *vpr* had relatively minor effects on virus replication in PBMCs (Dedera *et al.*, 1989; Ogawa *et al.*, 1989; J. J. Wang *et al.*, unpublished results). However, virions derived from a HIV-1 strain in which the C-terminal 17 amino acids of Vpr were deleted (CRST) exhibited markedly decreased levels of virion-associated Vpr. This finding is attributed to a reduction in Vpr packaging into virus particles, but additional defects in Vpr transport or stability cannot be excluded.

A mutant Vpr protein (SRIG), in which residues 79 to 85 were altered, was packaged normally into virions at intracellular sites, but was partially defective in incorporation into virions budding at the plasma membrane. Whereas the ratio of full-length Vpr incorporation into extracellular versus intracellular virions was approximately 1.6, the ratio for the SRIG mutant Vpr was 0.4. These results indicate that the altered sequences may be important for intracellular targeting of Vpr.

Our recent data indicated that when Vpr was expressed in the absence of other viral proteins, it was found primarily in the nucleus (Lu *et al.*, 1993). However, when Vpr was coexpressed with the HIV-1 Gag precursor protein, it was incorporated into virions. These findings provide further evidence that other viral proteins are critical for export of Vpr from infected cells.

In conclusion, our results show that Vpr is localized in

virions primarily beneath the viral envelope. Furthermore, Vpr is incorporated into HIV-1 virions on cellular vacuolar membranes as well as at the plasma membrane. An alteration of the highly conserved sequence at residues 79 to 85 results in redistribution of Vpr virion incorporation to favour intracellular rather than extracellular budding virions. Additional studies of the interaction of Vpr with the viral core structure will be necessary to decipher its contribution to HIV-1 replication.

We thank Ms Nancy Vander Heyden for technical assistance. This work was supported by grants NSC-81-0412-B-016-505 and NSC-83-0412-B-016-013 from the National Science Council of the Republic of China, ACS grant FRA 373, contract DAMD-90C-0125 and an American Foundation for AIDS Research Travel Award 200078-12-SG.

References

- ARYA, S. K., GUO, C., JOSEPHS, S. F. & WONG-STAAI, F. (1985). Trans-activator gene of human T-lymphotropic virus type III (HTLV-III). *Science* **229**, 69-73.
- COHEN, E. A., DEHNI, G., SODROSKI, J. G. & HASELTINE, W. A. (1990a). Human immunodeficiency virus vpr product is a virion-associated regulatory protein. *Journal of Virology* **64**, 3097-3099.
- COHEN, E. A., TERWILLIGER, E. F., JALINOS, Y., PROULX, J., SODROSKI, J. G. & HASELTINE, W. A. (1990b). Identification of HIV-1 vpr product and function. *Journal of Acquired Immunodeficiency Syndrome* **3**, 11-18.
- DEDERA, D., HU, W., VANDER HEYDEN, N. & RATNER, L. (1989). Viral protein R of human immunodeficiency virus types 1 and 2 is dispensable for replication and cytopathogenicity in lymphoid cells. *Journal of Virology* **63**, 3205-3208.
- GELDERBLOM, H. R., HAUSMANN, E. H., OZEL, M. & KOCH, M. A. (1987). Fine structure of human immunodeficiency virus (HIV) and immunolocalization of structural protein. *Virology* **156**, 171-176.
- GELDERBLOM, H. R. (1991). Assembly and morphology of HIV: potential effect on viral function. *AIDS* **5**, 617-638.
- GRIEF, C., FARRAR, G. H., KENT, K. A. & BERGER, E. G. (1991). The assembly of HIV within the Golgi apparatus and Golgi-derived vesicles of JM cell syncytia. *AIDS* **5**, 1433-1439.
- HART, T. K., KLINKNER, A. M., VENTRE, J. & BEGELSKI, P. J. (1993). Morphometric analysis of envelope glycoprotein gp120 distribution on HIV-1 virions. *Journal of Histochemistry and Cytochemistry* **41**, 265-271.
- HATTORI, N., MICHAELS, F., FARGNOLI, K., MARCON, L., GALLO, R. C. & FRANCHINI, G. (1990). The human immunodeficiency virus type 2 vpr gene is essential for productive infection of human macrophages. *Proceedings of the National Academy of Sciences, U.S.A.* **87**, 8080-8084.
- HAUSMANN, E. H. S., GELDERBLOM, H. R., CLAPHAM, P. R., PAULI, G. & WEISS, R. A. (1987). Detection of HIV envelope specific antibodies by immunoelectron microscopy and correlation with antibody titer and virus neutralizing activity. *Journal of Virological Methods* **16**, 125-137.
- LU, Y.-L., SPEARMAN, P. & RATNER, L. (1993). HIV-1 viral protein R localization in infected cells and virions. *Journal of Virology* **67**, 6542-6550.
- MYERS, G., KORBER, B., BERZOFKY, J. A., SMITH, R. F. & PAVLAKIS, G. N. (1992). Human Retroviruses and AIDS, 1992. *Report of the Theoretical Biology and Biophysics Group T-10*. Los Alamos: Los Alamos National Laboratory.
- OGAWA, K., SHIBATA, R., KIYOMASU, T., HIGUCHI, K., KISHIDA, Y., ISHIMOTO, A. & ADACHI, A. (1989). Mutational analysis of the human immunodeficiency virus vpr open reading frame. *Journal of Virology* **63**, 4110-4114.

- ORENSTEIN, J. M., MELTZER, M. S., PHIPPS, T. & GENDELMAN, H. E. (1988). Cytoplasmic assembly and accumulation of human immunodeficiency virus types 1 and 2 in recombinant human colony-stimulating factor-1-treated human monocytes: an ultrastructural study. *Journal of Virology* **62**, 2578-2586.
- PAUTRAT, G., SUZAN, M., SALAÜN, D., CORBEAU, P., ALLASIA, C., MOREL, G. & FILIPPI, P. (1990). Human immunodeficiency virus type 1 infection of U937 cells promotes cell differentiation and a new pathway of viral assembly. *Virology* **179**, 749-758.
- PAXTON, W., CONNOR, R. I. & LANDAU, N. R. (1993). Incorporation of Vpr into human immunodeficiency virus type 1 virions: requirement for the p6 region of gag and mutational analysis. *Journal of Virology* **67**, 7229-7237.
- ROSEN, C. A. (1991). Regulation of HIV gene expression by RNA-protein interaction. *Trends in Genetics* **7**, 9-14.
- STRANSKY, G. & GAY, S. (1991). Ultrastructural localization of HTLV-I gag protein p19 and p24 by single and double immunogold labeling. *Journal of Histochemistry and Cytochemistry* **39**, 185-191.
- WESTERVELT, P., HENKEL, T., TROWBRIDGE, D. B., ORENSTEIN, J., HEUSER, J., GENDELMAN, H. E. & RATNER, L. (1992). Dual regulation of silent and productive infection in monocytes by distinct HIV-1 determinants. *Journal of Virology* **66**, 3925-3931.
- YUAN, X., MATSUDA, Z., MATSUDA, M., ESSEX, M. & LEE, T.-H. (1990). Human immunodeficiency virus vpr gene encodes a virion-associated protein. *AIDS Research and Human Retroviruses* **6**, 1265-1271.

(Received 8 April 1994; Accepted 27 April 1994)

Alterations in Spliced and Unspliced HIV-1-Specific RNA Detection in Peripheral Blood Mononuclear Cells of Individuals with Varying CD4-Positive Lymphocyte Counts

MAX ARENS,¹ THERESA JOSEPH,¹ SUTAPA NAG,¹ J. PHILIP MILLER,² WILLIAM G. POWDERLY,³
and LEE RATNER^{3,4}

ABSTRACT

Reverse transcriptase-polymerase chain amplification reactions (RT-PCR) were used to identify transcripts for HIV-1 structural and regulatory proteins in peripheral blood mononuclear cells of a cohort of 48 patients. At least one set of PCR primers was capable of detecting HIV-1 transcripts in 94% of patients. Unspliced *gag-pol* transcripts were detected with *gag* or *pol* primer sets in 60 and 63% of samples, respectively. A significant inverse correlation was noted between transcript identification with the *gag* primer set and the number of CD4-positive lymphocytes in the blood sample and the clinical stage of infection. Single-spliced *env* transcripts were identified in 44% of individuals. Multiple-spliced *tat* or *nef* transcripts were detected in 6.2 and 53% of individuals, respectively. These findings indicate that viral transcripts are expressed throughout the course of HIV-1 infection.

INTRODUCTION

THE NATURAL HISTORY of HIV-1 infection is characterized by an acute phase of illness within the first few months after infection, a chronic and clinically indolent phase of disease lasting a few months to more than 10 years, and a late stage of illness characterized as AIDS with opportunistic infections and malignancies.¹ Progression from the chronic asymptomatic phase of disease to AIDS is characterized by a continual decline in the number of CD4⁺ lymphocytes, an increase in the level of viremia,²⁻⁴ an increase in the number of HIV-1 DNA-positive lymphocytes,⁴⁻⁵ and an increase in the number of infected cells that express viral gene products.^{6,7} The increase in virus gene expression associated with disease progression is likely critical to the pathogenesis of HIV-1.¹ Increased virus expression may result from changes in host immune regulation and virus-mediated regulatory influences. The goal of the current study was to examine the influence of viral regulatory genes in a cross-sectional cohort of patients at different stages of disease.

The HIV-1 genome includes overlapping reading frames for

structural genes (*gag*, *pol*, and *env*) and regulatory genes (*tat*, *rev*, *vif*, *vpr*, *vpu*, and *nef*) (Fig. 1A).⁸ Structural genes encode proteins found in the virus particle that are important for the assembly and enzymatic functions of the virus. Regulatory genes encode proteins that are generally not found in the virus particle (with the exception of *vpr*) and that are thought to be important for virus replication in the host cell.¹ Two regulatory gene products modulate virus transcription, and were therefore chosen as a major focus of the current study. These include Tat, which is a potent positive effector of virus gene expression⁹ and Nef, which appears to be a weak negative modulator of virus RNA synthesis.¹⁰ The Rev protein also exerts a regulatory effect on mRNA expression,¹ but was not included in our analysis.

Expression of the HIV-1 genome is mediated by three classes of viral mRNAs: unspliced (9.0 kb), single-spliced (4.5 kb), and multiple-spliced (1.8-2.2 kb) transcripts (Fig. 1B-D).¹¹ Structural genes are encoded by the first two classes of transcripts, with the unspliced mRNA producing Gag and Pol proteins and single-spliced mRNA producing Env proteins (as well as Vif, Vpr, and Vpu products).¹² Regulatory genes (with the exception

Departments of Pediatrics,¹ Biostatistics,² Medicine,³ and Molecular Microbiology,⁴ Washington University School of Medicine, St. Louis, Missouri 63110.

of *vif*, *vpr*, and *vpu* are expressed from multiple-spliced mRNAs. The single-spliced *vpu-env* mRNA utilizes splice donor and splice acceptor sites at nucleotides 287 and 5557 (Fig. 1C)¹³ (nucleotide positions according to Ref. 14). The multiple-spliced mRNAs all utilize splice donors at nucleotides 287 and 5625, and a splice acceptor at nucleotide 7956 (Fig. 1D). Utilization of a particular splice acceptor site in the central portion of the genome distinguishes *nef* mRNAs (splice acceptor at nucleotide 5557) from *tat* mRNAs (splice acceptor at nucleotide 5357), and from other regulatory gene transcripts. Additional exons in the central portion of the genome are utilized in regulatory gene transcripts.¹³

The current study has utilized these features of splicing to develop reverse transcriptase-polymerase chain (RT-PCR) assays capable of distinguishing transcripts for individual HIV-1 structural or regulatory genes. Primers complementary to sequences in different exons were utilized to amplify spliced but

not unspliced transcripts (Fig. 1C and D). The single-spliced *env* mRNA is distinguished from multiply spliced regulatory gene mRNAs by using a downstream primer (*Senv*) complementary to a sequence present in the *env* mRNA, but removed by splicing from regulatory gene mRNAs (Fig. 1C). Different regulatory gene transcripts are distinguished from one another by the use of primers complementary to the sequence spanning the splice acceptor site unique for the particular transcript (S4B at nucleotide 5357 for *tat* mRNA and S7B at nucleotide 5557 for *nef* mRNA).

In the current study, we have used nested sets of primers to perform PCR on RNA extracted from patient peripheral blood mononuclear cells (PBMCs) at various stages of disease, as characterized by the number of CD4⁺ lymphocytes. We have identified structural as well as regulatory poly(A)⁺ RNA transcripts in patients with a wide range of CD4 cell counts. We demonstrated active transcription of mRNA from several regions of the HIV-1 genome in patients who have no symptomatic disease as well as in those who have AIDS.

MATERIALS AND METHODS

Patients

Blood was drawn from 48 HIV-1-seropositive patients presenting to the Washington University AIDS Clinical Trials Unit (ACTU) between October 1991 and May 1992. Most patients were being screened for entry onto ACTU protocols and 37 patients had not previously received an antiretroviral drug (Table 1). All patients gave informed consent.

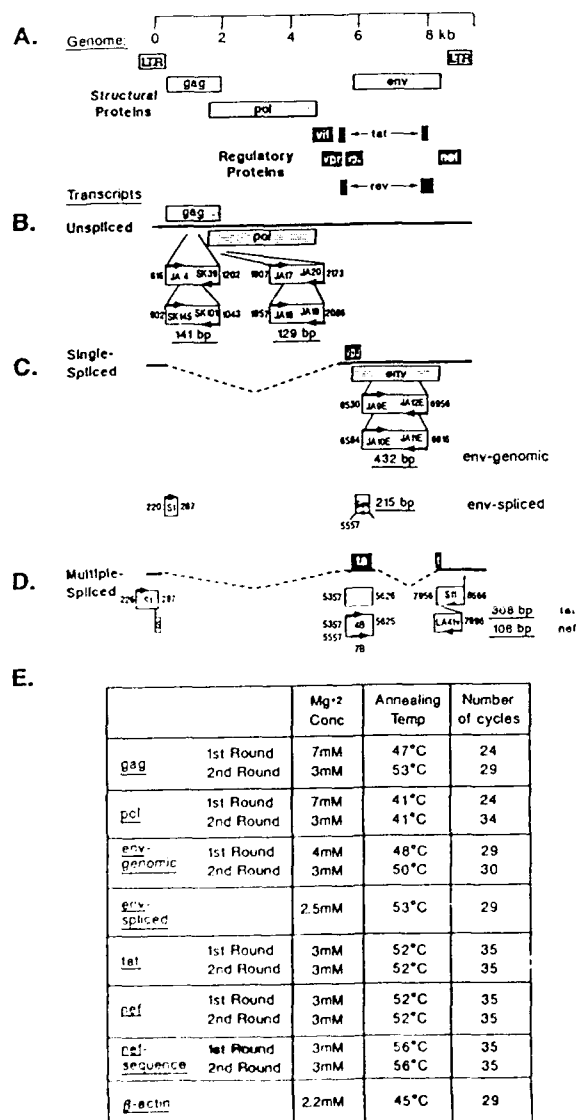


FIG. 1. HIV-1 RNA RT-PCR analysis. (A) The schematic drawing of the HIV-1 genome is shown with the nucleotide positions relative to the RNA initiation site indicated above. Genes encoding structural proteins and regulatory proteins are indicated separately. (B) The unspliced transcript that encodes Gag and Pol proteins is indicated as well as the positions of the nested primer sets in each gene. Arrows indicate positions of the primers, and the designation for each primer is shown in the box above or below the arrow. Nucleotide positions of the primers are indicated outside the boxes. The predicted sizes of the products of the nested PCR reactions are underlined and indicated below the boxes. In the case of *env*-genomic products, the actual product size was 22 bp larger than the genome locations would indicate because of the addition of 11 bp on each primer, including an *Eco*RI restriction enzyme site. (C) The single-spliced transcript encoding Env and Vpu products is indicated with the dotted line indicating the intron that is removed by splicing. The nested *env*-genomic primers are indicated, as well as the *env*-spliced primers. (D) The multiple-spliced transcripts are represented by a schematic showing one of the *tat* mRNAs. In each case, the first round of PCR was performed with primers S1 and S11 shown in the 5' and 3' most exons. The second round of PCR was performed with primers S4B (for *tat* mRNAs) or S7B (for *nef* mRNAs), both of which span the first splice site, and with primer LA41, found in the 3' most exon. The predicted nested PCR product sizes for *tat* and *nef* transcripts are underlined and indicated to the right. (E) Reaction conditions for PCR are listed.

TABLE 1. IMMUNOLOGICAL MEASUREMENTS AND POLYMERASE CHAIN REACTION RESULTS ON PATIENT COHORT

Patient No.	CDC class	Immunological						PCR results						
		CD4 ⁺ (No.)	CD4 (%)	CD8 (No.)	CD8 (%)	T4/T8	AVT ^a	gag	pol	env (genomic)	env (spliced)	tat	nef	nef-seq
1	C3	0	0	223	62	0.0	Yes	+	+	+	-	-	-	-
2	C3	0	0	529	55	0.0	Yes	+	+	+	+	-	-	-
3	C3	6	7	37	41	0.16	Yes	+	+	+	-	-	-	-
4	B3	8	1	424	51	0.02	Yes	+	+	+	+	-	-	-
5	C3	8	1	178	22	0.04	Yes	+	+	+	+	-	-	-
6	C3	10	5	119	57	0.08		+	+	+	-	-	-	-
7	C3	23	2	897	79	0.03		-	+	+	+	-	-	+
8	B3	24	2	722	59	0.03	Yes	+	-	-	-	-	-	-
9	B3	32	5	486	76	0.07	Yes	+	+	+	-	-	+	-
10	B3	62	4	1287	83	0.05		+	+	+	-	+	+	-
11	B3	86	8	713	66	0.12		+	-	-	-	-	-	-
12	B3	105	5	990	47	0.11	Yes	-	-	-	-	-	+	-
13	A3	137	6	1938	85	0.07		-	-	-	-	-	+	+
14	A3	177	12	854	58	0.21	Yes	-	+	+	-	-	+	-
15	B3	185	19	614	63	0.30		-	-	+	+	-	+	+
16	B3	191	11	1180	68	0.16		+	+	+	+	-	-	+
17	B3	195	21	492	53	0.40		+	+	+	-	+	+	-
18	A2	255	16	894	56	0.29		-	-	-	+	-	+	+
19	B2	259	16	875	54	0.30		+	+	+	-	-	+	-
20	A2	281	15	1161	62	0.24		+	+	+	+	-	+	-
21	A2	297	25	654	55	0.45		-	+	+	-	-	-	-
22	B1	306	29	444	42	0.69		-	-	+	+	-	-	-
23	B2	333	17	1420	58	0.29		-	+	-	+	-	+	-
24	B2	336	28	576	43	0.65		+	+	-	-	-	+	-
25	A2	358	23	935	60	0.38		+	+	+	-	-	+	-
26	B2	365	28	770	59	0.47		+	-	+	+	-	+	+
27	A2	370	22	959	57	0.39		+	+	+	+	-	-	-
28	B2	370	14	1614	61	0.23		+	+	+	+	-	-	-
29	B2	383	25	826	54	0.46		-	-	-	-	-	-	-
30	A2	390	29	685	51	0.57		-	-	-	-	-	+	-
31	A2	392	30	626	48	0.63		-	-	-	+	-	-	-
32	A2	408	17	1392	58	0.29	Yes	+	+	+	+	+	+	-
33	A2	421	20	1221	58	0.34		-	-	+	+	-	-	-
34	A2	424	16	1962	74	0.22		+	+	-	-	+	+	+
35	C2	426	36	463	39	0.92		+	+	-	-	-	-	-
36	A2	434	29	763	51	0.57		+	+	+	+	-	+	-
37	A2	460	31	728	49	0.63		+	-	-	-	-	-	-
38	A2	490	28	998	57	0.49		+	+	-	+	-	+	+
39	A1	535	25	1214	59	0.44		+	+	+	-	-	+	+
40	A1	560	32	980	56	0.57		-	-	-	+	-	-	-
41	B1	564	18	1942	62	0.29		+	+	-	-	-	+	-
42	A1	569	19	2065	69	0.28		-	+	+	+	-	-	-
43	B1	587	26	1331	59	0.44		-	-	-	-	-	-	-
44	B1	647	33	902	46	0.72		+	-	-	-	-	-	-
45	A1	686	26	1399	53	0.49	Yes	-	+	+	-	-	+	-
46	A1	822	31	1405	53	0.59		-	+	-	+	-	+	+
47	A1	902	52	520	30	1.73		-	-	-	-	-	-	-
48	A1	1280	49	706	27	1.81		-	-	+	-	-	-	-

^aAVT, antiviral therapy: yes, patients were known to have been on therapy within the previous 6 months; blanks indicate patient had not been on therapy.

Cells

Peripheral blood mononuclear cells were purified by Ficoll-Hypaque (LSM; Organon Teknika Corp., Durham, NC) gradient centrifugation from heparinized venous blood of patients. Separated cells were washed twice with phosphate-buffered saline (PBS) and aliquots were suspended in freeze medium

(10% dimethylsulfoxide [DMSO] and 40% fetal calf serum in RPMI medium) and viably frozen at -75°C.

Purification and quantitation of polyadenylated RNA

Samples of patient cells, frozen as described above, were thawed, and the number of viable cells counted in the presence

of trypan blue (>95% viable). Aliquots of 5×10^6 cells were used for isolation of poly(A)⁺ RNA according to the Micro-Fast Track procedure (Invitrogen, San Diego, CA). The purified poly(A)⁺ RNA was treated with RNase-free DNase I (40 units; Boehringer Mannheim, Indianapolis, IN) at 37°C for 10 min in the presence of 1 µg of carrier tRNA, 10 mM MgCl₂, 0.1 mM dithiothreitol, and 200 U of RNasin (Promega, Madison, WI). Each reaction was stopped by addition of 4 µl of 0.5 M ethylenediaminetetraacetic acid (EDTA) and 4 µl of 10% sodium dodecyl sulfate (SDS). DNase-treated poly(A)⁺ RNA was extracted once with phenol-chloroform-isoamyl alcohol (100:96:4) and the aqueous phase was precipitated by the addition of glycogen carrier (10 µl), 30 µl of 2 M sodium acetate, and 3 vol of cold ethanol and kept at -70°C overnight. The precipitate was collected by centrifugation, dried at room temperature, and dissolved in elution buffer.

Quantitation of poly(A)⁺ RNA was accomplished by measuring the incorporation of oligo(dT)-directed incorporation in the presence of Moloney murine leukemia virus (M-MuLV) reverse transcriptase (RT) of [³H]dCTP into DE81-retainable material, using purified globin mRNA (GIBCO/BRL/Life Technologies, Gaithersburg, MD) as a standard. A 2-µl sample of each purified RNA from above was denatured at 65°C for 3 min and then added to a reaction mixture (final volume, 20 µl) containing the following: 80 U of RNasin, 0.02 OD of oligo p(dT)₁₂₋₁₈, 0.4 mM each of dATP, dGTP, and dTTP, 5 µCi of [³H]dCTP (28 Ci/mmol; ICN Radiochemicals, Irvine, CA), 50 mM Tris-HCl (pH 8.3), 30 mM KCl, 8 mM MgCl₂, 1 mM dithiothreitol, and 20 U of M-MuLV RT (GIBCO/BRL, Gaithersburg, MD). The reaction was incubated at 37°C for 1 hr and stopped by the addition of 4 vol of 10 mM Tris-HCl (pH 7.5) containing 1 mM EDTA. Duplicate 50-µl samples were spotted onto DE81 filter paper disks and dried. Filters were washed five times in 5% sodium phosphate dibasic, once in 95% ethanol, dried, and counted in a liquid scintillation counter. A standard curve using 50 pg to 2.5 ng of purified globin mRNA was run with each assay and was used to calculate RNA concentrations of patient samples. Samples that did not fall within the linear portion of the standard curve were diluted appropriately and the assay repeated.

Reverse Transcriptase-Polymerase Chain Reaction

The RT reaction was performed using 1.5×10^5 cell equivalents of RNA in a final volume of 20 µl containing the following: 1 mM each of dATP, dCTP, dGTP, and dTTP, 6.5 mM MgCl₂, 10 mM Tris-HCl (pH 8.3), 50 mM KCl, 20 U of RNasin, 2.5 µM random primers (GIBCO/BRL) and 2.5 U of M-MuLV RT (GIBCO/BRL). The reaction was incubated at room temperature for 10 min and then at 42°C for 35 min and was terminated by heating at 99°C for 5 min.

For PCR, the 20-µl reaction from above was added to a final volume of 50 µl containing the following: 400 µM each of dATP, dCTP, dGTP, and dTTP, 10 mM Tris-HCl (pH 8.3), 50 mM KCl, 0.01% gelatin, 10 pmol of each primer, 1.25 units of *Taq* polymerase (Amplitaq; Cetus Corp., Emeryville, CA) and MgCl₂ as shown in Fig. 1E. Primers, annealing temperatures, cycle numbers, and expected product sizes for PCR amplifications are shown in Fig. 1B-E. The genomic locations of all JA primers were given by Albert and Fenyo.¹⁵ The *env* primer set

(JA9E, JA10E, JA11E, and JA12E) is as described by Albert and Fenyo, with the addition of an *Eco*RI site at the 5' end of each primer. SK primers were as described by Ou *et al.*¹⁶ β-Actin primers were described by Michael *et al.*¹⁷ The sequences of other primers are as follows:

S1: 5'-TCTCTCGACGCGAGCTCGGCTTGC-3' (HIV-1 nucleotides: 226-250)

Senv: 5'-CCACACAACCTATTGCTATTATT-3' (HIV-1 nucleotides: 5707-5686)

S11: 5'-TCCAGTCCCCCTTTCTTTTAAAAA-3' (HIV-1 nucleotides: 8641-8666)

S4B: 5'-GAGGGGCGGCGACTGAATTGGGTGTC-3' (HIV-1 nucleotides: 275-287, 5357-5368)

S7B: 5'-GGGGCGGCGACTGGAAGAAGCGGAGA-3' (HIV-1 nucleotides: 275-287, 5557-5569)

LA41v: 5'-CTTCGGGCTGTCTGGGTCCCCCTCGGG-3' (HIV-1 nucleotides: 7995-7970)

NefAS: 5'-AGCACTCAAGGCAAGCTTTATTGAG-3' (HIV-1 nucleotides: 9210-9186)

8306: 5'-TTCCGAATTCAAGCTTGTAGAGCTATTCCG C-3' (HIV-1 nucleotides: 8306-8325)

9134: 5'-TTCCGAATTGAGCTCCCAGGCTCAGATCT GG-3' (HIV-1 nucleotides: 9134-9113)

The initial RT-PCR assay on a particular RNA preparation included reactions with or without the RT, as a control. Only samples that yielded no product in the absence of RT, thus indicating the complete removal of DNA, were used for further analysis. DNA products were analyzed by agarose gel electrophoresis and ethidium bromide staining.

Sensitivity of *tat* and *nef* polymerase chain reaction

The plasmid pCV1, containing 1.8-kb insert of a cDNA copy of *tat* mRNA, and the plasmid pCV3, containing a 1.7-kb insert of a cDNA copy of *nef* mRNA,⁹ were used to determine the sensitivity of the *tat* and *nef* nested PCR reactions using DNA as a target. S1 and S11 were used in both cases as the outside primers (Fig. 1D). With pCV1, at least seven copies of *tat* DNA could be detected in a reaction mixture when S4B and LA41V were used as the inside primers. With pCV3 DNA as a target and S7B and LA41V as inside primers, at least seven copies of DNA could be detected by PCR.

The sensitivity of the nested PCR reaction for detection of *tat* and *nef* RNA transcripts was also determined. pCV1 and pCV3 were digested with *Pst*I and cloned into Bluescript KS (Pharmacia LKB Biotechnology, Piscataway, NJ). Bluescript plasmids were linearized using *Sma*I for the *tat* plasmid or *Eco*RI for the *nef* plasmid. *In vitro* transcription products were synthesized with T3 or T7 polymerase according to a standard protocol (Promega) using an *in vitro* transcription kit (Stratagene, La Jolla, CA). RNA products were treated with DNase I prior to analysis on ethidium bromide-stained formaldehyde gels. RNA was purified through two push columns (Stratagene) and the optical density of the final product was determined and used to calculate RNA copy number for PCR sensitivity analysis. Our

nested primer method could consistently detect 10 to 100 copies of *in vitro*-synthesized transcripts.

RESULTS

Immunological characteristics of study patients

Blood samples from the 48 patients were analyzed for immunological markers. CD4⁺ lymphocyte counts ranged from 0 to 1280/mm³ (mean, 352/mm³; normal range, 1000–1500/mm³); CD4 percentage ranged from 0 to 52% (mean 20%); CD8⁺ cell counts ranged from 37 to 2065/mm³ (mean, 924/mm³); CD8 percentage ranged from 22 to 85 (mean, 55%); and CD4/CD8 ratio ranged from 0 to 1.81 (mean, 0.21). The subjects are listed in Table 1 according to increasing CD4⁺ lymphocyte counts.

Strategy for the detection of HIV RNAs

As shown in Fig. 1, HIV RNAs were detected with nested sets of PCR primers. The locations of primers within the HIV genome and relative to each other are shown in Fig. 1B–D. Primer pairs for *gag* and *pol* were designed to amplify unspliced RNAs (Fig. 1B), and primer pairs for *env*-spliced (Fig. 1C), *tat* (Fig. 1D), *nef* (Fig. 1D), and *nef*-sequence (using primers S7B and NefAs in the first round and primers 8306 and 9134 in the second round, Fig. 1E) were designed to amplify spliced mRNA. Whereas primers for *env*-genomic are capable of amplifying both unspliced and single-spliced transcripts, primers for *env*-spliced amplify only spliced *env* mRNA. Two different sets of primers were utilized for *nef* mRNA which amplify products of 108 bp (*nef*) or 828 bp (*nef*-sequence). For RNA preparations in which HIV-specific transcripts were not detected, the quality of the RNA was confirmed by RT-PCR with β -actin primers (Fig. 1E).

Detection of HIV RNAs

The results of the nested PCR assays for HIV RNA with seven different sets of primers are shown in Table 1. Of the 48 patient samples that were analyzed with all 7 sets of nested primers, 45 (93.8%) were positive with at least 1 set of HIV-specific primers. The three samples in which no HIV-1 transcripts were detected were obtained from patients with CD4 cell counts of 383, 587, and 902/mm³, respectively. None of the latter three patients had received antiretroviral therapy.

When nested sets of primers were used for the detection of unspliced RNAs, the *gag* primer set yielded 29 of 48 (60%) positive results, the *pol* nested primer set yielded 30 of 48 (63%) positive results, and the *env*-genomic nested primer set yielded 31 of 48 (65%) positive. All of these primer sets should detect unspliced RNA, whereas the *env*-genomic primer set should also detect spliced *env* RNA species. There was good correlation between the results with *gag* and *pol* primer sets, with 23 samples yielding positive results with both primer sets, 6 samples yielding positive results with the *gag* primer set but not the *pol* primer set, and 7 samples yielding positive results with the *pol* primer set but not the *gag* primer set. Discordances may be due to sequence variation at sites of binding of individual primers. Twenty-two samples were positive with *env*-genomic

primers as well as both *gag* and *pol* primer sets, 5 samples were positive with *env*-genomic primers and *gag* or *pol* primer sets, 4 samples were positive with *env*-genomic primers but neither *gag* nor *pol* primers, and 11 samples negative with *env*-genomic primers were positive with *gag* and/or *pol* primers.

When nested sets of primers were used for the detection of spliced RNAs, the *env*-spliced primer set yielded 21 of 48 (44%) positive results, the *tat* set yielded 3 of 48 (6.2%) positive results, *nef* primers yielded 28 of 53 (53%) positive results, and the *nef*-sequence primer set yielded 9 of 48 (19%) positive results. Discrepancies between the two different *nef* primer sets may be due to sequence heterogeneity, as well as to the lower sensitivity of the *nef*-sequence primer set compared to the *nef* primer set.

Kendall Tau b correlation coefficients and *p* values of significant inverse correlations were determined between results of transcript detection and immunological parameters and clinical parameters. Table 2^{17a} shows the results of these calculations for transcripts that either approached or attained statistical significance when correlated with various immunological parameters. Statistical significance (at the level of *p* < 0.05) was achieved in the correlation of *gag* transcripts with CD4 cell count, CDC clinical stage, and CDC clinical/CD4 stage, *pol* transcripts with CD4%, *env*-genomic transcripts with CD4% and *nef*-sequence transcripts with CD8%.

DISCUSSION

Our results support and extend the conclusions of other investigators who have documented the presence of HIV-1 transcripts at all stages of disease. Thus, we and others have detected mRNA⁴ for structural proteins in a high percentage of patients, and at all levels of CD4 lymphocytes.^{6,18,19} In addition, our study is the first to examine the expression of *tat* and *nef* mRNAs in a cross-sectional cohort of subjects. We have shown that mRNAs for these regulatory proteins are also present in peripheral blood mononuclear cells of patients with CD4 cell counts in the range of 0 to 822 cells/mm³. Whereas *tat* mRNA is rarely detectable under the current assay conditions, *nef* mRNA is detectable in the majority of HIV-1-infected individuals. The higher level of *nef* than *tat* transcripts may be a reflection of similar results obtained in studies of HIV-1 infection *in vitro*.^{20–22} Rev is another important HIV regulatory protein, but has not been included in this present analysis of patient PBMCs.

Schnittman *et al.* used an RT-PCR technique to assess the transcriptional activity of HIV-1 in peripheral blood mononuclear cells from infected patients.⁶ They found viral transcripts in 84% of the individuals, regardless of the clinical status of their HIV disease or the use of antiretroviral therapies. In addition, they showed a significant inverse correlation between the presence of *gag* mRNA and CD4 counts of less than 30%. This finding is confirmed in the present study, and extended by demonstrating that *env*-genomic transcripts were also significantly associated with depressed CD4% and CD4/CD8 ratio. It remains to be determined by longitudinal studies whether the presence of any of these transcripts in the peripheral blood mononuclear cells of a single patient is predictive of more rapid progression or more severe disease.

TABLE 2. KENDALL TAU b CORRELATION ANALYSIS BETWEEN PRESENCE OF HIV-1 RNA TRANSCRIPTS AND IMMUNOLOGICAL PARAMETERS

Gene	Correlation coefficient (P)					CDC ^a clin	CDC ^b clin/CD4
	CD4	CD4 (%)	CD8	CD8 (%)	CD4/CD8		
<i>gag</i>	-0.25 (0.03)	-0.24 (0.05)	-0.18 (0.13)	-0.02 (0.90)	-0.21 (0.08)	0.36 (0.01)	0.38 (0.003)
<i>pol</i>	-0.17 (0.16)	-0.25 (0.04)	0.02 (0.88)	0.09 (0.47)	-0.22 (0.06)	0.16 (0.25)	0.16 (0.22)
<i>env-gen</i>	-0.22 (0.06)	-0.29 (0.02)	-0.07 (0.56)	0.20 (0.11)	-0.27 (0.02)	0.12 (0.40)	0.13 (0.31)
<i>nef</i>	0.09 (0.94)	0.006 (0.96)	0.20 (0.09)	0.10 (0.43)	0.009 (0.94)	-0.27 (0.05)	-0.15 (0.24)
<i>nef-seq</i>	-0.08 (0.95)	-0.02 (0.87)	0.21 (0.08)	0.28 (0.02)	-0.04 (0.72)	-0.09 (0.53)	-0.05 (0.71)

^aCDC classification of HIV infection based on clinical status. Categories are (1) asymptomatic, (2) symptomatic, non-AIDS, and (3) AIDS-indication illness.

^bCDC classification of HIV infection based on clinical status and CD4 cell count. Above categories are subdivided into three groups: CD4 count >500/mm³, 200–499/mm³, and <200/mm³.^{17a}

Schnittman *et al.* also detected spliced mRNAs containing the major splice junction (*msj*) and *tat/rev*.⁶ Only 6 of 49 patients had detectable *msj* transcripts whereas 29 of 49 had *tat/rev* transcripts but no significant correlations with other parameters were demonstrated. We detected *tat* mRNA in only 3 of 48 patients, *nef* was detected in 24 of 48, and, using *nef*-sequence primers, we detected *nef*RNA in 9 of 48. There was a significant ($p = 0.02$) correlation of CD8% with the presence of transcripts detectable with the *nef*-sequence primer set. The significance of this finding with respect to disease stage or progression is not certain at present. The ability of these PCR techniques to detect unspliced and spliced HIV RNAs in patient PBMCs at all stages of disease demonstrates the breadth of transcriptional activity of HIV.

Others have described analyses of PBMC RNA for *tat* mRNA. Furtado *et al.* performed PCR on 6.6×10^5 cell equivalents of total cellular RNA with an internal *tat* RNA control, and calculated a range of 2500–6500 copies of *tat* mRNA/10⁶ PBMC.²³ Patterson *et al.* used PCR-driven *in situ* hybridization on patient PBMCs, and detected *tat* RNA in <1 to 8% of cells.²⁴ The differences between these results and our data may be accounted for by the different RNA extraction methods, different amounts of RNA in the assay, different PCR techniques, or different primers used for PCR.

Michael *et al.* have demonstrated that progression of HIV disease is characterized by a conversion of transcripts from spliced to unspliced genomic RNA.¹⁷ Schsma and colleagues also reported higher ratios of levels of spliced and unspliced mRNAs in asymptomatic HIV-1-infected individuals compared to AIDS patients.²⁵ These findings reflect the findings obtained with an *in vitro* model of HIV-1 latency, which shows a preponderance of multiple-spliced over unspliced transcripts. When HIV-1 is activated from latency *in vitro*, the ratio of unspliced to multiple-spliced transcripts increases.²⁶ Although our data are not quantitative, the significant inverse correlations

of the presence of *gag* and *env*-genomic transcripts with CD4 number and percentage support these observations.

The current study is limited to examining cellular RNAs rather than free genomic RNA in the plasma. Ottmann and colleagues demonstrated HIV-1 genomic RNA in 95% of infected individuals,²⁷ and Bagnarelli and colleagues show the levels of plasma RNA correlated with disease stage better than did the levels of cell-associated RNAs.²⁸ The current study is also limited to examining viral transcripts in PBMCs, which may differ from mRNAs present in tissues. Analysis of viral transcription *in vivo* should provide further understanding of HIV-1 pathogenesis, and may serve as a marker for monitoring antiviral therapies.

ACKNOWLEDGMENTS

We thank David Starkey for technical assistance, Evan Sadler and Lisa Westfield (Howard Hughes Medical Institute) for oligonucleotides, the staff of the ACTG for collection of blood samples, Warren Seyfried for data collection, and Gregory Storch for his continuous advice and support. This work was supported by Contract DAMD-90C-0057, and Grants AI 25903, FRA 373 (ACS Research Faculty Award to L.R.), AMFAR 001709, and a grant from the McDonnell Douglas Employees Fund.

REFERENCES

1. Ratner L. Molecular biology and pathogenesis of HIV. *Curr Opin Infect Dis* 1993;6:181–190.
2. Coombs RW, Collier AC, Allan JP, Nikora B, Leuther M, Gierset G, and Corey L. Plasma viremia in human immunodeficiency virus infection. *N Engl J Med* 1989;321:1626–1636.

3. Ho DD, Moudgil T, and Alam M: Quantitation of human immunodeficiency virus type 1 in the blood of infected persons. *N Engl J Med* 1989;321:1621-1625.
4. Simmonds P, Balfe P, Ludlam CA, Bishop JO, and Brown AJL: Analysis of sequence diversity in hypervariable regions of the external glycoprotein of human immunodeficiency virus type 1. *J Virol* 1990;64:5840-5850.
5. Hsia K and Spector SA: Human immunodeficiency virus DNA is present in a high percentage of CD4+ lymphocytes of seropositive individuals. *J Infect Dis* 1991;164:470-475.
6. Schnittman SM, Greenhouse JJ, Lane HC, Pierce PF, and Fauci AS: Frequent detection of HIV-1-specific mRNAs in infected individuals suggests ongoing active viral expression in all stages of disease. *AIDS Res Hum Retroviruses* 1991;7:361-367.
7. Lewis DE, Minshall M, Wray NP, Paddock SW, Smith LC, and Crane MM: Confocal microscopic detection of human immunodeficiency virus RNA-producing cells. *J Infect Dis* 1990;162:1373-1378.
8. Bryant M and Ratner L: The biology and molecular biology of HIV. *Pediatr Infect Dis J* 1992;11:390-400.
9. Arya SK, Guo C, Josephs SF, and Wong-Staal F: Trans-activator gene of human T-lymphotropic virus type III (HTLV-III). *Science* 1985;229:69-73.
10. Niederman TMJ, Thielan BJ, and Ratner L: Human immunodeficiency virus type 1 negative factor is a transcriptional silencer. *Proc Natl Acad Sci USA* 1989;86:1128-1132.
11. Rabson AB, Daugherty DF, Venkatesan S, Boulukos KE, Benn SI, Folks TM, Fiorino P, and Martin MA: Transcription of novel open reading frames of AIDS retrovirus during infection of lymphocytes. *Science* 1985;229:1388-1390.
12. Schwartz S, Felber BK, Fenyo E-M, and Pavlakis GN: Env and Vpu proteins of human immunodeficiency virus type 1 are produced from multiple bicistronic mRNAs. *J Virol* 1990;64:5448-5456.
13. Schwartz S, Felber BK, Benko DM, Fenyo E-M, and Pavlakis GN: Cloning and functional analysis of multiply spliced mRNA species of human immunodeficiency virus type 1. *J Virol* 1990;64:2519-2529.
14. Ratner L, Fisher A, Jagodzinski LL, Mitsuya H, Liou R-S, Gallo RC, and Wong-Staal F: Complete nucleotide sequences of functional clones of the AIDS virus. *AIDS Res Hum Retroviruses* 1987;3:57-67.
15. Albert J and Fenyo EM: Simple, sensitive, and specific detection of human immunodeficiency virus type 1 in clinical specimens by polymerase chain reaction with nested primers. *J Clin Microbiol* 1990;28:1560-1564.
16. Ou C-Y, Kwok S, Mitchel SW, Mack DH, Sninsky JJ, Krebs JW, Feorino P, Warfield D, and Schoecketman G: DNA amplification for direct detection of HIV-1 in DNA of peripheral blood mononuclear cells. *Science* 1988;239:295-297.
17. Michael NL, Vahey M, Burke DS, and Redfield RR: Viral DNA and mRNA expression correlate with the stage of human immunodeficiency virus (HIV) type 1 infection in humans: evidence for viral replication in all stages of HIV disease. *J Virol* 1992;66:310-316.
- 17a. Centers for Disease Control and Prevention: 1993 revised classification system for HIV infection and expanded surveillance definition for AIDS among adolescents and adults. *MMWR* 1992;41(RR-17):1-19.
18. Davis GR, Blumeyer K, DiMichele J, Whitfield KM, Chappelle H, Riggs N, Ghosh SS, Kao PM, Fahy E, Kwok DY, Guatelli JC, Spector SA, Richman DD, and Gingeras TR: Detection of human immunodeficiency virus type 1 in AIDS patients using amplification-mediated hybridization analyses: reproducibility and quantitative limitations. *J Infect Dis* 1990;162:13-20.
19. Richman DD, McCutchan JA, and Spector SA: Detection human immunodeficiency RNA in peripheral blood mononuclear cells in peripheral blood mononuclear cells by nucleic acid hybridization. *J Infect Dis* 1987;156:823-827.
20. Guatelli JC, Gingeras TR, and Richman DD: Alternative splice acceptor utilization during human immunodeficiency virus type 1 infection of cultured cells. *J Virol* 1990;64:4093-4098.
21. Klotman ME, Kim S, Buchbinder A, DeRossi A, Baltimore D, and Wong-Staal F: Kinetics of expression of multiply spliced RNA in early human immunodeficiency virus type 1 infection of lymphocytes and monocytes. *Proc Natl Acad Sci USA* 1991;88:5011-5015.
22. Robert-Guroff M, Popovic M, Gartner S, Markham P, Gallo RC, and Reitz MS: Structure and expression of *tat*, *rev*, and *nef*-specific transcripts of human immunodeficiency virus type 1 in infected lymphocytes and macrophages. *J Virol* 1990;64:3391-3398.
23. Furtado MR, Murphy R, and Wolinsky SM: Quantification of human immunodeficiency virus type 1 *tat* mRNA as a marker for assessing the efficacy of antiretroviral therapy. *J Infect Dis* 1993;167:213-216.
24. Patterson BK, Till M, Otto P, Goolsby C, Furtado MR, McBride LJ, and Wolinsky SM: Detection of HIV-1 DNA and messenger RNA in individual cells by PCR-driven in situ hybridization and flow cytometry. *Science* 1993;260:976-979.
25. Sehnsam T, Bagasra O, Trono D, Baltimore D, and Pomerantz RJ: Blocked early-stage latency in the peripheral blood cells of certain individuals with human immunodeficiency virus type 1. *Proc Natl Acad Sci USA* 1992;89:10663-10667.
26. Pomerantz RJ, Trono D, Feinberg MB, and Baltimore D: Cells nonproductively infected with HIV-1 exhibit an aberrant pattern of viral RNA expression: a molecular model for latency. *Cell* 1990;61:1271-1276.
27. Ottmann M, Innocenti P, Tenadey M, Micoud M, Pelloquin F, and Seigneurin J-M: The polymerase chain reaction for the detection of HIV-1 genomic RNA in plasma from infected individuals. *J Virol Methods* 1991;31:273-284.
28. Bagnarelli P, Menzo S, Valenza A, Manzin A, Giacca M, Ancarani F, Scalise G, Varaldo PE, and Clementi M: Molecular profile of human immunodeficiency virus type 1 infection in symptomless patients and in patients with AIDS. *J Virol* 1992;66:7328-7335.

Address reprint requests to:

Max Arens

Department of Pediatrics

Washington University School of Medicine

1 Children's Place

St. Louis, Missouri 63110